U.S. Department
of Commerce

Volume 98
Number 3
July 2000

Fishery Bulletin

U.S. Department of Commerce
William M. Daley
Secretary

National Oceanic and Atmospheric Administration
D. James Baker
Under Secretary for Oceans and Atmosphere

National Marine Fisheries Service
Penelope D. Dalton
Assistant Administrator for Fisheries

Fishery Bulletin

Scientific Editor
Dr. John V. Merriner

Editorial Assistant
Sarah Shoffler

Southeast Fisheries Science Center
National Marine Fisheries Service, NOAA
101 Pivers Island Road
Beaufort, NC 28516

Managing Editor
Sharyn Matriotti
National Marine Fisheries Service
Scientific Publications Office
7600 Sand Point Way NE, BIN C15700
Seattle, Washington 98115-0070

Editorial Committee
Dr. Andrew E. Dizon National Marine Fisheries Service
Dr. Harlyn O. Halvorson University of Massachusetts, Boston
Dr. Ronald W. Hardy University of Idaho, Hagerman
Dr. Richard D. Methot National Marine Fisheries Service
Dr. Theodore W. Pietsch University of Washington, Seattle
Dr. Joseph E. Powers National Marine Fisheries Service
Dr. Harald Rosenthal Universität Kiel, Germany
Dr. Fredric M. Serchuk National Marine Fisheries Service

***Fishery Bulletin* web site: fishbull.noaa.gov**

The *Fishery Bulletin* (ISSN 0090-0656) is published quarterly by the Scientific Publications Office, National Marine Fisheries Service, NOAA, 7600 Sand Point Way NE, BIN C15700, Seattle, WA 98115-0070. Periodicals postage is paid at Seattle, WA, and at additional mailing offices. POSTMASTER: Send address changes for subscriptions to Fishery Bulletin, Superintendent of Documents, Attn.: Chief, Mail List Branch, Mail Stop SSOM, Washington, DC 20402-9373.

Although the contents of this publication have not been copyrighted and may be reprinted entirely, reference to source is appreciated.

The Secretary of Commerce has determined that the publication of this periodical is necessary according to law for the transaction of public business of this Department. Use of funds for printing of this periodical has been approved by the Director of the Office of Management and Budget.

For sale by the Superintendent of Documents, U.S. Government Printing Office, Washington, DC 20402. Subscription price per year: $50.00 domestic and $62.50 foreign. Cost per single issue: $19.00 domestic and $23.76 foreign. **See back for order form.**

The *Fishery Bulletin* carries original research reports and technical notes on investigations in fishery science, engineering, and economics. It began as the Bulletin of the United States Fish Commission in 1881; it became the Bulletin of the Bureau of Fisheries in 1904 and the *Fishery Bulletin* of the Fish and Wildlife Service in 1941. Separates were issued as documents through volume 46; the last document was No. 1103. Beginning with volume 47 in 1931 and continuing through volume 62 in 1963, each separate appeared as a numbered bulletin. A new system began in 1963 with volume 63 in which papers are bound together in a single issue of the bulletin. Beginning with volume 70, number 1, January 1972, the *Fishery Bulletin* became a periodical, issued quarterly. In this form, it is available by subscription from the Superintendent of Documents, U.S. Government Printing Office, Washington, DC 20402. It is also available free in limited numbers to libraries, research institutions, State and Federal agencies, and in exchange for other scientific publications.

U.S. Department of Commerce
Seattle, Washington

Volume 98
Number 3
July 2000

Fishery Bulletin

Contents

Articles

451–462 **Bolles, Karen L., and Gavin A. Begg**
Distinction between silver hake (*Merluccius bilinearis*) stocks in U.S. waters of the northwest Atlantic based on whole otolith morphometrics

463–473 **Broadhurst, Matt K., Pual E. McShane, and Roger B. Larsen**
Effects of twine diameter and mesh size in the body of prawn trawls on bycatch in Gulf St. Vincent, Australia

474–488 **Cappo, Mike, Peter Eden, Stephen J. Newman, and Simon Robertson**
A new approach to validation of periodicity and timing of opaque zone formation in the otoliths of eleven species of *Lutjanus* from the central Great Barrier Reef

489–506 **DeMartini, Edward E., James H. Uchiyama, and Happy A. Williams**
Sexual maturity, sex ratio, and size composition of swordfish, *Xiphias gladius*, caught by the Hawaii-based pelagic longline fishery

507–527 **Drass, Denice M., Kevin L. Bootes, Joanne Lyczkowski-Shultz, Bruce H. Comyns, G. Joan Holt, Cecilia M. Riley, and Ronald P. Phelps**
Larval development of red snapper, *Lutjanus campechanus*, and comparisons with co-occurring snapper species

528–538 **McBride, Richard S., and Kim A. McKown**
Consequences of dispersal of subtropically spawned crevalle jacks, *Caranx hippos*, to temperate estuaries

539–582 **Orr, James W., and Ann C. Matarese**
Revision of the genus *Lepidopsetta* Gill, 1862 (Teleostei: Pleuronectidae) based on larval and adult morphology, with a description of a new species from the North Pacific Ocean and Bering Sea

583–599 **Ortiz, Mauricio, Christopher M. Legault, and Nelson M. Ehrhardt**
An alternative method for estimating bycatch from the U.S. shrimp trawl fishery in the Gulf of Mexico, 1972–1995

The conclusions and opinions expressed in *Fishery Bulletin* are solely those of the authors and do not represent the official position of the National Marine Fisheries Service (NOAA) or any other agency or institution.

The National Marine Fisheries Service (NMFS) does not approve, recommend, or endorse any proprietary product or proprietary material mentioned in this publication. No reference shall be made to NMFS, or to this publication furnished by NMFS, in any advertising or sales promotion which would indicate or imply that NMFS approves, recommends, or endorses any proprietary product or proprietary material mentioned herein, or which has as its purpose an intent to cause directly or indirectly the advertised product to be used or purchased because of this NMFS publication.

600–611 **Pilling, Graham M., Richard S. Millner, Michael W. Easey, Christopher C. Mees, Shyama Rathacharen, and Roland Azemia**
Validation of annual growth increments in the otoliths of the lethrinid *Lethrinus mahsena* and the lutjanid *Aprion virescens* from sites in the tropical Indian Ocean, with notes on the nature of growth increments in *Pristipomoides filamentosus*

612–624 **Taylor, Ronald G., James A. Whittington, Harry J. Grier, and Roy E. Crabtree**
Age, growth, maturation, and protandric sex reversal in common snook, *Centropomus undecimalis,* from the east and west coasts of South Florida

625–641 **Yoklavich, Mary M., H. Gary Greene, Gregor M. Cailliet, Deidre E Sullivan, Robert N. Lea, and Milton S. Love**
Habitat associations of deep-water rockfishes in a submarine canyon: an example of a natural refuge

Notes

642–645 **Bolden, Stephania K.**
Long-distance movement of a Nassau grouper (*Epinephelus striatus*) to a spawning aggregation in the central Bahamas

646–649 **Dudley, Sheldon F. J., Michael D. Anderson-Reade, Greg S. Thompson, and Paul B. McMullen**
Concurrent scavenging off a whale carcass by great white sharks, *Carcharodon carcharias,* and tiger sharks, *Galeocerdo cuvier*

650–654 **Powell, Allyn B., Elisabeth H. Laban, Scott A. Holt, and G. Joan Holt**
Validation of age estimates from otoliths of larval and juvenile spotted seatrout, *Cynoscion nebulosus*

655–659 **Rooper, Christopher N., and Lewis J. Haldorson**
Consumption of Pacific herring (*Clupea pallasi*) eggs by greenling (Hexagrammidae) in Prince William Sound, Alaska

660 *Subscription form*

Distinction between silver hake (*Merluccius bilinearis*) stocks in U.S. waters of the northwest Atlantic based on whole otolith morphometrics

Karen L. Bolles

Gavin A. Begg

Northeast Fisheries Science Center
National Marine Fisheries Service, NOAA
166 Water Street, Woods Hole, Massachusetts 02543
Present address: (for K. L. Bolles): Marine Research Institute
Skulagata 4, P.O. Box 1390
121 Reykjavik, Iceland.

E-mail address (for K. L. Bolles): karen@hafro.is

Abstract.—A method for using whole otolith morphometrics to identify silver hake (*Merluccius bilinearis*) stocks in U.S. waters of the northwest Atlantic is described. Whole sagittal otolith morphometric variables of length, width, area, perimeter, circularity, and rectangularity were extracted by image processing and, in combination with age-specific discriminant analyses, were used to differentiate two stocks of silver hake: a northern stock from the Gulf of Maine to northern Georges Bank and a southern stock from southern Georges Bank to the Middle Atlantic. Further support for these groupings is supported by growth rate analyses: fish of the northern stock grew slower than those of the southern stock, resulting in typically larger otoliths for fish from the northern stock. This study demonstrates that whole otolith morphometrics, specific to fish age, are useful in identifying silver hake stocks and can be a useful tool in identifying other fish stocks.

Manuscript accepted 15 February 2000.
Fish. Bull. 98:451–462 (2000).

Accurate distinction between fish stocks is necessary for effective fisheries management to prevent overfishing of individual stocks, to preserve the reproductive and genetic diversity of stock complexes, and to determine optimal strategies for rebuilding stocks (Cushing, 1968; Booke, 1981; Grimes et al., 1987; Begg et al., 1999; Stephenson, 1999). Integral to attaining such management strategies and objectives, is the necessary requirement of reevaluating stock definitions when needed, particularly when the status of the resource changes, or when new technologies become available that may provide more effective stock discrimination tools than those already in use (Begg and Waldman, 1999). Because of the uncertainties surrounding the stock definitions for silver hake (*Merluccius bilinearis*) in U.S. waters of the northwest Atlantic, such a need for reevaluation of stock definitions arose. Furthermore, there was no efficient method for adequately discriminating between silver hake stocks that could also provide a fast and accurate way to determine levels of stock mixing for current fishery assessment and management. In our study, we focused on these issues by incorporating the technology and efficiency of image analysis systems, in combination with multivariate statistical analyses, to distinguish between silver hake stocks on the basis of phenotypic differences in whole otoliths.

Silver hake, (or whiting), is a principal groundfish species found along the continental shelf and slope from Newfoundland to South Carolina, inhabiting depths from shallow inshore waters to those greater than 400 m (Bigelow and Schroeder, 1953; Almeida, 1987; Helser et al., 1995). Silver hake are ecologically important both as a predator and prey in the northwest Atlantic ecosystem (Edwards and Bowman, 1979; Bowman and Michaels, 1984), and form an important part of the commercial fisheries throughout this region (Anonymous, 1998). With annual landings averaging 16,600 metric tons, silver hake are currently considered overexploited (Anonymous, 1998).

Two stocks of silver hake are currently defined in U.S. waters on the basis of analysis of research survey and commercial catch data, as well as multivariate analysis of external morphometric data: a northern stock (from the Gulf of Maine to northern Georges Bank) and a southern stock (from southern Georges Bank to the Middle Atlantic) (Almeida, 1987). Distributions of the two stocks vary seasonally and spatially, probably in response to temperature and depth (Helser et al., 1995). Silver hake that compose the northern stock overwinter in the deeper regions of the Gulf of Maine and during their peak spawning months of July and August, are found on northern Georges Bank and in coastal waters east of Cape Cod, north to Grand Manan (Big-

elow and Schroeder, 1953; Almeida, 1987). In contrast, the southern stock is found predominantly in waters from Cape Cod to Montauk Point, New York, and during peak spawning, which occurs in June and July, it is found on southern Georges Bank, in the New York Bight, and as far south as Cape Hatteras (Almeida, 1987; Helser et al., 1995).

Although silver hake in U.S. waters are currently assessed according to this two-stock scheme, uncertainty exists in the stock definitions. A variety of other stock identification techniques have also been used to identify these two stocks of silver hake, including examining external morphometrics (Conover et al., 1961), growth rate comparisons (Nichy, 1969), immunological analyses (Konstantinov and Noskov, 1969), research survey distribution studies (Anderson, 1974), and genetic analyses (Schenk, 1981). However, the stock boundaries suggested in each of these studies have all tended to vary from one another. More recently, Helser (1996) found that silver hake growth rates differed both between and within the two stocks—a finding that is inconsistent with the stock boundaries currently defined (Almeida, 1987) and that confounds the delineation of the stocks and the degree to which the two stocks mix. Given this finding, we believed further investigation into the stock structure of silver hake was needed to clarify the current management units defined for U.S. waters. In addition, we aimed to introduce a more efficient and accurate method for distinguishing between silver hake stocks than the previous methods that have been used, one which would have the potential to enable rapid and accurate in-season assessment of the degree of stock mixing for silver hake.

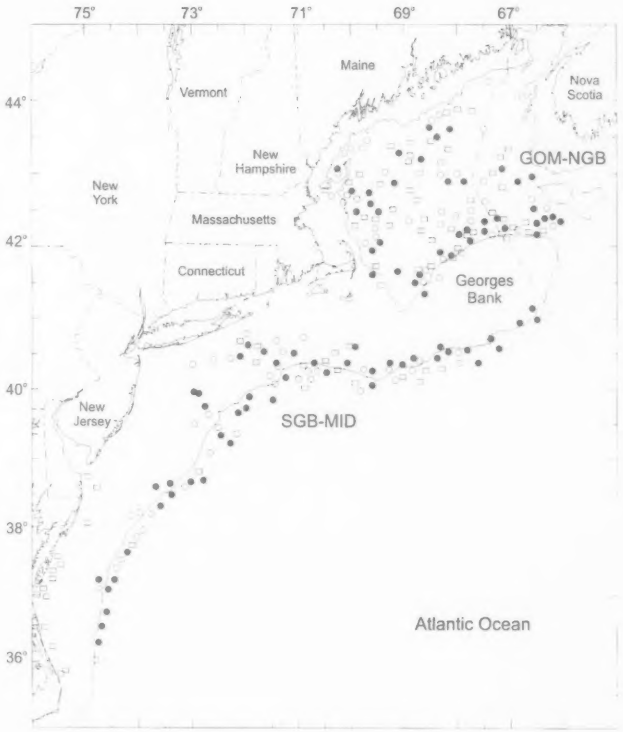

Figure 1

NEFSC spring survey stations where silver hake samples were collected for otolith morphometric-based stock discrimination analysis in 1992 (squares), 1994 (closed circles), and 1996 (open circles). GOM-NGB: Gulf of Maine to northern Georges Bank; SGB-MID: southern Georges Bank to the Middle Atlantic.

Otolith morphometric data have recently been used to identify stocks of marine fish, including Atlantic mackerel, *Scomber scombrus* (Dawson, 1991; Hopkins[1]), Atlantic herring, *Clupea harengus* (Messieh et al., 1989), and Atlantic salmon, *Salmo salar* (Friedland and Reddin, 1994). In contrast, otolith morphometric data have not been used to differentiate between stocks of silver hake, but because silver hake have been found to differ phenotypically (Almeida, 1987), and possibly genetically (Schenck, 1981), it was assumed that otolith morphometric characteristics may also vary. Dery (1988) observed that silver hake otoliths from the northern stock were narrower and thicker in cross-section than those of the southern stock, although no statistical analyses were used to test her observations. Accordingly, it was thought that otolith morphometrics could differ between the two silver hake stocks and could prove to be useful characters by which to differentiate stocks in the future. The collection of such data by means of image processing techniques has proven to be useful in stock identification, providing accurate and efficient measures that traditional morphometric methods have not been able to provide (Jearld, 1995; Cadrin and Friedland, 1999). Given these benefits and Dery's (1988) observations, our study aimed to identify whole otolith morphometric characteristics unique to silver hake stocks in U.S. waters of the northwest Atlantic by using image processing techniques. We address the advantages and limitations encountered when using this method to distinguish fish stocks, and reevaluate the current silver hake stock scheme given the recent within-stock growth differences observed by Helser (1996).

[1] Hopkins, P. J. 1986. Mackerel stock discrimination using otolith morphometrics. ICES Council Meeting 1986, 17 p.

Materials and methods

Sample collection

Silver hake were collected in 1992, 1994, and 1996 during the spring Northeast Fisheries Science Center (NEFSC) stratified random bottom-trawl surveys when the fish were assumed to be on their spawning grounds. Silver hake samples were obtained from the Gulf of Maine to northern Georges Bank (GOM–NGB), and from southern Georges Bank to the Middle Atlantic regions (SGB–MID) (Fig. 1, Table 1). Silver hake were measured (fork length [FL], cm),

sex was determined by macroscopic examination of the gonads, and sagittal otolith pairs were removed from each fish. One otolith from each pair was sectioned and assigned an age following methods in Dery (1988). The other otolith of the pair, either left or right, was then used for morphometric analysis. Samples were restricted to fish of ages 1 to 3 years, because older fish were infrequently collected in the surveys. This restriction also enabled both size- and age-related variation, which could have confounded discrimination analyses, to be minimized.

Otolith orientation was standardized by positioning the otolith with its proximal side down and the rostrum was used as a common starting point from which the perimeter was traced in a counterclockwise direction. Broken or visibly damaged otoliths were not measured. Whole otolith length, width, area and perimeter, and two shape indices—circularity and rectangularity, were collected for each otolith by using the OPTIMAS™ (version 6.2) image analysis system (OPTIMAS, 1996). Rectangularity is a measure of the otolith area divided by the area of its minimum enclosing rectangle, and circularity is the perimeter of the otolith squared divided by its area (OPTIMAS, 1996). All otolith measurements were performed at a magnification of 7×.

Data analysis

Bottom ocean temperatures measured throughout the NEFSC spring and autumn bottom-trawl surveys from 1989 to 1996 were compared between the northern and southern regions to determine whether different thermal regimes exist between the two regions that could effect growth rates and subsequent otolith morphometric characteristics of silver hake inhabiting each of these regions. A two-way, fixed-factor, unbalanced analysis of variance (ANOVA) was used to compare bottom temperatures between the regions and time of the survey. Following a significant interaction between these factors, unpaired *t*-tests were used to compare bottom temperatures between regions for each survey, and one-way ANOVAs were used to compare bottom temperatures between surveys for each region. Significance levels were corrected for multiple testing by using the Bonferroni adjustment factor. Tukey's honestly significant difference (HSD) tests were used for *a posteriori* comparisons.

Growth rates of silver hake sampled throughout the NEFSC spring bottom-trawl surveys were calculated by using linear regressions for samples of each sex, year, and region of capture to determine if growth differences existed that might be indicative of stock separation. Analysis of covariance (ANCOVA) was used to compare differences in growth rates of silver hake between the sexes (same year and region), sampling years (same sex and region), and regions (same year and sex).

All otolith morphometric variables were first examined for normality and homogeneity of variances, and were $\log_e$-transformed prior to statistical analysis if these criteria were not satisfied. ANCOVA was then used to determine the effect of fish length on the magnitude of each otolith morphometric variable. "Region" was treated as the main factor and "length" was the covariate. Morphometric variables for which "region-length" interactions were significant were not included in any further analyses because they could not be corrected for fish length. Variables that were significantly correlated with fish length were corrected for variable fish length by using the common within-group slope (b).

Multivariate analysis of variance (MANOVA) was used to compare otoliths sampled for each sex (same region, year class, and age group) by using the appropriate length-corrected variables. One-way ANOVAs were then used to examine individual morphometric variables to explain any significant differences detected by the MANOVAs. Significance levels were corrected for multiple testing with the Bonferroni adjustment factor. Likewise, multi- and univariate analyses were then used to test the effects of year class (samples from the same region and age group) on otolith structure. Following these analyses, similar tests were used to investigate morphological differences in otolith samples from the northern and southern regions. Spatial comparisons were made between samples from the different regions for fish of the same age group, sex, and year class. Canonical discriminant analysis was then used to detect morphometric differences in otoliths of silver hake sampled from the northern and southern regions. Significant ($P<0.05$) canonical variates represented the optimal combination of regions and morphometric variables that provided the best overall discrimination between the groups. Standardized coefficients provided for each sig-

Table 1
Sampling information on silver hake.

Region	Age group (years)	Year class	Sex	Length range (cm)	*n*
North	1	1991	Females	—	—
			Males	12–18	45
South	1	1991	Females	11–19	22
			Males	11–20	22
North	2	1990	Females	17–28	50
			Males	16–24	31
South	2	1990	Females	18–22	6
			Males	17–26	11
North	3	1989	Females	23–32	15
			Males	22–29	12
South	3	1989	Females	26–36	9
			Males	26–28	5
North	3	1991	Females	23–31	50
			Males	23–29	26
South	3	1991	Females	23–35	50
			Males	23–32	50
North	3	1993	Females	20–32	53
			Males	22–29	24
South	3	1993	Females	21–34	53
			Males	22–33	25

nificant variable represented the contribution of the respective morphometric variable to the discrimination of silver hake samples between regions. Jack-knifed cross-validation procedures were used to give unbiased estimates of classification success (SYSTAT, 1997).

Results

Bottom ocean temperatures differed significantly between region and time of survey (ANOVA interaction, F=11.7, df=15, 2931, P<0.0001). Generally, temperatures were significantly lower in the northern region than in the southern region for all surveys (t-tests, P<0.0001), except during the spring of 1994 and 1996 (although consistent differences were still maintained between regions during these times, albeit not significant) (Fig. 2). Within each region, bottom temperatures have a consistent seasonal pattern, tending to be significantly lower in spring than autumn for both regions (ANOVA, P<0.0001; HSD, P<0.05), with no apparent differences between years within seasons and regions (Fig. 2).

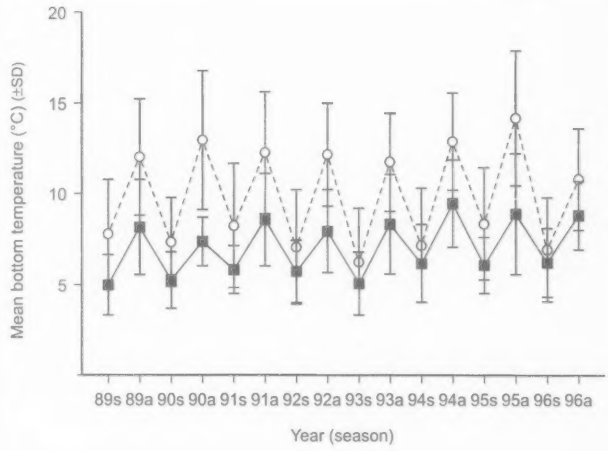

Figure 2

Mean ocean bottom temperatures (°C) (± standard deviation) of northern (squares) and southern (circles) regions collected from the spring (s) and autumn (a) NEFSC bottom-trawl surveys (1989–1996).

Silver hake had significantly different growth rates between sexes, year classes, and the regions from where they were sampled (Fig. 3). Female silver hake grew at a faster rate than males in both the northern and southern regions; and age-length differences between the sexes increased as the fish got older (ANCOVA, P<0.05). Growth rates of each sex, within each region, also differed between sampling years, indicative of the presence of a year class effect (ANCOVA, P<0.005). Likewise, significant differences in growth rates were found between silver hake from the northern and southern regions in each year for both males and females (ANCOVA, P<0.005).

The six otolith morphometric variables (length, width, area, perimeter, circularity, and rectangularity) that were measured for silver hake were $\log_e$-transformed, except for otolith width, to correct for non-normality and heterogeneity of variances. ANCOVAs detected significant (P<0.0001) "region-fish length" interactions for four (otolith area, length, width, and perimeter) of the six variables measured when all samples were examined together, irrespective of age group, year class, or sex. However, the use of individual ANCOVAs for fish of each age group reduced the number of interactions to only one variable for both 1-year-old (rectangularity) and 2-year-old silver hake (width), and two variables (area, length) for samples from 3-year-olds (Table 2). All the remaining variables for the different aged samples were significantly correlated with fish length (P<0.01), and therefore were corrected for variable fish length with their respective common within-group slope (Table 2). Consequently, length-corrected data determined from the individual ANCOVAs for each age group were used for the remaining analyses and indicated the strong effect different ages can have on these types of measurements. Typically, for any given fish length, silver hake from the northern region appeared to have larger otolith dimensions (area, length, width, and perimeter) than those fish from the southern region (Fig. 4).

Multi- and univariate analyses were used to examine confounding sources of variation that may have influenced regional patterns of silver hake (Table 3). In general, otolith morphometrics were not significantly different (P>0.05) between the sexes, indicating that their otoliths develop at a similar rate over the age range examined. In contrast, as for the growth rate analyses, significant differences were found among otolith morphometrics of the same-age silver hake sampled from different year classes for both males and females (Table 3). Likewise, similar year-class differences in otolith morphometrics were found when the sexes were pooled together, confirming congruency in rates of otolith development, and justifying assimilation of sexes for statistical purposes.

Silver hake sampled from the northern region tended to have larger otolith dimensions than those from the southern region (Fig. 4). Overall, when the appropriate length-corrected morphometric variables were examined together for silver hake of the same age group and year class, irrespective of sex, significant differences were found between samples from the northern and southern regions (MANOVA, P<0.001) (Table 4). Fewer multivariate significant differences were detected for samples from 3-year-olds, although these differences were probably the result of samples for this age group having fewer variables to examine compared with samples from the other age groups. This was supported by univariate tests where significant differences (P<0.05) between silver hake from the northern and southern regions were found for several variables, for all age groups, and for almost all of the age group, sex, and year class combinations (Table 4). Also, the oto-

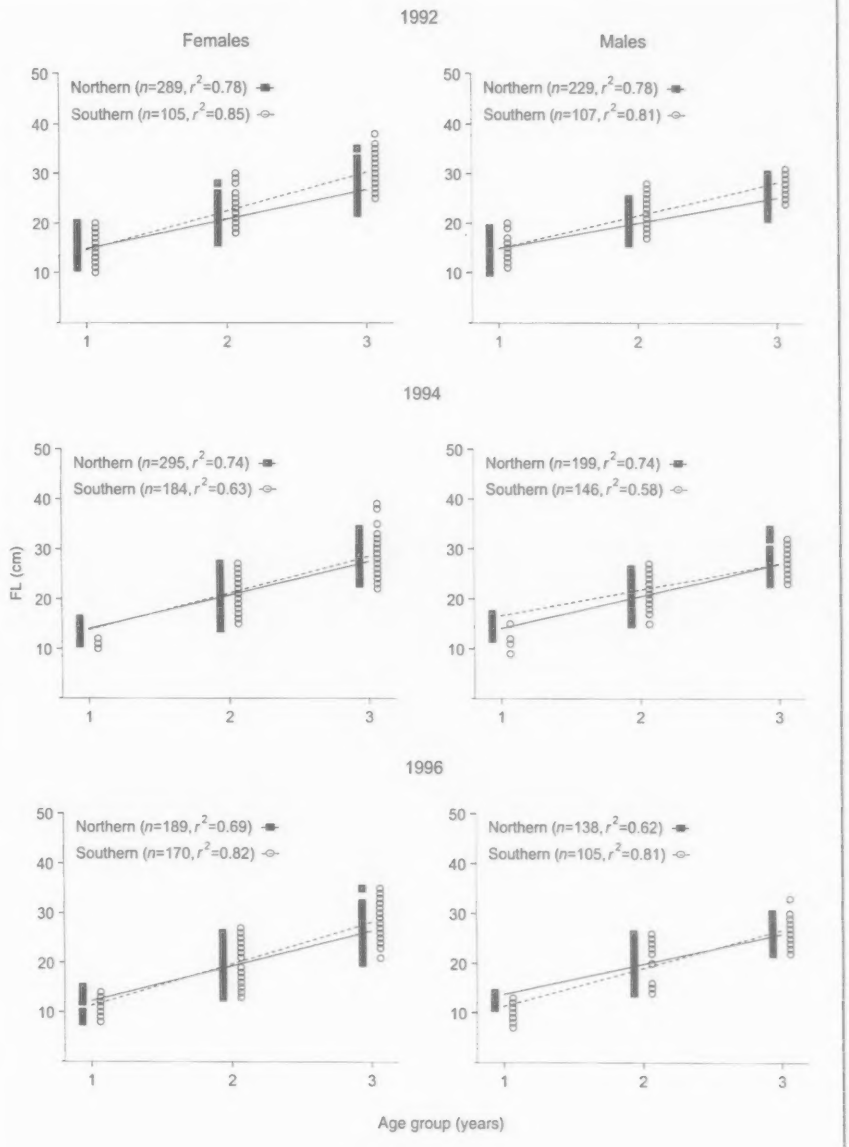

Figure 3

Linear growth relationships of silver hake samples (age groups 1 to 3) from the NEFSC 1992 (northern, F: S=6.41, I=8.15; M: S=4.97, I=9.98; southern, F: S=6.83, I=8.33, M: S=5.73, I=9.58), 1994 (northern, F: S=6.75, I=7.20; M: S=6.07, I=8.33; southern, F: S=7.10, I=6.99, M: S=4.84, I=12.25), and 1996 (northern, F: S=6.91, I=5.57; M: S=5.76, I=8.30; southern, F: S=8.03, I=3.72, M: S=7.15, I=4.65) spring surveys. (F=females; M=males; S=slope; I=intercept; n=sample size; r^2=coefficient of determination).

lith morphometric variables not included in the comparisons of 3-year-olds (those variables based on the ANCOVA results—area and length) were the most significant of the variables examined individually for the other age groups, emphasizing the potential importance of these two variables for stock discrimination.

Discriminant analyses provided further support for the separation between northern and southern stocks among

Table 2

Otolith morphometric variables that were significantly correlated with fish length for 1-, 2-, and 3-year-old silver hake samples. N.S. = not significant.

A 1-year-old silver hake

	Fish length × variable (df=2, 83)		Fish length (df=1, 85)		
Variable	*F*	*P*	*F*	*P*	*b*
Otolith length	0.10	N.S.	603.59	0.0001	0.0063
Width	2.65	N.S.	526.37	0.0001	0.0156
Area	1.24	N.S.	683.39	0.0001	0.0118
Perimeter	0.05	N.S.	471.07	0.0001	0.0067
Circularity	1.85	N.S.	15.99	0.0001	0.0016
Rectangularity	6.07	0.0035	—	—	—

B 2-year-old silver hake

	Fish length × variable (df=3, 90)		Fish length (df=1, 93)		
Variable	*F*	*P*	*F*	*P*	*b*
Otolith length	1.46	N.S.	621.48	0.0001	0.0047
Width	3.84	0.0123	—	—	—
Area	2.17	N.S.	715.78	0.0001	0.0084
Perimeter	0.78	N.S.	515.89	0.0001	0.0049
Circularity	0.80	N.S.	30.83	0.0001	0.0014
Rectangularity	1.11	N.S.	6.83	0.0104	–0.0002

C 3-year-old silver hake

	Fish length × variable (df=11, 348)		Fish length (df=1, 359)		
Variable	*F*	*P*	*F*	*P*	*b*
Otolith length	2.56	0.0040	—	—	—
Width	0.68	N.S.	561.32	0.0001	0.0102
Area	2.04	0.0239	—	—	—
Perimeter	1.10	N.S.	1024.62	0.0001	0.0037
Circularity	0.64	N.S.	144.02	0.0001	0.0020
Rectangularity	0.82	N.S.	12.78	0.0004	–0.0001

the silver hake samples, as indicated by the multi- and univariate analyses (Fig. 5). We found significant differences in the discriminant scores (CV I) between those samples from the northern and southern regions for both 1-year-old (t=-6.3075, df=87, P<0.0001) and 2-year-old fish (t=4.7654, df=95, P<0.0001). However, as in the preceding analyses, poor separation was observed between the samples of 3-year-olds (t=1.7827, df=370, not significant). This was again probably due to the reduced number of variables in the analyses, particularly that of otolith area and length. Variation in otolith area, length, and circularity was mainly responsible for the north–south separation in samples of 1- and 2-year-olds, whereas otolith width and circularity accounted for most of the variation in the samples of 3-year-olds (Table 5).

Classification success, based on each particular discriminant model, decreased with each age group. Overall, individual samples of 1-, 2-, and 3-year-old silver hake were correctly classified 75%, 69%, and 49% of the times, respectively (Table 6). Classification rates increased slightly when samples from each age group were analyzed separately by sex (1-year-old fish, males—78%; 2-year-old fish, females—68%, males—71%; 3-year-old fish, females—54%, males—56%) and year class (3-year-old fish: 1989 year class—54%; 1991 year class—64%; 1993 year class—61%), indicating the confounding affects that these variables can have on these types of analyses when used for stock discrimination.

Discussion

We confirmed that two stocks of silver hake exist in U.S. waters of the northwest Atlantic from differences in whole otolith morphometrics and growth rates. Our method of

Table 3

Examination of confounding sources of variation (sex and year class) on the length-corrected otolith morphometric variables. N.S. = not significant.

	MANOVA				ANOVA		
Comparison	*F*	df	*P*	Significant variable	*F*	df	*P*
Sex							
Females vs. males (South; 1991 year class; age 1)	0.18	4, 39	N.S.	—	—	—	—
Females vs. males (North; 1990 year class; age 2)	2.59	4, 76	0.0434	circularity	8.02	1, 79	0.0059
Females vs. males (South; 1990 year class; age 2)	0.36	4, 12	N.S.	—	—	—	—
Females vs. males (North; 1989 year class; age 3)	1.49	4, 22	N.S.	—	—	—	—
Females vs. males (South; 1989 year class; age 3)	2.54	4, 9	N.S.	—	—	—	—
Females vs. males (North; 1991 year class; age 3)	1.74	4, 71	N.S.	—	—	—	—
Females vs. males (South; 1991 year class; age 3)	7.32	4, 95	0.0001	rectangularity	8.43	1, 98	0.0046
Females vs. males (North; 1993 year class; age 3)	0.53	4, 72	N.S.	—	—	—	—
Females vs. males (South; 1993 year class; age 3)	0.57	4, 73	N.S.	—	—	—	—
Year class							
1989; 1991 vs. 1993 (Females; North; age 3)	4.97	8, 226	0.0001	—	—	—	—
1989; 1991 vs. 1993 (Males; North; age 3)	5.45	8, 114	0.0001	width	4.80	2, 59	0.0118
1989; 1992 vs. 1993 (Females; South; age 3)	2.37	8, 214	0.0183	perimeter circularity	6.67 6.13	2, 109	0.0018 0.0030
1989; 1992 vs. 1993 (Males; South; age 3)	2.86	8, 150	0.0055	perimeter	6.18	2, 77	0.0033
1989; 1991 vs. 1993 (Sexes pooled; North; age 3)	8.60	8, 350	0.0001	width	7.81	2, 177	0.0006
1989; 1992 vs. 1993 (Sexes pooled; South; age 3)	3.23	8, 374	0.0014	perimeter circularity	9.65 5.94	2, 189	0.0001 0.0031

using otolith morphometrics, coupled with discriminant function analysis, when analyzed with respect to fish age, enabled us to distinguish between a northern stock (from the Gulf of Maine to northern Georges Bank) and a southern stock (from southern Georges Bank to the Middle Atlantic), thus providing a more efficient and accurate method for discriminating between silver hake stocks than had been used previously.

Typically, silver hake of the northern stock grew at a slower rate, and had larger otoliths than fish of the southern stock. Otoliths of silver hake from the northern stock tended to be longer, wider, and greater in area and perimeter than similar-size fish from the southern stock because, for any given fish length, northern stock fish were older and therefore had more time to accumulate otolith material than had southern stock fish. These results were consistent with previous growth studies where slower growing fish generally had larger otoliths than those of similar-size, faster growing fish (Templeman and Squires, 1956; Reznick et al., 1989; Fowler and Short, 1996).

Likewise, Helser (1996) found that silver hake from the northern stock grew at slower rates than those fish of the southern stock, and like Nichy (1969), Almeida (1978) and Pentilla et al. (1989) found that the northern stock reached larger asymptotic lengths. However, Helser (1996) also found results that did not support the current stock

Table 4

Spatial comparisons of the length-corrected otolith morphometric variables. N.S. = not significant.

	MANOVA				ANOVA		
Spatial comparison	*F*	df	*P*	Significant variable	*F*	df	*P*
Same sex, age group, and year class							
North vs. South (Males; age 1; 1991)	6.98	4, 62	0.0001	length	13.71	1, 65	0.0004
				width	8.12		0.0059
				area	18.06		0.0001
North vs. South (Females; age 2; 1990)	1.24	4, 51	N.S.	—	—	—	—
North vs. South (Males; age 2; 1990)	6.30	4, 37	0.0006	area	8.68	1, 40	0.0053
				circularity	13.93		0.0006
North vs. South (Females; age 3; 1989)	1.98	4, 19	N.S.	—	—	—	—
North vs. South (Males; age 3; 1989)	2.40	4, 12	N.S.	—	—	—	—
North vs. South (Females; age 3; 1991)	5.80	4, 95	0.0003	—	—	—	—
North vs. South (Males; age 3; 1991)	3.84	4, 71	0.0070	perimeter	10.48	1, 74	0.0018
				circularity	7.35		0.0083
North vs. South (Females; age 3; 1993)	2.16	4, 101	N.S.	—	—	—	—
North vs. South (Males; age 3; 1993)	2.38	4, 44	N.S.	width	7.03	1, 47	0.0109
Same age group, year class; sexes combined							
North vs. South (age 1; 1991)	9.60	4, 84	0.0001	length	17.18	1, 87	0.0001
				width	9.04		0.0035
				area	22.16		0.0001
				circularity	10.61		0.0016
North vs. South (age 2; 1990)	5.05	4, 93	0.0010	length	11.15	1, 96	0.0012
				area	12.78		0.0006
North vs. South (age 3; 1989)	0.78	4, 36	N.S.	—	—	—	—
North vs. South (age 3; 1991)	5.18	4, 171	0.0006	perimeter	10.44	1, 174	0.0015
				circularity	8.47		0.0041
North vs. South (age 3; 1993)	4.05	4, 150	0.0038	width	11.49	1, 153	0.0009

scheme; growth rates differed between silver hake from northern Georges Bank and the Gulf of Maine and between fish from southern Georges Bank and the Middle Atlantic. Such within-stock differences further emphasizes the uncertainty that currently exists over both stock boundaries and the degree of mixing between silver hake stocks in U.S. waters of the northwest Atlantic.

Similarly, the uncertainty in stock boundaries and the degree of stock mixing was evident in most of the past silver hake stock discrimination studies (Conover et al., 1961; Konstantinov and Noskov, 1969; Nichy, 1969; Anderson, 1974), although we believe that our approach has the potential to resolve some of these questions. A major reason for this uncertainty has been due to a lack of intensive genetic studies to investigate the population structure of the species, and therefore a subsequent lack of knowledge concerning the actual reproductive isolation of the species. Schenk (1981) demonstrated two genetically distinct groups but, owing to a limited geographic sample area, was not able to define boundaries between the groups. However, it must be remembered that a "stock" in its working definition for practical fisheries management is a management unit and not a discrete biological population unit. Consequently, stocks of fish with different phenotypic (i.e. morphometric) characteristics or life history (i.e. growth) dynamics should be considered as separate management units and modeled separately regardless of genetic characteristics for stock assessment and management purposes (Cadrin and Friedland, 1999). Although our study did not delineate actual stock bound-

aries or determine the mixing components between the silver hake stocks, further investigation into the application of this technique may show that otolith morphometrics, when coupled with image processing and discriminant analysis, is capable of achieving these objectives.

Subsequently, to understand better the fishery dynamics of silver hake stocks and to manage them accordingly, we must question what caused these differences—whether they are differences in fish growth, or internal or external morphometric characters, both between and within stocks. Otolith morphometric differences between silver hake stocks are probably the result of both environmental and genetic influences. For example, the hydrodynamics of northwest Atlantic waters are considered to be heterogeneous; environmental conditions differ between the Gulf of Maine and the Middle Atlantic (Brooks, 1996). Certainly, we observed significant and consistent differences in the bottom temperatures between the two stock regions inhabited by silver hake, where those fish in the northern region experience lower temperatures than those in the southern region. Because fish growth and external body morphometrics are known to be influenced by such environmental factors (Ihssen et al., 1981; Pawson and Jennings, 1996), one would also expect that internal morphometrics, such as otolith length and width, would also differ in response to these variables because fish growth and otolith growth tend to be related. In accord with these assumptions, otolith shape has been found to vary in response to environmental conditions and is also highly correlated with fish growth (Campana and Casselman, 1993). Similarly, the results of our study showed significant correlations between fish and otolith growth for all the otolith morphometric characteristics measured. Therefore, it is likely that the differences found between silver hake stocks in growth rates (Helser, 1996; our study), external morphometrics (Conover et al., 1961; Almeida, 1987), and internal morphometrics (our study) are to some extent reflective of localized environmental conditions.

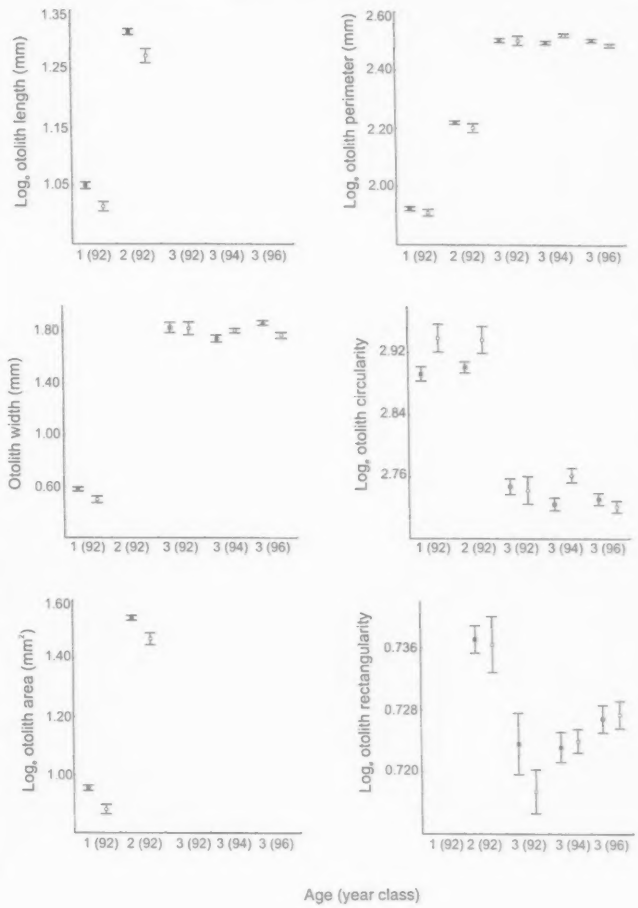

Figure 4

Otolith morphometrics (mean ±standard error) for 1-, 2-, and 3-year-old silver hake samples pooled across sexes for individual year classes showing differences between those fish from the northern (squares) and southern (circles) regions.

Assuming that environmental variables can effect otolith growth, we analyzed bottom ocean temperature between the two stock regions across the life history range of our samples to investigate whether the differences in otolith morphometrics found in this study were due to a weather phenomenon during any given sampling year (Fig. 2). Temperature was found to differ consistently on a seasonal basis during all years, as would be assumed, and there was no marked change in temperature between any given years, within any given season. As a result, the possibility of a severe temperature shift that could influence otolith morphometrics and make this method unsuitable for stock discrimination was not apparent in our study. However, because temperature was shown to differ between the proposed stock regions and because silver hake distribute themselves in response to temperature (Almeida, 1987; Helser, 1996), it can be assumed that this variable could effect otolith growth.

Alternatively, growth and otolith morphometric differences found between silver hake stocks could also be apparent, regardless of environmental variation, and reflect a genetic influence. This could be a valid assumption given

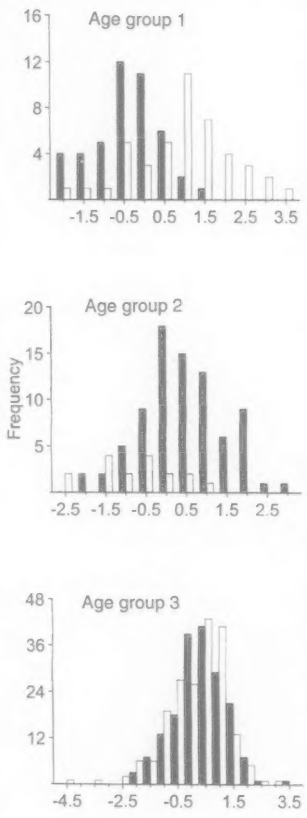

Figure 5

Discrimination of silver hake samples from the northern (solid bars) and southern regions (open bars) based on frequency of canonical variate scores (CV I) for 1-, 2-, and 3-year-old fish.

that a certain degree of reproductive isolation has been confirmed in spawning and postspawning silver hake (Almeida, 1987). Such isolation could restrict gene flow to a level that effectively isolates population units (Iles and Sinclair, 1982). However, some degree of intermixture probably occurs owing to the wide migratory patterns of silver hake (Almeida, 1987). Therefore, further investigations are required to interpret the degree to which morphological differences between silver hake stocks are caused by environmental or genetic influences, but as long as these differences persist between stocks, the use of otolith morphometrics remains a viable tool for stock discrimination.

Otolith morphometrics in combination with an image analysis system has been found to be a relatively inexpensive, objective, and efficient tool by which to distinguish fish stocks (Messieh et al., 1989; Jearld, 1995). Rapid and precise measurements can be obtained in less time with this technique, compared with alternative manual-based procedures, because all the measurements are automatically determined from an outline of the otolith perimeter traced with an edge-detection algorithm (OPTIMAS, 1996). In addition otolith morphometric data can easily be obtained because

Table 5

Length-corrected otolith morphometric variables responsible for the discrimination of 1-, 2-, and 3-year old silver hake samples determined by the standardized within-group variances of the canonical variates (CV I).

Otolith morphometric variable	Canonical variate I		
	Age group 1	Age group 2	Age group 3
Length	–1.01	0.57	—
Width	0.04	—	0.62
Area	0.10	0.38	—
Perimeter	—	—	–0.32
Circularity	0.82	–0.66	–0.59
Rectangularity	—	–0.16	0.09

Table 6

Jack-knifed classification matrix of the frequency of assigned cases in each region (pooled sexes and year classes) used to differentiate samples.

	Classification of individual silver hake								
	Age group 1			Age group 2			Age group 3		
	Correct %	North	South	Correct %	North	South	Correct %	North	South
North	80	36	9	70	57	24	54	98	82
South	70	13	31	65	6	11	43	109	83
Total	75	49	40	69	63	35	49	207	165

otoliths are routinely collected by most fisheries agencies to determine the age of their respective principal fish species for assessment and management purposes. However, one drawback in using otolith morphometrics for stock discrimination is that otoliths frequently are broken or lost during routine collection and processing, effectively limiting the number of samples available for analysis.

In these types of studies, it is also essential to consider any confounding variation that may be present owing to differences between samples in age group, year class, or sex, so as to not mistake stock differences for sample differences. Failure to account for such extraneous influences may result in falsely attributing morphological differences between separate stocks to a "stock effect," whereas the differences may in fact simply be reflecting variation between samples in age structure, sex ratio, or sampling year (Castonguay et al., 1991). Significant variation in otolith morphometrics of silver hake observed in our study between different age groups, year classes, and to a lesser extent sex, emphasized the need to examine these factors before evaluating the stock status of the species with this technique. Likewise, significant differences in these effects have been detected in other morphometric-based stock identification studies for marine fish species, such as Atlantic salmon (L'Abée-Lund, 1988), Atlantic mackerel (Castonguay et al., 1991), and Atlantic cod, *Gadus morhua* (Campana and Casselman, 1993). Thus, although it is clearly necessary to correct for these confounding variables, which can influence any stock identification procedure, they do not limit the use of otolith morphometrics for stock discrimination provided they are examined and accounted for before making any conclusions about the stock structure of a species. Indeed, calculating linear discriminant functions of otolith morphometric characteristics for 1-year-old silver hake on a yearly basis, differentiated by sex, should provide a level of discrimination not yet seen for silver hake stocks in U.S. waters of the northwest Atlantic and may assist in estimating levels of stock mixing (an objective yet to be realized for silver hake or for most of our commercially exploited fish stocks).

There was clearly a need for a more advanced and efficient method in distinguishing between silver hake stocks or in determining mixing levels between stocks. Assessment and management of silver hake stocks are currently based on stock structure results from the late 1970s and early 1980s, on discriminant analysis of external morphometric characters, coupled with a qualitative analysis of research survey and commercial catch data (Almeida, 1987). Since that time, the status of silver hake has certainly changed—spawning stock biomass and recruitment levels have declined (Helser and Brodziak, 1998)—and stock discrimination technologies through image processing have certainly improved (Cadrin and Friedland, 1999). We suggest that the use of whole otolith morphometrics in the analysis of silver hake stocks will give fishery scientists and managers greater logistical benefits (in terms of time and expense), not to mention greater discrimination success, than the stock discrimination methods used previously.

Our study indicated that successful identification of silver hake stocks can be achieved by using whole otolith morphometrics in combination with image processing and discriminant function analysis. We are confident that this is a relatively inexpensive, objective method which can facilitate routine discrimination of silver hake stocks, as well as other marine fish species, by efficiently obtaining accurate measurements to produce valid, repeatable results. This method may prove to be particularly useful for rapid (in-season) assessments for determining levels of stock mixing that are often a requirement of contemporary management plans. Discrimination between stocks is important for fisheries stock-rebuilding strategies, such as those for silver hake, because genetic and stock biodiversity of the species needs to be maintained to ensure all divisions of a stock contribute to the replenishment of the resource.

Acknowledgments

We thank Fred Nichy for his support and guidance; John Boreman, Frank Almeida, Kathy Lang, and two anonymous reviewers for reviews of this manuscript; Nina Shepherd for aging silver hake; Jay Burnett for his helpful suggestions; Donald Hoagland and Jim Phillips for their support during the initial phase of the study; and the staff of the Fishery Biology Program for their assistance with the image analysis. This work was performed while G. A. Begg held a National Research Council (NOAA/NMFS/NEFSC) Research Associateship.

Literature cited

Almeida, F. P.
1978. Determination of the Von Bertalanffy growth equation for the southern New England-Middle Atlantic, Georges Bank, and Gulf of Maine stocks of silver hake. Woods Hole Lab. Ref. Doc. 78-13, Northeast Fisheries Science Center, Natl. Mar. Fish. Serv., NOAA, 15 p.
1987. Stock definition of silver hake in the New England Middle Atlantic area. N. Am. J. Fish. Manage. 7:169–186.

Anderson, E. D.
1974. Comments on the delineation of red and silver hake stocks in the ICNAF Subarea 5 and Statistical Area 6. Int. Comm. NW Atl. Fish. Res. Doc. 74/100, 8 p.

Anonymous.
1998. Status of the fishery resources off the Northeastern United States for 1998. U.S. Dep. Commer., NOAA Tech. Memo. NMFS-NE-115, 149 p.

Begg, G. A., K. D. Friedland, and J. B. Pearce.
1999. Stock identification and its role in stock assessment and fisheries management—an overview. Fish. Res. 43:1–8.

Begg, G. A., and J. R. Waldman.
1999. An holistic approach to fish stock identification. Fish. Res. 43:35–44.

Bigelow, H. B., and W. C. Schroeder.
1953. Fishes of the Gulf of Maine. U.S. Fish and Wildl. Serv. Bull. 74, vol. 53, 577 p.

Booke, H. E.
1981. The conundrum of the stock concept—are nature and nurture definable in fishery science? Can. J. Fish. Aquat. Sci. 38:1479–1480.

Bowman, R. E., and W. L. Michaels.
1984. Food of seventeen species of northwest Atlantic fish. U.S. Dep. Commer., NOAA Tech. Memo. F/NEC-28, 196 p.

Brooks, D. A.
1996. Physical oceanography of the shelf and slope seas from Cape Hatteras to Georges Bank: a brief overview. *In* The northeast shelf ecosystem: assessment, sustainability, and management (K. Sherman, N. A. Jaworski, and T. J. Smayda, eds.), p. 47–74. Blackwell Science, Inc., Cambridge.

Cadrin, S. X., and K. D. Friedland.
1999. The utility of image processing techniques for morphometric analysis and stock identification. Fish. Res. 43:129–139.

Campana, S. E., and J. M. Casselman.
1993. Stock discrimination using otolith shape analysis. Can. J. Fish. Aquat. Sci. 50:1062–1083.

Castonguay, M., P. Simard, and P. Gagnon.
1991. Usefulness of Fourier analysis of otolith shape for Atlantic mackerel (*Scomber scombrus*) stock discrimination. Can. J. Fish. Aquat. Sci. 48:296–302.

Conover, J. T., R. L. Fritz,, and M. Viera.
1961. A morphometric study of silver hake. U.S. Fish Wildl. Serv., Spec. Sci. Report, Fisheries 368.

Cushing, D. H.
1968. Fisheries biology, a study in population dynamics. Univ. Wisconsin Press, Madison, WI, 200 p.

Dawson, W. A.
1991. Otolith measurement as a method of identifying factors affecting first-year growth and stock separation of mackerel (*Scomber scombrus* L.). J. Cons. Int. Explor. Mer 47:303–317.

Dery, L. M.
1988. Silver hake, *Merluccius bilinearis*. *In* Age determination methods for northwest Atlantic species (J. Pentilla and L. M. Dery, eds.), p. 41–47. U.S. Dep. Commer., NOAA Tech. Rep. NMFS 72.

Edwards, R. L., and R. E. Bowman.
1979. Food consumed by continental shelf fishes. *In* Predator-prey systems in fish communities and their role in fisheries management (H. Clepper, ed.), p. 387–407. Sports Fishing Institute, Washington, D.C.

Fowler, A. J., and D. A. Short.
1996. Temporal variation in the early life-history characteristics of the king george whiting (*Sillaginodes punctata*) from analysis of otolith microstructure. Mar. Freshwater Res. 47:809–818.

Freidland, K. D., and D. G. Reddin.
1994. Use of otolith morphology in stock discriminations of Atlantic salmon (*Salmo salar*). Can. J. Fish. Aquat. Sci. 51:91–98.

Grimes, C. B., A. G. Johnson, and W. A. Fable Jr.
1987. Delineation of king mackerel (*Scomberomorus cavalla*) stocks along the U.S. east coast and in the Gulf of Mexico. *In* Proceedings of the stock identification workshop November 5–7, 1985 Panama City Beach, Florida (H. E. Kumpf, R. N. Vaught, C. B. Grimes, A. G. Johnson, and E. L. Nakamura, eds.), p. 186–187. U.S. Dep. Commer., NOAA Tech. Memo. NMFS-SEFC-199.

Helser, T. E.
1996. Growth of silver hake within the U.S. continental shelf ecosystem of the northwest Atlantic Ocean. J. Fish. Biol. 48:1059–1073.

Helser, T. E., F. P. Almeida, and D. E. Waldron.
1995. Biology and fisheries of north-west Atlantic hake (silver hake: *M. bilinearis*). *In* Hake: biology, fisheries and markets (J. Alheit, and T. J. Pitcher, eds.), p. 203–237. Chapman and Hall, London.

Helser, T. E., and J. K. T. Brodziak.
1998. Impacts of density dependent growth and maturation on assessment advice to rebuild depleted U.S. silver hake (*Merluccius bilinearis*) stocks. Can. J. Fish. Aquat. Sci. 55:882–892.

Ihssen, P. E., H. E. Booke, J. M. Casselman, J. M. McGlade, N. R. Payne, and F. M. Utter.
1981. Stock identification: materials and methods. Can. J. Fish. Aquat. Sci. 38:1838–1855.

Iles, T. D., and M. Sinclair.
1982. Atlantic herring: stock discreteness and abundance. Science (Wash. D.C.) 215:627–633.

Jearld, A. Jr.
1995. Clinic overview. Image analysis systems. *In* Recent developments in fish otolith research (D. H. Secor, J. M. Dean and S. E. Campana, eds.), p. 655–670. Univ. South Carolina Press, Columbia, SC.

Konstantinov, K. G., and A. S. Noskov.
1969. U.S.S.R research report, 1968. ICNAF (International Commission for the Northwest Atlantic Fisheries) Redbook II:99–117.

L'Abée-Lund, J. H.
1988. Otolith shape discriminates between juvenile Atlantic salmon, *Salmo salar* L., and brown trout, *Salmo trutta* L. J. Fish Biol. 33:899–903.

Messieh, S. N., C. MacDougall, and R. Taylor.
1989. Separation of Atlantic herring (*Clupea harengus*) stocks in the southern Gulf of St. Lawrence using digitized otolith morphometrics and discriminant function analysis. Can. Tech. Rep. Fish. Aquat. Sci. 1647:iv + 22 p.

Nichy, F. E.
1969. Growth patterns on otoliths from young silver hake, *Merluccius bilinearis* (Mitchell). Int. Comm. NW Atl. Fish. Res. Bull. 6:107–117.

OPTIMAS. 6.
1996. User guide and technical reference, 8th ed., vol. I: xiii + 474 p. vol. II: viii + 630 p. Media Cybernetics, Silver Spring, MD.

Pawson, M. G., and S. Jennings.
1996. A critique of methods for stock identification in marine capture fishes. Fish. Res. 25:203–217.

Pentilla, J. A., G. A. Nelsen, and J. M. Burnett.
1989. Guidelines for estimating lengths at age for 18 northwest Atlantic finfish and shellfish species. U.S. Dep. Commer., NOAA Tech. Memo. NMFS-F/NEC-66, 30 p.

Reznick, D., E. Lindbeck, and H. Bryga.
1989. Slower growth results in larger otoliths: an experimental test with guppies (*Poecilia reticulata*). Can. J. Fish. Aquat. Sci. 46:108–112.

Schenk, R.
1981. Population identification of silver hake (*Merluccius bilinearis*) using isoelectric focusing. Woods Hole Lab. Ref. Doc. 81-44, Northeast Fisheries Science Center, NOAA, 31 p.

Stephenson, R. L.
1999. Stock complexity in fisheries management: a perspective of emerging issues related to population sub-units. Fish. Res. 43:247–249.

SYSTAT.
1997. SYSTAT 7.0 statistics. SPSS Inc., Chicago, IL., 751 p.

Templeman, W., and H. J. Squires.
1956. Relationship of otolith lengths and weights in the haddock *Melanogrammus aeglefinus* (L.) to the rate of growth of the fish. J. Fish. Res. Board Can. 13:467–487.

Effects of twine diameter and mesh size in the body of prawn trawls on bycatch in Gulf St. Vincent, Australia

Matt K. Broadhurst
Departamento de Pesca, Laboratório de Oceanografia Pesqueira
Universidade Federal Rural de Pernambuco-UFRPE
Av. Dom Manuel de Medeiros, s/n
Dois Irmãos, Recife-PE, Brasil, CEP: 52.171-900
E-mail address: fhvhazin@truenet.com.br

Paul E. McShane
South Australian Aquatic Sciences Centre
P.O. Box 120
Henley Beach, South Australia 5022, Australia

Roger B. Larsen
University of Tromsø
Breivika N-9037
Tromsø, Norway

Abstract.—The influences on catches and bycatches due to 1) an increase in size of mesh and 2) a reduction in twine diameter in the body of prawn trawls were investigated in Gulf St. Vincent, Australia. Compared with a conventional trawl body (mesh size 45 mm) attached to a composite square-mesh codend, two new trawl bodies, made with 53-mm mesh but with different twine diameters (1 and 1.7 mm, respectively) and each attached to identical composite square-mesh codends, were equally effective in significantly reducing the numbers of a range of small fish (by between 23.7% and 67%) and in not significantly reducing the weight of targeted prawns. Because there were no significant differences in the selectivity parameters of both new trawl bodies, these results indicated that the main cause of bycatch reduction was the increase in size of mesh in the body of the trawl. The escape of large numbers of unwanted small fish and prawns is discussed in terms of their probable behavior in the body of the trawl and the extent to which this behavior was influenced by the operational characteristics of the gear.

Manuscript accepted 1 December 1999.
Fish. Bull. 98:463–473 (2000).

In many of the world's prawn-trawl fisheries, large numbers of organisms are captured incidentally with the targeted catch (collectively termed "bycatch" *sensu* Saila, 1983). This bycatch comprises a diverse assemblage of small fish, cephalopods, and crustaceans, including prawns that are smaller than optimum size (for reviews see Saila, 1983; Andrew and Pepperell, 1992; Alverson et al., 1994). Concerns over the negative effects that the mortality of these fish and small organisms may cause on the yield of stocks has led to the application of various management strategies designed to minimize bycatch (Andrew and Pepperell, 1992). The most common approach has been to change the conventional trawls to improve overall selectivity of the gear. Depending on the sizes and species to be targeted and excluded, these changes have involved the sizes and types of mesh used, and the application of physical modifications, collectively termed bycatch reducing devices (BRDs) (see Broadhurst, 2000, for review).

Inherent variations among the characteristics of different prawn-trawl fisheries have resulted in a range of modifications to conventional trawls. Regardless of design, however, the majority of functional modifications have been applied within or immediately anterior to the codend (e.g. Isaksen et al., 1992; Thorsteinsson, 1992; Broadhurst and Kennelly, 1997; Rogers et al., 1997) mainly because observations suggest that most of the selection process for many species occurs in this area (Armstrong et al., 1990; MacLennan, 1992; Wileman et al., 1996). Moreover, because codends often are similar among the different trawl designs within a particular fishery (e.g. Broadhurst and Kennelly, 1997), any modifications to improve selectivity are more easily implemented, adopted, and regulated throughout the fishery.

Although alterations to codends have been successful in reducing various subsets of bycatch, there is evidence suggesting that individuals of some species, particularly those of prawns, escape from the bodies of prawn trawls (High et al., 1969; Sumpton et al., 1989; Vendeville, 1990). For example, High et al. (1969) attached various covers to the upper, lateral, and posterior bodies of trawls to isolate areas that could be modified to passively separate fish from prawns (*Pandalus* sp.). Although there was little evidence of fish escaping, large numbers of small prawns were retained in the covers, particularly in the posterior sections. Similarly, in one

of the few studies on the effects of changes in the types of twine used in the body of trawls on catches, Sumpton et al. (1989) showed that compared with multifilament twine (1.1 mm diameter), significantly more smaller-size prawns (*Penaeus* spp.) and squid (*Loligo* spp.) escaped through the bodies of trawls made from monofilament twine (0.9 mm diameter).

Despite these results and although nearly all prawn-trawl fisheries are regulated by means of legally defined minimum mesh sizes (typically ranging from 40 to 50 mm stretched mesh, Vendeville, 1990), there is a paucity of information on the effects of different sizes of mesh used in the bodies of trawls on selectivity. This is particularly the case in Australian prawn-trawl fisheries, where despite extensive research to develop BRDs (see Broadhurst, 2000), no published studies have quantified the effects of different sizes of mesh. In a recent experiment in Gulf St. Vincent, South Australia (Broadhurst et al., 1999), we provided evidence to suggest, however, that the minimum size mesh (45 mm) throughout the trawls was too small. As a first step in addressing this issue, we investigated modifications to the codends and demonstrated that new designs comprising composite panels of different-size square-shape mesh (52 and 80 mm mesh hung on the bar) were effective in significantly reducing bycatches of undersize western king prawns (*Penaeus latisulcatus*) and small fish without reducing the weight of the commercial catch.

These results, combined with the simplicity of the new codend, led to the immediate and unanimous adoption of a design, based on those tested, by Gulf St. Vincent prawn trawlers. Encouraged by the performance of simple changes in mesh type and size to improve selectivity, commercial fishermen sought assistance to examine other refinements to their trawls. Given evidence to suggest that the mesh size used in Gulf St. Vincent was inappropriate and that selection for some species may occur in the body of prawn trawls, our aims in the present study were to quantify the influences on selection in this area due to 1) increasing the mesh size (from approx. 45 mm to 53 mm) and 2) reducing the diameter of twine used.

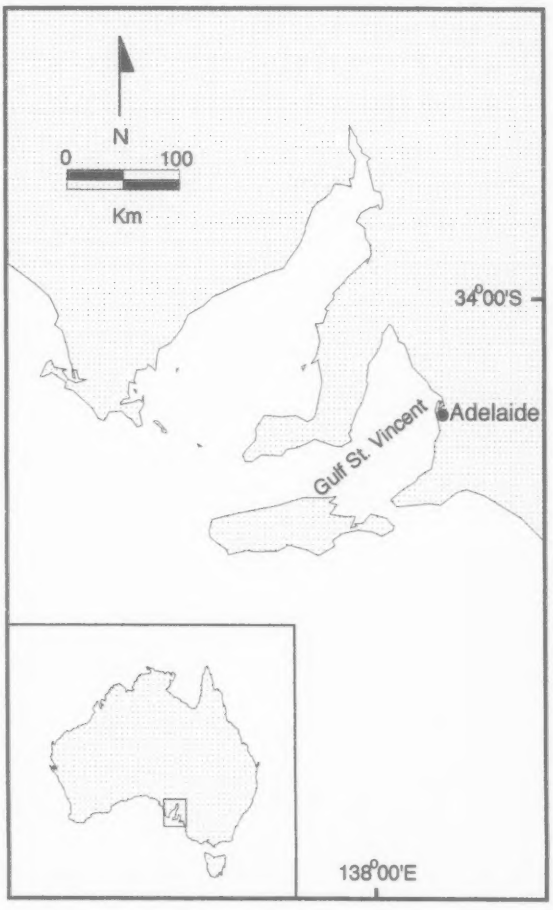

Figure 1
Location of study at Gulf St. Vincent, South Australia.

Materials and methods

Our work was done in Gulf St. Vincent, South Australia (Fig. 1), in October, 1998, with a chartered commercial prawn trawler rigged to tow three trawls in a standard triple gear configuration (see Andrew et al., 1991, for details). Three different trawl bodies were examined. The first (termed the "control") represented conventional trawl bodies (see Broadhurst et al., 1999, for specifications) and was constructed of 1.7-mm-diameter, 24-strand, polyethylene twisted twine with a mean mesh size (stretched distance between the knots) of 44.42 mm (see "Results" section). The second and third trawl bodies (termed "spectra-1-mm" and "momoi-1.7-mm") were identical in design, in headrope and footrope length, in rigging and tapers to the control trawl body but were made from 1-mm-diameter, polyethylene cabled twine (brand name "spectra") and 1.7-mm-diameter, 30-ply, polyethylene twisted twine (brand name "momoi"), respectively, with mean mesh sizes of 52.43 and 52.96 mm, respectively (see "Results" section).

All three trawl bodies were attached to identical composite square-mesh codends (Broadhurst et al., 1999) consisting of two sections, each measuring 80 bars in circumference, 70 bars in length, and constructed of 52-mm mesh (3-mm-diameter, braided polyethylene twine) cut on the bar (Fig. 2, A–C). Each square-mesh section consisted of an upper and lower panel sewn together so that the direction of the knots on the upper panel were opposite those on the lower panel (Fig. 2A). A panel of 104-mm netting, measuring 6 bars × 10 bars, was inserted into the tops of the posterior sections of each square-mesh codend, starting at the leading edge and ending about 1.3 m anterior to the last row of meshes (Fig. 2, A and B). Lengths of 12-mm-diameter, polyethylene 3-strand rope (termed "last-ridge ropes") were firmly laced at a hanging ratio of 0.9 to each of the two lateral seams of the codends (to provide length-wise strength) (Fig. 2B).

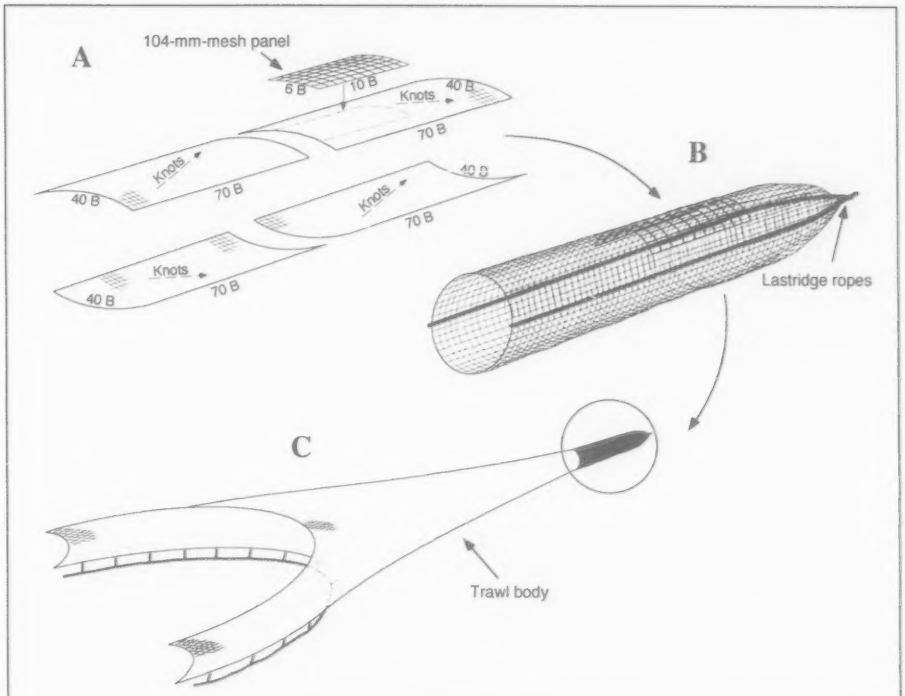

Figure 2

Diagrammatic representation of (**A**) panels and sections of the composite square-mesh codend (B=bars), (**B**) completed composite square-mesh codend, and (**C**) prawn-trawl body and codend used in the study. B = bars.

Experimental procedure

Before starting the experiment, all trawls were towed for a short period to allow knots and bindings to stretch. To obtain accurate information on mesh sizes, a set of dial calipers was used to measure 30 randomly located meshes (stretched length in mm, between the inside knots) at four separate locations (starboard wing, footrope, headrope, and posterior body) in each trawl body.

The spectra-1-mm and momoi-1.7-mm trawls were compared separately against the control trawl. In each paired comparison, the trawls were shackled to the outside sweeps of the sleds and otterboards of the triple rigged gear and towed simultaneously. A conventional trawl body was used as the center net in all comparisons, but because it was not rigged in exactly the same manner as the outside nets, its catch was excluded from analysis. The triple gear was towed in normal commercial tows of 25-min duration at 3 knots (1.5 m/s) over a combination of sandy and light coral bottoms. Each of the outside trawls were randomly assigned after each tow (to eliminate any potential biases), so that three paired comparisons of each new trawl against the control trawl were made on each night (i.e. a total of six tows per night). Over five nights, we completed a total of 15 replicate comparisons of each configuration.

After each tow, the catches from the two outside trawls were emptied onto a partitioned tray. Data collected from each tow were the following: the total weight of western king prawns and a subsample (100 prawns from each trawl) of their carapace lengths (to the nearest 1 mm); the total number of prawns (estimated from the weight of the subsample); the total weight of discarded bycatch and discarded noncommercial bycatch; the weights and numbers of commercially or recreationally (or both) important bycatch species; and the sizes (to the nearest 0.5 cm) of commercially or recreationally (or both) important fish. A random sample of prawns (approximately 12 kg) from each trawl in each tow was separated and sent to A. Raptis & Sons PTY LTD (seafood processing plant) in Adelaide for grading into "commercial categories" (based on a system of numbers per pound) with a locally built "dynamic grading machine."

Several commercially important species were caught in sufficient quantities to enable meaningful comparisons. These were western king prawns (*Penaeus latisulcatus*), blue swimmer crabs (*Portunus pelagicus*), sand trevally (*Pseudocaranx wrighti*), red mullet (*Upeneichthys porosus*), leatherjacket (*Thamnaconus degeni*), southern sand flathead (*Platycephalus bassensis*), small-toothed flounder (*Pseudorhombus jenynsii*), and southern calamari (*Sepioteuthis australis*). With the exception of western king prawns

and southern calamari (which fishermen are legally permitted to retain), all remaining species comprised those that are considered commercially important bycatch (e.g. to other fisheries) and that are normally discarded.

Analysis of mesh sizes

The mesh-size measurements collected from the trawl bodies were analyzed for heteroscedasticity with Cochran's test and a two-factor, balanced analysis of variance (ANOVA) with trawl body and location of meshes considered fixed and random factors, respectively. Significant differences detected in these analyses were investigated by Tukey's multiple comparisons of means test.

Analysis of catch data

Catch data for all replicates that had sufficient numbers of each variable (i.e. 1 individual in at least 10 replicates) were analyzed with paired *t*-tests ($P \leq 0.05$). Except for the weights and numbers of blue swimmer crabs and small-toothed flounder (species that could not pass through the meshes in any of the trawls), all variables were analyzed with one-tailed tests to test the hypothesis that the larger-mesh trawl bodies retained fewer individuals than the control. Catches of blue swimmer crabs and small-toothed flounder were compared with two-tailed tests. To examine the relative effectiveness of the spectra-1-mm and momoi-1.7-mm trawl bodies, differences in catches (between each trawl and their respective controls) for those variables that had data in all tows were analyzed by using Cochran's test for homogeneity of variances and a balanced, two-factor ANOVA. In these analyses, trawl-type and nights were considered fixed and random factors, respectively. Where there were sufficient data ($n>25$ in each trawl, pooled across all tows), size frequencies of commercially or recreationally important fish (or both) were plotted and compared with two-sample Kolmogorov-Smirnov tests ($P=0.05$).

Analysis of prawn sizes

Size-frequencies of prawns retained in each of the three trawls were combined across all tows. Using an estimated split model (Millar and Walsh, 1992), we fitted logistic curves to these data by maximum likelihood method (Pope et al., 1975). Logistic curve parameters, associated standard errors and 95% confidence limits were calculated for each large-mesh trawl body. Model deviance values were determined for a goodness-of-fit hypothesis (i.e. to test H_0: that the curves were logistic). Size categories of commercially graded prawns from each trawl were plotted and analyzed with two-sample Kolmogorov-Smirnov tests ($P=0.05$).

Results

Analysis of mesh sizes

There were significant differences detected in size of mesh between the three trawl bodies (Table 1). Tukey's comparison of means test showed no significant differences between the spectra-1-mm and momoi-1.7-mm trawl bodies (mean mesh sizes ±SE of 52.43 ±0.08 mm and 52.96 ±0.09 mm, respectively). The mean size of mesh in the control trawl was significantly less at 44.42 ±0.13 mm. Mesh size was not significantly different among the various locations (e.g. wing, footrope, head rope, and posterior body) examined in any of the trawl bodies.

Table 1

Summaries of *F* ratios from two-factor analysis of variance to determine differences in size of mesh in the trawls and at various locations and results of Tukey's comparison of means test for the significant difference detected in size of mesh between trawls (spectra-1-mm=momoi-1.7-mm>control). Data were treated in the raw form. ** = $P<0.01$.

Treatment	df	Mesh size (mm)
Trawls (T)	2	2494.7**
Location of mesh in trawl (L)	3	0.85
$T \times L$	6	1.4
Residual	346	

Analysis of catch data

Compared with the control, the spectra-1-mm and momoi-1.7-mm trawl bodies significantly reduced the numbers of western king prawns caught (means reduced by 13.7% and 15.6%, respectively), without significantly reducing the weights of prawns (although mean catch from the spectra-1-mm was 6.3% lower than that from the control) (Table 2; Fig. 3, A and B). The spectra-1-mm and momoi-1.7-mm trawl bodies also significantly reduced the weights of total discarded bycatch (by 29.3% and 20.3%); numbers of leatherjacket (by 32.5% and 23.7%) and their weights (by 24.2% and 19.6%); numbers of sand trevally (by 56.2% and 40.4%) and their weights (by 52.8% and 40.4%); and the numbers of southern sand flathead (by 59.8% and 40.2%) and red mullet (by 67.2% and 59.3%) (Fig. 3, C, E, F, G, and I; Table 2). The spectra-1-mm trawl body also significantly reduced the weights of southern sand flathead (by 31.8%), red mullet (by 57%), and the numbers of southern calamari (by 33.6%) (Fig. 3, H, J, and L; Table 2). ANOVA of the differences in catches between the new trawl bodies and their controls showed no significant interactions nor main effects for any of the variables examined (Table 3).

Two-sample Kolmogorov-Smirnov tests for comparing the size-frequency distributions of fish measured from the control and new trawl bodies detected significant differences in the relative size compositions of southern sand flathead retained by both new trawl bodies and in the relative size compositions of sand trevally retained by the momoi-1.7-mm trawl body (the new trawl bodies retained proportionally fewer small-size fish) (Fig. 4, A and B). There were no other significant differences detected.

Table 2

Summaries of paired *t*-tests in which the control and the new trawl bodies were compared. Weights and numbers of blue swimmer crabs and small-toothed flounder were analyzed with two-tailed paired *t*-tests whereas the remaining variables were analyzed with one-tailed paired *t*-tests. pt-v = paired *t*-value; *n* = number of replicates; disc = discarded; n-comm = noncommercial. * = $P<0.05$; ** = $P<0.01$.

	Spectra-1-mm versus control			Momoi-1.7-mm versus control		
	pt-v	*P*	*n*	pt-v	*P*	*n*
No. of prawns	–2.368	0.016*	15	–2.389	0.016*	15
Wt. of prawns	–1.755	0.051	15	–0.044	0.483	15
Wt. of total disc bycatch	–4.127	0.0005**	15	–2.662	0.009**	15
Wt. of disc n–comm bycatch	–1.709	0.055	15	–1.38	0.095	15
No. of leatherjacket	–3.627	0.001**	15	–2.447	0.014*	15
Wt. of leatherjacket	–4.542	0.0002**	15	–2.181	0.023*	15
No. of sand trevally	–1.987	0.033*	15	–2.491	0.013*	15
Wt. of sand trevally	–1.960	0.035*	15	–2.253	0.020*	15
No. of southern sand flathead	–3.516	0.002**	14	–2.939	0.006**	14
Wt. of southern sand flathead	–2.994	0.005**	14	0.445	0.668	14
No. of red mullet	–3.116	0.004**	15	–2.610	0.013*	11
Wt. of red mullet	–2.157	0.024*	15	–0.882	0.199	11
No. blue swimmer crab	1.505	0.156	14	0.725	0.482	13
Wt. of blue swimmer crab	1.524	0.152	14	1.462	0.169	13
No. of small–toothed flounder	–0.395	0.699	13	–1.977	0.068	15
Wt. of small–toothed flounder	–0.082	0.936	13	–0.150	0.883	15
No. of southern calamari	–2.210	0.022*	15	–0.846	0.206	15
Wt. of southern calamari	0.026	0.510	15	–0.837	0.208	15

Table 3

Summaries of *F* ratios from two-factor analyses of variance to determine effects on variables due to fishing with different trawl bodies on different nights. The transforms used to stabilize the variances where required are listed. N-comm = noncommercial, disc = discarded.

				Bycatch (wt. in g)							
		Prawns		Total	N-comm	Leatherjacket		Trevally		Southern calamari	
Treatment	df	no. 1/(x+1)	wt.	disc	disc	no. ln(x+1000)	wt.	no.	wt.	no.	wt.
Trawl bodies (*T*)	1	0.01	3.97	0.64	0.44	0.64	0.64	1.36	1.36	1.15	1.31
Nights (*N*)	4	1.50	1.79	0.40	0.41	0.40	0.42	0.72	0.72	1.47	0.18
$T \times N$	4	1.00	0.48	0.86	1.27	0.86	0.23	0.73	0.29	2.20	0.36
Residual	19										

Analysis of prawn sizes

The logistic length selection curves derived for each of the new trawl bodies are provided in Figure 5. Model deviance indicated sufficient goodness of fit for both curves (Table 4). The 95% confidence limits of the selectivity parameters showed that there were no statistically significant differences between the two new trawl bodies (Table 4).

Significant differences were detected in Kolmogorov-Smirnov tests on the commercial-size categories of prawns

graded from the control and new trawl bodies (Fig. 6). Both trawls with the larger meshed bodies retained proportionally fewer smaller prawns.

Discussion

The results from this study showed that both new trawl bodies were effective in excluding under-size prawns and large numbers of small fish (by up to almost 60%) and in not reducing the weight of targeted prawns. These results provide evidence to suggest that simple changes to the body of prawn trawls can have a contributing effect on overall trawl selectivity. The escape of large numbers of small fish and prawns from this area may be due to their behavior in the trawl and the extent to which they were influenced by the operational characteristics of the gear.

It is well established that fish exhibit specific responses to stimuli from trawls and attempt to avoid contact with the trawl body by maintaining position at the opening (Wardle, 1983; Watson, 1989). After some period, depending on species- and size-specific swimming abilities (Wardle, 1975), fish invariably tire and turn towards the codend, allowing the trawl to pass around them (Watson, 1989) or alternatively, maintain swimming in the direction of the tow, but gradually fall back along the taper of the body panel towards the codend opening (Wardle, 1983). As the taper of the trawl body narrows and the density of fish increases, some fish may rise in the trawl and attempt escape through the meshes or pass into the codend and resume swimming immediately anterior to the catch (Wardle, 1983). In contrast, benthic invertebrates like prawns tend to display limited responses during capture. SCUBA observations by Watson (1976) showed that after contact with the leading edge of the trawl, penaeid prawns contracted their abdomens ventrally, propelling themselves backwards. This initial response was repeated three to five times but because prawns are not capable of maintaining such activity, the speed of the trawl through the water quickly forced them against the meshes of the trawl body and they eventually tumbled down the net into the codend.

In view of these behavioral patterns, gear-related factors, such as the fast towing speed (1.5 m/s) and taper of the trawl body in our study, may have increased the probability of small fish and prawns being selected in this area. For example, the sizes of most of the fish encountered, and particularly sand trevally, leatherjackets, and small southern sand flathead (5–15 cm, [Fig. 4]), means that they would have been unable to maintain position in the moving trawls. Studies quantifying the swimming speeds of teleost fish suggest that although individuals 5 and 15 cm long may be expected to have burst speeds of 0.5 m/s and 1.5 m/s over very short periods, their normal maximum swimming performance (or maximum cruising speed, Wardle, 1983) would be much less (Bainbridge, 1958; Wardle, 1975, 1983; Beamish, 1978). As a consequence, in our study some fatigued individuals probably came in contact with meshes in the body panels as they were herded towards the codend opening. Further, the relatively steep tapers (i.e. 1N4B—see Broadhurst et al., 1999) of the trawl bodies (compared with those used in most other prawn-trawl fisheries, FAO,

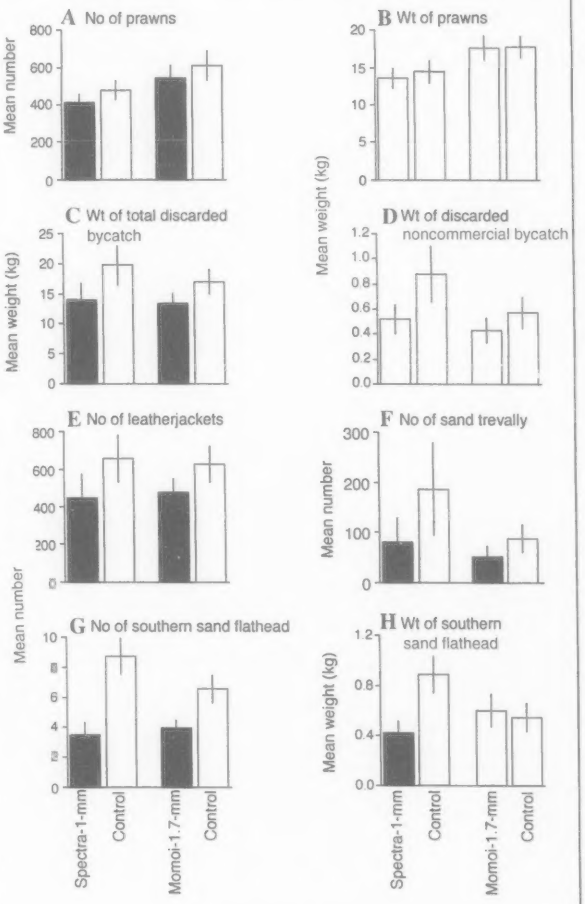

Figure 3

Differences in mean catches (per 25 min tow ±SE) between the new trawl bodies and control for the (**A**) numbers and (**B**) weights of king prawns (*Penaeus latisulcatus*); the weights of (**C**) total discarded bycatch and (**D**) discarded noncommercial bycatch; the numbers of (**E**) leatherjackets (*Thamnaconus degeni*), (**F**) sand trevally (*Pseudocaranx wrighti*) and (**G**) southern sand flathead (*Platycephalus bassensis*); the weights of (**H**) southern sand flathead; the numbers (**I**) and weights (**J**) of red mullet (*Upeneichthys porosus*); the numbers of (**K**) blue swimmer crabs (*Portunus pelagicus*); the numbers (**L**) and weights of (**M**) southern calamari (*Sepioteuthis australis*); and the numbers of small-toothed flounder (*Pseudorhombus jenynsii*). Significant differences are indicated by shaded histograms.

Table 4

Computed selectivity parameters for prawns (carapace length in mm) from the two new trawl bodies and deviance values for the goodness-of-fit logistic curve. Standard errors are given in parentheses. a, b = logistic parameters (Pope et al., 1975). P = split proportion from estimated split model

	Momoi-1.7-mm		Spectra-1-mm	
a	−8.99		−13.00	
b	0.26		0.39	
P	0.59		0.56	
		95% confidence limits		95% confidence limits
25% retention (L25)	30.26 (0.67)	25.43–34.91	29.92 (0.49)	26.72–32.92
50% retention (L50)	34.47 (0.92)	32.93–37.06	32.68 (0.57)	31.69–34.13
75% retention (L75)	38.68 (1.56)	34.11–45.51	35.44 (0.92)	32.46–39.55
Selection range (SR)	8.42 (0.44)	5.48–11.42	5.52 (0.16)	3.71–7.33
Deviance	22.58		29.49	
df	34		32	
P-value	0.932		0.594	

1972), probably contributed to contact of both fish and prawns with meshes in this section of the trawl. A combination of the above effects in the larger-mesh spectra-1-mm and momoi-1.7-mm trawl bodies may have facilitated the escape of smaller individuals.

It is also likely that a reduction in twine area associated with the larger mesh sizes in both new trawl bodies allowed a faster release of water than did the control trawl body,[1] possibly contributing to the effects discussed above. In partial support of this hypothesis and although no significant differences were detected between the spectra-1-mm and the momoi-1.7-mm trawl bodies for those variables examined (Table 3), the narrower-twine spectra-1-mm trawl body consistently reduced a larger percentage of bycatch across a greater range of variables. These variables included the weights of southern sand flathead and red mullet and the numbers of southern calamari (Table 2; Fig 3). Further investigation, involving a greater number of replicate tows would be required, however, to validate the potential for this effect.

A contributing operational factor towards the escape of fish from both large-mesh trawl bodies may have been the period between the time when the vessel was slowed and when the gear was hauled to the surface (termed "haulback") (Watson, 1989; Broadhurst et al., 1996). Watson (1989) showed that differences in geometry of the trawl and associated water flow during haulback caused fish (that were still swimming in the trawl) to become disorientated and to attempt escape through the surrounding meshes. More specifically, Workman and Taylor (1989) observed that numerous small individuals of schooling species such as Carangidae (e.g. *Trachurus lathami* and *Decapterus punctalus*) escaped during this period and that larger individuals were often caught by their gills in

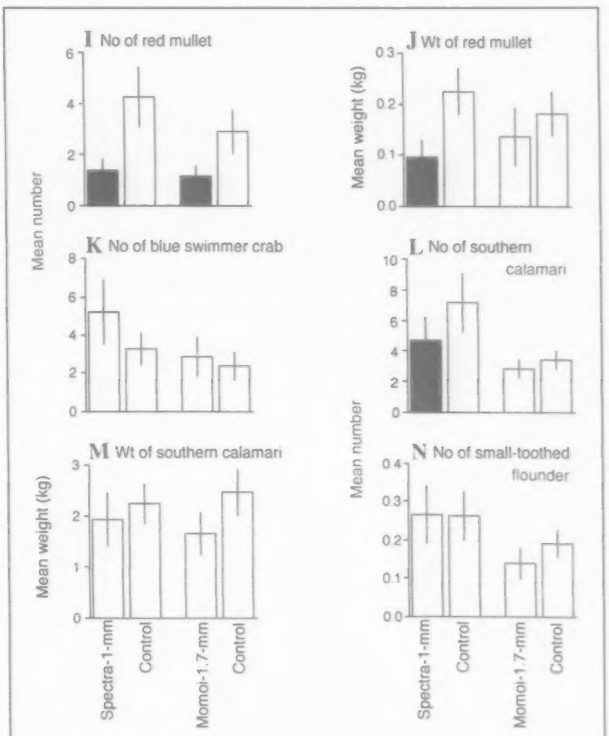

Figure 3 (continued)

[1] Harrington, D. L., J. W. Watson, L. G. Parker, J. B. Rivers, and C. W. Taylor. 1988. Shrimp trawl design and performance, 37 p. University of Georgia Marine Extension Service, 715 Bay St., Brunswick, Georgia 31520-4601.

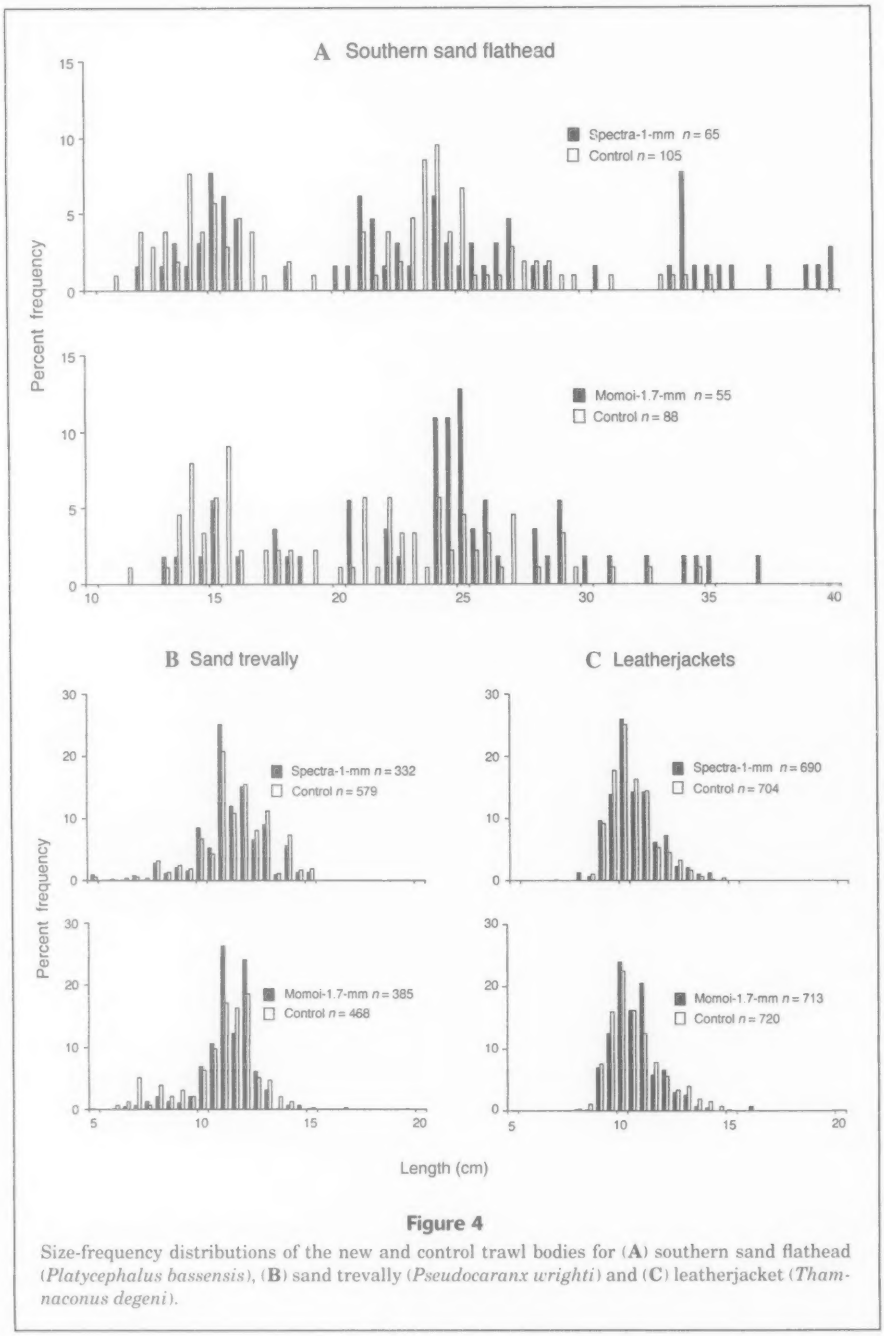

Figure 4

Size-frequency distributions of the new and control trawl bodies for (**A**) southern sand flathead (*Platycephalus bassensis*), (**B**) sand trevally (*Pseudocaranx wrighti*) and (**C**) leatherjacket (*Thamnaconus degeni*).

the meshes of the body panels. Likewise in our study, we observed numerous larger individuals of southern sand flathead, leatherjackets, and particularly larger sand trevally (10–15 cm) trapped in the meshes of the posterior sections of both large-mesh trawl bodies.

Although the results showed that significantly more smaller prawns escaped from the new trawl bodies than from the control trawl body, the selectivity parameters and associated 95% confidence limits (Fig 5; Table 4) were within the range calculated in a previous study (Broadhurst et al., 1999) for a

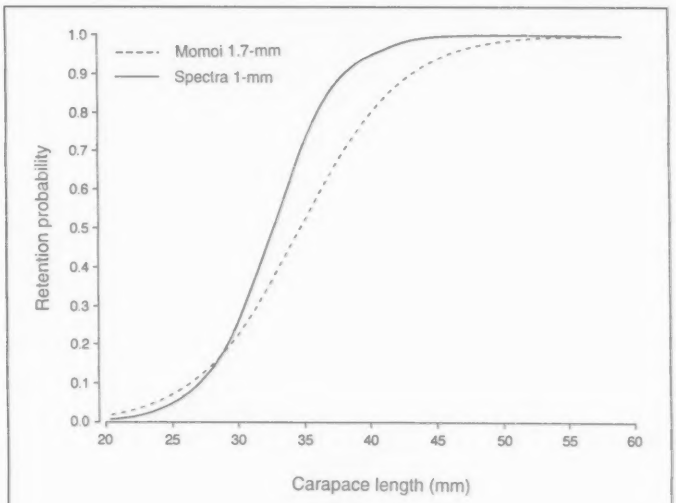

Figure 5

Plots of the selection curves of western king prawns (*Penaeus latisulcatus*) for the spectra-1-mm and momoi-1.7-mm trawl bodies.

trawl comprising a body of 45-mm mesh attached to a similar composite square-mesh codend. During this previous study, the codend that showed the most appropriate size-selectivity for prawns tapered from a circumference of 70 bars at the start of the anterior section to 58 bars at the end of the posterior section. After extensive commercial testing, however, it was reported that the slight taper in this codend occasionally "wedged" the catch in the posterior section, making it difficult to remove the catch when the codend was retrieved and the draw-strings were opened. To address this problem, fishermen widened the circumference to 80 bars throughout the codend. Although such an alteration solved the problems associated with buildup of catch in the codend (by allowing it to distribute more horizontally), it probably lowered the selectivity for prawns (Broadhurst and Kennelly, 1996). Any contributing effects on trawl selectivity due to the larger mesh in the spectra-1-mm and momoi-1.7-mm trawl bodies may have been slightly negated by a reduction in overall selectivity of the composite square-mesh codends. This result illustrates the need for ongoing assessments of influences on selectivity of trawls due to subtle modifications to facilitate operational procedures.

Like the results from other related studies, the significant reduction in numbers of prawns caught, but not in their weights, has shown that increases in mesh sizes or in openings (or in both) can facilitate an increase in catches of target-size individuals (Walsh et al., 1992; Broadhurst and Kennelly, 1997; Broadhurst et al., 1999). Possible hypotheses to explain this effect include 1) a faster release of water from the larger-mesh trawls resulted in prawns quickly passing into the trawl after initial contact, with less chance of escaping over the head rope and out through the mouth of the trawl or alternatively, 2) less drag in the larger-mesh trawls, due to less twine area and amount of bycatch, allowed the mouth of the trawl to spread wider, thereby covering more of the sea bed and capturing more prawns. Of these two hypotheses, the potential for an increase in spread is less likely because there were no significant differences in the catches of blue swimmer crabs or small-toothed flounder (species that could not pass through either the trawl bodies or composite square-mesh codends) between any of the trawls examined.

Because there were no significant differences detected in the weights of prawns captured between the various trawls, a further increase in the size of mesh in the body of the trawl (e.g. 60 mm) warrants investigation. Given the results presented in our study, this increase in mesh size could facilitate a greater release of small fish and further improve size selectivity for the targeted prawns. Alternatively, it may be feasible to examine the utility of trawl bodies comprising composite panels of larger mesh, particularly in the posterior section, because it is apparent that as fish are herded together in this area their densities increase, resulting in random attempts at escape through the sides of the trawl (Wardle, 1983). In addition, any fatigued fish still swimming in the posterior section of the trawl during haulback may have an opportunity to escape through these larger meshes.

Although not mandated, the results from our study have led to the use of large-mesh trawl bodies by many of the fishermen operating in Gulf St. Vincent. Combined with the contributing effects on bycatch reduction due to the composite square-mesh codend, this modification should result in a comparatively more selective prawn-trawl fishery. For example, in a review of literature quantifying bycatches from prawn-trawl fisheries throughout the world, Andrew and Pepperell (1992) reported that typical bycatch-to-prawn ratios in similar temperate fisheries were in the order of 5:1. From the mean catch per tow from the control and the new trawl bodies in our study,

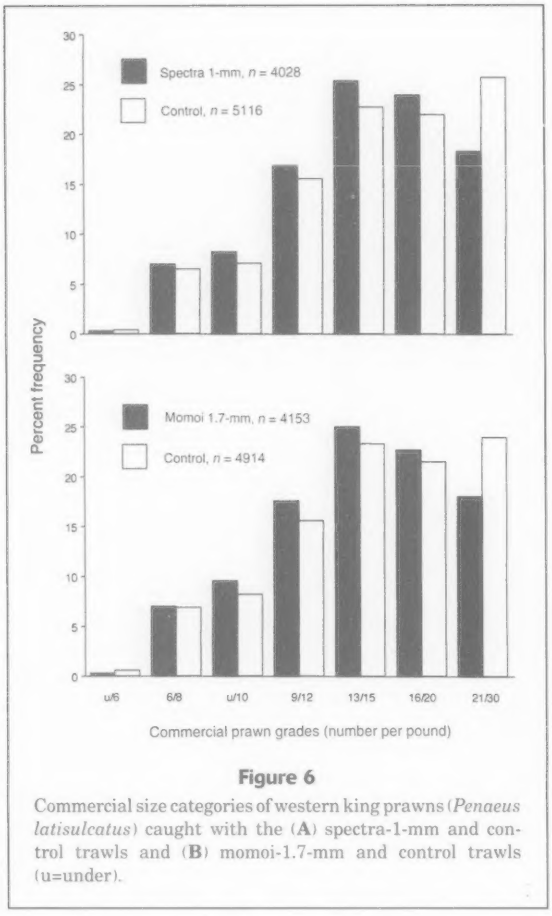

Figure 6

Commercial size categories of western king prawns (*Penaeus latisulcatus*) caught with the (**A**) spectra-1-mm and control trawls and (**B**) momoi-1.7-mm and control trawls (u=under).

discarded bycatch-to-prawn ratios were 1:1 for the spectra-1-mm and 1:1.3 for the momoi-1.7-mm trawl bodies. Ongoing monitoring is still required, however, to assess any potential effects on selectivity associated with operational refinements to the current trawl configurations.

Acknowledgments

This study was funded by the Australian Fishing Industry Research and Development Corporation. We thank Simon Boxshall and Brian McDonald for logistical support and assistance in the field and Jim Raptis (A. Raptis and Sons, PTY LTD) for the use of his vessel *Jillian Sandra*. We are grateful for the assistance and advice provided by Less Lowe (Gulf Net mending PTY LTD), Kim Redman, Hec Kavenagh, and all Gulf St. Vincent prawn trawlers. We would also like to acknowledge the Conselho National de Ensino e Pesquisa (CNPq) in Brazil for their contribution to the involvement of Matt Broadhurst.

Literature cited

Alverson, D. L., M. H. Freeberg, S. A. Murawski, and J. G. Pope.
1994. A global assessment of fisheries bycatch and discards. FAO Fish. Tech. Paper 339, Rome, 233 p.

Andrew, N. L., K. J. Graham, S. J. Kennelly, and M. K. Broadhurst.
1991. The effects of trawl configuration on the size and composition of catches using benthic prawn trawls off the coast of New South Wales, Australia. ICES J. Mar. Sci. 48:201–209.

Andrew, N. L., and J. G. Pepperell.
1992. The bycatch of shrimp trawl fisheries. Oceanogr. Mar. Biol. Annu. Rev. 30:527–565.

Armstrong, D. W., R. S. T. Ferro, D. N. MacLennan, and S. A. Reeves.
1990. Gear selectivity and the conservation of fish. J. Fish Biol. 37A:261–262.

Bainbridge, R.
1958. The speed of swimming of fish as related to size and to the frequency and amplitude of the tailbeat. J. Exp. Biol. 35:109–133.

Beamish, F. W. H.
1978. Swimming capacity. *In* Fish physiology, vol: VII, Locomotion (W. S. Hoar and D. J. Randall, eds.), p. 101–187. Academic Press, New York, NY.

Broadhurst, M. K.
In press. Modifications to reduce bycatch in prawn trawls: a review and framework for development. Rev. Fish Biol. Fish.

Broadhurst, M. K., and S. J. Kennelly.
1996. Effects of the circumference of codends and a new design of square-mesh panel in reducing unwanted bycatch in the New South Wales oceanic prawn-trawl fishery, Australia. Fish. Res. 27:203–214.
1997. The composite square-mesh panel: a modification to codends for reducing unwanted bycatch and increasing catches of prawns throughout the New South Wales oceanic prawn-trawl fishery. Fish. Bull. 95:653–64.

Broadhurst, M. K., S. J. Kennelly, and G. O'Doherty.
1996. Effects of square-mesh panels in codends and of haul-back-delay on bycatch reduction in the oceanic prawn-trawl fishery of New South Wales, Australia. Fish. Bull. 94:412–22.

Broadhurst, M. K., R. B. Larsen, S. J. Kennelly, and P. McShane.
1999. Use and success of composite square-mesh codends in reducing bycatch and in improving size-selectivity of prawns in Gulf St. Vincent, South Australia. Fish. Bull. 97:434–48.

FAO (Food and Agriculture Organization of the United Nations).
1972. Catalogue of fishing gear designs. Fishing news books Ltd., Farnham, Surrey, England, 160 p.

High, W. L., I. E. Ellis, and L. D. Lusz.
1969. A progress report on the development of a shrimp trawl to separate shrimp from fish and bottom-dwelling animals. Comm. Fish. Rev. 31:20–33.

Isaksen, B., J. W. Valdemarsen, R. B. Larsen, and L. Karlsen.
1992. Reduction of fish bycatch in shrimp trawl using a rigid separator grid in the aft belly. Fish. Res. 13:35–52.

MacLennan, D. N.
1992. Fishing gear selectivity: an overview. Fish. Res. 13: 201–204.

Millar, R. B., and S. J. Walsh.
1992. Analysis of trawl selectivity studies with an application to trouser trawls. Fish. Res. 13:205–220.

Pope, J. A., A. R. Margetts, J. M. Hamley, and E. F. Akyuz.
1975. Manual methods for fish stock assessment. Part III: selectivity of fishing gear. FAO Fisheries Technical Report 41 (revision 1), 65 p. FAO, Rome.

Rogers, D. R., B. D. Rogers, J. A. de Silva, and V. L. Wright.
1997. Effectiveness of four industry-developed bycatch reduction devices in Louisiana's inshore waters. Fish. Bull. 95:552–565.
Saila, S. B.
1983. Importance and assessment of discards in commercial fisheries. FAO Fish. Circ. 765, 62 p.
Sumpton, W. D., P. J. Smith, and B. G. Robotham.
1989. The influence on catch of monofilament and multifilament netting in otter prawn-trawls. Fish. Res. 8:35–44.
Thorsteinsson, G.
1992. The use of square mesh codends in the Icelandic shrimp (*Pandalus borealis*) fishery. Fish. Res. 13:255–266.
Vendeville, P.
1990. Tropical shrimp fisheries: types of fishing gear used and their selectivity. FAO Fish. Tech. Paper 261 (revision 1), 75 p. FAO, Rome.
Walsh, S. J., R. B. Millar, C. G. Cooper, and W. M. Hickey.
1992. Codend selection in American plaice: diamond versus square mesh. Fish. Res. 13:235–254.
Wardle, C. S.
1975. Limit of fish swimming speed. Nature (Lond.) 255: 725–7.
1983. Fish reactions to towed fishing gears. *In* Experimental biology at sea (A. MacDonald and I. G. Priede, eds.), p. 167–195. Academic Press, New York, NY.
Watson, J. W.
1976. Electrical shrimp trawl catch efficiency for *Penaeus duorarum* and *Penaeus aztecus*. Trans. Am. Soc. 105:135–148.
1989. Fish behaviour and trawl design: potential for selective trawl development. *In* Proceedings of the world symposium on fishing gear and fishing vessels (C. M. Campbell, ed.), p. 25–29. Marine Institute, St Johns, Canada.
Wileman, D. A., R. S. T. Ferro, R. Fonteyne, and R. B. Millar.
1996. Manual methods of measuring the selectivity of towed fishing gears. ICES, Copenhagen, 126 p.
Workman, I. K., and C. W. Taylor.
1989. The fish funnel: a trawl modification to reduce fish escapement. Mar. Fish. Rev. 51:23–27.

A new approach to validation of periodicity and timing of opaque zone formation in the otoliths of eleven species of *Lutjanus* from the central Great Barrier Reef*

Mike Cappo
Australian Institute of Marine Science, PMB 3
Townsville MC, Queensland, Australia 4810
E-mail address: m.cappo@aims.gov.au

Peter Eden
Mote Pty Ltd
423 Elizabeth Drive
Vincentia, Jervis Bay, New South Wales, Australia 2540

Stephen J. Newman
Western Australian Marine Research Laboratories
Fisheries Western Australia
PO Box 20, North Beach, Western Australia 6020

Simon Robertson
Central Ageing Facility
Marine and Freshwater Resources Institute
Queenscliff, Victoria 3225, Australia

Abstract.—A model was proposed for validation studies of the periodicity and timing of growth checks on fish otolith sections, based on measurements of otolith radii around tetracycline (OTC) marks. Continuous variables were obtained by expressing measurements of the marginal increment and distance between the OTC mark and the subsequent opaque zone as "fractions" of the width of a completed increment cycle within an otolith. The sum of these fractions and the counts of whole cycles completed outside the OTC mark, divided by the known time at liberty, produced estimates of the periodicity of opaque zone completion. Given this rate of completion and known dates of OTC marking and sacrifice, the marginal increment was used to estimate a date on which the outermost opaque zone was completed. The model was applied to 82 marked fish of 11 *Lutjanus* species recovered after 6–22 months at liberty, and an hypothesis of annual periodicity, about a mean of 0.96 ±0.32 cycles/yr, was retained for the pooled species along the best, ventral reading axis. Model estimates for *L. erythropterus*, *L. johnii*, *L. malabaricus*, and *L. sebae* were in the range of 0.78 ±0.22 cycles/yr to 1.03 ±0.29 cycles/yr along this axis. Median ages of these fish were 3+ for *L. erythropterus* and *L. sebae* and 5+ for *L. johnii*. A two-fold difference in somatic and otolith growth detected between field-tagged and captive fish did not affect periodicity. Extension of the model suggested false annuli were induced by changes in salinity or adverse weather. On average, annuli were completed within 1–3 months after the minima in water temperature, in the austral spring–early summer, around early September for *L. erythropterus* and *L. johnii*, late September for *L. malabaricus* and late October for *L. sebae*. Results from the model were only preliminary for the small samples of *L. argentimaculatus*, *L. bohar*, *L. carponotatus*, *L. monostigma*, *L. rivulatus*, and *L. vitta*, although the common validation approach indicated annual periodicity of opaque zone completion for these species.

Manuscript accepted 1 December 1999.
Fish. Bull. 98:474–488 (2000).

There have been recent developments in the use of thin sections of otoliths for counting annual increments in otolith macrostructure as accurate and precise indicators of age for a variety of tropical reef species (see Fowler, 1995 for review). Lifespans of 15–30 years were estimated for tropical snappers in Mexico (Rocha-Olivares, 1998) and the central Great Barrier Reef (GBR) region (Sheaves, 1995; Newman et al., 1996). In contrast, Milton et al. (1995) applied a radiometric aging technique and estimated longevities of <10 years for the "red snappers" *Lutjanus erythropterus*, *L. malabaricus* and *L. sebae* in the Gulf of Carpentaria (lat. <14°S). These results were one third to one half of the maximum ages estimated by Newman et al. (in press) from sectioned otoliths for the same species in the central GBR (lat. 18–20°S).

These differences have produced uncertainty about the nature of potential development of northern Australian fisheries and raised important questions regarding intraspecific, latitudinal variation in otolith interpretation and demographic parameters. There is a clear need to validate age estimates from both regions.

Francis (1995) proposed that validation is the process of estimating the accuracy of an aging method and that a first stage in the validation involves confirming the temporal meaning of the zones. A three-step conceptual approach to direct age validation studies with tetracycline (OTC) marking and recapture has also been used (Fowler, 1990, 1995; Fowler and Short, 1998), but no corresponding protocols have been published for the statistical analysis

* Contribution 930 of the Australian Institute of Marine Science, Townsville, Queensland, Australia.

and reporting of the periodicity and timing of annulus formation outside OTC marks.

The most common analysis of periodicity has been that of informally comparing the observed number and position of annuli distal to the OTC mark with an expected number of annuli chosen from the whole number of years or seasons elapsed between marking and recapture. The most extensive studies, comprising large numbers of long-term recoveries of marked fish, reported the results as either percentage agreement (MacLellan and Fargo, 1995) or as a *t*-test (McFarlane and Beamish, 1995). Both approaches could not include fish recovered at liberty for less than one year and did not allow exploration of the sources of error evident in the comparisons. Low recovery rates of fish at liberty for more than 2–3 years are a feature of such tagging programs (Campana and Jones, 1998) and sample sizes are usually small. A median of only 21 fish was reported by Francis et al. (1992) from 14 earlier OTC mark-recapture studies. Such characteristics prevent the use of linear regressions, such as those used in validating daily microincrements (e.g. Foreman, 1996). The timing of opaque zone formation is most commonly inferred by informally noting the relative position of opaque zones, OTC marks, and the otolith margins on diagrams and photomicrographs (Choat and Axe, 1996; Ferreira and Russ, 1992, 1994; Fowler and Doherty, 1992; Murphy et al., 1998).

We propose that validation can be formalized into models to develop separate estimators of both the periodicity and timing of formation of opaque zones based on ratios of increment measurements around OTC marks. Our primary goals were to determine directly if the distinct opaque zones in sectioned otoliths of 11 species of *Lutjanus* from the central GBR were formed once per year and to estimate the dates of completion of these zones. Long-term recovery of useful sample sizes of GBR lutjanids marked with OTC is difficult because of ontogenetic changes in habitat of many species, the low levels of fishing effort, and tag shedding. Therefore we held captive fish to complement recoveries from a field-tagging program.

Our objectives were to develop a model for otolith growth past OTC marks that would allow tests of the null hypothesis of annual periodicity of opaque zone formation and that would provide mean estimates and measures of variation of the date of completion of these zones for comparison with environmental variables. These objectives required that we compare interpretations of otoliths and otolith growth between captive and wild fish, that we compare different reading axes and readers, and that we compare model estimates with the earlier validation approaches.

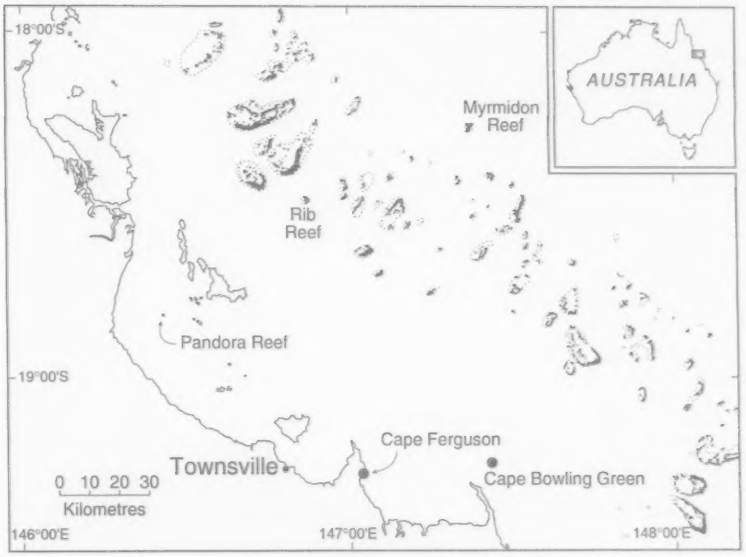

Figure 1
Central section of Great Barrier Reef Marine Park, showing sampling locations.

Materials and methods

Field techniques

Fish were collected with baited lines or traps (see Newman and Williams, 1995) in shallow water (<10 m) around the wharf at Cape Ferguson and Pandora Reef, and in deeper water (<37 m) in the GBR lagoon off Cape Bowling Green and the bases of Rib and Myrmidon Reefs (Fig. 1). There were two separate groups of fish used in the study. One group (n=170) of seven species were tagged and released in the shallow locations, where commercial and recreational fishing was prohibited, and repeated visits were made under research permits to recapture tagged fish. A second group (n=251) of 12 species were transported from the deeper locations and housed in two sea cages at Cape Ferguson wharf. The cages had a volume of 17.7 m^3 (cage dimensions: 2.95 m long × 2.45 m deep × 2.45 m wide) and were constructed from 25-mm galvanized steel tube covered in square, galvanized weldmesh (50 mm or 25 mm). Fish in each cage were fed with 2.5 kg of chopped pilchards (*Sardinops sagax*) each night.

Tetracycline was administered to both groups of fish in the form of Terramycin/MA injectable solution (oxytetracycline hydrochloride at 100 mg/mL) into the coelomic cavity at a dosage rate of 50 millilitres of Terramycin/MA per kilogram of estimated fish weight. In the field-tagging program, the fork length (FL mm) of all fish was measured and they were double-tagged below the spinous dorsal fin with numbered "T-bar" anchor tags or nylon-tipped dart tags. Tag legends advised retaining the whole fish upon recapture, but some fish recaptured after short times at liberty were injected and released again. Batches of captive fish were measured and injected once with OTC. Some *L. erythropterus* were injected

Table 1

Details of release, numbers of fish recovered (n), and ranges in age, length at recovery (FL mm) and time at liberty (months) of fish with visible OTC marks. Field = fish released in shallow locations where commercial and recreational fishing was prohibited; cage = fish held captive in sea cages.

Species	Release group	Place of capture	n	Age (yr)	FL	Liberty
L. argentimaculatus	field Sep 92–Mar 93	Cape Ferguson	3	6–7+	435–520	13.2–19.3
L. bohar	cage Mar 94	Myrmidon Reef	1	6+	386	11.6
L. carponotatus	cage Jul 93	Rib Reef	1	7+	326	19.9
L. carponotatus	cage Mar 94	Pandora Reef	1	4+	288	11.6
L. erythropterus	cage Aug 93	Cape Bowling Green	21[1]	2–5+	335–496	9.0–18.5
L. erythropterus	cage Nov 93	Cape Bowling Green	13[1]	3–4+	427–481	15.4
L. gibbus	cage Mar 94	Myrmidon Reef	1	4+	296	11.6
L. johnii	cage Feb 94	Cape Ferguson	10	4–7+	422–598	12.7
L. johnii	field Feb 93–Apr 94	Cape Ferguson	10[1]	3–7+	376–740	6.0–21.7
L. malabaricus	cage Mar 94	Pandora Reef	4	3+	402–466	11.2–11.6
L. monostigma	cage Mar 94	Pandora Reef	1	4+	306	11.6
L. rivulatus	cage Feb 94	Cape Ferguson	1	4+	312	12.7
L. rivulatus	cage Mar 94	Cape Ferguson	1	5+	401	12.0
L. sebae	field Mar 93	Pandora Reef	2	3+	280–296	12.3
L. sebae	cage Aug 93	Cape Bowling Green	3	2–4+	371–446	18.5
L. sebae	cage Mar 94	Pandora Reef	8	2–5+	331–444	11.6
L. vitta	cage Aug 93	Cape Bowling Green	2	4–6+	284–315	18.5

[1] Five of these fish were injected twice.

again about 3 months later. Most individuals were identified before release into the cages by tagging with anchor tags or by clipping of fin spines or rays. Some rarer species were not identified this way to reduce handling stress, and other individuals shed tags before recapture. The histories of these captive fish were recognizable from unique combinations of cage and species or, for some *L. erythropterus*, from twin OTC marks visible on otolith sections (Table 1).

Monthly measurements of surface seawater temperature and salinity recorded next to the cages and continuous records from the Australian Institute of Marine Science weather stations nearby on the GBR were used to derive information on environmental stressors and wind speed and direction. Caged fish were subject to extremes of wave energy, water temperature, turbidity, and salinity that are characteristic of the inshore habitat in the cyclone belt of the dry tropics. Water temperatures rose by 11°C from the austral winter to summer, and freshwater plumes from cyclonic rains caused fluctuations in salinity and turbidity. These influences extended out to Pandora Reef, but not to Rib and Myrmidon Reefs where there were clear waters and only a 6°C seasonal change in water temperature.

Laboratory techniques

For each fish after death, the FL was measured where possible and both sagittae (hereafter referred to as the otoliths) were removed, weighed, and measured. One otolith from each fish was randomly selected and embedded in soft epoxy resin. Three transverse sections were cut with a low-speed saw and diamond wafering blade in the vicinity of the primordium. The sections were 0.25–0.50 mm thick, depending on width of the otolith, and were lightly polished on wet ebony paper (1000 grade) and lapping film (9 and 3 µm). The sections were mounted on microscope slides under cover slips in a colorless epoxy casting resin and stored in darkness between short periods of examination.

The counts and measurements of otolith features made at the Australian Central Ageing Facility (CAF) were used in the analyses in our study to avoid possible bias from familiarity with the treatment of the individual fish. These data were compared with counts made by the senior author to assess precision and bias in otolith interpretation. Opaque zones were counted under magnifications from 7.5× to 25.2× with a stereo-dissecting microscope with transmitted white light, or under reflected light against a dark background (Newman et al., 1996). The position of the OTC mark was then measured by using epifluorescence illumination with a compound microscope at 20× to 40× magnification.

Video images were obtained, enhanced, and digitized with Bioscan's Optimas(TM) and Optimate(TM) software by using customized macros (Morison et al., 1998) along two planes (Fig. 2), from the primordium to the ventral apex of the otolith (ventral L1 axis), and from the primordium to the proximal edge parallel to the sulcus on the christa inferior (sulcal L3 axis). To define the position of the opaque

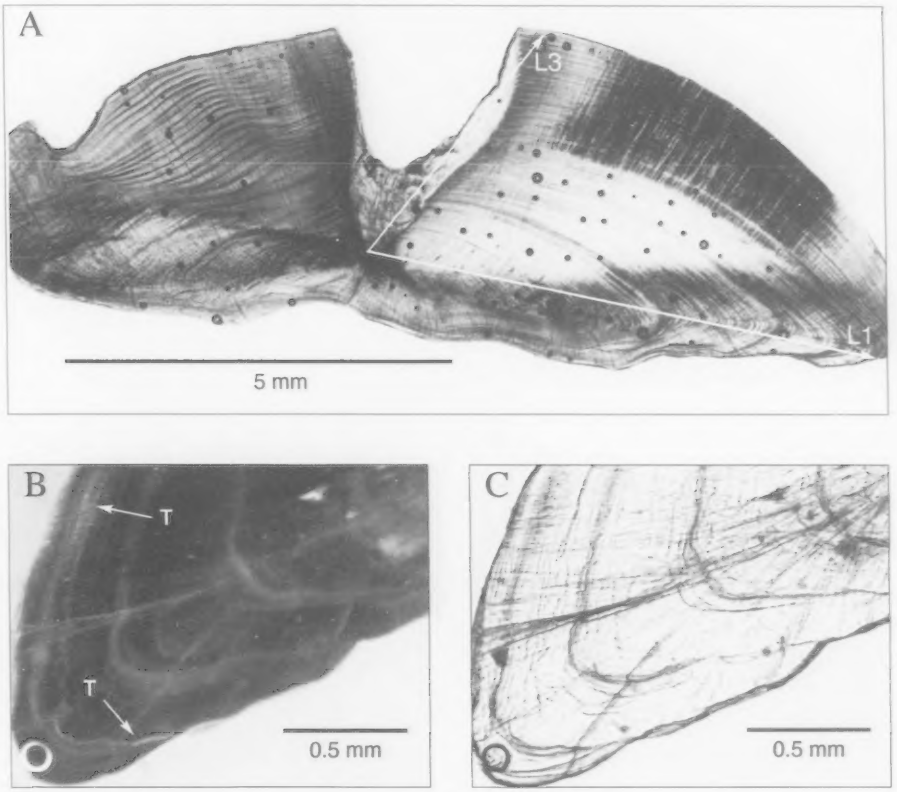

Figure 2

Photomicrographs of transverse sections of the sagittae of (**A**) *L. erythropterus* s1799 (21+yr) by transmitted white light showing the ventral L1 and sulcal L3 axes used for counting opaque zones; (**B**) the outer L1 axis of *L rivulatus* (s1996) showing the position of an OTC mark (T) by reflected ultraviolet light; (**C**) the same outer L1 axis of *L rivulatus* (s1996) showing narrow opaque zones by transmitted white light.

zones along these axes we recognized sharply defined "structural check rings" (sensu Gauldie, 1988) that could be followed from the ventral leading edge of the otolith around to the sulcus. These check rings were evident on the outermost edges of the opaque zones and were counted and measured after adjustment for aspect ratios. The position of the OTC mark was measured from the primordium to the outside edge of the mark and from there to the edge of the otolith along the L1 and L3 axes. The distance between twin OTC marks was measured from the distal edge of the first mark to the proximal edge of the second.

Data analyses

Analyses of the results for periodicity and timing of increment formation each comprised both an informal approach analogous to those used in earlier validation studies and a model of otolith growth. The informal validation of periodicity assumed a calendar date of 1 October for completion of opaque zones, based on previous Australian studies (Fowler, 1995), to report frequency distributions of the observed number of zones minus the expected number of zones formed outside OTC marks. The informal, "method of best fit" approach to estimate timing of completion of opaque zones was to assume that formation was completed annually on a particular day of the year. For each otolith section, and for every single day of the year, the number of opaque zones expected to be completed during time at liberty was calculated from the dates elapsed between marking and sacrifice. Only those dates for which the expected number of opaque zones formed past the OTC mark equalled the number actually observed were retained for analysis. The mean dates (MD) from frequency distributions of these possible calendar dates were selected as best informal estimates of time of completion of opaque zones.

We defined an "increment cycle" as the complete formation of adjacent translucent and opaque zones visible on an otolith section (Fig. 3). Two models were developed in a "direct method" to estimate the periodicity and timing

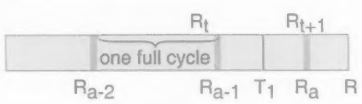

Figure 3

Positions of radii used to estimate initial and final fractions of otolith growth in Equations 1–3 shown across an otolith section of width R from a fish of age $a+$ with an OTC mark at T_1. In this example the radii of opaque zones at R_{a-1} and R_a are equivalent to radii of opaque zones immediately before (R_t) and after (R_{t+1}) the OTC mark. A full increment cycle is indicated.

of opaque zone completion based on the following observations. First, otoliths grow at a measurable rate that allows both counts of annuli and measurements of otolith weight to be converted to an estimate of age, with an associated error (Worthington et al., 1995). Second, this is a continuous process best represented by a continuous variable (*sensu* Zar 1996)—not a discrete variable such as the (whole) number of opaque zones. Third, the widths of outer increment cycles become similar for older fish (see figures in Fowler, 1995). We therefore proposed that ratios of otolith widths could be equated to ratios of corresponding time intervals in a model if two approximations were assumed:

1 the rate of otolith growth throughout the formation of an increment cycle was constant; and
2 the widths of increment cycles on outer margins of otoliths were the same.

We obtained continuous variables by expressing measurements of the marginal increment and distance between the OTC mark and subsequent opaque zone as "fractions" of widths of a completed increment cycle within an otolith. The sum of these fractions and the counts of whole cycles completed outside the OTC mark, divided by the known time at liberty, produced estimates of the rate, or periodicity, of opaque zone completion. Given this rate of completion, and known dates of OTC marking and sacrifice, the marginal increment could be used to estimate a date on which the outermost opaque zone was completed.

The number of increment cycles completed per year was the "cycle frequency" (V) and its inverse was the "cycle period" in units of years. The "closing date" (CD) of an increment cycle was defined as the date on which the formation of the opaque zone was completed. The time elapsed between OTC injection and the day on which the fish was sacrificed was referred to as the "time at liberty" (L) measured in decimal units of years.

The "initial fraction" (IF) and the "final fraction" (FF) of otolith growth were the two ratios of widths modelled to estimate time intervals with this direct method. Following the measurements shown in Figure 3, these two values were calculated as

$$IF = (R_{t+1} - T_1) / (R_{t+1} - R_t), \quad (1)$$

where R_t = the radius to the opaque zone formed immediately before OTC injection; and
R_{t+1} = the radius to the opaque zone formed immediately after OTC injection;

and as

$$FF = (R - R_a) / (R_a - R_{a-1}), \quad (2)$$

where a = age of the fish;
R_a = the radius to the final opaque zone; and
R_{a-1} = the radius to the penultimate opaque zone.

The terms R_a and R_{t+1} were equivalent, and R_{a-1} and R_t were equivalent, where there was only a single opaque zone measured past the OTC mark.

The cycle frequency (V) was estimated for all sections with at least one opaque zone past the OTC mark as

$$V = (IF + N + FF) / L, \quad (3)$$

where N = the number of full increment cycles visible outside the OTC mark; and
L = the time at liberty; the term N = an integer and $N = 0$ in Figure 3.

The "liberty fraction" (LF) was calculated as the sum of the full cycles and partial cycles that formed during time L, and was expressed in decimal fractions of cycles as

$$LF = IF + N + FF. \quad (4)$$

The cycle frequency was investigated using linear regression (SAS Institute Inc., 1989a) of the model

$$LF = \beta L. \quad (5)$$

This assumed an intercept value of zero (there was no time for otolith growth to occur when L=0) and the slope $\beta = 1$ when cycles had an annual periodicity. Confidence intervals for β were calculated from t distributions (Montgomery, 1991).

The second model, to estimate closing dates (CD) of the last cycle fully completed, assumed that for each otolith section the cycles that finished during time L had equal cycle periods. Closing dates were calculated as

$$CD = K - 365(FF/V), \quad (6)$$

where K = the date on which the fish was sacrificed, coded by SAS in units of days (SAS Institute Inc., 1989b).

The calendar day of the year on which the cycle ended (calendar closing date CCD) was derived from CD by

using SAS date functions as an integer between 1 and 365. The closing dates of anomalous extra cycles for comparison with environmental stressors were estimated by using

$$CD_{t+i} = TET_1IN + 365(i - 1 + IF) / V, \quad (7)$$

where TET_1IN = the date of the first OTC injection coded in SAS internal format in units of days; and

$t + i$ = the i_{th} opaque zone completed after the OTC mark.

The mean of the *CCD* estimates could be used as an estimate of the calendar date (*MCCD*) on which the opaque zones were most likely to have been completed. Days or months of the year are circular scales of measurement and best expressed in Polar coordinates as angles and radius unity. Means, angular deviations (analogous to the linear standard deviation), and confidence intervals were therefore calculated for circular von Mises distributions of *CCD* for each species by using the methods of Zar (1996). The Hotelling paired sample test was used to determine the significance of differences in angular *CCD* data between reading axes.

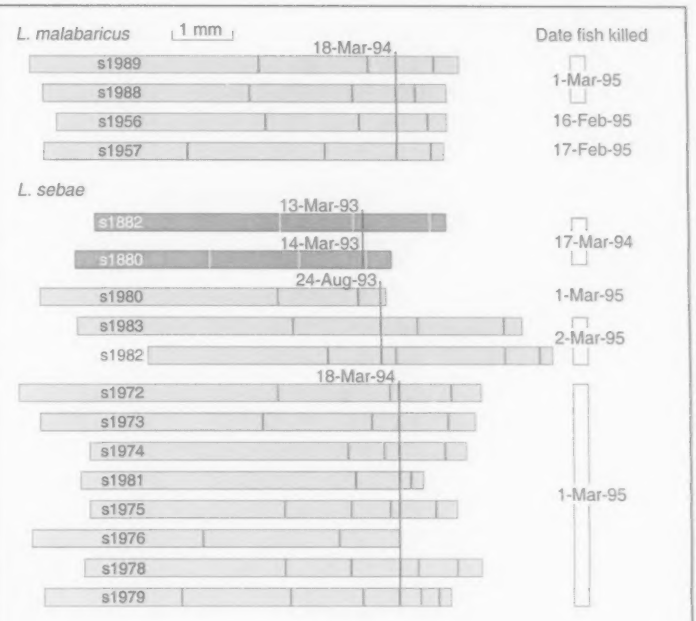

Figure 4

Measurements of the position of opaque zones and the OTC marks (unbroken or extended vertical bar) on the ventral L1 axis from the primordium to the otolith edge for *L. malabaricus* and *L. sebae*, identified by slide numbers. Bars representing field-tagged recaptures are shaded darker than those for captives. Dates of injection and sacrifice are shown. Otoliths marked on the same date are arranged with OTC marks aligned vertically, with a subjective horizontal scale for the spread of injection dates.

Results

Recoveries of marked fish

A total of 82 individuals from 11 species were recovered with OTC marks visible on sections of their otoliths (Table 1), equating to a recovery rate of less than 20% from the field-tagged and captive groups. Times at liberty were less than 22 months and the marked fish were all in younger year classes, less than 8+, in relation to the longevities estimated in some current studies (e.g. Williams et al.[1]). The median ages estimated for the most numerous species were only 3+ for *L. erythropterus*, *L. malabaricus*, and *L. sebae*, and 5+ for *L. johnii*. Apart from a few early recoveries of fatalities in the cages, all captive fish were sacrificed in the beginning of March 1995. Fish were recaptured in the field mainly over the summer period between September 1994 and April 1995.

Recoveries of field-tagged *L. johnii*, *L. argentimaculatus* and *L. sebae* were low (only 8–10% of the initial number released were recovered, and tag loss was evident (60% of field recoveries had lost one tag and three others, not included in our study, had an OTC mark but no tags). Of the captive group, only 60 fish from 10 species, including six dead fish, were recovered. None of the smallest species, *L. fulviflamma* and *L. kasmira*, and only 5% of the numerous *L. vitta* remained at the end of captivity. Only eight captive fish had retained anchor tags, and individual lengths at release for captive fish without tags were generally not distinguishable. One field-tagged *L. johnii* and four captive *L. erythropterus* had two OTC marks visible on their otoliths.

Otolith growth and interpretation near OTC marks

The strength of the working assumptions used in the models developed in our study depended on the sources of variability apparent in rate of growth of the otoliths outside the OTC mark amongst species, age classes, field-tagged and captive groups, and individuals in Figures 4–7. This region generally comprised only a small proportion of the otolith width, especially in the oldest fish, *L. johnii* (Fig. 6),

[1] Williams, D. McB., S. J. Newman, M. Cappo, and P. J. Doherty. 1995. Recent advances in the ageing of coral reef fishes. South Pacific Commission, Forum Fisheries Agency Workshop on the Management of South Pacific Inshore Fisheries. South Pacific Commission Integrated Coastal Fish Management Project Technical Document 12. Forum Fisheries Agency, P.O. Box 629, Honiara, Guadalcanal, Solomon Islands.

L. argentimaculatus, *L. gibbus*, and *L. bohar* (Fig. 7). There were no opaque zones visible past the OTC mark on both axes of one *L. gibbus*, and *L. monostigma* had no OTC mark visible on the ventral axis. An opaque zone was coincident with the OTC mark on the ventral axis, but not the sulcal axis, of *L. bohar*.

The ease of interpretation of opaque zones in the otolith preparations was tested by comparing the pairs of counts made by the two otolith readers. Nonparametric, Wilcoxon signed rank tests showed significant differences between readers in estimates of fish age along both reading axes (ventral axis n=82 S=285.0 $P>|S|=0.0001$; sulcal axis n=82 S=285.5 $P>|S|=0.0001$) but not in interpretation of the number of opaque zones past the OTC mark (ventral axis n=61 S=21.0 $P>|S|=0.5034$; sulcal axis n=62 S=15.0 $P>|S|=0.6476$). An age bias plot (Campana et al., 1995) showed that the mean and standard deviation of the CAF estimates were 2.9 ±0.5 for 2+ fish, 3.5 ±0.6 for 3+ fish and 4.2 ±0.4 for 4+ fish aged by the senior author. We inferred that there was similar interpretation amongst readers of the area of interest outside the OTC mark and that the definition of the first opaque zone was a source of bias for youngest fish.

Sections from *Lutjanus* otoliths have been read along the sulcal L3 axis in a protocol developed by Newman et al. (1996), but opaque zones may be closest together in this area and measurements of growth past OTC marks might best be made elsewhere. To justify our choice of measurement axes for subsequent analyses we compared the mean growth and variance from the two axes in Table 2. Growth rates along the ventral axis were consistently twice as high as those along the sulcal axis; therefore we judged that errors in measurement of zone radii would be least, and interpretation best, along the ventral axis. The coefficients of variation were similar for both axes, with the exception of those for *L. sebae*.

Lutjanus sebae showed the highest mean growth rates and variability along both reading axes (Table 2) which led us to investigate artifacts of captivity. The growth rates of otoliths of *L. johnii* and *L. sebae* in the field were much lower than those of captives (Figs. 4 and 6). Captive *L. johnii* had mean otolith growth rates of 0.78 mm/yr along the ventral axis—twice as high as those tagged in the field (0.36 mm/yr). These differences were highly significant (n=20 ndf=1 ddf=18 F=22.49 $P>F$=0.0002), but no significant difference in otolith weight was detected when fish length was used as a covariate (n=20, ndf=1 ddf=18 F=0.19 $P>F$=0.6704). This latter finding indicated that faster otolith growth rates were correlated with the faster somatic growth of captive fish.

Further evidence of this correlation and the effects of captivity on somatic growth were an increase in mean FL of captives by about 7 mm/month for *L. johnii* and about 12 mm/month for *L. sebae*, compared with field growth rates of 0.2–6.2 mm/month for *L. johnii* and only 2.6–3.9 mm/month for *L. sebae*. One field-tagged *L. johnii* (s6667, Fig. 6) showed both an apparent decline in FL and no otolith growth outside the OTC mark on the ventral axis.

Plots of increment cycle width (W) along the ventral axis against cycle number (a) were made to examine

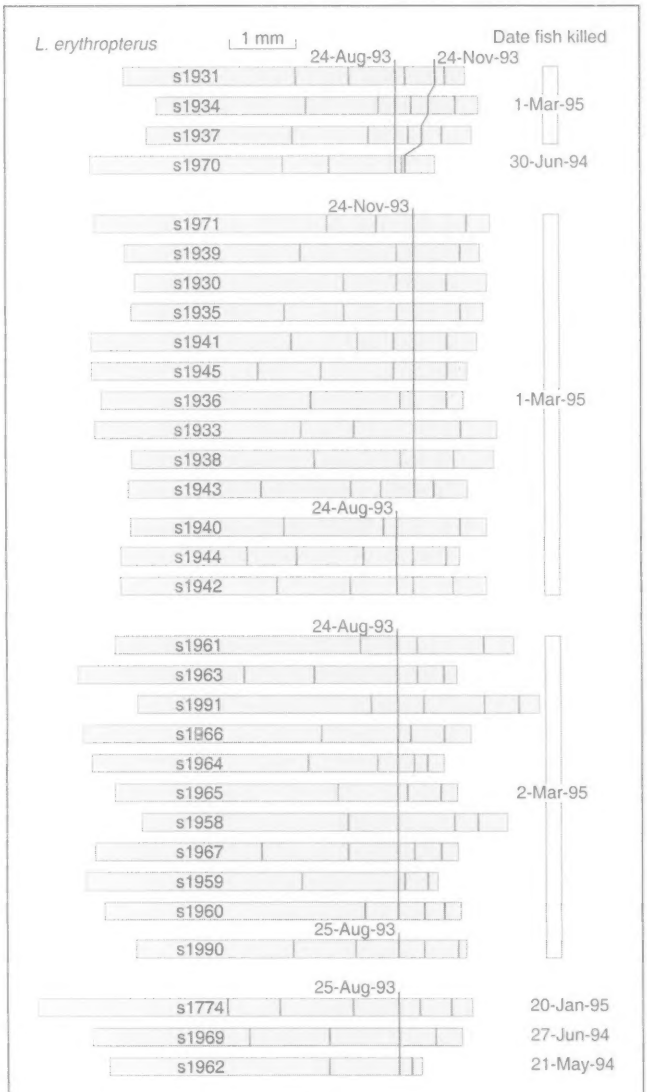

Figure 5

Measurements of the position of opaque zones and the OTC marks on the ventral L1 axis for *L. erythropterus*. Date of the second injection with OTC is shown to the right of the continuous line joining OTC marks. All conventions as in Figure 4.

Table 2

Mean growth rates of otoliths (mm/yr) outside OTC marks and measures of dispersion from sample size (n) of the most numerous species along the ventral L1 and sulcal L3 axes. Captive = fish held in sea cages; field = fish released in shallow locations where commercial and recreational fishing was prohibited.

Group	Age range (yr)	Axis	n	Growth rate	SD	CV (%)
L. johnii—captive	4–7+	L1	10	0.78	0.21	27
		L3	10	0.31	0.08	25
L. johnii—field	3–7+	L1	10	0.36	0.18	51
		L3	10	0.21	0.09	45
L. sebae—captive	2–5+	L1	11	1.00	0.61	61
		L3	11	0.43	0.15	36
L. sebae—field	3+	L1	2	0.91	0.62	69
		L3	2	0.52	0.17	33
L. erythropterus—captive	2–5+	L1	27	0.77	0.22	28
		L3	27	0.33	0.08	24
L. malabaricus—captive	3+	L1	2	0.94	0.15	16
		L3	2	0.36	0.07	20

our second working approximation that outer cycles had equal widths on the marked otoliths. The plots were fitted best by exponential curves: $W = 0.38 + 4.92e^{-0.81a}$ for species pooled; $W = 0.70 + 11.44e^{-1.68a}$ for *L. erythropterus*; $W = 0.30 + 3.21e^{-0.5a}$ for *L. johnii*; and $W = 0.75 + 9.12e^{-1.26a}$ for *L. sebae*. On average, there was a small decrease in cycle width from the third to the fourth cycle and then successive cycles were similar; however captivity or tagging may have caused anomalous growth of some otoliths. Two *L. sebae* showed no (s1976), or insignificant (s1980), growth along the ventral axis (Fig. 4) but their otoliths did continue to thicken. The largest *L. sebae* and *L. erythropterus* showed substantial growth along the ventral axis in relation to other individuals (Figs. 4 and 5), contributing to the high coefficients of variation shown in Table 2. For some captives this phenomenon led to a progressive or irregular increase in cycle width, most notable for *L. erythropterus* marked in August 1993 (eg. s1937, s1943, s1954, and s1958 in Fig. 5), that violated the second approximation of our model.

Periodicity of zone formation

Using the informal validation approach, and assuming a springtime completion date of 1 October, we estimated the frequency distributions shown in Table 3 that indicated an annual periodicity of deposition of opaque zones in the majority of otolith sections. However, there was a small minority of fish with more or less zones than expected, and information about the opaque zones counted for these individuals was available by applying the "direct method" developed in our study by rewriting Equation 3 as

$$V = (IF + FF)/L + N/L. \quad (8)$$

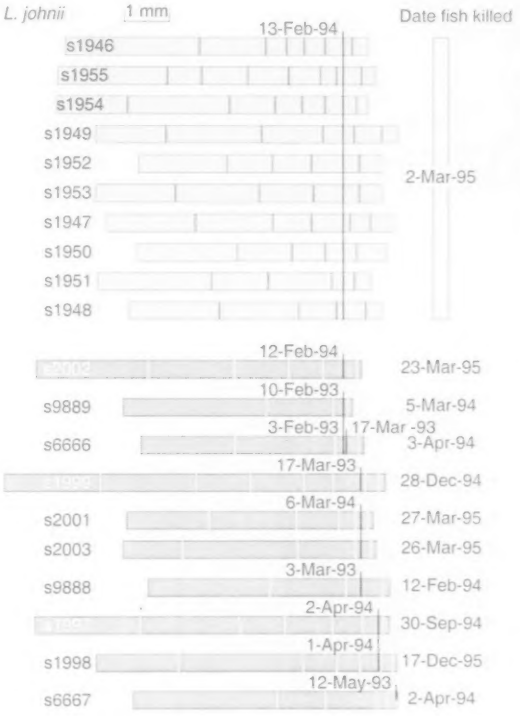

Figure 6

Measurements of the position of opaque zones and the OTC marks on the ventral L1 axis for *L. johnii*. All conventions are the same as those in Figures 4 and 5.

L. argentimaculatus, L. gibbus, and *L. bohar* (Fig. 7). There were no opaque zones visible past the OTC mark on both axes of one *L. gibbus*, and *L. monostigma* had no OTC mark visible on the ventral axis. An opaque zone was coincident with the OTC mark on the ventral axis, but not the sulcal axis, of *L. bohar*.

The ease of interpretation of opaque zones in the otolith preparations was tested by comparing the pairs of counts made by the two otolith readers. Nonparametric, Wilcoxon signed rank tests showed significant differences between readers in estimates of fish age along both reading axes (ventral axis n=82 S=285.0 $P>|S|=0.0001$; sulcal axis n=82 S=285.5 $P>|S|=0.0001$) but not in interpretation of the number of opaque zones past the OTC mark (ventral axis n=61 S=21.0 $P>|S|=0.5034$; sulcal axis n=62 S=15.0 $P>|S|=0.6476$). An age bias plot (Campana et al., 1995) showed that the mean and standard deviation of the CAF estimates were 2.9 ±0.5 for 2+ fish, 3.5 ±0.6 for 3+ fish and 4.2 ±0.4 for 4+ fish aged by the senior author. We inferred that there was similar interpretation amongst readers of the area of interest outside the OTC mark and that the definition of the first opaque zone was a source of bias for youngest fish.

Sections from *Lutjanus* otoliths have been read along the sulcal L3 axis in a protocol developed by Newman et al. (1996), but opaque zones may be closest together in this area and measurements of growth past OTC marks might best be made elsewhere. To justify our choice of measurement axes for subsequent analyses we compared the mean growth and variance from the two axes in Table 2. Growth rates along the ventral axis were consistently twice as high as those along the sulcal axis; therefore we judged that errors in measurement of zone radii would be least, and interpretation best, along the ventral axis. The coefficients of variation were similar for both axes, with the exception of those for *L. sebae*.

Lutjanus sebae showed the highest mean growth rates and variability along both reading axes (Table 2) which led us to investigate artifacts of captivity. The growth rates of otoliths of *L. johnii* and *L. sebae* in the field were much lower than those of captives (Figs. 4 and 6). Captive *L. johnii* had mean otolith growth rates of 0.78 mm/yr along the ventral axis—twice as high as those tagged in the field (0.36 mm/yr). These differences were highly significant (n=20 ndf=1 ddf=18 F=22.49 $P>F$=0.0002), but no significant difference in otolith weight was detected when fish length was used as a covariate (n=20, ndf=1 ddf=18 F=0.19 $P>F$=0.6704). This latter finding indicated that faster otolith growth rates were correlated with the faster somatic growth of captive fish.

Further evidence of this correlation and the effects of captivity on somatic growth were an increase in mean FL of captives by about 7 mm/month for *L. johnii* and about 12 mm/month for *L. sebae*, compared with field growth rates of 0.2–6.2 mm/month for *L. johnii* and only 2.6–3.9 mm/month for *L. sebae*. One field-tagged *L. johnii* (s6667, Fig. 6) showed both an apparent decline in FL and no otolith growth outside the OTC mark on the ventral axis.

Plots of increment cycle width (W) along the ventral axis against cycle number (a) were made to examine

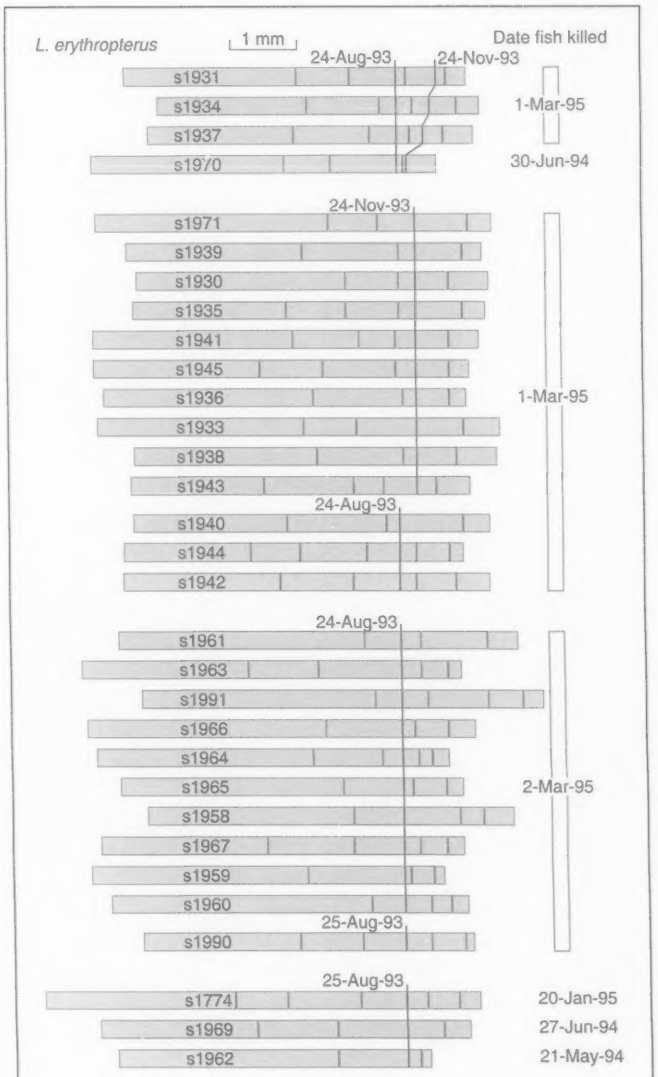

Figure 5

Measurements of the position of opaque zones and the OTC marks on the ventral L1 axis for *L. erythropterus*. Date of the second injection with OTC is shown to the right of the continuous line joining OTC marks. All conventions as in Figure 4.

Table 2

Mean growth rates of otoliths (mm/yr) outside OTC marks and measures of dispersion from sample size (n) of the most numerous species along the ventral L1 and sulcal L3 axes. Captive = fish held in sea cages; field = fish released in shallow locations where commercial and recreational fishing was prohibited.

Group	Age range (yr)	Axis	n	Growth rate	SD	CV (%)
L. johnii—captive	4–7+	L1	10	0.78	0.21	27
		L3	10	0.31	0.08	25
L. johnii—field	3–7+	L1	10	0.36	0.18	51
		L3	10	0.21	0.09	45
L. sebae—captive	2–5+	L1	11	1.00	0.61	61
		L3	11	0.43	0.15	36
L. sebae—field	3+	L1	2	0.91	0.62	69
		L3	2	0.52	0.17	33
L. erythropterus—captive	2–5+	L1	27	0.77	0.22	28
		L3	27	0.33	0.08	24
L. malabaricus—captive	3+	L1	2	0.94	0.15	16
		L3	2	0.36	0.07	20

our second working approximation that outer cycles had equal widths on the marked otoliths. The plots were fitted best by exponential curves: $W = 0.38 + 4.92e^{-0.81a}$ for species pooled; $W = 0.70 + 11.44e^{-1.68a}$ for *L. erythropterus*; $W=0.30 + 3.21e^{-0.5a}$ for *L. johnii*; and $W = 0.75 + 9.12e^{-1.26a}$ for *L. sebae*. On average, there was a small decrease in cycle width from the third to the fourth cycle and then successive cycles were similar; however captivity or tagging may have caused anomalous growth of some otoliths. Two *L. sebae* showed no (s1976), or insignificant (s1980), growth along the ventral axis (Fig. 4) but their otoliths did continue to thicken. The largest *L. sebae* and *L. erythropterus* showed substantial growth along the ventral axis in relation to other individuals (Figs. 4 and 5), contributing to the high coefficients of variation shown in Table 2. For some captives this phenomenon led to a progressive or irregular increase in cycle width, most notable for *L. erythropterus* marked in August 1993 (eg. s1937, s1943, s1954, and s1958 in Fig. 5), that violated the second approximation of our model.

Periodicity of zone formation

Using the informal validation approach, and assuming a springtime completion date of 1 October, we estimated the frequency distributions shown in Table 3 that indicated an annual periodicity of deposition of opaque zones in the majority of otolith sections. However, there was a small minority of fish with more or less zones than expected, and information about the opaque zones counted for these individuals was available by applying the "direct method" developed in our study by rewriting Equation 3 as

$$V = (IF + FF)/L + N/L. \quad (8)$$

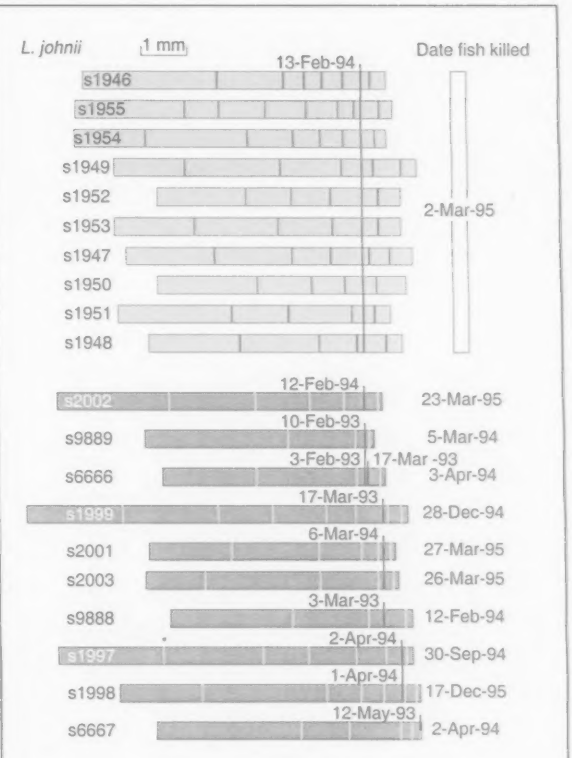

Figure 6

Measurements of the position of opaque zones and the OTC marks on the ventral L1 axis for *L. johnii*. All conventions are the same as those in Figures 4 and 5.

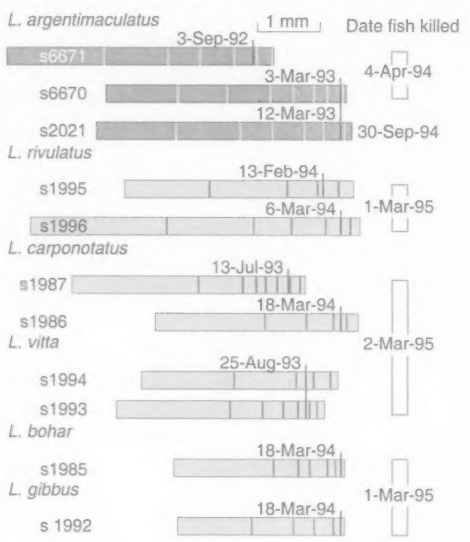

Figure 7

Measurements of the position of opaque zones and the OTC marks on the ventral L1 axis for six species represented by three individuals or less in the study. All conventions are the same as those in Figure 4.

Table 3

Frequency distribution of the difference between observed (obs) and expected (exp) number of opaque zones past the first OTC mark where a nominal date of 1 October was used for completion of zone formation.

			Difference between obs and exp no. of opaque zones			
Species	*n*	Axis	−2	−1	0	1
L. argentimaculatus	3	L1	0	0	3	0
		L3	0	0	3	0
L. bohar	1	L1	0	1	0	0
		L3	0	0	1	0
L. carponotatus	2	L1	0	0	2	0
		L3	0	0	2	0
L. erythropterus	31	L1	0	1	29	1
		L3	0	2	27	2
L. gibbus	1	L1	0	1	0	0
		L3	0	1	0	0
L. johnii	20	L1	0	0	16	4
		L3	0	0	16	4
L. malabaricus	4	L1	0	0	4	0
		L3	0	0	4	0
L. monostigma	1	L1	—	—	—	—
		L3	0	0	1	0
L. rivulatus	2	L1	0	0	2	0
		L3	0	0	2	0
L. sebae	13	L1	1	1	8	3
		L3	1	0	8	4
L. vitta	2	L1	0	0	2	0
		L3	0	0	2	0

This procedure allowed us to determine objectively outliers in the values of N estimated for fish in groups with similar times at liberty. Fish with the same values of liberty, L, and number of complete increment cycles, N, lay on a line of slope $1/L$ in the plot of cycle frequency (V) against the sum of the initial and final fractions ($IF+FF$) in Figure 8. Fish with the same value of L and an estimate of N larger or smaller by one complete increment cycle were offset from this line by $1/L$ cycles per year.

In addition, this procedure allowed us to exclude 18 fish from the "direct method" of estimating periodicity along either reading axis, under three criteria. First, fish with anomalies in opaque zone formation, such as "false annuli" (e.g. *L. erythropterus* s1991, *L. johnii* s1947, *L. sebae* s1982), or with other errors in otolith interpretation were included only in analyses exploring the possible relationships between formation of false annuli and environmental conditions. Second, fish with $FF>1.0$ (e.g. *L. erythropterus* s1958, s1964 in Fig. 5) were excluded because they violated our second working approximation of the equal spacing of outer zones. Third, other fish were excluded because the OTC marks were absent along one axis (*L. monostigma*) or were visible outside the outermost opaque zones (*L. sebae* s1980, *L. gibbus*).

When these outliers were removed, the "direct method" produced a normal distribution of cycle frequency along the ventral axis about a mean of 0.96 ±0.32 cycles/yr (n=66 Shapiro-Wilk w=0.98 $P<w$=0.71) for all species pooled. Data from the sulcal axis produced a mean of 1.02 cycles/yr (n=64 w=0.95 $P<w$=0.04), but this was not normally distributed.

The estimated cycle frequencies were grouped loosely about one cycle/yr for *L. erythropterus*, *L johnii*, *L. rivulatus*, and *L. sebae*, with *L. malabaricus*, *L. argentimaculatus*, and *L. bohar* having a lower estimate and *L. carponotatus* and *L. vitta* having a higher frequency (Fig. 9). All means lay within the range 0.78–1.21 cycles/yr; apparently a lower cycle frequency was estimated when radii measured along the ventral axis (Table 4) were used. Analysis of variance showed no significant differences in cycle frequencies among these species and between reading axes, but a nonparametric Wilcoxon signed-rank test for paired data found significant differences between axes (n=61 S=−363.5 prob > |S| =0.008).

Simple linear regression of the number of whole and partial cycles formed after OTC marking (liberty fraction LF) on time at liberty showed significant linear relationships along both the ventral axis (n=66 ndf=1 ddf=64 F=739.37 $P>F$=0.0001) (Fig. 10) and the sulcal axis (n=64 ndf=1 ddf=62 F=913.36 $P>F$=0.0001). The slopes were β=1.01

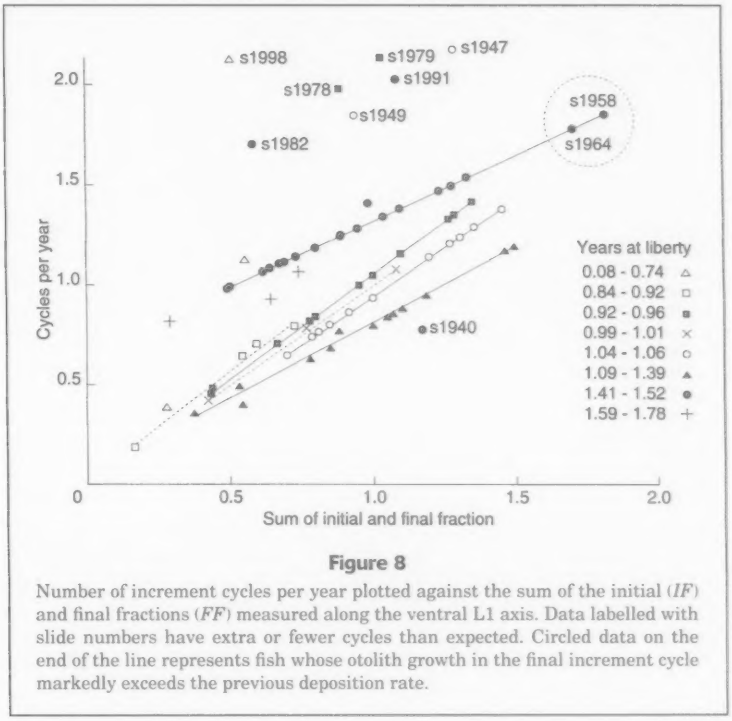

Figure 8

Number of increment cycles per year plotted against the sum of the initial (*IF*) and final fractions (*FF*) measured along the ventral L1 axis. Data labelled with slide numbers have extra or fewer cycles than expected. Circled data on the end of the line represents fish whose otolith growth in the final increment cycle markedly exceeds the previous deposition rate.

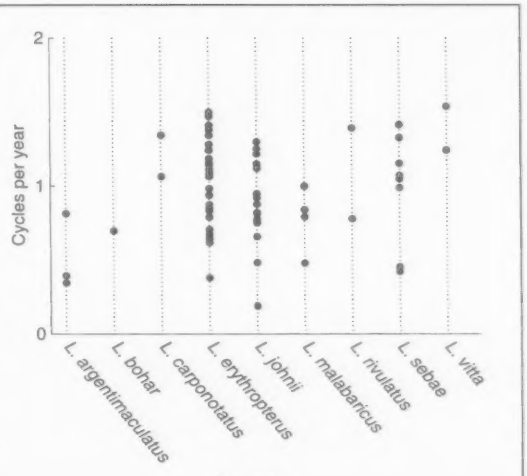

Figure 9

Number of increment cycles per year along the ventral L1 axis estimated for 61 fish of nine study species with the direct method.

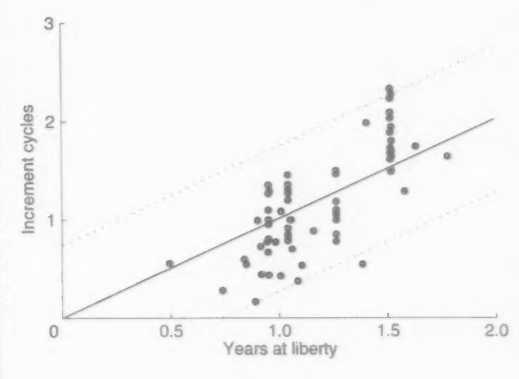

Figure 10

Linear regression and 95% confidence intervals ($LF=\beta L$) for the number of whole and partial increment cycles formed during time at liberty *LF* (liberty fraction, ventral L1 axis) against time at liberty *L* for 66 fish of 9 species from Figure 9.

along the ventral axis ($t_{0.025,\,64}$=1.99; confidence interval $0.94<\beta<1.09$) and β=1.09 along the sulcal axis ($t_{0.025,\,62}$=1.99; confidence interval $1.02<\beta<1.16$). The regression residuals were normally distributed only along the ventral axis (n=66 w=0.981428 $P<w$=0.7105), and were influenced by a group of positive residuals around 1.5 years at liberty, corresponding to $V > 1$ cycles/yr. These were mainly *L. erythropterus*, for which Equation 6 consistently estimated

that the 1993 zones were completed later in the calendar year than those formed in 1994. The hypothesis that the frequency of zone completion, as the slope of the regression, was equal to one cycle/yr was therefore retained for the ventral axis for all species pooled.

Timing of zone formation

Four *L. erythropterus* had otoliths with two OTC marks that bracketed a fully formed opaque zone (Fig. 5), indicating that these annuli were formed in the austral spring in September–November 1993. A Hotelling paired sample test for equality of means in circular distributions showed that there were significant differences in estimates of calendar closing dates (*MCCD*) from the direct method between reading axes (n=60 ndf=2 ddf=58 F=3.41 $P>F$=0.04). There was also variability amongst species, with the most numerous species completing an annulus along the ventral axis in mid-August by *L. johnii*, in early September by *L. erythropterus*, and in early November by *L. sebae*.

Table 4

Mean increment cycle frequency (increment cycles/yr) and standard deviation along the ventral L1 and sulcal L3 axes for the species represented by four or more marked individuals.

Species	L1 axis	L3 axis
L. erythropterus	1.03 ±0.29	1.15 ±0.25
L. johnii	0.88 ±0.29	0.85 ±0.22
L. malabaricus	0.78 ±0.22	0.88 ±0.15
L. sebae	0.99 ±0.37	1.21 ±0.33

By pooling data from the ventral and sulcal axes by taking the mean of each pair we were able to overcome problems associated with anomalous otolith growth, resolve differences in the estimates, and not significantly change the degrees of freedom in any subsequent tests for significance of timing of zone formation. This procedure tightened the estimates of closing date for *L. sebae* and generally gave a best estimate of spring–early summer for formation of the annulus in the most numerous species (Table 5). Results from the "method of best fit" were inside the bounds of the confidence limits of the direct method for *L. johnii* and *L. sebae* and were similar for *L. malabaricus*, *L. monostigma*, and *L. rivulatus* but were significantly later in the year for *L. erythropterus* (Table 5). The discrepancies between methods for *L. argentimaculatus*, *L. bohar*, *L. carponotatus*, and *L. vitta* reflected both the small number of fish and difficulties in measurement and interpretation of their smaller otoliths. The estimates for the less numerous species must be considered to be tentative.

There was a marked coincidence between the August 2nd minimum in water temperature and a peak in August for frequency of 1994 closing dates (Fig. 11). Extra opaque zones counted or deemed to be false annuli may have formed after storms and salinity fluctuations at Cape Ferguson. To investigate this possibility, we estimated closing dates using Equation 7 from the radii of anomalous "extra" opaque zones visible on both reading axes in otoliths of *L. johnii* (s1947, s1949, s1998, Fig. 6), *L. sebae* (s1979, s1982, Fig. 4), and *L. erythropterus* (s1991, Fig. 5) identified as outliers on Figure 8. All but one of these fish (s1998) were in the group of captives. Compared with salinity and sea state during the months of captivity, there appeared to be a relationship between a sharp fall and rise in salinity of at least 1.4 ppt for March–May 1994 and the completion of these "extra" zones in the following month, although periods of rough and very rough sea conditions also occurred most commonly at this time. Salinity dropped

Table 5

Mean calendar closing dates (*MCCD*), angular deviation (s) in days, and lower (*LCL*) and upper (*UCL*) 95% confidence limits pooled and averaged for the ventral and sulcal axes, from the "direct method," compared with the mean date (*MD*) estimated from the "method of best fit" for n fish of each study species.

Species	n	(*LCL* < *MCCD* <*UCL*)	s	*MD*
L. argentimaculatus	3	26 Oct	54	26 Dec
L. bohar	1	14 May	—	8 Sep
L. carponotatus	2	14 Aug	13	29 Oct
L. erythropterus	27	14 Aug< 2 Sep<20 Sep	42	31 Oct
L. gibbus	1	—	—	9 Mar
L. johnii	17	3 Aug< 5 Sep <8 Oct	53	16 Aug
L. malabaricus	4	30 Sep	26	3 Sep
L. monostigma	1	8 Sep	—	8 Sep
L. rivulatus	2	27 Aug	5	23 Aug
L. sebae	9	9 Sep < 19 Oct < 29 Nov	47	23 Oct
L. vitta	2	17-Sep	71	27 Nov

from 36.0 ppt on 3 February to 34.8 ppt on 1 April and rose again to 36.2 ppt on 1 May. The closing dates for these false annuli were distributed in March (n=1), April (n=2), and May (n=3).

Discussion

The use of increment widths on otolith sections to examine timing of opaque zone formation underpins marginal increment analysis (Fowler and Short, 1998) and informal inferences made from the relative position of OTC marks (Choat and Axe, 1996; Ferreira and Russ, 1992, 1994; Francis et al., 1992). The direct method developed in our study has essentially formalized and extended this use to allow for robust parametric tests and has three advantages over previous approaches to direct validation. First, the use of fractions of otolith growth allows linear regression of the number of whole or partially completed (or whole *and* partially completed) increment cycles on time at liberty, and both measures are expressed correctly as continuous variables. This method allows periodicity to be estimated directly from all recaptures with at least one opaque zone outside the OTC mark, including those fish at liberty for less than one year. Second, there is no need for subjective choice of a fixed date of completion of opaque zones to allow for comparisons between expected and observed counts of opaque zones. Third, the calendar date of completion of outer opaque zones can be estimated independently of the dates of marking or sacrifice for all recaptures with at least one opaque zone outside the OTC mark. Previous inferences about timing have been limited to the opaque zones that are immediately adjacent to OTC marks. Such contrasts are not always readily available, especially when tagging and recaptures cannot be spread throughout the year because of seasonal differences in fishing effort or vulnerability of fish to capture.

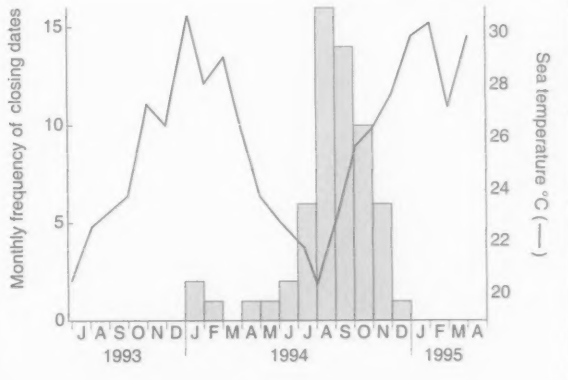

Figure 11

Monthly sea surface temperature (°C) in the cages during captivity of marked fish, plotted with the monthly frequency of closing dates (*CD*) in 1994 estimated with the "direct method" with Equation 6 for nine species from Figure 9. The estimates have been pooled and averaged for the ventral and sulcal axes for each of 61 fish.

Periodicity and timing of opaque zones

We tested, and retained, the hypothesis that there was an annual periodicity of formation of opaque zones for the pooled study species, around a mean of 0.96 ±0.32 increment cycles/yr. Anomalous sections and "false" annuli were identified objectively and could be related to periods of environmental stress in six cases. The model also identified interannual difference in timing of zone completion by a group of *L. erythropterus*, which clearly inflated overall estimates of periodicity. Despite this difference, estimates of periodicity in the range of 0.78–1.21 cycles/yr for both reading axes, accompanied by confidence intervals, were robust for *L. erythropterus*, *L. johnii*, *L. malabaricus*, and *L. sebae*. This result supported the use of thin sections of otoliths for accurate age estimates of lutjanids in the central GBR and supported estimates of longevity proposed for some of our study species (eg Sheaves, 1995; Newman et al., in press; Loubens[2]). The results for the other species showed similar trends, and no interspecific differences in periodicity were detected, but the numbers of marked fish were low for *L. argentimaculatus*, *L. bohar*, *L. carponotatus*, *L. gibbus*, *L. monostigma*, *L. rivulatus*, and *L. vitta*. Twofold differences in otolith growth rate between captive and tagged *L. johnii* and *L. sebae* did not affect the periodicity of annulus formation, further demonstrating the capacity of these otoliths to accurately reflect age under varying conditions of somatic growth.

Substantial variability in the timing of opaque zone formation has been noted by Beckman and Wilson (1995), at the individual, population, and species levels. Our best estimates of closing dates indicated that, on average, opaque zones recognized as annuli in lutjanid otoliths were completed within months of the austral spring and early summer, around early September for *L. erythropterus* and *L. johnii*, late September for *L. malabaricus*, and late October for *L. sebae*. These differences were significant and indicated a timing of formation that is somewhat earlier for *L. erythropterus* and *L. johnii* than the spring–summer peak of opaque zone formation in tropical fishes identified by Fowler (1995) and Beckman and Wilson (1995). Other studies have concluded that lutjanids and serranids on the GBR form opaque zones in winter–spring (Ferreira and Russ, 1992, 1994; Newman et al., 1996).

Lack of definition of the term "formation" makes it difficult to compare our results with those of previous studies. Our use of single OTC marks and measurements of only the outside edges of opaque zones allowed inferences about the timing of completion, not commencement, of annuli. We could

[2] Loubens, G. 1980. Biologie de quelques de poissons du lagon Neo-Caledonian. III. Croissance. Cahiers de l'Indo-pacifique 2(2): 101–153. Foundation Singer-Polignac, 43, avenue Georges-Mandel, 75016 Paris. ISSN 0180-9954.

estimate a formation time of less than 3 months for opaque zones on otoliths from *L. erythropterus* marked twice in 1993. Those individuals clearly showed springtime formation of the opaque zones in that year, but we also concluded that completion occurred earlier in the following year, about 1–2 months after the minimum water temperature in August, indicating that commencement and formation could have occurred during winter 1994. This difference was not explained by interannual variation in the occurrence of minimum water temperatures and may have been due to changes in metabolism and physiology induced by capture, transport, handling, and captivity. These are plausible artifacts, given that opaque zone formation is under control of a poorly understood combination of environmental and endogenous factors that influence endolymph fluid chemistry (Beckman and Wilson, 1995; Romanek and Gauldie, 1996). The location of the cages may have contributed to mortality or lack of growth of the otoliths of *L. bohar*, *L. fulviflamma*, *L. gibbus*, *L. kasmira*, and *L. vitta* transported inshore from their reef habitats, whereas the other inshore species were expected to be more tolerant of the cage environment.

The models produced similar, but more informative, conclusions to the application of the informal approaches. Analyses following MacLellan and Fargo (1995) indicated an annual periodicity of opaque zone formation for 10 study species with few exceptions. The "method of best fit" estimated mean calendar completion dates that were inside the confidence intervals of the direct method, with the exception of *L. erythropterus*, for which the method was sensitive to the interannual variability in timing of annulus completion.

Sources of bias

Assumptions concerning otolith growth rate in the direct method were the best available approximations, given both our observations and the current understanding of otolith growth, and we were confident that their main effects were accounted for by excluding outliers and by measures of variation reported about the mean results.

Earliest models of otolith growth presumed that no net accretion occurred when fish stopped growing, and these "no-growth" horizons provided the foundation for the recognition of annual winter marks in otoliths (Romanek and Gauldie, 1996). However, otolith growth is not directly coupled to somatic growth (e.g. Mosegaard et al., 1988) and has been observed to show complexities correlated by various authors with factors such as food intake, life-history stage, temperature, and metabolic rate (Romanek and Gauldie, 1996; Schirripa and Goodyear, 1997). Most recently, Romanek and Gauldie (1996) proposed that otolith growth along the main growth axis is continuous, with the rate of deposition (that is, the microincrement width) being modulated by temperature and pH of the endolymph. This model was based on the known physiology of the endolymph and the physical chemistry of aragonite, and was tested by Payan et al. (1997) and Gauldie and Romanek (1998).

We therefore assumed a constant rate of otolith growth, while recognizing that a number of factors might be expected to vary regularly during continuous growth of the otolith, including the widths of daily micro-increments, trace element concentrations, matrix proteins, and aragonite crystal structure (Gauldie and Nelson, 1990; Gauldie et al., 1990). It remains unknown which combination of such variable characteristics integrate into the optical macrostructure of otolith sections viewed as opaque and translucent zones (Fowler, 1995).

If alternating periods of slow and fast otolith growth occurred regularly throughout each increment cycle, in violation of our working approximation, errors would tend to cancel one another during calculation of periodicity. In Equations 1–3, the initial fraction of otolith growth (*IF*) was estimated by using a numerator from the last part of a cycle, but the final fraction (*FF*) was estimated from the first part of a cycle by using the marginal increment as a numerator. If *IF* was underestimated because the otolith grew slowly at the end of a cycle, it would be countered by an overestimation of *FF* caused by faster otolith growth at the start of a cycle. Our method was most vulnerable to interannual differences in otolith growth rate, which were evident for some fish as anomalous otolith growth, possibly as a physiological response to captivity or tagging.

The widths of outer increment cycles were assumed to be the same in our second working approximation because an exponential decrease in growth along otolith reading axes and equidistant outer zones are a feature of several families from the central GBR, including lutjanids (Fowler and Doherty, 1992; Choat and Axe, 1996; Newman et al., 1996). The exponential curves presented in our study supported the approximation for the 50 marked fish that had completed their fourth increment cycle but did not support so well for the younger fish sacrificed during their fourth (n=28) and third cycles (n=4). Finally, the model assumption that the increment cycles had the same time period of formation in an individual otolith was supported for our estimation of closing dates by the determination of the annual periodicity of opaque zone formation.

There was bias in interpretation of the position of the first annulus, causing significantly higher estimates of total age by the unfamiliar reader, but not of the number of annuli past the OTC marks. The structural check rings at the outer edges of opaque zones were the best feature of the large lutjanid otoliths, and the potential for errors in interpreting the annuli on outer margins (Francis et al., 1992) was reduced by sacrificing most fish in late summer and autumn. The longer ventral axis was the most useful because of the variability in growth, measurement errors, and significant differences in estimates of closing dates from measurements along the shorter sulcal axis. However, growth in older otoliths with complex prismatic structure becomes restricted by the otic cleft (Gauldie and Nelson, 1990), and the sulcal axis may provide the only straight axis for measurement in future applications of the models.

Related studies

In contrast to our results for the "red snappers" *L. erythropterus*, *L. malabaricus*, and *L. sebae*, Milton et al. (1995)

concluded from disequilibria in ^{210}Pb to ^{226}Ra ratios of pooled otoliths that shorter lifespans obtained from whole otolith readings (*sensu* McPherson and Squire, 1992) were more accurate than the higher estimates from section counts. This independent method of age determination had previously helped differentiate between very different age interpretations of deep-water *Hoplostethus* and *Sebastes* that were thought to attain high longevities. However, Campana and Jones (1998) noted that radiochemical dating was too imprecise for detailed or individual age determinations, and West and Gauldie (1994) also concluded that the method held promise but was inadequate to validate fish ages.

Regional differences in the ease of interpretation of otolith macrostructure have been reported in tropical species separated by only four degrees of latitude (Fowler, 1995) and may partly explain the differences between our results. The lack of interpretable macrostructure in an otolith section from *L. erythropterus* from the Gulf of Carpentaria is evident when Figure 5b in Milton et al. (1995) is compared with the well-defined incremental structure for the same species in our Figure 2A. Alternatively, there may be real latitudinal differences in the demography of these species. Comparisons of the relationships between otolith weight and age estimates from the Gulf of Carpentaria and the central GBR, and further validation with the "radiocarbon bomb chronometer" (Kalish, 1995; Campana and Jones, 1998), OTC marking, or other independent techniques, may account more precisely for the differences between the validation studies.

Models with ratios of increment measurements around OTC marks in order to estimate time intervals could provide a statistical protocol to accompany the emerging definitions of various levels of validation. Francis (1995) proposed that the highest degree of validation requires demonstration that inner and outer zones are formed annually and that quantitative estimates of accuracy are provided for the process of converting a count of zones to an age estimate. This method requires knowledge of hatching dates and the age at completion of the first annulus, as well as decisions about the nominal calendar dates when opaque zones can be distinguished on otolith margins. The approach presented in our study could allow precise estimates of the timing of some of these latter events if improved theoretical models of growth of opaque zones are developed. We conclude that, for at least the three "reds" species and *L. johnii*, we have attained Francis's (1995) second level of validation—namely, that the opaque zones were formed annually and completed from spring through early summer, but there remains a need to produce quantitative estimates of the accuracy of this aging method.

Acknowledgments

This work was supported by grants to D. McB. Williams and G. Russ from the Australian Research Council. Fieldwork was greatly assisted by the fishing skills of S. Boyle, J. Dalling, A. Mead, G. Muller and D. Moore. The sea cages were designed and built by P. Speare, and we are grateful to the officers of Argus Security Pty Ltd for feeding the captive fish. At the Central Ageing Facility we wish to thank K. Hall for sample registration and database entry and C. Green for advice on interpretation and photomicrography of otoliths. M. Fimeri offered support with image analysis and M. Eden and T. Simmonds drafted the figures. We are particularly grateful for the improvement of the manuscript by three anonymous referees, and for critique of our first working approximation by A. J. Fowler and R. W. Gauldie.

Literature cited

Beckman, D. W., and C. A. Wilson.
1995. Seasonal timing of opaque zone formation in fish otoliths. *In* Recent developments in fish otolith research (D. H. Secor, J. M. Dean, S. E. Campana, eds.), p. 27–44. Univ. South Carolina Press, Columbia, SC.

Campana, S. E., M. C. Annand, and J. I. McMillan.
1995. Graphical and statistical methods for determining the consistency of age determinations. Trans. Am. Fish. Soc. 124:131–138.

Campana, S. E., and C. M. Jones.
1998. Radiocarbon from nuclear testing applied to age validation of black drum, *Pogonias cromis*. Fish. Bull. 96:185–192.

Choat, J. H., and L. M. Axe.
1996. Growth and longevity in acanthurid fishes; an analysis of otolith zones. Mar. Ecol. Prog. Ser. 134:15–26.

Ferreira, B. P., and G. R. Russ.
1992. Age, growth and mortality of the inshore coral trout *Plectropomus maculatus* (Pisces: Serranidae) from the central Great Barrier Reef, Australia. Aust. J. Mar. Freshwater Res. 43:1301–1312.
1994. Age validation and estimation of growth rate of the coral trout, *Plectropomus leopardus*, (Lacepede 1802) from Lizard Island, northern Great Barrier Reef. Fish. Bull. 92:46–57.

Foreman, T.
1996. Estimates of age and growth, and an assessment of ageing techniques, for northern bluefin tuna, *Thunnus thynnus*, in the Pacific Ocean. Int.-Am. Trop. Tuna Comm. Bull. 21(2):123.

Fowler, A. J.
1990. Validation of annual growth increments in the otoliths of a small, tropical coral reef fish. Mar. Ecol. Progr. Ser. 64:25–38.
1995. Annulus formation in otoliths of coral reef fish—a review. *In* Recent developments in fish otolith research (D. H. Secor, J. M. Dean, S. E. Campana, eds.), p. 45–64. Univ. South Carolina Press, Columbia, SC.

Fowler, A. J., and P. J. Doherty.
1992. Validation of annual growth increments in the otoliths of two species of damselfish from the southern Great Barrier Reef. Aust. J. Mar. Freshwater Res. 43:1057–1068.

Fowler, A. J., and D. A. Short.
1998. Validation of age determination from otoliths of the King George whiting *Sillaginodes punctata* (Perciformes). Mar. Biol. 130:577–587.

Francis, R. I. C. C.
1995. The analysis of otolith data—a mathematician's perspective (what, precisely, *is* your model). *In* Recent developments in fish otolith research (D. H. Secor, J. M. Dean, S. E. Campana, eds.), p. 81–95. Univ. South Carolina Press, Columbia, SC.

Francis, R. I. C. C., L. J. Paul, and K. P. Mulligan.
1992. Ageing of adult snapper (*Pagrus auratus*) from otolith annual ring counts: validation by tagging and oxytetracycline injection. Aust. J. Mar. Freshwater Res. 43:1069–1089.

Gauldie, R. W.
1988. Similarities in fine structure of annual, and non-annual, check rings in the otolith of the New Zealand snapper (*Chrysophrys auratus*). N.Z. J. Mar. Freshwater Res. 22:273–278.

Gauldie, R.W., N. M. Davies, G. Coote, and I. Vickridge.
1990. The relationship between organic material and check rings in fish otoliths. Comp. Biochem. Physiol. 97A:461–474.

Gauldie, R. W., and D. G. A. Nelson.
1990. Otolith growth in fishes. Comp. Biochem. Physiol. 97A:119–135.

Gauldie, R. W., and C. R. Romanek.
1998. Orange roughy otolith growth rates: a direct experimental test of the Romanek-Gauldie otolith growth model. Comp. Biochem. Physiol. 120A:649–653.

Kalish, J. M.
1995. Radiocarbon and fish biology. *In* Recent developments in fish otolith research (D. H. Secor, J. M. Dean, S. E. Campana, eds.), p. 637–654. Univ. South Carolina Press, Columbia, SC.

MacLellan, S. E., and J. Fargo.
1995. Validation of age and growth for English sole (*Parophrys vetulus*) in Hecate Strait, British Columbia. *In* Recent developments in fish otolith research (D. H. Secor, J. M. Dean, S. E. Campana, eds.), p. 341–355. Univ. South Carolina Press, Columbia, SC.

McFarlane, G. A., and F. W. H. Beamish.
1995. Validation of the otolith cross-section method of age determination for sablefish (*Anoploma fimbria*) using oxytetracycline. *In* Recent developments in fish otolith research (D. H. Secor, J. M. Dean, S. E. Campana, eds.), p. 319–329. Univ. South Carolina Press, Columbia, SC.

McPherson, G. R., and L. Squire.
1992. Age and growth of three dominant *Lutjanus* species of the Great Barrier Reef inter-reef fishery. Asian Fish. Sci. 5:25–36.

Milton, D. A., S. A. Short, M. F. O'Neill, and S. J. M. Blaber.
1995. Ageing of three species of tropical snapper (Lutjanidae) from the Gulf of Carpentaria, Australia, using radiometry and otolith ring counts. Fish. Bull. 93:103–115.

Montgomery, D. C.
1991. Design and analysis of experiments, 3rd ed. Wiley, New York, NY, p. 486–489.

Morison, A. K., S. G. Robertson, and D. C. Smith.
1998. An integrated system for production fish ageing: image analysis and quality assurance. N. Am. J. Fish. Manage. 18:587–598.

Mosegaard, H., H. Svedang, and K. Taberman.
1988. Uncoupling of somatic and otolith growth rates in Arctic char (*Salvelinus alpinus*) as an effect of differences in temperature response. Can. J. Fish. Aquat. Sci. 45:1514–1524

Murphy, M. D., D. H. Adams, D. M. Tremain, and B. L. Winner.
1998. Direct validation of ages determined for adult black drum, *Pogonias cromis*, in east-central Florida, with notes on black drum migration. Fish. Bull. 96:382–387.

Newman, S. J., and D. McB. Williams.
1995. Mesh size selection and diel variability in catch of fish traps on the central Great Barrier Reef, Australia: a preliminary investigation. Fish. Res. 23:237–253.

Newman, S. J., D. McB. Williams, and G. R. Russ.
1996. Age validation, growth and mortality rates of the tropical snappers (Pisces; Lutjanidae) *Lutjanus adetii* (Castelnau, 1873) and *L. quinquelineatus* (Bloch, 1790) from the central Great Barrier Reef, Australia. Mar. Freshwater Res. 47:575–584.

Newman, S. J., M. Cappo, and D. McB. Williams.
In press. Comparison of age, growth, mortality rates and corresponding yield estimates using counts of annuli in whole and sectioned otoliths of the tropical red snappers *Lutjanus erythropterus*, *L. malabaricus* and *L. sebae* from the central Great Barrier Reef, Australia. Fish. Res.

Payan, P., H. Kossmann, A. Watrin, N. Mayer-Gostan, and G. Bouef.
1997. Ionic composition of endolymph in teleosts: origin and importance of endolymph alkalinity. J. Exp. Biol. 200:1905–1912.

Rocha-Olivares, A.
1998. Age, growth, mortality, and population characteristics of the Pacific red snapper, *Lutjanus peru*, off the southeast coast of Baja California, Mexico. Fish. Bull. 96:562–574.

Romanek, C. S., and R. W. Gauldie.
1996. A predictive model of otolith growth in fish based on the chemistry of the endolymph. Comp. Biochem. Physiol. 114A:71–79.

SAS Institute Inc.
1989a. SAS/STAT user's guide, version 6, 4th ed., vol. 2. SAS Institute Inc., Cary, NC, p. 1352–1455.
1989b. SAS language and procedures: usage, version 6, 1st ed. SAS Institute Inc., Cary, NC, p. 185–197.

Schirripa, M. J., and C .P. Goodyear.
1997. Simulation of alternative assumptions of fish otolith-somatic growth with a bioenergetics model. Ecol. Modelling 102:209–223.

Sheaves, M. J.
1995. Large lutjanid and serranid fishes in tropical estuaries: Are they adults or juveniles? Mar. Ecol. Progr. Ser. 129:31–40.

West, I. F., and R. W. Gauldie.
1994. Determination of fish age using ^{210}Pb:^{225}Ra disequilibrium methods. Can. J. Fish. Aquat. Sci. 51:2333–2340.

Worthington, D. G., A. J. Fowler, and P. J. Doherty.
1995. Determining the most efficient method of age determination for estimating the age structure of a fish population. Can. J. Fish. Aquat. Sci. 52:2320–2326.

Zar, J. H.
1996. Biostatistical analysis, 3rd ed. Prentice Hall, Upper Saddle River, NJ, p. 591–662.

Sexual maturity, sex ratio, and size composition of swordfish, *Xiphias gladius*, caught by the Hawaii-based pelagic longline fishery

Edward E. DeMartini

James H. Uchiyama

Happy A. Williams

Honolulu Laboratory
Southwest Fisheries Science Center
National Marine Fisheries Service, NOAA
2570 Dole Street
Honolulu, Hawaii 96822-2396

E-mail address (for E. E. DeMartini): Edward.Martini@noaa.gov

Abstract.–Swordfish (*Xiphias gladius*) caught by the Hawaii-based pelagic longline fishery during March 1994–June 1997 were examined at sea by observers of the National Marine Fisheries Service, Southwest Region. Observers provided unbiased size and sex composition data for 4.8% of the swordfish catch and 4.9% of the effort in number of hooks of the fishery during the 40-mo. period. Observers measured body lengths for more than 8600 swordfish brought aboard participating vessels; sex, based on macroscopic appearance of gonads, was identified aboard ship for 77% of measured fish. Sex identifications were later verified (0.5% error rate) and gonadal developmental stage described for 1336 fish whose sex was identified in the field. Logistic regression was used to estimate sex-specific, median body size at sexual maturity (L_{50}) by using microscopic morphological evidence for gonadal development. L_{50} was 102 cm ±2.5 (95% CI) cm eye-to-fork length (EFL) and 144 ±2.8 cm EFL for males (n=506) and females (n=822), respectively. Sex ratios were an increasing power function between 100 and 220 cm, and nearly all fish >220 cm EFL were females. Sex composition and body size varied temporally and spatially, especially the latter. Relatively more males were caught south of 27°N; females dominated catches north of 27°N. Small-bodied fish of both sexes prevailed year-round below 22°N. A greater percentage of large-bodied (>156-cm [males], >172-cm [females] EFL) fish were caught north of 35°N during the late summer–early winter. The latter observations are consistent with several nonmutually exclusive hypotheses of migration energetics and body muscle heat conservation, both of which are discussed.

Manuscript accepted 1 December 1999.
Fish. Bull. 98: 489–506 (2000).

Rapid expansion of the Hawaii-based pelagic longline fishery for swordfish (*Xiphias gladius*) during the late 1980s and early 1990s has generated a need for an explicit management plan and assessment of swordfish stocks in the Pacific. Assessments for swordfish might be improved by using size- or age-structured, rather than surplus production, models for several reasons. Size- and age-structured models are less dependent on effort statistics (Gulland and Rosenberg, 1992) and in the Pacific as in the Atlantic, adequate effort statistics are largely unavailable for pelagic longline catches. Effort data are further complicated by geographically separated fisheries that differentially target swordfish or other pelagic fishes and by multiple jurisdictions with varying data collection standards. In the Atlantic these difficulties might be overcome by using nonequilibrium production models and virtual population analyses (ICCAT, 1997).

Estimates of body size and age at sexual maturity are of fundamental importance for the determination of fishery management thresholds based on size- and age-structured stock assessments. In particular, determination of the spawning potential ratio (SPR: Goodyear, 1993) depends on size at maturity. Sex-specific size composition data are also needed to stratify catch and effort statistics, thereby reducing the variances of CPUE estimates.

Information on reproductive biology is inadequate for swordfish in the Pacific. Nakamura et al. (1951) were the first to infer spawning seasonality in the western Pacific based on net collections of swordfish larvae. Yabe et al. (1959) further described swordfish eggs and larvae and used plots of gonad weight versus body length for fish on spawning grounds to approximate body size at sexual maturity for female swordfish in the western Pacific. Kume and Joseph (1969) estimated body size at sexual maturity for female swordfish in the eastern Pacific, and Sosa-Nishizaki (1990) estimated body size at sexual maturity for female swordfish throughout the North Pacific. Uchiyama and Shomura (1974) estimated total fecundities for eight fish and provided anecdotal evidence of swordfish spawning near the Hawaiian Archipelago. Adult-size swordfish caught in the eastern North Pacific were described by Weber and Goldberg (1986) as reproductively inactive during late August–November. Hinton and Deriso's (1998) more recent evaluation of swordfish gonadal index data from the Japanese longline fishery, however, has documented the seasonal presence of reproductively active swordfish near Baja California during May–August. Although largely nonexistent for the Pacific, reproductive and related growth parameters have recently been estimated for swordfish in the Northwest Atlantic (Arocha et al., 1994; Arocha and Lee, 1995, 1996; Ehrhardt et al., 1996; Arocha, 1997).

Catch and effort data for swordfish in Pacific fisheries have been summarized by Miyabe and Bayliff (1987) and Nakano and Bayliff (1992) and reviewed

by Sosa-Nishizaki (1990) and Sosa-Nishizaki and Shimizu (1991). DiNardo and Kwok (1998) have provided a preliminary description of catch statistics and the body size and sex composition of swordfish caught by the Hawaii-based longline fishery in the central North Pacific.

Our study had several complementary objectives, and the ultimate goal of providing accurate and precise information for stock assessments of Pacific swordfish. In our study, we estimated size at sexual maturity for swordfish captured by the Hawaii-based pelagic longline fishery in the central North Pacific. Because the growth rates of adult male and female swordfish differ in the Pacific (Uchiyama et al., 1998), as elsewhere (Ehrhardt et al., 1996), size at maturity was characterized separately for males and females. We classified maturity on the basis of histological analyses of gonads subsampled from a larger sample of field-sexed fish and used this maturity classification as the basis for our estimates of size at maturity. The latter are compared with a complementary characterization of reproductive activity using gonad indices (Hinton et al., 1997). Data on body size (length), date, and location of capture of swordfish in the parent sample of field-sexed fish were used to provide preliminary descriptions of temporal and spatial patterns of size- and sex-specific catch. These patterns of sex and size composition identified factors that could be used for stratifying catch and effort data for the Hawaii-based longline fishery, thereby reducing the variance of population parameter estimates based on logbook records used in future stock assessments. Finally, we interpreted spatial and temporal variations in catch in terms of possibly different migratory behaviors by swordfish of different body sizes and sexes.

Methods and materials

Shipboard collections and measurements

About 90% of the swordfish analyzed were caught by commercial vessels fishing pelagic longlines in the central North Pacific from March 1994 to June 1997. Most (65%: Ito and Machado, 1996,[1] 1997,[2] 1999[3]) swordfish were caught on trips on which swordfish were targeted. Another 34% were caught on "mixed sets" (both tuna and swordfish targeted), and the remaining 1% on "tuna sets" (Boggs and Ito, 1993; He et al., 1997). The remaining 10% of swordfish examined were caught on swordfish research cruises of the NOAA ship *Townsend Cromwell* during 1992–97 in the region of the commercial fishery.

Commercial fishermen dressed all swordfish as the fish were brought aboard ship; observers noted that about 10% were alive and 90% moribund or dead upon retrieval. Viability of fish when sampled is important for interpreting the quality of histological specimens. Observers (NMFS SWR) were assigned to participating longline vessels according to a stratified random design based on vessel size (effort). Observers recorded eye-to-fork length (EFL, cm) for most swordfish caught. For most swordfish that were measured, sex was identified on the basis of macroscopic appearance of the gonads, and, for a random subsample of sexed fish, a gonad tissue sample (2 cm^3, including gonad wall) was collected from the middle of either gonad lobe and immediately fixed in 10% buffered formalin. Swordfish gonad samples were collected during most months of four consecutive years (172 trips sampled during March 1994–June 1997), complemented by specimens collected by research cruises in April–May of 1992 and 1993, September 1996, and March–April 1997. Specimens examined histologically thus spanned several annual cycles; overall 81% of the fish examined were collected during March–July spawning periods (Fig. 1). Fish were sampled throughout the spatial range of the longline fishery during March 1994–June 1997, mostly between lat. 17–41°N and long. 141–180°W (Fig. 2).

During spring 1997, SWR observers collected whole ovaries of approximately 100 swordfish as they were being dressed aboard ship. For each pair of ovaries, a fresh tissue specimen was collected and fixed for later histological evaluation of developmental stage (as described below), and the remainder of the ovaries were frozen for weighing ashore. The latter samples were used in analyses of gonad indices.

Laboratory processing

Field-classified sex was verified and reproductive condition evaluated based on gonadal developmental stage determined by microscopic examination of histological preparations and oocyte size frequencies. Fixed gonad specimens were stored for at least 60 days before oocytes were measured or a subsample was prepared for histological analyses. A single series of sequential, histological sections (6 µm thick) (2–8: mode=3[ovaries], mode=4[testes]) was cut and stained with Harris's hematoxylin, followed by eosin counterstain (Hunter and Macewicz, 1985). Slide sections were examined with a compound microscope at 60–300× and developmental stage categorized following the stage criteria of Murphy and Taylor (1990). For females, the following characteristics were noted for the largest size mode of oocytes present: presence and relative quantity of eosinophilic yolk, partly to moderately yolked oocytes, and fully yolked oocytes. If oocytes were fully yolked, we further noted the presence of hydrating or hydrated oocytes (HYDs), postovulatory follicles (POFs), and fully

[1] Ito, R. Y., and W. A. Machado. 1996. Annual report of the Hawaii-based longline fishery for 1995. Southwest Fish. Sci. Cent. Admin. Rep. H-96-12, Honolulu Laboratory, Southwest Fish. Sci. Cent., Natl. Mar. Fish. Serv., NOAA, Honolulu, HI 96822-2396, 45 p.

[2] Ito, R. Y., and W. A. Machado. 1997. Annual report of the Hawaii-based longline fishery for 1996. Southwest Fish. Sci. Cent., Admin. Rep. H-97-12, Honolulu Laboratory, Southwest Fish. Sci. Cent., Natl. Mar. Fish. Serv., NOAA, Honolulu, HI 96822-2396, 48 p.

[3] Ito, R. Y., and W. A. Machado. 1999. Annual report of the Hawaii-based longline fishery for 1998. Southwest Fish. Sci. Cent. Admin. Rep. H-99-06, Honolulu laboratory, Southwest Fish. Sci. Cent., Natl. Mar. Fish. Serv., NOAA, Honolulu, HI 96822-2396, 62 p.

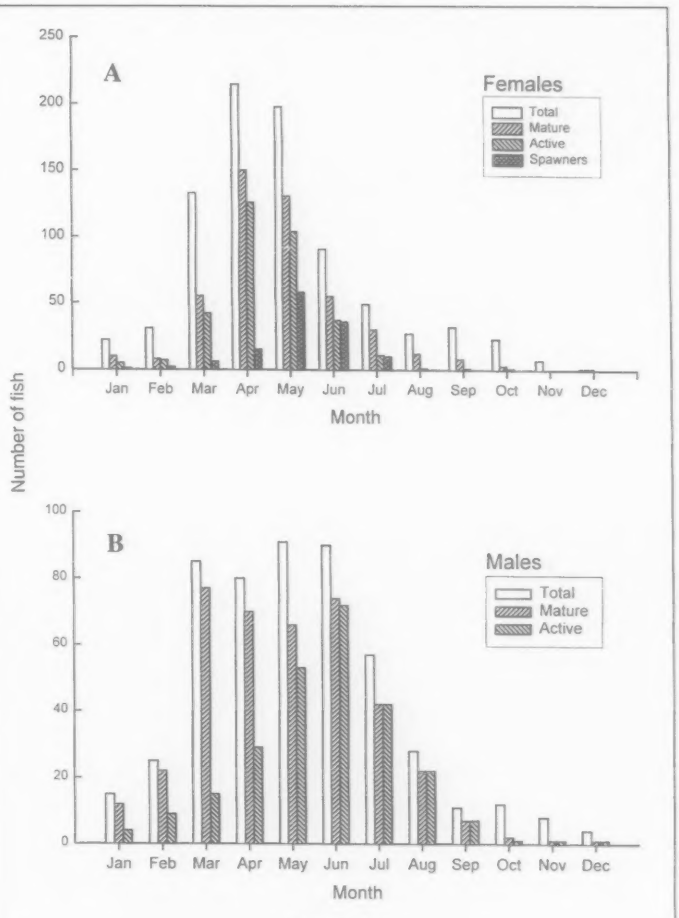

Figure 1

Numbers of (**A**) female and (**B**) male swordfish (*Xiphias gladius*) that were immature, mature, active, or imminent spawners (females only), which were caught on occasional research cruises and by the Hawaii-based pelagic longline fishery each month during March 1994–June 1997. Maturity and reproductive activity were assessed based on gonad developmental stages scored histologically.

yolked oocytes undergoing α-, or β- and later atresia (Table 1). Female individuals were designated as "immature" if their most advanced oocytes were unyolked or only partly to moderately yolked without substantial atresia, or as "mature" if their most advanced oocytes were fully yolked with or without atresia ("active-mature") or if their most advanced oocytes were less than fully yolked but with alpha or beta atretic stages present. Developmental stages were further described according to the diameters of the largest size class mode of oocytes present. Among mature females, fish were deemed "ripening mature" if fully yolked but lacking HYDs or POFs, "ripe mature" (imminent spawners) if POFs or HYDs were present, or "resting mature" if a majority of yolked oocytes were atretic.

Oocyte diameters were measured by using formalin-fixed whole oocytes or oocyte cross sections on histological slides. For formalin-fixed specimens, diameters of 25 of the largest oocytes were measured with a dissecting microscope (random axis, 25–50×). The median of 25 random diameters provides a cost-efficient estimator of average maximum oocyte size for multiple-spawning fishes (Lau and DeMartini, 1994); swordfish are multiple-spawners (Uchiyama and Shomura, 1974; Arocha, 1997). Histological slides were prepared for a random subset of these specimens; diameters of oocyte cross sections on slides were measured at 60–300× and for each fish ovary examined, maximum and minimum diameters were averaged for 5–10 of the largest oocyte sections present

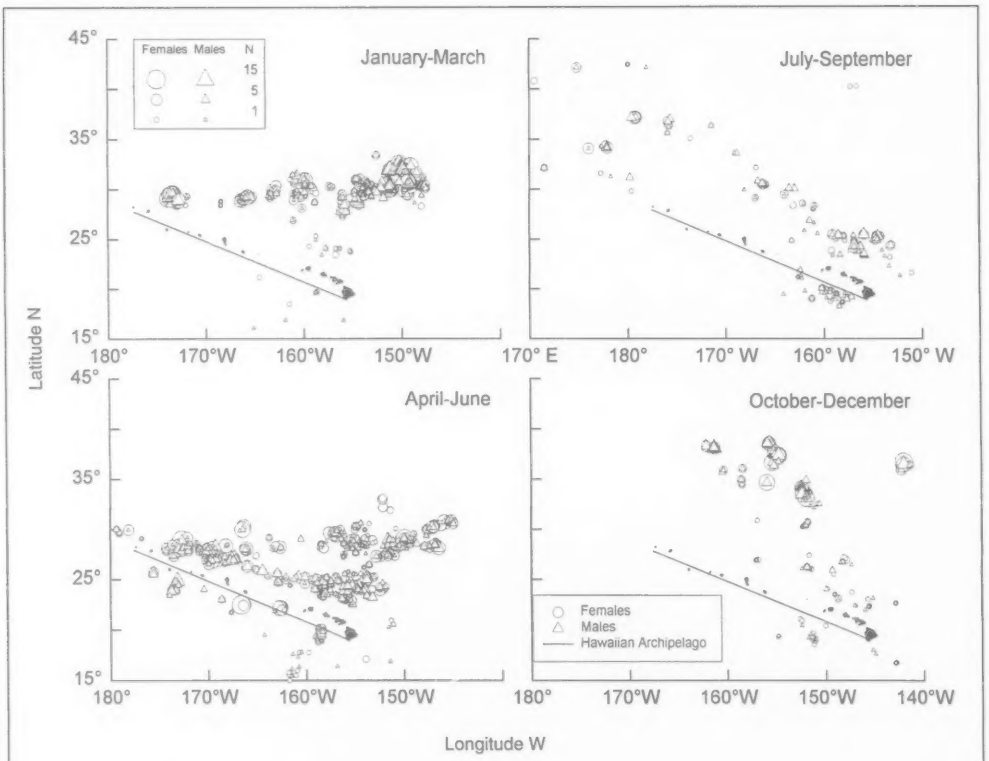

Figure 2

Spatial distributions of known-sex (female: hollow circles; male: hollow triangles) swordfish (*Xiphias gladius*), caught by the Hawaii-based pelagic longline fishery during January–March, April–June, July–September, and October–December periods, between March 1994 and June 1997, illustrating seasonal geographic shifts in the fishery. Areas of symbols are proportional to catch-per-unit-of-effort (CPUE, number of fish per set); CPUEs are scaled continuously from a minimum of 1 to a maximum of 17 fish per set.

that included a central nucleus and were spherical (least deformed by processing), so that the coefficient of variation (CV) of the diameter estimate was <10%. Diameters measured for a subset of matched (formalin-fixed, histology) specimens were used to convert between the two types of measurements.

The gonadal development of males was classified by using the criteria of Grier (1981) as specified for billfish by de Sylva and Breder (1997). Males were scored as "immature" if spermatogenesis (meiosis) was absent or, when occurring, if ripe (fully tailed) spermatozoa were restricted to crypts and lobules (tubules) of testes. Males were deemed mature only if ripe sperm were present in spermatic ducts, as well as in crypts and lobules, or as spent or resting if they had developed lobules but no spermatogenesis present (Table 1).

Sex was histologically verified for 506 males and 830 females. The sex of only 23 swordfish (8 males: 70–153 cm EFL, March–December; 15 females: 98–212 cm EFL, April–December) was misclassified from gross visual inspection of gonads by observers aboard commercial longliners. Misclassification error was unrelated to true sex (χ^2=0.02; df=1; P=0.9), and appeared unrelated to fish size or period of capture, although the data were too few to formally evaluate size and period effects. Because the misclassification rate was so low (0.5%), we ignored it in further analyses of the sex composition of swordfish catch where field-sexed fish were used.

For ovary specimens collected in spring 1997, frozen specimens were thawed overnight in a refrigerator. Each lobe of bilobed ovaries was weighed damp; accuracy was 1 g (if total ovary weight ≤500 g) or 20 g (if >500 g). Seven of 95 females caught during the spring 1997 spawning period lacked weights for one ovary lobe; total ovary weights of these fish were estimated by using the relationship between both ovaries (total gonad weight, GW) and right (RO) and left (LO) ovary weights (in g): $GW = 1.807RO$, and $GW = 2.170LO + 133.6$ (both r^2>0.98; n=88). Right ovaries of the swordfish examined were 28% heavier than left ovaries (matched-pair t-test; t=6.9; n=88).

Table 1

Histological criteria for classification of gonadal developmental stages and maturation in male and female swordfish, *Xiphias gladius*, caught in the central North Pacific during the period April 1992–June 1997. Maturity stages are based on the criteria of Murphy and Taylor (1990). Median observed oocyte diameters are for 10% formalin-fixed (sea water) specimens.

Maturity stage by sex		Histological appearance of the most advanced gamete stage present in gonads
Females		
1	vestigial	Primitive oogonia only; 80 µm
2	developing	Primary oocytes (basophilic) only present; 133 µm
3	maturing	Early vitellogenesis; beginnings of nucleus breakdown and development of fat inclusions; no chorionic membrane (zona pellucida); 211 µm
4	ripening	Oocytes well-yolked (completely eosinophilic); nuclear membrane indistinct; prominent chorionic membrane, with fat inclusions distributed throughout cytoplasm; 547 µm
5	spawning	Migratory (eccentric) nucleus, hydrating or hydrated oocytes present; 1012 µm
6	recently spawned	Postovulatory follicles present; 1197 µm
7	spent or resting	A majority of classes 4–5 yolked oocytes present undergoing α- β-, or later atresia; 201 µm
Males		
1	undeveloped	Spermatocytes only present; spermatogenesis (meiosis) lacking
2–3	maturing	Spermatogenesis present; some to many ripe (fully tailed) spermatozoa present in crypts and lobules (tubules), but none in spermatic ducts
4	ripe	Ripe sperm present in spermatic ducts as well as crypts and lobules; relatively little spermatogenic activity
5	spent	Developed lobules containing few remaining sperm

Statistical analyses

We estimated body length at median sexual maturity (L_{50}) for males and females separately using nonlinear regression. A derivative-free maximum likelihood method (Proc NLIN; SAS, 1989) was used to fit percentage maturity by 5-cm length class to the two-parameter logistic model,

$$P_x = 100 / (1+\exp^{(a-bEFL)}),$$

where P = percentage mature at length x; and
L_{50} = $(-a/b)$.

Sex ratios (females/total) also were related to 5-cm length class by using nonlinear regression. Regressions were weighted by the square root of the number of fish examined in each length class. Ninety-five percent confidence intervals on L_{50}'s were calculated by using SAS Proc PROBIT. Logistic regression (STATISTIX, vers. 4.1; Analytical Software, 1994) was used to relate ovarian developmental stage to oocyte diameter and to predict reproductive readiness with gonad weight plus body size. Contingency chi-square and unbalanced fixed-factor ANOVAs (Zar, 1984; SAS, 1989) were used to compare sex ratios and the relative body size compositions of swordfish catches, pooled by 1° lat. by 1° long. bins, during spawning (March–July) and nonspawning (August–February; see "Results" section) periods. Least-squares regression was used to regress median body length versus latitude after body length distributions were made linear by rank transformation. Analyses of sex ratios and size composition were limited to observer-sampled trips and should be considered a first approximation of patterns for the total Hawaii-based longline catches of swordfish during March 1994–June 1997. Significance was based on an alpha level of 0.05.

Results

Sex and maturity composition of sampled fish

During the 40-mo. sampling period, an estimated 142,000 swordfish were caught by the Hawaii-based pelagic longline fishery (2.26 million hooks: Ito and Machado, 1996,[1] 1997,[2] 1999[3]). Data for the 6639 field-sexed fish examined herein thus represent about 4.8% of the commercial landings of swordfish, with the samples reflecting about 4.9% of the total longline effort (2.26 million out of 45.7 million hooks) expended during the period. The sex ratio (females as fraction of total) of the field-sexed commercial catch was 0.533 (SE=0.006; P<0.001). About 64% of the 1336 swordfish examined histologically were sexually mature (stages ≥4, Table 1). The two sexes differed in maturity composition based on histological classification (χ^2=67.4; P<0.001): 78% of 506 confirmed males but only 56% of 828 confirmed females were mature.

About 73% of 463 mature females were reproductively active (stages 4–6; including 28% stages 5–6 imminent spawners) and 27% were spent or resting (stage 7, Table 1). Of a total 130 spawning females, 33 had ovaries containing oocytes that were hydrating or hydrated, indicating imminent spawning. The ovaries of 122 fish contained POFs, suggesting ovulation within several days prior to capture. The exact age of POFs was inestimable because the likely temperature-dependent (Fitzhugh and Hettler, 1995) degradation rate of swordfish POFs is unknown and because gonad samples were collected from fish that had been hooked for differing lengths of time at varying water temperatures. Twenty-five of the 130 fish had ovaries containing both unovulated, hydrated oocytes and POFs from a previous spawning (Fig. 3, A and B). Of a total 395 mature (stage ≥4) males, 65% were reproductively active (stage 4) and 35% were spent or resting (stage 5, Table 1).

Oocyte size and developmental stage

Ovarian developmental stage was closely related to diameter of the largest size class mode of oocytes present in ovaries. The diameters of formalin-fixed whole oocytes (OD, in μm) and oocyte cross sections (XS, in eyepiece units [epu], where 1 epu=0.1544 μm) on histological slides were best related by the linear regression

$$OD = 11.9 + 6.320XS \qquad (r^2=0.948,\ n=182,\ P<0.001).$$

With logistic regression, ovarian development as an indicator of reproductive activity (where active=stages 4–6; inactive=stages 1–3, 7) was predicted with 97.5% accuracy for 828 fish collected during both spawning and nonspawning periods. The predictive relationship was

$$\ln(p/(1-p)) = -6.318 + 0.0180OD,$$

where OD = whole oocyte diameter (in μm); and
p = the probability of active stages 4–6.

The threshold (p=0.5) for stages 4–6 is predicted at a whole oocyte diameter of 351 μm. Oocyte size distributions are related graphically to ovarian stages in Figure 4. Median oocyte diameters for the respective stages are listed in Table 1.

Body lengths at sexual maturity

Estimates of L_{50} with all females were indistinguishable (<1 cm different: G-test; P=0.3) from those where females were used that had been caught during the 5-mo. (March–July) spawning periods when reproductively active females (stages 4–6) were present. L_{50} estimates for males were improved if immature (most likely less-than-year-old) fish, many of which were available only during nonspawning periods, were included. We therefore felt it preferable to describe L_{50}'s using all gonad sample fish collected year-round.

L_{50}'s were 102.0 ± 2.5 (95% CI) cm EFL for males (r^2=0.98; n=506) and 143.6 ± 2.8 cm EFL for females (r^2=0.97; n=816; Fig. 5). Fits to the logistic model were as follows:

$$\text{Males:} \quad \%\,Mature = 100/(1 + e^{(14.4011 - 0.1412EFL)})$$
$$\text{Females:} \quad \%\,Mature = 100/(1 + e^{(14.8569 - 0.1034EFL)}).$$

Females attained ≥95% sexual maturity at 173 cm EFL. The corresponding value for males was 123 cm EFL. The smallest reproductively active female whose ovaries contained hydrated oocytes or postovultory follicles was 134 cm EFL. Sample sizes ranged from 2 to 45 fish of each sex per 5-cm EFL class; only 6 out of 36 and 12 out of 31 classes contained <10 fish for females and males, respectively. Median sample sizes were 22 (for females) and 17 (for males) for each 5-cm class (Fig. 5).

Indices of spawning readiness

Reproductive readiness (verified by histological staging of ovaries) of female swordfish in the Hawaii-based fishery could be predicted by logistic regressions with body size (length, weight) and ovary weight (or with length- or weight-based gonad indices). Although the spawning activity of female swordfish was predictable from body size and ovary weight alone, the accuracy of prediction was improved if a measure of ovary maturation (such as size of the largest oocytes present) was included. Overall, about 96% of 95 females (range 8–295 kg, 76–247 cm EFL; Table 2A) were correctly classified (with reference to histological stages 4–6) as either reproductively active (1) or not (0) by the logistic regression

$$\ln(p/(1-p)) = \ln(RW) + \ln(GW) + \ln(EV),$$

where RW = round weight in kg;
GW = gonad weight in g; and
EV = oocyte volume in $mm^3 = 4/3\pi r^3$; and
r = diameter/2 (Table 2A).

The fit of this model was similar to those where oocyte volume plus any of several length- or weight-based gonad indices were used. Among the latter, the index, $GI(2') = [\ln(GW)/\ln(RW)]$, was best (90% accurate), and overall classification accuracy increased to 97% if oocyte volume was added to the model (Table 2B). The index, $GI(2) = [\ln(GW)/\ln(EFL)]$ of Hinton et al. (1997), plus oocyte volume, showed comparable accuracy (94%; Table 2C), and retained 87% accuracy even if oocyte volume was excluded (Table 2D). The latter length-based gonad index itself (Table 2D) should have the widest applicability, despite some loss in predictive power because an oocyte volume term is lacking, because data on swordfish body lengths and gonad weights are often available but body weight and egg size data are not. We also provide (Table 3) several key regressions of swordfish length-on-length and weight-on-length, summarized from Uchiyama et al. (1999), to enable conversions between the different index-based predictors of reproductive readiness.

Temporal and spatial spawning patterns

Swordfish caught by the Hawaii-based longline fishery during March 1994–June 1997 included both reproductively inactive and active adult fish, in addition to imma-

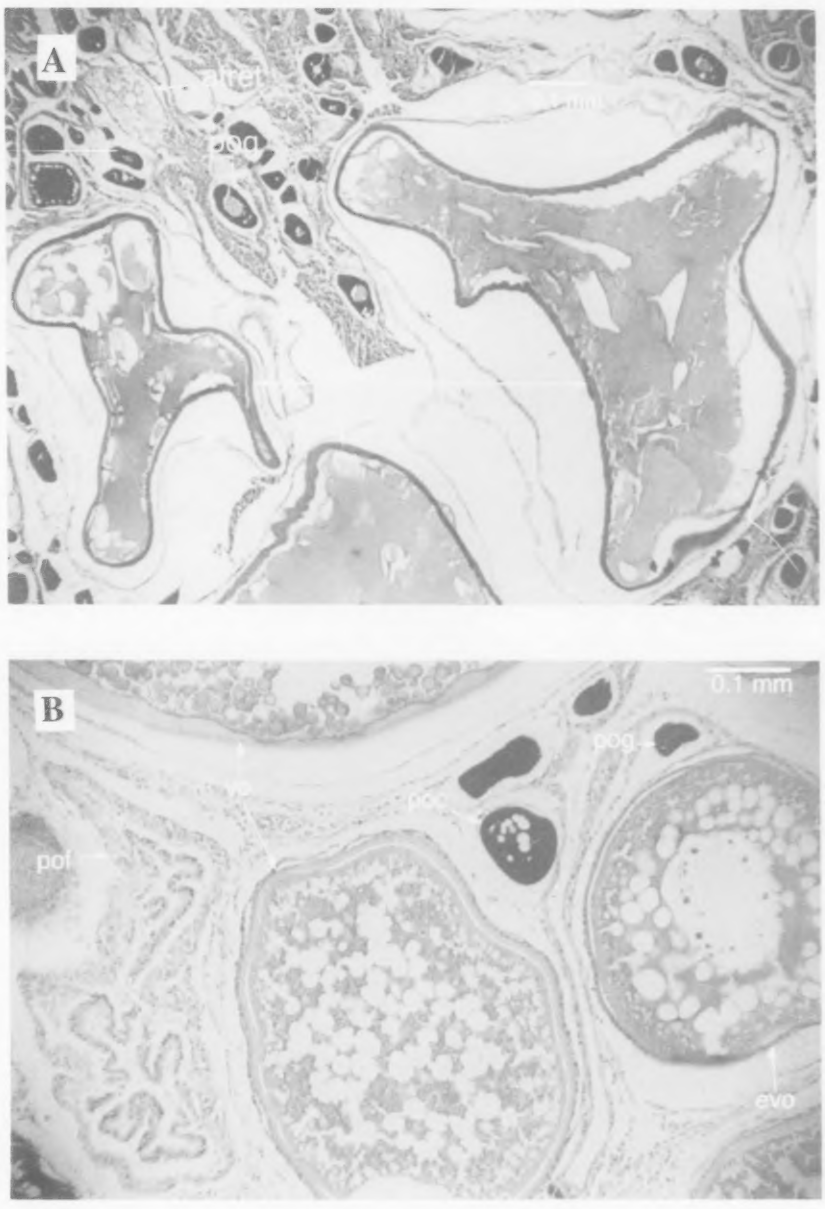

Figure 3

Histological sections of the ovaries of imminently spawning swordfish (*Xiphias gladius*) illustrating (**A**) hydrated oocytes (hyd; stage 5) and (**B**) postovulatory follicles (pof; stage 6). Several other developmental stages of oocytes are also present, including primitive oogonia (pog; stage 1); previtellogenic oocytes (poc; stage 2); early vitellogenic (evo: stage 3) and vitellogenic (vo; stage 4) oocytes; and atretic oocytes (atret; stage 7; an α-atretic, vitellogenic oocyte indicated by arrow in 3A).

ture, mostly female fish. Reproductively active females (stages 4–6) were caught primarily during spring (Fig. 6). Ninety-eight percent of all imminently spawning females were caught during March–July periods, and 73% were caught during May–June (Fig. 6). POFs and hydrated oocytes often co-occurred in ovaries (in 25 out of 33 cases;

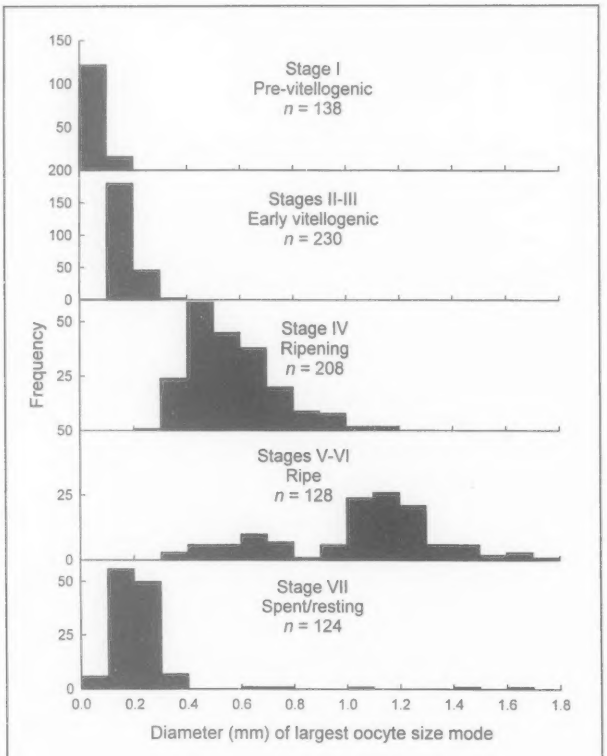

Figure 4

Size distribution of oocyte stages in ovaries of swordfish (*Xiphias gladius*) caught by the Hawaii-based pelagic longline fishery during March 1994–June 1997, which were examined histologically. Diameters (mm) are for the largest size class mode of viable (not atretic) oocytes present. Sample sizes refer to the numbers of specimens with ovaries in each stage.

χ^2=23.1; df=1; P<0.001). The relative numbers of active females and imminent spawners were independent of moon phase (Table 4), although indicating no lunar spawning periodicity. Eighty-two percent of all reproductively active (stage 4) males were caught during March–July. Many imminently spawning females were caught within several hundred km of the Hawaiian Archipelago (Fig. 6), not far beyond the borders of the 75- and 50-mile closures to pelagic longlining in the main Hawaiian and Northwestern Hawaiian Islands, respectively.

Size, sex, and maturity composition of catches

The size and sex composition of swordfish catches were related (Table 5; Fig. 7). Most (0.55) of the swordfish caught that were <140 cm were male, most (0.64) of those >150 cm were female, whereas the sex ratio (females/total) of fish between 140 and 150 cm EFL was indistinguishable from 0.5 (Fig. 8). Sex ratios fluctuated around 0.5 without pattern at lengths <100 cm, were an increasing power function of fish length between 100 and 220 cm (proportion female=$0.0018EFL^{1.1418}$; r^2=0.87; n=24 5-cm classes; P<0.001) and were consistently >0.9 at lengths >220 cm EFL (Fig. 7). Overall, males represented about 39.5% of the March 1994–June 1997 observer-sampled swordfish catch by weight. The female catch by weight was 60.5%.

The maturity composition of swordfish catches differed between the sexes. During March 1994–June 1997, mature fish represented about 56% and 77% of the sampled female catch in terms of numbers and weight, respectively. Mature fish comprised 88% (numbers) and 96% (weight) of the sampled male catch. Overall, 71% and 85% of the total sampled catch (both sexes) were mature by numbers and weight, respectively.

Both the sex and size composition of swordfish catches varied spatially (Fig. 9; Table 6). Latitude had a stronger influence on sex ratio and size composition than did longitude (Table 6, A and B). A large majority (61%) of all swordfish caught south of 27°N were males. The body size (hence sex) of swordfish caught might vary with depth and time

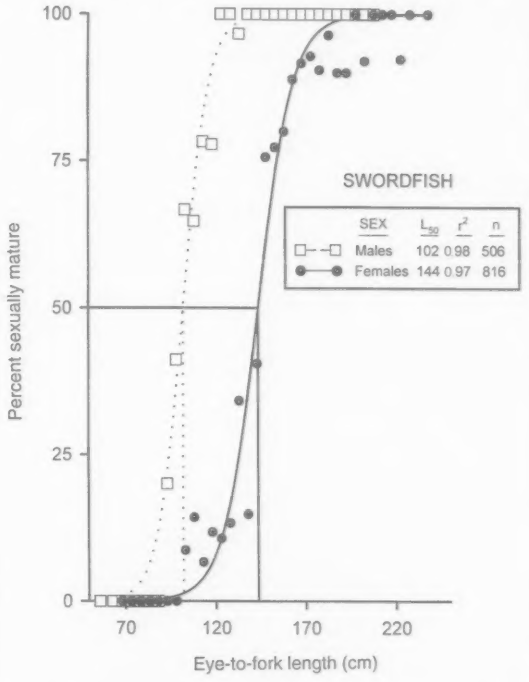

Figure 5

Nonlinear regression fits of the logistic model for percentage sexually mature versus eye-to-fork length (5-cm EFL class), weighted by square root of sample size per length class, for male and female swordfish (*Xiphias gladius*) caught by the Hawaii-based pelagic longline fishery during March 1994–June 1997. Solid and dashed best-fit lines are predicted relationships, and analogous perpendicular lines are median body size at sexual maturity (L_{50} intercepts), for females and males, respectively. Symbols represent mean percentages mature per 5-cm EFL class.

of day fished, and relatively more "tuna sets" (deep, daytime soak) are made during the peak summertime tuna season, particularly at latitudes at and below the Hawaiian Archipelago (He et al., 1997). We therefore reevaluated the sex composition of swordfish catches south and north of 27°N using only the fish caught on sets on which swordfish were targeted (He et al., 1997). A total of 5547 fish were caught on swordfish sets, representing 84% of all swordfish present in the parent sample. The male proportion of 585 swordfish caught on swordfish sets south of 27°N was the same (61%) as for all observer-sampled sets. Proportions of females in catches at and north of 27°N also were the same (56%) for total and swordfish-targeted sets.

Sex and size composition of the swordfish catch varied with season (Table 6A). Small-bodied males and females dominated lower-latitude catches during spawning as well as nonspawning periods (Table 6B). Overall, about 64% by numbers and 65% by weight of all swordfish were caught during March–July spawning periods.

Several interesting spatial patterns were apparent in the size composition data. Relatively greater numbers of "small-bodied" (<25th length percentile; females: <126 cm; males: <118 cm EFL) swordfish were caught south of 22°N (Table 6B). Relatively greater numbers of "large-bodied" (>75th percentile; females: >172 cm; males: >156 cm EFL) fish were caught north of 35°N (Table 6C). Median body sizes of swordfish caught increased with latitude (regressions of ranked median EFL on 1° bins, r^2>0.8 for each sex, n=21, P<0.001) with the proportions of catch that were small-bodied (and mostly male) greater south of about 22°N (Fig. 9).

Discussion

Sex-specific sizes at maturity

Effects of methods Ninety-five percent confidence intervals on our estimates of median body size (L_{50}) at sexual

Table 2

Summary results of logistic regressions predicting reproductive activity (histological stages 4–6) versus inactivity (stages 1–3, 7; see Table 1) based on (**A**) round weight (RW), gonad weight (GW), plus egg volume (EV); (**B**) a weight-based gonad index [GI(2')] plus EV; (**C**) a length- based gonad index [GI(2)] plus EV; or (**D**) GI(2) alone; for female swordfish, *Xiphias gladius,* sampled from the Hawaii-based pelagic longline fishery during May–June of 1997.

A $\ln(p/(1-p)) = \ln(RW) + \ln(GW) + \ln(EV)$

Predictor variables	Coefficient	Standard error	*P*-value
$\ln(RW)$	–10.740	3.437	0.0018
$\ln(GW)$	4.228	1.899	0.0260
$\ln(EV)$	2.073	0.610	0.0007

Classification table			Proportion correctly classified		
	Predictions				
Actual	0	1	0	1	overall
0	18	2	0.900	0.973	0.958
1	2	73			

B $\ln(p/(1-p)) = GI(2') + \ln(EV)$, where $GI(2') = [\ln(GW)/\ln(RW)]$

Predictor variables	Coefficient	Standard error	*P*-value
GI (2')	–21.464	5.176	0.0001
$\ln(EV)$	2.822	0.610	0.0001

Classification table			Proportion correctly classified		
	Predictions				
Actual	0	1	0	1	overall
0	17	3	0.850	1.000	0.968
1	0	75			

C $\ln(p/(1-p)) = GI(2) + \ln(EV)$, where $GI(2) = [\ln(GW)/(\ln(EFL)]$

Predictor variables	Coefficient	Standard error	*P*-value
GI (2)	–15.916	3.847	0.0001
$\ln(EV)$	1.934	0.444	0.0001

Classification table			Proportion correctly classified		
	Predictions				
Actual	0	1	0	1	overall
0	14	6	0.700	1.000	0.937
1	0	75			

D $\ln(p/(1-p)) = GI(2)$

Predictor variables	Coefficient	Standard error	*P*-value
GI (2)	20.559	4.823	0.0001
Intercept	–24.968	6.008	0.0001

Classification table			Proportion correctly classified		
	Predictions				
Actual	0	1	0	1	overall
0	13	7	0.650	0.933	0.874
1	5	70			

Table 3

Predictive equations and summary statistics for best-fit regressions relating various body length and weight metrics for swordfish, *Xiphias gladius*, in the central North Pacific. Source: Uchiyama et al. (1999). Eye-to-fork length (EFL) and lower jaw-to-fork length (LJFL) are cm; and round weight (RW) and dressed weight[1] (DW) are kg. Sample size (n) is number of fish (sexes pooled). All equations are significant at $P<0.001$.

Model	Equation	SE b	SE a	n	r^2
$EFL = a + b \times LJFL$	$EFL = -6.543 + 0.927 \times LJFL$	0.006	0.849	179	0.992
$LJFL = a + b \times EFL$	$LJFL = 8.009 + 1.071 \times EFL$	0.007	0.865	179	0.992
$RW = a \times EFL^b$	$RW = 1.299 \times 10^{-5} \times EFL^{3.074}$	0.041	3.010×10^{-6}	166	0.967
$DW = a \times RW^b$	$DW = 0.646 \times RW^{1.032}$	0.051	0.016	73	0.987

[1] Dressed weight is defined as round (total) weight minus the head, entrails, vertical and pectoral fins, and with caudal fin (including caudal peduncle and keel) removed by a cut make between the 22nd and 23rd vertebrae (Uchiyama et al., 1999).

maturity were within ±2–3% of their respective estimate and provide reasonably precise input parameters for stock assessment. Occasional estimates of less-than-complete maturity in some larger length classes of females (Fig. 5) likely reflect chance indetection of relatively rare, large atretic oocytes in the ovaries of inactive but mature females. Such may be expected when only a single region of ovary is examined histologically. We feel that the evalu-

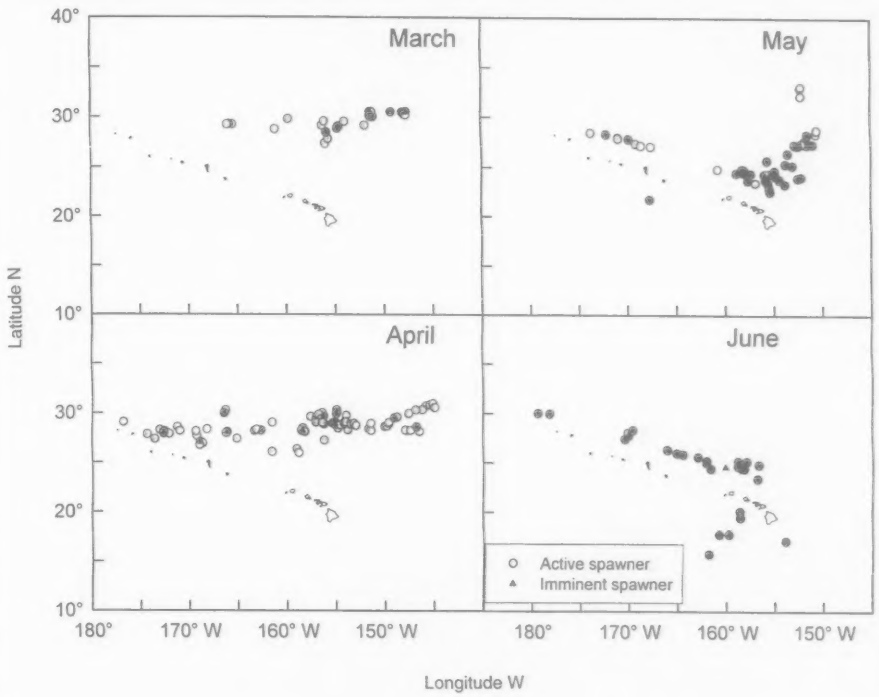

Figure 6

Capture locations of imminent spawners (stages 5–6; solid triangles) overlaid on locations of all reproductively active females (stages 4–6; shaded circles), for swordfish (*Xiphias gladius*) caught by the Hawaii-based pelagic longline fishery during March 1994–June 1997. Monthly plots from March, April, May, and June depict the increasing proximity of imminent spawners to the Hawaiian Archipelago as the spawning season progresses.

ation of greater numbers of females by using only a single ovary section offsets the rare failure to detect maturity in mature but inactive females.

Histological examination of gonadal developmental stage is the most accurate and expensive method of characterizing sexual maturity, and cost-effective alternatives are desirable (West, 1990). Gonad indices (GIs) represent one such general (West, 1990) and specific (Hinton et al., 1997) option. Our findings indicate that swordfish body weight plus ovary weight together can predict reproductive activity with >90% accuracy in swordfish caught by the Hawaii-based fishery. Our observations support the conclusion of Hinton et al. (1997) that GIs can provide useful proxies of reproductive activity in swordfish. We reiterate, however, that GIs alone are limited to detection of reproductive activity (Hinton et al., 1997); without ancillary data such as gonad development or oocyte size, GIs are often not reliable measures to distinguish reproductively inactive but mature females from immature females during the nonspawning season (West, 1990; Mejuto and Garcia, 1997). GIs are most often used for determining spawning seasons; if nonspawning season fish are to be included in a size-at-maturity evaluation, a relatively inexpensive alternative to histological staging (such as oocyte size) should be used for deducing maturation stages. Oocyte size can provide an accurate proxy for gonadal developmental stage

Table 4

Results of 2×3 χ^2 test comparing relative frequency with which imminently spawning (stages 5–6) female swordfish, *Xiphias gladius*, were caught, among all reproductively active females (stages 4-6) caught during new, quarter, and full moon periods by the Hawaii-based pelagic longline fishery during March 1994–June 1997. $\chi^2 = 3.28$, df = 2, $P = 0.20$.

Period	Active	Spawning	Both
New	34	27(44%)	61
Quarter	76	39(34%)	115
Full	74	59(44%)	133
All	184	125	309

Table 5

Monthly sex ratios (females/total), effort (positive swordfish sets), and summary statistics for body sizes of female and male swordfish, *Xiphias gladius*, used to describe sex and size composition of catch. *n* = number of fish in sample. EFL = eye-to-fork length (cm).

Month	Sex	*n*	Sex ratio	Trips (sets)	25th percentile	Median EFL	75th percentile
Jan	F	182	0.56	3 (35)	132	153	176
	M	142		3 (32)	125	144	163
Feb	F	334	0.56	9 (66)	129	148	165
	M	264		11 (60)	125	141	159
Mar	F	883	0.55	13 (161)	129	151	175
	M	723		13 (165)	121	136	159
Apr	F	746	0.58	15 (170)	128	150	175
	M	531		17 (164)	118	134	152
May	F	359	0.51	14 (110)	120	151	181
	M	340		14 (108)	115	129	148
Jun	F	183	0.44	12 (71)	118	148	171
	M	237		14 (83)	118	139	160
Jul	F	174	0.46	11 (51)	118	152	178
	M	204		10 (60)	114	135	157
Aug	F	39	0.39	4 (17)	106	136	152
	M	62		7 (29)	102	125	151
Sep	F	41	0.53	6 (24)	93	105	122
	M	36		6 (21)	68	102	126
Oct	F	159	0.45	11 (50)	120	140	155
	M	193		10 (50)	119	138	164
Nov	F	283	0.56	6 (49)	124	151	167
	M	218		5 (47)	108	133	152
Dec	F	156	0.51	7 (36)	136	159	180
	M	150		6 (39)	121	140	160
All	F	3539	0.533	111 (840)	126	149	172
	M	3100		116 (858)	118	136	156

in swordfish (Taylor and Murphy, 1992; Arocha and Lee, 1995; our study). Gonad weights scaled for body length (because body lengths, not weights, are typically collected for swordfish at sea) deserve further evaluation as predictors of spawning readiness, particularly because our findings for swordfish in the central North Pacific are so similar to those of Hinton et al. (1997) for Atlantic swordfish.

Other maturity estimates Prior reported estimates of body size at sexual maturity for female swordfish in the Pacific in general do not agree with ours, but dissimilarities likely reflect the different measures used to gauge sexual maturity used by various researchers. For example, Yabe et al. (1959) concluded, from length distributions and gonad weights, that "most [female] swordfish" in the western Pacific mature sexually between 150 and 170 cm EFL. Kume and Joseph (1969) observed that female swordfish "in spawning condition" (defined as having a greater than defined threshold value of gonad index) were not "regularly encountered" until about 170 cm EFL. Sosa-Nishizaki's (1990, p. 64) estimate of sexual maturity at about 160 cm EFL for "most individuals" was also inferred from a length-based GI. In contrast to females, ours is the first estimate of any kind for body size at sexual maturity of male swordfish in the Pacific Ocean. Our results overall underscore the importance of sex-specific, histologically validated estimates of median body size at sexual maturity as data for stock assessments.

Our estimates of L_{50} for swordfish caught by the Hawaii-based longline fishery appear comparable (for males) to slightly smaller (females) than estimates for swordfish caught in several regions of the Atlantic. For swordfish from the Straits of Florida, Taylor and Murphy (1992) observed L_{50}'s of 112 and 182 cm lower jaw-to-fork length (LJFL) for males and females, respectively, equivalent to 96 and 161 cm EFL. Arocha and Lee (1996) estimated L_{50}'s of 129 (males) and 179 cm LJFL (females), equivalent to 112 and 158 cm EFL, respectively, for swordfish caught throughout the western Atlantic. We caution that these L_{50} estimates for swordfish in the Atlantic may not be totally comparable to ours because studies might differ in whether estimates apply to fish caught throughout the entire year or during spawning periods only.

Female swordfish in the Mediterranean presently mature at an L_{50} of about 142 cm LJFL (de la Serna et al., 1996),

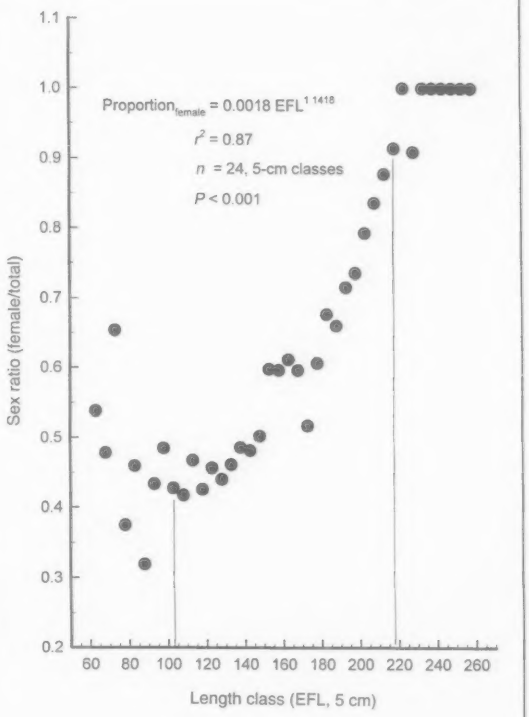

Figure 7

Relationship between sex ratios (females/total) estimated from catches and eye-to-fork length (EFL, 5-cm classes) for swordfish (*Xiphias gladius*) caught by the Hawaii-based pelagic longline fishery during March 1994–June 1997. Vertical lines depict the bounds ($100 \leq EFL \leq 220$ cm) used to regress proportion female on fish length.

equivalent to an estimated 124 cm EFL, considerably smaller than that documented for females in any other fishery. This estimate by de la Serna et al. (1996) was based on length-based gonad indices that were histologically validated.

For swordfish caught by the Hawaii-based longline fishery, the disparate body lengths at median sexual maturity of males and females are equivalent to a threefold difference between 55 kg RW (40 kg dressed-head off weight, DW) for females and 19 kg RW (14 kg DW) for males. Corresponding ratios of female:male body weights at L_{50} for swordfish in the tropical and western North Atlantic are 4.4 (Taylor and Murphy, 1992) and 2.7 (Arocha and Lee, 1996). Details of computation notwithstanding, these disparities in mass clearly represent biologically meaningful differences between the sexes in swordfish. Sexual differences in rates of biomass accrual—likely due to sexually dimorphic growth rates—translate to important differences in the sustainable fisheries yield provided by each sex. With later maturation, the period of rapid prereproductive somatic growth of female swordfish extends several or more years longer than that of males. Taylor and Murphy (1992) for example estimate ages-at-sexual maturity of swordfish from the Straits of Florida, corresponding to median sizes-at-maturity, as 5.5 yr (for females) and 1.4 yr (for males).

At present our characterization of maturity in North Pacific swordfish is limited to body size. Age-at-maturity estimates must await completion of size-at-age studies being conducted at the Honolulu Laboratory of the National Marine Fisheries Service.

Sex and size composition

Sex ratios of swordfish caught by the Hawaii-based longline fishery vary temporally and spatially. These variations may partly reflect different availabilities or catchabilities resulting from sexual differences in behavior that change seasonally (e.g. during spawning periods). Variations in the sex composition of catches must partly reflect different natural distributions of the sexes. Sex ratios of catches follow recurrent seasonal patterns among years, and spatial differences in the sex composition of catches repeat annually. Neither of these two observations would be likely if, for example, the sex composition of catches represented simple targeting of larger (female) fish by fishermen.

Similarities in sex ratios-at-length between North Atlantic (Stone and Porter, 1997) and central North Pacific swordfish (our study) suggest that size-specific sex ratios of swordfish catches can be predicted with adequate precision from data on the length composition of catches. If true, this could obviate the need for a direct characterization of the sex composition of swordfish catches—a task complicated in fisheries like Hawaii's in which swordfish are landed fully dressed. Sex ratios of swordfish caught by the Hawaii-based fishery are identical for swordfish-targeted and nonswordfish-targeted sets. Estimates of the sex ratio of swordfish catches in the Hawaii-based fishery thus seem robust to the specifics of capture, at least for the period sampled. Further comparisons of sex ratio estimates for catches with different gear types over a longer sampling period would be required to thoroughly evaluate possible sexual differences in catchability and expand inferences on sex ratios beyond catch to stock.

Seasonal patterns Temporal changes in the sex ratios and related size composition of swordfish catches in the Hawaii-based longline fishery resemble those observed for swordfish in other known spawning areas. Taylor and Murphy (1992) observed analogous temporal differences in catches of male and female swordfish in and near the Straits of Florida, where the fraction of males in catches was significantly greater than that of females only during peak (spring–summer) spawning periods. Temporal patterns of changes in sex ratios thus are consistent with sexual differences in migratory and spawning or other reproductive behaviors such as the greater propensity for males to aggregate in group-spawning pelagic species (Hunter and Macewicz, 1986) and other fishes.

Spatial patterns Arocha and Lee (1995) observed spatial variations, complementary to Taylor and Murphy's (1992)

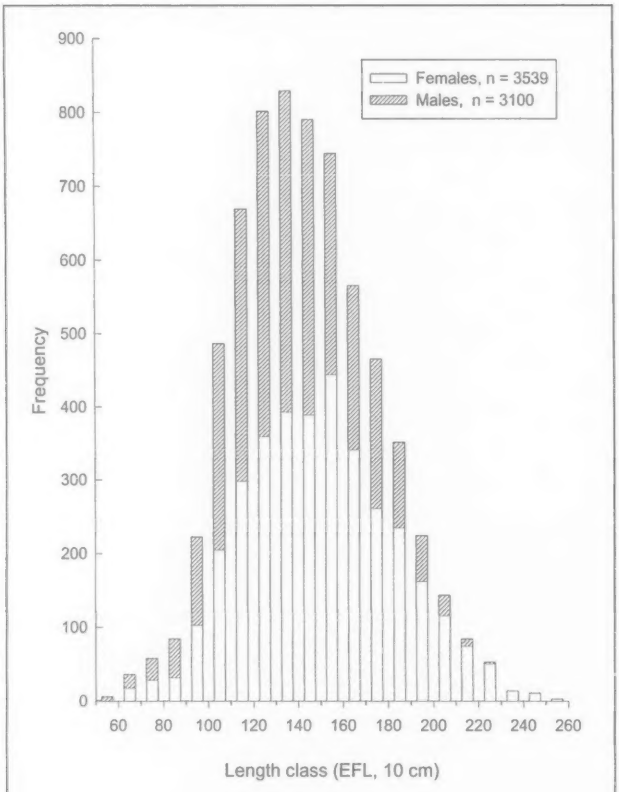

Figure 8

Size-specific sex ratios of swordfish (*Xiphias gladius*), used to evaluate sex and size composition of catch of the Hawaii-based pelagic longline fishery during March 1994–June 1997. For readability, lengths (EFL) have been pooled by 10-cm classes.

temporal variations in swordfish sex ratios elsewhere in the western Atlantic. The sex ratios of adult-size swordfish (>125 cm LJFL, but smaller than very large adults [>195 cm], the size at which the numbers of males diminish greatly in Atlantic swordfish stocks) are strongly male-biased only in the subtropical region (19–35°N) in which most spawning occurs (Arocha et al., 1994; Arocha and Lee, 1995). Spatial patterns similar to the latter also have been observed in spawning regions of the tropical western Atlantic (Mejuto et al., 1998) and western Indian Ocean (Mejuto et al., 1995).

Spatial differences in the sex and size composition of swordfish also may be related to sex-specific foraging migrations. Differences in the sex and size composition of swordfish catches have been noted by others in western Atlantic fisheries. Males predominate in catches made at tropical latitudes but females dominate in waters <18°C (Beckett, 1974). Most swordfish caught in the western North Atlantic off New England and the Canadian maritime provinces are large female fish (Tibbo et al., 1961).

Distributional ecology and energetics of migration

Limited tag-recapture data[4] suggest that some swordfish move great distances within the North Pacific. Swordfish also display marked diel vertical migrations that appear to vary among fish of different sizes and that inhabit continental shelf versus open ocean areas (Carey and Robison, 1981; Carey, 1990). As they migrate between warm mixed layer and cold subthermocline waters, swordfish encounter changes in water temperature as great as 19° in 2.5 h (8–27°C: Carey and Robison, 1981). A vascular rete system enables swordfish to dampen the rate of temperature loss in swimming muscles on deep dives, and it is likely that body mass importantly influences this ability (Carey, 1990) and the metabolic costs of inhabiting cold water masses

[4] Boggs, C. H. 1998. Unpubl. data. Honolulu Laboratory, Southwest fish. Sci. Cent., Natl. Mar. Fish. Serv., NOAA, Honolulu, HI 96822-2396.

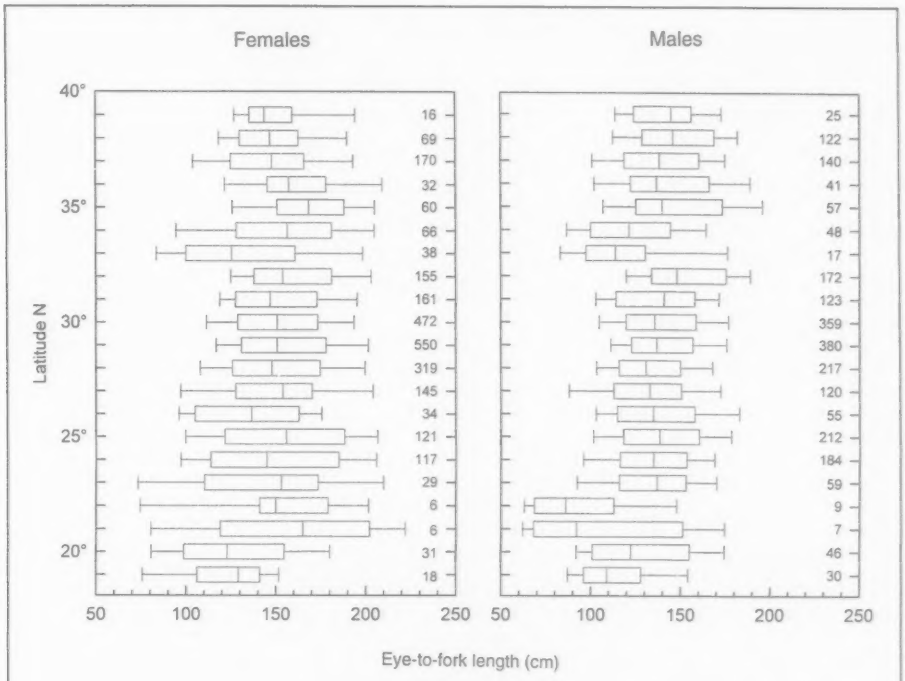

Figure 9

Median body lengths (EFL, cm) plotted by 1-degree north latitude increments for female and male swordfish (*Xiphias gladius*), caught by the Hawaii-based pelagic longline fishery during March 1994–June 1997. Also indicated are the respective 5th, 25th, 75th, and 95th percentiles, and sample sizes (number of fish; arrayed along right-hand abscissa).

(first hypothesized as a "size-temperature mediated physiological mechanism" by Hoey, 1991).

Horizontal movements also incur different energetic costs, as well as other types of costs, for fishes of different body sizes (Roff, 1988). It is plausible that feeding and spawning migrations involve different costs for individual swordfish ranging over the broad spectrum of body sizes (90–210 cm EFL, 13–180 kg; Fig. 8) commonly caught by the Hawaii-based fishery. Because most small swordfish are males and most large swordfish are females, it is further likely that the costs of migration differ between the sexes as well as among fish of varying body sizes that might migrate different distances. The significant relationships observed between latitude and sex ratio and between latitude and body size for swordfish of both sexes in the central North Pacific are consistent with the latter hypothesis.

Recurrent patterns of variation in the sex composition of swordfish catches throughout the world's longline fisheries remain poorly understood. Observed patterns may reflect natural differences in distributions of the sexes, may represent consistent artifacts of different catchabilities of the sexes during spawning periods, or both. A challenging topic for future research will be the evaluation of whether the differences reflect sexually distinct costs versus benefits for vertical or horizontal migration that result from the disparate body masses of males and females.

Implications for stock assessment

It is clear that stratifying swordfish catch statistics by sex could appreciably reduce the variances of catch and effort estimates, and future research should include simulation studies that explore the quantitative effects of sex stratification on stock assessments (Restrepo, 1991). Further, if our observations for swordfish caught by the Hawaii-based longline fishery have identified patterns that are relevant to swordfish caught elsewhere, age-structured stock assessments for swordfish in the Pacific should evaluate explicitly the potentially great importance of temporal and spatial dynamics in the sex and size composition of catches. It will likely be necessary to stratify catches by latitude of capture (and perhaps spawning and nonspawning period), in addition to standardizing CPUE statistics for environmental variables and targeting (e.g. see He et al., 1997; Hinton and Deriso, 1998; Bigelow et al., 1999), in order to reduce the variances of abundance indices used in stock assessments.

Table 6

Results of fixed-factor ANOVAs relating (**A**) sex ratio (females/total) versus period (spawning = Mar–Jul, nonspawning = Aug–Feb), latitude class (North: ≥27°N, South: <27°N) and longitude class (East: ≤160°W, West: >160°W); (**B**) the relative number of fish smaller than the 25th length percentile (RNQ1, see text) versus period and latitude class (Far S: ≤22°N, Other: >22°N); and (**C**) the relative number of fish larger than the 75th percentile (RNQ3, see text) vs sex and latitude class (Far N: ≥35°N, Other: <35°N) on sets with swordfish present, for swordfish, *Xiphias gladius*, caught by the Hawaii-based pelagic longline fishery during March 1994–June 1997. NS terms (e.g. longitude) are unspecified. SS = sum of squares; MS = mean square; LSMEAN = least square mean; SE LSMEAN = Standard error of least square mean.

A Source		df	SS	MS	*F*-value	*Pr>F*
Latitude		1	6.634	6.634	23.13	0.0001
Period × Latitude		2	4.297	2.149	7.49	0.0006
			Sex ratio			
Case	Period × Latitude		LSMEAN	SE LSMEAN	Contrasts	
1	Nonspawning	N	0.532	0.012		
2	Nonspawning	S	0.472	0.048	3>1=2=4	
3	Spawning	N	0.584	0.009		
4	Spawning	S	0.392	0.016		
B Source		df	SS	MS	*F*-value	*Pr>F*
Period		1	2.634	2.634	10.64	0.0011
Latitude		1	14.179	14.179	57.29	0.0001
Period × Latitude		1	2.009	2.009	8.12	0.0044
			RNQ1			
Case	Period × Latitude		LSMEAN	SE LSMEAN	Contrasts	
1	Nonspawning	FarS	0.696	0.073		
2	Nonspawning	Other	0.248	0.011	1>3>2=4	
3	Spawning	FarS	0.433	0.043		
4	Spawning	Other	0.230	0.008		
C Source		df	SS	MS	*F*-value	*Pr>F*
Sex		1	0.486	0.486	2.31	0.13
Latitude		1	1.569	1.569	7.47	0.0063
Sex × Latitude		1	1.254	1.254	5.97	0.0146
			RNQ3			
Case	Sex × Latitude		LSMEAN	SE LSMEAN	Contrasts	
1	Female	FarN	0.253	0.023		
2	Female	Other	0.248	0.008	3>1=2=4	
3	Male	FarN	0.321	0.023		
4	Male	Other	0.232	0.009		

Acknowledgments

We thank Don Peterson, Tim Price, and Lyle Enriquez of the NMFS, Southwest Region (SWR, Long Beach, CA) office and Tom Shearer, Kevin Busscher, and numerous shipboard observers (anonymous for confidentiality) of the SWR, Honolulu Office, for the organized collection of specimens and data management necessary to complete our study. Eric Yamanoha (Pathology Department, Queen's Hospital, Honolulu) ably supervised the histological work. We also thank Chris Boggs, Gerard DiNardo, Kurt Schaefer, and two anonymous reviewers for constructive criticisms of manuscript drafts and Debra Yamaguchi for help with the figures.

Literature cited

Analytical Software, Inc.
1994. STATISTIX, user's manual, vers. 4.1. Analytical Software, P.O. Box 12185, Tallahassee, Florida, 329 p.

Arocha, F.
1997. The reproductive dynamics of swordfish *Xiphias gladius* L. and management implications in the northwestern Atlantic. Ph.D. diss., Univ. Miami, Florida, 383 p.

Arocha, F., and D. W. Lee.
1995. The spawning of swordfish from the Northwest Atlantic. Int. Comm. Conserv. Atl. Tunas, Coll. Vol. Sci. Pap., vol. 44(3):179–186.
1996. Maturity at size, reproductive seasonality, spawning frequency, fecundity and sex ratio in swordfish from the Northwest Atlantic. Int. Comm. Conserv. Atl. Tunas, Coll. Vol. Sci. Pap., vol. 45(2):350–357.

Arocha, F., D. W. Lee, and J. R. Grubich.
1994. Observations on sex ratio, maturity stages, and fecundity estimates of swordfish, *Xiphias gladius*, in the Northwest Atlantic Ocean. Int. Comm. Conserv. Atl. Tunas, Coll. Vol. Sci. Pap., Vol. 42(1):309–318.

Beckett, J. S.
1974. Biology of swordfish, *Xiphias gladius* L., in the Northwest Atlantic Ocean. *In* Proc. Int. Billfish Symp., Part 2, Review and contributed papers (R. S. Shomura, and F. Williams, eds.), p. 105–106. U. S. Dep. Commer., NOAA Tech. Rep. NMFS SSRF-675.

Bigelow, K. A., C. H. Boggs, and X. He.
1999. Environmental effects on swordfish and blue shark catch rates in the U.S. North Pacific longline fishery. Fish. Oceanogr. 8:179–198.

Boggs, C. H., and R. Y. Ito.
1993. Hawaii's pelagic fisheries. Mar. Fish. Rev. 55:69–82.

Carey, F. G.
1990. Further acoustic telemetry observations of swordfish. *In* Planning the future of billfishes: research management in the 90s and beyond, Proc. 2nd Int. Billfish Symp., Kailua-Kona, Hawaii, August 1–5, 1988; Part 2: Contributed papers (R. H. Stroud, ed.), p. 103–122.

Carey, F. G., and B. H. Robison.
1981. Daily patterns in the activities of swordfish, *Xiphias gladius*, observed by acoustic telemetry. Fish. Bull. 79:277–292.

de la Serna, J. M., J. M. Ortiz de Urbina, and D. Macias.
1996. Observations on sex ratio, maturity and fecundity by length-class for swordfish (*Xiphias gladius*) captured with surface longline in the Western Mediterranean. Int. Comm. Conserv. Atl. Tunas, Coll. Vol. Sci. Pap., vol. 45(1): 115–139.

de Sylva, D. P., and P. R. Breder.
1997. Reproduction, gonad histology, and spawning cycles of North Atlantic billfishes (Istiophoridae). Bull. Mar. Sci. 60:668–697.

DiNardo, G. N., and W. Kwok.
1998. Spatiotemporal dynamics of swordfish (*Xiphias gladius*) landings in the Hawaii-based North Pacific longline fishery. *In* Biology and fisheries of swordfish, *Xiphias gladius* (I. Barrett, O. Sosa-Nishizaki, and N. Bartoo, eds.), p. 51–64. U.S. Dep. Commer., NOAA Tech. Rep. NMFS 142.

Ehrhardt, N. M., R. J. Robbins, and F. Arocha.
1996. Age validation and growth of swordfish, *Xiphiasgladdius*, in the Northwest Atlantic. Int. Comm. Conserv. Atl. Tunas, Coll. Vol. Sci. Pap., vol. 45(2):358–367.

Fitzhugh, G. R., and W. F. Hettler.
1995. Temperature influence on postovulatory follicle degeneration in Atlantic menhaden, *Brevoortia tyrannus*. Fish. Bull. 93:568–572.

Goodyear, C. P.
1993. Spawning stock biomass per recruit in fisheries management: foundation and current use. *In* Risk evaluation and biological reference points for fisheries management (S. J. Smith, J. J. Hunt, and D. Rivard, eds.), p. 67–81. Can. Spec. Publ. Fish. Aquat. Sci. 120.

Grier, H. J.
1981. Cellular organization of the testis and spermatogenesis in fishes. Am. Zool. 21:345–367.

Gulland, J. A., and A. A. Rosenberg.
1992. A review of length-based approaches to assessing fish stocks. FAO Fish. Tech. Pap. 323, 100 p. FAO, Rome.

He, X., K. R. Bigelow, and C. H. Boggs.
1997. Cluster analysis of longline sets and fishing strategies within the Hawaii-based fishery. Fish. Res. 31:147–158.

Hinton, M. G., and R. B. Deriso.
1998. Distribution and stock assessment of swordfish, *Xiphias gladius*, in the eastern Pacific Ocean from catch and effort data standardized on biological and environmental parameters. *In* Biology and fisheries of swordfish, *Xiphias gladius* (I. Barrett, O. Sosa-Nishizaki, and N. Bartoo, eds.), p. 161–179. U.S. Dep. Commer., NOAA Tech. Rep. NMFS 142.

Hinton, M. G., R. G. Taylor, and M. D. Murphy.
1997. Use of gonad indices to estimate the status of reproductive activity of female swordfish, *Xiphias gladius*: a validated classification method. Fish. Bull. 95:80–84.

Hoey, J.
1991. Sex ratio data for western North Atlantic swordfish. Int. Comm. Conserv. Atl. Tunas, Coll. Vol. Sci. Pap., vol. 35(2):429–436.

Hunter, J. R., and B. J. Macewicz.
1985. Measurement of spawning frequency in multiple spawning fishes. *In* An egg production method for estimating spawning biomass of pelagic fish: application to the northern anchovy, *Engraulis mordax* (R. Lasker, ed.), p. 79–94. U.S. Dep. Commer., NOAA Tech. Rep. NMFS 36.
1986. The spawning frequency of skipjack tuna, *Katsuwonus pelamis*, from the South Pacific. Fish. Bull. 84:895–903.

ICCAT (International Commission for the Conservation of Atlantic Tunas).
1997. 1996 detailed report on swordfish. Report of the ICCAT Swordfish Stock Assessment Session (Halifax, N.S., Canada, October 2–9, 1996). ICCAT Coll. Vol. Sci. Pap., vol. 46(3):165–188.

Kume, S., and J. Joseph.
1969. Size composition and sexual maturity of billfish caught by the Japanese longline fishery in the Pacific Ocean east of 130°W. Bull. Far Seas Fish. Res. Lab. (Shimizu) 2:115–162 [In Engl., Jpn. summ.]

Lau, B. B., and E. E. DeMartini.
1994. An evaluation of oocyte size in multiple regressions predicting gonad weight from body weight: a test using Hawaiian ehu, *Etelis carbunculus*. U.S. Dep. Commer., NOAA Tech. Memo. NMFS-SWFSC-212, 17 p.

Mejuto, J., J. M. de la Serna, and B. Garcia
1995. An overview of the sex ratio at size of the swordfish (*Xiphias gladius*) around the world: similarity between different strata. Int. Comm. Conserv. Atl. Tunas, Coll. Vol. Sci. Pap., vol. 44(3):197–205.
1998. Some considerations on the spatial and temporal variability in the sex-ratio at size of the swordfish (*Xiphias gla-*

dius). Int. Comm. Conserv. Atl. Tunas, Coll. Vol. Sci. Pap., vol. 48(4):205–215.

Mejuto, J., and B. Garcia.
1997. A preliminary analisis [sic] of gonadal indices of the swordfish (*Xiphias gladius* L.) in the Atlantic Ocean. Int. Comm. Conserv. Atl. Tunas, Coll. Vol. Sci. Pap., vol. 46(3):336–344.

Miyabe, N., and W. H. Bayliff.
1987. A review of the Japanese longline fishery for tunas and billfishes in the eastern Pacific Ocean, 1971–1980. Inter-Am. Trop. Tuna Comm., Bull. 19(1):1–163.

Murphy, M. D., and R. G. Taylor.
1990. Reproduction, growth, and mortality of red drum *Sciaenops ocellatus* in Florida waters. Fish. Bull. 88:531–542.

Nakamura, H., T. Kamimura, Y. Yabuta, A. Suda, S. Ueyanagi, S. Kikawa, M. Honma, M. Yukinawa, and S. Morikawa.
1951. Notes on the life history of the sword-fish, *Xiphias gladius* Linnaeus. Jpn. J. Ichthyol. 1:264–271.

Nakano, H., and W. H. Bayliff.
1992. A review of the Japanese longline fishery for tunas and billfishes in the eastern Pacific Ocean, 1981–1987. Inter-Am. Trop. Tuna Comm., Bull. 20(5):183–355.

Restrepo, V.
1991. Some possible biases in swordfish VPAs due to sexually dimorphic growth. Int. Comm. Conserv. Atl. Tunas, Coll. Vol. Sci. Pap., vol. 35(2):338–345.

Roff, D. A.
1988. The evolution of migration and some life history parameters in marine fishes. Environ. Biol. Fish. 22:133–146.

Sosa-Nishizaki, O.
1990. A study of the swordfish *Xiphias gladius* stocks in the Pacific Ocean. Ph.D. diss., Fac. Agric., Univ. Tokyo, Tokyo, 246 p.

Sosa-Nishizaki, O., and M. Shimizu.
1991. Spatial and temporal CPUE trends and stock unit inferred from them for the Pacific swordfish caught by the Japanese tuna longline fishery. Bull. Nat. Res. Inst. Far Seas Fish. (Shimizu) 28:75–89.

SAS (Statistical Analysis System).
1989. SAS/STAT user's guide, version 6, 4th ed., vol. 2. SAS Inst., Cary, NC, 846 p.

Stone, H. H., and J. M. Porter.
1997. Development of a swordfish sex ratio-at-size relationship for catches from the Canadian fishery. Int. Comm. Conserv. Atl. Tunas, Coll. Vol. Sci. Pap., vol. 46(3):311–314.

Taylor, R. G., and M. D. Murphy.
1992. Reproductive biology of the swordfish *Xiphias gladius* in the Straits of Florida and adjacent waters. Fish. Bull. 90:809–816.

Tibbo, S. N., L. R. Day, and W. F. Doucet.
1961. The swordfish (*Xiphias gladius* L.), its life-history and economic importance in the northwest Atlantic. Fish. Res. Board Can. Bull. 130:1–47.

Uchiyama, J. H., E. E. DeMartini, and H. A Williams.
1999. Length-weight interrelationships for swordfish, *Xiphias gladius* L. caught in the central North Pacific. U.S. Dep. Commer., NOAA Tech. Memo. NMFS NOAA-TM-NMFS-SWFSC-284, 82 p.

Uchiyama, J. H., and R. S. Shomura.
1974. Maturation and fecundity of swordfish, *Xiphias gladius*, from Hawaiian waters. *In* Proc. Int. Billfish Symp., part 2, Review and contributed papers (R. S. Shomura and F. Williams, eds.), p. 142–147. U.S. Dep. Commer., NOAA Tech. Rep. NMFS SSRF-675.

Uchiyama, J. H., R. A. Skillman, J. D. Sampaga, and E. E. DeMartini.
1998. A preliminary assessment of the use of hard parts to age central Pacific swordfish, *Xiphias gladius*. *In* Biology and fisheries of swordfish, *Xiphias gladius* (I. Barrett, O. Sosa-Nishizaki, and N. Bartoo, eds.), p. 261–273. U.S. Dep. Commer., NOAA Tech. Rep. NMFS 142.

Weber, E. C., and S. R. Goldberg.
1986. The sex ratio and gonad indices of swordfish, *Xiphias gladius*, caught off the coast of southern California in 1978. Fish. Bull. 84:185–186.

West, G.
1990. Methods of assessing ovarian development in fishes: a review. Austr. J. Mar. Freshwater Res. 41:199–222.

Yabe, H. S., S. Ueyanagi, S. Kikawa, and H. Watanabe.
1959. Studies of the life history of the swordfish, *Xiphias gladius* Linnaeus. Rep. Nankai Reg. Fish. Res. Lab., 10:107–150. [In Jpn., Engl. summ.; transl. by CEP Multilingual Serv. Div., Dep. Sec. of State, Canada.]

Zar, J. H.
1984. Biostatistical analysis, 2nd ed. Prentice-Hall, Englewood Cliffs, NJ, 718 p.

Larval development of red snapper, *Lutjanus campechanus*, and comparisons with co-occurring snapper species

Denice M. Drass
National Marine Fisheries Service, NOAA
3209 Frederick St.
Pascagoula, Mississippi 39567
E-mail address: ddrass@triton.pas.nmfs.gov

Kevin L. Bootes
Marine Science Institute
University of Texas at Austin
750 Channel View Drive
Port Aransas, Texas 78373

Joanne Lyczkowski-Shultz
National Marine Fisheries Service, NOAA
3209 Frederick St.
Pascagoula, Mississippi 39567

Bruce H. Comyns
Gulf Coast Research Laboratory
E. Beach Blvd.
Ocean Springs, Mississippi 39564

G. Joan Holt
Marine Science Institute
University of Texas at Austin
750 Channel View Drive
Port Aransas, Texas 78373

Cecilia M. Riley
Gulf Coast Bird Observatory
103 West Highway 332
Lake Jackson, Texas 77566

Ronald P. Phelps
Department of Fisheries and Allied Aquaculture
Auburn University
Auburn, Alabama 36849

Abstract.—The larval development of red snapper, *Lutjanus campechanus*, is described from reared larvae and from specimens collected in the Gulf of Mexico (GOM). Snapper larvae are pelagic and are characterized by the following features: a deep and compressed, lightly pigmented body; moderately short gut; 24 myomeres; and elongated dorsal and pelvic fins that form early in development. Specimens of *L. campechanus* (1.9 to 26.1 mm) also showed the presence of weak serrations on pelvic-fin spines, absence of serrations on preopercular or dorsal spines, early forming pigment in dorsal and pelvic fins, and notochord flexion between 3.6 and 5.5 mm. Preflexion larvae of the snapper subfamily Lutjaninae in GOM collections cannot be reliably identified to species despite recent larval descriptions. Species-specific differences in number, spacing, and size of melanophores in the postanal ventral series are evident in the youngest larvae of species from the GOM whose development has been described (*Ocyurus chrysurus*, *L. analis*, *L. synagris*, *L. griseus*, *L. campechanus*, and *Rhomboplites aurorubens*) but further evaluation of the utility of these characters is needed. Characteristics that distinguish mid- to late-flexion larvae of these species are compiled in our study and discussed. Among known GOM lutjanine larvae, body depth, pelvic-ray length and serrations on the angle spine of the preopercle can be used in combination with pigmentation to identify larvae to species. Presence of melanistic pigment (and size at first appearance) or absence of melanistic pigment in the following locations are useful characters for larval snapper identification: anterior surface of the visceral mass, ventral to notochord flexure; internal area over the notochord; dorsal midline of caudal peduncle; soft dorsal fin; anal-fin base or membrane; and pelvic fin.

Manuscript accepted 7 February 2000.
Fish. Bull. 98:507–527 (2000).

In the Gulf of Mexico (GOM), the red snapper, *Lutjanus campechanus*, supports lucrative commercial and recreational fisheries that have been under increasingly restrictive regulation since the 1980s (Workman and Foster, 1994; Schirripa and Legault[1]). Responsible management decisions should be based on an understanding of all life history stages, but until recently the larval development of only three of the 18 species of snappers found in the GOM were known. Collins et al. (1980) described *L. campechanus* from wild larvae with substantial fin development that allowed identification by meristic counts and Rabalais et al. (1980) described reared red snapper eggs and larvae that developed only until 4 days after hatching. Substantial fin development also allowed identification by meristic counts for larvae of the vermilion snapper, *Rhomboplites aurorubens* (Laroche, 1977), and a third lutjanid, the gray snapper (*L. griseus*), was described by Richards and Saksena (1980) from reared specimens. More recently, descriptions by Clarke et al., 1997 (*Ocyurus chrysurus*, *L. analis* and *L. synagris*), Riley et al., 1995 (*O. chrysurus*), Leis and Lee, 1994 (*Etelis* spp., *Pristipomoides aquilonaris* and *P. freemani*?) and the summary compilation by Richards et al. (1994) added three genera and four species to the list of known snapper larvae. Our paper describes for the first time the complete sequence of larval development of red snapper from reared specimens and compares the structure and shape of reared and wild larvae. Additionally, we present a summary of developmental characteristics to separate snapper larvae in field collections from the Gulf of Mexico.

[1] Schirripa, M. J., and C. M. Legault. 1997. Status of the red snapper in U.S. waters of the Gulf of Mexico: updated through 1996. Unpublished contribution report MIA-97/98-05, 37 p. Miami Laboratory, Southeast Fish. Sci. Cent., Natl. Mar. Fish. Serv., NOAA.

Materials and methods

A total of 96 reared larvae, ranging in body length (BL) from 1.9 to 26.1 mm, and a total of 118 wild larvae, ranging from 2.6 to 20.0 mm BL, were used to describe larval development of red snapper. Reared larvae came from the Marine Science Laboratory, University of Texas at Austin, Port Aransas, Texas (TX), and the Claude Peteet Mariculture Center in Gulf Shores, Alabama (AL). Spawning and rearing methods used are described by Riley et al. (1995) at the Texas facility and by Bootes (1998) at the Alabama facility. Notable differences in the rearing methods at the two facilities that could have contributed to different developmental rates include higher salinities in the TX study (33–38 ppt vs. 31–33 ppt), higher temperatures in the AL study (27–32°C vs. 27–28°C) and natural light conditions in the AL study. Several larvae were preserved each day during the Texas rearing study whereas only one larva was preserved each day during the Alabama rearing experiments. Specimens from AL were fixed in 2% formalin and specimens from TX were fixed in 80% ethanol (EtOH) and together formed the developmental series described in our study. Age in days after hatching (DAH) is included in parentheses after BL for reared larvae. In addition, observations on the development of pigment characters were augmented with 96 larvae reared at the Gulf Coast Research Laboratory (GCRL) in Ocean Springs, MS, under conditions similar to the AL study.

Wild red snapper larvae were obtained from plankton samples collected in the GOM by the Southeast Area Monitoring and Assessment Program (SEAMAP) and GCRL. Samples were collected with bongo and neuston nets at stations 56 km apart by using standard SEAMAP collection procedures (Richards, 1984; Richards et al., 1993). Samples were fixed in 10% formalin and transferred to 70% EtOH after 48 h.

All specimens described in our study are considered larvae because they exhibit specializations for pelagic life (head spination, long fin elements) and are pigmented differently than juveniles and adults are pigmented (Leis, 1987; Leis and Trnski, 1989; Leis et al., 1997). Myomere and fin-ray counts were made on the left side of the body. Illustrations were made with a camera lucida. Preserved eggs and larvae were measured to the nearest 0.1 mm with an ocular micrometer fitted to a dissecting microscope. Body length (BL) as defined in Leis and Rennis (1983) is equivalent to notochord length or standard length depending on the stage of development of the larvae. Notochord length is the straight line distance from the tip of the snout to the posterior tip of the notochord and is used as the standard measurement before and during flexion. Standard length is the distance from the tip of the snout along the midline to a vertical line through the posterior edge of the hypural plate. Other common measurements and abbreviations follow Leis and Rennis (1983). Additional abbreviations used here are as follows:

avm = anterior surface of the visceral mass;
BD = body depth;
IPo = inner border of the preopercle (=anterior border of some authors);
OPo = outer border of the preopercle (=posterior border of some authors);
pav = postanal-ventral.

Results

Description of reared larvae

General development (Table 1, Figs. 1–5) Red snapper eggs (AL) were 0.72–0.76 mm in diameter (n=4) at one hour after fertilization and contained a single oil globule (diameter 0.11–0.13 mm). Larvae hatched in approximately 24 h and had a large, elongate yolk sac extending anteriorly beyond the head with a single oil globule. The oil globule was the last portion of the yolk to be absorbed at 4 days after hatching (DAH). Body lengths of the youngest larvae measured were 1.9 mm at hatching (n=1), 2.5 mm at 12 h (n=1), and 2.8 mm at 28 h (n=1). The eyes were pigmented and the mouth was functional by the end of 2 DAH when larvae began to swim actively and feed. Larvae were initially elongate (10% BD at 2.9 mm) but became deeper bodied (43% BD at 4.9 mm) and laterally compressed with development. The smallest larvae (2.5–3.1 mm) showed no fin development or spination. Head length increased from 9% BL in preflexion larvae (2.4 mm) to 42% BL in postflexion larvae (7.5 mm). Teeth appeared along the premaxilla and dentary by 3.5 mm. The gut was initially straight but began to coil at 2.4 mm (6 DAH) and was fully coiled by 3.6 mm (9 DAH). Preanal length increased from 38% BL (2.4 mm) in preflexion larvae to 69% BL in postflexion larvae (16.5 mm). Gas bladder inflation occurred at 4 DAH, and in our study the gas bladder was visible in the 2.4-mm (6 DAH) larva. Notochord flexion began at 3.8 mm (12 DAH) and was complete by 5.5 mm (15 DAH). Scales were present on the largest specimen (26.3 mm, 34 DAH).

Spination (Figs. 1–5) All spines described here were easily visible without clearing and staining. Head spination began by 3.0 mm with the development of preopercular spines, with one spine on the inner border of the preopercle (IPo) and two spines (including the angle spine) on the outer border of the preopercle (OPo). At 3.6 mm, there were two spines on the IPo and four spines on the OPo, one above the angle spine and two below. Spines increased to three on the IPo and five on the OPo by 3.8 mm. At 5.6 mm, there were four spines on the IPo and six spines on the OPo, four below and one above the angle. Spines on the IPo increased to six by 12.2 mm, and on the OPo increased to eight with six below and one above the angle. Spines on the preopercle in the two largest specimens were smaller (reduced in size) and more numerous than in smaller specimens. One interopercular spine was observed between the angle spine and the upper OPo spine by 3.5 mm and was present throughout the rest of the series. An opercular spine was present by 4.4 mm and a postcleithral spine was present just above the pectoral-fin base by 9.6 mm. One supracleithral spine formed by 3.6 mm on the 9-DAH specimen and two supracleithral spines were present on the 3.6-mm (10-DAH) specimen. There were three supra-

Table 1

Measurements (mm) of reared larval red snapper. — = not measured owing to damage. TX = Texas; AL = Alabama.

Source	Age (DAH)	Body length (BL)	Head length	% Head length/BL	Preanal length	% Preanal length/BL	Body depth at cleithrum	% Body depth/BL	Eye diameter	% Eye diameter/BL
TX	4–6	1.93	0.48	24.87	0.84	43.52	0.35	18.13	0.21	10.88
TX	1	2.02	0.20	9.90	1.01	50.00	0.56	27.72	—	—
TX	5	2.06	0.42	20.39	0.80	38.83	0.30	14.56	0.18	8.74
TX	4–6	2.07	0.42	20.29	0.83	40.10	0.35	16.91	0.23	11.11
TX	1	2.10	0.24	11.43	0.99	47.14	0.38	18.10	—	—
TX	4–6	2.16	0.51	23.61	1.11	51.39	0.32	14.81	0.21	9.72
AL	6	2.16	0.46	21.30	1.03	47.69	0.39	18.06	0.22	10.19
AL	6	2.16	0.52	24.07	1.05	48.61	0.43	19.91	0.25	11.57
TX	4–6	2.21	0.39	17.65	0.93	42.08	0.35	15.84	0.21	9.50
TX	5	2.24	0.50	22.32	0.90	40.18	0.32	14.29	0.20	8.93
TX	3	2.30	0.39	16.96	0.90	39.13	0.29	12.61	0.20	8.70
AL	6	2.33	0.42	18.03	0.95	40.77	0.37	15.88	0.22	9.44
AL	6	2.34	0.48	20.51	1.08	46.15	0.40	17.09	0.23	9.83
AL	6	2.35	0.46	19.57	1.02	43.40	0.43	18.30	0.25	10.64
TX	1	2.35	0.21	8.94	1.17	49.79	0.51	21.70	—	—
TX	10	2.40	0.59	24.58	0.92	38.33	0.35	14.58	0.24	10.00
TX	4–6	2.40	0.41	17.08	0.99	41.25	0.30	12.50	0.20	8.33
AL	6	2.42	0.49	20.25	1.08	44.63	0.46	19.01	0.25	10.33
TX	1	2.44	0.29	11.89	1.19	48.77	0.42	17.21	—	—
TX	4–6	2.44	0.42	17.21	1.08	44.26	0.33	13.52	0.23	9.43
TX	1	2.44	0.35	14.34	1.17	47.95	0.56	22.95	—	—
TX	4–6	2.44	0.53	21.72	1.14	46.72	0.36	14.75	0.23	9.43
TX	5	2.47	0.53	21.46	0.96	38.87	0.38	15.38	0.23	9.31
TX	1	2.49	0.27	10.84	1.19	47.79	0.42	16.87	—	—
TX	4–6	2.49	0.48	19.28	1.11	44.58	0.36	14.46	0.20	8.03
AL	6	2.53	0.54	21.34	1.11	43.87	0.43	17.00	0.26	10.28
AL	6	2.53	0.51	20.16	1.09	43.08	0.46	18.18	0.25	9.88
TX	3	2.53	0.50	19.76	1.13	44.66	0.32	12.65	0.23	9.09
AL	6	2.53	0.52	20.55	1.08	42.69	0.45	17.79	0.25	9.88
TX	3	2.54	0.44	17.32	0.99	38.98	0.32	12.60	0.21	8.27
TX	1	2.54	0.30	11.81	1.20	47.24	0.44	17.32	—	—
TX	1	2.54	0.33	12.99	1.25	49.21	0.53	20.87	—	—
TX	1	2.54	0.27	10.63	1.22	48.03	0.42	16.54	—	—
TX	1	2.54	0.32	12.60	1.22	48.03	0.53	20.87	—	—
TX	3	2.59	0.41	15.83	1.08	41.70	0.36	13.90	0.21	8.11
TX	4–6	2.59	0.51	19.69	1.11	42.86	0.32	12.36	0.22	8.49
TX	3	2.59	0.35	13.51	1.11	42.86	0.32	12.36	0.18	6.95
TX	3	2.59	0.47	18.15	1.14	44.02	0.29	11.20	0.20	7.72
TX	4–6	2.59	0.49	18.92	1.08	41.70	0.38	14.67	0.21	8.11
TX	4–6	2.59	0.50	19.31	1.16	44.79	0.33	12.74	0.20	7.72
AL	6	2.60	0.55	21.15	1.12	43.08	0.48	18.46	0.25	9.62
AL	7	2.60	0.70	26.92	1.20	46.15	0.60	23.08	0.31	11.92
TX	3	2.63	0.51	19.39	1.26	47.91	0.32	12.17	0.17	6.46
TX	3	2.63	0.51	19.39	1.17	44.49	0.30	11.41	0.23	8.75
TX	4–6	2.63	0.48	18.25	1.08	41.06	0.38	14.45	0.21	7.98
TX	1	2.63	0.29	11.03	1.23	46.77	0.45	17.11	—	—
TX	1	2.63	0.27	10.27	1.19	45.25	0.39	14.83	—	—

continued

Table 1 (continued)

Source	Age (DAH)	Body length (BL)	Head length	% Head length/BL	Preanal length	% Preanal length/BL	Body depth at cleithrum	% Body depth/BL	Eye diameter	% Eye diameter/BL
TX	10	2.63	0.62	23.57	1.10	41.83	0.40	15.21	0.26	9.89
TX	12	2.65	0.63	23.77	1.22	46.04	0.44	16.60	0.18	6.79
TX	10	2.67	0.63	23.60	1.17	43.82	0.38	14.23	0.27	10.11
TX	4–6	2.68	0.53	19.78	1.13	42.16	0.40	14.93	0.21	7.84
TX	4–6	2.68	0.54	20.15	1.13	42.16	0.36	13.43	0.24	8.96
TX	3	2.68	0.47	17.54	1.08	40.30	0.32	11.94	0.18	6.72
TX	4–6	2.68	0.56	20.90	1.20	44.78	0.35	13.06	0.20	7.46
TX	4–6	2.68	0.54	20.15	1.16	43.28	0.39	14.55	0.23	8.58
TX	1	2.68	0.26	9.70	1.23	45.90	0.51	19.03	—	—
TX	3	2.68	0.51	19.03	1.13	42.16	0.30	11.19	0.21	7.84
TX	4–6	2.68	0.47	17.54	1.10	41.04	0.34	12.69	0.21	7.84
TX	6	2.73	0.60	21.98	1.22	44.69	0.33	12.09	0.23	8.42
TX	3	2.73	0.50	18.32	1.17	42.86	0.33	12.09	0.23	8.42
TX	6	2.73	0.60	21.98	1.20	43.96	0.36	13.19	0.23	8.42
TX	3	2.73	0.48	17.58	1.11	40.66	0.32	11.72	0.23	8.42
TX	10	2.73	0.65	23.81	1.23	45.05	0.41	15.02	0.27	9.89
TX	3	2.73	0.41	15.02	1.31	47.99	0.30	10.99	0.23	8.42
TX	3	2.77	0.51	18.41	1.17	42.24	0.30	10.83	0.21	7.58
TX	5	2.80	0.54	19.29	1.17	41.79	0.30	10.71	0.20	7.14
TX	3	2.82	0.45	15.96	1.17	41.49	0.30	10.64	0.21	7.45
TX	13	2.91	0.83	28.52	1.23	42.27	0.66	22.68	0.36	12.37
TX	3	2.91	0.53	18.21	1.26	43.30	0.30	10.31	0.23	7.90
TX	12	2.99	0.70	23.41	1.37	45.82	0.45	15.05	0.30	10.03
TX	17	3.00	0.77	25.67	1.43	47.67	0.59	19.67	0.30	10.00
TX	12	3.05	0.68	22.30	1.34	43.93	0.48	15.74	0.30	9.84
TX	12	3.11	0.69	22.19	1.28	41.16	0.47	15.11	0.29	9.32
TX	13	3.20	0.81	25.31	1.39	43.44	0.63	19.69	0.33	10.31
TX	13	3.28	0.82	25.00	1.41	42.99	0.53	16.16	0.32	9.76
TX	16	3.30	0.96	29.09	1.49	45.15	0.65	19.70	0.36	10.91
AL	11	3.38	1.06	31.36	1.73	51.18	1.18	34.91	0.43	12.72
TX	16	3.42	0.96	28.07	1.59	46.49	0.72	21.05	0.31	9.06
AL	9	3.51	1.06	30.20	1.68	47.86	1.03	29.34	0.41	11.68
AL	10	3.51	1.06	30.20	1.70	48.43	1.01	28.77	0.41	11.68
TX	13	3.52	0.95	26.99	1.68	47.73	0.68	19.32	0.33	9.38
AL	12	3.64	1.22	33.52	1.93	53.02	1.41	38.74	0.52	14.29
TX	16	3.65	1.08	29.59	1.70	46.58	1.00	27.40	0.41	11.23
TX	16	3.80	1.16	30.53	1.82	47.89	1.00	26.32	0.50	13.16
AL	13	4.42	1.73	39.14	2.50	56.56	1.80	40.72	0.62	14.03
AL	14	4.81	1.74	36.17	2.68	55.72	2.07	43.04	0.66	13.72
AL	15	5.27	2.07	39.28	3.01	57.12	2.16	40.99	0.75	14.23
AL	16	5.40	1.97	36.48	3.15	58.33	2.16	40.00	0.75	13.89
AL	19	7.54	3.15	41.78	4.70	62.33	2.91	38.59	1.03	13.66
AL	17	9.49	3.42	36.04	5.58	58.80	3.42	36.04	1.35	14.23
AL	26	12.20	4.23	34.67	7.74	63.44	4.23	34.67	1.53	12.54
AL	21	15.34	5.20	33.90	9.23	60.17	5.59	36.44	1.95	12.71
AL	33	16.50	6.63	40.18	11.44	69.33	6.76	40.97	2.47	14.97
AL	35	18.10	6.37	35.19	11.57	63.92	6.89	38.07	2.47	13.65
AL	26	20.50	7.02	34.24	13.00	63.41	7.28	35.51	2.60	12.68
AL	34	26.10	9.62	36.86	16.90	64.75	9.62	36.86	3.25	12.45

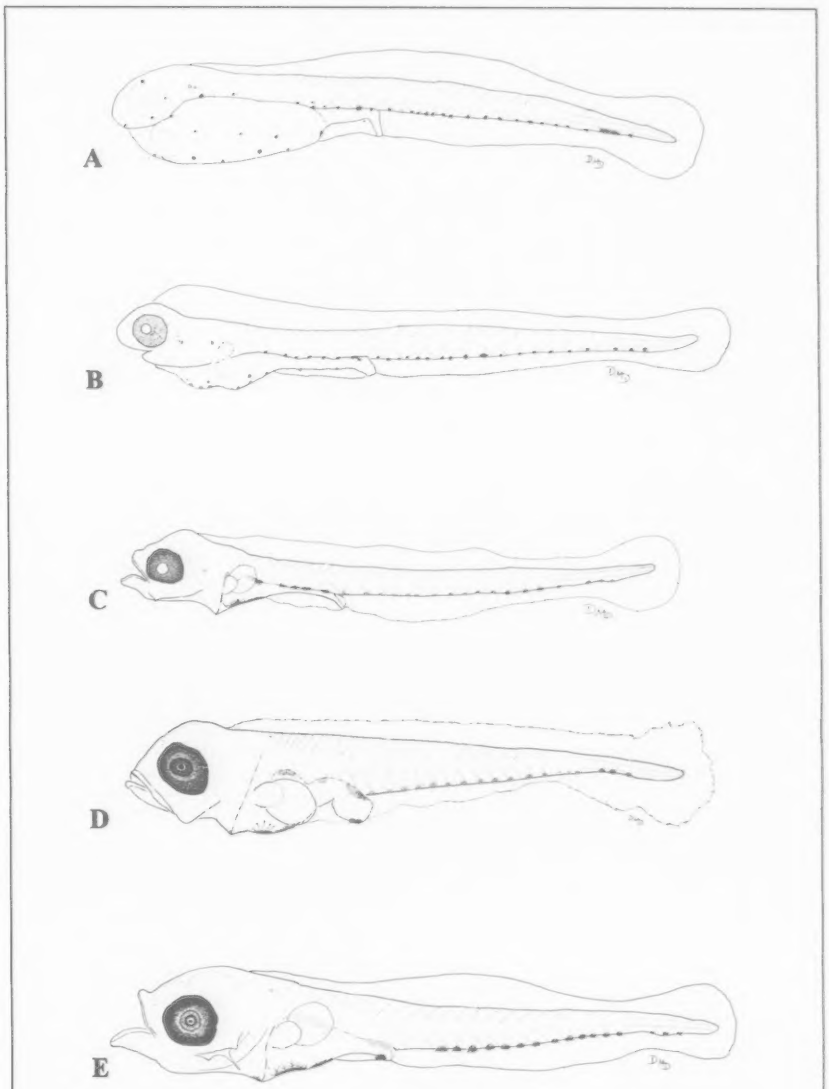

Figure 1

Preflexion larvae of reared *Lutjanus campechanus:* (**A**) 2.5 mm, 1 DAH, from TX; (**B**) 2.6 mm, 3 DAH, from TX; (**C**) 2.8 mm, 5 DAH, from TX; (**D**). 2.4 mm, 6 DAH, from AL; (**E**) 3.1 mm, 12 DAH, from TX.

cleithral spines on the 3.5-mm (11-DAH) specimen and by 4.9 mm (14 DAH), four supracleithral spines were present. A posttemporal spine had developed by 3.8 mm (12 DAH), and by 5.5 mm (15 DAH) there were two posttemporal spines. A supraocular ridge formed by 3.8 mm and one spine developed on the ridge by 4.4 mm (13 DAH). Two, three, and four additional spines were present on the supraocular ridge by 4.9 mm (14 DAH), 5.6 mm (16 DAH), and 9.6 mm (17 DAH), respectively.

Fin development (Table 2, Figs. 1–5) Sequence of fin-ray formation can be characterized either by initial or completed development of fin elements. The order of development, based on initial development as reported by Potthoff et al. (1988), for red snapper is first dorsal, then pelvic, caudal, second dorsal, anal, pectoral. Order by completed development as reported by Johnson (1984) for lutjanids in general is first dorsal, then pelvic, second dorsal, anal, pectoral. Elements of the dorsal and pelvic fins began forming

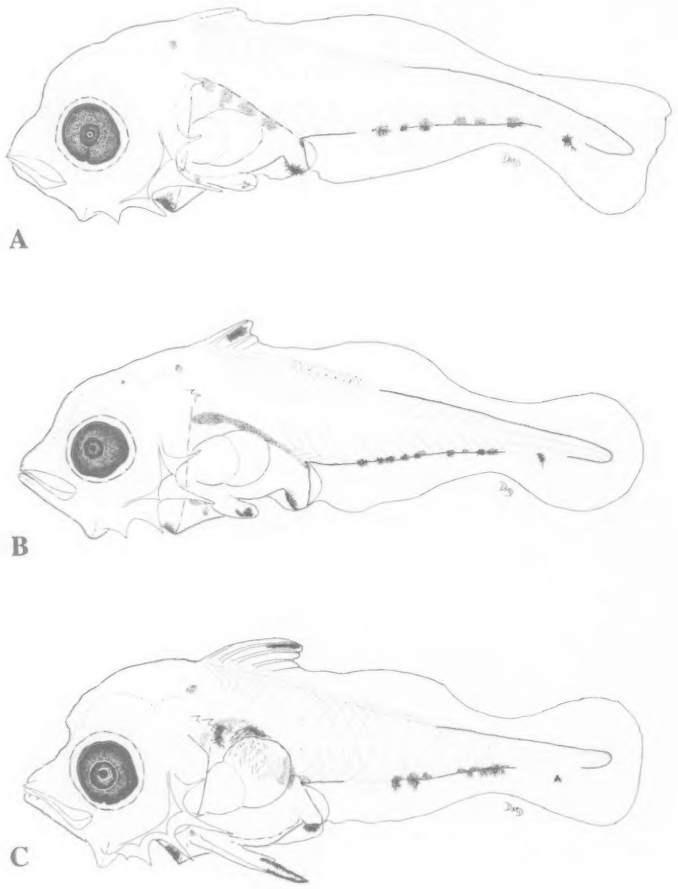

Figure 2

Preflexion reared *Lutjanus campechanus* larvae. (**A**) 3.6 mm, 9 DAH, from AL; (**B**) 3.6 mm, 10 DAH, from AL; (**C**) 3.5 mm, 11 DAH, from AL.

at >3.6 mm between 9 and 11 DAH. The second spine of the dorsal fin was first to develop followed by the third, then the first and fourth spines. Development of the remaining dorsal-fin elements proceeded posteriorly; the tenth dorsal spine initially formed as a raylike element. Fine serrations were present on the leading edge of the pelvic spine at 3.8 mm (12 DAH). Anal-fin development began by 3.6 mm (11 DAH) and by 3.8 mm (12 DAH) the first anal spine began to form. Development of the remaining anal-fin elements proceeded posteriorly; the third anal spine initially forming as a raylike element. All fin spines were V-shaped in cross section. Caudal rays were first noticeable at 4.4 mm (13 DAH) and pectoral-fin rays began forming at 5.5 mm (15 DAH). By 9.6 mm (17 DAH), all elements in the dorsal, pelvic, and anal fins were formed. Formation of pectoral rays and both principal and procurrent rays of the caudal fin was completed by 12.2 mm.

Pigmentation (Figs. 1–5) *Head* Small melanophores were scattered over the head of day-old yolksac larvae at 2.5 mm. These melanophores were not present in 3 DAH larvae but small melanophores were present in the otic capsule of 2.6- and 2.8-mm larvae (3 and 5 DAH). A melanophore appeared over the midbrain at 3.6 mm and with development, both internal and external head pigment increased until at 9.6 mm, most of the surface of the head above the midbrain was covered with small melanophores. Pigment on the surface of the head over the forebrain was

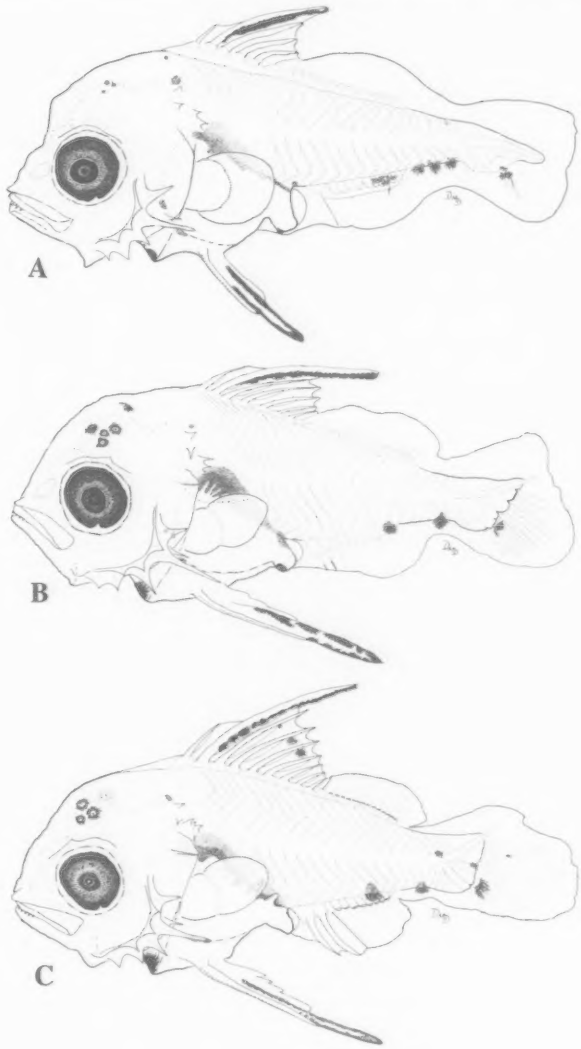

Figure 3

Early flexion and flexion reared *Lutjanus campechanus* larvae: (**A**) 3.8 mm, 12 DAH, from AL; (**B**) 4.4 mm, 13 DAH, from AL; (**C**). 4.9 mm, 14 DAH, from AL.

present by 9.6 mm, and by 12.2 mm the forebrain region was covered with many small melanophores. An internal nape melanophore was present at 3.1 mm and persisted until overlying tissue obscured it. Pigment did not appear on the operculum until 5.5 mm, and by 9.6 mm additional small melanophores were present dorsal to the operculum pigment and posterior to the orbit. Pigment first appeared on the tip of the premaxilla at 9.6 mm and increased over the snout and on the lower jaw by 12.2 mm. The head region and jaws of the 26.3-mm specimen were densely covered with pigment. A melanophore lying just anterior to the cleithral symphysis first appeared by 2.4 mm (6 DAH) and remained visible throughout the developmental series until becoming obscured by tissue in fish larger than 12.0 mm.

Body Numerous melanophores were scattered over the yolk sac and dorsal surface of the gut in the smallest larvae. The number of melanophores over the gut and

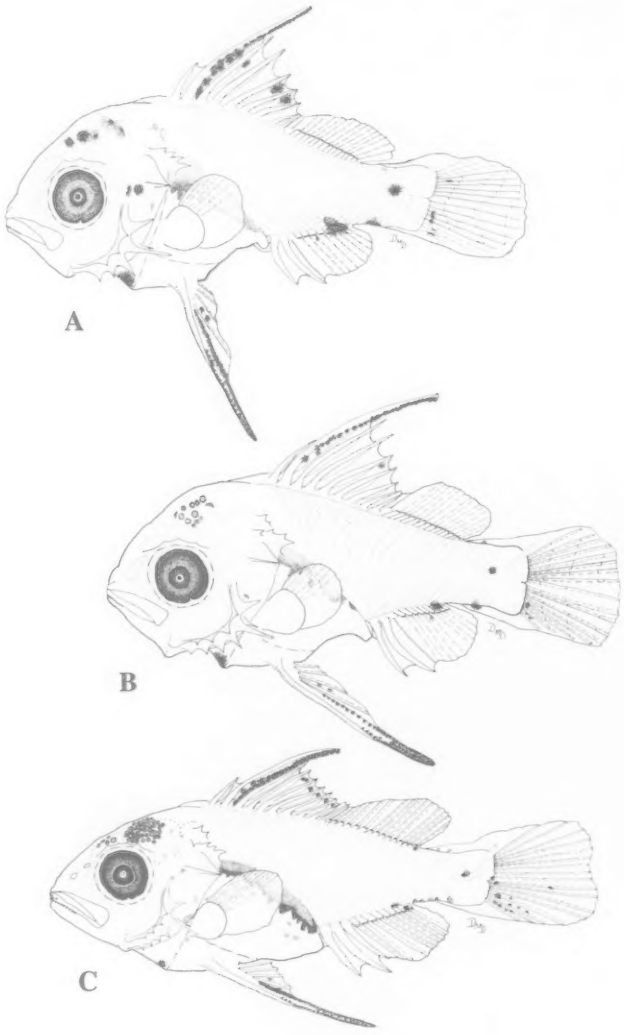

Figure 4

Flexion and postflexion reared *Lutjanus campechanus* larvae: (**A**) 5.5 mm, 15 DAH, from AL; (**B**) 5.6 mm, 16 DAH, from AL; (**C**). 9.6 mm, 17 DAH, from AL.

gas bladder increased until 3.6 mm when this pigment appeared as a solid melanistic patch. Pigment on the ventral surface of the trunk (between the cleithrum and the anus) consisted of one or two melanophores that were present until the pelvic fin bud emerged. As the pelvic fin developed, this pigment migrated internally to a position anterodorsal to the insertion of the pelvic fin and remained discernible through the body wall of specimens up to 4.9 mm. One melanophore was also present on the ventral surface of the hindgut just anterior to the anus over the size range of 2.4 mm to 4.4 mm. A melanophore was present in the peritoneum on the anterior surface of the visceral mass (avm) at the level of the pectoral-fin base and was visible through the operculum in the 3.6-, 3.8-, 4.4-, and 5.6-mm specimens. This melanophore was more easily observed when the operculum was lifted. Additional data from larvae (n=96) raised at GCRL showed that the avm melanophore was first present in larvae as small as

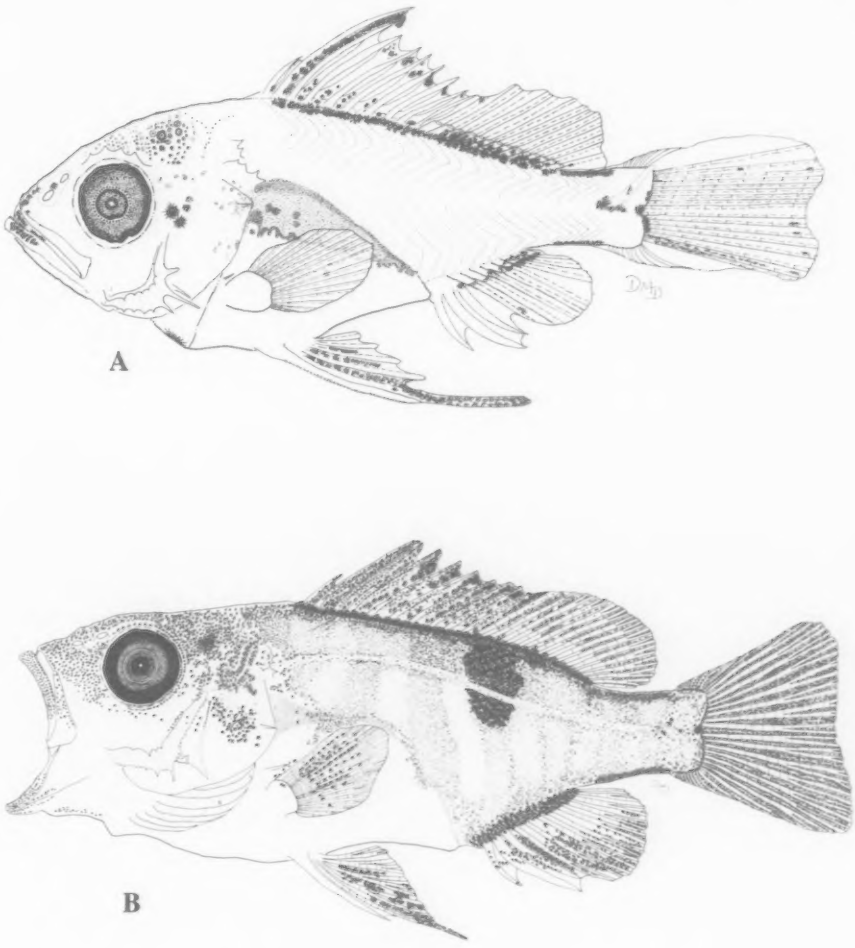

Figure 5

Postflexion reared *Lutjanus campechanus* larvae: (**A**) 12.2 mm, 26 DAH, from AL; (**B**) 26.3 mm, 34 DAH, from AL. Scales omitted from illustration.

3.4 mm (preflexion) and was found in all specimens ≥3.6 mm. When present, this spot lies above the internal melanophore that is located anterodorsal to the insertion of the developing pelvic fin.

Melanophores that form a postanal ventral (pav) series on the tail were most numerous (18–20) in the smallest larvae and decreased in number with development. The pav series is further characterized by the presence of a gap posteriorly and by the presence of one to four melanophores (typically three) located after the gap in the hypural area. As flexion began (3.8 mm), three melanophores were present on the caudal peduncle, but these melanophores coalesced to form a single ventral spot on the caudal peduncle in postflexion larvae up to 9.6 mm. In larger larvae, additional melanophores lined the entire ventral edge of the caudal peduncle. At the beginning of flexion, one to three melanophores were present over the ventral edge of the hypural plate anlagen. As flexion progressed, this pigment bent up with the hypural elements and came to lie at the base of the ventral caudal rays. A melanophore at the flexure of the notochord on the caudal peduncle first appeared in the 4.9-mm larva. It remained prominent until extensive surface pigment on the body obscured it in the largest specimen. Dorsal pigment on the caudal peduncle appeared in the 3.8-mm early flexion larva in the form of a single internal melanophore. This

Table 2

Meristics and spine lengths of reared larval red snapper. nd = not developed, i = incipient ray(s) or spine(s). AL = Alabama; TX = Texas. P_2 = pelvic fin.

Source	Body length (BL)	Dorsal fin spines and rays	2nd dorsal spine length	% 2nd dorsal spine length/BL	3rd dorsal spine length	% 3rd dorsal spine length/BL	P_2 spine length	% P_2 spine length/BL	P_2 ray length	% P_2 ray length/BL	Anal fin spines and rays
AL	3.57	ii	nd	nd	nd	nd	bud	nd	bud	nd	nd
AL	3.57	IIi	0.32	8.96	0.21	5.88	bud	nd	bud	nd	nd
AL	3.57	IIIii	0.53	14.85	0.38	10.64	0.24	6.72	0.45	12.61	nd
TX	3.65	III	0.36	9.86	0.21	5.75	0.26	7.12	0.42	11.51	nd
AL	3.76	Vii	0.89	23.67	0.60	15.96	0.55	14.63	0.86	22.87	i
TX	3.80	IIIi	0.54	14.21	0.29	7.63	0.27	7.11	0.50	13.16	nd
AL	4.40	VIIi	1.45	32.95	0.91	20.68	1.05	23.86	1.64	37.27	Iii
AL	4.85	IXi,(14i)	1.75	36.08	1.06	21.86	1.22	25.15	1.82	37.53	II,(9i)
AL	5.47	IXi,(14i)	1.85	33.82	1.32	24.13	1.32	24.13	2.16	39.49	II,(9i)
AL	5.64	IXi,(14i)	2.16	38.30	1.42	25.18	1.37	24.29	2.09	37.06	II,(10i)
AL	7.54	IXi,(14i)	2.49	33.02	1.74	23.08	2.11	27.98	3.02	40.05	III,8
AL	9.59	X,15	2.91	30.34	2.02	21.06	2.07	21.58	3.10	32.33	III,9
AL	12.20	X,14	3.15	25.82	2.44	20.00	2.82	23.11	3.38	27.70	III,8
AL	15.34	X,14	3.71	24.19	3.06	19.95	2.96	19.30	4.61	30.05	III,9
AL	16.50	X,13	3.76	22.79	3.24	19.64	3.71	22.48	4.95	30.00	III,8
AL	18.10	IXi,14	3.71	20.50	3.20	17.68	3.10	17.13	12.87	71.10	III,9
AL	20.50	X,14	4.42	21.56	3.90	19.02	4.51	22.00	2.91	14.20	III,9
AL	26.10	X,14	4.56	17.47	4.47	17.13	4.32	16.55	6.75	25.86	III,8

pigment was absent in the next two larvae in the series (4.4 and 4.9 mm) but it was present in the remaining larvae of the series. Additional melanophores were added until the entire dorsal surface of the caudal peduncle was lined with pigment by 12.2 mm.

Fins Melanophores were present on the pelvic fin bud at its emergence in the 3.6-mm (9 DAH) specimen. This pigment became concentrated on the first ray and in the membrane between the first and second rays as fin elements developed. Melanophores appeared on the membrane between the second and third rays by 5.5 mm and continued to increase until pigment was present between the first four pelvic rays by 12.2 mm. Pigment appeared in the dorsal-fin membrane behind the second dorsal spine by 3.6 mm (10 DAH) and continued to increase as that spine grew, so that pigment extended out along the entire length of the spine. At 4.9 mm, additional melanophores were present near the distal margin of the dorsal-fin membrane between the third and fourth, fourth and fifth, and fifth and sixth spines. This latter condition was not consistent over the series; the 5.5-mm specimen had pigment between the third and fourth, fifth and sixth, sixth and seventh spines, whereas the 5.6-mm specimen had pigment only between the fifth and sixth spines. As seen in the largest specimens of the series, pigment eventually developed in the membrane between all of the dorsal spines but pigment was consistently most extensive behind the second dorsal spine. By 12.2 mm, melanophores appeared in the proximal region of the fin membrane at the base of the spines. One melanophore was present at the base of the last dorsal ray by 9.6 mm, and by 12.2 mm pigment covered the entire base of the dorsal fin. As the anal fin formed, one to four melanophores from the pav series persisted over the posterior pterygiophores. At sizes larger than 9.6 mm, additional melanophores began to form on the anal fin base, and by 12.2 mm the pterygiophores of the last six rays were pigmented and eventually the entire anal-fin base was covered. The distal region of the anal fin and the pectoral fin were extensively pigmented in the 26.3-mm specimen. Pigment on the caudal-fin rays first developed on the ventralmost rays and subsequently near the posterior margin of the fin until in the 26.3-mm specimen, the membrane between the rays was pigmented from the base out to the edge of the fin.

Comparison of reared and wild larvae

Reared and wild red snapper larvae were examined and compared to determine variability and usefulness of various developmental characters (Figs. 1–6; Tables 1–4). Field-collected larvae were identified as red snapper by the presence of morphological and pigmentational features described in Collins et al. (1980) and Richards et al. (1994), as well as by their general resemblance to the reared larvae described in our study. All wild larvae were collected in shelf waters in the northcentral GOM, where

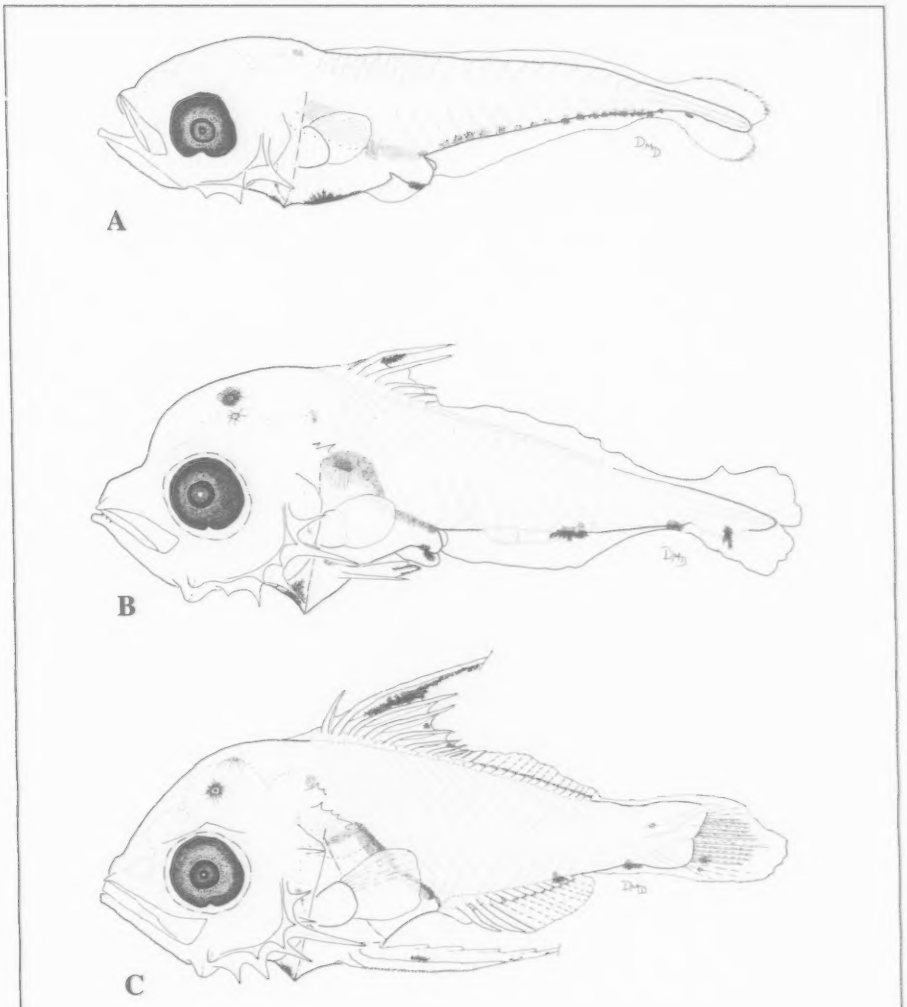

Figure 6

Preflexion and flexion wild *Lutjanus campechanus*: (**A**) 2.6 mm., GCRL 1708; (**B**) 3.5 mm, SEAMAP 14766; (**C**) 5.2 mm, GCRL 1753B.

relatively few species of lutjanids (larvae or adults) occur in abundance [SEAMAP Atlas 1985–1995 (Thompson et al., 1988; Sanders et al., 1990a, 1990b, 1991a, 1991b, 1992; Donaldson et al. 1993, 1994, 1996, 1997a, 1997b); longline data, (Jones[2]); video data, (Gledhill[3])].

There were no notable or consistent differences between laboratory-reared and field-caught red snapper larvae in pigmentation, development or morphometry at similar stages of development. Presence of avm pigment, number of pav spots, and arrangement of median fin pigment among wild larvae matched the appearance of these features in reared larvae at about the same stage of development (Figs. 2–6). Differences in size at stage of development that were evident were probably caused by net-related shrinkage or abrasion, or by both (Theilacker, 1980). We observed no consistent differences in pigment that could have been caused by rearing conditions. Median fin element development in wild red snapper larvae appeared at smaller sizes

[2] Jones, L. M. 1998. Personal commun. Mississippi Laboratories, Southeast Fisheries Science Center, National Marine Fisheries Service, PO Drawer 1207, Pascagoula, MS 39568-1207.

[3] Gledhill, C. T. 1998. Personal commun. Mississippi Laboratories, Southeast Fisheries Science Center, National Marine Fisheries Service, PO Drawer 1207, Pascagoula, MS 39568-1207.

Table 3

Measurements (mm) of wild larval red snapper. — = not measure owing to damage. GCRL = Gulf Coast Research Laboratory; SEAMAP = Southeast Area Monitoring and Assessment Program.

Source	Body length (BL)	Head length	% Head length/BL	Preanal length	% Preanal length/BL	Body depth at cleithrum	% Body depth/BL	Orbit diameter	% Orbit diameter/BL
GCRL	2.60	0.79	30.38	1.39	53.46	0.77	29.62	0.34	13.08
GCRL	2.60	0.75	28.85	1.36	52.31	0.66	25.38	0.30	11.54
GCRL	2.60	0.77	29.62	1.27	48.85	0.79	30.38	0.34	13.08
GCRL	2.73	0.79	28.94	1.30	47.62	0.74	27.11	0.29	10.62
GCRL	2.73	0.84	30.77	1.44	52.75	0.79	28.94	0.36	13.19
GCRL	2.86	0.72	25.17	1.25	43.71	0.77	26.92	0.31	10.84
GCRL	2.86	0.77	26.92	1.44	50.35	0.72	25.17	0.34	11.89
SEAMAP	2.86	1.27	44.41	1.41	49.30	1.18	41.26	0.47	16.43
GCRL	2.99	0.89	29.77	1.46	48.83	0.82	27.42	0.43	14.38
GCRL	2.99	0.91	30.43	1.61	53.85	0.89	29.77	0.36	12.04
GCRL	2.99	0.99	33.11	1.74	58.19	1.08	36.12	0.38	12.71
SEAMAP	2.99	1.08	36.12	1.63	54.52	0.98	32.78	0.38	12.71
SEAMAP	2.99	1.10	36.79	1.56	52.17	1.15	38.46	0.41	13.71
SEAMAP	2.99	1.37	45.82	1.97	65.89	1.32	44.15	0.46	15.38
GCRL	3.12	0.85	27.24	1.46	46.79	0.89	28.53	0.33	10.58
GCRL	3.12	0.91	29.17	1.56	50.00	0.86	27.56	0.41	13.14
GCRL	3.12	0.98	31.41	1.56	50.00	0.89	28.53	0.38	12.18
GCRL	3.12	0.89	28.53	1.42	45.51	0.86	27.56	0.31	9.94
SEAMAP	3.12	1.08	34.62	1.63	52.24	0.96	30.77	0.41	13.14
SEAMAP	3.12	1.13	36.22	1.50	48.08	1.18	37.82	0.47	15.06
SEAMAP	3.12	1.27	40.71	1.65	52.88	1.13	36.22	0.52	16.67
GCRL	3.25	1.13	34.77	1.61	49.54	1.01	31.08	0.38	11.69
GCRL	3.25	0.89	27.38	1.55	47.69	0.89	27.38	0.38	11.69
GCRL	3.25	1.13	34.77	1.79	55.08	1.22	37.54	0.42	12.92
SEAMAP	3.25	1.27	39.08	1.69	52.00	1.13	34.77	0.47	14.46
GCRL	3.38	0.91	26.92	1.61	47.63	1.03	30.47	0.36	10.65
GCRL	3.38	0.94	27.81	1.49	44.08	0.91	26.92	0.36	10.65
GCRL	3.38	1.20	35.50	1.68	49.70	1.03	30.47	0.41	12.13
SEAMAP	3.38	0.98	28.99	1.51	44.67	1.13	33.43	0.41	12.13
SEAMAP	3.38	1.15	34.02	1.58	46.75	1.15	34.02	0.43	12.72
SEAMAP	3.38	1.13	33.43	1.70	50.30	1.22	36.09	0.38	11.24
SEAMAP	3.38	1.27	37.57	1.75	51.78	1.25	36.98	0.48	14.20
SEAMAP	3.38	1.41	41.72	1.83	54.14	1.41	41.72	0.45	13.31
SEAMAP	3.38	1.41	41.72	1.93	57.10	1.36	40.24	0.52	15.38
GCRL	3.51	1.13	32.19	1.75	49.86	0.98	27.92	0.43	12.25
GCRL	3.51	1.22	34.76	1.83	52.14	1.13	32.19	0.38	10.83
GCRL	3.51	1.15	32.76	1.85	52.71	1.20	34.19	0.43	12.25
SEAMAP	3.51	1.25	35.61	—	—	1.20	34.19	0.41	11.68
SEAMAP	3.51	1.22	34.76	1.69	48.15	1.22	34.76	0.47	13.39
SEAMAP	3.51	1.41	40.17	1.93	54.99	1.36	38.75	0.52	14.81
SEAMAP	3.51	1.41	40.17	2.07	58.97	1.41	40.17	0.47	13.39
GCRL	3.64	0.79	21.70	1.44	39.56	0.86	23.63	0.38	10.44
GCRL	3.64	1.10	30.22	1.75	48.08	1.08	29.67	0.43	11.81
GCRL	3.64	1.10	30.22	1.75	48.08	1.13	31.04	0.41	11.26
SEAMAP	3.64	1.32	36.26	1.88	51.65	1.27	34.89	0.47	12.91
SEAMAP	3.64	1.50	41.21	1.97	54.12	1.50	41.21	0.52	14.29

continued

Table 3 (continued)

Source	Body length (BL)	Head length	% Head length/BL	Preanal length	% Preanal length/BL	Body depth at cleithrum	% Body depth/BL	Orbit diameter	% Orbit diameter/BL
SEAMAP	3.64	1.27	34.89	1.83	50.27	1.22	33.52	0.52	14.29
GCRL	3.77	1.18	31.30	1.80	47.75	1.15	30.50	0.43	11.41
GCRL	3.77	1.03	27.32	1.74	46.15	1.18	31.30	0.42	11.14
GCRL	3.77	1.13	29.97	1.83	48.54	1.13	29.97	0.47	12.47
GCRL	3.77	1.27	33.69	1.87	49.60	1.22	32.36	0.46	12.20
SEAMAP	3.77	1.66	44.03	2.28	60.48	1.56	41.38	0.53	14.06
SEAMAP	3.77	1.20	31.83	1.73	45.89	1.42	37.67	0.58	15.38
SEAMAP	3.77	1.56	41.38	2.11	55.97	1.49	39.52	0.55	14.59
SEAMAP	3.77	1.41	37.40	1.88	49.87	1.46	38.73	0.56	14.85
SEAMAP	3.77	1.41	37.40	2.02	53.58	1.50	39.79	0.52	13.79
SEAMAP	3.77	1.65	43.77	2.21	58.62	1.55	41.11	0.52	13.79
SEAMAP	3.81	1.55	40.68	2.21	58.01	1.41	37.01	0.52	13.65
SEAMAP	3.84	1.50	39.06	2.12	55.21	1.46	38.02	0.47	12.24
SEAMAP	3.90	1.36	34.87	1.97	50.51	1.46	37.44	0.47	12.05
GCRL	3.90	1.46	37.44	2.16	55.38	1.46	37.44	0.56	14.36
SEAMAP	3.90	1.32	33.85	1.93	49.49	1.36	34.87	0.56	14.36
SEAMAP	3.90	1.46	37.44	2.07	53.08	1.55	39.74	0.52	13.33
SEAMAP	3.90	1.41	36.15	2.02	51.79	1.55	39.74	0.52	13.33
GCRL	4.03	1.36	33.75	1.97	48.88	1.27	31.51	0.52	12.90
SEAMAP	4.03	1.32	32.75	2.11	52.36	1.44	35.73	0.43	10.67
GCRL	4.03	1.41	34.99	2.16	53.60	1.46	36.23	0.52	12.90
SEAMAP	4.03	1.50	37.22	2.12	52.61	1.55	38.46	0.56	13.90
SEAMAP	4.03	1.60	39.70	2.21	54.84	1.55	38.46	0.61	15.14
SEAMAP	4.03	1.50	37.22	2.07	51.36	1.46	36.23	0.56	13.90
SEAMAP	4.03	1.56	38.71	2.23	55.33	1.63	40.45	0.60	14.89
GCRL	4.16	1.27	30.53	2.02	48.56	1.22	29.33	0.47	11.30
GCRL	4.16	1.20	28.85	1.63	39.18	1.10	26.44	0.41	9.86
GCRL	4.16	1.41	33.89	2.21	53.13	1.50	36.06	0.52	12.50
GCRL	4.16	1.60	38.46	2.26	54.33	1.50	36.06	0.56	13.46
SEAMAP	4.16	1.55	37.26	2.16	51.92	1.60	38.46	0.56	13.46
SEAMAP	4.16	1.55	37.26	2.30	55.29	1.69	40.63	0.56	13.46
SEAMAP	4.16	1.65	39.66	2.30	55.29	1.55	37.26	0.56	13.46
SEAMAP	4.16	1.65	39.66	2.16	51.92	1.65	39.66	0.56	13.46
SEAMAP	4.29	1.50	34.97	2.07	48.25	1.41	32.87	0.52	12.12
SEAMAP	4.29	1.65	38.46	2.35	54.78	1.65	38.46	0.56	13.05
GCRL	4.29	1.50	34.97	2.30	53.61	1.46	34.03	0.56	13.05
SEAMAP	4.42	1.50	33.94	2.26	51.13	1.50	33.94	0.51	11.54
SEAMAP	4.42	1.60	36.20	2.07	46.83	1.65	37.33	0.56	12.67
SEAMAP	4.42	1.79	40.50	2.49	56.33	1.79	40.50	0.56	12.67
SEAMAP	4.42	1.50	33.94	2.44	55.20	1.69	38.24	0.61	13.80
GCRL	4.42	1.79	40.50	2.54	57.47	1.79	40.50	0.71	16.06
SEAMAP	4.55	1.55	34.07	2.44	53.63	1.65	36.26	0.52	11.43
SEAMAP	4.55	1.55	34.07	2.35	51.65	1.74	38.24	0.61	13.41
GCRL	4.55	1.79	39.34	2.49	54.73	1.74	38.24	0.66	14.51
SEAMAP	4.55	1.88	41.32	2.54	55.82	2.02	44.40	0.66	14.51
GCRL	4.68	1.65	35.26	2.54	54.27	1.74	37.18	0.56	11.97
GCRL	4.68	1.55	33.12	2.44	52.14	1.69	36.11	0.61	13.03
SEAMAP	4.68	1.69	36.11	2.44	52.14	1.65	35.26	0.56	11.97

continued

Table 3 (continued)

Source	Body length (BL)	Head length	% Head length/BL	Preanal length	% Preanal length/BL	Body depth at cleithrum	% Body depth/BL	Orbit diameter	% Orbit diameter/BL
SEAMAP	4.68	1.83	39.10	2.59	55.34	1.79	38.25	0.66	14.10
SEAMAP	4.81	1.69	35.14	2.44	50.73	1.74	36.17	0.56	11.64
SEAMAP	4.81	1.97	40.96	2.82	58.63	1.97	40.96	0.71	14.76
SEAMAP	4.81	1.93	40.12	2.77	57.59	1.97	40.96	0.56	11.64
SEAMAP	4.94	1.93	39.07	2.63	53.24	1.93	39.07	0.66	13.36
SEAMAP	4.94	1.97	39.88	2.73	55.26	2.12	42.91	0.71	14.37
GCRL	5.07	1.79	35.31	2.68	52.86	1.79	35.31	0.71	14.00
SEAMAP	5.07	1.88	37.08	2.73	53.85	1.88	37.08	0.61	12.03
SEAMAP	5.07	1.65	32.54	2.44	48.13	2.02	39.84	0.61	12.03
SEAMAP	5.07	1.93	38.07	2.73	53.85	1.79	35.31	0.71	14.00
GCRL	5.20	1.74	33.46	2.73	52.50	1.83	35.19	0.66	12.69
SEAMAP	5.20	1.93	37.12	2.77	53.27	1.93	37.12	0.71	13.65
SEAMAP	5.20	1.88	36.15	2.82	54.23	2.02	38.85	0.71	13.65
GCRL	5.46	1.97	36.08	3.01	55.13	1.97	36.08	0.71	13.00
SEAMAP	5.46	2.35	43.04	3.29	60.26	2.21	40.48	0.71	13.00
GCRL	5.46	1.88	34.43	3.15	57.69	2.16	39.56	0.61	11.17
SEAMAP	5.46	2.12	38.83	3.10	56.78	2.12	38.83	0.71	13.00
GCRL	5.59	1.97	35.24	3.15	56.35	2.16	38.64	0.71	12.70
SEAMAP	5.59	2.16	38.64	3.10	55.46	2.21	39.53	0.80	14.31
SEAMAP	5.85	1.97	33.68	3.10	52.99	2.54	43.42	0.71	12.14
GCRL	6.37	2.26	35.48	3.57	56.04	2.26	35.48	0.85	13.34
GCRL	9.49	3.85	40.57	5.67	59.75	3.57	37.62	1.36	14.33
SEAMAP	10.01	4.03	40.26	5.85	58.44	3.48	34.77	1.32	13.19
SEAMAP	20.02	7.15	35.71	12.09	60.39	7.02	35.06	2.60	12.99

(2.9 mm) than in reared larvae, whereas fin pigmentation seemingly appeared later in development (Tables 1–4). Comparisons of the ratios of head length, preanal length, body depth, and orbit diameter to body length indicated that development in the laboratory resulted in larvae that mirrored development in the wild.

Discussion

The larvae of as many as eighteen species of snappers in three subfamilies can occur in the western Central Atlantic which includes the Gulf of Mexico and Caribbean Sea. The early life stages of the subfamily Apsilinae are mostly unknown but the low number of dorsal soft rays (10, rarely 9) should separate late-stage larvae and juveniles of *Apsilus dentatus* from larvae of species in the other two subfamilies (Leis et al., 1997; Leis and Lee, 1994; Richards et al., 1994). Eteline snappers are represented by four species in GOM collections, *Etelis oculatus* and three species of *Pristipomoides*. The larvae of these taxa should be separable from lutjanine larvae by body shape and spine structure because eteline larvae are slender bodied and have weaker median fin spines (Leis and Lee, 1994; Richards et al., 1994). The lower dorsal count of etelines (21) will also distinguish larvae from lutjanines (22–24) in specimens whose total dorsal elements can be counted (Leis and Lee, 1994; Richards et al., 1994). The majority of snappers (13 species) found in the area belong to the subfamily Lutjaninae (Richards et al., 1994). Distinguishing the lutjanine larvae from each other is difficult despite published larval descriptions for six taxa: *Rhomboplites aurorubens* (Laroche, 1977); *Lutjanus griseus* (Richards and Saksena, 1980); *Ocyurus chrysurus* (Riley et al., 1995; Clarke et al., 1997); *L. synagris* (Clarke et al., 1997); *L. analis* (Clarke et al., 1997); and *L. campechanus* (Rabalais et al., 1980; Collins et al., 1980; and our study). We undertook a synthesis of these published descriptions and illustrations to better evaluate the usefulness of various characters in distinguishing the larvae of lutjanine species occurring in the Gulf of Mexico (Table 5).

Our tabulated character list is not exhaustive and represents only those features for which known GOM lutjanine larvae appear to differ. Dorsal-fin meristics can be used to narrow the possible choices among species once total fin element number is established and even before spines and rays are completely differentiated. Only four species have 22 or 23 total dorsal elements and of these, *R. aurorubens* is the only species with 12 dorsal spines; the other three usually have 10 spines. Body shape may also

Table 4

Meristics and spine lengths of wild larval red snapper. nd = not developed, — = not measured owing to damage, i = incipient ray(s) or spine(s), P_2 = pelvic fin. SEAMAP = Southeast Area Monitoring and Assessment Program; GCRL = Gulf Coast Research Laboratory.

Source	Body length (BL)	Dorsal fin spines and rays	2nd dorsal spine length	2nd dorsal spine length/BL	3rd dorsal spine length	3rd dorsal spine length/BL	P_2 spine length	P_2 spine length/BL	P_2 ray length	P_2 ray length/BL	Anal fin spines and rays
SEAMAP	2.86	II	0.30	10.49	0.24	8.39	bud	nd	bud	nd	anlage
SEAMAP	2.99	i	0.09	3.01	nd	nd	bud	nd	bud	nd	nd
SEAMAP	2.99	IIi	0.44	14.72	0.36	12.04	0.21	7.02	0.29	9.70	anlage
SEAMAP	2.99	IVi	0.58	19.40	0.38	12.71	0.26	8.70	0.26	8.70	anlage
SEAMAP	3.12	ii	0.17	5.45	0.12	3.85	bud	nd	bud	nd	nd
SEAMAP	3.12	IIii	0.44	14.10	0.36	11.54	0.23	7.37	0.23	7.37	anlage
SEAMAP	3.12	IVi	0.54	17.31	0.39	12.50	0.32	10.26	0.38	12.18	anlage
GCRL	3.25	IIIi	0.29	8.92	0.18	5.54	bud	nd	bud	nd	anlage
SEAMAP	3.25	IIIi	0.48	14.77	0.36	11.08	0.26	8.00	0.38	11.69	anlage
SEAMAP	3.38	IIi	0.38	11.24	0.32	9.47	0.18	5.33	0.38	11.24	anlage
SEAMAP	3.38	IIii	0.50	14.79	0.41	12.13	0.19	5.62	0.26	7.69	anlage
SEAMAP	3.38	IVii	0.53	15.68	0.36	10.65	0.22	6.51	0.26	7.69	anlage
SEAMAP	3.38	IVii	0.55	16.27	0.38	11.24	0.26	7.69	0.31	9.17	anlage
SEAMAP	3.38	V	0.66	19.53	0.42	12.43	0.42	12.43	0.47	13.91	anlage
SEAMAP	3.38	Vi	0.80	23.67	0.52	15.38	0.52	15.38	0.61	18.05	anlage
GCRL	3.51	IIii	0.29	8.26	0.22	6.27	1.06	30.20	0.58	16.52	na
SEAMAP	3.51	IIii	0.38	10.83	0.24	6.84	0.19	5.41	0.19	5.41	anlage
SEAMAP	3.51	IIIii	0.55	15.67	0.36	10.26	0.29	8.26	0.34	9.69	anlage
SEAMAP	3.51	V	0.61	17.38	0.56	15.95	0.38	10.83	0.52	14.81	anlage
SEAMAP	3.51	VIi	0.99	28.21	0.61	17.38	0.33	9.40	0.56	15.95	i
SEAMAP	3.64	IIIii	0.66	18.13	0.38	10.44	0.56	15.38	—	—	anlage
SEAMAP	3.64	Vi	0.72	19.78	0.48	13.19	0.50	13.74	0.50	13.74	anlage
SEAMAP	3.64	VI	0.55	15.11	0.38	10.44	0.26	7.14	0.34	9.34	anlage
GCRL	3.77	II	0.20	5.31	0.17	4.51	bud	nd	bud	nd	nd
GCRL	3.77	IIi	0.31	8.22	0.24	6.37	bud	nd	bud	nd	nd
GCRL	3.77	IIii	0.24	6.37	0.17	4.51	bud	nd	bud	nd	anlage
GCRL	3.77	IVi	0.36	9.55	0.29	7.69	bud	nd	bud	nd	anlage
SEAMAP	3.77	Vi	1.08	28.65	0.70	18.57	0.70	18.57	0.89	23.61	anlage
SEAMAP	3.77	VI	0.87	23.08	0.53	14.06	0.53	14.06	0.56	14.85	anlage
SEAMAP	3.77	VI	0.94	24.93	0.67	17.77	—	—	—	—	anlage
SEAMAP	3.77	VIi	0.82	21.75	0.55	14.59	0.48	12.73	0.50	13.26	anlage
SEAMAP	3.77	VIi	1.08	28.65	0.65	17.24	0.70	18.57	0.79	20.95	anlage
SEAMAP	3.77	VIi	1.18	31.30	0.75	19.89	0.80	21.22	0.99	26.26	ii
SEAMAP	3.81	Vi	0.56	14.70	0.47	12.34	0.21	5.51	0.68	17.85	anlage
SEAMAP	3.84	Vi	0.71	18.49	0.42	10.94	0.47	12.24	0.66	17.19	anlage
SEAMAP	3.90	IVii	0.82	21.03	0.53	13.59	0.55	14.10	0.77	19.74	anlage
GCRL	3.90	Vi	0.72	18.46	0.46	11.79	0.43	11.03	0.43	11.03	anlage
SEAMAP	3.90	Vii	0.89	22.82	0.50	12.82	0.60	15.38	0.63	16.15	anlage
SEAMAP	3.90	VIi	1.03	26.41	0.61	15.64	0.65	16.67	0.70	17.95	anlage
SEAMAP	3.90	VIi	1.03	26.41	0.71	18.21	0.71	18.21	0.89	22.82	i
GCRL	4.03	IVi	0.54	13.40	0.35	8.68	0.30	7.44	0.57	14.14	anlage
SEAMAP	4.03	IVii	0.68	16.87	0.44	10.92	0.29	7.20	0.60	14.89	anlage
GCRL	4.03	Vi	0.66	16.38	0.48	11.91	0.50	12.41	0.57	14.14	anlage
SEAMAP	4.03	Vi	0.94	23.33	0.56	13.90	0.66	16.38	1.03	25.56	anlage
SEAMAP	4.03	VIi	1.03	25.56	0.65	16.13	0.62	15.38	0.82	20.35	anlage

continued

Table 4 (continued)

Source	Body length (BL)	Dorsal fin spines and rays	2nd dorsal spine length	2nd dorsal spine length/BL	3rd dorsal spine length	3rd dorsal spine length/BL	P_2 spine length	P_2 spine length/BL	P_2 ray length	P_2 ray length/BL	Anal fin spines and rays
SEAMAP	4.03	VIiii	0.85	21.09	0.49	12.16	0.52	12.90	0.80	19.85	anlage
SEAMAP	4.03	VIIIi	1.22	30.27	0.77	19.11	0.94	23.33	1.22	30.27	i
GCRL	4.16	IVii	0.53	12.74	0.33	7.93	0.26	6.25	0.33	7.93	anlage
GCRL	4.16	Vi	0.62	14.90	0.47	11.30	0.45	10.82	0.45	10.82	anlage
GCRL	4.16	Vi	0.82	19.71	0.50	12.02	0.46	11.06	0.55	13.22	anlage
GCRL	4.16	Vi	0.70	16.83	0.43	10.34	0.31	7.45	0.53	12.74	anlage
SEAMAP	4.16	VIi	1.13	27.16	0.38	9.13	0.75	18.03	0.89	21.39	ii,(9i)
SEAMAP	4.16	VIi	1.27	30.53	0.85	20.43	0.94	22.60	0.85	20.43	anlage
SEAMAP	4.16	VIIi,(16i)	1.13	27.16	0.80	19.23	0.80	19.23	0.99	23.80	anlage
SEAMAP	4.16	VIIii,(15i)	1.32	31.73	0.85	20.43	0.42	10.10	0.75	18.03	ii,(9i)
SEAMAP	4.29	Vi	0.82	19.11	0.67	15.62	0.54	12.59	0.72	16.78	anlage
SEAMAP	4.29	Vii	0.94	21.91	0.66	15.38	0.75	17.48	0.80	18.65	anlage
GCRL	4.29	VIi	0.86	20.05	0.58	13.52	0.53	12.35	0.79	18.41	anlage
SEAMAP	4.42	VIi	0.94	21.27	0.52	11.76	0.56	12.67	0.71	16.06	anlage
SEAMAP	4.42	VIi,(17i)	1.25	28.28	0.82	18.55	0.72	16.29	0.96	21.72	ii,(9i)
SEAMAP	4.42	VIii,(16i)	1.18	26.70	0.79	17.87	—	—	—	—	II,(9i)
SEAMAP	4.42	VIIIi	0.33	7.47	0.89	20.14	1.03	23.30	1.32	29.86	IIi
GCRL	4.42	VIIIii,(13i)	1.44	32.58	0.96	21.72	1.15	26.02	1.49	33.71	ii,(8i)
SEAMAP	4.55	VIi	1.00	21.98	0.65	14.29	0.77	16.92	0.78	17.14	anlage
SEAMAP	4.55	VIIi	1.13	24.84	0.71	15.60	0.56	12.31	1.03	22.64	i
SEAMAP	4.55	VIIIi	1.65	36.26	0.80	17.58	0.38	8.35	1.41	30.99	IIi,(8i)
GCRL	4.55	VIIii,(14i)	1.04	22.86	0.69	15.16	0.93	20.44	1.41	30.99	ii,(9i)
SEAMAP	4.68	IXi,(14i)	1.74	37.18	1.08	23.08	1.20	25.64	1.46	31.20	IIi,(8i)
GCRL	4.68	VIi	0.98	20.94	0.46	9.83	0.62	13.25	0.77	16.45	anlage
GCRL	4.68	VIi,(16i)	0.98	20.94	0.65	13.89	0.91	19.44	0.98	20.94	ii
SEAMAP	4.68	VIIIi,(15i)	1.55	33.12	0.94	20.09	1.03	22.01	1.34	28.63	ii,(9i)
SEAMAP	4.81	IXi,(14i)	1.60	33.26	0.94	19.54	1.20	24.95	1.78	37.01	ii,(9i)
SEAMAP	4.81	VIi,(15i)	1.18	24.53	0.80	16.63	0.94	19.54	1.08	22.45	ii,(9i)
SEAMAP	4.81	VIIIii,(14i)	0.61	12.68	0.89	18.50	0.24	4.99	1.22	25.36	ii,(8i)
SEAMAP	4.94	IXi,(14i)	0.94	19.03	1.08	21.86	1.36	27.53	1.83	37.04	IIi,(9i)
SEAMAP	4.94	VIIii	1.46	29.55	0.94	19.03	1.03	20.85	1.60	32.39	ii,(10i)
GCRL	5.07	VIIi,(16i)	1.20	23.67	0.79	15.58	0.93	18.34	0.82	16.17	ii,(9i)
SEAMAP	5.07	VIIIi,(13i)	1.27	25.05	0.89	17.55	0.99	19.53	1.13	22.29	ii,(9i)
SEAMAP	5.07	VIIIii	1.55	30.57	1.03	20.32	1.18	23.27	1.70	33.53	IIi,(8i)
SEAMAP	5.07	VIIIii,(14i)	1.66	32.74	1.01	19.92	1.08	21.30	1.75	34.52	IIi,(8i)
SEAMAP	5.20	IXi,(14i)	1.74	33.46	0.99	19.04	1.27	24.42	1.32	25.38	IIi,(8i)
GCRL	5.20	VIIii,(15i)	1.32	25.38	0.84	16.15	0.86	16.54	1.42	27.31	II,(9i)
SEAMAP	5.20	VIIIii,(14i)	1.54	29.62	0.94	18.08	1.08	20.77	1.39	26.73	IIi,(8i)
SEAMAP	5.46	IXi,(14i)	1.88	34.43	1.13	20.70	1.36	24.91	1.32	24.18	IIi,(8i)
SEAMAP	5.46	VIIii,(15i)	1.58	28.94	1.06	19.41	1.22	22.34	1.89	34.62	IIi,(8i)
GCRL	5.46	VIIii,(15i)	1.39	25.46	0.89	16.30	0.94	17.22	1.15	21.06	II,(9i)
GCRL	5.46	VIIIi,(15i)	1.10	20.15	0.91	16.67	0.74	13.55	0.74	13.55	II,(9i)
SEAMAP	5.59	IX,(15i)	1.92	34.35	1.32	23.61	1.61	28.80	2.04	36.49	IIi,(8i)
GCRL	5.59	VIIIii,(14i)	2.96	52.95	1.06	18.96	1.15	20.57	1.49	26.65	II,(9i)
SEAMAP	5.85	IXi,(14i)	1.74	29.74	1.32	22.56	1.46	24.96	1.97	33.68	IIi,(8i)
GCRL	6.37	IXi,(14i)	1.61	25.27	1.13	17.74	0.89	13.97	1.37	21.51	II,(9i)
GCRL	9.49	X,14	3.20	33.72	1.74	18.34	1.79	18.86	0.80	8.43	III,8
SEAMAP	10.01	X,14	2.96	29.57	2.26	22.58	2.87	28.67	3.85	38.46	III,9
SEAMAP	20.02	X,14	6.63	33.12	3.64	18.18	2.73	13.64	5.20	25.97	III,9

Table 5

Morphological comparison of *Rhomboplites aurorubens*, *Ocyurus chrysurus*, and *Lutjanus* spp. larvae based on presence (+), absence (–), and specimen size (BL in mm) at the first noted appearance of selected characters from published descriptions and illustrations. Abbreviations: D = dorsal; D_2 = soft dorsal fin; BD= body depth; sp = spine; a = anterior; p = posterior; P_2 = pelvic fin; Pr An sp = preopercular angle spine; avm = anterior visceral mass; pav = postanal ventral melanophore series; nv = not visible in published illustrations; ? = no published illustrations. "Spots" refer to melanophores. Dorsal fin counts in parentheses are rare values (Richards et al., 1994).

	Dorsal-fin count	BD to BL ratio	P_2 ray length	Avm pigment	Pr An sp serrations	D sp serrations	No. of pav spots in preflexion	Enlarged pav spot in preflexion	Gap in pav series in preflexion
R. aurorubens	XII,(10)11(12)	35% at 4.0	=P_2sp	–	+	+	8–18	–	–
L. apodus	X,14	?	?	?	?	?	?	?	?
L. cyanopterus	X,14	?	?	?	?	?	?	?	?
L. griseus	X,14	34% at 4.2	=P_2sp	nv	–	+	23–27	–	–
L. jocu	X,(13)14	?	?	?	?	?	?	?	?
L. mahogani	X,(11)12	?	?	?	?	?	?	?	?
O. chrysurus	(IX)X(XI),12-13(14)	26% at 4.5	2×P_2sp	3.3–4.0	–	+	13–19	–	–
L. synagris	X,12(13)	29% at 4.6	2×P_2sp	3.3–4.0	–	+	15–25	+	–
L. analis	X(XI),(13)14	23% at 4.6	2×P_2sp	3.3–4.0	–	+	13–23	+	+
L. buccanella	X,14	?	?	?	?	?	?	?	?
L. campechanus	(IX)X,(13)14(15)	36% at 4.2	2×P_2sp	3.4	–	–	8–22	–	+
L. purpureus	(IX)X,(13)14(15)	?	?	?	?	?	?	?	?
L. vivanus	X(XI),(13)14	?	?	?	?	?	?	?	?

	Spot ventral to notochord flexure	Internal spots over notochord	Dorsal midline caudal pigment	D_2 pigment	Anal-fin pigment base and membrane	Pelvic-fin pigment during flexion	Data sources
R. aurorubens	–	–	4.5	nv	5.1/nv	membrane ray 1	1,2,3
L. apodus	?	?	?	?	?	?	
L. cyanopterus	?	?	?	?	?	?	
L. griseus	–	–	–	by 9.6	by 6.2/by 7.1	spine+ray tips (?)	2,4
L. jocu	?	?	?	?	?	?	
L. mahogani	?	?	?	?	?	?	
O. chrysurus	–	6.3	6.3	11.5	5.3/6.3	membrane all rays	5,6
L. synagris	–	6.2	6.2	6.2	4.7/9.8	membrane ray 1	6
L. analis	5.8	–	8.1	11.5	6.2/16	membrane ray 1	6
L. buccanella	?	?	?	?	?	?	
L. campechanus	–	–	3.8 or 5.5	12.2	3.8/12.2	membrane ray 1	2,7,8
L. purpureus	?	?	?	?	?	?	
L. vivanus	?	?	?	?	?	?	

[1] Laroche (1977).

[2] Richards et al. (1994).

[3] Comyns, B.H., and J. Lyczkowski-Shultz. 1993. Spawning and early life history of snappers in the northcentral Gulf of Mexico. Final Report. MARFIN grant NA17FF0382-01, NMFS Southeast Regional Office, St. Petersburg, FL 33701.

[4] Richards and Saksena (1980).

[5] Riley et al. (1995).

[6] Clarke et al. (1997).

[7] Collins et al. (1980).

[8] Our study.

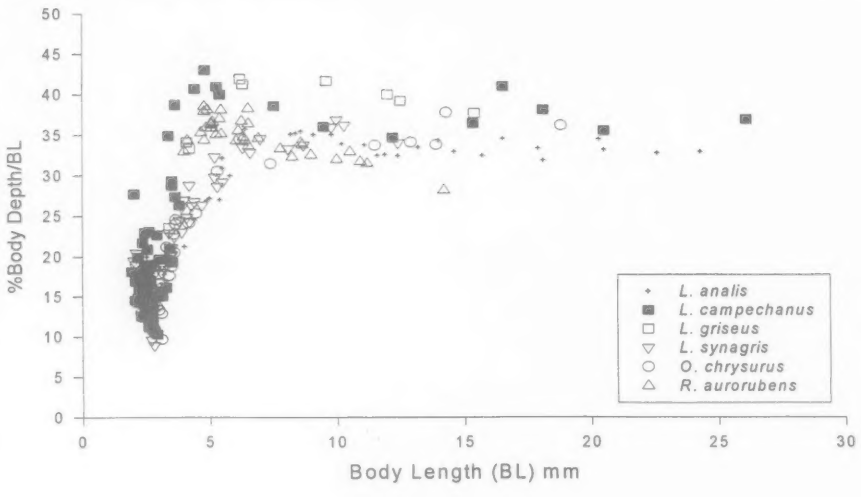

Figure 7

Comparison of body depth ratios among larvae of *L. analis*, *L. campechanus*, *L. griseus*, *L. synagris*, *O. chrysurus*, and *R. aurorubens*.

provide important diagnostic characters. Flexion larvae of *O. chrysurus*, *L. analis*, and *L. synagris* are shallow-bodied ranging from 23% to 29% of body length (Fig. 7), whereas body depth in flexion larvae of *L. campechanus*, *L. griseus*, and *R. aurorubens* is from 34% to 36% of body length. The approximately equal length of the longest pelvic-fin ray and pelvic spine helps distinguish *R. aurorubens* and *L. griseus* from *O. chrysurus*, *L. synagris*, *L. analis*, and *L. campechanus* larvae in which the longest pelvic ray is nearly twice the length of the pelvic spine.

Small preflexion larvae of *L. campechanus* can be consistently distinguished from larvae of *R. aurorubens* in northcentral GOM waters by the presence of the avm melanophore. This character first appeared in reared specimens at 3.4 mm but would be seen in somewhat smaller wild specimens because of the shrinkage experienced by net-captured larvae (Theilacker, 1980). Larvae of *O. chrysurus*, *L. synagris*, and *L. analis* also develop avm pigment at BLs between ~3 and 4 mm. The presence or absence of this character in *L. griseus* larvae could not be ascertained from published illustrations (Richards and Saksena, 1980), but avm pigment was present in all specimens of *L. griseus* that we examined. The presence of serrations on the angle spine of the preopercle in *R. aurorubens* larvae at sizes >3.4 mm distinguishes them from *O. chrysurus* and all *Lutjanus* larvae currently known in the GOM. Snapper larvae may develop serrations on the median fin spines to some degree or another, but at least three species of lutjanine snappers (*Hoplopagrus gunteri*, *L. novemfasciatus*, and *L. peru*) from the Pacific do not develop serrations on any fin spines (Brogan, 1996; Watson and Brogan, 1996). Larvae of the six species compared in Table 5 develop serrations on the pelvic spine and all species, except *L. campechanus*, develop serrations on dorsal-fin spines. Although not shown in the illustrations of Richards and Saksena (1980), the larvae of *L. griseus* do develop pronounced serrations on both dorsal and pelvic spines (Clarke et al., 1997; Richards et al., 1994). The relative size and extent of these serrations vary among species; *R. aurorubens* has the stoutest serrations among snapper larvae on both the leading and trailing edges of the spines (Laroche, 1977).

The postanal series of melanophores (pav) along the ventral midline is characteristic of many percoid larvae, including those of snappers. In snapper larvae, postanal pigmentation decreases dramatically during the flexion stage. Despite the dynamic nature of this pigment during development and the considerable overlap in number of pav melanophores among preflexion larvae (Table 5), Clarke et al. (1997) suggested that the "usual" number (not overall range) of pav melanophores would distinguish the larvae of *L. synagris* and *L. analis* from each other. Yolksac and preflexion larvae of these two species are further distinguished from other known lutjanine larvae by the presence of an enlarged melanophore in the pav series (Clarke et al., 1997). An additional pav-related character that differs among known lutjanine larvae is the gap in the pav series posteriorly, as seen in *R. aurorubens*, *L. campechanus*, and *L. analis*. The pav series of melanophores in *L. griseus*, *O. chrysurus*, and *L. synagris* is continuous in preflexion larvae.

Pigmentation associated with the notochord can be used to distinguish the larvae of *O. chrysurus*, *L. synagris*, and *L. analis* from other described GOM lutjanine larvae (Table 5). Although pigment overlying the point of notochord flexure develops by ~6 mm in all described GOM

lutjanine larvae, only *L. analis* simultaneously acquires pigment ventral to notochord flexure. Only the larvae of *O. chrysurus* and *L. synagris* develop internal melanophores over the notochord. Both species first acquire this pigment by ~6 mm but it becomes more extensive with development in *O. chrysurus* than in *L. synagris*. Pigment on the dorsal midline of the caudal peduncle develops in all lutjanine larvae except *L. griseus*. There is some interspecific variation in the size when this pigment first develops (Table 5). *Rhomboplites aurorubens* larvae as small as 4.5 mm have dorsal pigment on the caudal peduncle (Richards et al., 1994) and this pigment does not develop in *L. analis* larvae until ~8 mm. A single melanophore first appeared on the dorsal midline of the caudal peduncle in the 3.8-mm *L. campechanus* of our series. It was not present in the next two specimens but was present in the 5.5-mm specimen and all subsequent larvae.

Interspecific differences among known lutjanine larvae are apparent in the amount, location, and size at first appearance of dorsal-fin pigment. Pigment in the spinous dorsal fin first appears in the membrane behind the second spine in *L. campechanus, O. chrysurus, L. synagris,* and *L. analis*. Additional melanophores develop posteriorly behind successive spines in *L. synagris* throughout flexion, whereas in the other three species, pigment develops posteriorly behind successive spines only in late flexion or after flexion. It appears from the illustrations of Clarke et al. (1997) that although pigment between the first and second spines is present in *L. synagris* from 4.7 to 6.2 mm, it is consistently present only in *O. chrysurus* larvae from preflexion onward. Spinous dorsal-fin pigment in *L. griseus* differs notably from the other species of lutjanines; melanophores first form low in the fin at the base of the second or third spines, or at the base of both, and as development proceeds, melanophores are added distally (farther out onto the fin) and posteriorly. Pigment was present between the second and third dorsal-fin spines in the few *R. aurorubens* larvae that had intact dorsal-fin membranes. Dorsal-fin pigment was not indicated in illustrations by Laroche (1977), probably because these specimens did not have intact fin membranes. Among known GOM lutjanine larvae, only *L. synagris* larvae develop pigment in the second (soft) dorsal fin before ray formation is complete, at ~6 mm. In larvae of the remaining species, pigment in the second dorsal-fin first appears at larger sizes when fin ray development is well advanced (Table 5).

Anal- and pelvic-fin pigmentation is also useful in separating the larvae of GOM lutjanines. Pigment on the anal-fin base develops in all six species whose larvae have been described and of these, *L. campechanus* larvae develop this pigment at the smallest size, <4 mm (Table 5). There are greater differences among larvae in size at first appearance of pigment in the anal-fin membrane than in the anal base. *Lutjanus campechanus* and *L. analis* larvae can be distinguished from the other described larvae by later development of anal-fin pigment at sizes ≥12 mm (Table 5). Pigment on the pelvic fin bud has been indicated in all illustrated lutjanine larvae except *L. griseus*. It is likely that this exception is due, not to true absence of this feature in *L. griseus*, but to the limited number of larvae in the described series (Richards and Saksena, 1980). The 4.2-mm *L. griseus* larva illustrated by these authors had pigment at the distal tips of the pelvic fin, but this pigment was not present in larger larvae of the series or in the 7.1-mm specimen illustrated in Richards et al. (1994). Pelvic-fin pigment distinguishes *O. chrysurus* and *L. griseus* from other lutjanine larvae once the spine and first ray are formed. From illustrations in Clarke et al. (1997), it appears that starting in the preflexion stage, *O. chrysurus* larvae have pigment throughout the pelvic-fin membrane and not just around the first fin ray as in *L. campechanus, L. synagris,* and *L. analis*. The unique condition of pelvic-fin pigmentation that characterizes *L. griseus* is the "candycane stripe" pattern of melanophores that overlay the pelvic spine. Pigment on the pelvic spine is present in *L. griseus* larvae as small as 4.2 mm and the striped pattern is evident by at least 6.2 mm (Richards and Saksena, 1980).

In Table 9 of their recent publication, Clarke et al. (1997) provided a summary of distinguishing characters for the known larvae and juveniles of western Central Atlantic lutjanine snappers. We have noted some discrepancies in that summary that may cause confusion for those attempting to identify lutjanine snapper larvae from our area. In Table 9, the "usual" number of pav melanophores listed for *L. campechanus* was given as 16–18. The modal number of pav spots among preflexion *L. campechanus* larvae (2.2–3.8 mm BL; n=70) from the GCRL rearings was 15, and 50 specimens had 14 to 19 pav spots. Also in Table 9, for the character "serrations on dorsal and pelvic fin spines," the entry for *L. campechanus* states, "on anterior spine margin only." Larvae of *L. campechanus* develop serrations on the anterior margin of the pelvic spine only, not on the dorsal spines (Collins et al., 1980; Potthoff et al., 1988). Clarke et al. (1997) also note that *L. griseus* larvae develop internal melanophores ventral to the point of notochord flexure (their character "O"). This feature is not visible in any of the published illustrations of *L. griseus* larvae or in specimens we have examined. Finally, information in Table 9 that pertains to character "P"—"internal melanophores on antero-ventral surface of gut (peritoneum) dorsal to pelvic bone" noted as being absent in four species—was clearly present in the *R. aurorubens* and *L. campechanus* larvae that we examined and is visible in illustrations of *L. analis* and *O. chrysurus* in Clarke et al. (1997).

The descriptions of larval lutjanine snapper development now available will allow scientists to identify mid- to late-flexion and postflexion larvae of the most common lutjanids in the Gulf of Mexico. In an examination of over 1500 snapper larvae from Gulfwide collections in 1992 and 1993, we found that the larvae of *R. aurorubens, L. campechanus,* and *P. aquilonaris* made up 23%, 13%, and 13% of all snapper larvae captured, respectively. Other identified taxa consisted of *Lutjanus* spp. (3%), *L. griseus* (<1%), and *L. synagris* (<1%). However, 47% of snapper larvae in these collections, typically <3.5–4.0 mm in length, could not be identified beyond the family level because diagnostic characters are present only after flexion has begun.

Closer scrutiny of characters, such as the number of pav spots, the enlarged pav spot, and the gap in the pav series, may allow identification of preflexion and early flexion snapper larvae, if not to a single species, at least to a reduced number of possibilities. Of course, larvae of the remaining snapper species need to be described before all small "undifferentiated snapper larvae" can be reliably and consistently identified to the species level. Investigation of additional characters among preflexion larvae such as the presence and location of other chromatophores, may yield further useful species-specific traits (Riley et al., 1995). Initial observations of *L. campechanus* show yellow chromatophores in similar locations (head and gut area) as those reported for *O. chrysurus* (Riley et al., 1995). Among larger *L. campechanus* specimens, additional chromatophores were present in locations not noted for *O. chrysurus* larvae. More specific comparisons will have to await a larger sample size to determine variability in numbers of chromatophores and size at development. Additionally, biochemical techniques are currently being investigated for the purpose of species-specific identification of snapper larvae (Chow et al., 1993; Sarver et al., 1996; Schultz et al., 1996). Initial results seem to indicate that no single technique will distinguish between all species in the subfamily Lutjaninae. Use of these biochemical assay methods for routine identification of snapper larvae may not be feasible for specimens taken during broadscale surveys. Yet a positive species identification of subsamples of field-caught snapper larvae with biochemical methods may lead to recognition of morphological features that have been previously overlooked and determination of the error rate of morphologically based identifications.

Acknowledgments

Most of the work for this study was done while the primary author was employed by Johnson Controls World Services. Gratitude is expressed to the following individuals for their able assistance during the course of this study and the support of the institutions they represent: the staff of the Claude Peteet Mariculture Center, particularly Jim Duffy; John Ogle, Casey Nicholson, Jeff Lotz, Donald Barnes, Mae Blake and Pam Bond of the Gulf Coast Research Laboratory, University of Southern Mississippi; and Kim Williams of the SEAMAP Archiving Center at the Florida Marine Research Institute, St. Petersburg, FL. The Texas study was funded by Grant NA16RGO457-03 from the National Oceanic and Atmospheric Administration through The Texas Sea Grant College Program. We thank W. J. Richards for reading an earlier draft and two anonymous reviewers for comments on the manuscript.

Literature cited

Bootes, K. L.
1998. Culture and description of larval red snapper, *Lutjanus campechanus*. M.S thesis, Department of Fisheries and Allied Aquacultures, Auburn Univ., Auburn, AL, 155 p.

Brogan, M. W.
1996. Larvae of the Eastern Pacific snapper *Hoplopagrus guntheri* (Teleostei: Lutjanidae). Bull. Mar. Sci. 58(2):329–343.

Chow, S., M. E. Clarke, and P. J. Walsh.
1993. PCR-RFLP analysis on thirteen western Atlantic snappers (subfamily Lutjaninae): a simple method for species and stock identification. Fish. Bull. 91:619–627.

Clarke, M. E., M. L. Domeier, and W. A. Laroche.
1997. Development of larvae and juveniles of the mutton snapper (*Lutjanus analis*), lane snapper (*Lutjanus synagris*) and yellowtail snapper (*Lutjanus chrysurus*). Bull. Mar. Sci. 61(3):511–537.

Collins, L. A., J. H. Finucane, and L. E. Barger.
1980. Description of larval and juvenile red snapper, *Lutjanus campechanus*. Fish. Bull. 77:965–974.

Donaldson, D. M., N. J. Sanders, and P. A. Thompson.
1993. SEAMAP environmental and biological atlas of the Gulf of Mexico, 1991. Gulf States Marine Fisheries Commission 29, 321 p.
1994. SEAMAP environmental and biological atlas of the Gulf of Mexico, 1992. Gulf States Marine Fisheries Commission 30, 293 p.

Donaldson, D. M., N. J. Sanders, P. A. Thompson, and R. Minkler.
1996. SEAMAP environmental and biological atlas of the Gulf of Mexico, 1993. Gulf States Marine Fisheries Commission 34, 284 p.
1997a. SEAMAP environmental and biological atlas of the Gulf of Mexico, 1994. Gulf States Marine Fisheries Commission 40, 277 p.
1997b. SEAMAP environmental and biological atlas of the Gulf of Mexico, 1995. Gulf States Marine Fisheries Commission 41, 280 p.

Johnson, G. D.
1984. Percoidei: development and relationships. *In* Ontogeny and systematics of fishes (H. G. Moser, W. J. Richards, D. M.Cohen, M. P. Fahay, A. W. Kendall Jr. and S. L. Richardson, eds.), p. 464–498. Am. Soc. Ichthyol. Herpetol. Spec. Publ. 1.

Laroche, W. A.
1977. Description of larval and early juvenile vermilion snapper, *Rhomboplites aurorubens*. Fish. Bull. 75:547–554.

Leis, J. M.
1987. Review of the early life history of tropical groupers (Serranidae) and snappers (Lutjanidae). *In* Tropical snappers and groupers: biology and fisheries management (J. J. Polovina and S. Ralston, eds.), p. 189–237. Westview Press, Boulder, Colorado.

Leis, J. M., and K. Lee.
1994. Larval development in the lutjanid subfamily Etelinae (Pisces): the genera *Aphareus*, *Aprion*, *Etelis* and *Pristipomoides*. Bull. Mar. Sci. 55(1):46–125.

Leis, J. M., and D. S. Rennis.
1983. The larvae of Indo-Pacific coral reef fishes. Univ. Hawaii Press, Honolulu, HI, 269 p.

Leis, J. M., and T. Trnski.
1989. The larvae of Indo-Pacific shorefishes. Univ. Hawaii Press, Honolulu, HI, 371 p.

Leis, J. M., S. Bullock, D. J. Bray, and K. Lee.
1997. Larval development in the lutjanid subfamily Apsilinae (Pisces): the genus *Paracaesio*. Bull. Mar. Sci. 61(3):697–742.

Potthoff, T., S. Kelley, and L. A. Collins.
1988. Osteological development of the red snapper, *Lutjanus campechanus* (Lutjanidae). Bull. Mar. Sci. 43(1):1–40.

Rabalais, N. N., S. C. Rabalais, and C. R. Arnold.
1980. Description of eggs and larvae of laboratory reared red snapper (*Lutjanus campechanus* Poey). Copeia 1980:704–708.

Richards, W. J.
1984. Kinds and abundances of fish larvae in the Caribbean Sea and adjacent areas. U.S. Dep. Commer., NOAA Tech. Rep. NMFS-SSRF-776, 54 p.

Richards, W. J., and V. P. Saksena.
1980. Description of larvae and early juveniles of laboratory-reared gray snapper, *Lutjanus griseus* (Linnaeus)(Pisces, Lutjanidae). Bull. Mar. Sci. 30:515–521.

Richards, W. J., M. F. McGowan, T. Leming, J. T. Lamkin, and S. Kelley.
1993. Larval fish assemblages at the Loop Current boundary in the Gulf of Mexico. Bull. Mar. Sci. 53(2):475–537.

Richards, W. J., K. C. Lindeman, J. L-Shultz, J. M. Leis, A. Ropke, M. E. Clarke, and B. H. Comyns.
1994. Preliminary guide to the identification of the early life history stages of lutjanid fishes of the western central Atlantic. U.S. Dep. Commer., NOAA Tech. Memo. NMFS-SEFSC-345, 49 p.

Riley, C. M., G. J. Holt and C. R. Arnold.
1995. Growth and morphology of larval and juvenile captive bred yellowtail snapper, *Ocyurus chrysurus*. Fish. Bull. 93:179–185.

Sanders, N. J., D. M. Donaldson, and P. A. Thompson.
1991a. SEAMAP environmental and biological atlas of the Gulf of Mexico, 1988. Gulf States Marine Fisheries Commission 23, 320 p.
1991b. SEAMAP environmental and biological atlas of the Gulf of Mexico, 1989. Gulf States Marine Fisheries Commission 25, 318 p.
1992. SEAMAP environmental and biological atlas of the Gulf of Mexico, 1990. Gulf States Marine Fisheries Commission 27, 311 p.

Sanders, N. J., P. A. Thompson, and D. M. Donaldson.
1990a. SEAMAP environmental and biological atlas of the Gulf of Mexico, 1987. Gulf States Marine Fisheries Commission 22, 337 p.

Sanders, N. J., P. A. Thompson, and T. Van Devender.
1990b. SEAMAP environmental and biological atlas of the Gulf of Mexico, 1986. Gulf States Marine Fisheries Commission 20, 328 p.

Sarver, S. K., D. W. Freshwater, and P. J. Walsh.
1996. Phylogenetic relationships of western Atlantic snappers (Family Lutjanidae) based on mitochondrial DNA sequences. Copeia 1996(3):715–721.

Schultz, D. R., P. I. Arnold, T. R. Capo, C. B. Paris-Limouzy, J. E. Serafy, and W. J. Richards.
1996. Immunologic methods for species identification of early life stages of lutjanid fishes from the western central Atlantic. Part I: Characterization of an interspecies protein. Fish. Bull. 94:734–742.

Theilacker, G. H.
1980. Changes in body measurements of larval northern anchovy, *Engraulis mordax*, and other fishes due to handling and preservation. Fish. Bull. 78:685–692.

Thompson, P. A., T. Van Devender, and N. J. Sanders Jr.
1988. SEAMAP environmental and biological atlas of the Gulf of Mexico, 1985. Gulf States Marine Fisheries Commission 17, 338 p.

Watson, W., and M. W. Brogan
1996. Lutjanidae: snappers. *In* The early stages of fishes in the California Current region (H. G. Moser, ed.), p. 977–989. California Cooperative Oceanic Fisheries Investigations Atlas 33.

Workman, I. K., and D. G. Foster.
1994. Occurrence and behavior of juvenile red snapper, *Lutjanus campechanus*, on commercial shrimp fishing grounds in the northeastern Gulf of Mexico. Mar. Fish. Rev. 56(2):9–11.

Consequences of dispersal of subtropically spawned crevalle jacks, *Caranx hippos*, to temperate estuaries*

Richard S. McBride
Rutgers University Marine Field Station
Institute of Marine and Coastal Sciences
800 Great Bay Boulevard
Tuckerton, New Jersey 08087
Present address: Florida Marine Research Institute
100 Eighth Avenue Southeast
St. Petersburg, Florida 33701-5095
E-mail address: richard.mcbride@fwc.state.fl.us

Kim A. McKown
New York State Department of Conservation
205 Belle Meade Road
East Setauket, New York 11733

Abstract.—*Caranx hippos* spawn at subtropical and tropical latitudes, but some of their propagules are dispersed hundreds of kilometers north of Cape Hatteras into temperate waters of the western North Atlantic. The effect that this northward dispersal pattern has upon the population depends on whether these juveniles return south during autumn to overwinter or whether they become expatriated from the spawning population and die from hypothermal winter conditions at temperate latitudes. We evaluated whether repatriation was possible by comparing *C. hippos* seasonal abundance and size-structure from New York to Florida. Young-of-the-year *C. hippos* occurred annually during summer and autumn but were uncommon in relation to other species in subtropical and temperate estuaries. Sizes of *C. hippos* at temperate latitudes were as large as conspecifics at subtropical latitudes and juveniles of other species that are known to migrate during autumn from temperate nursery grounds to subtropical latitudes. As *C. hippos* disappeared from estuaries of the middle Atlantic states in autumn, similar-size fish appeared on the inner continental shelf. We postulate that at least some of the *C. hippos* observed migrating from temperate estuaries during the autumn eventually overwinter at subtropical latitudes, where they can return to the spawning population. This is unusual, because individuals of many other species whose larvae are transported north of Cape Hatteras do not appear to successfully migrate back to subtropical overwintering habitats. This life-history pattern, in which fish begin their first year in the Carolinian biogeographic province, are dispersed to the Virginian province, and return to the Carolinian province before their first winter, has been demonstrated for only one other western North Atlantic finfish species: bluefish (*Pomatomus saltatrix*). A few other species are likely to occupy and reproduce within such large-scale oceanographic systems because they have a combination of spawning, larval, and juvenile traits that is similar to that of *P. saltatrix* and *C. hippos*.

Manuscript accepted 15 December 1999.
Fish. Bull. 98: 528–538 (2000).

In the western North Atlantic, many species spawn at tropical and subtropical latitudes, and their larvae are dispersed to temperate and even boreal regions (e.g. Gill, 1904; Markle et al., 1979; Curran, 1989). This transport of larvae occurs in association with the Gulf Stream (Wroblewski and Cheney, 1984; Hare and Cowen, 1991, 1996) and disperses propagules from the Carolinian to the Virginian biogeographic province (Briggs, 1974, 1996). This process, which involves the entrainment of eggs and larvae into oceanographic currents and the dispersal of propagules to various water masses, is understood for only a few species and may vary considerably between species. Perhaps the most famous example is that of catadromous freshwater eels (*Anguilla anguilla* and *A. rostrata*), which spawn in the Sargasso Sea and whose larvae are transported to coastal nurseries in North America and Europe (McCleave et al., 1987). Larval *A. rostrata* drift for up to one year (Kleckner and McCleave, 1985) through gyres in the southwestern Sargasso Sea, the Antilles Current, and the Florida Current and its Gulf Stream extension before moving into coastal waters (McCleave, 1993). In the case of a wrasse, *Xyrichtys novacula*, northward transport across hundreds of kilometers occurs in as little as eight days, and cross-shelf transport in the northern portion of the Carolinian province is aided by interactions between western-edge, warm-core eddies and the Gulf Stream itself (Hare and Cowen, 1991). Similar northward transport in association with the Gulf Stream occurs for "spring-spawned" bluefish, *Pomatomus saltatrix*, except that for this species dispersal time is longer—about 2 months (McBride and Conover, 1991)—and its juveniles may actively swim out of the Gulf Stream system (Hare and Cowen, 1996). Although some species are transported annually in this manner (e.g. *Pomatomus*), others are transported less regularly (*Xyrichtys*, *Bothus*, *Syacium*), and still other species do not move between slope and shelf water masses (Cowen et al., 1993).

Those individuals dispersed across biogeographic boundaries become expatriated, in terms of passing on their genes if they do not return to spawning grounds to reproduce. *Anguilla* species remain in coastal habitats for several years before migrating back to the Sargasso Sea (Tesch, 1977), but many species that spawn at subtropical latitudes are physiologically incapable of overwintering at temperate latitudes. To our knowledge, only *P. saltatrix* spawns at

* Contribution 2000-06 of the Institute of Marine and Coastal Sciences, Rutgers Univerisity, Tuckerton, New Jersey 08087.

subtropical latitudes and its propagules, once dispersed to temperate latitudes, are known to migrate south within the same year. This species is successful largely because it spawns early in the year in the subtropics and juveniles enter temperate estuaries at a time when their principal prey is becoming available (Juanes et al., 1994). Direct evidence of a successful autumn migration by young-of-the-year *P. saltatrix* is available from recaptures of tagged individuals and size-frequency analyses (Lund and Maltezos, 1970; McBride et al., 1993). This "spring-spawned" cohort of *P. saltatrix* was more abundant than other intraspecific cohorts in the western North Atlantic during the 1980s and early 1990s (Chiarella and Conover, 1990; McBride et al., 1993), and this species repeats this life-history pattern in several oceanographic systems worldwide (Juanes et al., 1996).

The effects of this transport process, from the Carolinian province to the Virginian province, is known for few other species and these examples suggest a different fate for these species than for *P. saltatrix*. Moss (1973) concluded that the "sluggish" swimming ability and the critical thermal minimum of 8.7°C for planehead filefish, *Monocanthus hispidus*, prevented individuals of this species from surviving once they had been dispersed to temperate latitudes. Hare and Cowen (1991) observed a wrasse, *Xyrichtys novacula*, settling on the continental shelf at temperate latitudes, but successive cruises could not find survivors from the initially observed cohort. And McBride and Able (1998) reported on the annual appearance of butterflyfishes (*Chaetodon* spp.) at temperate latitudes, but field collections and laboratory experiments led them to conclude that none of these individuals survived through their first winter. Sinclair (1988) would categorize these unfortunate individuals as "vagrants" from, as opposed to "members" of, a population.

Although the ecological information about these tropical forms as they occur in temperate waters is limited, the common paradigm is that "[the] Gulf Stream has a profound effect upon the distribution of shore animals in the western Atlantic . . . many tropical forms are left stranded along the inhospitable shores of northeastern North America." (Briggs, 1996; p. 238). We believe that Briggs's conclusion can be applied to most of these species; nonetheless, juveniles of several "southern" species grow and survive well at temperate latitudes during the summer and, based on their size by autumn and their general mobility, may migrate successfully back to subtropical latitudes before winter (see also Hare and Cowen, 1993). We propose that at least one other species is capable of following a dispersal-migration pattern that links the temperate and subtropical latitudes during its first year. The crevalle jack, *Caranx hippos* (Linnaeus), is a migratory, coastal species that is distributed worldwide at subtropical and tropical latitudes (Briggs, 1960; Kwei, 1978; Grosslein and Azarovitz, 1982). In the western North Atlantic, it occurs primarily in the southeastern United States and the Gulf of Mexico (U.S. Department of Commerce, 1986), and spawning is known to occur only in the subtropical Straits of Florida (Berry, 1959; Fahay, 1975) and in the tropical Caribbean Sea (Montolio, 1978). Young-of-the-year (YOY) *C. hippos* occur in subtropical estuaries of the south Atlantic states, and they use these habitats as nurseries before presumably migrating offshore in autumn (Berry, 1959). However, YOY *C. hippos* are also reported from many temperate estuaries north of Cape Hatteras (McBride[1]). Despite the broad geographic distribution of YOY *C. hippos*, little is known about their early life history at any latitude. From archived museum collections, recent field collections, and the literature, we assembled data about *C. hippos* in both southern and northern estuaries and postulate on the significance of dispersal of YOY *C. hippos* across two biogeographic provinces.

Materials and methods

Archival collections were examined at the New York State Museum, the American Museum of Natural History, and the Academy of Natural Sciences of Philadelphia, and collection dates, locations, and sizes of *C. hippos* from coastal habitats of New York and New Jersey were recorded (material examined is listed in McBride[1]). Similar data for *C. hippos* in subtropical estuaries (from Cape Hatteras, North Carolina, to Cape Sable, Florida) were taken from Berry (1959). Densities and size data from samples collected in Great South Bay (New York) and southern New Jersey embayments during 1987 and 1988 were also examined (see McBride and Conover [1991] for seine-survey design; weir-sample data from Rountree et al.[2]). Fish densities in these other estuaries and from the published literature were calculated as

$$CPUE = (\textit{Catch per unit of effort [number of fish per seine haul]})$$

for the period May–October unless stated otherwise. Field sampling (described below) of temperate coastal habitats was also completed, and abundance, habitats, seasonality, and sizes of *C. hippos* were examined. Unless noted otherwise, fish size is reported to the nearest cm fork length (FL). A Gompertz model was used to model growth:

$$FL = L_{\infty} \exp\left(-\exp\left\{-G[DOY - X_0]\right\}\right),$$

where FL = fork length in mm;
L_{∞} = asymptotic length;
G = instantaneous rate of growth at age X_0;
DOY = day of the year, and
X_0 = inflection point of the curve.

[1] McBride, R. S. 1995. Perennial occurrence and fast growth rates by crevalle jacks (Carangidae: *Caranx hippos*) in the Hudson River estuary. *In* Final reports of the Tibor T. Polgar Fellowship Program, 1994 (E. A. Blair and J. R. Waldman, eds.), p. VI1–VI29. Hudson River Foundation, New York, NY.

[2] Rountree, R. A., K. J. Smith, and K. W. Able. 1992. Length frequency data for fishes and turtles from polyhaline subtidal and intertidal marsh creeks in southern New Jersey. Institute of Marine and Coastal Science (IMCS) report 92-34, Rutgers, the State Univ. of New Jersey, New Brunswick, NJ, 08903, 165 p.

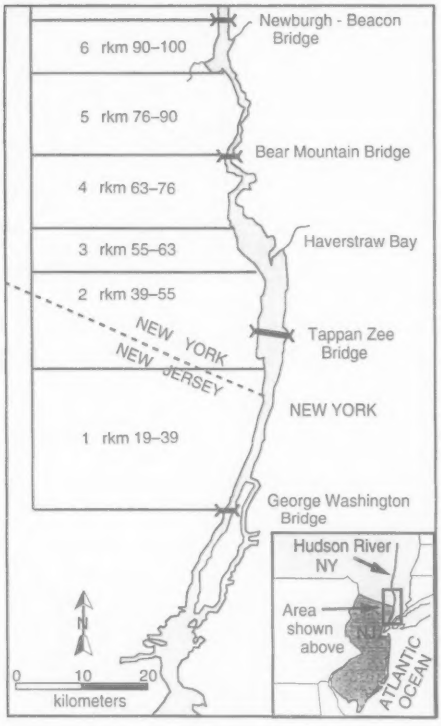

Figure 1

Sampling strata (1–6) in the Hudson River region where *Caranx hippos* was common. Haverstraw Bay is within strata 2–4. Strata 7–12 (river kilometers 100–246) are not shown. Jamaica Bay is located just east of the mouth of the Hudson River.

Growth modeling and other statistical analyses were performed by using SAS (SAS, 1990).

Field sampling—Hudson River

Recent data (1986–1993) were analyzed from an ongoing (since 1974) survey of the entire Hudson River (Fig. 1). Fish were collected during daylight over a 1-wk period every other week between mid-June and mid-November. During each sampling week, a 30.5-m × 2.4-m (max. mesh=10 mm) beach seine was set in an arc from a boat at approximately 100 stations. Station locations were selected in a stratified random design by using 12 strata between Manhattan and Albany, New York (from river kilometer [rkm] 19 to 246). The length of each stratum varied from 8 to 44 km, and typically 5–20 hauls were completed in each stratum during each biweekly period. Mean abundance, by month or stratum, was calculated from transformed values of the number of fish in each seine haul ($\log_e [n+1]$) and was expressed as a geometric mean (antilogged mean values of −1). Annual abundances were also calculated as geometric means but only for data from August to September (when *C. hippos* were consistently collected).

Field sampling—Haverstraw and Jamaica bays

Further analyses of the ecology of *Caranx hippos* in the Hudson River were based on data from an independent survey for the same 8-yr period (1986–1993) as the survey of the entire river. This additional survey focused on two subregions of the estuary: Haverstraw Bay and Jamaica Bay. Haverstraw Bay corresponds to strata numbers 2–4 of the Hudson River survey (Fig. 1); Jamaica Bay is a satellite embayment close to the mouth of the Hudson River.

Seining in Haverstraw Bay occurred biweekly from July to November (see also McKown and Young, 1992). Typically, 25 stations were sampled during daylight over a 2-d period; at each station, a single haul was made with a 61-m × 3-m beach seine (max. mesh=6.4 mm) set in an arc from a boat. This seine was used similarly in Jamaica Bay from May to November, but sampling frequency was generally monthly and only 4–5 stations were sampled each time. Temperature and salinity were measured with a hand-held thermometer and refractometer from surface-water samples after the net was hauled. Abundance of *C. hippos* was calculated as above (i.e. by geometric means).

Field sampling—the continental shelf

To determine seasonal abundance of *C. hippos* above the U.S. east coast continental shelf, we examined data collected during 1972–1996 in the National Marine Fisheries Service's bottom-trawling program. This program followed a stratified random statistical design to survey fish stocks of the continental shelf (9–366 m) from Cape Fear, North Carolina, to Nova Scotia, Canada. Standard methods were to tow a 24.4- or 30.5-m otter trawl (13-mm codend liner) for 30 min at randomly assigned stations within fixed strata (strata were delimited largely by depth and latitude). All samples combined covered all seasons, but sampling intensity was greatest during spring (March–May) and autumn (September–November), when about 350 stations were sampled during each 6–8 wk period. Fish were measured to the nearest cm. General survey design and its specific applications for other species can be found in many other studies (e.g. Grosslein and Azarovitz, 1982; Despres-Patanjo et al., 1988; McBride et al., 1998).

Results

Latitudinal comparisons

Young-of-the-year *C. hippos* occurred in subtropical estuaries between North Carolina and Florida from June to November and in temperate estuaries of New York and New Jersey during July–November (Fig. 2). On average, we observed only about one fish collected in three or more seine hauls, and these arithmetic mean densities were the same for temperate and subtropical estuaries (Fig. 3).

At subtropical latitudes, individuals <4.0 cm FL were present in all months, June–November (Fig. 2). Small individuals were also present for three months, July–September, at temperate latitudes. In both biogeographic regions,

some individuals had reached approximately 20 cm FL by October and November, suggesting that absolute growth could exceed 1 mm/d. The prolonged appearance of small fish in southern estuaries, in particular, and the lack of age-specific data precluded more detailed comparisons of growth rates.

Estuarine residency

In the Hudson River system, *C. hippos* occurred annually but its density varied by an order of magnitude among years (Table 1). This species occurred as far upstream as rkm 102 (i.e. lower part of stratum 7) but was most abundant in the upper portion of Haverstraw Bay (Fig. 4A). Seasonally, *C. hippos* resided in the Hudson River system from July to November and was most common from late July to early October (Figs. 4B, 5A). The median temperature for collections of *C. hippos* was 26°C in Haverstraw Bay and 24°C in Jamaica Bay (Fig. 6). Near Haverstraw Bay, where salinities were much lower than those of Jamaica Bay, *C. hippos* was capable of invading nearly freshwater regions of the Hudson River (Fig. 6). Abundance measured with a 61-m net, set in a comparable manner in both bays, showed that the abundance of *C. hippos* was much higher in Jamaica Bay than in Haverstraw Bay. Abundance in Great South Bay, New York, was also consistently higher than in Haverstraw Bay (Fig. 5A), even though a smaller, 30-m net was used.

Fork length of fish collected during 1986–1993 in the Hudson River estuary ranged from 2.9 to 17.6 cm. Growth rate was modeled by using data for New York and New Jersey estuaries (Fig. 5B; n=439), and the resulting equation,

$$FL = 136.6\exp\left(-\exp\{-0.0315[DOY - 211]\}\right), \quad (r^2=0.75),$$

predicted a peak instantaneous growth rate for July 30, after which growth slowed and fish reached a mean asymptotic length of 13.7 cm. The distribution of residuals for this growth model suggested that the asymptotic length was biased (i.e. lowered) by the presence of small, presumably young, juveniles in August–September; therefore we consider these growth estimates to be preliminary.

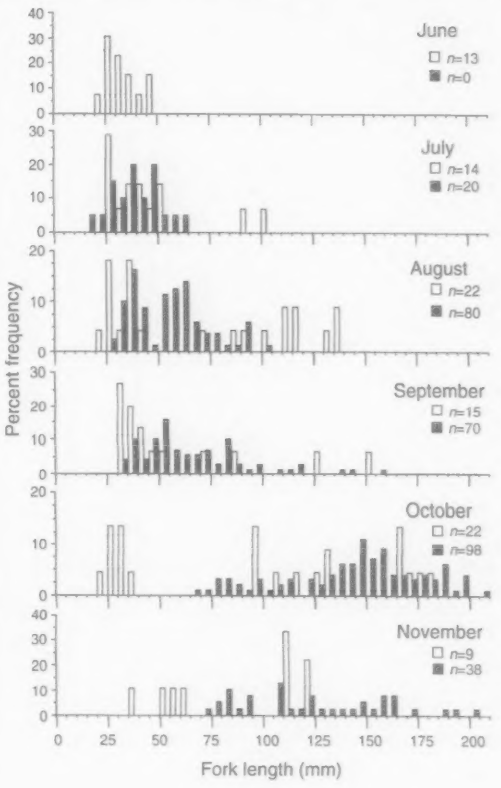

Figure 2

Monthly length frequencies of young-of-the-year *Caranx hippos* in estuaries from North Carolina to Florida (open bars) and New York or New Jersey (filled bars). Data for southern states are taken from Berry (1959; Table 23, Addenda, p: 534–535), and data for northern states are from material archived at the New York State Museum, Academy of Natural Sciences in Philadelphia, and American Museum of Natural History (listed in McBride[1]). n = number of fish measured.

Continental shelf distributions

A total of 657 *C. hippos* were collected at 134 stations between 33°47'N and 41°00'N and at depths from 6 to 38 m (Fig. 7A). Although present in all but four years during 1972–1996, *C. hippos* were collected only in the months of July (1 of 134 stations=0.8%), September (84.3%), October (14.2%), and November (0.8%) during this period. Fish ranged in size from 3 to 29 cm FL, and modal size (17 cm) was the same for fish collected both north and south of 36°00'N (Fig. 7B).

Discussion

Densities of *C. hippos* in Haverstraw Bay, where our study was focused, were generally low compared with other New York estuaries. We did observe considerable variation in densities of *C. hippos* between months, years, and estuaries, which we believe is at least partially the result of this species' relatively low density and shoaling (e.g. aggregating) behavior (Kwei, 1978). Larval dispersal processes or habitat may also affect juvenile *C. hippos* densities between temperate estuaries. This variability appears to have led to contradictory reports of *C. hippos* abundance at temperate latitudes: some investigators concluded that this species is "rare" or "scarce" (e.g. Bean, 1900; Greeley, 1937), whereas others have considered it to be "common" or "abundant" (DeKay, 1842; Smith, 1985).

Our review of seining data across a latitudinal range from 27°N to 41°N demonstrated that densities of *C. hippos* propagules transported to subtropical estuaries were not

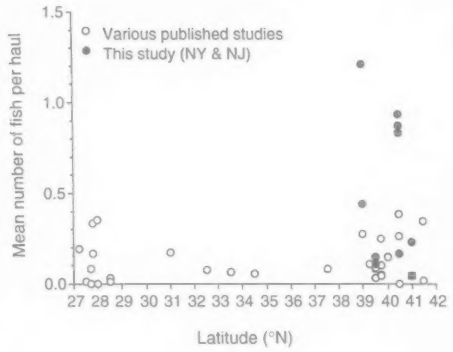
Various published studies
This study (NY & NJ)
Mean number of fish per haul
1.5
1.0
0.5
0.0
27 28 29 30 31 32 33 34 35 36 37 38 39 40 41 42
Latitude (°N)

Figure 3

Densities (arithmetic mean number of fish caught per seine haul) of young-of-the-year *Caranx hippos* by sampling latitude (Rhode Island to Florida). Data were limited to seines from 10- to 90-m long, set during May–October and calculated per year if a study was conducted for multiple years. Data were taken from the following surveys (open circles), listed here by decreasing latitude (with seine length): Hoff and Ibara, 1977 (12 m); Briggs and O'Connor, 1971 (91 m); Briggs, 1975 (91 m); Ecological Analysts, Inc. 1981. Ecological studies at Oyster Creek Nuclear Generating Station. Feb. 1981 EA Report JCP91I3 Progress Report. September 1979–August 1980, prepared for Jersey Central Power and Light Company, Appendix D, E, unpaginated (46 m); Marcellus, 1972 (11 m); Thomas, D. L., and C. B. Milstein 1973. Ecological studies in the bays and other waterways near Little Egg Inlet and in the ocean in the vicinity of the proposed site for the Atlantic generating station, NJ. Progress Report for January–December, 1972, vol. I: Fishes and volume II: Appendices, Ichthyological Associates, Inc. Absecon, NJ, 1065 p. (76 m); Thomas, D. L., C. B. Milstein, T. R. Tatham, R. C. Bieder, D. J. Danila, H. K. Hoff, D. P. Swiecicki, R. P. Smith, G. J. Miller, J. J. Gift, and M. C. Wyllie. 1975. Ecological studies in the bays and other waterways near Little Egg Inlet and in the ocean in the vicinity of the proposed site for the Atlantic generating station, NJ. Progress Report for January–December, 1974. Volume I: Fishes, 490 p. Ichthyological Associates, Inc. Absecon, NJ. (76 m); de Sylva, D. P., F. A. Kalber, and C. N. Shuster. 1962. Fishes and ecological conditions in the shore zone of the Delaware River Estuary, with notes on other species collected in deeper water. University of Delaware Marine Laboratory. Information Series Publication 5. Technical Report to Delaware Board of Game and Fish Commissioners under Dingell-Johnson Federal Aid in Fish and Wildlife Restoration. Delaware Project F-13-R-1-2-3, 150 p. Contact senior Richard McBride (senior author) for data of this report (18 m); Richards and Castagna, 1970 (12 m); Tagatz and Dudley, 1961 (21 m); Ogburn et al., 1988 (15 m); Anderson et al., 1977 (20 m); Miller, G. L., and S. C. Jorgenson. 1969. Seasonal abundance and length frequency distribution of some marine fishes in coastal Georgia, 103 p. U. S. Fish Wildl. Ser. Data Rep. 35. Washington, D.C. (on two microfische) (21 m); Gilmore, 1988 (62 m); Schooley, 1977 (12 m); Peters, 1984 (9 m); Futch and Dwinell, 1977 (15 m); and Gunter and Hall, 1963 (15 m). Data from the present study, restricted to the years 1987 and 1988, are shown separately (filled circles) and include two southern New Jersey locales and Haverstraw, Jamaica, and Great South bays, New York (30 and 61 m seine nets). There was no significant relationship among the data (Spearman correlation coefficent, r_s=0.24, n=40; P=0.14).

higher, as would be expected for a "subtropical" species, than densities of those propagules transported to temperate estuaries. Not all CPUE values we examine in our study were directly comparable because of potential differences in deployment procedures, sampling habitats, and range of seine sizes. We hope that others will report more data for such comparative purposes in the future. We are also unaware of comparative data for tropical regions to determine if this species is more abundant in a more central portion of its latitudinal range. Young-of-the-year *C. hippos* abundance is generally low compared with other estuarine finfishes from Massachusetts to Florida (e.g. Ayvazian et al., 1992; Tremain and Adams, 1995; Able et al., 1996), and we conclude that this species is uncommon throughout this range.

Having found juvenile *C. hippos* in reasonable densities in temperate estuaries, we also observed them to occupy habitats similar to those of juvenile *C. hippos* in subtropical estuaries. In both temperate and subtropical regions, juveniles of this species appear to use estuaries as nurseries (see also Berry, 1959; Kwei, 1978). We observed individuals as far upstream as the freshwater interface (about 1 ppt), at about rkm 90–100 in the Hudson River during July–October (Cooper et al., 1988; Geoghegan et al., 1992). Several others have reported YOY *C. hippos* in oligohaline habitats (Christensen, 1965; Tagatz, 1968; Smith, 1985; Beebe and Savidge, 1988) but none in fresh water. The presence of *C. hippos* within the Hudson River was associated with warm temperatures; this species occurred in similarly warm temperatures in subtropical estuaries (18–33°C: Tagatz and Dudley, 1961; Christensen, 1965; Tagatz, 1968). The concentration of fish in and near Haverstraw Bay is probably due to this region's broad width and shallow bathymetry, which slows waterflow rates and responds rapidly to solar radiation (Cooper et al., 1988). In addition, three power plants that release heated effluent are located near Haverstraw Bay (Cooper et al., 1988). Temperature eventually becomes a very important parameter affecting YOY *C. hippos* distribution, and cold temperatures have been implicated in several cases of overwintering mortality for *C. hippos*. We know of no experimental study to document the lower lethal temperature for this species, but Bean (1903) noted that *C. hippos* could overwinter in aquarium conditions above 10°C, and Hoff (1971) observed dead *C. hippos* in waters colder than 9°C, whereas conspecifics in a downstream portion of the same Massachusetts river survived in waters above 9°C. Water temperatures fall below 10°C for at least the 4-mo. period of December–April near Haverstraw Bay and above the continental shelf of the middle Atlantic states (Cooper et al., 1988; Mountain and Holzwarth, 1989); therefore there is no suitable overwintering habitat for *C. hippos* north of Cape Hatteras. Yet although the predictability of the seasonal cycle may be an important determinant of a species' latitu-

Table 1

Catch data for all Hudson River sampling sites; a 30.5-m seine or 61-m seine net was used. Geometric mean (GM) number of *C. hippos* per seine haul is calculated only from collections during peak abundance (August–September).

Year	Total no. of hauls	No. of hauls containing *C. hippos*	Total no. of *C. hippos* collected	GM	Total no. of hauls	No. of hauls containing *C. hippos*	Total no. of *C. hippos* collected	GM
Entire Hudson River (30.5-m seine)	All sampling strata				Haverstraw Bay (strata 2–4)			
1986	1000	6	10	0.0058	429	4	8	0.0135
1987	1101	2	3	0.0038	473	2	3	0.0089
1988	1100	12	22	0.0235	407	6	12	0.0344
1989	1100	15	40	0.0198	429	14	39	0.0468
1990	1000	19	32	0.0284	364	13	23	0.0395
1991	1000	11	58	0.0134	364	11	58	0.0341
1992	1000	9	53	0.0084	364	8	50	0.0130
1993	1000	17	30	0.0171	364	15	27	0.0403
Total	8301	91	248	—	3,194	73	220	—
Haverstraw and Jamaica bays (61-m seine)	Haverstraw Bay				Jamaica Bay			
1986	222	6	21	0.0398	38	2	10	0.732
1987	225	7	9	0.0406	56	4	14	0.468
1988	220	21	45	0.1578	42	4	54	1.151
1989	225	17	64	0.0730	49	2	2	0.000
1990	217	16	39	0.1274	48	7	11	0.475
1991	215	9	20	0.0649	58	4	6	0.000
1992	221	5	5	0.0140	44	2	3	0.292
1993	225	11	20	0.0437	43	3	11	0.000
Total	1770	92	223	—	378	28	111	—

dinal range, sudden and irregular freezes are more likely agents for actual hypothermal mortality, regardless of latitude (Storey, 1937). There are, for example, several instances of hypothermal mortality of *C. hippos* on Florida's Atlantic and Gulf coasts (Storey and Gudger, 1936; Miller, 1940; Galloway, 1941; Gilmore et al., 1978; Snelson and Bradley, 1978; Provancha et al., 1986). If individuals dispersed to temperate estuaries react in a similar manner to those dispersed to subtropical estuaries and emigrate from estuaries during autumn, then they may successfully migrate south to suitable overwintering habitats. We observed similar sizes of YOY *C. hippos* disappearing from estuaries and appearing on the continental shelf during September and October, which is strong circumstantial evidence of a migration pattern before hypothermal temperatures are reached.

During the summer, coastal water temperatures at temperate and subtropical latitudes are similar (e.g. Mountain and Holzwarth, 1989) and produce a favorable growth climate for *C. hippos* across a wide latitudinal range. Monthly sizes of YOY *C. hippos* were similar across latitudes, and the apparent growth rates were high in relation to other YOY estuarine fish species in temperate waters (Rountree and Able, 1992). Our comparative data suggested no size disadvantage for individuals dispersed to temperate estuaries. Overwintering mortality is size-dependent for some species that migrate offshore (Conover, 1990), so that if *C. hippos* in temperate waters were smaller by autumn than those in subtropical estuaries, then their overwinter survival could be lower. Nevertheless, individuals in temperate waters may be at a disadvantage to equal-size individuals in subtropical waters because the latter do not need to migrate as far to reach overwintering habitats. Our preliminary growth model was confounded by a prolonged (about 3 months) presence of small fish, and presumably there was considerable age variation within our late-summer samples. The continued presence of small fish into September confounded analysis of length frequencies and created the appearance of sudden shifts in average fish size in late summer. The discrepancy between predicted size in temperate estuaries during autumn and the modal size observed on the shelf (e.g. 14 vs. 17 cm FL) could be the result of smaller fish having a higher mortality rate during this habitat shift. Further work with growth modeling will improve with age-specific data. The growth and size data of our study, however, suggest that *C. hippos* emigrated from estuaries largely as YOY and at the same time and sizes across latitudes. These data suggest that the same behavioral cue to migrate operated on individuals dispersed to both biogeographic regions.

By the time YOY *C. hippos* reach shelf habitats during autumn, we postulate that they are of adequate size to continue south to subtropical latitudes. For example, YOY *C. hippos* are as large as "summer-spawned" YOY *P. saltatrix*; McBride et al. (1993) concluded the latter migrate from temperate nursery grounds to subtropical overwintering habitats at sizes of 10–15 cm FL. Moreover, several fish species have been tagged in temperate waters and recaptured in subtropical waters at sizes similar to those of *C. hippos* in autumn, including Atlantic croaker, *Micropogonias undulatus* (Pearson, 1932; Haven, 1959); spot, *Leiostomus xanthurus* (Pearson, 1932); weakfish, *Cynoscion regalis* (Nesbit, 1954); Atlantic thread herring, *Opisthonema oglinum* (Pristas and Cheek, 1973); bluefish, *P. saltatrix* (Lund and Maltezos, 1970); and Atlantic menhaden, *Brevoortia tyrannus* (Kroger and Guthrie, 1973). We reject the hypothesis that YOY *C. hippos* migrate offshore to the shelf edge, because they are distributed close to shore (<38 m) during autumn and they are not collected in winter or spring sampling out to 366 m depths by the National Marine Fisheries Service's trawling program. We similarly reject the hypothesis that the YOY *C. hippos* observed in coastal habitats during autumn have moved inshore from "offshore" nursery grounds. This cohort was not evident in summer trawl samples and such a hypothesis would require an alternative life history tactic for using shelf habitats as nurseries—a tactic that up until now has not been reported for this species.

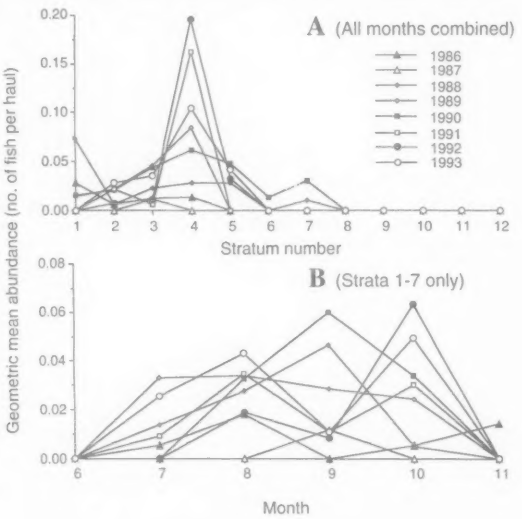

Figure 4

Variations in abundance of *Caranx hippos* from late June to early November: (**A**) Geometric mean abundance by sampling strata and year; (**B**) geometric mean abundance by month and year. All samples were collected with a 30.5-m seine and symbols denoting sampling year (1986–1993) in both A and B are the same. See Figure 1 for reference strata.

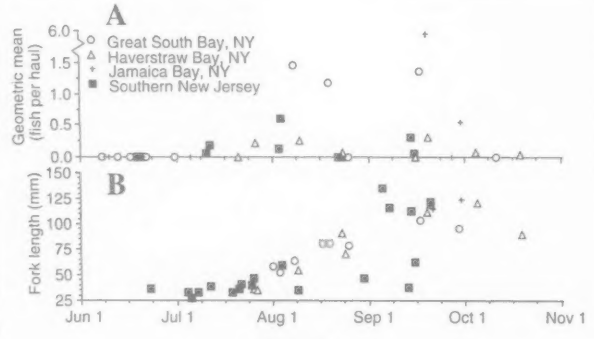

Figure 5

(**A**) Geometric mean abundance of *Caranx hippos* plotted for each sampling day during 1988 (seine-net collections only) for four estuarine systems in the New York and New Jersey region. (**B**) Mean length of *C. hippos* plotted for each sampling day during 1988 (same symbols used to denote each embayment as in A). Sampling gears differ between bays: Great South Bay—30.5-m seine, Haverstraw Bay—61-m seine, Jamaica Bay—61-m seine, and two southern New Jersey areas— 30.5-m seine plus lengths from weir samples.

Direct evidence (e.g. mark-recapture) of successful migrations by marine fishes is rare, and the migration patterns of many species are inferred from seasonal changes in distribution (Leggett, 1977), as we have done in our study. In addition, we have examined growth rates and sizes to link the seasonal changes in geographic distribution to the YOY cohort. The above evidence indirectly links some YOY *C. hippos* that have dispersed to temperate estuaries back to suitable overwintering habitats and suggests that these individuals retain "membership" in the spawning population (*sensu* Sinclair, 1988). We do not, however, assume that all individuals leave temperate estuaries before hypothermal conditions can develop, nor that all individuals survive an autumn migration to subtropical latitudes. The relative importance of temperate estuaries over subtropical estuaries for YOY *C. hippos* depends on the relative contribution to future spawning by individuals dispersed to each biogeographic region, but this contribution can not be calculated without further study.

Cape Hatteras represents a major faunal (and floral) break along the U.S. east coast (Pielou, 1979; Briggs, 1996), but the larvae of many species that spawn in coastal habitats, particularly of those that broadcast their eggs into the water column and have moderate-to-long planktonic larval durations, are capable of being transported around this geographic barrier (e.g. Curran, 1989). Among these species, we postulate that there is a subset of species that have juvenile traits that allow them to exploit nursery habitats in both biogeographic provinces, and an additional subset of species for which some individuals can return

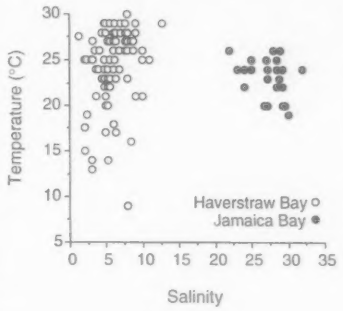

Figure 6

Scattergram of temperature and salinity measured at stations where young-of-the-year *Caranx hippos* were collected in Haverstraw (open circles) and Jamaica (filled circles) bays. Data were collected with 61-m seine nets and pooled for all years, 1986–1993.

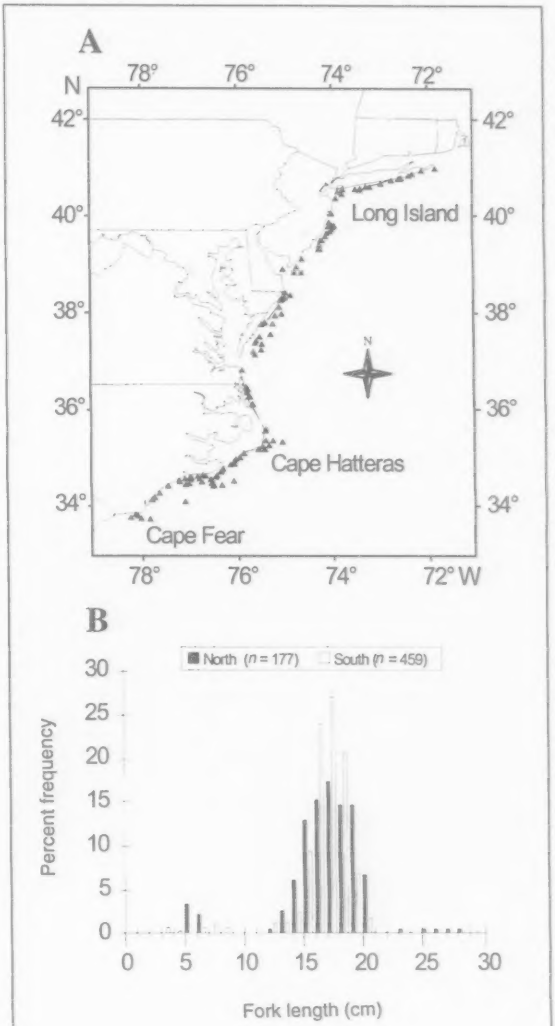

Figure 7

(**A**) Distribution of tows containing *Caranx hippos* based on sampling of the continental shelf between Cape Fear and southern New England. (**B**) Size frequency of *C. hippos* collected north (filled bars) and south (open bars) of 36°N. Samples are from bottom trawl collections for the years 1972–1996. There were no records of *C. hippos* farther north or east of Long Island (but see Bigelow and Schroeder, 1953). *n* = number of fish measured.

from temperate estuaries to reproduce. Traits such as early spawning season (i.e. winter or spring), fast growth rate, large YOY body size, generalized habitat requirements, and fast swimming speeds are favorable traits for any species attempting to complete a life-history circuit within one year between subtropical and temperate waters of the western North Atlantic. These traits are found in several finfish species in the Carangidae, Scombridae, and Mugilidae. Grouping species by spawning, larval, and juvenile characteristics and comparing their fate in these large oceanographic systems will help define the appropriate spatial scale for sampling these populations in the western North Atlantic, as well as in other systems such as the Sea of Japan (Nishimura, 1965), the Agulhas Current (Beckley, 1985), and the East Australian Current (Miskiewicz, 1981) where similar dispersal patterns of subtropically spawned species to temperate waters have been described. An initial screening for such characters allows researchers to begin to evaluate whether a specific "subtropical" species can or cannot survive once dispersed to temperate habitats.

Some of these subtropically spawned species are dispersed to temperate waters during less favorable conditions (e.g. winter) and, presumably, others do not grow to a sufficient size or have the behavior characteristics to migrate in autumn. A nonadaptive outcome of dispersal for many species on an ecological timescale is not, however, necessarily surprising. An examination of the paleontological record, which is most complete for invertebrates, shows that biogeographic assemblages lag notably behind environmental changes at an evolutionary timescale (Briggs, 1974; Pielou, 1979). A modeling and theoretical method, such as that used by Hare and Cowen (1993), could help explain why the larvae of so many species are dispersed into large oceanographic systems even when expatriation is likely, but more natural history data are necessary before such a method can be widely applied. A more complete record of which species are and are not expatriated within large-scale systems will contribute to understanding the processes underlying these biogeographic patterns, provide opportunities to examine further the evolution of

reproductive strategies, and help explain oceanographic effects on population dynamics.

Acknowledgments

R. Daniels, W. Saul, and C. L. Smith assisted with the collections at the New York State Museum, the Academy of Natural Sciences of Philadelphia, and the American Museum of Natural History, respectively. Data for the entire Hudson River were collected for Consolidated Edison and were made available by J. Young and G. Sentell of EA Engineering, Science, and Technology. B. Young, L. Pasciutti, M. Penski, and other biologists of the New York State Department of Environmental Protection helped collect data for Haverstraw Bay and Jamaica Bay. Trawling data were collected by the Northeast Fishery Science Center, National Marine Fisheries Service, and made available by T. Azarovitz and B. O'Gorman. Valuable discussions or comments were provided by K. Able, F. Berry, E. Blair, D. Conover, R. Crabtree, J. Hare, S. Kaiser, R. Loveland, W. Smith-Vaniz, and J. Waldman. Final data analyses and manuscript preparation were completed while R.S.M. was employed at he Florida Marine Research Institute. Editorial assistance was provided by L. French, J. Leiby, and J. Quinn. This research was supported in part by a Tibor T. Polgar Fellowship to R.S.M. from the Hudson River Foundation. We are grateful to all of the above.

Literature cited

Able, K. W., D. A. Witting, R. S. McBride, R. A. Rountree, and K. J. Smith.
1996. Fishes of polyhaline estuarine shores in Great Bay-Little Egg Harbor, New Jersey: a case study of seasonal and habitat influences. *In* Estuarine shores: environments and human alterations (K. F. Nordstrom and C. T. Roman, eds.), p. 335–355. John Wiley and Sons, Ltd. New York, NY.

Anderson, W. D., Jr., J. K. Dias, R. K. Dias, D. M. Cupka, and N. A. Chamberlain.
1977. The macrofauna of the surf zone off Folly Beach, South Carolina. U.S. Dep. Commer., NOAA Tech. Rep. NMFS-SSRF 704, 23 p.

Ayvazian, S. G., L. A. Deegan, and J. T. Finn.
1992. Comparison of habitat use by estuarine fish assemblages in the Acadian and Virginian zoogeographic provinces. Estuaries 15:368–383.

Bean, T. H.
1900. Report on the fishes of Long Island collected in the summer of 1898. N.Y. State Mus. Rep. 52. vol. 1, p. r103.
1903. Catalogue of the fishes of New York. Bull. N. Y. State Mus. 60, Zoology 9:428–429.

Beckley, L. E.
1985. The fish community of East Cape tidal pools and an assessment of the nursery function of the habitat. South African J. Zool. 20:21–27.

Beebe, C. A., and I. R. Savidge.
1988. Historical perspective on fish species composition and distribution in the Hudson River estuary. Am. Fish. Soc. Monogr. 4:25–36.

Berry, F. H.
1959. Young jack crevalles (*Caranx* species) off the southeastern Atlantic coast of the United States. Fish. Bull. 59:417–535.

Bigelow, H. B., and W. C. Schroeder.
1953. Fishes of the Gulf of Maine. U.S. Fish and Wildl. Serv. Bull.74, vol. 53, 577 p.

Briggs, J. C.
1960. Fishes of worldwide (circumtropical) distribution. Copeia 1960:171–180.
1974. Marine zoogeography. McGraw-Hill Book Co, New York, NY, 475 p.
1996. Global biogeography. Elsevier, Amsterdam, The Netherlands, 452 p.

Briggs, P. T.
1975. Shore-zone fishes of the vicinity of Fire Island Inlet, Great South Bay, New York, N.Y. Fish Game J. 22:1–12.

Briggs, P. T., and J. S. O'Connor.
1971. Comparison of shore-zone fishes over naturally vegeetated and sand-filled bottoms in Great South Bay. N. Y. Fish Game J. 18:16–41.

Chiarella, L. A., and D. O. Conover.
1990. Spawning season and first-year growth of adult bluefish from the New York Bight. Trans. Am. Fish. Soc. 119:455–462.

Christensen, R. F.
1965. An ichthyological survey of Jupiter Inlet and Loxahatchee River, Florida. M.S. thesis. Fla. State Univ., Tallahassee, FL, 318 p.

Conover, D. O.
1990. The relation between capacity for growth and length of growing season: evidence for the implications of countergradient variation. Trans. Am. Fish. Soc. 119:416–430.

Cooper, J. C., F. R. Cantelmo, and C. E. Newton.
1988. Overview of the Hudson River estuary. Am. Fish. Soc. Monogr. 4:11–24.

Cowen, R. K., J. A. Hare, and M. P. Fahay.
1993. Beyond hydrography: can physical processes explain larval fish assemblages within the Middle Atlantic Bight? Bull. Mar. Sci. 53:567–587.

Curran, M. C.
1989. Occurrence of tropical fishes in New England waters. *In* Proceedings of the American Academy of Underwater Science; Ninth Ann. Sci. Diving Symp. Sept. 28–Oct. 1, 1989 (M. A. Lang and W. C. Jaap, eds.), p. 71–82. Am. Academy of Underwater Sciences, Costa Mesa, CA.

DeKay, J. E.
1842. Zoology of New York or the New York Fauna. Part III: reptiles and amphibia, p: 120–121. W. & A. White & J. Visscher, Albany, NY.

Despres-Patanjo, L. I., T. R. Azarovitz, and C. J. Byrne.
1988. Twenty-five years of fish surveys in the northwest Atlantic: the NMFS Northeast Fisheries Center's Bottom Trawl Survey Program. Mar. Fish. Rev. 50:69–71.

Fahay, M. P.
1975. An annotated list of larval and juvenile fishes captured with surface-towed meter net in the South Atlantic Bight during four RV *Dolphin* cruises between May 1967 and February 1968. U.S. Dep. Commer., NOAA Tech. Rep. NMFS-SSRF-685, 39 p.

Futch, C. R., and S. E. Dwinell.
1977. Nearshore marine ecology at Hutchinson Island, Florida: 1971–1974. IV: Lancelets and fishes. Fla. Mar. Res. Publ. 24, 23 p.

Galloway, J. C.
1941. Lethal effect of the cold winter of 1939–40 on marine fishes at Key West, Florida. Copeia 1941:118–119.

Geoghegan, P., M. T. Mattson, J. J. Reichle, and R. G. Keppel.
1992. Influence of salt front position on the occurrence of uncommon marine fishes in the Hudson River Estuary. Estuaries 15:251–254.
Gill, T.
1904. State ichthyology of Massachusetts. Science (new series) 20:321–338.
Gilmore, R. G., Jr.
1988. Subtropical seagrass fish communities: population dynamics, species guilds and microhabitat associations in the Indian River Lagoon, Florida. Ph.D. diss., Fla. Inst. Tech. Melbourne, FL, 199 p.
Gilmore, R. G., Jr., L. H. Bullock, and F. H. Berry.
1978. Hypothermal mortality in marine fishes, south-central Florida, January, 1977. Northeast Gulf Sci. 2:77–97.
Greeley, J. R.
1937. Fishes of the area with annotated list. *In* Survey of the lower Hudson watershed, p. 45–103. State of New York Conservation Department, Albany, NY.
Grosslein, M. D., and T. R. Azarovitz.
1982. Fish distribution. MESA New York Bight Atlas Monograph 15. New York Sea Grant Institute, Albany, NY, 182 p.
Gunter, G., and G. E. Hall.
1963. Biological investigations of the St. Lucie estuary (Florida) in connection with Lake Okeechobee discharges through the St. Lucie canal. Gulf Res. Rep. 1:189–307.
Hare, J. A., and R. K. Cowen.
1991. Expatriation of *Xyrichtys novacula* (Pisces: Labridae) larvae: evidence of rapid cross-slope exchange. J. Mar. Res. 49:801–823.
1993. Ecological and evolutionary implications of the larval transport and reproductive strategy of bluefish, *Pomatomus saltatrix*. Mar. Ecol. Prog. Ser. 98:1–16.
1996. Transport mechanisms of larval and pelagic juvenile bluefish (*Pomatomus saltatrix*) from South Atlantic Bight spawning grounds to Middle Atlantic Bight nursery habitats. Limnol. Oceanogr. 41:1264–1280.
Haven, D. S.
1959. Migration of the croaker, *Micropogon undulatus*. Copeia 1959:25–30.
Hoff, J. G.
1971. Mass mortality of the crevalle jack, *Caranx hippos* (Linnaeus) on the Atlantic coast of Massachusetts. Chesapeake Sci. 12:49.
Hoff, J. G., and R. M. Ibara.
1977. Factors affecting the seasonal abundance, composition and diversity of fishes in a southeastern New England estuary. Estuarine Coastal Marine Sci. 5:665–678.
Juanes, F., J. A. Buckel, and D. O. Conover.
1994. Accelerating the onset of piscivory: intersection of predator and prey phenologies. J. Fish Biol. 45 (suppl. A):41–54.
Juanes, F., J. A. Hare, and A. G. Miskiewicz.
1996. Comparing early life history strategies of *Pomatomus saltatrix*: a global approach. Mar. Freshwater Res. 47:365–79.
Kleckner, R. C., and J. D. McCleave.
1985. Spatial and temporal distribution of American eel larvae in relation to North Atlantic ocean current systems. Dana 4:67–92.
Kroger, R. L., and J. F. Guthrie.
1973. Migrations of tagged juvenile Atlantic menhaden. Trans. Am. Fish. Soc. 102:417–422.
Kwei, E. A.
1978. Food and spawning activity of *Caranx hippos* (L.) off the coast of Ghana. J. Nat. Hist. 12:195–215.
Leggett, W. C.
1977. The ecology of fish migrations. Ann. Rev. Ecol. Syst. 8:285–308.
Lund, W. A., and G. C. Maltezos.
1970. Movements and migrations of the bluefish, *Pomatomus saltatrix*, tagged in waters of New York and Southern New England. Trans. Am. Fish. Soc. 99:719–725.
Marcellus, K. L.
1972. Fishes of Barnegat Bay, New Jersey, with particular reference to seasonal influence and the possible effect of thermal discharge. Ph.D. diss., Rutgers Univ., New Brunswick, NJ, 172 p.
Markle, D. F., W. B. Scott, and A. C. Kohler.
1979. New and rare records of Canadian fishes and the influence of hydrography on resident and nonresident Scotian shelf ichthyofauna. Can. J. Fish. Aquat. Sci. 37:49–65.
McBride, R. S., and K. W. Able.
1998. Ecology and fate of butterflyfishes *Chaetodon* spp. in the temperate, western North Atlantic. Bull. Mar Sci. 63(2):401–416.
McBride, R. S., and D. O. Conover.
1991. Recruitment of young-of-the-year bluefish (*Pomatomus saltatrix*) to the New York Bight: Variation in abundance and growth of spring- and summer-spawned cohorts. Mar. Ecol. Prog. Ser. 78:205–216.
McBride, R. S., J. B. O'Gorman, and K. W. Able.
1998. Interspecific comparisons of searobins (*Prionotus* spp.) movements, size structure, and abundance in the temperate western North Atlantic. Fish. Bull. 96:303–314.
McBride, R. S., J. L. Ross, and D. O. Conover.
1993. Recruitment of bluefish (*Pomatomus saltatrix*) to estuaries of the South Atlantic Bight. Fish. Bull. 91:389–395.
McCleave, J. D.
1993. Physical and behavioural controls on the oceanic distribution and migration of leptocephali. J. Fish Biol. 43 (suppl. A):243–273.
McCleave, J. D., R. C. Kleckner, and M. Castonguay.
1987. Reproductive sympatry of American and European eels and implications for migration and taxonomy. Am. Fish. Soc. Symp. 1:286–297.
McKown, K. A., and B. H. Young.
1992. Effects of year class strength on size of young-of-the-year striped bass. *In* Estuarine research in the 1980's (C. L. Smith, ed.), p. 265–276. State Univ. New York Press. Albany, NY.
Miller, E. M.
1940. Mortality of fishes due to cold on the southeast Florida coast. Ecology 21:420–421.
Miskiewicz, A. G.
1981. The distribution of tropical/coral reef fish larvae in temperate waters along the New South Wales coast of Australia. Rapp. P.-V. Cons. Int. Explor. Mer 191:452.
Montolio, M.
1978. Algunos aspectos sobre el desove y las concentraciones larvarias de las especies de la familia Carangidae en el Mar Caribe. Rev. Cubana Invest. Pesqueras 3:29–49.
Moss, S. A.
1973. The responses of planehead filefish, *Monocanthus hispidis* (Linnaeus), to low temperature. Chesapeake. Sci. 14:300–303.
Mountain, D. G., and T. J. Holzwarth.
1989. Surface and bottom temperature distribution for the northeast continental shelf. U.S. Dep. Commer., NOAA Tech. Memo. NMFS-F/NEC-73, 32 p.
Nesbit, R. A.
1954. Weakfish migration in relation to its conservation. U.S. Fish Wildl. Spec. Sci. Rep.-Fish. 115, 81 p.

Nishimura, S.
1965. The zoogeographical aspects of the Japan Sea, part 1. Publ. Seto Mar. Biol. Lab. 13:35–79.
Ogburn, M. V., D. M. Allen, and W. K. Michener.
1988. Fishes, shrimps, and crabs of the North Inlet Estuary, SC: a four-year seine and trawl survey. Baruch Institute Tech. Rep. 88-1, Univ. South Carolina. Columbia, SC, 299 p.
Pearson, J. C.
1932. Winter trawl fishery off the Virginia and North Carolina coasts. U.S. Bur. Fish. Invest. Rep. 10, 31 p.
Peters, D. J.
1984. Seasonality, residency, and spatial distribution of juvenile surf zone fishes of the Florida east coast. M.S. thesis, Fla. Inst. Tech., Melbourne, FL, 66 p.
Pielou, E. C.
1979. Biogeography. John Wiley & Sons. New York, NY, 351 p.
Pristas, P. J., and R. P. Cheek.
1973. Atlantic thread herring (*Opisthonema oglinum*) movements and population size inferred from tag returns. Fish. Bull. 71:297–301.
Provancha, M. J., P. A. Schmalzer, and C. R. Hall.
1986. Effects of the December 1983 and January 1985 freezing air temperatures on select aquatic poikilotherms and plant species of Merritt Island, Florida. Fla. Sci. 49:199–212.
Richards, C. E., and M. Castagna.
1970. Marine fishes of Virginía's eastern shore (inlet and marsh, seaside waters). Chesapeake Sci. 11:235–248.
Rountree, R. A., and K. W. Able.
1992. Fauna of polyhaline subtidal marsh creeks in southern New Jersey: composition, abundance, and biomass. Estuaries 15:178–220.
SAS Institute, Inc.
1990. SAS/STAT user's guide, vols. 1 and 2. SAS Institute, Inc., Cary, NC, 1686 p.
Schooley, J. K.
1977. Factors affecting the distribution of the nearshore fishes in the lagoonal waters of the Indian River, Florida. M.S. thesis, Univ. Florida. Gainesville, FL, 165 p.
Sinclair, M.
1988. Marine populations: an essay on population regulation and speciation. Washington Sea Grant Program. Seattle, WA, 252 p.
Smith, C. L.
1985. The inland fishes of New York State. The New York State Department of Environmental Conservation. Albany, NY, 522 p.
Snelson, F. F., and W. K. Bradley Jr.
1978. Mortality of fishes due to cold on the east coast of Florida, January, 1977. Fla. Sci. 41:1–12.
Storey, M.
1937. The relation between normal range and mortality of fishes due to cold at Sanibel Island, Florida. Ecology 18:10–26.
Storey, M., and E. W. Gudger.
1936. Mortality of fishes due to cold at Sanibel Island, Florida, 1886–1936. Ecology 17:640–648.
Tagatz, M. E.
1968. Fishes of the St. Johns River, Florida. Quart. J. Fla. Acad. Sci. 30:25–50.
Tagatz, M. E., and D. L. Dudley.
1961. Seasonal occurrence of marine fishes in four shore habitats near Beaufort, N.C., 1957–60. U. S. Fish Wildl. Spec. Sci. Rep. Fish 390, 19 p.
Tesch, F.-W.
1977. The eel: biology and management of Anguillid eels. Chapman and Hall. London, United Kingdom, 434 p.
Tremain, D. M., and D. H. Adams.
1995. Seasonal variations in species diversity, abundance, and composition of fish communities in the northern Indian River Lagoon, Florida. Bull. Mar. Sci. 57:171–192.
U. S. Department of Commerce.
1986. Marine recreation fishery statistics survey, Atlantic and Gulf coasts, 1985. Current Fishery Statistics 8327. Natl. Mar. Fish. Serv. Washington, D.C., 21 p.
Wroblewski, J. S., and J. Cheney.
1984. Ichthyoplankton associated with a warm core ring off the Scotian Shelf. Can. J. Fish. Aquat. Sci. 41:294–303.

Revision of the genus *Lepidopsetta* Gill, 1862 (Teleostei: Pleuronectidae) based on larval and adult morphology, with a description of a new species from the North Pacific Ocean and Bering Sea

James W. Orr

Ann C. Matarese

Resource Assessment and Conservation Engineering Division
Alaska Fisheries Science Center
National Marine Fisheries Service, NOAA
7600 Sand Point Way NE
Seattle, Washington 98115-0070
E-mail address (for J. W. Orr): James.Orr@noaa.gov

Abstract.—The endemic North Pacific pleuronectid genus *Lepidopsetta* Gill is revised to include three species: *L. bilineata* (Ayres), *L. polyxystra* n. sp., and *L. mochigarei* Snyder. Adults of *L. bilineata* can be distinguished by a low gill-raker count and high supraorbital pore count; larvae may be distinguished by four dorsal midline melanophores, heavy finfold pigment, a short snout-to-anus length, and a deep body. The species ranges from Baja California to the eastern Aleutian Islands and the extreme southeastern Bering Sea. Adults of *L. mochigarei* are distinguished from all other members of *Lepidopsetta* by higher scale and preopercular pore counts and lower gill-raker and supraorbital pore counts. Larvae are similar to larvae of *L. bilineata* but can be distinguished by their postanal pigment pattern and melanophores on pectoral-fin rays. *Lepidopsetta mochigarei* ranges from the southern Sea of Okhotsk to Korea. Adults of *L. polyxystra* n. sp. are diagnosed by a high gill-raker count and low supraorbital pore count; larvae are diagnosed by two dorsal midline melanophores, light finfold pigment, long snout-to-anus length, and a slender body. The species is found from Puget Sound through the Bering Sea and Aleutian Islands to the Kuril Islands, overlapping with *L. bilineata* from the extreme southeastern Bering Sea to Puget Sound and with *L. mochigarei* in the southern Sea of Okhotsk. Synonymies, diagnoses, descriptions, and geographic distributions are provided for adults and larvae of all species; keys are provided for adults. Descriptions of early juveniles of eastern North Pacific species are also presented. Under the name of *L. bilineata*, *L. polyxystra* n. sp. has been the subject of many studies of eastern North Pacific *Lepidopsetta*. All previous studies of specimens from the southeastern Bering Sea into Puget Sound should be considered applicable at the generic level only, unless voucher specimens are verifiable.

Manuscript accepted 22 February 2000.
Fish. Bull. 98:539–582 (2000).

The flatfishes (Pleuronectiformes) of the eastern North Pacific Ocean constitute a major component of the commercial fisheries of the region. In the Bering Sea, which encompasses the largest fisheries resource of the United States, the rock soles of the genus *Lepidopsetta* are the second most abundant flatfishes and the third most abundant commercial groundfish species, second only to yellowfin sole (*Limanda aspera*) and walleye pollock (*Theragra chalcogramma*) (NMFS, 1999).

At the species level, eastern North Pacific pleuronectids have been considered well known. Nearly all species were recognized and described during the latter half of the 1800s, primarily through the activities of California ichthyologists. Among the names that remain valid, the last species to be described was *Limanda sahkalinensis* Hubbs, 1915, although in the western Pacific *Microstomus shuntovi* Borets, 1983, was most recently described from the northwestern Hawaiian ridge. However, these earlier works were based on adult morphology, and only recently has a knowledge of the ontogeny of these species been acquired. Among the descriptions of early life history stages of eastern North Pacific pleuronectids, one morphological form could not be traced to a recognized species. Examination of this form led to the following revision of the genus *Lepidopsetta*.

Four nominal species have been described and allocated to the genus *Lepidopsetta*: *Platessa bilineata* Ayres, 1855a, was described from San Francisco material, and apparently without the knowledge of Ayres' slightly earlier description, a specimen collected near Puget Sound was described as *Platichthys umbrosus* Girard, 1856. Gill (1862) erected *Lepidopsetta* to contain *Platichthys umbrosus* and later (1864) indicated that *Platessa bilineata* Ayres, 1855a, was allied and perhaps congeneric. Lockington (1879b) published a redescription of *L. umbrosa*, describing the misidentified new species *Isopsetta isolepis* (Lockington, 1880a), which he ultimately removed from *Lepidopsetta* to his new genus *Isopsetta* (Lockington, 1883). In his description of *Lepidopsetta isolepis*, he treated *Platichthys umbrosus* Girard as a synonym of *L. bilineata*. Nearly 20 years after Gill's erection of *Lepidopsetta*, Cope (1873) described *Pleuronectes perarcuatus* from Alaska, later considered a synonym of *L. bilineata* by Jordan and Gilbert (1881). Jordan and Evermann (1898) considered each of these nominal species members of *Lepidopsetta* and further as synonyms of *L. bilineata*, although they recognized the northern populations ("Puget Sound and northward") as *L. bilineata umbrosa*. Finally, Japanese *Lepidopsetta* were described by Snyder (1911) as *L. mochigarei* and Jordan and Hubbs (1925) considered all Japanese *Lepidopsetta* to be representatives of this species.

More recently, the genus has been envisioned as containing either two spe-

cies, *L. bilineata* of the eastern North Pacific Ocean and Bering Sea and *L. mochigarei* of the western North Pacific around Japan (Hubbs, 1915; Sakamoto, 1984b), or a single species, *L. bilineata*, with two subspecies *L. b. bilineata* and *L. b. mochigarei* in the Bering Sea and western Pacific (Taranets, 1937; Schmidt, 1950). A third subspecies in the southeastern North Pacific was recognized by Moiseev (1953) and Wilimovsky et al. (1967). Although both authors split eastern Pacific populations into two subspecies, Moiseev (1953) considered the northern subspecies to be *L. b. bilineata* and the southern subspecies to be *L. b. umbrosa*, whereas Wilimovsky et al. (1967) applied the names *L. b. perarcuata* and *L. b. bilineata* to northern and southern populations, respectively.

Our study arose from an examination of collections from ichthyoplankton surveys conducted from the Bering Sea to northern California by the Recruitment Processes Task (referred to simply as "Task" in the following account) of the Alaska Fisheries Science Center (AFSC). In 1985, ichthyoplankton taxonomists began to routinely separate an unidentified pleuronectid from numerous collections. Larvae from the developmental series of this unidentified pleuronectid most closely resembled larvae previously described as *Psettichthys melanostictus* (Hickman, 1959; Pertseva-Ostroumova, 1961) and, for the following few years, larval pigment patterns and morphological characters were used to separate what were then considered *Psettichthys* into two readily distinguishable morphotypes. Thus in 1986, an early draft of the Task's laboratory guide (Matarese et al., 1989) included illustrations of an unidentified series referred to as a variant of *Psettichthys* ("*Psettichthys* 2").

During winter and spring 1987, larvae of both morphotypes of "*Psettichthys*" were collected from Puget Sound and reared through transformation and settlement stages, and upon examination of the reared juveniles, Kendall and Matarese[1] determined that larvae previously referred to as "*Psettichthys* 2" were, in fact, another form of *Lepidopsetta*. From the early results of this work, Matarese et al. (1989) decided to include a partial description of the unknown pleuronectid (referred to as "*Lepidopsetta* 2") and compared various stages with larvae of *Psettichthys* and other *Lepidopsetta*. Mulligan et al. (1995) finally verified the identity of *Lepidopsetta* 2 by rearing larvae spawned from *Lepidopsetta* adults collected in Puget Sound and conducted a morphological study of adults. Although they reported significant heterogeneity in shape, structure, and allozymes, they recommended the retention of Wilimovsky et al.'s (1967) subspecies designations.

Although previous authors (Townsend, 1936, 1937; Wilimovsky et al., 1967; Mulligan et al., 1995) concluded that observed variation represented a cline smoothly grading from California through the Bering Sea to Japan and supported subspecific designations, new data became available in 1992 with the development of a fishery for *Lepidopsetta* in the northern Gulf of Alaska. Domestic fisheries observers (see "Acknowledgments" section) experienced in sampling in the Bering Sea flatfish fisheries began to report the presence of two syntopic adult forms of *Lepidopsetta* in the northern Gulf of Alaska, one distinctly different from the form in the eastern Bering Sea. These observations spurred a further examination into the morphological differences of all life stages of *Lepidopsetta*. Our revision therefore incorporates evidence from adult, juvenile, and larval morphology and distribution to support the recognition of three species, one described as new, in the North Pacific. We describe morphological variation in adults, juveniles, and larvae; differentially diagnose adults, juveniles, and larvae; and describe geographic and bathymetric distributions of the three species.

Materials and methods

Unless indicated otherwise, standard length (SL) is used throughout. Institutional abbreviations follow Leviton et al. (1985) and Leviton and Gibbs (1988), as modified by Poss and Collette (1995), except for the Kamchatka Institute of Ecology, abbreviated as KIE.[2]

Adult morphology

Meristic data, except gill-raker counts, and morphometric data were taken from the ocular-side of adult material, following Hubbs and Lagler (1958) with the following exceptions. Standard, head, and snout length were measured from the anterior margin of the maxilla, with the mouth closed. Body depth was the greatest depth measured at the origin of the anal fin. Head length included only the opercle and not the opercular membrane. Snout length was measured to the anterior edge of the dorsal orbit. Cheek length was the greatest distance from the posterior rim of the ventral orbit to the edge of the preopercle, often the posterior angle of the preopercle. Interorbital width equals the least bony width. Pectoral-fin length was the length of the longest ray, often the third ray, and was measured for both ocular-side and blind-side fins. Lateral-line arch length was the distance between anterior and posterior flexion points, and this straight line was used as the base for the depth measurement. Greatest caudal peduncle depth was measured at the base of the caudal fin.

All rayed elements were included in counts of fin rays. The last two rays of the dorsal and anal fins were counted separately. Scales above the lateral line were counted on a diagonal at the greatest depth between the dorsal-fin base and lateral line. Scales below the lateral line were counted from the anal-fin origin on a diagonal to the lateral line. Total scales above and below the lateral line is the sum of the two counts. Cheek scales were counted at greatest cheek length. Ocular-side suborbital pores were counted

[1] Kendall, A. W., Jr., and A. C. Matarese. 1987. Unpubl. data. Resource Assessment and Conservation Engineering Division, Alaska Fisheries Science Center, Natl. Mar. Fish. Serv., NOAA, 7600 Sand Point Way NE, Seattle, WA 98115.

[2] Sheiko, B. 1997. Personal commun. Kamchatka Institute of Ecology, Partizanskaya 6, Petropavlovsk-Kamchatsky 683000, Russia. Present address: Department of Ichthyology, Zoological Institute, Russian Academy of Sciences, Universitetskaynab. 1, St. Petersburg 199034, Russia.

from the first pore branching from the temporal canal to the anteriormost pore; all pores were counted, including those dorsal and ventral to the canal. Blind-side suborbital pores were counted from the first pore branching from the postorbital canal to the anteriormost pores. Pore counts of the dorsal anterior and posterior branches of the accessory dorsal branch of the lateral line (ADB) began with the first pore of each branch and did not include the single pore typically found at the intersection of the two branches. Supraorbital pores include the first pore dorsal to the postorbital canal and include those pores at the posterior rim of the dorsal orbit (Fig. 1). Preopercular pores begin with the first pore posterior to the mandibular articulation and end at the last pore before the temporal canal. Caudal-fin terminology follows Sakamoto (1984a).

Larval collections

Most data were garnered from samples collected by the AFSC with standard bongo gear during ichthyoplankton surveys of the Bering Sea and Gulf of Alaska (1971–1994, Table 1, Appendix Table 1). In most cases, the identities of specimens collected prior to 1985 (when the unidentified pleuronectid developmental series was first separated) have been verified. All larval specimens used for illustrations and morphological descriptions have been cataloged at the University of Washington Fish Collection (UWFC); other material will be archived at the UWFC as well (see Appendix Table 1). Additional data for *Lepidopsetta* in Canadian waters were obtained from the Canadian Department of Fisheries and Oceans, Pacific Biological Station, Nanaimo (W. Shaw), and Vancouver Public Aquarium (J. Marliave; these specimens are now deposited at UWFC). The Washington Department of Fisheries also provided distribution and life history data for Puget Sound.[3] In addition, dip-net sampling in Puget Sound conducted by the AFSC from 1985 through 1995 resulted in 16 collections of *Lepidopsetta* larvae (Busby et al., 2000). Two larvae from the Washington, Oregon, and northern California survey area were examined—the only two *Lepidopsetta* larvae collected during the eight years (from 1980 to 1987) during which the AFSC conducted ichthyoplankton cruises in the region. Geoff Moser, NMFS Southwest Fisheries Science Center (SWFSC), provided data for *Lepidopsetta* collected during California Cooperative Fisheries Investigations (CalCOFI) cruises conducted along the coast of California.

Identification of juveniles

Recently transformed juveniles present particular problems in identification because adult characters, such as meristics and pigment patterns, are not completely developed and some aspects of larval shape, structure, and pigment patterns are retained. Thus, early juveniles (approximately 20–35 mm SL) were identified by a combination of characters, including gill-raker counts of the first arch, larval pigment characters retained on the blind side, and size at transformation. Although gill rakers were not fully formed, specimens with counts greater than seven on the lower arch were assumed to be the new species. Juveniles with counts of seven or less were identified in conjunction with other characters. Postsettlement juveniles greater than 30 mm SL were separated by using the above characters in addition to counts of the number of supraorbital pores. *Lepidopsetta bilineata* typically has 4–6 head pores along the supraorbital canal, whereas the new species typically has 1–3. Differences in gill-raker structure useful in distinguishing adults are usually not evident at sizes less than 200 mm SL.

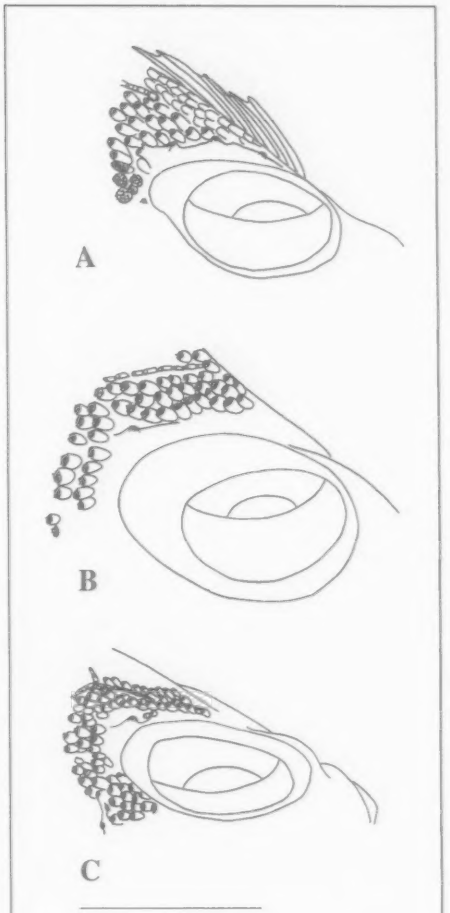

Figure 1

Supraorbital pores of *Lepidopsetta* species: **(A)** *L. bilineata*, UW 29670, 187.5 mm; **(B)** *L. polyxystra* n. sp., UW 044023, 239.5 mm; **(C)** *L. mochigarei*, USNM 68245, 174.0 mm, holotype. View of dorsal (right lateral) side. Scale bar equals 15 mm.

[3] Penttila, D. 1996. Personal commun. Puget Sound Forage Fish Unit, Washington Department of Fish and Wildlife, 1702 Anderson Road, Bay 4, Mt. Vernon, WA 98173.

Table 1

Collections of *Lepidopsetta* larvae examined for this study. AFSC = Alaska Fisheries Science Center, Seattle, WA; VPA = Vancouver Public Aquarium, Vancouver, BC; PBS = Pacific Biological Station, Nanaimo, BC; CalCOFI = California Current Oceanic Fisheries Investigations, La Jolla, CA.

General location	Source of data	Years	Months sampled	No. of samples
Bering Sea	AFSC	1971, 1977, 1979, 1988, 1992–94	Apr–Aug	152
Gulf of Alaska	AFSC	1972, 1978–79, 1981-94	Mar–Oct	1896
British Columbia	VPA, PBS	1983–88, 1991–93	Mar–July	72
Puget Sound	AFSC	1985–95	Mar–July	16
WA, OR, and N. CA	AFSC	1980–87	Apr–May	2
California	CalCOFI	1951–84	Feb–July	21

Identification of larvae

Identification of *Lepidopsetta* larvae was accomplished by a variety of methods because the more traditional serial approach was not possible. Initially, our unidentified pleuronectid series was grouped together on the basis of a continuous sequence of shared characters. This series, however, could not be linked with a recognized pleuronectid taxon whose larvae had not already been described. The unidentified series (*Psettichthys* 2) was similar to larvae previously described for *P. melanostictus*. Larvae of *Psettichthys* 2 were determined to be *Lepidopsetta* by rearing wild-caught larvae[1] and finally confirmed to be *Lepidopsetta* by rearing larvae spawned from *Lepidopsetta* adults collected in Puget Sound (Mulligan et al., 1995).

Nomenclature of larval developmental stages follows Kendall et al. (1984) where each stage is based on widespread, fundamental features of development. The early life history stages used in our study were based on the flexion of the notochord that accompanies the hypochordal development of the homocercal caudal fin. The onset of the juvenile stage is defined in our study as completion of eye migration and attainment of the adult complement of fin elements. Early juveniles (approximately 20–35 mm SL) are defined as those collected in the water column; many had remnants of larval pigmentation on their blind side. Postsettlement juveniles were collected with bottom gear and rarely retained any larval pigmentation on their blind side.

Only melanistic pigment is described in our study because formalin fails to preserve other pigments (live larvae have yellow, orange, and brown chromatophores associated with the melanophores). Previous descriptions of larval pigment patterns, particularly those of pleuronectids, have used confusing terminology. Postanal pigment patterns have been variously described as vertically oriented bands (Pertseva-Ostroumova, 1961; Moser et al., 1984; Matarese et al., 1989) and bars (Charter and Moser, 1996). The number of postanal bands and bars may or may not include the caudal or terminal notochord pigment. For clarity, in the descriptions of pigment patterns, the terms "band" and "bar" refer to aggregations of melanophores that approximate vertically oriented rectangles (including the caudal pigment). A band is always complete and a bar incomplete. A "stripe" approximates a line or elongate rectangle and is horizontally oriented. A "spot" is an approximately circular aggregation of melanophores. A "patch" is any other distinguishable aggregation of melanophores.

Larval morphology

A total of 115 eastern North Pacific *Lepidopsetta* larvae were measured with a calibrated digital image analysis system (larvae of the western North Pacific *L. mochigarei* were not available). This system consists of a video camera attached to a dissecting stereomicroscope or camera lens, a microcomputer with digital imaging board, and a video monitor. All measurements of larvae were taken from the left side. Unless otherwise noted, standard length (SL) is used throughout and is defined in our study as the length from snout tip to notochord tip (prior to development of the caudal fin) or to the posterior margin of hypural elements. Other measurements are defined as follows: head length (HL), snout tip to posterior edge of opercle (to pectoral-fin base in small larvae before opercular margin is visible); snout length (SNL), snout tip to anterior margin of orbit; orbit length (OL), greatest length of orbit; body depth (BD), vertical distance from dorsal to ventral body margin at a vertical line through center of anal opening; snout-to-anus length (SAL), distance along body midline from snout tip to a vertical line through center of anal opening. Standard proportional measurements were calculated (Table 2).

Distributional analysis of larvae

The dataset used for mapping and calculation of mean density of larvae (number per 10 m^2; Appendix Table 1) was a subset of the AFSC ichthyoplankton historical database (1972–1994) from the Bering Sea and Gulf of Alaska. This subset included all reidentified samples that had been originally identified as *Psettichthys* 2, *Lepidopsetta* 2, and *L. bilineata* and thus provided the only historic distributional records for larvae of *L. polyxystra* n. sp. Maps of material examined and distribution and mean density

Table 2

Proportional measurements for *Lepidopsetta* larvae. SL = standard length; HL = head length. Statistical significance of raw data was evaluated by an ANCOVA analysis. See Table 10 for *P*-values. NS = not significant; S = significant.

Developmental stage	*L. polyxstra* n. sp.	*L. bilineata*	Significance
Yolksac			
Sample size	6	13	
Snout-to-anus length /SL	32.1 ±1.7 (30.6–34.8)	32.9 ±1.8 (30.1–36.8)	NS
Body depth/SL	3.8 ±0.6 (2.7–4.3)	4.7 ±0.8 (3.9–6.7)	S
Head length/SL	11.6 ±1.0 (10.1–12.6)	13.3 ±1.4 (10.0–15.1)	NS
Snout length/HL	24.7 ±2.4 (21.2–27.1)	22.6 ±7.8 (13.1–36.5)	NS
Orbit length/HL	51.8 ±5.6 (43.8–58.9)	51.9 ±6.6 (36.7–61.5)	NS
Preflexion			
Sample size	11	13	
Snout-to-anus length /SL	33.5 ±1.3 (32.3–36.0)	30.7 ±2.3 (26.8–34.3)	S
Body depth/SL	4.8 ±0.7 (3.2–5.8)	5.0 ±0.9 (3.3–6.7)	NS
Head length/SL	13.0 ±1.3 (10.6–15.6)	12.7 ±1.8 (10.4–15.8)	NS
Snout length/HL	20.5 ±5.3 (13.3–29.7)	23.5 ±6.3 (15.1–35.8)	NS
Orbit length/HL	48.1 ±6.7 (34.1–61.9)	45.3 ±5.6 (37.1–53.0)	S
Flexion			
Sample size	26	17	
Snout-to-anus length /SL	35.5 ±2.5 (31.3–40.0)	33.8 ±2.1 (29.9–38.2)	S
Body depth/SL	10.5 ±4.1 (4.6–18.0)	11.1 ±5.1 (5.5–21.9)	S
Head length/SL	19.1 ±3.6 (13.3–26.4)	17.9 ±3.0 (14.6–24.4)	NS
Snout length/HL	20.5 ±3.3 (12.8–26.2)	22.5 ±4.7 (13.5–29.3)	NS
Orbit length/HL	31.1 ±6.9 (20.6–44.9)	33.6 ±4.1 (27.8–40.6)	NS
Postflexion			
Sample size	10	19	
Snout-to-anus length /SL	39.3 ±3.3 (35.3–45.7)	34.6 ±2.9 (29.3–38.2)	S
Body depth/SL	28.5 ±6.4 (20.0–38.6)	35.7 ±3.0 (27.8–39.9)	S
Head length/SL	26.7 ±2.4 (22.4–30.6)	29.3 ±1.7 (26.7–32.7)	S
Snout length/HL	22.8 ±2.1 (19.3–26.0)	20.7 ±2.3 (16.8–24.2)	NS
Eye length/HL	20.9 ±2.4 (17.5–24.0)	23.8 ±3.2 (19.6–31.8)	S
Total larvae measured	53	62	

of species were generated by using the geographic information system Arc/Info and ArcView (Environmental Systems Research Institute, 1996). Tables were produced with ArcView and Systat software (SPSS, Inc., 1996). Densities were mapped by dividing the geographic area into contiguous square polygons, 625 km^2 each. Catches per unit of effort (CPUEs) from all tows (including 0 catches) within each square polygon were averaged, yielding a mean density. Polygons were shaded according to their mean density, or left unshaded when no tows occurred within a polygon.

Adult statistical analyses

The software programs S-Plus (Statistical Sciences, 1993) or Statgraphics Plus 2.1 (Manugistics, 1997) were used in statistical analyses performed on juveniles and adults. Unless otherwise indicated, tests were considered significant at $P < 0.05$, as adjusted by the Bonferroni correction (Sokal and Rohlf, 1995). For all characters, Bartlett's test of homogeneity of variances (Sokal and Rohlf, 1995) was used to determine the appropriateness of an ANOVA to test for differences between species. When Bartlett's test found significant differences in variances, pairwise comparisons were made. Pairs with significant differences in variances were then tested for differences in medians by using the nonparametric Kruskal-Wallis test (Sokal and Rohlf, 1995). The following meristic characters did not differ significantly in variance among species pairs and were subjected to an ANOVA: gill rakers of the upper and lower first arch and lower second arch; dorsal- and anal-fin rays; ocular-side and blind-side pectoral-fin rays; posterior and anterior ADB pores; interorbital scales; cheek scales; scales above, below, and total around the lateral line; ocular-side and blind-side suborbital pores; supraorbital pores.

Table 3

Counts of gill rakers for species of *Lepidopsetta*.

	Upper first arch								
Species	1	2	3	4	5	6	*n*	*x*	SD
L. bilineata	12	167	104	4			287	2.3	0.58
L. mochigarei	1	18	8				27	2.3	0.53
L. polyxystra n. sp.			135	183	15	3	336	3.7	0.61

	Lower first arch								
	4	5	6	7	8	9	*n*	*x*	SD
L. bilineata	5	105	160	17			287	5.7	0.62
L. mochigarei	1	5	18	3			27	5.9	0.66
L. polyxystra n. sp.			13	204	114	5	336	7.3	0.57

	Lower second arch											
	5	6	7	8	9	10	11	12	13	*n*	*x*	SD
L. bilineata	1	52	170	38	12	2				275	7.1	0.76
L. mochigarei		2	14	10	1					27	7.4	0.69
L. polyxystra n. sp.			4	17	125	139	40	10	1	336	9.7	0.92

For morphometric characters, significant differences between species were identified using an ANOVA of arcsine-transformed ratios of the measurement divided by SL or HL (Sokal and Rohlf, 1995) and an analysis of covariance (ANCOVA) with SL or HL as covariates when assumptions of homogeneity of slopes were satisfied. The following morphometric characters did not significantly differ in variances among species pairs and were subjected to an ANOVA: head length, snout length, ocular-side maxilla length, blind-side maxilla length, ocular-side mandible length, cheek length, interorbital width, dorsal orbit length, ocular-side pectoral-fin length, body depth, caudal peduncle depth, and caudal-fin length. Snout length, blind-side maxilla length, ocular-side mandible length, and interorbital width were also subjected to ANCOVA.

To aid in the discrimination and classification of species, standard principal components analysis (PCA) was conducted on all morphometric and meristic characters for adults of all species together and on the eastern North Pacific material separately. Raw morphometric data were log-transformed and the covariance matrix was subjected to PCA, as was the correlation matrix of raw meristics. Differences between species were illustrated by separately plotting principal components (PC) 2 and 3 of the morphometric analyses, PC1 and PC2 of the meristic analyses, and PC1 of the meristic analyses against PC2 of the morphometric analyses (Stauffer and Hert, 1992). For eastern North Pacific species, data points were also identified by reference to 11 geographic regions: Sea of Okhotsk, western Bering Sea, eastern Bering Sea, Aleutian Islands, Gulf of Alaska, British Columbia, Puget Sound, Washington coast, Oregon coast, California coast, and Baja California coast.

Larval statistical analyses

In an effort to identify additional characters to distinguish larvae of the two eastern North Pacific species, morphometric characters of yolksac preflexion, flexion, and postflexion larvae were further analyzed. Scatter plots for each measurement versus SL were made. Morphometric data were analyzed by the ANCOVA model for each parameter at each developmental stage and at all stages combined, which included species as a factor, standard length as a covariate, and a species/SL interaction (e.g. $BD = C + Species + SL + (Species \times SL)$). A residual analysis was done for each model to determine the appropriateness of the model. Whenever the interaction was not significant (at the 5% level), a reduced model was used, and the interaction was dropped and the slopes were forced to be the same ($BD = C + Species + SL$). This procedure removed the effect of SL and allowed testing for significant differences between species. When the species were significantly different, the *P*-value was reported and graphs were generated to illustrate differences between elevations of the two regressions. Principal components analysis was also used to highlight differences.

Results

Adults

All three species differed significantly from each other in three meristic characters (Tables 3–7): posterior ADB pores (Table 5), total scales above and below the lateral

Table 4

Fin-ray counts for species of *Lepidopsetta*.

	Dorsal-fin rays																							
Species	64	67	68	69	70	71	72	73	74	75	76	77	78	79	80	81	82	83	84	85	86	89	*n*	*x*	SD
L. bilineata		1			4	1	6	5	10	7	15	22	21	11	8	5	3	1	1	1	4	1	127	77.14	3.57
L. mochigarei								1	5	3	10		3	1		3	1						27	76.52	2.46
L. polyxystra n. sp.	1	3	5	6	12	9	13	12	13	8	20	14	10	14	7	4	1	2					154	74.60	3.84

	Anal-fin rays																					
	49	50	51	52	53	54	55	56	57	58	59	60	61	62	63	64	65	66	*n*	*x*	SD
L. bilineata							7	2	13	26	17	29	15	9	4	1	2	1	126	59.3	2.15
L. mochigarei								1	3	5	4	5	6	1	1		1		27	59.6	2.02
L. polyxystra n. sp.	1	3	6	4	5	6	14	20	11	17	17	20	15	9	3	2			153	57.5	3.28

	Blind pectoral-fin rays								
	8	9	10	11	12	13	*n*	*x*	SD
L. bilineata			10	52	62	2	126	11.4	0.66
L. mochigarei			2	17	6	2	27	11.3	0.72
L. polyxystra n. sp.	1	2	36	82	30	2	153	10.9	0.77

	Ocular pectoral-fin rays							
	9	10	11	12	13	*n*	*x*	SD
L. bilineata	5	12	69	32	5	123	11.2	0.81
L. mochigarei		5	14	7	1	27	11.1	0.77
L. polyxystra n. sp.	5	47	74	25	2	153	10.8	0.79

line (Table 6), and ocular-side suborbital pores (Table 7). *Lepidopsetta polyxystra* n. sp. also differed from *L. bilineata* in number of gill rakers of the upper and lower first arch and lower second arch (Table 3), dorsal-fin rays (Table 4), ocular-side and blind-side pectoral-fin rays (Table 4), anterior ADB pores (Table 5), blind-side suborbital pores (Table 7), and supraorbital pores (Table 7), and differed from *L. mochigarei* in number of gill rakers of the upper and lower first arch and lower second arch (Table 3), blind-side pectoral-fin rays (Table 4), anterior and posterior ADB pores (Table 5), and cheek scales (Table 6).

All three species were found to differ significantly in the means of two morphometric characters with either ANOVA or ANCOVA: interorbital width and ocular-side mandible length (Table 8). *Lepidopsetta polyxystra* n. sp. also differed from *L. bilineata* in seven additional characters: head length, blind-side maxilla length, cheek length, body depth, ocular-side pectoral-fin length, caudal-fin length, and caudal peduncle depth; and differed in medians in ocular-side maxilla length, blind-side pectoral-fin length, and body depth. *Lepidopsetta polyxystra* n. sp. also differed from *L. mochigarei* in means of two characters: dorsal orbit length and cheek length; and in medians of head length, body depth, depth at caudal base, and caudal length. *Lepidopsetta bilineata* also differed from *L. mochigarei* in means of two additional characters: blind-side maxilla length and dorsal orbit length; and differed in medians in head length, ocular-side maxilla length, cheek length, body depth, caudal peduncle depth, and depth at caudal base. No differences in means were found in snout length or ocular-side maxilla length.

In the standard PCA of all three species together, loadings of morphometric PC1 were all positive and thus exhibited a strong size effect (Table 9), accounting for 95% of morphometric variation. Principal components 2 and 3 accounted for 56% of the remaining morphometric variation. Principal component 2 loadings described a gradient based on interorbital width and dorsal orbit length; PC3 loadings, a gradient on caudal peduncle depth, cheek depth, caudal depth at hypural margins, and body depth. The plot of PC2 versus PC3 revealed extensive overlap in morphometric characters (Fig. 2A). Principal components 1 and 2 of the meristics analysis accounted for 46% of the meristic variance: PC1 strongly loaded on lateral line pores and scales above and below the lateral line, preopercle pores, and suborbital pores, whereas PC2 strongly

Table 5

Counts of lateral-line and supratemporal pores for species of *Lepidopsetta*.

Species	Lateral-line pores																					
	70	71	72	73	74	75	76	77	78	79	80	81	82	83	84	85	86	87	88	89	90	91
L. bilineata	1			2		2	5	4	9	9	15	15	18	17	11	12	11	8	4	2	2	1
L. mochigarei																						
L. polyxystra n. sp.							2		2	1	5	6	3	12	12	24	15	14	16	10	7	10

Species	Lateral-line pores (cont'd)																							
	92	93	94	95	96	97	98	99	100	101	102	103	104	105	106	107	108	109	115	117	119	*n*	*x*	SD
L. bilineata																						148	82.1	3.67
L. mochigarei				1	1			3	2	2	3	2	1	2	1	4		2	1	1	1	27	104.4	5.84
L. polyxystra n. sp.	5	6	2	4		1	1	1	1													160	86.8	4.28

Species	Posterior supratemporal pores																															
	6	8	9	10	11	12	13	14	15	16	17	18	19	20	21	22	23	24	25	26	27	28	29	30	31	33	34	35	*n*	*x*	SD
L. bilineata		1	1	1		4	7	6	13	5	15	14	12	11	6	8	5	6	7	4	1	2		4				1	134	19.1	4.73
L. mochigarei	2	3	2	1	3	2	3	3	3	1				1		2													26	12.6	4.28
L. polyxystra n. sp.				3	2	2		4	2	8	14	8	13	16	16	6	11	10	8	2	4	7	1	4	5	1	3	1	151	21.4	5.21

Species	Anterior supratemporal pores																
	2	3	4	5	6	7	8	9	10	11	12	13	14	15	*n*	*x*	SD
L. bilineata	1	4	11	33	19	23	23	7	9	2	2				134	6.6	1.99
L. mochigarei		1	5	1	6	5	1	3	2	1	1				26	6.8	2.38
L. polyxystra n. sp.		1	1	9	15	30	25	30	25	8	3	1	2	1	151	8.3	1.99

Table 6

Counts of total scales above and below lateral line, scales above lateral line, scales below lateral line, and cheek scales for species of *Lepidopsetta*.

Total body scales

Species	65	66	67	68	69	70	71	72	73	74	75	76	77	78	79	80	81	82	83	84	85	86	87	88
L. bilineata	2	1	2	5	3	2	4	2	4	7	5	3	9	6	3	7	4	4	1	5	3	1	1	1
L. mochigarei																								
L. polyxystra n. sp.		1		1	1	1	3		1	3	6	6	4	5	5	9	10	3	7	7	3	1	3	1

Total body scales (cont'd)

	89	90	91	92	93	94	95	96	97	98	99	100	101	102	103	104	105	106	107	108	*n*	*x*	SD
L. bilineata																					85	76.3	5.59
L. mochigarei			1	1	1			1	5	2		3	1	3	3	2	1	1	1	1	27	100.1	4.42
L. polyxystra n. sp.	5	2	2	2	1			1													94	80.8	5.95

Scales above lateral line

	25	26	27	28	29	30	31	32	33	34	35	36	37	38	39	40	41	42	43	44	45	*n*	*x*	SD
L. bilineata	1	5	8	5	8	8	13	12	9	6	4	4			1			1	1			85	31.0	3.13
L. mochigarei											1	3		4	2	6	4	4	1	1	1	27	39.9	2.49
L. polyxystra n. sp.			5	5	5	11	9	16	17	7	9	6	2	1		1						94	32.2	2.69

Scales below lateral line

	32	38	39	40	41	42	43	44	45	46	47	48	49	50	51	52	53	54	55	56	58	59	60	61	62	63	64	65	67	*n*	*x*	SD
L. bilineata	1	1	1	3	10	5	6	5	9	11	10	7	6	3	3	2	2													85	45.3	3.74
L. mochigarei																1		1		2	3	4	2	4	3	4	1	1	1	27	60.2	3.33
L. polyxystra n. sp.		1		2	1	3	1	2	7	7	15	5	12	11	11	4	2	1	2	5	1	1								94	48.6	3.95

Cheek scales

	7	8	9	10	11	12	13	14	15	16	*n*	*x*	SD
L. bilineata			7	14	18	21	15	6	2	1	84	11.6	1.55
L. mochigarei				2	8	9	7		1		27	11.9	1.11
L. polyxystra n. sp.	3	5	14	36	29	10	2				99	10.2	1.21

Table 7

Counts of ocular- and blind-side suborbital pores, preopercle pores, and supraorbital pores for species of *Lepidopsetta*.

	Ocular-side suborbital pores																												
Species	13	14	15	16	17	18	19	20	21	22	23	24	25	26	27	28	29	30	31	32	33	34	35	36	37	38	*n*	*x*	SD
L. bilineata		1		1		9	8	7	16	15	2	3	6		2	1	1										72	21.2	2.71
L. mochigarei										1			1			2	8	3	2	3	3		1		2	1	27	30.7	3.51
L. polyxystra n. sp.	1		2		2	4	2	7	11	11	17	10	11	6	3	3	3										93	22.7	3.10

	Blind-side suborbital pores																	
	6	7	8	9	10	11	12	13	14	15	16	17	18	19	20	*n*	*x*	SD
L. bilineata	1	2	12	24	21	9	3	2								74	9.5	1.32
L. mochigarei					2	3	7	8	4	2					1	27	12.9	1.94
L. polyxystra n. sp.			5	17	32	31	3	4	1							93	10.3	1.16

	Supraorbital pores											
	1	2	3	4	5	6	7	8	9	*n*	*x*	SD
L. bilineata		2	6	20	70	91	51	10	5	255	5.8	1.19
L. mochigarei	17	1	1							19	1.2	0.50
L. polyxystra n. sp.	118	105	29	7	2	3	2			266	1.8	1.03

	Preopercle pores											
	5	6	7	8	9	10	11	12	13	*n*	*x*	SD
L. bilineata	2	60	9							71	11.6	1.55
L. mochigarei			1	4	2	8	6	1	2	24	11.9	1.11
L. polyxystra n. sp.	1	32	53	3						89	10.2	1.21

Table 8

Proportional morphometrics of adults of *Lepidopsetta*. HL = head length; SL = standard length. Data are in hundreds of SL or HL with mean ± standard deviation (range). Statistical significance was evaluated by ANOVA and ANCOVA, when appropriate, at 0.05 level. All = Differences between all three species were significant; bp = Differences between *L. bilineata* and *L. polyxystra* n. sp. were significant; pm = Differences between *L. polyxystra* n. sp. and *L. mochigarei* were significant; ns = No significant differences were found.

	Species			Significance	
	L. bilineata	*L. mochigarei*	*L. polyxystra*	ANOVA	ANCOVA
Sample size	83	26	94		
Head length/SL	28.20±1.64 (24.01-32.86)	26.23±1.71 (23.23–30.54)	27.24±1.62 (21.75–31.54)	bp	
Snout length/HL	16.09±2.07 (12.37-22.45)	16.13±1.69 (12.72–20.21)	16.02±1.84 (12.06–20.12)	ns	ns
Ocular-side maxilla length/HL	27.88±1.25 (25.26-32.53)	27.21±1.41 (24.63–29.41)	26.30±1.89 (20.42–31.47)	ns	
Ocular-side mandible length/HL	41.91±1.69 (38.33-46.10)	39.61±1.83 (36.57–44.64)	40.73±2.20 (34.39–50.00)	bm	All
Interorbital width/HL	3.54±0.79 (2.14-6.02)	2.68±0.69 (1.32–4.17)	4.35±0.80 (2.49–6.56)	All	All
Dorsal orbit length/HL	28.06±1.91 (23.38-32.46)	30.08±1.83 (26.09–34.74)	28.13±1.95 (22.18–32.86)	pm/bm	
Ventral orbit length/HL	3.54±0.79 (2.14-6.02)	2.68±0.69 (1.32–4.17)	4.35±0.80 (2.49–6.56)		
Cheek length/HL	34.17±2.84 (28.06-41.84)	31.09±1.71 (28.57–34.98)	32.54±2.77 (26.67–38.52)	bp/pm	
Body depth/SL	46.98±2.84 (40.80-57.04)	51.79±3.23 (45.54–61.04)	49.02±3.44 (41.17–58.93)	bp	
Ocular-side pectoral length/SL	15.19±1.34 (12.20-18.20)	14.58±1.24 (12.60–17.42)	14.66±1.52 (10.73–18.23)	bp	
Caudal-fin length/SL	20.79±1.57 (17.62-23.63)	21.22±1.69 (18.77–25.14)	22.72±1.77 (17.78–29.13)	bp	
Caudal peduncle depth/SL	10.20±0.80 (8.18-12.29)	11.03±0.94 (9.71–13.96)	10.91±0.71 (9.36–13.13)	bp	
Caudal peduncle length/SL	9.11±0.72 (7.18-10.87)	8.89±0.54 (7.77–10.28)	8.90±0.62 (7.01–10.12)		
Ocular-side pelvic length/SL	9.83±0.98 (7.64-12.50)	9.82±0.94 (7.40–11.75)	9.95±0.97 (7.84–12.15)		
Sample size	77	26	93		
Blind-side maxilla length	31.26±2.25 (25.16-41.18)	29.73±1.56 (27.30–32.87)	28.70±2.01 (22.22–35.66)	bp/bm	bp/bm
Sample size	78	26	93		
Blind-side pectoral length/SL	9.91±0.77 (7.33-12.22)	9.58±0.90 (7.89–11.69)	10.16±1.17 (6.58–12.66)		
Sample size	67	26	92		
Cheek depth/HL	19.15±2.13 (13.92-24.19)	19.64±2.60 (14.83–25.53)	18.62±2.17 (13.56–22.73)		
Caudal depth at hypurals/SL	12.13±0.69 (10.46-14.25)	13.12±0.70 (11.66–14.61)	12.35±0.88 (10.06–16.91)		
Sample size	8	6	15		
Lateral line length/ lateral line depth	30.20±3.78 (24.84-37.06)	33.42±3.78 (27.86–38.98)	31.72±3.41 (26.29–38.20)		

Table 9

Character loadings for principal component analysis of morphometric characters of adult *Lepidopsetta bilineata*, *L. mochigarei*, and *L. polyxystra* n. sp.

	Loadings		
Characters	PC1	PC2	PC3
Standard length	0.22484	0.06236	0.15282
Head length	0.22819	0.03318	–0.06512
Snout length	0.21789	0.00863	–0.04715
Ocular-side maxilla length	0.23138	0.05417	–0.30392
Blind-side maxilla length	0.23849	0.0835	–0.30268
Ocular-side mandible length	0.2334	0.03438	–0.20318
Dorsal orbit length	0.21415	0.11385	–0.09032
Ventral eye length	0.20185	0.09275	–0.20682
Interorbital width	0.22077	–0.96363	–0.03502
Cheek length	0.24796	0.00482	–0.13585
Cheek depth	0.25623	0.08324	–0.39732
Body depth	0.23716	0.08671	0.33759
Ocular-side pectoral length	0.24489	0.0723	–0.01453
Blind-side pectoral length	0.24277	0.01015	0.184878
Ocular-side pelvic length	0.22725	0.0275	0.076978
Caudal peduncle length	0.22574	0.08882	0.121448
Caudal peduncle depth	0.22183	0.00716	0.401018
Caudal depth at hypurals	0.22707	0.07164	0.377584
Caudal-fin length	0.20981	–0.00818	0.20981

Table 10

Character loadings for principal component analysis of meristic characters for *Lepidopsetta bilineata*, *L. mochigarei*, and *L. polyxystra* n. sp. ADB = supratemporal branch of the lateral line.

	Loadings	
Characters	PC1	PC2
Upper 1st arch gill rakers	0.0722	0.4021
Lower 1st arch gill rakers	0.0646	0.4414
Upper 2nd arch gill rakers	0.0067	0.1393
Lower 2nd arch gill rakers	0.0181	0.406
Dorsal-fin rays	–0.1314	–0.1926
Anal-fin rays	–0.1265	–0.1939
Ocular-side pectoral-fin rays	–0.0975	–0.1331
Blind-side pectoral-fin rays	–0.0759	–0.1527
Lateral-line pores	–0.4017	0.1027
ADB1 pores	0.2092	0.1578
ADB2 pores	0.0079	0.1962
Interorbital scales	–0.0508	0.2163
Cheek scales	–0.1907	–0.2532
Scales above lateral line	–0.384	0.0291
Scales below lateral line	–0.392	0.0873
Ocular-side suborbital pores	–0.3635	0.0177
Blind-side suborbital pores	–0.3007	0.0961
Preopercle pores	–0.3643	0.0394
Supraorbital pores	0.203	–0.3731

loaded on gill rakers of the lower first and second arches and upper first arch and supraorbital pores (Table 10). By plotting PC1 of the meristic analysis and PC2 of the morphometric analysis (Fig. 2C), we found a distinct cluster representing *L. mochigarei* and an overlap of clusters representing *L. bilineata* and *L. polyxystra* n. sp.

In the PCA of only the eastern North Pacific species, loadings of morphometric PC1 were all positive and thus exhibited a strong size effect, accounting for 96% of morphometric variation. Principal components 2 and 3 accounted for 33% and 19% of the remaining morphometric variation, respectively. Principal component 2 loadings described a gradient based primarily on interorbital width, as well as on ventral orbit length and blind-side maxilla length; PC3 loadings described a gradient on interorbital width, caudal peduncle depth, and body depth. The plot of PC2 versus PC3 revealed extensive overlap in morphometric characters (Fig. 3A). Principal components 1 and 2 of the meristics analysis accounted for 28% and 17%, respectively, of the meristic variance: PC1 strongly loaded on gill rakers and supraorbital pores and PC2 strongly loaded on dorsal-fin rays, anal-fin rays, and cheek scales. The plot of meristic PC1 versus PC2 revealed two distinct clusters (Fig. 3B). By plotting PC1 of the meristic analysis and PC2 of the morphometric analysis (Fig. 3C), we found two distinct clusters representing *L. bilineata* and *L. polyxystra* n. sp.

When data points of eastern North Pacific species were identified by geographic regions, no significant clustering was apparent within groups of either *L. bilineata* or *L. polyxystra* n. sp. Extensive overlap was found between clusters representing each of these general geographic areas.

Larvae

Raw morphometric data were subjected to an ANCOVA analysis, which indicated differences in several morphological characters (snout-to-anus length, body depth, and orbit length) between larvae of *L. bilineata* and *L. polyxystra* n. sp. at various stages of development (Table 11). Several characters showed significant differences in postflexion larvae ($P<0.0001$), including snout-to-anus length, head length, and orbit length. Snout-to-anus length is shorter in larvae of *L. bilineata* during the preflexion, flexion, and postflexion stages (Fig.4). Larvae of *L. bilineata* are deeper-bodied during the yolksac, preflexion, and flexion stages of development (Fig. 5). The PCA plots of PC2 and PC3 for each developmental stage produced broadly overlapping clusters.

Systematics

Genus *Lepidopsetta* Gill, 1862

Lepidopsetta Gill, 1862:330 (type species *Platichthys umbrosus* Girard, 1856 [originally cited as *Psettichthys umbrosus* but subsequently corrected by Gill (1864)], by monotypy).

Diagnosis

Pleuronectid genus *Lepidopsetta* is distinguished by the following combination of characters in adults: lateral line with a high arch, 6–8 scale rows between highest point of arch and base of arch over the pectoral fin; supratemporal branch of lateral line with a moderately elongate posterior extension of up to 35 pored scales; mouth small, maxilla extending to anterior quarter of ventral orbit; expanded anteriormost anal pterygiophore ("anal spine") present, often projecting beyond body wall in damaged specimens; supraorbital pores present; scales on ocular side often tuberculate, especially on the head and anterior portion of body; scales on blind side always cycloid anteriorly.

Larvae are distinguished from other pleuronectid genera by the following combination of characters: dorsal and anal finfold pigment present, 1–3 postanal bars (2–4 distinctive pigment regions along dorsal midline), a series of ventral midline melanophores, absence of slashlike hypaxial pigment along the postanal body, few to many pigment spots around the notochord tip, and 37–44 total myomeres (Table 12).

Description of adults

Body ovate, greatest depth 31.7–61.0% SL, scales above lateral line 25–45, scales below lateral line 27–67; head acute to rounded, length 21.8–32.9% SL; dorsal margin of head concave to nearly linear, snout length 3.1–6.2% SL (12.1–22.4% HL); mouth small, premaxilla with fleshy lips and prominent, broad-based posterior lobe, maxilla extending to anterior rim of ventral orbit, ocular-side maxilla shorter than blind-side maxilla, ocular-side maxilla length 20.4–32.5% HL, blind-side maxilla length 22.2–41.2% HL; ocular-side mandible length 34.4–50.0% HL, about equal in length to blind-side mandible; teeth conical and slightly lobate or truncate, largest are anterior becoming gradually smaller posteriorly, fewer on ocular-side premaxilla and dentary, 4–10 on ocular-side premaxilla, 20–27 on blind-side premaxilla, 8–15 on ocular-side dentary, 20–29 on blind-side dentary; gill rakers of first arch moderately slender to broad and robust, 6–14 total, 1–6 on upper and 4–9 on lower arch; gill rakers of second arch broad and robust, 6–14 total, 0–4 on upper and 5–13 on lower arch; dorsal orbit round (nearly equal to eye length) to elliptical (posterior rim elongate and much greater than eye length), orbit lenth 22.2–34.7% HL,

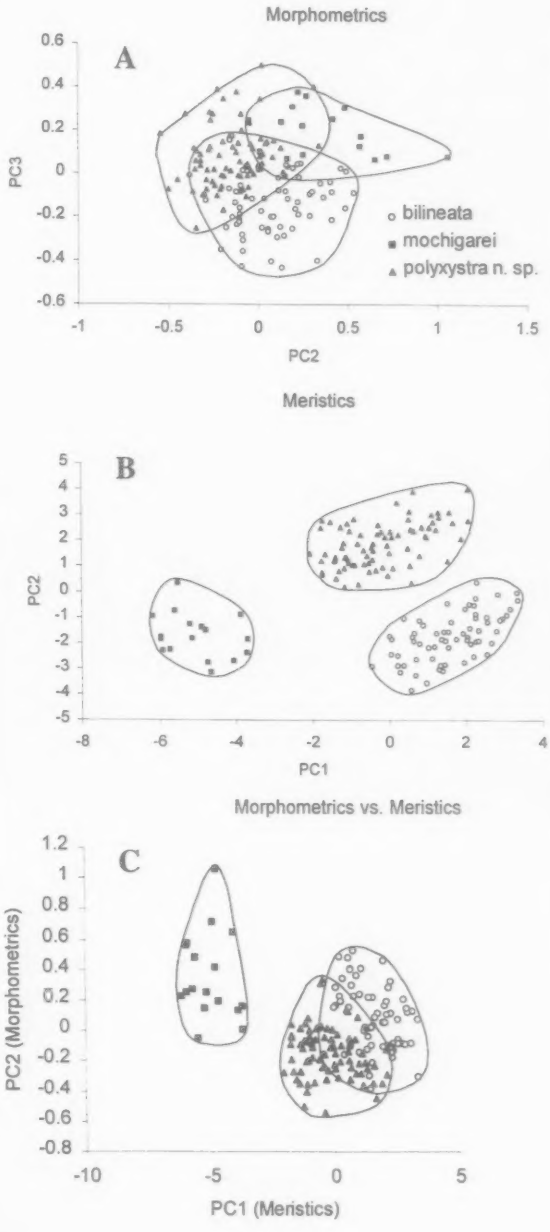

Figure 2

Plots of principal component scores for morphometric and meristic characters for *Lepidopsetta* species: *L. bilineata* (circle), *L. mochigarei* (square), *L. polyxystra* n. sp. (triangle). **(A)** Morphometric characters only; **(B)** meristic characters only; **(C)** morphometric characters (PC2) versus meristic characters (PC1).

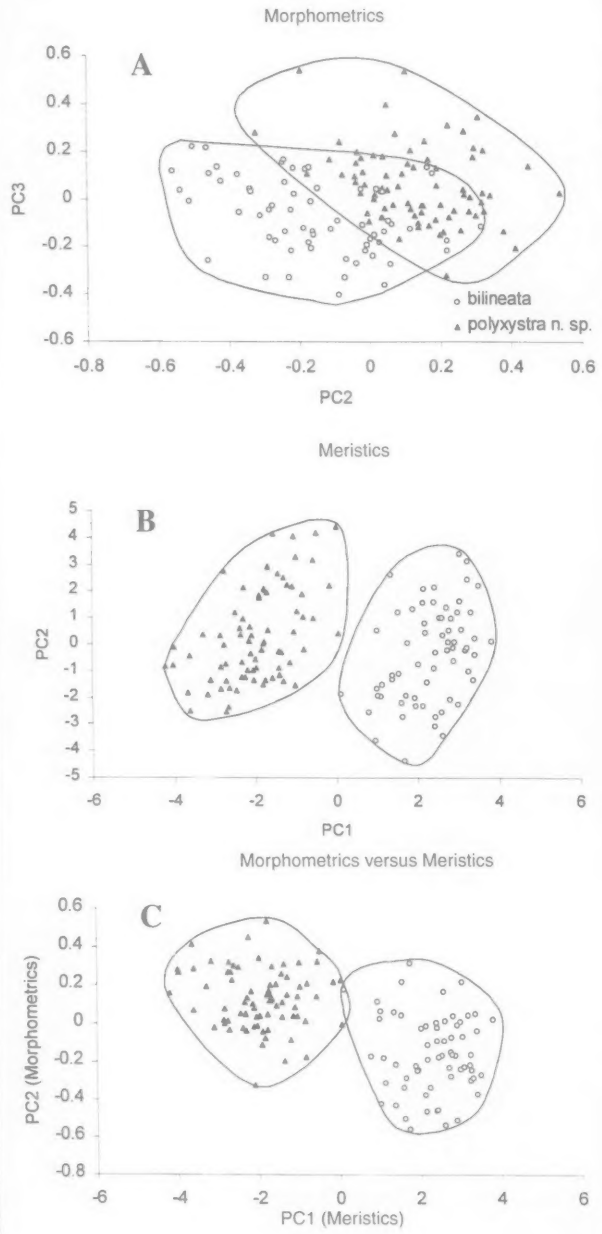

Figure 3

Plots of principal component scores for morphometric and meristic characters for eastern North Pacific *Lepidopsetta* species: *L. bilineata* (circle), *L. polyxystra* n. sp. (triangle). **(A)** Morphometric characters only; **(B)** meristic characters only; **(C)** morphometric characters (PC2) versus meristic characters (PC1).

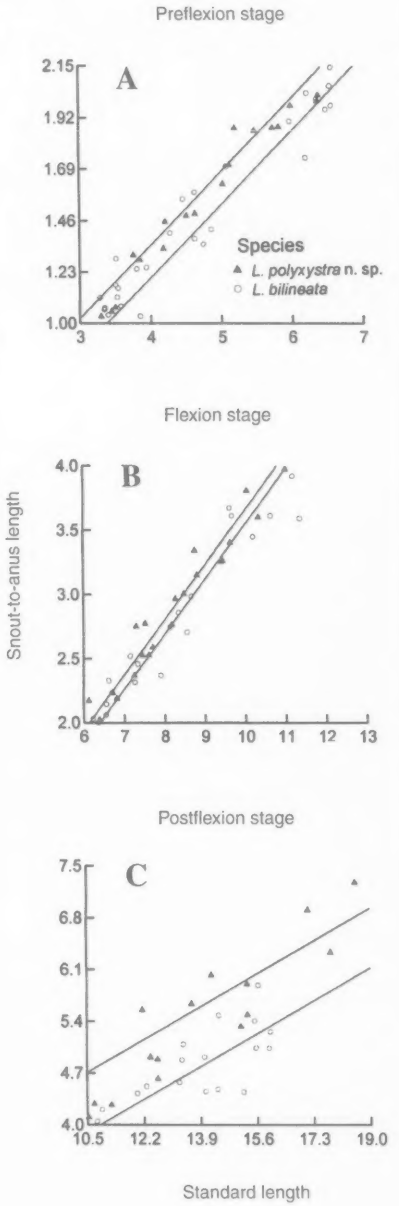

Figure 4

Comparison of snout-to-anus length versus standard length in developmental stages of *Lepidopsetta bilineata* (open circle) and *L. polyxystra* n. sp. (triangle). The lines represent a linear regression with both species having similar slopes: **(A)** preflexion, **(B)** flexion, **(C)** postflexion.

Table 11

P-values for ANCOVA of larvae of *Lepidopsetta bilineata* and *L. polyxystra* n. sp. Bold values indicate that the species are different from each other at the 0.05 significance level.

	Stage of development			
Character	Yolksac	Preflexion	Flexion	Postflexion
Snout-to-anus length	NS	***P*=0.001**	***P*=0.035**	***P*<0.001**
Body depth	***P*=0.001**	NS	***P*=0.037**	***P*<0.001**
Head length	NS	NS	NS	***P*=0.001**
Snout length	NS	NS	NS	NS
Orbit length	NS	***P*=0.020**	NS	***P*<0.001**

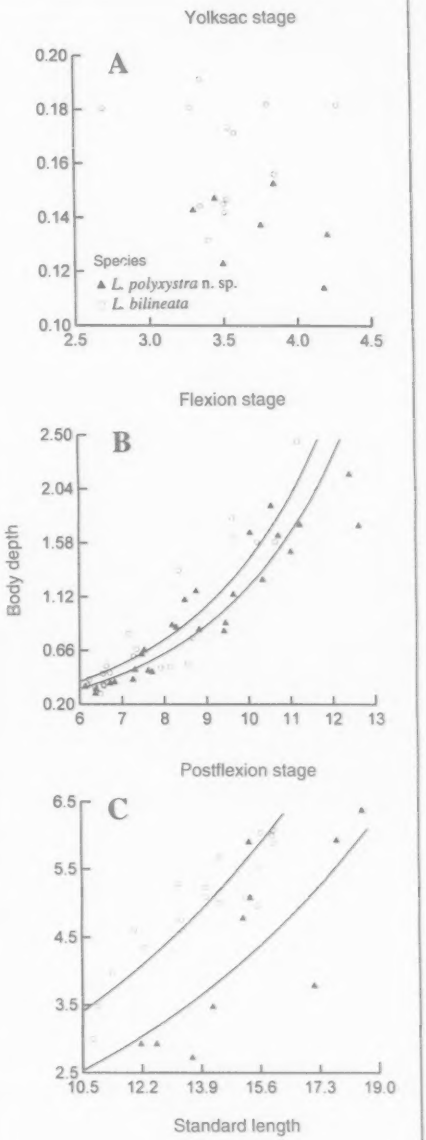

Figure 5

Comparison of body depth versus standard length in developmental stages of *Lepidopsetta bilineata* (open circle) and *L. polyxystra* n. sp. (triangle). The lines represent a nonlinear relationship between body depth and standard length: **(A)** yolksac (no relationship between body depth and standard length), **(B)** flexion, **(C)** postflexion.

dorsal eye length 17.9–32.9% HL; ventral eye approximately equal in length to ventral orbit, length 17.2–35.4% HL; interorbital with up to 5 scales (often lost in preserved material), width 1.3–6.6% HL; cheek with 7–16 scales, length 26.7–65.9% HL, depth 13.6–33.6% HL; preopercular pores 5–13; ocular-side suborbital pores 13–38; blind-side suborbital pores 6–20; lateral line with a high arch, 6–8 scale rows high over the pectoral fin, arch length about three times its depth, length 26.1–69.9% HL, lateral line pores 70–119; anterior supratemporal short, pores 2–15; posterior supratemporal branch moderately elongate, pores 6–35; supraorbital canal short or long, pores 1–9; pectoral fins with 8–13 rays, dorsal 2–3, and ventralmost simple and all others branched, ocular-side pectoral fin longer than blind-side pectoral fin, length 10.7–18.2% SL (38.3–70.4% HL), blind-side pectoral fin about equal in length to pelvic fins, length 6.6–12.7% SL (23.2–49.6% HL); pelvic fins with 6 branched rays, ocular-side pelvic-fin length about equal to blind-side pelvic-fin length, 7.4–12.5% SL (26.7–45.9% HL); dorsal-fin origin over anterior portion of dorsal orbit, dorsal fin with 64–89 simple soft rays, smallest rays anterior and posterior, longest rays at midbody, height 10.2–16.6% SL; dorsal-fin pterygiophores 68–78 in specimens with 64–83 dorsal-fin rays, 8–11 anterior to first neural spine, the first bifurcate and supporting two rays; anal fin with 49–77 simple soft rays in specimens with 54–63 anal-fin rays supported by 53–63 pterygiophores, fin about equal in height to dorsal fin; anal-fin rays 1 and 2 supported by greatly expanded anterior pterygiophore, sharp point of which often projects through skin between anal-fin origin and anus; caudal peduncle length 7.0–10.9% SL (25.5–42.2% HL); least caudal peduncle depth 8.2–14.0% SL (29.6–50.3% HL; 90.0–172.0% caudal peduncle length); greatest caudal peduncle depth 10.1–16.9% SL (37.2–57.7% HL); caudal fin truncate to rounded, with 18–19 rays, total of 8–10 both dorsally and ventrally, five on each of complex hypurals 1+2 and 3+4, 3 on hypural 5, one on the epural or preural 2 neural spine, and four on the parhypural, length 15.3–29.1% SL; vertebrae 39–42, 11 precaudal and 28–31 caudal, neural spines 1–3 and haemal spines 1–4 anteroposteriorly expanded, epineurals present on vertebrae 2–11, ribs present on vertebrae 3–11. Meristics are summarized in Tables 3–7.

Table 12

Summary of selected larval characters helpful in distinguishing eastern North Pacific pleuronectid larvae during preflexion and early flexion stages (Matarese et al., 1989, in part). Characters are presented for taxa where at least some early life-history stages are known. Only general trends are presented because pigment may vary among specimens. When specimens were not available, subjective decisions were based on previously published material. PVM = postventral melanophores.

	Pigment characters							
Genus	Postanal bars	Hypaxial	PVM	Notochord tip	Dorsal finfold	Anal finfold	Head spines	Total myomeres
Embassichthys	3	Absent	Absent	Present	Present	Present	Absent	57–65
Eopsetta	3	Absent	Absent	Present	Absent	Absent	Preopercular	41–45
Glyptocephalus	4	Absent	Absent	Present	Present/ absent	Present/ absent	Preopercular	52–66
Hippoglossoides	3–4	Present	Absent	Present	Present	Present	Absent	44–51
Isopsetta	3	Absent	Absent	Present	Absent	Present	Absent	41–42
Lepidopsetta	1–3	Absent	Present	Present	Present	Present	Absent	37–44
Microstomus	3–4	Absent	Absent	Present	Present	Present	Otic	50–55
Psettichtys	1	Absent	Absent	Present	Present	Present	Absent	38–41
Acanthopsetta	Absent	Present	Present	Present	Absent	Absent	Absent	39–40
Atheresethes	Absent	Absent	Absent	Present/ absent	Absent	Absent	Preopercular/ supraocular crest	47–50
Hippoglossus	Absent	Present	Absent	Present	Present	Present	Absent	49–51
Limanda	Absent	Present	Present	Absent	Absent	Present	Absent	40–41
Liopsetta	Absent	Absent	Absent	Present	Absent	Absent	Absent	37–41
Lyopsetta	Absent	Present	Absent	Present	Present	Present	Absent	43–47
Parophrys	Absent	Present	Present	Present	Absent	Present	Absent	42–47
Platichthys	Absent	Absent	Present	Present	Present	Present	Absent	35–38
Pleuronectes	Absent	Absent	Present	Absent	Absent	Present	Absent	41–42
Pleuronichthys	Absent	Absent	Absent	Present	Present	Present	Absent/otic	38–41
Reinhardtius	Absent	Present	Absent	Present	Present	Present	Absent	61–64

Ocular-side scales ctenoid, often tuberculate, especially on anterior portion of the body around the head and pectoral girdle; tubercules columnar, narrow from base to tip, up to 10 tubercules on scales of head, fewer on tuberculate body scales; blind-side scales nearly always cycloid except in ambicolored specimens, never tuberculate, posterior scales occasionally with central cteni along lateral midline; broad, flaplike urogenital pore on ocular side, dorsal to anus; anus just anterior to anal-fin origin; color of ocular side varies with substrate, in life olivaceous greenish brown with various blotches of dark brown and spots of light areas scattered over body, brown streaks in dorsal, anal, and caudal fins, often with a series of four to five large light spots at base of dorsal fin and four similar spots at base of anal fin; in preservation ocular side yellowish brown with blotches; blind side bright white to cream in life, cream to yellowish in preservation. Moderate sized pleuronectids, reaching a standard length of 600 mm (Hart, 1973).

Description of larvae

Snout-to-anus length remaining constant during development, length 32.1–39.3% SL; preflexion body slender, body depth increasing with development, sharply after flexion, from a depth of 3.8 to 35.7% SL; finfolds of moderate size; head length increasing with development, sharply after flexion, from a length of 11.6 to 29.3% SL; snout length remaining constant during development, length 20.5–24.7% HL; orbit length decreasing with development, from 51.9 to 20.9% HL.

Size at stage of development variable among species (Table 13). Larvae hatching at less than 3.0–4.45 mm; yolk absorbed by 2.7–4.5 mm. Preflexion larvae ranging in size from 3.8 to 6.6 mm; flexion larvae between 6.4 and 11.1 mm; postflexion larvae between 10.8 and 18.6 mm. Transformation occurring at sizes as small as 10.0 mm; juvenile stage usually attained by 35.0 mm (Table 13).

Preanal pigment present initially along lower jaw, increasing posteriorly with development. Pigment occurring ventrally along gut and dorsally on anus; by flexion a distinct patch of melanophores occurring along the posterior edge of the gut, with pigment increasing laterally with development. Pigment may be present or absent on pectoral-fin rays and base.

Postanal pigment in preflexion larvae may be present as melanophores along distal edges of dorsal and anal finfolds, but typically with isolated patches along finfolds and pigment spots or patches along distal edges of anal finfold; when present, two to four distinct pigment regions along

Table 13

Length at stage of development for species of *Lepidopsetta* (mm SL). For a more complete explanation of each developmental stage, see Kendall et al. (1984).

Stage	*L. bilineata*	*L. mochigarei*	*L. polyxystra* n. sp.
Egg	~1.0	0.90	~1.0
Hatch	<3.0	3.95–4.48	>3.0
Yolk absorption	2.7–4.5	unknown	3.3–4.2
Preflexion	3.8–6.6	unknown	4.2–6.2
Flexion	6.4–11.1	~8.9–10.6	6.2–12.6
Postflexion	10.8–16.0	unknown	12.2–18.6
Transformation	as small as 10.0	as small as 15.3	as small as 15.0
Early juvenile	complete as small as 13.0 (13.0–33.9)	unknown	complete as small as 26.0
Postsettlement juvenile	<35.0	unknown	>35.0

dorsal midline; a series of melanophores present from the gut along the ventral midline posterior to anus to just posterior to ventral stripe of posteriormost bar; a few melanophores on the caudal peduncle and above and below the notochord tip.

Distribution

The genus is endemic to the North Pacific and is widespread on the continental shelf (Figs. 6–13). Its range extends from Yongil Bay, Korea, in the southern Sea of Japan and along the northern coasts of Japan, north through the Sea of Okhotsk and the Bering Sea, the most northerly record being from the Gulf of Anadyr and the vicinity of St. Lawrence Island. It is recorded from the Aleutian Islands and into the eastern North Pacific throughout the Gulf of Alaska, south into Puget Sound and along the west coast of Washington, Oregon, California, and Mexico. Its most southerly record in the eastern Pacific is from the Cortez Banks of Baja California, Mexico.

Larvae of the eastern North Pacific species range from the Bering Sea and Aleutian Islands along the Pacific coast to Baja California (Figs. 12-13). Both species co-occur in the eastern Aleutian Islands to the Washington coast; only larvae of *L. polyxystra* n. sp. have been routinely collected from the Bering Sea and only larvae of *L. bilineata* have been collected from California and south in California Cooperative Oceanic Fisheries Investigations (CalCOFI) samples. A subset of larvae collected by AFSC surveys in the Gulf of Alaska and Bering Sea was examined to compare differences in temporal distribution and mean density (number/10 m^2; Appendix Table 1). During the 22-year sampling period, larvae of *L. polyxystra* n. sp. appear first in our March collections (Table 14), whereas larvae of *L. bilineata* first appear in April. The largest catches of *L. polyxystra* n. sp. occurred in May, whereas the largest catches of *L. bilineata* occurred in June. Overall, in the subset of cruises from 1972 to 1994 considered in our study, *L. polyxystra* n. sp. were more abundant and mean density was higher (5.34/10 m^2) than that of *L. bilineata* (0.414/10 m^2).

Habitat

Species of the continental shelf were collected over sand and gravel, commonly at depths of 200 m and less, to as deep as 575 m (Allen and Smith, 1988). For eastern North Pacific species, highest densities of larvae were found over depths of less than 500 m, although they were also collected over deeper water.

Life history

Described eggs of *Lepidopsetta* are demersal, off-round, and have a sticky chorion, causing them to adhere to each other or to a substrate, and range in size from 0.86 to 1.08 mm in diameter (Yusa, 1958; Pertseva-Ostroumova, 1961; Penttila, 1995). The reproductive season extends from winter to early summer, generally earlier in southern species, and spawning occurs at depths of less than 220 m. All sexually mature *Lepidopsetta* apparently migrate from shallow shelf areas in the fall to deeper upper slope waters during winter and migrate back into shallower shelf waters during spring and summer. Immature *Lepidopsetta* remain in shallow waters throughout the winter and migrate into shallower coastal waters in the spring and summer.

Garrison and Miller (1982) provided a summary of reproductive characteristics of *Lepidopsetta* from the western and eastern Pacific Ocean, which included *L. bilineata* and *L. polyxystra* n. sp. Blackburn (1973) described the ichthyoplankton from Skagit Bay, Washington, located in the northernmost region of Puget Sound and included descriptions and illustrations of larvae of *Lepidopsetta*. The Washington Department of Fisheries (WDF) has reported eggs of *Lepidopsetta* (*L. bilineata* or *L. polyxystra* n. sp., or both) from late December through early March in sandy gravel of upper intertidal beaches in several sites in central and

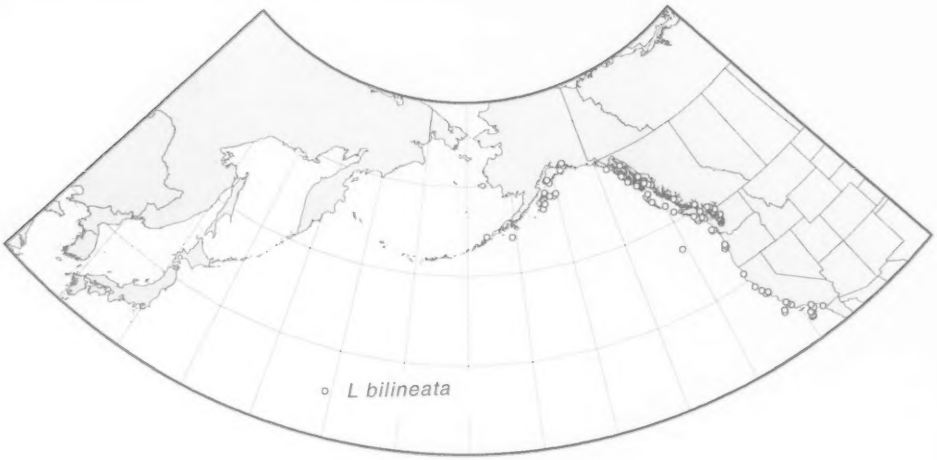

Figure 6

Distribution of adults of *Lepidopsetta bilineata* based on material examined. Each symbol may represent more than one capture.

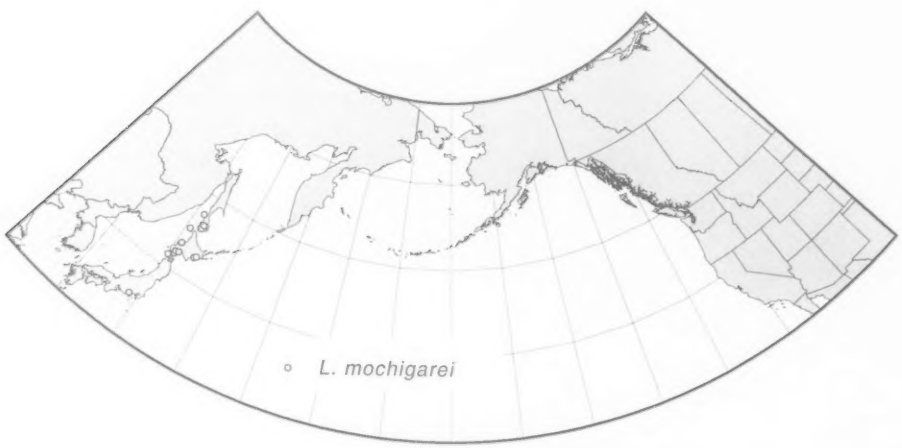

Figure 7

Distribution of adults of *Lepidopsetta mochigarei* based on material examined. Each symbol may represent more than one capture.

southern Puget Sound (Penttila, 1995). These eggs were described as demersal and adhesive ("clinging to upper beach surface material," p. 238). Eggs were collected at the same times and location as those of surf smelt (*Hypomesus pretiosus*) and Pacific sand lance (*Ammodytes hexapterus*).

Etymology

The name *Lepidopsetta* is derived from the Greek *lepido* meaning "scaled," a probable reference to the strongly ctenoid scales found on the ocular side of most individuals, and *psetta*, meaning "flatfish".

Comments

Sakamoto (1984a) synonymized *Lepidopsetta* (as well as five other pleuronectid genera: *Limanda*, *Parophrys*, *Isopsetta*, *Pseudopleuronectes, and Liopsetta*) with *Pleuronectes*, based on a phenetic analysis of detailed morphological data. Several recent authors have criticized Sakamoto's (1984a) phylogenetic techniques (Chapleau [1993]; Rass

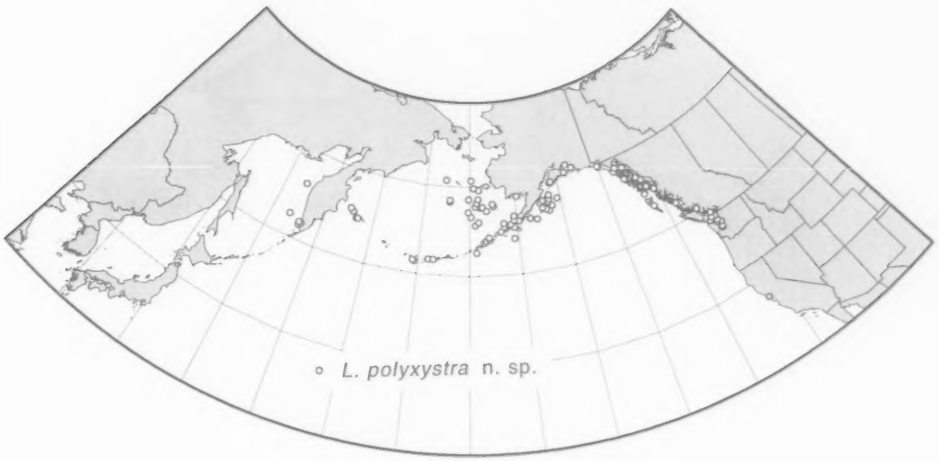

Figure 8

Distribution of adults of *Lepidopsetta polyxystra* n. sp. based on material examined. Each symbol may represent more than one capture.

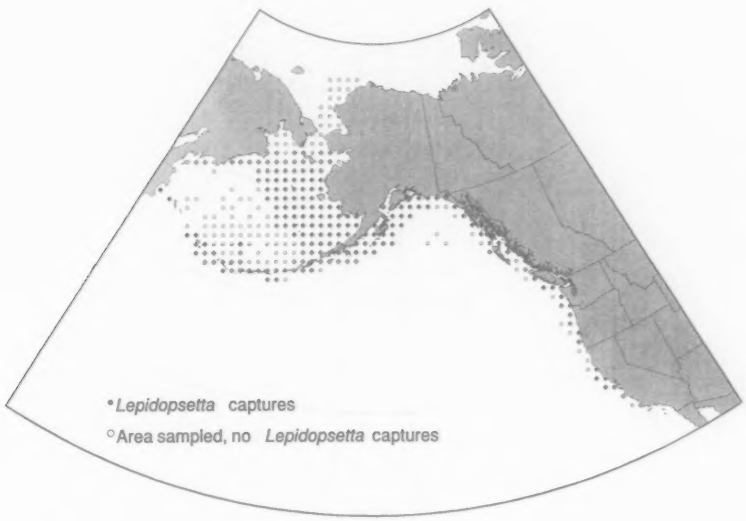

Figure 9

Records of *Lepidopsetta* from the National Marine Fisheries Service, Alaska Fisheries Science Center, Resource Assessment and Conservation Engineering survey database 1948–1997.

[1996]; Berendzen, [1998]; Cooper and Chapleau [1998]) and have refuted the monophyly of *Pleuronectes sensu* Sakamoto (Rass [1996]; Cooper and Chapleau [1998]). Cooper and Chapleau (1998) recently conducted a cladistic analysis and resurrected these genera from synonymy with *Pleuronectes*. We follow the consensus among most current scientists (Nelson, 1994; Cooper and Chapleau, 1996, 1998; Rass, 1996) and recognize each of these genera as distinct.[4]

[4] We do not recognize two other generic nomenclatural changes recommended by Cooper and Chapleau (1998) and have chosen to retain *Embassichthys* and *Atheresthes* as separate genera, distinct from *Microstomus* and *Reinhardtius*, respectively.

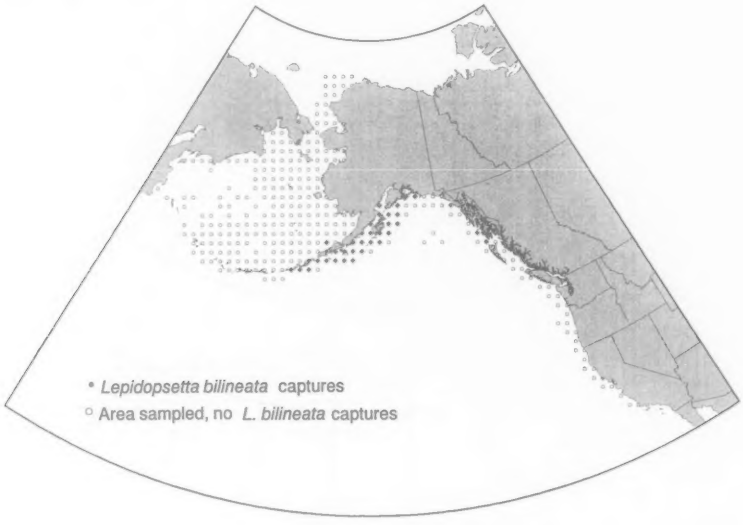

Figure 10

Records of *Lepidopsetta bilineata* from the National Marine Fisheries Service, Alaska Fisheries Science Center, Resource Assessment and Conservation Engineering survey database, 1995–1998.

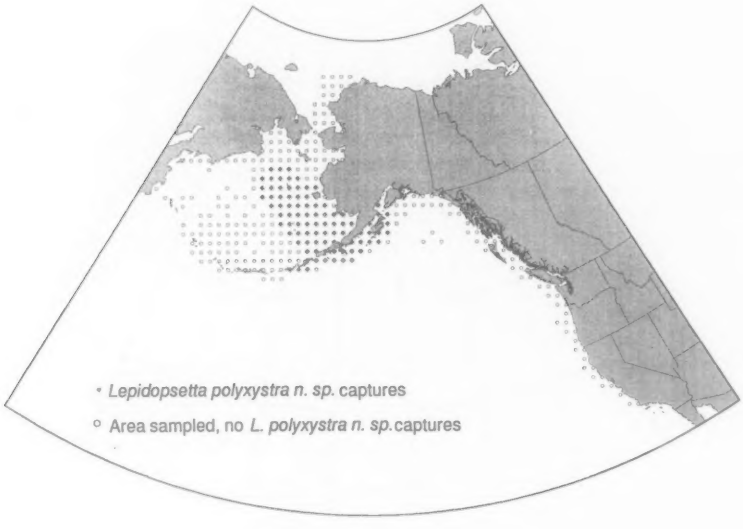

Figure 11

Records of *Lepidopsetta polyxystra* n. sp. from the National Marine Fisheries Service, Alaska Fisheries Science Center, Resource Assessment and Conservation Engineering survey database, 1995–1998.

Supraorbital pores have not been reported in other flatfishes. The supraorbital canal is an extension of a nerve branch arising from between the frontals at the posterior rim of the dorsal orbit. In *Lepidopsetta* the pores of the canal are supported by a series of 1–6 bones (Fig. 14), similar in size and shape to the suborbitals. Typically each bone shares in the support of one or two pores.

Among other North Pacific pleuronectids examined, *Parophrys vetulus*[5] has 6–11 pores and *Isopsetta isolepis* 2–12 pores, whereas *Limanda aspera* and *L. pinnifasciatus*,

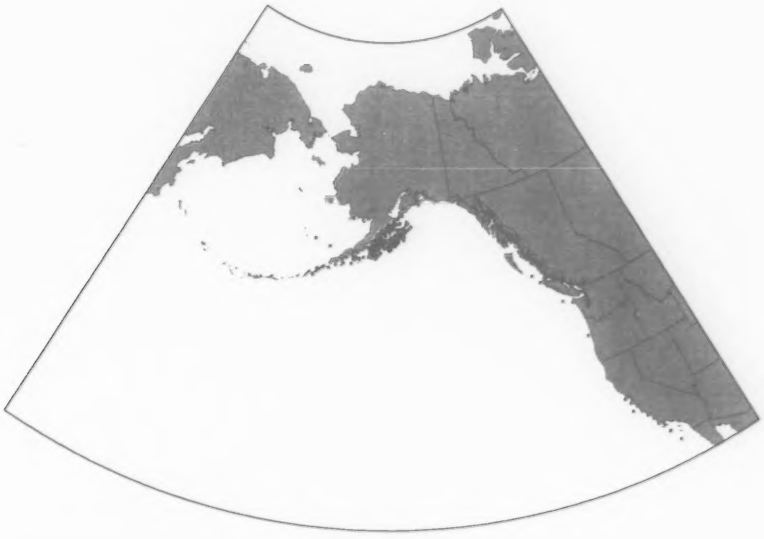

Figure 12

Distribution of larvae of *Lepidopsetta bilineata* based on material examined. Each symbol may represent more than one capture. Sampling effort by the National Marine Fisheries Service, Alaska Fisheries Science Center, was limited in regions between Kodiak and Vancouver Islands; other data are not available from alternate sources.

Figure 13

Distribution of larvae of *Lepidopsetta polyxystra* n. sp. based on material examined. Each symbol may represent more than one capture. Sampling effort by the National Marine Fisheries Service, Alaska Fisheries Science Center, was limited in regions between Kodiak and Vancouver Islands; other data are not available from alternate sources.

[5] Cooper and Chapleau (1998) changed the specific epithet of *Parophrys vetulus* to *vetula* to agree in gender with *Parophrys*. However, because Girard's (1854) original description did not specify his treatment of *vetulus* and because it may also be treated as a noun in apposition, we consider this change an incorrect subsequent spelling and retain *P. vetulus*.

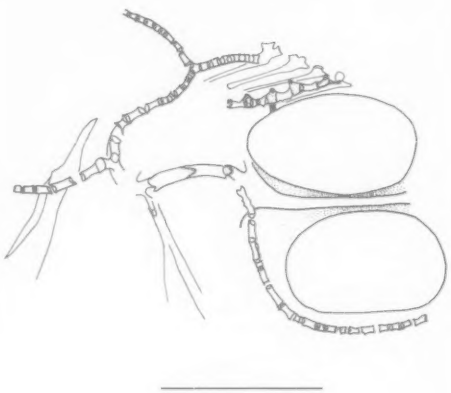

Figure 14

Supporting elements of the pores of the supraorbital canal of *Lepidopsetta bilineata*, UW 025197, 77.3 mm, Puget Sound, WA. View of dorsal (right lateral) side. Scale bar equals 5 mm.

Psettichthys melanostictus, and *Inopsetta ischyra* (a possible hybrid of *Platichthys stellatus* and *Parophrys vetulus*) have a single pore. In *Hippoglossoides elassodon* and *H. robustus*, a series of pores is found at the anterior extension of the supratemporal line, as depicted by Lindberg and Fedorov (1993) for *H. elassodon* (their Fig. 33). These pores are apparently part of the anterior extension of the trunk lateral line, but ventrally the pores extend near the dorsal orbital rim. In one specimen of *H. elassodon* examined (UW 040271), the pores extended nearly the same length along the rim of the dorsal orbit as the length for the same pores in some *L. bilineata*.

Pleuronectid larvae are difficult to diagnose on the basis of a simple set of characters. Pleuronectids are oviparous and spawn planktonic or demersal eggs (about 0.66–4.5 mm), with homogenous yolk that is either pigmented or not, and usually contains no oil. Among eastern North Pacific pleuronectids, *Lepidopsetta* is the only genus that produces demersal eggs, which are off-round and have a sticky chorion that causes them to adhere to each other or to a substrate (Pertseva-Ostroumova, 1961; Penttila, 1995). Pleuronectid larvae hatch between 1.7 and 16.0 mm; yolksac and preflexion larvae are slender, becoming deeper-bodied during the postflexion stage. Larvae of *Lepidopsetta* hatch at <3.0–4.5 mm; preflexion larvae are slender and have moderate-size finfolds.

Larval pigmentation (including finfold) varies considerably in pleuronectids. A combination of pigment pattern (postanal bands, bars, and finfold), meristic characters, and size at development is needed for identification (Matarese et al., 1989; Charter and Moser, 1996). Larvae with special characters (e.g. *Atheresthes* larvae with head spines) or high myomere counts (e.g. *Embassichthys*) are easily distinguished. Other pleuronectid larvae are usually distinguished by a combination of pigmentation characters including the number of postanal bands and bars and finfold pattern (Table 12).

No single early life history character distinguishes larvae of *Lepidopsetta* from other pleuronectid genera. Depending on developmental stage, larvae of *Lepidopsetta* generally are categorized by the presence of at least one postanal bar (Table 12). Larvae of *L. bilineata* have a postanal pigment pattern with four dorsal pigment patches (the posteriormost aligning with a ventral patch forming a caudal bar), larvae of *L. mochigarei* have three dorsal patches (the posteriormost aligns with a ventral pigment patch approximating a caudal bar), whereas larvae of *L. polyxystra* n. sp. have two dorsal pigment patches (the posteriormost aligns with a ventral pigment patch forming a bar located at about 2/3 of body length). Among other pleuronectid genera that have a postanal band and bar pattern, preflexion and early flexion larvae of *Lepidopsetta* may be distinguished by the presence of a series of postanal ventral midline melanophores and fewer pigment spots along the notochord tip (Table 12).

In general, larvae of *L. bilineata* closely resemble those of *Psettichthys* among other genera (Table 12). Both have alternating patches of pigment on dorsal and ventral body margins, although *Psettichthys* has a series of small patches on the dorsal and ventral finfold margins whereas *L. bilineata* has isolated patches along the finfolds. A series of postanal ventral melanophores is present in *L. bilineata* and absent in *Psettichthys*, in which postanal pigment is usually restricted to three or four large spots. Larvae of *L. bilineata* generally have much less pigment on the jaws and isthmus than do larvae of *Psettichtys*.

Size at stage of development varies among species (Table 13). Larvae of *L. bilineata* begin transformation at smaller lengths than larvae of *L. polyxystra* n. sp. or *L. mochigarei*. Larvae of *L. bilineata* also have a larger orbit, shorter snout-to-anus length, and a slenderer body (see Table 2).

The juvenile stages of most eastern North Pacific pleuronectids are poorly known. Traditional early life history descriptions typically describe developmental stages on the basis of eggs and larvae captured in plankton nets and usually do not include transitional larvae that undergo changes associated with a benthic existence. Plankton surveys routinely use nets that do not effectively sample bottom waters where many pleuronectid juveniles eventually settle.

Pleuronectid juveniles can be separated by several characters. Perhaps the most important character is the size at which transformation occurs, although data are scarce on when transformation is completed. Among taxa for which data are available, eastern North Pacific pleuronectids can be grouped into three categories based on approximate transformation sizes: <15 mm SL, 15–30 mm SL, and >30 mm SL. Genera with at least one species transforming at sizes <15 mm SL include *Limanda*, *Platichthys*, *Pleuronectes*, and *Pleuronichthys (sensu* Cooper and Chapleau, 1998). Genera with larvae that transform at much larger sizes (>30 mm SL) include *Atheresthes*, *Embassichthys*, *Glyptocephalus*, *Hippoglossoides*, *Microstomus*, and *Reinhardtius*. Larvae of *Lepidopsetta* generally undergo transformation between 15 and 25 mm SL. Other eastern North

Pacific pleuronectids that undergo transformation at similar sizes include *Acanthopsetta*, *Eopsetta*, *Hippoglossus*, *Isopsetta*, *Lyopsetta*, *Parophrys*, and *Psettichthys*.

Characters that separate juveniles further include meristics of vertebrae, median fin elements, and gill rakers (although gill rakers may not be fully formed); mouth size; and the shape of the lateral line. Generally juveniles of *Lepidopsetta* have lower meristics than juveniles of *Atheresethes*, *Eopsetta*, *Hippoglosssoides*, and *Hippoglossus*. Juveniles of *Lepidopsetta* develop the highly arched lateral line during this stage (15–25 mm SL). A combination of mouth size, residual larval pigment on the blind side of early juveniles, lateral line shape, and, in larger juveniles, number of gill rakers may help to separate other similar-looking eastern North Pacific pleuronectids (*Acanthopsetta*, *Isopsetta*, *Lyopsetta*, *Parophrys*, and *Psettichthys*).

Identification of early life history stages of *Lepidopsetta* has been confused in the literature for many years. Hickman (1959) described egg and larval development of the sand sole, *Psettichthys melanostictus*, on the basis of material collected from Puget Sound, Washington. He illustrated six larvae identified as *Psettichthys* from specimens reared from eggs (his Figs. 1 and 2) and from larvae collected by net (his Figs. 3–6). His Figures 3 and 4 can be identified as *L. bilineata* from the alignment of dorsal and ventral midline melanophores on the postanal body.

In her extensive study of reproduction and development in North Pacific flatfishes, Pertseva-Ostroumova (1961) described the early life history stages of *L. bilineata* and *L. mochigarei*. The description of *L. bilineata* is based on material from collections off the Kuril Islands, off the eastern and western coasts of Kamchatka, and in the western Bering Sea. Larvae from these geographic areas are *L. polyxystra* n. sp.

Blackburn (1973) provided figures of two specimens of *L. bilineata* (his appendix Fig. C-2, A and B) in his survey of ichthyoplankton from Skagit Bay, Puget Sound. His discussion, however, is clearly based on the larvae of both eastern North Pacific species.

Garrison and Miller (1982) reviewed the reproductive characteristics of *L. bilineata*, but their sources either represent both species (Smith, 1936; Forrester, 1969; Forrester and Thompson, 1969) or *L. polyxystra* n. sp. alone (Shubnikov and Lisovenko, 1964; Shvetsov, 1979). Ahlstrom et al. (1984) correctly illustrated *Psettichthys* larvae but presented data and a figure for *L. bilineata* (their Fig. 351b) based on Figure 22 (4) of Pertseva-Ostroumova (1961), now identified as *L. polyxystra* n. sp. Okiyama (1988) also presented material for *L. bilineata*, based on Figure 23(1) of Pertseva-Ostroumova (1961), which therefore represents *L. polyxystra* n. sp.

Matarese et al. (1989) separated larvae of *Lepidopsetta* from *Psettichthys*. Their description and figures of *L. bilineata* are based on what we now refer to as *L. polyxystra* n. sp., whereas the descriptions and figures of "*Lepidopsetta* 2" are now referred to as *L. bilineata*. Charter and Moser (1996) presented figures of both *Psettichthys melanostictus* and *L. bilineata* but, because Pertseva-Ostroumova (1961) was cited as a source for *L. bilineata*, some descriptive data are suspect. Data for *L. bilineata*, particularly in the introductory tables, may be based in part on *L. polyxystra* n. sp. (see tables "Pleuronectidae," pages 1370–1373, Charter and Moser, 1996).

Key to juveniles and adults >30 mm of species of *Lepidopsetta*

1a Preopercular pores 8–13; lateral-line pores 95–119; sum of scales above and below lateral line 91–103; supraorbital pores 1–3; total gill rakers on first arch ≤10, on upper part of first arch ≤3..... ***L. mochigarei***
southern Sea of Okhotsk to Korea

1b Preopercular pores 5–7; lateral-line pores 70–91; sum of scales above and below lateral line 65–88; supraorbital pores 1–8; total gill rakers on first arch 6–14... **2**

2a Total gill rakers on first arch typically ≥10, on upper part of first arch ≥3; supraorbital pores 1–2, rarely 3–7; blind side creamy white ..... ***L. polyxystra* n. sp.**
Puget Sound to Sea of Okhotsk

2b Total gill rakers on first arch typically ≤10, on upper part of first arch ≤3; supraorbital pores 3–8; blind side with extensive bright white highlights... ***L. bilineata***
Baja California to southeastern Bering Sea

Lepidopsetta bilineata (Ayres, 1855a)
Southern rock sole
Figs. 1–6, 10, 12, 14–18; Tables 2–11, 13–14

Platessa bilineata Ayres, 1855a:2 (original description, one specimen, apparently lost, sex and size unknown, fish markets of San Francisco Bay, California).

Platichthys umbrosus Girard, 1856:136 (original description, one specimen, apparently lost, sex unknown, ca. 190 mm TL, Cape Flattery, Washington).

Pleuronectes perarcuatus Cope, 1873:32 (original description, one specimen; holotype, ANSP 8725, sex undetermined, 108 mm SL, Gulf of Alaska, "Sitka" or "Unalaska").

Lepidopsetta bilineata umbrosa (in part) Jordan and Evermann, 1898:2643 (new combination, "Puget Sound and northward").

Lepidopsetta bilineata bilineata Taranets, 1937:144 (new combination, keys).

Pleuronectes bilineata Sakamoto, 1984a:99 (new combination, phylogenetics).

Neotype

CAS 42650, 1(207.6 mm), Calif., Gulf of the Farallones, Sta. F43(2)N, M. Moriguchi, August–September 1978.

Other material examined

A total of 380 adult and juvenile specimens, 22.7–426 mm, including the neotype listed above, was examined. Sixty-four larvae were examined.

Adults Bering Sea: UW 041696, 3(222–245 mm), N of Unimak I., 55.0213°N, 164.6009°W. Aleutian Islands: SIO 94-164, 1(167 mm) of 10(103–193 mm), Unimak Pass, 54°15.1'N, 165°57.6'W, 4 June 1994; UW 041695, 3(170-210), Aleutian Is., NE of Umnak I., 53.44°N, 168.4944°W; Gulf of Alaska: ABL uncat, 1(153 mm), Ursus Channel, San Fernando I., 1 November 1956; ABL 64-696, 1(138 mm), Gore Point, S of Kenai Peninsula, 28 July 1963; ABL 67-211, 4(197–234 mm), Auke Bay, 19.2 km NW of Juneau, 22 May 1962; ABL 71-5, 2(200.5–205.5 mm), Baranof I., Point Conclusion, 17 May 1971; OS 6447, 3(166.1–184.6 mm), 57°10'N, 151°40.5'W, 77 m, 20 September 1978; OS 2156, 1(75.0 mm), Revillagigedo I., Ward Cove, 26 July 1949; OS 2175, 1(102.4 mm), Revillagigedo I., Ward Cove, 26 August 1949; SIO 72-219, 1(251 mm), Lituya Bay, 9.3 km SW of Harbor Pt., 25 June 1961; SIO 72-258, 1(289 mm), Baranof I., Katlian Bay, 57°10'N, 135°20'W; SIO 72-225, 1(288 mm), 2°E of Kodiak I., 6 May 1962; SIO 76-300, 1(187.5 mm) of 28(145–280 mm), Kodiak shelf, 57°40'N, 150°37'W, 23 June 1976; SIO 69-478, 3(112–170 mm) of 7(51–195 mm), Afognak I., Kitoi Bay, NE of Kodiak I., 16–21 April 1968; UW 040267, 1(330 mm), off Kodiak; UW 044021, 1(255 mm), 55.8088°N, 158.7503°W, 67 m, 10 June 1996; USNM 054286, 1(358 mm), Ketchikan, Sta. TT2120, RV *Albatross*; USNM 130739, 1(252 mm), Prince William Sound, Macleod Harbor, 16 March 1941; UW 01666, 1(132 mm), Alexander Archipelago, off Wrangell I., 1 December 1931; UW 008376, 1(240 mm), Ketchikan, 23 September 1949; UW 040902, 1(182 mm), Prince William Sound, 1989; UW 008292, 1(162 mm), Southeast Alaska, 26–31 March 1950; UW 018837, 2(222.5–230.5 mm), 11.7 km NNW of Triangle I., 50°58.1'N, 129°4.9'W, 19 August 1960; UW 40264, 1(342 mm), 54.039°N, 165.8153°W; UW 27679, 23(20.5–57.4 mm), Prince William Sound; UW 044010, 1(240 mm), 59.4918°N, 151.6185°W, 41 m, 27 February 1996; UW 044028, 1(292 mm), 59.4885°N, 151.6062°W, 30 m, 27 February 1996; UW 044025, 2(210–285 mm), Kachemak Bay, 12 May 1996; UW 040268, 1(290 mm), Kodiak I.; UBC 65-525, 1(290 mm), off Baranof I.; UW 044013, 7(287–426 mm), 56.5°N, 153.5°W, R. Bonaduhr; UW 041801, 6(270–335 mm), 54°N, 160.74°W, British Columbia: UW 083483, 33.5 mm, off Vancouver Island, 48°39.5'N, 125°55.2'W, 19 September 1977. SIO 63-202, 1(247 mm), Strait of Georgia, Fraser R.; USNM 31993, 1(158.5 mm), Carter Bay, June 1882; UBC 53-85, 1(172 mm), Vancouver I.; UBC 53-50, 1(57.3 mm), Vancouver I.; UBC 53-68, 1(105 mm), Vancouver I.; UBC 53-50, 1(57.3 mm), Vancouver I., Departure Bay, 49.2167°N, 123.95°W; UBC 53-301, 7(101.5–177 mm), Vancouver I., Baynes Sound; UBC 53-245, 1(144.8 mm), Vancouver I., Burrard Inlet; UBC 55-281, 1(32.9 mm), Vancouver I., Departure Bay, 49.2167°N, 123.95°W; UBC 56-8, 1(220.5 mm); UBC 55-496, 3(217–235 mm), Point Gray, 3.2 km SE of North Arm of Fraser R.; UBC 56-519, 5(205–233 mm), Vancouver fish docks; UBC 61-393, 3(59–88 mm), Bute Inlet; UBC 61-484, 2(145–167 mm), Vancouver I., Burrard Inlet, 25 October 1961; UBC 61-609, 9(38.5–123 mm), Bute Inlet; UBC 61-232, 2(245 mm and one head only), Hecate Strait; UBC 60-416, 1(205 mm), Queen Charlotte Is., Gillat Arm; UBC 63-910, 1(148 mm), Howe Sound; UBC 63-732, 10(68–140 mm), off Keats I.; UW 044026, 1(306.5 mm), 48.57723°N, 124.7803°W, 25 August 1995; UW 044027, 2(293–308 mm), 48.74507°N, 125.9744°W, 28 August 1995; UBC 65-676, 6(44–142 mm), Graham I., McIntyre Bay; UBC 62-93, 6(80–142 mm), Nass Bay; UBC 61-686, 1(62.8 mm), S of Vargas I., 5 July 1934; UBC 61-621, 1(50.5 mm), Snake I., near Nanaimo, 8 May 1933; UBC 61-610, 2(139–142 mm), Work Channel, head of Trail Bay, 16 July 1951; UBC 61-674, 1(60 mm), Dean Channel, off Nescall Bay; UBC 62-94, 1(94 mm), Sydney Inlet; UBC 81-3, 1(201 mm), Vancouver I., Grappler Inlet; UBC 76-7, 1(135 mm), English Bay, 20 January 1962. Washington, Oregon, and California: USNM 054392, 1(292 mm), near Port Townsend, TT2838, RV *Albatross*; USNM 27299, 2(150-246 mm), Puget Sound, 1880; UW 041090, 2(196.0–196.5 mm), Agate Pass, 3 April 1950; UW 041089, 1(229 mm), Agate Pass, 3 April 1950; UW 6070, 7(61–133 mm), San Juan Islands, East Sound, 3 March 1937; UW 06134, 2(53–63.5 mm), N of Maury I., 4 December 1948; UW 014838, 2(65-68 mm), Golden Gardens Beach, 14–15 May 1952; UW 014380, 2(101–108 mm), near Hat I., 29 May 1936; UW 044011, 1(145 mm), San Juan Islands, East Sound, 18 February 1964; UW 017115, 1(178 mm), Port Orchard Channel, 2 February 1964; UW 015423, 1(169 mm), Shilshole Bay; UW 000782, 2(147–156.5 mm), Alki Point, 8 March 1930; UW 005522, 11(46.6–159.5 mm), Edmonds, 18 August 1947; UW 018663, 1(60.5 mm), San Juan Islands, East Sound, 11 December 1964; UW 040665, 2(54–58 mm), Port Townsend Bay, 5 January 1979; UW 040686, 6(114.3–167.3 mm), West Point, 3 October 1978; UW 025723, 4(52.1–230.5 mm), Port Townsend Bay, 5 December 1978–5 January 1979; UW 025721, 3(166–208 mm), Golden Gardens, 22 July 1981; UW 006109, 1(154.5 mm), Alki Point, 3 March 1939; UW 017840, 1(211 mm), S end of Port Susan, 6 May 1950; UW 025719, 12 (103.2–164.5 mm), Murden Cove, 22 April 1980; UW 025727, 2(116.5–169.5 mm), West Point, 29 March 1979; UW 005135, 8(22.7–70.6 mm), Alki Point, 5 April 1938; UW 025197, 1(77.3 mm; cleared-and-stained), Meadow Point; UW 044006, 11(135–250.5 mm), Nisqually, 47.1578°N, 122.6693°W, 16 May 1996; UW 040269, 10(209–259 mm), Puget Sound, 47°19.48'N, 122°33.8'W, 10 May 1996; UW 029670, 49(125.3–283.5 mm), Colvos Passage off Vashon I., 47.5°N, 122.4167°W, 18 July 1949; UW 025726, 5(125–175 mm), Puget Sound, West Point, 3 October 1978; UW 025720, 7(130–185 mm), Puget Sound, West Point, 3 April 1979; UW 041319, 6(122–202 mm), Puget Sound, West Point; UW 041330, 1(225 mm), Puget Sound, Portage Bay; UW 041301, 1(245 mm), Puget Sound, Port Townsend Bay; OS 15509, 4(226.5–287.4 mm), Cobb Seamount, 46°50'N, 130°50'W, 20 August 1992; OS 13792, 1(180.3 mm), 44°54.2667'N, 124°10.0667'W; OS 13500, 1(417 mm), Cobb Seamount, 46°50'N, 130°50'W; OS 13499, 1(330 mm), 44°52.2667'N, 124°09.55'W; OS 7482, 1(223.3 mm), off Newport; OS 14732, 1(132.2 mm), 44°40.7'N, 124°09'W; OS 14690, 1(189.4 mm), 44°37'N, 124°11.1'W; OS 6208, 4(137.3–222.8 mm), off Newport, 30 September 1978; OS 7477, 1(173.7 mm), 44°37.4'N, 124°08.9'W; CAS 18553, 1(198.5 mm), Calif., San Francisco Bay, 14 May 1931; CAS 31832, 1(205 mm), Calif., Gulf of the Farallones, 37°44'N,122°40'W, October 1973; CAS 40341, 1(347.4 mm), Calif., 22.6 km NW of Pt. Pinos, 34°47.5'N, 122°7.8167'W; CAS-SU 111615, 1(335.0 mm),

San Francisco Market, May 1895; CAS 49152, 1(229.5 mm), Calif., Sonoma, Bodega Bay, 18 October 1981; SIO 88-119, 1(277 mm), Calif., south of La Jolla; SIO H48-22, 1(261 mm), Calif., south of La Jolla; SIO 63-241, 1(243 mm), Tanner Bank, Calif., 32°42.5'N, 119°6.5'W, 17 May 1963; SIO 65-460, 1(284 mm), Calif., ridge between Tanner and Cortez Banks, 26 September 1965; SIO 65-6-64A, 1(210 mm), Calif., Tanner Bank, 32°42'N, 119°08'W, 15 January 1965; SIO 63-732-64A, 1(183 mm), Calif., Catalina I., off Avalon, 22 March 1962; SIO 85-145, 2(74–86 mm), Calif., Navarro Head, 39°05.7'N, 123°E44.95'W, 60.4–110.5 m, 17 August 1985; LACM W54-382, 7(178.5–247 mm), 1.6 km W of Santa Barbara I., 33°08.15'N, 119°04.1333'W, 31 October 1954; LACM W66-67, 1(198.5 mm), off San Simeon Point, 13 November 1966; LACM W54-380, 2(274–275 mm), 1.6 km E of Santa Barbara I., 30 October 1954; LACM 44390-1, 1(282 mm), off Palos Verdes, 22 February 1988; LACM 31966-8, 8(176.5–357 mm), Humboldt Co., 8 km S of Shelter Cove, 7 August 1971; LACM 241, 4(153–320 mm), Calif., San Francisco; OS 972, 1(201.2 mm), southern Calif.; LACM 35690-3, 2(83–164.5 mm), Calif., S end of Tanner Bank; UW 044009, 9(143–252.5 mm), 37.781°N, 122.9288°W, 26 June 1995; UW 040262, 1(250 mm), 48.74317°N, 125.7785°W, 27 September 1992; UW 041698, 1(223 mm), 35.0935°N, 120.7774°W, 15 June 1995; UW 041803, 1(358 mm), 47.0839°N, 124.748°W, 8 August 1995; UW 041802, 1(376 mm), 46.91147°N, 124.7292°W, 3 August 1995; UW 041903, 2(290–347 mm), 46.91308°N, 124.4756°W, 5 August 1995; Mexico: CAS 2484, 1(226.3 mm), Baja California, off Cortez Banks, 21 August 1932.

Larvae 64 specimens (2.7–19.0 mm) examined: Western Gulf of Alaska: UW 083400, 2(10.8–12.3 mm), 54°10.8'N, 165°24.3'W, 0–55 m depth, Methot net, 30 July 1991; UW 083401, 1(10.9 mm), 54°38.5'N, 160°51.2'W, 0–98 m depth, Methot net, 30 July 1991; UW 083402, 1(12.0 mm), 56°11.6'N, 157°21.7'W, 0–129 m depth, Methot net, 27 July 1991; UW 083403, 1(14.0 mm), 54°36.2'N, 162°16.2'W, 0–87 m depth, Methot net, 30 July 1991; UW 083404, 1(14.1 mm), 55°43.8'N, 157°34.6'W, 0–105 m depth, Methot net, 27 July 1991; UW 083405, 2(14.4–15.6 mm), 55°43.0'N, 159°49.4'W, 0–108 m depth, Methot net, 25 July 1991; UW 083406, 1(15.5 mm), 53°59.8'N, 165°51.0'W, 0–50 m depth, Methot net, 31 July 1991; UW 083407, 2(15.9–16.0 mm), 55°18.0'N, 160°11.4'W, 0–115 m depth, Methot net, 24 July 1991; UW 083408, 1(16.0 mm), 55°17.7'N, 160°11.7'W, 0–115 m depth, Methot net, 24 July 1991; UW 083445 1(13.3 mm), 56°11.6'N, 158°03.6'W, 0–141 m depth, Methot net, 25 July 1991; UW 072255, 5 of 6(2.7–8.6 mm), 57°01.1'N, 156°19.2'W, 0–95 m depth, bongo net, 3 June 1990; UW 072453, 2 of 4(6.2–6.5 mm), 57°17.2'N, 155°27.6'W, 0–102 m depth, bongo net, 5 June 1990; UW 072126, 2(6.6–7.3 mm), 56°54.0'N, 156°29.5'W, 0–84 m depth, bongo net, 3 June 1990; UW 071455, 1(6.7 mm), 57°60.0'N, 153°59.3'W, 0–103 m depth, bongo net, 28 May 1990; UW 072087, 1(8.1 mm), 56°39.8'N, 156°20.0'W, 0–102 m depth, bongo net, 3 June 1990; UW 072264, 1(8.7 mm), 57°09.1'N, 156°09.1'W, 0–100 m depth, bongo net, 3 June 1990; Gulf of Alaska: UW 083484, 1(19.0 mm), 59°37.8'N, 151°44.2'W, 34 m depth, 17 July 1996; UW 083409, 1(16.4 mm), 58°19.5'N, 150°53.0'W, 64 m depth, bongo net, 22 July 1977; UW 083410, 1(6.3 mm), 57°61.1'N, 151°17.4'W, 0–35 m depth, Tucker net, 26 June 1978; UW 083411, 1(9.7 mm), 56°42.3'N, 153°33.4'W, 28–70 m depth, Tucker net, 28 June 1978; UW 083412, 1(11.0 mm), 57°00.8'N, 153°28.3'W, 0 m depth, neuston net, 14 September 1978; UW 083413, 2(5.1–6.2 mm), 57°10.7'N, 156°01.3'W, 0–100 m depth, Tucker net, 4 June 1988; UW 083414, 1 (6.6 mm), 56°21.0'N, 157°03.8'W, 0–100 m depth, Tucker net, 6 June 1988; UW 083415, 1(6.4 mm), 56°47.3'N, 155°26.0'W, 0–105 m depth, Tucker net, 23 May 1988; UW 083416, 1(6.5 mm), 57°03.8'N, 156°01.8'W, 0–101 m depth, Tucker net, 4 June 1988; UW 083417, 1(6.6 mm), 56°47.3'N, 155°25.9'W, 0–101 m depth, Tucker net, 4 June 1988; UW 083418, 1(7.1 mm), 57°10.8'N, 156°29.9'W, 0–102 m depth, Tucker net, 4 June 1988; UW 083419, 1(8.3 mm), 56°38.9'N, 156°31.5'W, 0–101 m depth, Tucker net, 2 June 1988; UW 083420, 1(10.2 mm), 56°46.7'N, 156°18.3'W, 0–91 m depth, Tucker net, 2 June 1988; UW 083421, 1(10.6 mm), 57°15.0'N, 155°53.6'W, 0–101 m depth, Tucker net, 4 June 1988; UW 083422, 3(3.3–3.4 mm), 57°55.6'N, 151°02.3'W, 0–76 m depth, bongo net, 13 May 1991; UW 083423, 1(3.9 mm), 5°43.8'N, 154°02.1'W, 0–100 m depth, bongo net, 24 May 1991; UW 083424, 1(4.7 mm), 55°53.9'N, 155°59.8'W, 0–75 m depth, bongo net, 23 May 1991; UW 083425, 1(4.9 mm), 57°36.9'N, 155°28.3'W, 0–101 m depth, bongo net, 24 May 1991; UW 083426, 1(3.6 mm), 56°40.7'N, 155°10.7'W, 0–61 m depth, bongo net, 8 May 1992; UW 083427, 1(6.0 mm), 56°58.4'N, 156°06.2'W, 0–100 m depth, bongo net, 14 May 1992; UW 083428, 2(3.5–4.3 mm), 55°27.2'N, 157°39.3'W, 0–88 m depth, bongo net, 19 May 1992; UW 083429, 1(3.8 mm), 55°17.0'N, 157°44.8'W, 0–72 m depth, bongo net, 19 May 1992; UW 083430, 1(4.6 mm), 55°22.5'N, 156°56.8'W, 0–80 m depth, bongo net, 19 May 1992; UW 083431, 1(7.9 mm), 55°16.0'N, 156°15.0'W, 0–102 m depth, bongo net, 18 May 1992; UW 083432, 1(7.3 mm), 55°55.3'N, 156°15.3'W, 0–216 m depth, bongo net, 21 May 1992; UW 083443, 1(3.2 mm), 57°01.1'N, 156°19.2'N, 0–95 m depth, bongo net, 3 June 1990; Puget Sound: UW 083433, 1(9.6 mm), 47°34.15'N, 122°32.3'W, 0 m depth, dip net, 9 May 1994; UW 083434, 1(9.7 mm), 47°34.15'N, 122°32.3'W, 0 m depth, dip net, 5 May 1989; UW 083435, 1(11.2 mm), 47°34.15'N, 122°32.3'W, 0 m depth, dip net, 27 March 1991; UW 083436, 1(11.4 mm), 47°34.15'N, 122°32.3'W, 0 m depth, dip net, 16 July 1987; UW 083437, 1(13.3 mm), 48°1.0'N, 123°0.0'W, reared, 4 May 1989; UW 083438, 1(13.4 mm), 48°1.0'N, 123°0.0'W, reared, 4 May 1989; UW 083439, 1(14.4 mm), 48°1.0'N, 123°0.0'W, 0 m depth, dip net (26 April 1989), reared (20 May 1989); UW 083440, 1(15.2 mm), 48°1.0'N, 123°0.0'W, 0 m depth, dip net (26 April 1989), reared (20 May 1989); UW 083441, 1(15.6 mm), 48°1.0'N, 123°0.0'W, 0 m depth, dip net, 1 July 1989; UW 083442, 1(11.4 mm), 47°34.15'N, 122°32.3'W, 0 m depth, dip net, 16 July 1987; UW 083444, 1(9.3 mm), 47°34.15'N, 122°32.3'W, 0 m depth, dip net, 1 June 1989.

Diagnosis

This species of *Lepidopsetta* has the following combination of characters in adults: total gill rakers on first arch 6–11; on upper arch 1–3, rarely 4, with at least one rudi-

mentary; total gill rakers on second arch 6–11; supraorbital pores 3–9; preopercular pores 5–7; lateral-line pores 70–91; sum of scales above and below lateral line 65–88; interorbital narrow; blind-side coloration white, with glossy highlights along myotome margins increasing anteriorly.

Larvae are distinguished from other species of *Lepidopsetta* by the following characters: body deep, snout-to-anus length short; hatching, flexion, and transformation at comparatively smaller sizes; preflexion pigment pattern with pigment patches along distal edges of dorsal and anal finfolds, four prominent spots along dorsal midline (in a pattern resembling alternating dorsal and ventral spots, with posteriormost dorsal spot coalescing with a corresponding ventral patch to form a bar), and a series of small ventral midline melanophores extending from gut to last myomere; flexion pigment pattern with distinctive anterior dorsal midline spot and posteriormost dorsal spot forming a bar with corresponding ventral patch; pectoral-fin rays unpigmented.

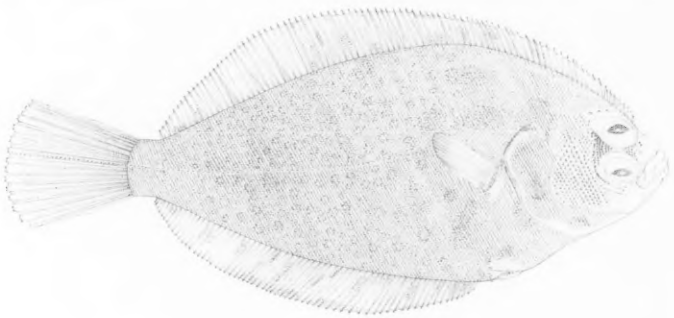

Figure 15

Lepidopsetta bilineata (Ayres), neotype, CAS 42650, 207.6 mm, Calif., Gulf of the Farallones, M. Moriguchi, August-September 1978. Illustration by B. Vinter, under contract to the National Marine Fisheries Service, Alaska Fisheries Science Center.

Description of adults (Fig. 15)

Body ovate, greatest depth 40.8–57.0 (47.0)% SL, scales above lateral line 25–43 and scales below lateral line 27–53; head relatively acute, length 24.0–32.9 (28.2)% SL; dorsal margin of head at dorsal-fin origin concave, snout length 3.1–6.1 (4.5)% SL (12.4–22.4 (16.1)% HL); ocular-side maxilla length 25.3–32.5 (27.9)% HL; blind-side maxilla relatively long, length 25.2–41.2 (31.3)% HL; ocular-side mandible length 38.3–46.1 (41.9)% HL; teeth 5–10 on ocular-side premaxilla, 20–27 on blind-side premaxilla and 10–12 on ocular-side dentary, 23–29 on blind-side dentary; gill rakers of first arch typically broad and robust, 6–11 total, 1–4 on upper arch, 5–7 on lower; gill rakers of second arch 6–11 total, 1 on upper and 5–10 on lower arch; dorsal orbit larger than eye length, orbit length 23.4–32.5 (28.1)% HL, dorsal eye length 17.9–30.3 (24.2)% HL; ventral eye length 18.2–35.4 (24.8)% HL; interorbital narrow, up to 3 scales at narrowest portion, 2.1–6.0 (3.5)% HL; cheek with 9–16 scales, length 28.1–41.8 (34.2)% HL, depth 13.9–24.2 (19.2)% HL; preopercular pores 5–7; ocular-side suborbital pores 14–29; blind-side suborbital pores 6–13; lateral-line pores 70–91, lateral-line arch length 49.3–58.1 (54.3)% HL, its depth 24.8–37.1 (30.2)% of its length; both anterior and posterior supratemporal branches relatively long, anterior pores 2–12, posterior pores 8–30; supraorbital canal long, extending to dorsal rim of dorsal orbit near insertions of dorsal-fin rays 3–4, pores 3–9; ocular-side pectoral-fin length 12.2–18.2 (15.2)% SL (43.6–66.2 (53.9)% HL); blind-side pectoral-fin length 6.7–12.2 (9.9)% SL (23.2–44.3 (35.0)% HL), about equal to ocular-side pelvic-fin length 7.6–12.5 (9.8)% SL (26.7–44.7 (34.8)% HL); dorsal fin with 67–89 rays, height 10.7–16.5 (13.3)% SL, in specimens with 72-79 rays supported by 71–78 pterygiophores, 9–11 anterior to first neural spine; anal fin with 54–77 rays, in specimens with 54–62 rays supported by 53–60 pterygiophores; caudal peduncle relatively slender, least depth 8.2–12.3 (10.2)% SL (29.6–43.0 (36.2)% HL; 90.0–152.4 (112.6)% caudal peduncle length); greatest depth 10.5–14.3 (12.1)% SL (37.2–53.0 (42.8)% HL); caudal peduncle length 7.2–10.9 (9.1)% SL (25.5–42.2 (32.4)% HL); caudal-fin length 15.3–23.6 (20.8)% SL. Vertebrae 40–41, with 11 precaudal and 29–30 caudal.

Scales around head and those scattered posteriorly on ocular side moderately rough with columnar tubercles in large adults; strong spines in small adults and juveniles. Urogenital flap darkly pigmented in 21–58 mm juveniles.

In life, blind side in adults translucent to bright white, with glossy highlights along edges of myotomes; in juveniles, primarily translucent, and having reduced glossy areas especially prominent over the head. When preserved, blind side of all individuals uniform creamy white to yellow-brown. Ocular side slightly more green than that of congeneric in Puget Sound.

Remaining description as for genus. Largest specimen examined 426 mm (UW 044012). Maximum size reported ca. 540 mm (580 mm TL[6]).

Description of juveniles (Fig. 16)

Most individuals were collected on bottom (Fig. 16A) by 19.0 mm; newly settled juveniles with dorsal eye completely migrated; median fin rays formed; lateral line nearly formed; expanded anteriormost anal-fin pterygiophore well devel-

[6] Resource Assessment and Conservation Engineering (RACE) Division. 1996. Unpubl. data from RACE database. Alaska Fisheries Science Center, Natl. Mar. Fish. Serv., NOAA, 7600 Sand Point Way NE, Seattle, WA 98115.

oped. Preanal pigment increased along head and gut; postanal pigment smaller and distributed in random patches; urogenital papilla darkly pigmented throughout its length. Blind side with pigment similar to that of postflexion larvae. Orbit length larger, mouth smaller, body depth less, gill-raker counts on lower arch less, and distance from pelvic-fin origin to anal-fin origin greater than in *L. polyxystra* n. sp. Pelvic- and pectoral-fin rays formed.

By 30.0 mm, pigmentation has increased along body, with darker patches and spots throughout (Fig. 16B) obscuring pigmented urogenital papillae. Lateral line more fully developed; supraorbital canal pores visible.

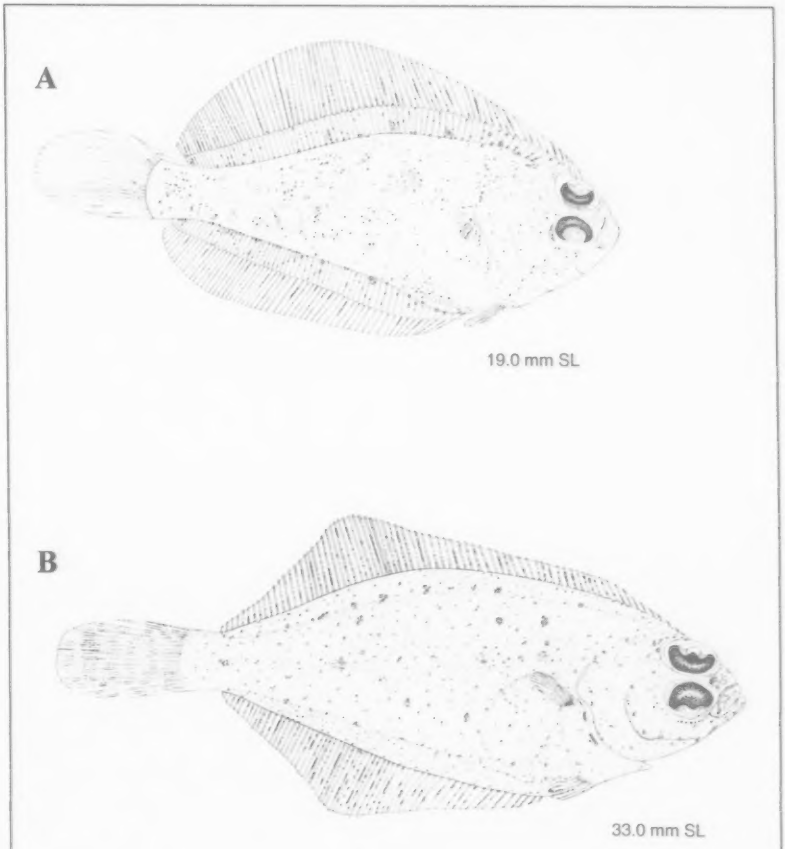

Figure 16

Juveniles of *Lepidopsetta bilineata* (Ayres): **(A)** UW 083484, 19.0 mm, Kachemak Bay, Alaska, 59°37.8'N, 151°44.2'W, 34 m depth, 17 July 1996; **(B)** UW 083483, 33.0 mm, off Vancouver Island, 48°39.5'N, 125°55.2'W, 19 September 1977. Illustrations by B. Vinter, under contract to the National Marine Fisheries Service, Alaska Fisheries Science Center.

Description of larvae (Fig. 17)

Snout-to-anus length is 32.9–34.6% SL, remaining constant during development; body depth 4.7–35.7% SL, increasing with development, sharply after flexion; head length 13.3–29.3% SL, increasing with development, sharply after flexion; snout length 22.6–20.7% HL, remaining constant during development; orbit length 51.9–23.8% HL, decreasing with development (Table 2). Total myomeres 37–44.

Larvae hatching at small lengths, at sizes less than 3.0 mm, yolk absorbed by 2.7–4.5 mm. Preflexion larvae ranging in size from 3.8 to 6.6 mm; flexion larvae, from 6.4 to 11.1 mm; postflexion larvae from 10.8 to 16.0 mm. Transformation occurring at lengths as small as 10.0 mm (often accompanied by a decrease in total body length); postsettlement juvenile stage usually attained by 20.0 mm (Table 13).

Preanal pigment present initially along lower jaw and ventral side of cleithral region, increasing with development to snout, upper jaw, and isthmus. Pigment ventrally along gut and dorsally on anus; by flexion a distinct patch of melanophores along the posterior edge of the gut; pigment increases laterally with development.

Postanal pigment present as melanophores along distal edges of dorsal and anal finfolds; four distinct pigment areas along the dorsal midline, anterior (first) spot begins 1–5 myomeres after anus at about myomere 12–16, second spot begins at about myomere 23–26, third spot begins at about myomere 33–46, and the fourth spot begins at about myomere 41–42 (after initially forming as a dorsal midline patch, the posteriormost spot coalesces with ventral patch to form a caudal bar); series of melanophores from the gut along the ventral midline beginning in a double row, changing to a single row posterior to the ventral stripe of the caudal bar; several additional melanophores along the ventral midline posterior to the caudal bar, pigment above and below the tip of the notochord. By transformation, the third dorsal midline patch and opposing ventral patch expand to form an indistinct bar; other patches of pigment form in myosepta and continue into the dorsal and anal pterygiophores and fin rays.

Distribution (Figs. 6, 10, 12, 18)

Lepidopsetta bilineata ranges from the continental shelf north and south of the Islands of Four Mountains in the eastern Aleutian Islands and in the southern Bering Sea

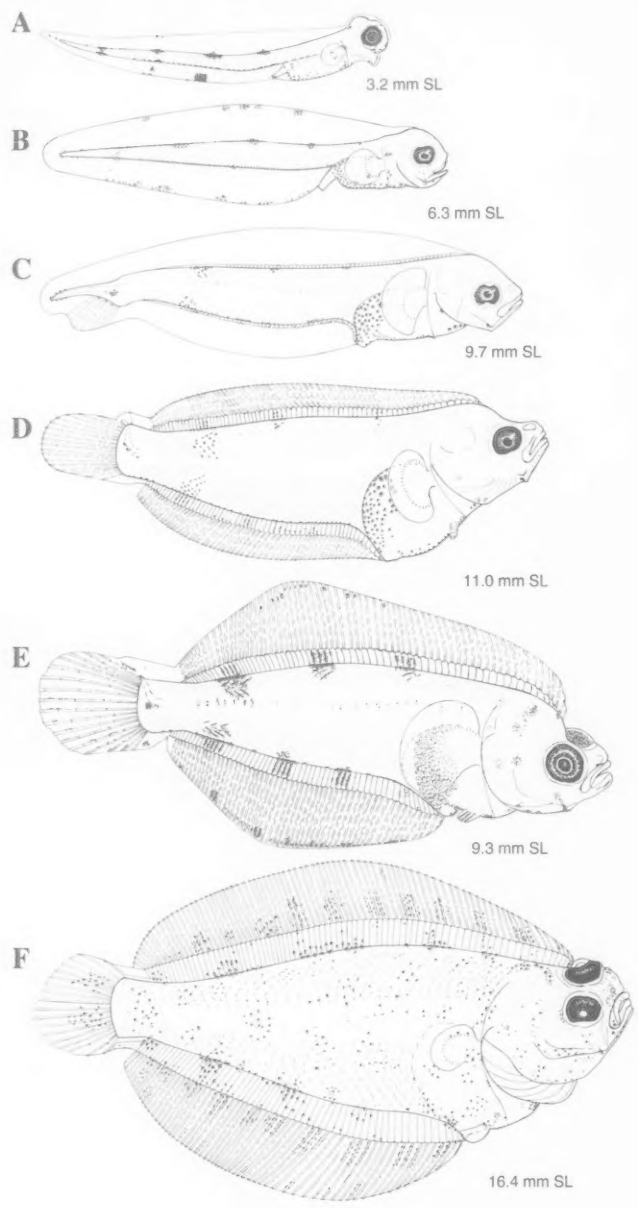

Figure 17

Larvae of *Lepidopsetta bilineata* (Ayres): **(A)** UW 083443, 3.2 mm, Gulf of Alaska, AFSC, 3 June 1990 ; **(B)** UW 083410, 6.3 mm, Gulf of Alaska, AFSC, 26 June 1978 (Matarese et al., 1989); **(C)** UW 083411, 9.7 mm, Gulf of Alaska (Matarese et al., 1989), AFSC, 28 June 1978; **(D)** UW 083412, 11.0 mm, Gulf of Alaska, AFSC, 14 Sept 1978; **(E)** UW 083444, 9.3 mm, Puget Sound, AFSC, 1 June 1989; **(F)** UW 083409, 16.4 mm, Gulf of Alaska, AFSC, 22 July 1977 (Matarese et al., 1989). Illustrations by B. Vinter, under contract to the National Marine Fisheries Service, Alaska Fisheries Science Center.

on the Slime Bank north of Unimak I., to Cortez Banks, Baja California, Mexico. It is common from the northern Gulf of Alaska to Puget Sound and is locally abundant along the coasts of Washington, Oregon, and California. Larvae have been collected from just south of the Aleutian Islands to Tanner Bank, Mexico (Moser et al., 1993; Charter and Moser, 1996).

Habitat

Adults were collected over sand and gravel substrates to depths of 339 m (RACE[6]). Larvae were collected over depths <1000 m.

During our 22-year sampling period, larvae were less common than those of *L. polyxystra* n. sp. in spring ichthyoplankton surveys conducted in the Gulf of Alaska. Larvae appeared in larger numbers later in the season (June) and the highest densities occurred from Kodiak Island to the eastern Gulf of Alaska (Table 14; Fig. 18). In the CalCOFI region, larvae were collected from February to July; peak abundance was in May (Charter and Moser, 1996). Larvae were collected more frequently and in higher densities closer to the coastline (within 55.6 km, Moser et al., 1993).

Life history

In *L. bilineata* taken off the coast of Oregon, brittlestars of the genus *Ophiura* dominated the diet, and polychaetes and mollusks constituted much of the remainder (Kravitz et al. 1976). Adults from the Gulf of Alaska and Aleutian Islands are often infested with the parasitic copepods *Nectobrachia indivisa* and *Naobranchia occidentalis*.[7] Both parasites were previously recorded in *Lepidopsetta* by Kabata (1988). For both parasite species, *L. bilineata* was significantly less infested than *L. polyxystra* n. sp.[6] The maximum recorded age for female *Lepidopsetta* is 18 yr at 49 cm FL and for a male is 17 yr at 40 cm FL (Levings, 1967; Forrester, 1969). For early life history information, see generic account.

[7] Zimmermann, M. and R. Harrison. 1998. Personal commun. Resource Assessment and Conservation Engineering Division, Alaska Fisheries Science Center, Natl. Mar. Fish. Serv., NOAA, 7600 Sand Point Way NE, Seattle, WA 98115.

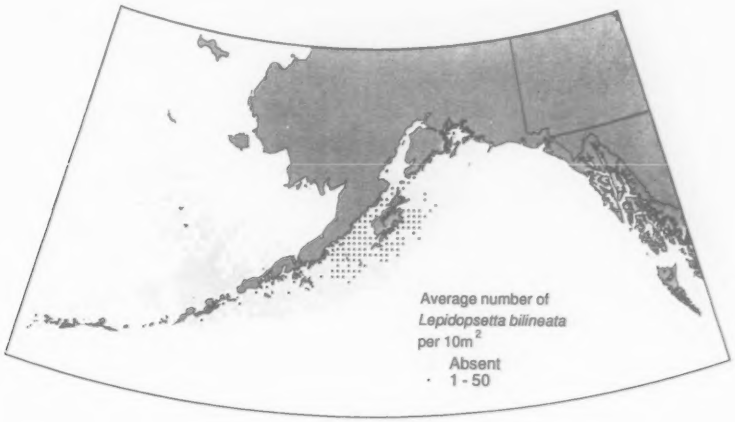

Figure 18

Distribution and density (average number per 10 m^2) of *Lepidopsetta bilineata* in the Gulf of Alaska and Bering Sea, 1972–1994.

Table 14

Monthly collections of larvae of *Lepidopsetta* in the Gulf of Alaska and Bering Sea (1972–1994). Mean density (number per 10 m^2) followed below by the standard deviation of the mean in parentheses.

	Month												
Taxon	Jan	Feb	Mar	Apr	May	Jun	Jul	Aug	Sep	Oct	Nov	Dec	Overall
L. bilineata	0	0	0	0.0139	0.568	1.73	0.15	0	0.116	0.0311	0	0	0.414
	(0)	(0)	(0)	(0.0059)	(0.0592)	(0.243)	(0.0553)	(0)	(0.0872)	(0.0311)	(0)	(0)	(0.0357)
L. polyxystra n. sp.	0	0	0.456	5.80	7.06	4.44	0.659	0	0.09	0.0386	0	0	5.34
	(0)	(0)	(0.204)	(0.633)	(0.383)	(0.481)	(0.018)	(0)	(0.0634)	(0.0386)	(0)	(0)	(0.289)
Total observations	115	163	704	2926	2678	861	333	0	144	138	585	11	7502

Etymology

The specific name is derived from the Latin *bilineata*, meaning "two lined", a reference to the bifurcate supratemporal branch of the lateral line.

Comments

Basing his work on an account first published in *The Pacific* (Ayres, 1855a) and subsequently reprinted in the Proceedings of the California Academy of Sciences (Ayres, 1855b), Ayres described his specimen of *Platessa bilineata* at the California Academy of Natural Sciences (CAS) in 1855. The specimen has not been located at CAS[8] (where it may have been destroyed in the 1906 San Francisco earthquake and subsequent fire, Springer and Anderson, 1998), ANSP,[9] LACM,[10] or USNM.[11] Because *L. bilineata* may be easily confused with *L. polyxystra* n. sp., especially in the Gulf of Alaska and Puget Sound, we therefore designated CAS 42650, collected in the Gulf of Farallones off California, as the neotype of *L. bilineata*. Ayres obtained his specimen from the San Francisco fish market and noted that, although not common, the species was taken in San Francisco Bay. Lockington (1879a) noted that *L. bilineata* was most commonly caught "at or near the Farallone Islands" for the San Francisco markets.

[8] Catania, D. 1996. Personal commun. Ichthyology Department, California Academy of Sciences, Golden Gate Park, San Francisco, CA 94118.

[9] Saul, W. 1996. Personal commun. Academy of Natural Sciences, 19th and The Parkway, Philadelphia, PA 19103.

[10] Feeney, R. 1996. Personal commun. Natural History Museum of Los Angeles County, 900 Exposition Blvd., Los Angeles, CA 90007.

[11] Jewett, S. 1995. Personal commun. Division of Fishes, Smithsonian Institution, Washington, D.C. 20560.

Girard (1856) described *Platichthys umbrosus* on the basis of a single specimen deposited at the USNM, which was collected at Cape Flattery, Washington, by Lieutenant W. P. Trowbridge. One lot listed in the catalog, USNM 607, bears the collector's name as Trowbridge and a collection date of 1856, and thus the single specimen of this lot appears to have been the one examined by Girard for his original description. From the original description, the specimen is approximately 190 mm TL. Unfortunately, this lot cannot be found and is presumed missing or destroyed.[11]

Girard was apparently unaware of Ayres' (1855a, 1855b) description of *L. bilineata* (Leviton and Aldrich, 1997). Although Günther (1862) considered *Platichthys umbrosus* distinct (basing his conclusion on the dried skins identified as *P. umbrosus* taken off Vancouver Island, Canada, and on the descriptions of *L. bilineata* provided by Ayres), later authors have treated *P. umbrosus* as a synonym of *L. bilineata* (Lockington, 1880a, 1880b; Jordan and Gilbert, 1881; Jordan and Evermann, 1898; Norman, 1934; Schmidt, 1950), and the name has not been used at the species level since Lockington's (1879b) misidentification of *Isopsetta isolepis*. *Lepidopsetta polyxystra* n. sp. also ranges south along the east coast of Vancouver Island, the "Inside Passage," to Puget Sound, and larvae of the new species have been recorded from the extreme northwest coast of Vancouver Island. Although *L. bilineata* is present, but uncommon, off the west coast of Vancouver Island, no adults or larvae of *L. polyxystra* n. sp. have been collected off Washington (Cape Flattery and south), despite the intensive survey efforts of the 1995 and 1998 NMFS triennial surveys, during which all captured *Lepidopsetta* were examined. Although the original description is insufficient to refer it to either of these species, the type locality lies well within the known range of *L. bilineata* and outside that of *L. polyxystra* n. sp. and we therefore consider *Platichthys umbrosus* to be a synonym of *L. bilineata*.

Cope's (1873) description of *Pleuronectes perarcuatus*, from a specimen taken somewhere along the eastern Pacific Ocean coast of Alaska, perhaps near Sitka or Unalaska Island, included a comparison with Girard's *Platichthys umbrosus* but not with Ayres's *Platessa bilineata*. Although the holotype is badly damaged, especially about the head, the gill-raker count and structure, as well as presence of at least one supraorbital pore at the dorsal margin of the orbit,[8] indicate the holotype is *L. bilineata*. The specimen has a high lateral-line pore count at the upper range of counts for *L. bilineata*. The name has been considered synonymous with, or a subspecies of, *L. bilineata* by later authors (Jordan and Gilbert, 1881; Jordan and Goss, 1889; Jordan and Evermann, 1898; Wilimovsky et al., 1967).

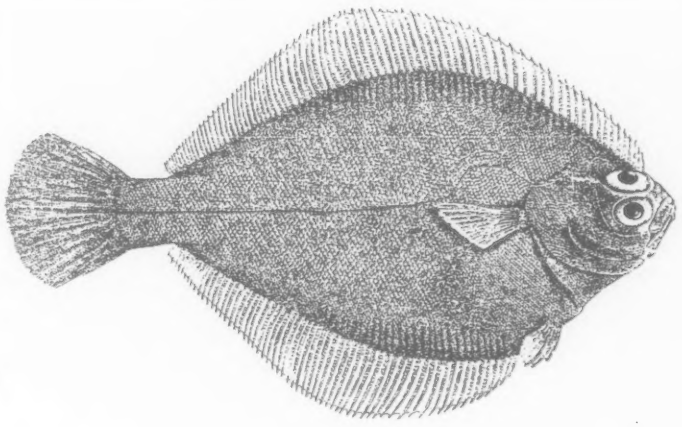

Figure 19

Lepidopsetta mochigarei Snyder, holotype, USNM 68245, 1(174 mm), Japan, Hokkaido, Otaru Market, 1906. After Snyder (1912).

Lepidopsetta mochigarei Snyder, 1911
Ricecake sole
Asabagarei
Figs. 1–2, 7, 19–20; Tables 3–10, 13

Lepidopsetta mochigarei Snyder, 1911:547 (original description, two specimens: holotype by original designation, USNM 68245, male, 174 mm, and "cotype." SU 21430, 145 mm TL, both from the market at Otaru, Hokkaido, Japan).

Lepidopsetta bilineata mochigarei Taranets, 1937:144 (new combination, keys).

Pleuronectes mochigarei Sakamoto, 1984a:99 (new combination, phylogenetics).

Material examined

Adults 27 specimens, 90.7–280.3 mm, including holotype listed above. Japan: CAS-SU 113378, 1(257.5 mm), Bomasiri Shima, off N end of Rebun To., 45°25.5'N,140°53'E, 22 September 1906; CAS-SU 122548, 1(146.7 mm), Tsugaru Strait/Sea of Japan, between Hakodate, Hokkaido and Ebisu, Sado I., S of Cape Tsiuka, 41°35.8333'N, 140°36.75'E, 16 July 1906; HUMZ 56717, 1(154 mm), Hokkaido, off Kushiro; HUMZ 58576, 1(189 mm), Hokkaido, off Otanoshike; HUMZ 58566, 1(197.5 mm), Otanoshike, off Hokkaido, 20 m; HUMZ 58563, 1(200.5 mm), Otanoshike, off Hokkaido, 20 m; HUMZ 58568, 1(171.5 mm), Otanoshike, off Hokkaido; HUMZ 58567, 1(184 mm), Hokkaido, off Otanoshike; HUMZ 87820, 1(175 mm), Hokkaido, off Muroran, 135 m; HUMZ 80974, 1(190.5 mm), Hokkaido, off Muroran; HUMZ 81056, 1(167.5 mm), Hokkaido, Usujiri, Minamikayabe; HUMZ 90912, 1(142.5 mm), Hokkaido, off Tomakomai, 300 m; HUMZ 64730, 1(116.6 mm), Hokkaido, Funkawan; HUMZ 15505, 1(107.2 mm), Hokkaido, Funka Bay; HUMZ

15456, 1(130.5 mm), Hokkaido, Funka Bay; HUMZ 15506, 1(90.7 mm), Hokkaido, Funka Bay; HUMZ 94034, 1(193.5 mm), Hokkaido, off Tomakomai, 300 m; UBC 58-355, 2(204–240 mm), Japan; USNM 150380, 1(130.6 mm), Hokkaido; USNM 077125, 1(166.1 mm), 104 km S of OseSaki, *Albatross* Sta. 5067, 35.0972°N, 138.6875°E, 536 m; Russia: USNM 77126, 1(244.2 mm), Gulf of Tartary, off SW coast of Sakhalin I., *Albatross* Sta. 4999, 47.6389°N, 141.65°E; USNM 77127, 1(247.4 mm), Aniwa Bay, approaching Korsokov, Sakhalin I., 73 m, *Albatross* Sta. 5008, 46.1306°N, 142.6222°E; USNM 77130, 1(280.3 mm), Gulf of Tartary, off SW coast of Sakhalin I., 57 m, *Albatross* Sta. 5000, 46.55°N, 142.7083°E; USNM 77128, 1(257 mm), Aniwa Bay, approaching Korsokov, Sakhalin I., 77 m, *Albatross* Sta. 5007, 46.05°N, 142.5167°E; USNM 77135, 1(246.8 mm), Sakhalin I., off Korsokov Lt., 39-56 m, *Albatross* Sta. 5010, 46.55°N, 142.725°E.

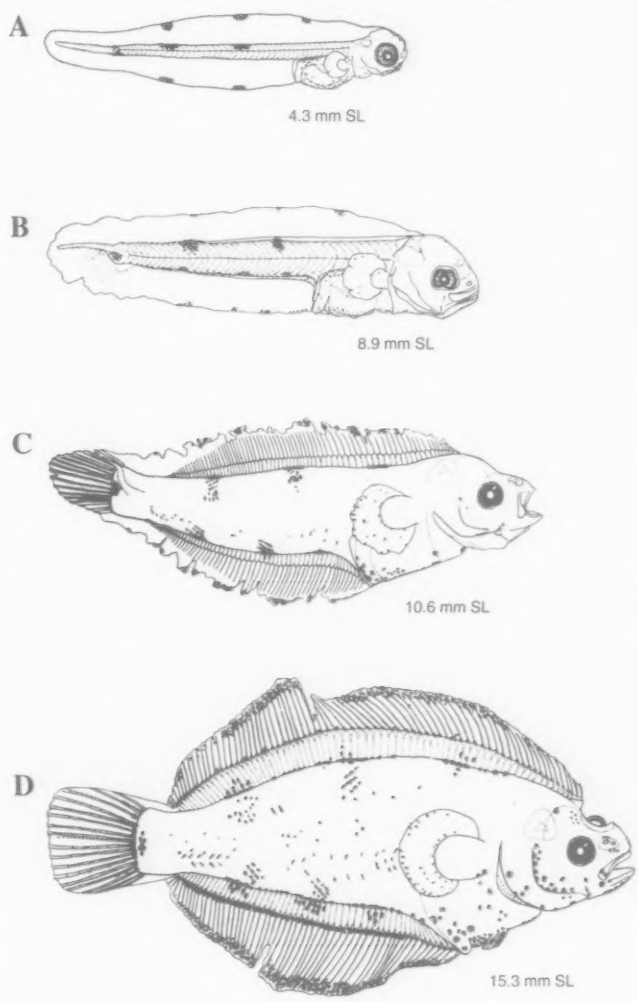

Figure 20

Larvae of *Lepidopsetta mochigarei* Snyder (figures reproduced from Okiyama, 1988): **(A)** 4.3 mm, Japan Sea (Okiyama and Takahashi, 1976); **(B)** 8.9 mm, Sea of Japan (Okiyama and Takahashi, 1976); **(C)** 10.6 mm, Sea of Japan (original illustration of Nagasawa, cited in Okiyama, 1988, locality implied in text); **(D)** 15.3 mm, Sea of Japan (original illustration of Nagasawa, cited in Okiyama, 1988, locality implied in text).

Diagnosis

Lepidopsetta mochigarei is a species of *Lepidopsetta* with the following combination of characters in adults: total gill rakers on first arch 6–10, on upper arch 1–3; total gill rakers on second arch 7–10; supraorbital pores 1–3; preopercular pores 8–13; lateral-line pores 95–119; sum of scales above and below lateral line 91–108; interorbital narrow; blind-side coloration white, and glossy highlights along myotome margins increasing anteriorly.

Larvae are distinguished from other species of *Lepidopsetta* by having the following combination of characters: body deep, increasing rapidly with development and snout-to-anus length moderate; larvae undergoing notochord flexion at comparatively larger sizes; preflexion pigment pattern with three prominent spots along margin of dorsal finfold and two spots along ventral finfold, three patches along postanal dorsal midline aligned with finfold spots to form slightly offset opposing patches, posteriormost dorsal spot coalescing with a corresponding ventral spot to form a bar; pectoral-fin rays pigmented (Okiyama and Takahashi, 1976; Nagasawa, cited in Okiyama, 1988).

Description of adults

Body ovate, relatively deep, greatest depth 45.5–61.1 (51.7)% SL, scales above lateral line 35–45 scales below lateral line 52–67; head relatively short and robust, length 23.3–30.5 (26.2)% SL; dorsal margin of head at dorsal-fin origin nearly linear, snout length 3.3–6.2 (4.3)% SL (12.7–20.2 (16.1)% HL); ocular-side maxilla length 24.6–29.4 (27.2)% HL; blind-side maxilla length 27.3–32.9 (29.7)% HL; ocular-side mandible length 36.6–44.6 (39.7)% HL; teeth 6–10 on ocular-side premaxilla, 23 on blind-side premaxilla and 8–15 on ocular-side dentary, 21–28 on blind-side dentary; gill rakers of first arch broad and robust, 6–10 total, 1–3 on upper arch, 4–7 on lower; gill

rakers of second arch 7–10 total, 1 on upper and 6–9 on lower arch; eyes relatively large, dorsal orbit slightly longer than eye length, orbit length 26.1–34.7 (30.1)% HL, eye length 21.4–30.0 (25.3)% HL; ventral eye length 21.6–31.1 (25.5)% HL; interorbital a narrow ridge, up to 2 scales at narrowest portion, 1.3–4.2 (2.7)% HL; cheek with 10–15 scales, length 28.6–35.0 (31.1)% HL, depth 14.8–25.5 (19.7)% HL; preopercular pores 8–13; ocular-side suborbital pores 22–38; blind-side suborbital pores 10–20; lateral line pores 95–119, lateral-line arch relatively long, 53.7–69.9 (62.7)% HL, its depth 23.8–35.7 (30.9)% its length; both anterior and posterior supratemporal branches relatively short, anterior pores 3–12, posterior pores 6–22; supraorbital canal short, reaching only to the posterior rim of the dorsal orbit at about the insertion of dorsal-fin rays 5–6, pores 1–3; ocular-side pectoral-fin length 12.6–17.4 (14.6)% SL (47.9–60.2 (55.6)% HL); blind-side pectoral-fin length 7.9–11.7 (9.6)% SL (30.3–42.8 (36.5)% HL); ocular-side pelvic-fin length 7.4–11.8 (9.8)% SL (31.8–43.5 (37.4)% HL); dorsal fin with 73–82 rays, height 11.2–14.7 (12.9)% SL, in specimens with 75–81 rays supported by 71–77 pterygiophores, typically 8 or rarely 9 anterior to first neural spine; anal fin with 56–65 rays, in specimens with 56–63 rays supported by 57–61 pterygiophores; caudal peduncle relatively deep, least caudal peduncle depth 9.7–14.0 (11.0)% SL (36.2-50.3 (42.2)% HL; 105.1–172 (124.3)% caudal peduncle length), greatest caudal peduncle depth 12.0–14.6 (13.2)% SL (44.7–56.0 (50.5)% HL); caudal peduncle length 7.8–10.3 (8.9)% SL (27.5–39.4 (34.1)% HL); caudal-fin length 18.8–25.1 (21.2)% SL. Vertebrae 39–42, with 11 precaudal and 28–31 caudal.

Scales on head, pectoral region, and those scattered posteriorly on ocular side slightly rough and having columnar tubercles in larger adults. Small spines present in small adults.

In life, blind side of adults translucent to white with glossy highlights along edges of myotomes (Amaoka et al., 1983, Fig. 220 as *L. bilineata*; Amaoka et al., 1995, Fig. 524 as *Pleuronectes bilineatus*). When preserved, blind side uniform creamy white to yellow-brown. Ocular side brownish with faint yellow highlights around small dark spots near bases of dorsal and anal fins and at midline (Amaoka et al., 1995, Fig. 524).

Remaining description as for genus. Largest specimen examined 280.3 mm (USNM 77130). Maximum size reported 400 mm SL (Sakamoto, 1984b).

Description of juveniles

No juveniles were examined for this study. Juveniles are not described in available literature.

Description of larvae

No larvae were examined in our study. The following description is based on Okiyama and Takahasi (1976, based on 3 specimens of 4.12–8.59 mm) and Pertseva-Ostroumova (1961; number and size of specimens examined not stated).

Snout-to-anus length 32.8–37.0% SL, decreasing with development according to Pertseva-Ostroumova, 1961 (34.2–32.5% SL); body depth 9.0–17.0% SL, increasing with development; head length 15.0–20.0% SL, increasing with development; orbit length 41.0–28.0% HL, decreases with development. Total myomeres 41–43.

Hatching occurring at relatively large sizes, at 3.95–4.48 mm (Yusa, 1958); flexion beginning by 8.9 mm (Fig. B of Okiyama, 1988); postflexion size between 10.6 mm and 15.3 mm (Figs. C and D of Okiyama, 1988); transformation occurring at sizes larger than 15.3 mm (Fig. D of Okiyama, 1988).

Preanal pigment (Fig. 20, based on Okiyama, 1988) present initially along lower jaw, extending ventrally along gut to anus. By flexion, melanophores appearing on pectoral-fin rays; pectoral-fin rays and base not pigmented in all earlier developmental stages; pectoral fin pigmented more heavily than *L. polyxystra* n. sp. by later stages (Pertseva-Ostroumova, 1961).

Postanal pigment of preflexion larvae in prominent patches of melanophores along finfold edges, three along dorsal and two along anal finfold, becoming more dispersed and less prominent with development; three distinct pigment patches along the dorsal midline, anterior patch begins at about myomere 20–22, posterior patch begins at about 33–36, and caudal patch, which aligns with a ventral patch to form a caudal bar, begins in the range of myomeres 40–44; these dorsal midline patches align vertically with the two posteriormost dorsal and both ventral finfold patches; a series of melanophores may occur along the postanal ventral midline (additional descriptions cannot be found in the literature); additional pigment spots above and below the notochord tip.

Distribution

Lepidopsetta mochigarei ranges in the western Pacific Ocean from the east coast of Korea, Yoglin Bay, in the Sea of Japan (Kim and Youn, 1994) to Iturup Island of the Kuril Islands in the southern Okhotsk Sea (Nikiforov et al., 1983), and to the west coast of northern Japan. Larvae have been collected in March along the coast of northern Honshu in the Sea of Japan (Okiyama, 1988).

Habitat

Adults have been collected over the continental shelf; spawning may occur in depths of about 120 m (Okada, 1955).

Life history

Fecundity ranges from 510,000 to 550,000 eggs (Okada, 1955). Spawned eggs are demersal and adherent, about 0.87–0.95 mm in diameter (Yusa, 1958; Pertseva-Ostroumova, 1961); oocytes at maturation stage IV were 0.440–0.655 mm in diameter (Nikiforov et al., 1983). Spawning occurs from December to June in waters around Hokkaido and the southern Kuril Islands (Minami, 1995). Embryonic and larval development to about 5.0 mm has been described by Yusa (1958).

Etymology

The species name *mochigarei* is derived from the Japanese, meaning "rice-cake flounder" (Snyder, 1911), probably a reference to the bright white blind side similar to white rice-cake common in Japan.[12]

Comments

Masutomi and Hamada (1966) described a fossil of *L. mochigarei*. It was subsequently described as the extinct *Chibapsetta dolichurostyli* by Sakamoto and Uyeno (1988).

Because early life history material was not available for examination, descriptions were based on the available literature (Yusa, 1957, 1958; Pertseva-Ostroumova, 1961; Okiyama and Takahashi, 1976; Okiyama, 1988). Several potentially important characters could not be gleaned from the available sources: an anterior pigment spot along the dorsal midline, important in distinguishing *L. bilineata* from *L. polyxystra* n. sp. (Figs. 17C, 17D), is not present in preflexion larvae (Figs. 20A and 20B). Because the sources were different, we needed verification that these figures constitute a series. Although present, the extent of the postanal ventral melanophores, important in distinguishing *Lepidopsetta* from *Psettichthys* in particular as well as from other pleuronectids, is not known. Additional data for morphological characters were also needed for all developmental stages. Larvae of *L. mochigarei* appear more similar to those of *L. bilineata* than *L. polyxystra* n. sp., but they are not sympatric with *L. bilineata*. Based on the present descriptions, larvae of *L. mochigarei* can be distinguished from those of *L. polyxystra* n. sp. by the distinctive vertically aligned dorsal midline and finfold pigment.

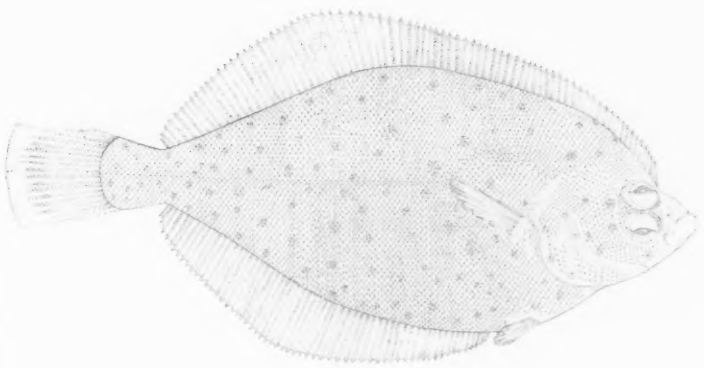

Figure 21

Lepidopsetta polyxystra n. sp., holotype, UW 14826, 169.7 mm, Alaska, Aleutian Islands, Amchitka I., Constantine Harbor, 19–42 m, 19 August 1955. Illustration by B. Vinter, under contract to the National Marine Fisheries Service, Alaska Fisheries Science Center.

Lepidopsetta polyxystra n. sp.
Northern rock sole
Figs. 1–5, 8, 11, 13, 21–24; Tables 2–11, 13–14

Lepidopsetta bilineata var. *umbrosa* Jordan and Evermann, 1898:2643 (in part, Fig. 928).

Lepidopsetta bilineata bilineata Taranetz, 1937:144 (in part, new combination, keys).

Holotype

UW 014826, 1(169.7 mm), Alaska, Aleutian Is., Amchitka I., Constantine Harbor, 19–42 m, 19 August 1955.

Material examined

A total of 843 adults and juveniles, including the holotype listed above, was examined. Sixty larvae were examined.

Paratypes

Adults 219 specimens, 26–427.5 mm. Okhotsk Sea: UW 042341 (orig. KIE 1147), 2(105.5–109.5 mm), western Kamchatka, 51°57'N, 156°25'E; UW 042342 (orig. KIE 1149), 3(144.5–195 mm), western Kamchatka, 52°02'N, 155°58'E, 6 June 1992; UW 042343 (orig. KIE 1151), 10(186–247 mm), 52°29'N, 153°40'E, 24 June 1992; KIE 1148, 1(89.5 mm), 51°43'N, 156°04'E, 5 June 1992; Southeast Kamchatka: CAS-SU 122549, 1(112.3 mm), Kamchatka, off Petropavlovsk, 18 June 1906; Bering Sea: KIE 1415, 1(289.5 mm), Bering I., SW of Cape Monati, 54°37'N, 166°31'E, 27 April 1996; KIE 1417, 1(258.5 mm), Bering I., SW of Cape Monati, 54°39'N, 166°29'E, 8 May 1996; KIE 1414, 1(260.5 mm), SW of Cape Monati, 54°40'N, 166°29'E; KIE 1268, 1(338.6 mm), NW of Bering I., 55°34'N, 164°55'E, 7 January 1994; KIE 1418, 1(289 mm), Bering I., SE of Cape Monati, 54.6667°N, 166.8333°E, 9 May 1996; KIE 1416, 1(261 mm), Kamchatka, SW of Cape Northwestern, 55.2833°N, 165.5333°E, 4 May 1996; KIE 1150, 1(238.5 mm), Kamchatka, 56.2333°N, 154.3°E, 18 June 1992; ABL 93-37, 1(193 mm), St. Paul I., Pribilof Is.; ABL 60-15, 1(265 mm), N of Pribilof Is., 58°33'N, 170°12'W, 17 July 1960; UW 041694, 3(150-177), Aleutian Is., NE of Umnak I., 53.44°N, 168.4944°W; SIO 94-164, 9(103–190 mm), Aleutian Is., off Unalaska I., 54°15.1'N, 165°57.6'W, 4 June 94; UW 041199, 1(267 mm), 60.6667°N, 169.65°W, 16 July 1979; UW 041697, 1(245 mm), Bering Sea, N of Unimak I., 55.0213°N, 164.6009°W; CAS 45562, 1(240.8 mm), WNW of Pribilof Is., NE end of Zhenchug Canyon, 58°15.8667'N,

[12] Amaoka, K. 1997. Personal commun. Laboratory of Marine Zoology, Faculty of Fisheries, Hokkaido University, Hakodate, Hokkaido, Japan.

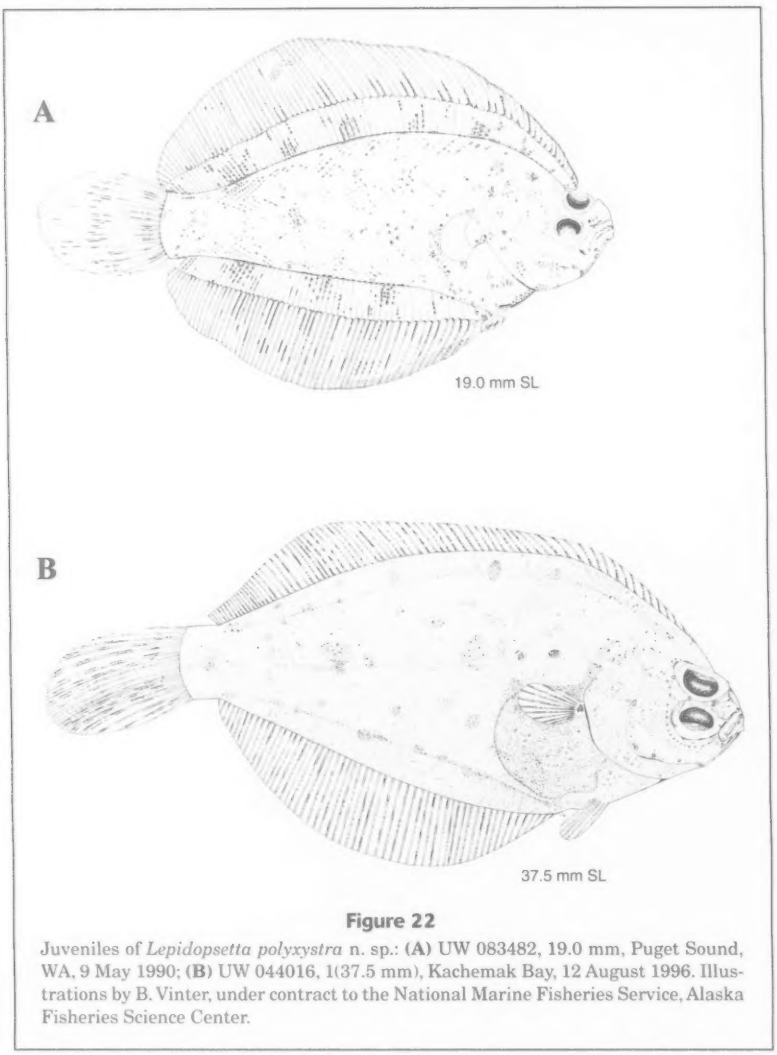

Figure 22

Juveniles of *Lepidopsetta polyxystra* n. sp.: **(A)** UW 083482, 19.0 mm, Puget Sound, WA, 9 May 1990; **(B)** UW 044016, 1(37.5 mm), Kachemak Bay, 12 August 1996. Illustrations by B. Vinter, under contract to the National Marine Fisheries Service, Alaska Fisheries Science Center.

174°0.3'W, 21 June 79; CAS 45567, 1(272.1 mm), SSW of Pribilof Is., 55°38.8667'N, 168°39.9833'W, 16 June 79; CAS 46676, 1(87.7 mm), Pribilof Is., St. George I., 56°35'N, 169°36'W, 27 July 1977; CAS 47531, 5(181.4–199.4 mm), Aleutian Is., 51°43.9'N,177°57.8833'W, 10 August 1980; CAS-SU 105731, 5(132.6–182.9 mm), Aleutian Is., Umnak I., off Nikolski, 31 July 1896; USNM 130725, 3(287–310 mm), 40 mi above Port Moller, 8 May 1941; USNM 060905, 1(316.5 mm), Karluk, TT2204, RV *Albatross*; UW 001378, 1(175.5 mm), Unalaska I., 1930; UW 003656, 1(100.5 mm), Alaska Peninsula, Cold Bay, 13 June 1932; UW 013667, 1(208.1 mm), Unimak I., False Pass, 1 July 1957; UW 016609, 1(191 mm), Pribilof Is., St. George I.; UW 025736, 3(28–45.7 mm), Port Moller; UW 016600, 3(83.9–130.9 mm), 58.5833°N, 168.1°W, 4 July 1949; UW 003100, 3(86.7–164.6 mm), Captains Bay, Unalaska I.; UW 10650, 2(81.6–112.8 mm), off Nunivak I., 59°36'N, 167°56'W; UW 14831, 1(83 mm), off Nunivak I., 59.82°N, 169.13°W, 4 July 1949; UW 25760, 1(193 mm), 57.65°N, 167.65°W; UW 25731, 1(178.9 mm), 57.6667°N, 167.2°W, 27 April 1987; UBC 65-39, 1(175 mm), Izembeck Bay, 31 August 1964; UBC 62-565, 2(198–229 mm), 120 km E of St. George I.; UBC 65-730, 2(220–245 mm), 57°45'N, 164°45'W, 16 August 1965; UBC 65-714, 1(160 mm), 57°45'N, 168°45'W, 1 August 1965; UBC 65-729, 1(150 mm), 55°45'N, 162°45'W, 14 August 1965; Gulf of Alaska: ABL 72-74, 6(26–59.3 mm), SE shore of Favorite Channel, 10 November 1972; ABL Uncat, 1(195 mm), Unalaska I., 18 June 1958; 86ABL 62-202, 3(83.5–88 mm), Auke Bay, ca. 17.6 km NW of Juneau, 23 May 1962; ABL 62-199, 1(52.3 mm), 19.2 km NW of Juneau; ABL 64-996, 2(65.6–69.5 mm), Auke Bay, ca. 17.6 km NW of Juneau, 30 April 1964; ABL 67-32,

1(265 mm), Baranof I., Katlian Bay, 19 April 1967; OS 17158, 20(227–315 mm), 55.3323°N, 161.3186°W, 32 m, 3 June 1996; OS 17157, 3(230–262 mm), Aleutian Is., 51.88373°N 179.7202°E, 95 m, 16 July 1997; OS 3497, 1(213 mm), False Pass, Ikatan Bay, 19 June 1956; OS out of 6447, 2(166.1–170.2 mm), 57°10'N, 151°40.5'W, 77 m, 20 September 1978; OS 2157, 1(92 mm), Kodiak I., Shelikof St., mouth of Sturgeon R., 9–10 September 1954; OS 2169, 1(64 mm), Moffet Pt. to Black Hill, 28 May 1957; OS 2173, 1(63.5 mm), Moffet Pt. to Black Hill, 3 June 1957; OS 3979, 1(94.6 mm), Little Port Walter, 8 August 1964; SIO 69-748, 3(51–195 mm) of 7(51–195 mm), Afognak I., Kitoi Bay, 16–21 April 1968; SIO 76-299, 1(270 mm), Kodiak shelf, 56°43'N, 153°22'W, 25 June 1976; SIO 72-227, 1(235 mm), 40 km NW of Juneau, Lynn Canal, 16 February 1963; USNM 130734, 1(254.5 mm), Ivanof Bay, 3 April 1941; USNM 27602, 1(261.8 mm), Kodiak I., 12 July 1880; USNM 27942, 1(260.2 mm), Cook Inlet, Port Chatham; USNM 116332, 2(293–295 mm), Canoe Bay, 17 September–15 October 1940; UW 003854, 1(355 mm), Alitak Bay, Kodiak I., 9 June 1932; UW 040498, 1(195 mm), Prince William Sound, 1989; UW 025740, 1(68.4 mm), Ugak Bay, Kodiak I.; UW 044029, 1(276 mm), 59.5743°N, 151.325°W, 11 m depth, 26 February 1996; UW 044001, 18(52.7–99 mm) [3(30–40 mm) of 18 used for illustration], Prince William Sound; UBC 59-485, 2(71–116.2 mm), Chief Cove, Spiridon Bay; UBC 65-572, 1(74 mm), Boussole Bay, 29 June 1965; UBC 63-174, 1(290 mm), Prince William Sound, off Cordova; UBC 65-148, 1(205 mm), W of Chirikof I., 3 August 1964. British Columbia: SIO 63-206-64B, 1(97 mm), Vancouver I., Stanley Park at Lumberman's Arch, 15 March 1963; UBC 56-83, 3(83.5–121.3 mm), Strait of Georgia, off Saturna I.; UBC 62-874, 1(120 mm), off Sooke, 20 June 1962; Puget Sound: OS 3565, 1(224 mm), Puget Sound, 3 February 1943; UW 041078, 2(126–144 mm), Nisqually Reach, 25 February 1949; UW 004411, 1(36 mm), Edmonds, 1 June 1938; UW 000203, 1(45.9 mm), Lopez I., 12 August 1929; UW 041678, 1(67.2 mm), San Juan Islands, East Sound, 11 December 1964; UW 041675, 3(53.7–166.5 mm), Port Townsend Bay, 5 December 1978–5 January 1979; UW 018096, 1(182.4 mm), Bellingham Bay, Chuckanut Bay, May 1964; UW 044014, 29(121–223 mm), 47°19.48'N,

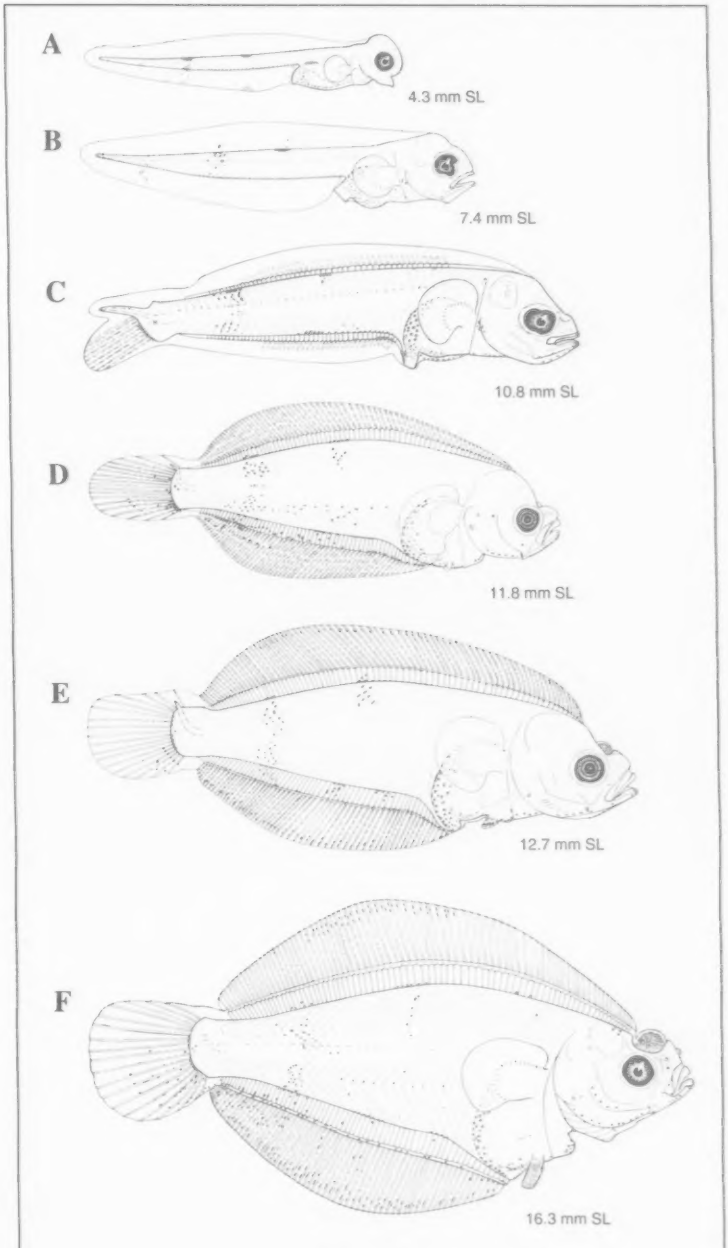

Figure 23

Larvae of *Lepidopsetta polyxystra* n. sp.: **(A)** UW 069346, 4.3 mm, Gulf of Alaska, 30 March 1978 (Matarese et al., 1989); **(B)** UW 083455, 7.4 mm, Gulf of Alaska, 15 May 1979 (Matarese et al., 1989); **(C)** UW 083446, 10.8 mm, Bering Sea, 26 July 1971 (Matarese et al., 1989); **(D)** UW 063735, 11.8 mm, Gulf of Alaska, 25 May 1985; **(E)** UW 083453, 12.7 mm, Gulf of Alaska, 24 June 1978; **(F)** UW 083454, 16.3 mm, Gulf of Alaska, 24 June 1978 (Matarese et al., 1989). Illustrations by B. Vinter, under contract to the National Marine Fisheries Service, Alaska Fisheries Science Center.

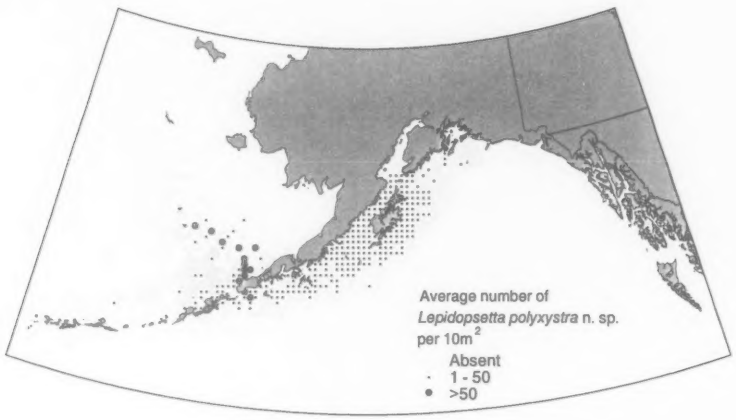

Figure 24

Distribution and density (average number per 10 m^2) of *Lepidopsetta polyxystra* n. sp. in the Gulf of Alaska and Bering Sea, 1972–1994.

122°33.8'W, 10 May 1996; UW 044007, 9(135–200 mm), Nisqually, 47°9.47'N, 122°40.16'W, 16 May 1996.

Larvae 18 specimens, 3.3–18.6 mm, examined. Bering Sea: UW 083475, 1(3.7 mm), 55°47.0'N, 165°59.0'W, 0–117 m depth, bongo net, 19 April 1991; Gulf of Alaska: UW 083456, 1(3.3 mm), 58°22.0'N, 150°06.0'W, 0–52 m depth, bongo net, 9 April 1991; UW 083479, 1(11.2 mm), 57°19.0'N, 156°09.0'W, 0–100 m depth, bongo net, 4 June 1990; UW 083457, 1(4.2 mm), 56°30.0'N, 157°00.2'W, 0–43 m depth, bongo net, 24 April 1991; UW 083476, 1(5.2 mm), 56°54.3'N, 156°15.3'W, 0–100 m depth, bongo net, 9 May 1992; UW 083461, 1(6.4 mm), 56°46.1'N, 156°47.9'W, 0–47 m depth, bongo net, 24 May 1991; UW 083472, 1(7.2 mm), 56°46.2'N, 156°33.6'W, 0–99 m depth, bongo net (333 mesh), 13 May 1992; UW 083471, 1(8.8 mm), 56°46.2'N, 156°33.6'W, 0–99 m depth, bongo net, 13 May 1992; UW 083478, 2 of 10 (10.0–10.7 mm), 56°56.7'N, 154°43.2'W, 0–42 m depth, bongo net, 5 June 1990; UW 083481, 2(13.6–14.2 mm), 56°54.0'N, 156°29.5'W, 0–84 m depth, bongo net, 3 June 1990; UW 083477, 1(5.7 mm), 55°57.0'N, 158°33.1'W, 0–100 m depth, bongo net, 21 May 1991; UW 083480, 2(12.4–12.6 mm), 55°39.1'N, 156°3.4'W, 0–100 m depth, bongo net, 31 May 1990; UW 083451, 1(17.8 mm), 55°18.1'N, 160°12.0'W, 0–115 m depth, Methot net, 24 July 1991; UW 083450, 1(15.3 mm), 54°39.2'N, 159°23.0'W, 0–54 m depth, Methot net, 29 July 1991; UW 083452, 1(18.6 mm), 54°36.2'N, 162°16.2'W, 0–87 m depth, Methot net, 30 July 1991.

Other material examined

Adults 629 adults and juveniles. Bering Sea: UW 044023, 6(173–292 mm), 60.6869°N, 175.4609°W, 11 July 1995; UW 044020, 2(331–368.5 mm), 58.45°N, 174.33°W; UW 044003, 2(226–249 mm), 58.12°N, 168.43°W; UW 041699, 1(108 mm), 58.66°N, 159.47°W; Gulf of Alaska: UW 044015, 307(18.2–190 mm), Kachemak Bay; UW 044016, 1(37.5 mm), Kachemak Bay; UW 044018, 54(26–90 mm), Kachemak Bay; SIO 76-300, 3(161–200 mm) of 28(145–280 mm), Kodiak shelf, 57°40'N, 150°37'W, 15 March 1963; ABL 68-505, 2(128–140 mm) of 15(15–140 mm) examined, Glacier Bay, 8 August 1968; UW 025735, 2(35.8–61.8 mm), "6/10/83, Sta. 14, Haul 52"; UW 04321, 1(230 mm), Fishing Vessel *Sulak*, Cruise 436, Robin Scheid; UW 002688, 83(56–107 mm), Shumagin Is., Baralof Bay, 27 June 1931; UW 002032, 30(75–137 mm), Yakutat Bay, 21 June 1932. UW 041674, 11(67.5–139 mm), Alexander Archipelago, off Wrangell I., 1 December 1931; UW 003841, 13(72–99 mm), Yakutat Bay, 21 June 1932; UW 004004, 7(77–100 mm), Yakutat Bay, 21 June 1932; UW 005047, 6(97–120 mm), Alitak Bay, 9 June 1932; UW 041681, 1(119.5 mm), Prince William Sound, 1989; UW 002069, 8(106–157.3 mm), Cold Bay, 6-26 May 1932; UW 022413, 5 cleared and stained of 14(53–110 mm), Adak I., Aleutian Is.; UW 040265, 16(159–350 mm), 54.03899°N, 165.8153°W; UW 003913, 5(113.4–167 mm), Prince William Sound, Orca Inlet, 2 April 1935; UW 044012, 6(275–384 mm), 56.5°N, 153.5°W, Bonaduhr; UW 020658, 7(56.1–135.7 mm), Kodiak I., Ugak Bay; UW 025763, 1(139.7 mm), off Amchitka I.; UW 040263, 3(214–255 mm), 54°N, 160.74°W. British Columbia: UBC out of 61-609, 3(44.8–56.6 mm), Bute Inlet; UBC out of 60–416, 6(181–230 mm), Queen Charlotte Is., Gillat Arm; UBC out of 62-93, 7(75–111 mm), Nass Bay; UBC out of 61-674, 7(64–81 mm), Dean Channel, off Nescall Bay. Washington, Oregon, and California: UW 041673, 5(68–110.5 mm), San Juan Is., East Sound, 3 March 1937; UW 047270, 6(60–240 mm), Puget Sound, Port Townsend Bay; CAS 19305, 1(246.5 mm), San Francisco (see comments).

Larvae 42 specimens (4.2–20.0 mm) examined: Bering Sea: UW 083446, 1(10.8 mm), 57°30.0'N, 169°30.0'W, depth unknown, bongo net, 26 July 1971; UW 083447, 1(4.5 mm), 54°01.3'N, 166°33.9'W, 0–100 m depth, bongo net, 25 April 1993; Western Gulf of Alaska: UW 083448, 1(15.1 mm),

55°17.7'N, 160°11.7'W, 0–115 m depth, Methot net, 24 July 1991; UW 083449, 1(15.3 mm), 54°39.2'N, 159°23.0'W, 0–54 m depth, Methot net, 29 July 1991; UW 071740, 1(12.0 mm; 11.0 mm as measured in this study), 55°38.6'N, 153°30.1'W, 0–102 m depth, bongo net, 31 May 1990; UW 071752, 1(10.0 mm; 9.4 mm as measured in this study), 55°31.6'N, 156°16.3'W, 0–100 m depth, bongo net, 31 May 1990; UW 072106, 1 of 2(17.1 mm), 56°46.2'N, 156°33.6'W, 0–100 m depth, bongo net, 3 June 1990; Gulf of Alaska: UW 069346, 1(4.3 mm) of 9, 58°22.0'N, 150°12.8'W, 0–47 m depth, bongo net, 30 March 1978; UW 083453, 1(12.7 mm), 56°41.9'N, 154°33.2'W, 0–16 m depth, bongo net, 24 June 1978; UW 083454, 1(16.3 mm), 57°19.5'N, 152°23.9'W, 0–48 m depth, bongo net, 24 June 1978; UW 083455, 1(7.4 mm), 56°23.7'N, 155°45.0'W, 0–79 m depth, bongo net, 15 May 1979; UW 063735, 1 of 12 (11.8 mm), 56°35.1'N, 153°43.6'W, 0–70 m depth, bongo net, 25 May 1985; UW 072459, 1 of 10 (9.4 mm), 57°10.7'N, 155°12.9'W, 0–100 m depth, bongo net, 5 June 1990; UW 072497, 6 of 10 (7.4–12.6 mm), 56°56.7'N, 154°43.2'W, 0–42 m depth, bongo net, 5 June 1990; UW 072502, 4 of 9 (7.3–10.3 mm), 56°49.4'N, 154°30.3'W, 0–60 m depth, bongo net, 5 June 1990; UW 072511, 1(12.2 mm), 57°28.6'N, 154°42.4'W, 0–60 m depth, bongo net, 5 June 1990; UW 072546, 1(8.1 mm), 57°40.6'N, 155°10.5'W, 0–287 m depth, bongo net, 6 June 1990; UW 083458, 1(6.8 mm), 57°15.6'N, 155°55.4'W, depth unknown, Mocness net, 14 May 1991; UW 083460, 1(6.4 mm), 56°16.4'N, 158°04.9'W, 0–64 m depth, bongo net, 22 May 1991; UW 083463, 1(4.2 mm), 57°52.3'N, 155°0.1'W, 0–82 m depth, bongo net, 7 April 1992; UW 083464, 1(5.0 mm), 57°42.2'N, 154°47.3'W, 0–219 m depth, bongo net, 7 April 1992; UW 083465, 1(5.5 mm), 57°16.5'N, 155°55.0'W, 0–100 m depth, bongo net, 8 May 1992; UW 083466, 1(5.8 mm), 56°54.3'N, 156°15.3'W, 0–100 m depth, bongo net, 9 May 1992; UW 083467, 3(4.6–6.0 mm), 56°51.8'N, 156°21.4'W, 0–99 m depth, bongo net, 9 May 1992; UW 083468, 1(6.1 mm), 56°53.3'N, 156°23.9'W, 0–102 m depth, bongo net, 9 May 1992; UW 083469, 1(8.5 mm), 56°42.2'N, 156°32.3'W, 0–100 m depth, bongo net, 13 May 1992; UW 083470, 1(6.7 mm), 56°44.4'N, 156°28.7'W, 0–102 m depth, bongo net, 13 May 1992; UW 083473, 1(7.6 mm), 56°09.4'N, 157°14.3'W, 0–101 m depth, bongo net, 22 May 1992; UW 083474, 1(7.5 mm), 56°40.6'N, 155°10.4'W, 0–59 m depth, bongo net, 15 May 1992; UW 083482, 2(19.0–20.0 mm), 47°34.15'N, 122°32.30'W, 0 m depth, dip net, 9 May 1990.

Diagnosis

Lepidopsetta polyxystra is a species of *Lepidopsetta* with the following combination of characters in adults: total gill rakers on first arch 9–14, on upper arch 2–6; total gill rakers on second arch 8–14; supraorbital pores 1–3, rarely 4–7; preopercular pores 5–8; lateral-line pores 76–100; sum of scales above and below lateral line 66–96; interorbital wide; blind side coloration in life creamy, without glossy highlights along margins of myotomes.

Larvae are distinguished from other species of *Lepidopsetta* by the following characters: body slender; snout-to-anus length long; larvae undergo hatching, flexion, and transformation at comparatively larger sizes; preflexion pigment pattern with light pigmentation along finfolds, limited mainly to the ventral finfold, and two pigment spots along the dorsal midline (the posteriormost aligning with a ventral patch forming a bar), a series of small melanophores extending from just posterior to the anus to just beyond the postanal bar (about 2/3 body); and flexion pigment pattern with a single bar located on the postanal body; pectoral-fin rays unpigmented.

Description of adults

Body ovate, greatest depth 41.2-58.9 (49.0)% SL, scales above lateral line 27–40, scales below lateral line 38–59; head relatively acute, length 21.8–31.5 (27.2)% SL; dorsal margin of head at dorsal-fin origin slightly concave, snout length 3.1–5.7 (4.4)% SL (12.1–20.1 (16.0)% HL); ocular-side maxilla length 20.4-31.5 (26.3)% HL; blind-side maxilla length 22.2–35.7 (28.7)% HL; ocular-side mandible length 34.4–50.0 (40.7)% HL; teeth 4–5 on ocular-side premaxilla, 23–24 on blind-side premaxilla and 8–9 on ocular-side dentary, 20–24 on blind-side dentary; gill rakers of first arch relatively slender, 9–14 total, 3–6 on upper arch, 6–9 on lower arch; gill rakers of second arch 8–14 total with 0–4 on upper and 7–13 on lower arch; dorsal orbit length often with posteriorly elongate rim and much longer than eye length, orbit length 22.2–32.9 (28.1)% HL, dorsal eye length 18.5–32.9 (23.0)% HL; ventral eye length 17.2–31.1 (24.2)% SL; interorbital wide, up to 5 scales at narrowest portion, 2.5–6.6 (4.4)% HL; cheek with 7–12 scales, length 26.7–38.5 (32.5)% HL, depth 13.6–22.7 (18.7)% HL; preopercular pores 5–8; ocular-side suborbital pores 13–29; blind-side suborbital pores 8–14; lateral line pores 76–100, lateral-line arch length 26.1–64.5 (52.3)% HL, its depth 26.3–38.2 (31.7)% its length; both anterior and posterior supratemporal branches relatively long, anterior pores 3–15, posterior pores 10–35; supraorbital canal short, reaching only to the posterior rim of the dorsal orbit at about the insertion of dorsal-fin rays 5–6, pores 1–3, rarely 4–7; ocular-side pectoral-fin length 10.7–18.2 (14.7)% SL (38.3–70.4 (53.9)% HL); blind-side pectoral-fin length 6.6–12.7 (10.2)% SL (24.2–49.6 (37.4)% HL); ocular-side pelvic-fin length 7.8–12.2 (9.9)% SL (27.6–45.9 (36.6)% HL); dorsal fin with 64–83 rays, height 10.2–16.6 (13.5)% SL, in specimens with 69–80 rays supported by 68–78 pterygiophores, typically 9 or rarely 8 anterior to first neural spine; anal fin with 49–64 rays, in specimens with 55–61 rays supported by 53–63 pterygiophores; caudal peduncle relatively slender, least depth 9.4–13.1 (10.9)% SL (32.2-48.8 (40.2)% HL, 101.2-144.2 (123)% caudal peduncle length), greatest depth 10.1–16.9 (12.3)% SL (38.1–57.7 (45.2)% HL); caudal peduncle length 7.0–10.1 (8.9)% SL (27.6–42.0 (32.7)% HL); caudal-fin length 17.8–29.1 (22.7)% SL. Vertebrae 39–41, with 10–11 precaudal and 29–30 caudal.

Scales around head and those scattered posteriorly on ocular side very rough, with columnar tubercles in large adults; strong spines in small adults and juveniles. Urogenital flap unpigmented or lightly pigmented in 23–80 mm juveniles.

In life, blind side in moderate to large adults creamy white, skin opaque (Amaoka et al., 1995, Fig. 525); in juveniles, blind side nearly completely translucent, with small, white glossy areas on head. When preserved, blind side of all individuals uniform creamy white to yellow-brown. Ocular

side slightly less green than that of congeneric in Puget Sound, often with faint yellow highlights around darker spots near bases of dorsal and anal fins and at midline.

Remaining description as for genus. Largest specimen examined 340 mm (427.5 mm TL) (UW 040265). Maximum size reported 588 mm (Fadeev, 1965) to 690 mm TL.[6]

Description of juveniles

Individuals of about 20 mm collected in water column (one 19.0-mm individual examined, UW 083482, not completely transformed; see comments); lateral line and pectoral-fin rays undeveloped; body pigmentation increasing throughout; bars and patches of postflexion larval pigmentation pattern visible; urogenital papilla light or speckled with an unpigmented tip. Eye length smaller, mouth larger, body deeper, gill-raker counts on lower arch higher, distance from pelvic-fin origin to anal-fin origin shorter, expanded anteriormost anal-fin pterygiophore less developed (not protruding beyond body wall in our material) than in similar-size *L. bilineata*.

By 35 mm, many individuals collected near bottom. Postsettlement juveniles (Fig. 22B) as developed as similar-size *L. bilineata*: increased body pigmentation giving juveniles a darker appearance (obscuring urogenital papillae pigment), rays of paired and median fins formed, lateral line formed, supraorbital pores present, expanded anteriormost anal-fin pterygiophore strongly developed.

Description of larvae

Snout-to-anus length 32.1–39.3% SL, remaining constant during development; body depth 3.8–28.5% SL, increasing with development, sharply increasing after flexion; head length 11.6–26.7% SL, increasing with development; snout length 22.8–24.7% HL, remaining constant during development; orbit length 51.8–20.9% HL, decreasing with development (Table 2). Total myomeres 38–42.

Larvae hatching at greater than 3.0 mm (3.6–4.0 mm, Pertseva-Ostroumova, 1961); yolk absorbed by 3.3–4.2 mm. Preflexion larvae ranging in size from 4.2 to 6.2 mm; flexion larvae, 6.2–12.6 mm; postflexion larvae, 12.2–18.6 mm. Transformation occurring at sizes as small as 15.0 mm; postsettlement stage usually not complete by 20.0 mm (Table 13).

Head pigment present initially along lower jaw and underside of chin (Fig. 23); increasing with development to snout, upper jaw, and isthmus. Pigment ventrally along gut and dorsally on anus; by flexion a distinct patch of melanophores along posterior edge of gut; pigment increasing laterally with development.

Postanal pigment light along the anal finfold, melanophores absent on dorsal finfold (Fig. 23); two pigment patches along the dorsal midline, anterior patch beginning about midbody at myomere 18–20, posterior patch beginning about myomere 30, posterior patch aligning with a ventral patch forming a postanal bar; series of melanophores along the ventral body midline beginning just posterior to the anus, extending to just beyond the postanal bar (about 2/3 body length); a few melanophores on caudal peduncle and above and below the notochord tip.

Distribution (Figs. 8, 11, 13, 24)

Ranging from the northern coast of Hokkaido throughout the Kuril Islands and the Okhotsk Sea of the western North Pacific, through the Bering Sea, from the Gulf of Anadyr[13] to off St. Lawrence Island (Allen and Smith, 1988), to Puget Sound, Washington, in the eastern North Pacific. Large concentrations have been reported from the west and southeast of the Kamchatka Peninsula, where it once composed 90% of the fisheries catches of pleuronectids (Shubnikov and Lisovenko, 1964), and from the southeastern Bering Sea. Minami and Nakamura (1978) also reported a single specimen of *L. bilineata* (=*L. polyxystra* n. sp. based on distribution) among many *L. mochigarei* from Wakasa Bay, Japan (ca. 35.7°N, 135.5°E); this specimen could not be located.[14] Larvae have been collected from Puget Sound, the east coast and northern tip of Vancouver Island, Hecate Strait, and north along the coasts of Alaska into the Bering Sea. According to Okiyama (1988), larvae occur along the coast of the Kuril Islands, the coast of Kamchatka, and into the Bering Sea.

The recorded locality of one adult (CAS 19305) from San Francisco Bay, over 1200 km south of the nearest verified capture in Puget Sound, is questionable. Although no evidence from catalog records[8] indicates that the specimen had been misplaced, the specimen was collected in 1888 and has an original catalog number from the Indiana University collection. Its morphology and meristics are distinctively that of more northerly populations.

Habitat

Lepidopsetta collected in the eastern Bering Sea are most commonly associated with sand, and least with "sand and mud," when compared with all other measured substrate types in the Bering Sea, including combinations of sand, gravel, and mud.[15] The maximum depth of collection was 246 m.[16] During the 22-year ichthyoplankton sampling period (all previously unidentified pleuronectid larvae were re-examined, thus providing the only historic distributional records for larvae of *L. polyxystra* n. sp.), larvae were common in spring surveys conducted in the Gulf of Alaska and Bering Sea, when they first appear in March collections; largest catches have been taken in May.

---

[13] Kessler, D. 1997. Personal commun. Under contract to Resource Assessment and Conservation Engineering Division, Alaska Fisheries Science Center, Natl. Mar. Fish. Serv., NOAA, 7600 Sand Point Way NE, Seattle, WA 98115.

[14] Saruwatari, T. 1997. Personal commun. Ocean Research Institute, University of Tokyo, Tokyo, Japan. Shinohara, G. 1997. Personal commun. Fish Section, Department of Zoology, National Science Museum (Natural History), Huankunin-cho, Shinjuku-ku, Tokyo, Japan.

[15] McConnaughey, R. 1997. Personal commun. Resource Assessment and Conservation Engineering Division, Alaska Fisheries Science Center, Natl. Mar. Fish. Serv., NOAA, 7600 Sand Point Way NE, Seattle, WA 98115.

[16] Resource Assessment and Conservation Engineering (RACE) Division. 1998. Unpubl. data from the RACE database. Alaska Fisheries Science Center, Natl. Mar. Fish. Serv., NOAA, 7600 Sand Point Way NE, Seattle, WA 98115.

Highest densities of larvae occur in the Bering Sea (Fig. 24), compared with the western Gulf of Alaska.

Life history

Lepidopsetta collected from the eastern Bering Sea and Sakhalin Island, presumed to be *L. polyxystra* n. sp., fed primarily on polychaetes and other marine worms; molluscs (Skalkin, 1959, 1963; Lang et al., 1995) or fishes, primarily *Ammodytes hexapterus* in depths >50 m (Lang et al., 1995), were a second significant component of the diet. Feeding took place primarily from May to September, falling to low levels during the winter (Shubnikov and Lisovenko, 1964) when spawning occurs (Fadeev, 1965). Spawning occurs in areas with good water circulation over hard bottoms of sand with gravel and peaks from early March to mid-April in waters off Kamchatka, possibly occurring as late as mid-June in the western Pacific (Pertseva-Ostroumova, 1961). Fecundity ranges from 151,700 to 404,200 eggs (Fadeev, 1965). Life history including spawning and development was discussed by Pertseva-Ostroumova (1961, as *L. bilineata bilineata*) and larval development was described by Okiyama (1988, as *L. bilineata*).

The Washington Department of Fisheries reported *Lepidopsetta* from late December through early March in sandy gravel of upper intertidal beaches at several sites in central and southern Puget Sound (Penttila, 1995). In January 1991, one beach site on the south shore of Dana Passage (the center of a relatively large area of documented *Lepidopsetta* spawning) was the source of six batches of field-collected spawned eggs (each about 1 mm in diameter) that were subsequently reared through hatching. We identified the reared larvae as *L. polyxystra* n. sp. Egg batches ranged in size from 40 to several hundred eggs and were incubated over about 14 days with ambient central Puget Sound water (about 9.0°C[3]). Larvae hatched between 4 and 5 mm and had yellow pigmentation associated with the melanophores. For additional early life history information, see generic account.

The maximum recorded age for female *L. polyxystra* n. sp. captured in the Bering Sea is 18 yr at 49 cm FL, and for males is 17 yr at 40 cm FL (Alton and Sample[17]). The gills of adults from the Gulf of Alaska have been found to be heavily infested with copepod parasites *Nectobrachia indivisa*, and *Naobranchia occidentalis*, previously recorded in *Lepidopsetta* by Kabata (1988). For both parasites, *L. polyxystra* n. sp. was significantly more heavily infested than *L. bilineata*.[7] The parasites *Acanthochondria vancouverensis* and *Haemobaphes* sp. were also recorded.

Etymology

The specific name *polyxystra* is derived from the Greek *poly*, meaning many, and *xystrus*, meaning raker, referring to the gill rakers being more numerous than those of congeneric species.

Comments

Under the name of *L. bilineata*, *L. polyxystra* n. sp. has been the subject of many studies. Work on specimens collected north of the extreme southeastern Bering Sea and west of the eastern Aleutian Islands in the western North Pacific may be presumed to be based on *L. polyxystra* n. sp. However, all studies conducted on specimens from the Gulf of Alaska into Puget Sound, regions of extensive overlap in the distributions of *L. polyxystra* n. sp. and *L. bilineata*, should be considered applicable at the generic level only, unless voucher specimens were collected and can be verified.

According to Pertseva-Ostroumova (1961), juveniles as small as 20 mm SL have been collected on the bottom. However, the species exhibits much plasticity in settling size, with specimens much greater than 20 mm SL routinely collected in plankton nets.

A widely published illustration identified as *L. bilineata* is based on a specimen of *L. polyxystra* n. sp. taken off Kodiak Island, Alaska ("St. Paul, Kodiak," USNM 27602), now badly damaged. First published in Goode (1884), it was subsequently reprinted in Jordan and Goss (1889), Jordan and Evermann (1900), Jordan and Starks (1906), and Evermann and Goldsborough (1907) among other publications.

Acknowledgments

Beverly Vinter first noticed an unidentified pleuronectid in our ichthyoplankton samples almost 15 years ago. With support from A. W. Kendall Jr., she persisted over the years in her belief that these larvae represented a new species of pleuronectid. We thank her for her insight as well as her identifications, illustrations, measurements, and numerous examinations of larvae. Early in our study, A. W. Kendall Jr. arranged for the collection of adults, the rearing of larvae (with D. Misitano, formerly of NWFSC), and electrophoretic analysis of samples (with F. Utter formerly of NWFSC). Helen Mulligan (first working at AFSC and later on contract to Humboldt State University) made several significant contributions to the study including a preliminary analysis of the geographic distribution of larval and adult *Lepidopsetta* that provided evidence supporting a taxonomic basis for the observed differences in larval shape and structure. Maryjane Cleveland, a domestic fisheries observer, provided detailed notes of her observations of *Lepidopsetta*, sparking independent early collections of adult samples. Other samples and data have been provided over the years by the AFSC's RACE Division (W. Flerx, G. R. Hoff, R. MacIntosh, G. Walters, and K. Weinberg), Resource Ecology and Fisheries Management Division's Observer Program (S. Barbeaux, M. Brown, S. Corey, K. Kruse, M. Loefflad, R. Narita, N. Raring, and K. Scott), and by the Alaska Department of Fish and Game (H. Sanborn and D. Urban). Biologists of the Washington Department of Fish and Wildlife, including W. A. Palsson, R. Pacunski, and G. Lippert, provided comparative photographs, specimens, and data for the Puget Sound. Jeff Marliave

[17] Alton, M. A., and T. Sample. 1976. Rock sole (family Pleuronectidae). *In* Demersal fish and shellfish resources of the eastern Bering Sea in the baseline year 1975 (W. T. Pereyra, J. E. Reeves, and R. G. Bakkala), p. 461–474. Northwest and Alaska Fish. Center Proc. Rep., Seattle, WA.

(Vancouver Public Aquarium) also provided Canadian larval material. Data on distribution and abundance of larvae and juveniles have been provided by H. G. Moser (SWFSC), W. Shaw (DFO, PBS), B. L. Norcross, A. A. Abookire, and B. Holladay (UA, Fairbanks), and D. Penttila (WDF). Several scientists at AFSC assisted throughout this study: D. M. Blood and M. S. Busby (collections at sea and technical assistance), L. Ciannelli (measurements), K. Mier (statistical analyses), S. Picquelle (mapping software and CPUE calculations), R. C. Harrison (translations), and W. Rugen (database support). For discussions on pleuronectid characters, osteology, and phylogeny, we thank J. A. Cooper and P. Berendzen. The following curators and collection managers generously provided loans and information on specimens under their care: D. Catania (CAS), W. G. Saul (ANSP), B. A. Brown (AMNH), R. F. Feeney and J. Seigel (LACM), J. D. McPhail, G. Haas, and E. Keeley (UBC), D. F. Markle (OS), B. Sheiko (KIE), T. W. Pietsch and B. K. Urbain (UWFC), S. Jewett and S. J. Raredon (NMNH), R. H. Rosenblatt, H. J. Walker, and C. Klepadlo (SIO), K. Amaoka (HUMZ), G. Shinohara (NSMT), I. Kinoshita (FRSKU), T. Minami (Japan Sea National Fisheries Institute), and B. L. Wing (ABL). We thank the following individuals for their reviews of the manuscript: T. W. Pietsch, W. Aron, G. R. Hoff, M. S. Busby, A. W. Kendall Jr., C. W. Mecklenburg, E. S. Brown, and H. H. Zenger.

Literature cited

Ahlstrom, E. H., K. Amaoka, D. A. Hensley, H. G. Moser, and B. Y. Sumida.
1984. Pleuronectiformes: Development. *In* Ontogeny and systematics of fishes (H. G. Moser, W. J. Richards, D. M. Cohen, M. P. Fahay, A. W. Kendall Jr., and S. L. Richardson, eds.), p. 640–670. Am. Soc. Ichthy. Herpet. Spec. Publ. 1.

Allen, M. J., and G. B. Smith.
1988. Atlas and zoogeography of common fishes in the Bering Sea and northeastern Pacific. U.S. Dep. Commer., NOAA Tech. Rep., NMFS 66, 151 p.

Amaoka, K., K. Nakaya, and M. Yabe.
1995. The fishes of northern Japan. Kitanihon Kaiyo Center Co., Sapporo, Hokkaido, 387 p.

Amaoka, K., K. Nakaya, and H. Yamamoto.
1983. Fishes and marine algae of northern Japan. Kitanihon Kaiyo Center Co., Sapporo, Hokkaido, 371 p.

Ayres, W. O.
1855a. [Description of new fishes from California.] The Pacific 4(18).
1855b. [Description of a new flounder.] Proc. Calif. Acad. Sci. 1:39–40.

Berendzen, P. B.
1998. Phylogenetic analysis of the order Pleuronectiformes using molecular and morphological evidence. M.S. thesis, Univ. Kansas, Lawrence, KS, 61 p.

Blackburn, J. E.
1973. A survey of the abundance, distribution, and factors affecting distribution of ichthyoplankton in Skagit Bay. M.S. thesis, Univ. Washington, Seattle, WA, 136 p.

Busby, M. S., A. C. Matarese, and K. L. Mier.
2000. Annual, seasonal, and diel composition of larval and juvenile fishes collected by dip-net in Clam Bay, Puget Sound, Washington, from 1985 to 1995. U.S. Dep. Commer., NOAA Tech. Memo. NMFS-AFSC-111, 36 p.

Chapleau, F.
1993. Pleuronectiform relationships: a cladistic reassessment. Bull. Mar. Sci. 52(1):516–540.

Charter, S. R., and H. G. Moser.
1996. Pleuronectidae: righteye flounders. *In* The early stages of fishes in the California Current Region (H. G. Moser, ed.), p. 1369–1403. CalCOFI Atlas 33.

Cooper, J., and F. Chapleau.
1996. The monophyletic status of *Pleuronectes* (Pleuronectidae: Pleuronectiformes). *In* Abstracts of the 1996 Annual Meeting of the American Society of Ichthyologists and Herpetologists, New Orleans, LA, p. 114.
1998. Monophyly and intrarelationships of the family Pleuronectidae (Pleuronectiformes), with a revised classification. Fish. Bull. 96:686–726.

Cope, E. D.
1873. A contribution to the ichthyology of Alaska. Proc. Am. Phil. Soc. 13:24–32.

Environmental Systems Research Institute.
1996. Arcview GIS, ver. 3.0. Environmental Systems Research Institute, Redlands, CA, 614 p.

Evermann, B. W., and E. L. Goldsborough.
1907. The fishes of Alaska. Bull. Bur. Fish. 26:219–360.

Fadeev, N. S.
1965. Comparative outline of the biology of flatfishes in the southeastern part of the Bering Sea and condition of their resources. Soviet Fisheries Investigations in the northeast Pacific, Part 4. Pacific Scientific Research Institute of Marine Fisheries and Oceanography (TINRO). Izvestiya 58:112–129. [1968 transl. by Israel Prog. Sci. Transl.]

Forrester, C. R.
1969. Life history information on some groundfish species. Fish. Res. Board Can. Tech. Rep. 105, 17 p.

Forrester, C. R., and J. A. Thompson.
1969. Population studies on the rock sole (*Lepidopsetta bilineata* (Ayres)) of northern Hecate Strait, B.C. Fish. Res. Board Can., Tech. Rep. 108, 104 p.

Garrison, K. J., and B. S. Miller.
1982. Review of the early life history of Puget Sound fishes. Report FRI-UW-8216 of the Fish. Res. Inst., Univ. Washington, Seattle, WA, 729 p.

Gill, T. N.
1862. Note on some genera of fishes of western North America. Proc. Acad. Nat. Sci. Phila. 14:329–332.
1864. Synopsis of the pleuronectoids of California and northwestern America. Proc. Acad. Nat. Sci. Phila. 16:194–198.

Girard, C. F.
1854. Descriptions of new fishes, collected by Dr. A. L. Heermann, naturalist attached to the survey of the Pacific railroad route, under Lieut. R. S. Williamson, U.S.A. Proc. Acad. Nat. Sci. Phila. 7:129–140.
1856. Contributions to the ichthyology of the western coast of the United States, from specimens in the collection of the Smithsonian Institution. Proc. Acad. Nat. Sci. Phila. 8:131–137.

Goode, G. B.
1884. The fisheries and fishery industries of the United States. Section I. Natural history of useful aquatic animals with an atlas of two hundred and seventy-seven plates. Plates. Government Printing Office, Washington, D.C., 215 p.

Günther, A.
1862. Catalogue of the fishes in the British Museum. Catalogue of the Acanthopterygii Pharyngognathi and Anacanthini in the collection of the British Museum, vol. 4, 534 p.

Hart, J. L.
1973. Pacific fishes of Canada. Bull. Fish. Res. Board Can. 180, 740 p.

Hickman, C. P., Jr.
1959. The larval development of the sand sole (*Psettichthys melanostictus*). Wash. Dep. Fish. Res. Pap. 2:38–47.
Hubbs, C. L.
1915. Flounders and soles from Japan collected by the United States Bureau of Fisheries steamer "*Albatross*" in 1906. Proc. U.S. Natl. Mus. 48:449–496.
Hubbs, C. L., and K. F. Lagler.
1958. Fishes of the Great Lakes region. Cranbrook Inst. Sci., Ann Arbor, MI, 213 p.
Ivankov, V. N.
1996. Review of the book by G. U. Lindberg and V. V. Fedorov, The fishes of the Sea of Japan and adjacent parts of the Sea of Okhotsk and the Yellow Sea. Part 6. Teleostomi, Osteichthyes, Actinopterygii. XXXI. Pleuronectiformes—Family Psettodidae—CCICFamily Cynoglossidae. J. Ichthyol. 36(7):549–550. [Transl. by P. A. Aleinikov.]
Jordan, D. S., and B. W. Evermann.
1898. The fishes of North and Middle America: a descriptive catalogue of the species of fish-like vertebrates found in the waters of North America, north of the Isthmus of Panama. Part III. Bull. U.S. Natl. Mus. 47:2183–3136.
1900. The fishes of North and Middle America: a descriptive catalogue of the species of fish-like vertebrates found in the waters of North America, north of the Isthmus of Panama. Part IV. Bull. U.S. Natl. Mus. 47:3137–3313.
Jordan, D. S., and C. H. Gilbert.
1881. List of the fishes of the Pacific Coast of the United States, with a table showing the distribution of the species. Proc. U.S. Natl. Mus. 3:452–458.
Jordan, D. S., and D. K. Goss.
1889. A review of the flounders and soles (Pleuronectidae) of America and Europe. Rep. U.S. Fish Comm. 14:225–342.
Jordan, D. S., and C. L. Hubbs.
1925. Record of fishes obtained by David Starr Jordan in Japan, 1922. Mem. Ann. Carnegie Mus. 10(2):93–346.
Jordan, D. S., and E. C. Starks.
1906. A review of the flounders and soles of Japan. Proc. U.S. Natl. Mus. 31(1484):161–246.
Kabata, Z.
1988. Copepoda and Branchiura. *In* Guide to the parasites of fishes of Canada, part II— Crustacea (L. Margolis and Z. Kabata, eds.), p. 3–127. Can. Spec. Publ. Fish. Aquat. Sci. 101.
Kendall, A. W., Jr., E. H. Ahlstrom, and H. G. Moser.
1984. Early life history stages of fishes and their characters. *In* Ontogeny and systematics of fishes (H. G. Moser, W. J. Richards, D. M. Cohen, M. P. Fahay, A. W. Kendall Jr., and S. L. Richardson, eds.), p. 11–22. Am. Soc. Ichthy. Herpet. Spec. Publ. 1.
Kim, I. S., and C. H. Youn.
1994. Taxonomic revision of the flounders (Pisces: Pleuronectiformes) from Korea. Korean J. Ichthy. 6(2):99–131.
Kravitz, M., W. G. Pearcy, and M. P. Guin.
1976. Food of five species of co-occurring flatfishes on Oregon's continental shelf. Fish. Bull. 74:984–990.
Lang, G. M., P. A. Livingston, and B. S. Miller.
1995. Food habits of three congeneric flatfishes: yellowfin sole (*Pleuronectes asper*), rock sole (*P. bilineatus*), and Alaska plaice (*P. quadrituberculatus*) in the eastern Bering Sea. Proc. InterNatl. Symp. N. Pac. Flatfish, Alaska Sea Grant Prog. Report AK-SG-95-04, p. 225–245.
Levings, C. D.
1967. A comparison of growth rates of the rock sole (*Lepidopsetta bilineata*) Ayres, in northeast Pacific waters. Fish. Res. Board Can., Tech. Rep. 36, 43 p.
Leviton, A. E., and M. L. Aldrich.
1997. Theodore Henry Hittell's "The California Academy of Sciences, a narrative history: 1853–1906." Calif. Acad. Sci., San Francisco, CA, 623 p.
Leviton, A. E., and R. H. Gibbs Jr.
1988. Standards in herpetology and ichthyology. Standard symbolic codes for institutional resource collections in herpetology and ichthyology. Suppl. 1: additions and corrections. Copeia 1988:280–282.
Leviton, A. E., R. H. Gibbs Jr., E. Heal, and C. E. Dawson.
1985. Standards in herpetology and ichthyology: part I. Standard symbolic codes for institutional resource collections in herpetology and ichthyology. Copeia 1985:802–832.
Lindberg, G. U., and V. V. Fedorov.
1993. The fishes of the Sea of Japan and adjacent parts of the Sea of Okhotsk and the Yellow Sea. Part 6. Teleostomi, Osteichthyes, Actinopterygii. XXXI. Pleuronectiformes—Family Pleuronectidae. Zool. Inst. Rossiiskoi Akad. Nauk, 271 p.
Lockington, W. N.
1879a. The flounders of our markets, No. 2. Mining and Scientific Press 39(4):70.
1879b. Review of the Pleuronectidae of San Francisco. Proc. U.S. Natl. Mus. 2:69–108.
1880a. Note on a new flat-fish (*Lepidopsetta isolepis*) found in the markets of San Francisco. Proc. U.S. Natl. Mus. 3:325.
1880b. Notes on new and rare fishes of the Pacific Coast. Am. Nat. 14:595–600.
1883. *Isopsetta isolepis*. *In* 1883 synopsis of the fishes of North America (D. S. Jordan and C. H. Gilbert, eds.), p. 1–1018. Bull. U. S. Natl. Mus. 16.
Manugistics.
1997. Statgraphics plus 2.1. Manugistics, Inc., Rockville, MD, 882 p.
Masutomi, K., and T. Hamada.
1966. Fossils in colour. Hoikusha Publishing Co., Osaka, 268 p. [Not seen; cited in Sakamoto and Uyeno (1988).]
Matarese, A. C., A. W. Kendall Jr., D. M. Blood, and B. M. Vinter.
1989. Laboratory guide to early life history stages of northeast Pacific fishes. U.S. Dep. Commer., NOAA Tech. Rep., NMFS 80, 652 p.
Minami, T.
1995. Spawning season of pleuronectid flatfishes in the coastal waters of Hokkaido, Japan [Review]. Bull. Hokkaido Natl. Fish. Res. Inst. 59:69–80.
Minami, T., and I. Nakamura.
1978. Seasonal occurrence of pelagic stages of flatfishes in the coastal waters of western Wakasa Bay. Mem. Coll. Agriculture, Kyoto Univ. 112:29–47.
Moiseev, P. A.
1953. [Cod and flounders of Far-Eastern Seas.] Izv. Tikhook. N.-I. Inst. Rybn.-Khoz. I Okeanogr. 40:1–287. Fish. Res. Board Can. Transl. 119.]
Moser, H. G., W. J. Richards, D. M. Cohen, M. P. Fahay, A. W. Kendall Jr., and S. L. Richardson, eds.
1984. Ontogeny and systematics of fishes. Am. Soc. Ichthy. Herpet. Spec. Publ. 1, 760 p.
Moser, H. G., R. L. Charter, P. E. Smith, D. A. Ambrose, S. R. Charter, C. A. Meyer, E. M. Sandknop, and W. Watson.
1993. Distributional atlas of fish eggs and larvae in the California Current region: taxa with 1000 or more total larvae, 1951 through 1984. CalCOFI Atlas 31, 233 p.
Mulligan, H. L., A. W. Kendall Jr., and A. C. Matarese.
1995. The significance of morphological variation in adults and larvae of the rock sole, *Pleuronectes bilineatus*, from the Bering Sea and northeastern Pacific Ocean. Proc. Int.

Symp. N. Pac. Flatfish, Alaska Sea Grant Coll. Prog. Report AK-SG-95-04, p. 133–150.

NMFS (National Marine Fisheries Service).
1999. Our living oceans: report on the status of U.S. living marine resources, 1999. U.S. Dep. Commer., NOAA Tech. Memo. NMFS-F/SPO-41, 301 p.

Nelson, J. S.
1994. Fishes of the world, 3rd ed. Wiley & Sons, New York, NY, 600 p.

Nikiforov, S. N., S. N. Safronov, and N. S. Fadeev.
1983. Distinguishing characters of rock sole, *Lepidopsetta bilineata*, and mochigar sole, *L. mochigarei* (Pleuronectidae). J. Ichthyol. 23:36–44.

Norman, J. R.
1934. A systematic monograph of the flatfishes (Heterosomata). Brit. Mus. Nat. Hist. 1:1–459.

Okada, Y.
1955. Fishes of Japan, illustrations and descriptions of fishes of Japan. Maruzen Co., Tokyo, 434 p.

Okiyama, M., ed.
1988. An atlas of the early stages of fishes in Japan. Tokai Univ. Press, Tokyo, 1154 p. [In Japanese.]

Okiyama, M., and K. Takahashi.
1976. Larval stages of right eye flounders (subfamily Pleuronectinae) occurring in Japan Sea. Bull. Japan. Sea. Reg. Fish. Res. Lab. 27:11–34.

Penttila, D. E.
1995. The WDFW's Puget Sound intertidal baitfish spawning beach survey project. *In* Puget Sound Research 95 Proceedings, vol. 1, Jan. 12–14, 1995, p. 235–241.

Pertseva-Ostroumova, T. A.
1961. The reproduction and development of far eastern flounders. Tr. Inst. Okeanol. Akad. Nauk SSR. [In Russian; English transl., Fish. Res. Board Can., Transl. Serv. 856, 1967.]

Poss, S. G., and B. B. Collette.
1995. Second survey of fish collections in the United States and Canada. Copeia 1995:48–70.

Rass, T. S.
1996. On taxonomy of Pleuronectini (Pleuronectidae). J. Ichthyol. 36:546–548.

Sakamoto, K.
1984a. Interrelationships of the family Pleuronectidae (Pisces: Pleuronectiformes). Mem. Fac. Fish., Hokkaido Univ. 31(1/2):95–215.
1984b. Pleuronectidae. *In* The fishes of the Japanese Archipelago (H. D. Masuda, K. Amaoka, C. Araga, T. Uyeno, and T. Yoshino, eds.), p. 351–354. Tokai Univ. Press, Tokyo, Japan.

Sakamoto, K., and T. Uyeno.
1988. A new righteye flounder from the late Pleistocene Togane Formation, Chiba Prefecture, Japan. Bull. Nat. Sci. Mus., Tokyo, ser. C, 14(3):135–142.

Schmidt, P. Y.
1950. Fishes of the Sea of Okhotsk. Academy of Sciences of the USSR, Transactions of the Pacific Committee, vol. 6, Moscow-Leningrad, 392 p. [In Russian, 1965 transl. by Israel Prog. Sci. Trans. Available from the National Technical Information Service, Springfield, VA.]

Shubnikov, D. A., and L. A. Lisovenko.
1964. Data on the biology of rock sole of the southeastern Bering Sea. Soviet Fisheries Investigations in the northeast Pacific, Part 2. Pacific Scientific Research Institute of Marine Fisheries and Oceanography (TINRO). Izvestiya 49:220–226. [1968 transl. by Israel Prog. Sci. Transl.]

Shvetsov, F. C.
1979. Reproduction of the flounder *Lepidopsetta bilineata* *bilineata*, off the Okhotsk Sea coast near Paramoshiro and Shumushu Islands. J. Ichthyol. 19(5):61–62.

Skalkin, V. A.
1959. [Diet and food relations of flatfish on the Il'inskii Shoal.] Pacific Scientific Research Institute of Marine Fisheries and Oceanography (TINRO). Izvestiya 47. [In Russian; cited by Skalkin, 1963.]
1963. Diet of flatfishes in the southeastern Bering Sea. Soviet Fisheries Investigations in the Northeast Pacific, Part 1. Pacific Scientific Research Institute of Marine Fisheries and Oceanography (TINRO). Izvestiya 50:235–250. [1968 transl. by Israel Prog. Sci. Transl.]

Smith, R. T.
1936. Report on the Puget Sound otter trawl investigations. Wash. Dept. Fish. Biol. Rep. 36B:1–61.

Snyder, J. O.
1911. Descriptions of new genera and species of fishes from Japan and Riu Kiu Islands. Proc. U.S. Natl. Mus. 40:525–549.
1912. Japanese shore fishes collected by the United States Bureau of Fisheries Steamer "*Albatross*" expedition of 1906. Proc. U.S. Natl. Mus. 42:437–441.

Sokal, R. R., and F. J. Rohlf.
1995. Biometry, 3rd ed. W. H. Freeman and Co., New York, NY, 859 p.

Springer, V., and M. E. Anderson.
1998. Catalog of type specimens of recent fishes in the National Museum of Natural History, 8: Suborder Zoarcoidei (Anarhichadidae, Bathymasteridae, Pholidae, Ptilichthyidae, Scytalinidae, Stichaeidae, Zoarcidae). Smiths. Contr. Zool. 589, 27 p.

SPSS, Inc.
1996. SYSTAT for Windows, version 6.0. SPSS, Inc., Chicago, IL, 751 p.

Statistical Sciences.
1993. S-Plus for Windows, version 3.3. Statistical Sciences, Seattle, WA, 819 p.

Stauffer, J. R., Jr., and E. Hert.
1992. *Pseudotropheus callainos*, a new species of mbuna (Cichlidae), with analyses of changes associated with two intra-lacustrine transplantations in Lake Malawi, Africa. Ichthyol. Explor. Freshwaters 3:253–264.

Taranets, A. J.
1937. Handbook for identification of fishes of the Soviet Far East and adjacent waters. Bull. Pac. Sci. Fish. Inst. Vladivostok. 11:1–200+map.

Townsend, L. D.
1936. Variations in the meristic characters of flounders from the northeastern Pacific. Rep. Intern. Fish. Comm. 11:1–24.
1937. Geographical variation and correlation in Pacific flounders. Copeia 1937:92–103.

Wilimovsky, N. J., A. Peden, and J. Peppar.
1967. Systematics of six demersal fishes of the North Pacific Ocean. Fish. Res. Board Can. Tech. Rep. 34, 95 p.

Yusa, T.
1957. Eggs and larvae of flatfishes in the coastal waters of Hokkaido. II. Early development of the flatfish (*Lepidopsetta mochigarei* Snyder). Bull. Hokkaido Reg. Fish. Res. Lab. 15(2):15–21.
1958. Eggs and larvae of flatfishes in the coastal waters of Hokkaido. II. Post-embryonic development and larvae of the flatfish *Lepidopsetta mochigarei* Snyder. Bull. Hokkaido Reg. Fish. Res. Lab. 18:1–10.

Appendix Table 1

Summary of Alaska Fisheries Science Center cruises with positive tows for larvae of *Lepidopsetta* (1971–72, 1977–94). Cruises in boldface were not used in calculations of mean density. BS = Bering Sea; GA = Gulf of Alaska; WA = Washington. Bongo = bongo net of 60 cm diameter, 0.505-mm mesh (larvae were occasionally collected using alternative frame sizes, including 20-cm net diameter and 0.333-mm mesh, but these collections were not used for abundance calculations); Meth = Methot trawl net of 5-m2 frame (2 × 3 mm oval mesh); Tuck = Tucker trawl net of 1-m frame and 0.505-mm mesh.

						Total occurrences	
Year	Cruises	Region	Month	Gear[1]	Total stations	*L. polyxystra* n. sp.	*L. bilineata*
1971	**4DE71**	**BS**	**Jul–Aug**	**bongo**	**10**	**8**[2]	**0**
1972	2KE72	GA	Apr–May	bongo	67	27	0
1977	**MF77B-5,6**	**BS**	**Apr–May**	**bongo**	**75**	**35**	**0**
	9SEI77	**GA**	**Jul**	**bongo**	**99**	**0**	**1**[2]
1978	4DI78	GA	Mar–Apr	bongo,Tuck	225	80	0
	2MF78	GA	Jun–Jul	bongo,Tuck	267	41	66
	3MF78	GA	Sep	bongo	26	1	1
	4MF78	GA	Sep–Oct	bongo	66	2	0
	5MF78	GA	Oct–Nov	bongo	19	0	1
1979	1PO79	GA	Sep	bongo	18	0	1
	3MF79	BS	Jun–Jul	bongo, Tuck	271	35	0
	5TK79	GA	May	bongo	58	15	3
1980	**1MF80**	**BS**	**Jan–Feb**	**bongo**	**8**	**2**[2]	**0**
1981	**1PO81**	**WA**	**May–Jun**	**bongo**	**131**	**0**	**1**
	1SH81	GA	Mar	bongo	131	4	0
	2MF81	GA	Mar–Apr	bongo	89	1	0
	2SH81	GA	Apr	bongo	60	31	2
	3MF81	GA	Apr–May	bongo	79	37	2
	3SH81	GA	May	bongo	57	37	10
	4MF81	GA	May	bongo	80	52	8
1982	1DA82	GA	Apr	bongo	83	20	0
	2DA82	GA	May	bongo	62	29	1
1983	1CH83	GA	May	bongo	70	19	5
	1EQ83	**WA**	**Apr–May**	**bongo**	**124**	**0**	**1**
1984	1SH84	GA	Apr–May	bongo	157	22	1
1985	1PO85	GA	Mar–Apr	bongo	154	37	0
	2MF85	GA	May	bongo	62	4	0
	2PO85	GA	May–Jun	bongo	189	52	17
1986	1GI86	GA	Apr	bongo	149	53	0
	1MF86	GA	Apr	bongo	80	4	0
	2MF86	GA	May	bongo	107	53	0
1987	1BB87	GA	Mar–Apr	bongo	117	12	1
	2MF87	GA	Apr	bongo	142	9	0
	3MF87	GA	May	bongo	60	14	8
1988	1DN88	BS and GA	Mar–May	bongo	203	17	0
	1MF88	GA	Apr	bongo,Tuck	196	51	0
	2MF88	GA	Apr–May	bongo,Meth,Tuck	84	41	1
	3MF88	GA	May	bongo	13	2	0
	4MF88	GA	May–Jun	bongo,Meth,Tuck	209	69	75
1989	1MF89	GA	Apr	bongo,Tuck	140	21	0
	2MF89	GA	Apr–May	bongo,Tuck	107	55	1
	3MF89	GA	May	bongo,Meth,Tuck	221	127	2
	4MF89	GA	May–Jun	Tuck	95	87	9

Continued

Appendix Table 1 (continued)

Year	Cruises	Region	Month	Gear[1]	Total stations	Total occurrences	
						L. polyxystra n. sp.	*L. bilineata*
1990	1MF90	GA	Apr	bongo	107	17	0
	2MF90	GA	May	bongo,Tuck	92	52	2
	3MF90	GA	May	bongo	17	9	0
	4MF90	GA	May–Jun	bongo	130	83	21
1991	1MF91	GA	Apr	bongo,Tuck	98	5	0
	2MF91	GA	Apr	bongo,Tuck	156	24	0
	3MF91	GA	May	bongo	119	28	0
	4MF91	GA	May	bongo	98	19	8
	5MF91	WGA	July	Meth	62	40	12
1992	1MF92	GA	Apr	bongo,Tuck	103	7	0
	1MM92	BS and GA	Jul	Meth	11	3	2
	3MF92	GA	May	bongo,Tuck	188	59	7
	4MF92	GA	May	bongo, Meth,Tuck	154	46	31
1993	2MF93	GA	Apr	bongo, Meth,Tuck	135	12	0
	3MF93	BS	Apr	bongo,Tuck	135	21	0
	4MF93	GA	May	bongo, Meth,Tuck	168	44	7
	5MF93	GA	May–Jun	bongo,Meth	119	25	22
	6MF93	GA	Sep	Tuck	24	0	2
1994	3MF94	GA	Mar–Apr	bongo, Tuck	49	2	0
	4MF94	BS	Apr	bongo,Tuck	144	37	0

[1] Although larvae of *Lepidopsetta* were collected in neuston and Mocness tows (see "Material examined" section), these collections were not used for abundance calculations and are not listed here.

[2] Total occurrences for these cruises represent the minimum number collected. Complete records for these cruises are unavailable at this time.

An alternative method for estimating bycatch from the U.S. shrimp trawl fishery in the Gulf of Mexico, 1972–1995

Mauricio Ortiz

Christopher M. Legault

Nelson M. Ehrhardt

Division of Marine Biology and Fisheries
Rosenstiel School of Marine and Atmospheric Sciences
University of Miami
4600 Rickenbacker Causeway
Miami, Florida 33149
Present address (for M. Ortiz): Miami Laboratory
Southeast Fisheries Science Center
National Marine Fisheries Service, NOAA
75 Virginia Beach Dr., Miami, Florida 33149

E-mail address (for M. Ortiz): mauricio.ortiz@noaa.gov

Abstract.–Finfish bycatch taken by the U.S. Gulf of Mexico shrimp fishery is an important issue in the management of fisheries resources given the perceived high mortality of the different fish stocks taken as bycatch in the region. Bycatch data are characterized by a high number of low catches, a few high catches, and depending on the finfish species, a significant proportion of observations with zero bycatch. An evaluation of the current general linear model for generating bycatch estimates indicates that the bycatch data do not conform to the assumptions of this model because bycatch estimates depend upon choices within the model that can significantly change the results of the model. These choices include the constant value added to catch-per-unit-of-effort (CPUE) values prior to the logarithmic transformation (to avoid undefined logarithms with zero CPUEs) and the standard time-unit selection for calculating CPUE values from catch in numbers and variable tow times. Currently a value of one is added to observed CPUE, and a constant time unit of one hour has been used; however, these choices are somewhat arbitrary.

An alternative approach to model bycatch data is to use a delta distribution that has two components. Component one models the proportion of zeros, and component two models the positive catches. In our study, we applied the delta lognormal model to estimate finfish bycatch in the shrimp fishery. This model avoids the problems of 1) the addition of a constant positive value to log-transformed CPUEs, and 2) the selection of a standard time unit for CPUE calculations. Bycatch estimates determined with the current general linear model were compared with those determined with the delta lognormal model for Atlantic croaker (*Micropogonias undulatus*), red snapper (*Lutjanus campechanus*), Spanish mackerel (*Scomberomorus maculatus*), and all finfish from 1972 through 1995. Analysis and evaluation of the performance of the delta lognormal model indicated that this model fits the bycatch database better than the current general linear model.

Manuscript accepted 10 January 2000.
Fish. Bull. 98:583–599 (2000).

In recent years shrimp bycatch has become one of the most important issues in fishery management in the southeastern United States, including the U.S. Gulf of Mexico. In 1990, the U.S. Congress requested a 3-year research program to assess the impact of bycatch by the shrimp fishery on federally managed fishery resources along the south Atlantic and the U.S. Gulf of Mexico coasts (Public Law 101-627, sec110c[1]). As a result, the National Marine Fisheries Service (NMFS) created the Cooperative Shrimp Bycatch Characterization Project (NOAA[1]), a four-year program which focused on 1) characterizing onboard shrimp trawl bycatch, 2) developing and testing bycatch reduction devices (BRDs), and 3) evaluating alternative bycatch management options. Among the major objectives identified in this project were those of updating and expanding temporal and spatial bycatch estimates (offshore and inshore waters) (NOAA[1]).

Since 1987, the NMFS has provided bycatch estimates for several finfish species in the Gulf of Mexico by using a catch-per-unit-of-effort (CPUE) method, where bycatch CPUEs are estimated following a general linear approach (Nichols et al.[2]). Briefly, a bycatch CPUE rate is estimated for each fish species by year (1972–95), area, season, and depth-zone stratum. These bycatch CPUEs are multiplied by an estimated annual shrimping effort within the stratum, and the total annual bycatch is the sum of the bycatch for each stratum. To estimate bycatch, the sample unit is defined as the number of fish of a given species caught each net-hour during a tow. The current general linear model was evaluated by considering two main topics: 1) the assumptions entailed with using the model and the theoretical basis for generating the estimates, and 2) the appropriateness of the available data to the configuration and analysis of the model. More specifically, we examined the matrix structure used in the general linear model, the logarithm usage in the general linear model, and the standardization of effort in the CPUE's in the current general linear model.

[1] NOAA. 1995. Cooperative research program addressing finfish bycatch in the Gulf of Mexico and South Atlantic shrimp fisheries: a report to congress. National Marine Fisheries Service Southeast Regional Office, 9721 Executive Center Dr. N., St. Petersburg, FL 33702.

[2] Nichols S., A. Shah, G. J. Pellegrin, and K. Mullin. 1987. Estimates of annual shrimp fleet bycatch for thirteen finfish species in the offshore waters of the Gulf of Mexico. Report to the Gulf of Mexico Fishery Management Council. The Commons at Rivergate, 3018 U.S. Highway 301 N., Tampa, FL 33619.

Procedure for estimating bycatch with the general linear model

In the bycatch estimation procedure with CPUE, it is assumed that the estimated annual shrimping effort is known and no variance is associated with this value. Therefore, we restricted our evaluation to the general linear model method to estimate the bycatch rates (CPUE) within each stratum. The general linear model is defined for each bycatch species by Nichols et al. (1987[2]) as

$$\text{Log}_{10}(CPUE + 1)_{ijklm} = mean + dataset_i + year_j + season_k + area_l + depth_m + \varepsilon_{ijklm}, \quad (1)$$

where CPUE = the catch in numbers per trawl for each hour of shrimp fishing;
mean = the overall mean;
dataset (i) = a fixed effect term differentiating commercial shrimp fishing from research trawls; and
the terms *year (j)*, *season (k)*, *area (l)*, and *depth (m)* = also fixed-effect terms characterizing the spatiotemporal variability of shrimp bycatch.

This model assumes that the error terms are random, independent, and normally distributed, with equal variance throughout. Predicted catch per trawl net for each hour of shrimp fishing is then estimated for each stratum for the commercial shrimp fishery as

$$CPUE = 10^{\hat{Y} + 1.1513 \times RMS/1} - 1, \quad (2)$$

where $\hat{Y}$ = the general linear model predicted $\log_{10}$ *(CPUE+1)*; and
RMS = the residual mean square from the general linear model.

The *RMS* term is required to estimate the arithmetic mean from the geometric mean of the assumed lognormal distribution. The constant 1.1513 is a correction factor for estimations derived with log base 10 instead of the natural log.

The predicted CPUE in each stratum is then multiplied by the estimated shrimping effort in the corresponding stratum. CPUEs are estimated for each trawl net. An average of two trawl nets per commercial shrimp vessel for the 1972–95 time series is assumed owing to the lack of information on number of nets per boat for each stratum (cell in the matrix configuration) or other grouping category. Total annual bycatch estimates for a given species are then simply the sum of the commercial bycatch (i=1) in all strata for that year (j) as

$$Bycatch_j = 2 \times \sum_{klm} CPUE_{1jklm} \times f_{jklm}, \quad (3)$$

where f_{jklm} = the estimated total shrimping effort (hours of fishing) for year j, area k, season l, and depth zone m.

The general linear model estimates an approximate variance for the arithmetic mean CPUE for each cell as

$$\left(10^{2/\hat{Y} + 1.15 \times RMS/+2.3/S^2_{\hat{Y}} + 2.65 \times RMS^2/rdf/}\right)\left(10^{2.3/S^2_{\hat{Y}} + 2.65 \times RMS^2/rdf/} - 1\right),$$

where $\hat{Y}$ and *RMS* = the predicted $\log_{10}$ *(CPUE+1)* and the residual mean square respectively;
$S^2_{\hat{Y}}$ = the estimate of variance of the predicted $\log_{10}$ *(CPUE+1)* for the cell; and
rdf = the residual degrees of freedom.

No variance estimates for the estimated shrimping effort are included in this model; thus effort is considered as if it were known exactly (Nichols et al.[2]).

The database for estimating shrimp bycatch CPUEs was derived from information collected in several projects. The current database comprises two types of data sources: 1) direct measurements of finfish catch by observers onboard of commercial shrimp vessels, and 2) catch rates from research surveys. Direct observations came from four main programs: the Sea Turtle Incidental Catch and Mortality Project (Henwood and Stuntz, 1987), the Excluder Trawl Device Evaluation Project (Henwood and Stuntz, 1987), the Shrimp Fleet Discards Project (Pellegrin, 1982), and the Cooperative Shrimp Bycatch Characterization Project (NOAA[1]). Direct observations were discontinuous in time and space; in particular, no onboard commercial vessels observations occurred between 1982 and 1991. Research observations came primarily from two annual trawling projects: the Fall Groundfish Surveys and the Summer SEAMAP Program. With over 22,000 tows documented from 1972 through 1995, research observations were the main source of the bycatch database. Research observations were restricted to tow surveys with the RV *Oregon II* equipped with a standard 40-ft shrimp trawl (Nichols et al.[3]).

For estimating bycatch, the U.S. Gulf of Mexico was divided into four geographic areas, two depth zones, and three seasons. Area 1 covered the Texas coastline, area 2 covered the Louisiana coast, area 3 covered the Alabama and Mississippi coasts, and area 4 covered to the Florida West Coast and the Lower Florida Keys. Two depth strata were defined by using the 10-fathom depth as the divider of inshore and offshore regions. Temporal variability of shrimp bycatch was taken into account by including three seasons: 1) January–April, 2) May–August, and 3) September–December.

Annual estimates of bycatch for the finfish category (i.e. all fish species, in weight units instead of numbers of fish), and for three fish species (Atlantic croaker, Spanish mack-

[3] Nichols S., A. Shah, G. J. Pellegrin and K. Mullin. 1990. Updated estimates of shrimp fleet bycatch in the offshore waters of the US Gulf of Mexico 1972–1989. Report to the Gulf of Mexico Fishery Management Council. The Commons at Rivergate 3018 U.S. Highway 301 N., Tampa, FL 33619.

Table 1

Distribution of number of cells and observations per cell for the general linear model and the modified models. The 3-area model refers to a reduced number of levels in the area factor of the general linear model (from 4 to 3) by combining areas 2 and 3 into a single area (see text for description of each area). The 2-season model refers also to a reduced number of levels in the season factor of the general linear model where season 1 is from September to April and season 2 is from May to August. The no-depth-zone model refers to the general linear model without the depth zone factor. The combined model refers to a model of 3 areas, 2 seasons, and no depth zone. The year and dset (data set) refers to a general linear model with only these two factors (i.e. excluding season, area, and depth-zone factors). Percent coverage refers to the proportion of cells in the matrix that have tow observations, both by type of data (commercial, research, and combined) as well as the number of positive bycatch tows with Spanish mackerel.

	Matrix structure of general linear model								
	Research			Commercial			Total		
Scenario	No. cells of matrix	Cells with tows	Cells with Spanish	No. cells of matrix	Cells with tows	Cells with Spanish	No. cells of matrix	Cells with tows	Cells with Spanish
General linear model	576	274	175	576	181	77	1152	455	252
3 areas	432	176	129	432	148	68	864	324	197
2 seasons	384	236	153	384	152	69	768	388	222
No depth zone	288	143	110	288	112	61	576	255	171
Combined	144	80	66	144	71	41	288	151	107
Year dset only	24	24	24	24	15	10	48	39	34
	Percentage coverage								
General linear model		47.6%	30.4%		31.4%	13.4%		39.5%	21.9%
3 areas		40.7%	29.9%		34.3%	15.7%		37.5%	22.8%
2 seasons		61.5%	39.8%		39.6%	18.0%		50.5%	28.9%
No depth zone		49.7%	38.2%		38.9%	21.2%		44.3%	29.7%
Combined		55.6%	45.8%		49.3%	28.5%		52.4%	37.2%
Year dset only		100.0%	100.0%		62.5%	41.7%		81.3%	70.8%

erel, and red snapper) were used to compare results of the sensitivity analysis. Atlantic croaker is a species commonly caught as bycatch, found in about 61% of tows. Red snapper and Spanish mackerel are important commercial and recreational fisheries in the U.S. Gulf of Mexico; the directed fishery management actions for these fisheries are influenced by the level of bycatch in the shrimp trawl fishery. Red snapper is caught as bycatch in the shrimp fishery in about 28% of tows, whereas Spanish mackerel is less commonly caught in only 5% of tows.

To evaluate the general linear model, we first describe some characteristics of the database that are important regarding assumptions entailed with the use of the model and analysis of the model , then we present a sensitivity analysis on the model structure and parameters. Three main analyses were performed: 1) analysis of the general linear model matrix structure, 2) analysis of the logarithmic scaling of the observed CPUE values, and 3) analysis of the standard tow time unit used to calculate observed CPUE values.

Evaluation of the general linear model

The present general linear model configuration for estimating bycatch created a matrix of 1152 cells, comprising data for 24 years, 2 datasets, 4 areas, 3 seasons, and 2 depth zones. Although there were a relatively large number of observations in the database (26,380), the percentage of cells in the matrix that had observations was only 39%, only 4160 tows (16%) were from commercial vessels during normal shrimp fishing operations, and the remaining 22,220 (84%) tows were from research vessels. In addition, the number of observations per cell varied largely, from 1 to 466 within research tows, and from 1 to 181 within the commercial tows.

Given the unbalanced distribution of observations per cell, we investigated the effects of the matrix structure on the general linear model. Our approach was to fit the model to scenarios with a reduced number of levels within factors or a reduced number of factors in the model (or to scenarios with both). For example, we combined seasons 1 and 3 to reduce the season factor to two levels or we eliminated the season factor from the model. Table 1 describes all the scenarios evaluated. Correspondingly, shrimping effort was adjusted to the new general linear model matrix by adding the annual shrimping effort within the modified strata, and annual bycatch was estimated as the product of the predicted CPUEs and the shrimping effort for each cell. Defining the percentage of coverage as the number of cells with observations divided by the total number of cells

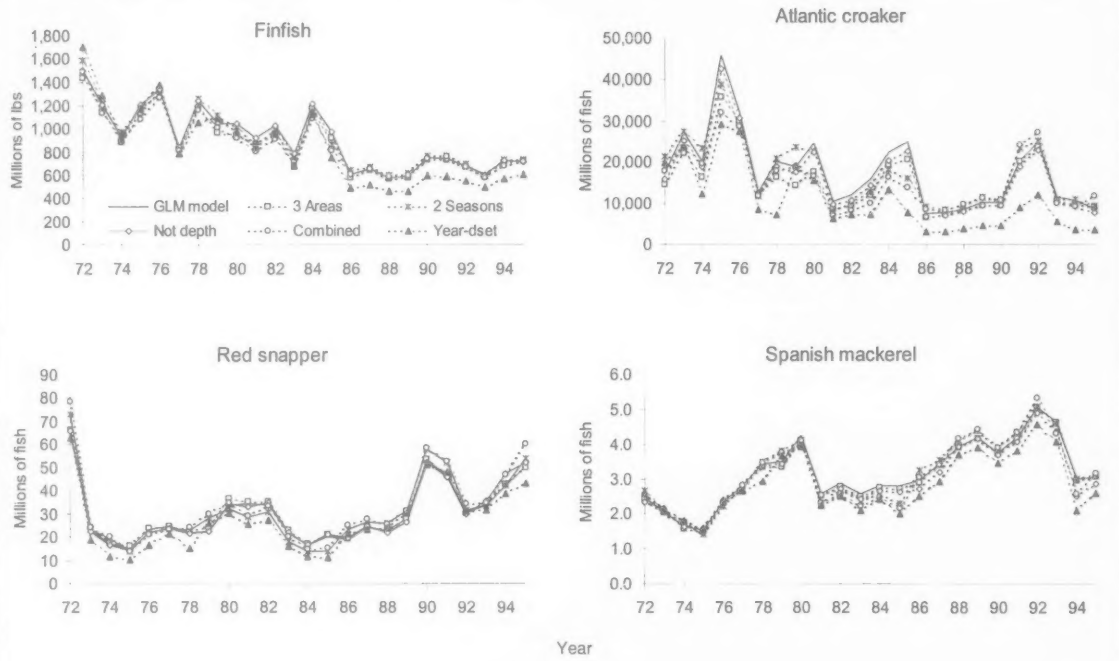

Figure 1

Estimated total bycatch with the general linear model and modified models of the general linear model for the finfish group, Atlantic croaker, red snapper, and Spanish mackerel. (See Table 1 for descriptions of the modified models.)

in the matrix, we found that this value increased from 39% in the base scenario of the current general linear model to 81%, in what was defined as the "minimum model" where only the factors year and dataset were included.

Overall, the results showed that total bycatch estimates did not vary substantially, although the assumed model was radically modified (Fig. 1). These results suggest that season, area, and depth zone are factors that do not significantly contribute to the explanation of the observed variability in the data. Although the F-values from the ANOVA tables were highly significant ($P<0.05$) for each factor in all general linear model matrix scenarios, this significance may be a response to the large number of degrees of freedom. Alternatively, it is possible that the structure of the general linear model does not reflect all the main factors that account for bycatch variability among years, except for dataset source. Indeed, interactions between the main factors may also be important. Given the limited data coverage, however, the inclusion of other factors or interactions among factors in the general linear model is clearly not advisable.

In summary, the simple model with year and dataset as factors produced similar estimates of bycatch in relation to the complex model, including season, area, and depth zone factors. In particular, for species that are not common as shrimp bycatch, a simple model avoids empty cells and highly unbalanced input matrix designs.

Use of logarithms in the general linear model

One of the assumptions in the linear regression model is that the error within the matrix cells should follow a normal distribution and have a constant equal variance. In the bycatch dataset, the CPUE variance increases as the mean CPUE increases, indicating a constant coefficient of variation. This condition suggests a logarithmic transformation of mean CPUE values. To avoid the problem of undefined logarithms for zero catches, a constant value c of 1 was added to all observed CPUE (Eq. 1) in the model. Then the linearization procedure was carried out on the log base 10 of the modified CPUE. This c value was then subtracted in the back transformation of the predicted means (Eq. 2). No particular explanation for the choice of 1 in the current general linear model has been given.

Thus, we considered the effects of using different c values in the general linear model. Three different c values where used: 10, 0.5, and the smallest positive CPUE-value for each species (i.e. 0.0178 for finfish, 0.0779 for Atlantic croaker, 0.0685 for red snapper, and 0.0685 for Spanish mackerel). The results showed that annual bycatch estimates vary dramatically depending upon the c value used in the algorithm (Fig. 2). Although the magnitudes varied with changes in the c value, the trends were the same for each species. However, the direction of change was not the same among spe-

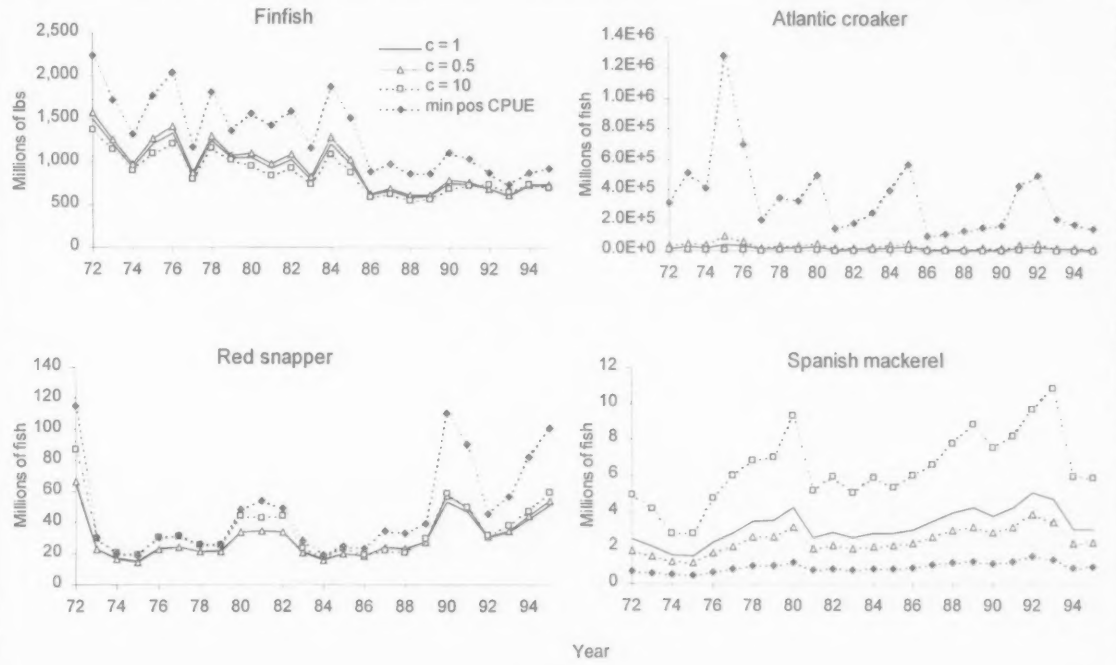

Figure 2

Estimated total with the general linear model with different c-values used in the logarithmic transformation of bycatch CPUE. Base scenario (c=1).

cies. For Spanish mackerel and red snapper, using c=10 increased the estimates of bycatch (100% and 15%, respectively). In contrast, bycatch estimates decreased for Atlantic croaker and finfish (75% and 6%, respectively). When the c was the smallest positive value of the data, annual estimates increased on average 47% for red snapper, 43% for finfish, and 1694% for Atlantic croaker, whereas bycatch estimates decreased on average 70% for Spanish mackerel.

These results show that the general linear model is highly sensitive to the logarithmic c value added to the observed CPUE values. Although it is known that logarithm transformations are affected by the selection of a c value, the large variations in magnitude of estimates for bycatch species should at least merit a review and analysis of the criteria for choosing an appropriate c value. In a review of logarithmic transformations, Berry (1987) suggested choosing a c that normalizes the log-transformed data. He specified an additive function of the skewness and the kurtosis of the data, where skewness and kurtosis are defined as

$$g_1(c) = \sum (y - \bar{y})^3 / (n\hat{\sigma}^3) \text{ and}$$

$$g_2(c) = \sum (y - \bar{y})^4 / (n\hat{\sigma}^4) - 3$$

respectively,

where $\bar{y}$ = the predicted means;
y = the observations; and
$\hat{\sigma}$ = the estimated standard deviation within the defined strata.

When the observations are normally distributed, then the g_1 function has a mean of zero, and the function g_2 has a mean equal to $-6/(d+2)$, where d is the number of degrees of freedom of the error. The additive function of skewness and kurtosis is then defined as

$$g_0(c) = |g_{1c}| + |g_2(c) + 6/(d+2)|.$$

Thus, the c value that minimizes $g_0(c)$ will make the residuals closer to a sample that follows a normal distribution. Using CPUE values for Spanish mackerel, we evaluated several c values ranging from 1.0E – 8 up to 1.0E + 3. We did not find a minimum solution for $g_0(c)$, but rather an asymptotic behavior with c values less than 0.05, indicating that it is not possible to normalize the Spanish mackerel bycatch data by using a logarithm transformation. Therefore, there is not an objective criterion for selecting a particular c value, and as shown before, even relatively small changes of the c value could cause significant variation of the annual bycatch estimates. Furthermore, independent of the method used to select the c constant in

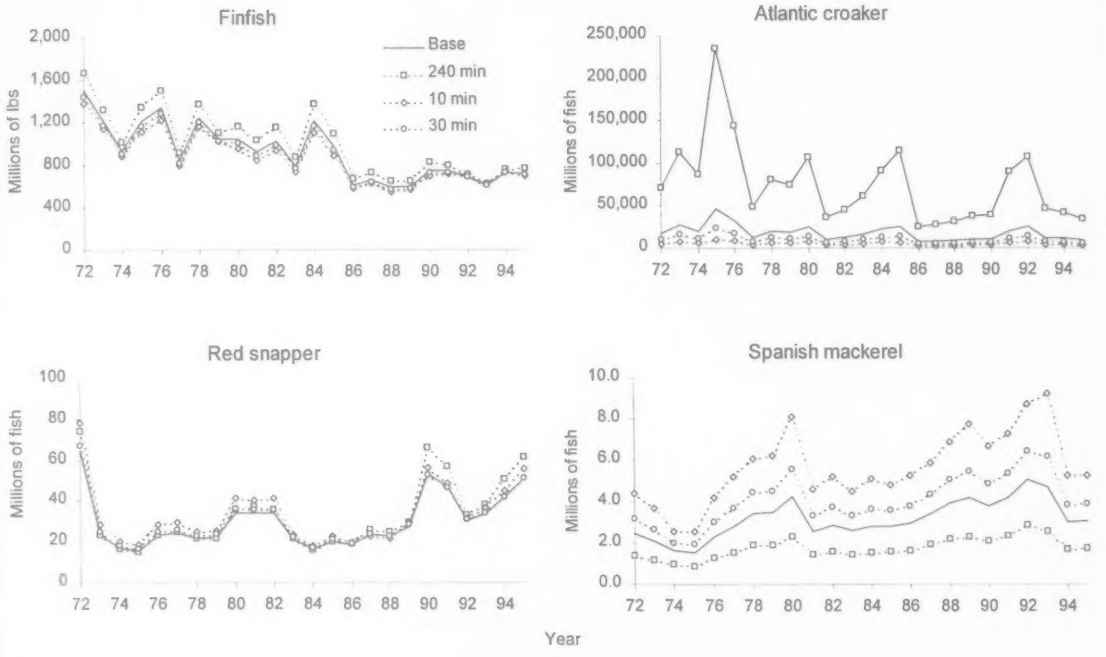

Figure 3

Estimated total bycatch with the general linear model when using different tow-time standard units. The current general linear model uses a one-hour tow time (base scenario).

the logarithmic transformation of the CPUE, the c values must be selected for each species independently. Therefore, the same c value might not be appropriate for different bycatch species, and if new bycatch data are added, then the c value must be re-evaluated.

Standardizing effort in the general linear model

The general linear model predicts bycatch CPUE by cell in units of number of fish caught in one shrimp trawl net per hour. Because actual observations of bycatch are the number of fish caught in a shrimp net during a tow and because tow times are variable, observations are converted to a standard unit of one hour tow time. This standardization procedure implies a direct linear relation between number of fish caught and tow time for all observations (i.e. if 10 fish were caught in a 30-min tow, the CPUE would be 20 fish per hour). However, the average tow time and the tow time distribution from commercial observations are considerably different from those from research observations. Most of the commercial tows range from 1 to 7 hours and have a mode of approximately 4 hours; a few tows are over 12 hours. In contrast, research tows are predominantly of 10-minute duration (73%), and the rest last 1 hour or less.

Given these differences in fishing and sampling time-effort between commercial and research observations, we estimated total bycatch by using different time units to convert the observed catch to CPUE values. We selected 10-, 30-, and 240-minute time units instead of the currently used one-hour unit. These were chosen on the basis of the most frequent tow time for research observations (10 min), the mean tow time of research observations (30 min), and the mode tow time for commercial observations (240 min). The predicted CPUEs were then multiplied by the shrimping effort per cell in the modified time units. Shrimping effort was given in 24-hour-day fishing effort. Therefore, if the predicted CPUE units were 0.5 hour (30 min), the 24-hour shrimping effort would be multiplied by 2. The c value was 1.0 for all these calculations.

Modifying the time unit for calculating CPUE values also had an effect on the annual estimates of shrimp bycatch from the general linear model (Fig. 3). Similar to the results of the evaluation of the logarithmic constant, the changes of estimated bycatch were different for each species and varied in the direction of the change. For example, for finfish and Atlantic croaker, a time unit of 10 minutes decreased estimated annual bycatch (5% and 68% on average, respectively). By contrast, red snapper and Spanish mackerel estimated bycatch increased with the 10 minute unit (12% and 78%, respectively). With the commercial mean tow time (240 min), bycatch estimates of Atlantic croaker increased on average 300%, and 10% for finfish. For red snapper, estimates changed only in the most recent

years (1990–95) by 20%. In contrast, the estimated bycatch of Spanish mackerel was reduced by 44% on average.

The estimated CPUE should be independent of the time unit used (because it is a constant factor for all observations). However, the differences seen in our study in estimated bycatch were due to the presence of zero CPUE values. By dividing by different time units, the relative distance between the groups of zero CPUE values and the positive CPUE values is changed; as a result, estimators of the central tendency for these data will vary. Although the end results of the time-unit and c value choices are similar (biased estimates), their mathematical origin is different. The time-unit choice is a multiplier of the positive catch data (zero catch /any time unit=zero CPUE), whereas the c value choice adds the c value to all CPUE data. Although a change in time unit could be exactly matched by the appropriate change on the c value, addition of more data, with the same time unit, would require recalculating the appropriate c value.

Procedure for estimating bycatch with the delta lognormal model

Delta models have been used to analyze fisheries data, in particular when there is a predominant group of zero observations. These models have been used to obtain estimates of abundance for highly aggregated organisms, such as planktonic samples (Pennington, 1983), in the analysis of catch-per-unit-of-effort data for the development of CPUE indices (Lo et al., 1992; Cooke and Lankester[4]), as well as in the analysis of ground trawl surveys to estimate total or relative abundance (Pennington, 1996; Stefánsson, 1996). The main advantage of delta models is that they allow for an explicit and finite probability of zero catch. In a delta model, the estimated values are the product of two independent components: the probability of nonzero observations, and the probability of effective density if there is a positive observation. In the case of fishery surveys, the nonzero probability can be analogous to the probability of encountering a fish aggregation, whereas the probability within the positive observations would correspond to the estimated density of a given fish aggregation (Cooke and Lankester[4]).

Delta models are multivariate distributions with a nonzero probability mass at the origin (Shimizu, 1988). Stefánsson (1996) presented a mathematical model based on a generalized delta lognormal model for analyzing groundfish survey data. This model defines the cumulative density function of abundance at a given sampling station as

$$F_i(\omega) = P[Y_i \leq \omega] = (1 - p_i) + p_i G_i(\omega),$$

where G_i = a continuous cumulative density function describing the distribution of positive values in a station I; and

p_i = the probability of finding fish in that station.

If p_i is constant and G_i is a lognormal distribution within a stratum, the function is the delta lognormal model. If p_i is set to one (i.e. excluding zero values), and G_i is set to a gamma or other exponential function with a parameterized mean, this model becomes a generalized linear model (GliM, Stefánsson, 1996). The advantage of this formulation is that each component in the delta model can be expressed in terms of a GLiM (McCullagh and Nelder, 1989). Thus, the choice of a particular density function in each of the delta model components can be related to other measured variables, such as tow times, location effects, and seasonal or year effects, through assumptions on distribution.

Bycatch data derived from observers in the Gulf of Mexico shrimp trawl fishery typically have a high proportion of zero bycatches and a skewed distribution of the positive bycatch CPUE rates, with a large number of low bycatches and very few large bycatches. The large catches most likely reflect the spatial-temporal distribution characteristics of fish stocks rather than are outliers of the data. This type of distribution is far from normal, and commonly used transformations are unable to make the data comply with the normal assumptions with the classical regression models. Furthermore, in the case of so-called "non-frequent bycatch species," the proportion of zero observations is markedly increased (above 95%); this significantly biases and reduces the efficiency of statistical estimators of central tendency and overestimates the variance (Pennington, 1996).

The delta lognormal model was used in our study to generate annual bycatch estimates for all finfish combined, as well as for three specific finfish species: Atlantic croaker, red snapper, and Spanish mackerel in the U.S. Gulf of Mexico shrimp trawl fishery. Briefly, bycatch CPUE rates of a given fish species in a given cell were estimated as the product of two components: 1) the proportion of tows with positive catch and 2) the mean catch rate if at least one fish was caught. Bycatch per cell is then the product of the estimated CPUE and the corresponding shrimping effort for that particular cell. Total annual bycatch is then the sum over all strata within a year for the commercial component, as in the general linear model (see Eq. 3).

Each component of the delta lognormal model, the proportion of positive tows and the mean bycatch rate, was estimated by following a general linear model approach with the procedure GENMOD in the SAS statistical software package (SAS Institute Inc., 1993). General linear models consist of three elements: 1) the *random* component which defines the error structure of the model, 2) the *systematic* component which defines a set of explanatory variables $x_1, x_2, \ldots, x_q$, and 3) the *link* function which defines the relation between the random and the systematic components (McCullagh and Nelder, 1989). We described the delta lognormal model for estimating shrimp bycatch on the basis of the assumptions entailed with each component of the model. To compare models, the same explanatory variables used in the current general linear model were used with the delta lognormal model.

[4] Cooke, J. G., and K. Lankester. 1995. Consideration of statistical models for catch-effort indices for use in tunning VPA's. ICCAT Collect. Vol. Sci. Pap. 45(2):125–131.

Proportion of positive tows

The proportion of positive tows for a particular fish species was estimated after classifying each tow as either 0 (no fish caught) or 1 (at least one fish caught). For the shrimp bycatch data, the model assumes that the data are independent results from n successive trials of a Bernoulli-type random variable with a probability p of catching a given fish species. In this case, it is assumed that the frequency distribution of observed zero and positive tows in each cell follows a binomial distribution. The error term is assumed to be constant and independent among the cells. The binomial distribution is then defined in terms of the proportion (y) of positive tows (r) to total tows (n) per cell, and the probability density function $f(y)$ and associated variance $Var\ (y)$ function are given by

$$\text{for } y = r/n,\ f(r) = \binom{n}{r}\mu^r(1-\mu)^{n-r} \text{ where } r = 1, 1, 2, \ldots\ldots, n$$

$$Var(y) = \mu(1-\mu)/n$$

where μ = the mean of y. The response variables y_i are independent for i=1,2,..., n tow trials.

The systematic component defines the set of explanatory variables $x_1, x_2, \ldots, x_q$ which produce a linear predictor η given by

$$\eta = \sum_{j=1}^{q} x_j \beta_j + \beta_0.$$

For the shrimp bycatch data, the linear predictor is a linear function of the fixed explanatory variables dataset, year, season, area, and depth zone, such that

$$\eta = \beta_0 + \beta_1 \cdot dataset + \beta_2 \cdot year + \beta_3 \cdot season + \beta_4 \cdot area + \beta_5 \cdot depth\ zone,$$

where the β_j are parameters to be estimated.

The link function that relates the linear predictor η to the expected value μ of observations y in each cell of the model must be a monotonic differentiable function g such that

$$g(\mu_1) = \eta.$$

In this case, the logit or logistic function expresses the relationship between the assumed binomial error distribution of μ and the given linear function of explanatory variables η, as

$$\eta = \log\left[\frac{\mu}{(1-\mu)}\right].$$

The GENMOD algorithm uses maximum-likelihood estimates for assumed binomial distributions, which are unbiased to a first order of approximation (McCullagh and Nelder, 1989)

Mean bycatch rate

In this section only positive tows were considered. The delta lognormal model assumed that for a given species the number of fish caught as bycatch relates to fixed variables: data source (commercial or research), year, season, area, and depth zone. The mean bycatch CPUE given a nonzero catch was also estimated following a generalized linear model approach. In this case, the random component for the estimated CPUE was assumed to follow a lognormal error distribution within cells. The probability density function is given by the normal function

$$f(y) = \frac{1}{\sqrt{2\pi\sigma^2}} e^{\left(-\frac{(y-\mu)^2}{2\sigma^2}\right)},$$

where μ = $E[y]$; and
σ^2 = $Var(y)$ with a logarithmic link function.

This specification is mathematically equivalent to defining the random component as lognormal with the identity as the link function.

The systematic component is defined as

$$\text{Log}(CPUE) = \beta_0 + \beta_1 \cdot dataset + \beta_2 \cdot year + \beta_3 \cdot season + \beta_4 \cdot area + \beta_5 \cdot depth,$$

where $CPUE$ = the catch rate in numbers of fish per net hour for nonzero catches;
β_0 = the overall mean;
$dataset$ = a fixed effect differentiating data sources from commercial shrimp fishing from those in research trawls, the terms *year*, *season*, *area*, and *depth* are also fixed effects; and
the β_j = parameters to be estimated.

The link function between the random and systematic components is the identity function:

$$\eta = \mu.$$

Estimation of bycatch

The overall model is then referred to as the delta lognormal model. This model generates the estimated proportion of positives tows ($\hat{p}_{ijklm}$) and the mean bycatch rate ($\hat{CPUE}_{ijklm}$) for a given species. Estimates of bycatch are calculated as the product of the proportion of positives tows ($\hat{p}_{ijklm}$) multiplied by the mean bycatch rate ($\hat{CPUE}_{ijklm}$) multiplied by the shrimping effort (f_{jklm}) multiplied by the two nets (assumed) per boat. Shrimping effort data are the same as those used in the current general linear model. Annual estimates of bycatch are simply the sum of bycatch per cell over the season, area and depth zone strata, for the commercial sector (i=1).

$$Bycatch_j = 2 \times \sum_{klm} \hat{p}_{1jklm} \times \hat{CPUE}_{1jklm} \times f_{jklm}.$$

Evaluation of the delta lognormal model

Before comparing the annual bycatch estimates of total finfish, Atlantic croaker, red snapper, and Spanish mackerel from the general linear model (Nichols[5]) and the delta lognormal model, the delta lognormal model was evaluated and assessed. Because there is not yet a formal strategy for model verification, acceptance of a particular model should not be based exclusively on "goodness of fit" scores (McCullagh and Nelder, 1989).

In general, model assessments can be classified into two main groups. The first group checks for systematic departure from the underlying model, testing for additional factors, factor interactions, or covariates that could explain a significant proportion of the residual model variation. The second group involves evaluation of particular or isolated points in the data. McCullagh and Nelder (1989) and O'Brien and Kell[6] have described six specific tests for evaluating generalized linear models: 1) assessment of the scale of independent variables; 2) assessment of the link function adequacy; 3) assessment of variance function adequacy; 4) investigation of systematic departure from the assumed model; 5) investigation of outliers; and, 6) investigation of omitted predictor variables. Most of these analyses are based on the behavior of the model residuals, either as graphical or informal tests, rather than an exact statistical test. For the delta lognormal model, only tests evaluating systematic departure from the assumed model were performed on each of the model components (i.e. an estimation of the proportion of positive tows and the estimation of bycatch rates) separately.

With the delta lognormal model, an evaluation of the proportion of positive tows was restricted to a graphical analysis of the frequency distribution of positive tows of observed and predicted data. This restriction was warranted because most of the tests suggested for assessing model adequacy are uninformative for binomial data (McCullagh and Nelder, 1989; O'Brien and Kell[6]). Figure 4 shows the standardized frequency distributions of proportion of positive tows per cell for the combined finfish category, Atlantic croaker, red snapper, and Spanish mackerel. Each plot shows the observed and the predicted proportions estimated by the binomial distribution of the delta lognormal model. The predicted frequencies fitted closely those observed in all four cases. The assumed binomial distribution is able to predict appropriately the proportion of positive tows in a broad range (from the combined finfish category case where almost all tows were positive [97%] to the case of Spanish mackerel where only 5% of the tows were positive).

The suitability of the delta lognormal general linear model component for the positive tows was evaluated by the following graphical tests: 1) adequacy of the link function, 2) adequacy of the variance function, and 3) systematic departure from the assumed model.

By plotting the adjusted dependent variable (log CPUE) we were able to assess the link function against the estimated linear predictor ($\hat{\eta}$). A linear configuration is expected for normal, assumed Poisson or gamma error distributions. In our case, the delta lognormal model assumed a normal error distribution for log CPUE of positive catch. Figure 5A shows the plots of the linear predictor (lp-logcp) against the adjusted dependent variable (log CPUE) for red snapper. In the case of high density of points as in Figure 5A, locally weighted regression smoothing procedures (i.e LOESS smoothing) have been suggested for showing the trend of the response variable (McCullagh and Nelder, 1989).

Adequacy of the variance or assumed error distribution function was evaluated by using a plot of residuals against fitted values. The spread of residuals is expected to be approximately constant and independent of the fitted values, confirming the adequacy of the assumed error distribution in the model. Figure 5B shows the plots of residuals (R-logcpu) against the fitted values (P-logcpu) for red snapper. The residuals are evenly distributed about the zero line and are without any apparent trend with respect to the fitted values. Likewise, a plot of residuals versus the normalized cumulative residuals (QQ plot) can be used to assess the variance function adequacy. A linear relationship is expected for residuals from a normal error distribution.

A plot of standardized residuals (rs-logcp) against fitted values (log CPUE) was used to identify possible trends or curvatures that would suggest a departure from the assumed model (Fig. 5C). The null pattern of this plot is a linear configuration of the standardized residuals (O'Brien and Kell[6]). In conclusion, assessments of each of the delta lognormal model components did confirm the model choices and assumptions for the finfish group and the fish species examined (similar plots were created for finfish, Spanish mackerel, and Atlantic croaker but are not presented here for briefness).

As shown before, bycatch estimates from the current general linear model depend upon the standard time unit chosen to convert catches in numbers to CPUE values. Similarly, the same tow time evaluation with the delta lognormal model was performed as with the general linear model. CPUE values were calculated by using 10-, 30- and 240-min tow times, and concurrently, shrimping effort unit, given in hours, were multiplied by a scale factor to make the time unit compatible with the modified CPUE values. With the delta lognormal model, the annual bycatch estimates were exactly the same, independent of the time unit used to calculate the CPUE values, further demonstrating the benefits of using a model that separates the zero catch observations from the positive catch. In addition, delta models do not require adding a constant value to logarithmic transformed values because the estimated density component is restricted to positive catch only, thus avoiding the uncertainty in selecting a c value to log transform CPUE values as required in the general linear model.

Results and discussion

Because the bycatch database complied with the delta lognormal model specifications, a stepwise analysis of devi-

[5] Nichols, S. 1996. Estimates of annual shrimp fleet bycatch in the offshore waters of the Gulf of Mexico. Personal commun. NMFS Pascagoula laboratory. 3209 Frederic St. Pascagoula, MS 39567.

[6] O'Brien, C. M., and L. T. Kell. 1996. The use of generalized linear models for the modelling of catch-effort series. I. Theory. ICCAT Collect. Vol. Sci. Pap. 46(4):476–482.

ance was performed to assess the importance of the factors selected in the delta model. Table 2 gives the percent change in deviance as each factor is added to the binomial fitted proportion of the zero versus positive tows component of the delta lognormal model. The deviance explained by the model is equivalent to the r^2 concept in linear models (McCullagh and Nelder, 1989; Stefánsson, 1996). Tests of significance were based on the χ^2 statistic for the binomial distribution of the proportion of positive tows (McCullagh and Nelder, 1989). Overall, the delta lognormal model, with all factors, explained between 55% and 75% of the total deviance for the finfish group and the three fish species. However, as expected, the percentage of deviance explained by each factor differed for each species. For example, the *dataset* factor appeared to be unimportant in estimating the proportion of positive tows for red snapper and Atlantic croaker. Instead, area and season factors were more important for red snapper, and area and depth zone for Atlantic croaker.

Table 3 shows the lognormal component of the delta model r^2 values, sum of squares error or residual deviance, residual degrees of freedom, and the P values. Similarly to the proportion of positive tows, a stepwise analysis of the r^2 shows that dataset, year, season, area, and depth zone are significant factors in explaining the overall variability of the model. An exception is the depth zone factor in estimating bycatch CPUE rates for red snapper. The delta lognormal estimated density model explained from 17% (Atlantic croaker) to 36% (Spanish mackerel) of the total variation, indicating that a significant portion of the bycatch CPUE variability is still unexplained by the model.

The annual shrimp bycatch estimates for the four species groups in the U.S. Gulf of Mexico differed in several aspects between the delta lognormal model and the current general linear model. Results varied for the finfish group and the fish species analyzed. Differences were found both in the absolute magnitude of bycatch estimates and in the trend over the time series 1972–95. For the total finfish bycatch, the delta lognormal model estimated an average of 795 million lbs. for the period 1972–95, or 14% lower than the equivalent general linear model estimate of 916

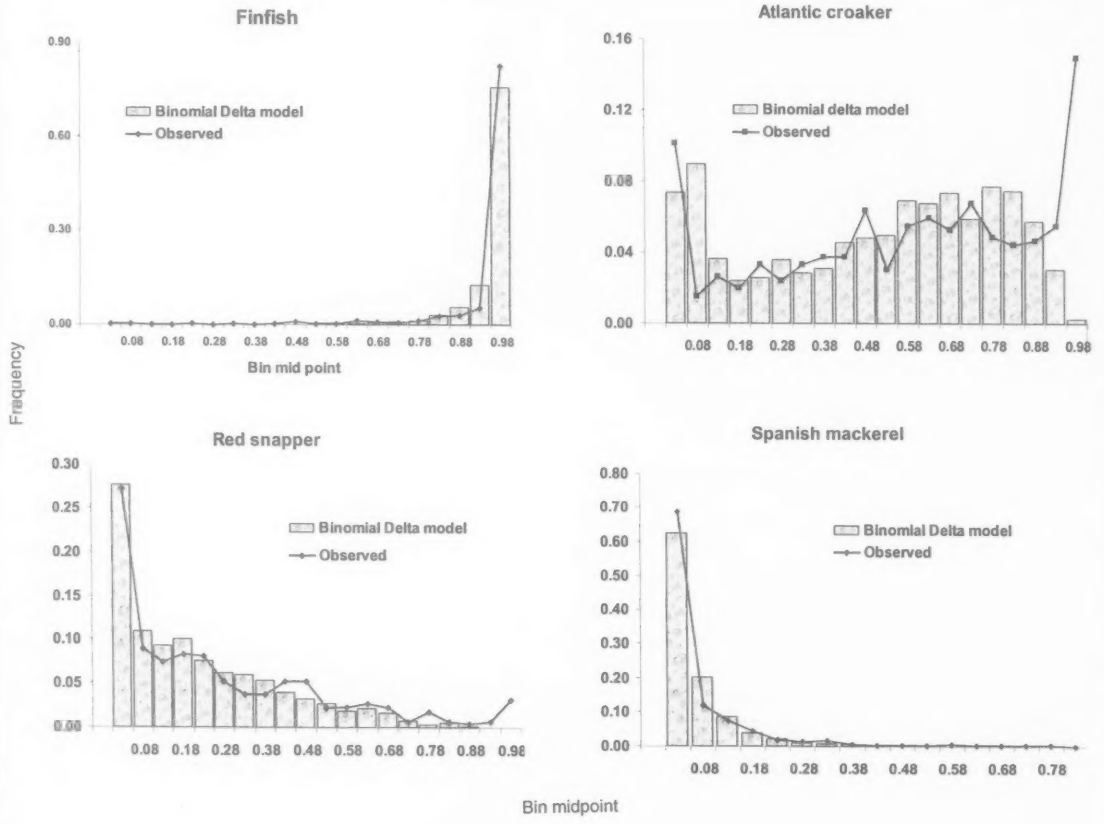

Figure 4

Standardized frequency distribution of the proportion of positive tows from the bycatch data 1972–95 and the proportions estimated by the binomial-based delta lognormal model component.

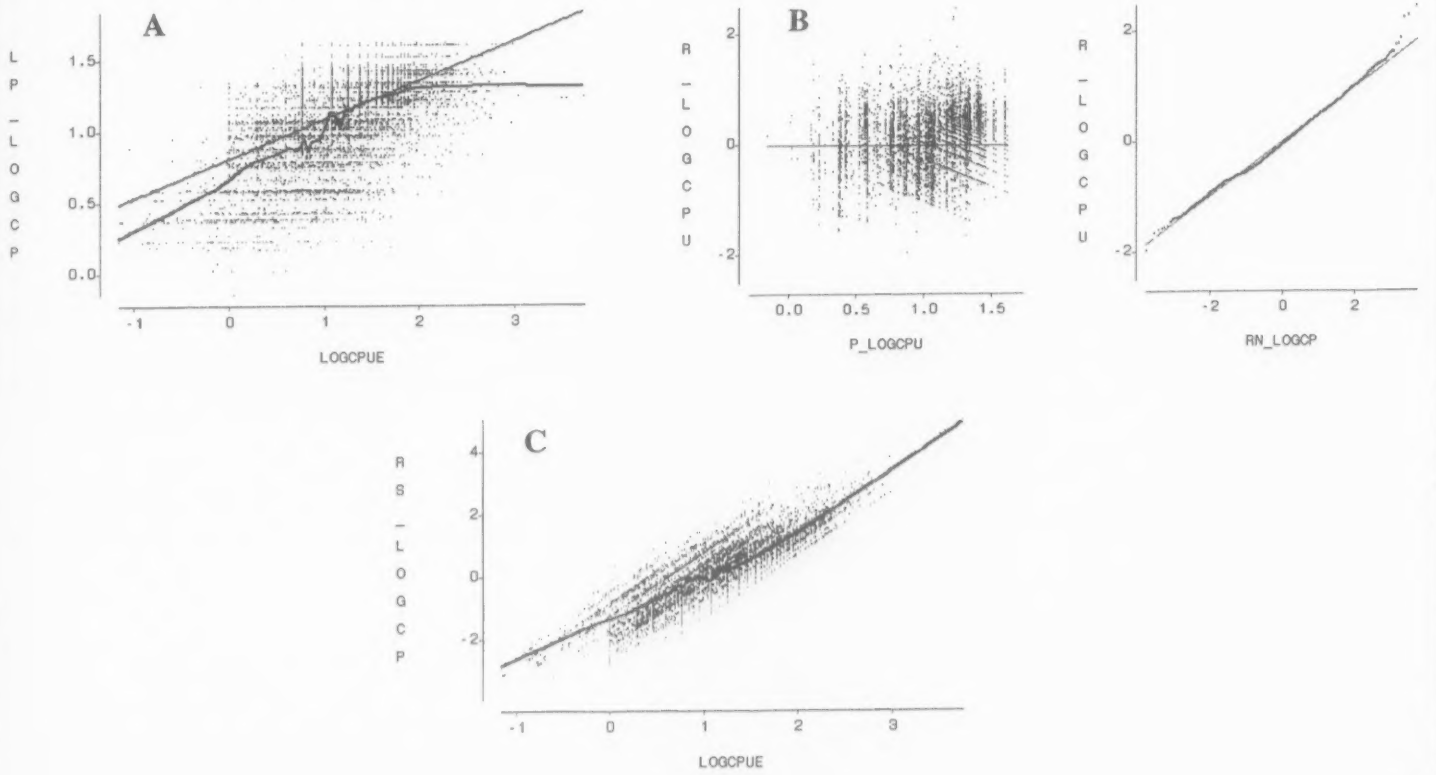

Figure 5

Evaluation plots for the positive catch component for red snapper with the delta lognormal model. (**A**) Plot of the linear predictor (lp_logcp) against the dependent variable (logCPUE). The straight line is the linear function of the variables for comparison purposes, the dark line is the LOESS smoothing procedure of the data. (**B**) Plot of the residuals (r_logcpu) against predicted values (p_logcpu) and the cumulative normalized-residuals or QQ plot. (**C**) Plot of the standardized residuals (rs_logcp) against the fitted values (logCPUE). The line represents the LOESS smoothing procedure to evaluate the data trend.

Table 2

Analysis of deviance table for different binomial-based delta lognormal models fitted to positive/total tows of each fish species and finfish category in the bycatch database for the U.S. Gulf of Mexico 1972–95. The models are fitted sequentially and the columns give the residual degrees of freedom for each model, the residual deviance, the resulting change in deviance, the percentage of total deviance change, and the *P*-value when χ^2 test was used for significance. Model 1 refers to estimating only the overall mean.

Model factors	Residual df	Residual deviance	Change in deviance	% of total deviance	*P*	Residul deviance	Change in deviance	% of total deviance	*P*
	Finfish					Atlantic croaker			
1	454	2403				8869			
Data set	453	1676	726.05	0.30	<0.001	8866	3.38	0.00	<0.0660
Data set + year	430	1113	563.93	0.23	<0.001	7890	976.05	0.11	<0.001
Data set + year + season	428	1079	33.70	0.01	<0.001	6194	1696.32	0.19	<0.001
Data set + year + season + area	425	1026	52.80	0.02	<0.001	3866	2327.89	0.26	<0.001
Data set + year + season + area + depth zone	424	1016	9.66	0.00	<0.001	3849	17.22	0.00	<0.001
	Red snapper					Spanish mackerel			
1	454	6390				2356			
Data set	453	6389	0.34	0.00	<0.5605	2086	270.00	0.11	<0.001
Data set + year	430	4935	1454.20	0.23	<0.001	1810	275.91	0.12	<0.001
Data set + year + season	428	4013	921.97	0.14	<0.001	1550	260.29	0.11	<0.001
Data set + year + season + area	425	2770	1243.33	0.19	<0.001	1468	81.92	0.03	<0.001
Data set + year + season + area + depth zone	424	1633	1136.46	0.18	<0.001	1065	402.92	0.17	<0.001

million lbs. (Table 4, Fig. 6). Total finfish bycatch estimates from the delta lognormal model were consistently lower for all years, and overall followed the same trend as the estimates from the current general linear model. The normalized plot of total finfish bycatch (i.e. year estimate minus the mean divided by the standard deviation of the time period) shows that the trends are identical between the two models up to 1990, but in 1991–95 some discrepancies were observed (Fig. 7). However, both models show a decreasing trend in the total finfish bycatch estimates from about 1,100 million lbs. (1972–84) to less than 700 million lbs. during the last 10 years (1985–95). This decline can be attributed to improvements in the selectivity of the shrimp trawl gear to retain less bycatch (i.e. introduction of TEDs and BRDs) or to an overall reduction of the trawlable fish stock biomass in the U.S. Gulf of Mexico.

For Atlantic croaker, bycatch estimates from the delta lognormal model were on average 4.5 billion fish for the 1972–95 period, 74.5% lower than estimates of 17.7 billion fish from the general linear model (Table 4, Fig. 6). Once more, the normalized plot shows a similar decreasing trend in bycatch estimates from both models in the 1972–95 period (Fig. 7). Atlantic croaker, together with longspine porgy (*Stenotomus caprinus*), are the most common finfish bycatch species in the Gulf of Mexico shrimp fishery, therefore a significant reduction in bycatch estimates of Atlantic croaker most likely correlates with a reduction in total estimated finfish bycatch.

Bycatch estimates of red snapper from the delta lognormal model were slightly greater in general from 1972 to 1982, and much lower from 1987 to 1995 compared with estimates yielded with the general linear model (Fig. 6). On average, the delta lognormal model bycatch estimates were 22.1 million fish for the years 1987–95, 40% lower than the equivalent average of 36.8 million fish estimated with the general linear model (Table 4). The normalized plot shows that since 1987, there has been an overall increasing trend in red snapper bycatch according to both the general linear model and delta model estimates, a peak in bycatch in 1990, subsequent low in 1992, and an increasing trend since then (Fig. 7). Prior to 1987, red snapper bycatch was relatively lower, with an exception of the highest bycatch peak in 1972 and some above average bycatch in 1980–82.

Delta lognormal estimates of Spanish mackerel bycatch were 97% higher on average than those from the general linear model (Fig. 6, Table 4) for the time period 1972–95. Spanish mackerel bycatch estimated by the delta lognormal model was on average 6.5 million fish, compared with 3.2 million fish estimated by the general linear model. In

Table 3

Analysis of deviance table for different lognormal-based delta models fitted to the positive bycatch CPUEs of each finfish species and the finfish category in the bycatch database for the US Gulf of Mexico 1972–95. The models were fitted sequentially and the columns give the residual degrees of freedom for each model, the residual deviance, the resulting change of deviance, the r^2 values, and the P-value when the F-test was used for significance. Model 1 refers to estimating only the overall mean.

Model factors	Residual df	Residual deviance	Change in deviance	% of total deviance	P	Residual df	Residul deviance	Change in deviance	% of total deviance	P
	Finfish					Atlantic croaker				
1	25,636	10,040.40				15,985	16,036			
Data set	25,635	8870.06	1170.34	0.12	<0.0001	15,984	15,238	798.03	0.05	<0.0001
Data set + year	25,612	7809.32	1060.74	0.22	<0.0001	15,961	13,855	1382.60	0.14	<0.0001
Data set + year + season	25,610	7685.07	124.25	0.23	<0.0001	15,959	13,790	65.09	0.14	<0.0001
Data set + year + season + area	25,607	7440.94	244.13	0.26	<0.0001	15,956	13,463	326.60	0.16	<0.0001
Data set + year + season + area + depth zone	25,606	7436.59	4.35	0.26	<0.0001	15,955	13,308	154.96	0.17	<0.0001
	Red snapper					Spanish mackerel				
1	7377	2491.32				1240	430.90			
Data set	7376	2122.94	368.38	0.148	<0.0001	1239	369.80	61.10	0.142	<0.0001
Data set + year	7353	1889.23	233.71	0.242	<0.0001	1216	329.53	40.27	0.235	<0.0001
Data set + year + season	7351	1847.03	42.20	0.259	<0.0001	1214	305.09	24.43	0.292	<0.0001
Data set + year + season + area	7348	1803.48	43.55	0.276	<0.0001	1211	288.32	16.77	0.331	<0.0001
Data set + year + season + area + depth zone	7347	1803.26	0.22	0.276	<0.0001	1210	273.54	14.78	0.352	<0.0001

our study, the delta lognormal model showed a larger year variability of bycatch with prominent peaks in 1980 and 1992. The normalized plot of Spanish mackerel bycatch illustrates that estimates from the general linear model and delta lognormal model followed similar trends from 1972 to 1981, and from 1988 to 1995 (Fig. 7). The time period from 1984 to 1987, the period of greatest oscillation in bycatch estimates for the delta lognormal model, corresponds with the years of no bycatch observations in the commercial fishery. Although delta lognormal bycatch estimates show a comparable trend to the general linear model estimates in the later years (1987–95), the magnitude of bycatch is much greater; the peak estimate of 14.4 million fish in 1993 is twice as high as the reported estimates from the general linear model (Nichols[5]).

The delta lognormal model protocol appears to be an improved alternative procedure for estimating shrimp bycatch in the U.S. Gulf of Mexico compared with the currently used general linear model. In theory, the delta model allows for an explicit probability for zero catches, which are highly common in the bycatch data set, especially when dealing within single species cases. Myers and Pepin (1990) stated that lognormal-based estimators are sensitive to violations of model assumptions, in particular if the number of observations is below 40 or if there is no confirmation that the sample came from a true lognormal distribution (or if both situations occur). However, their arguments are restricted to the positive tows (i.e. nonzero observations); they concluded that lognormal estimators should be used only in cases where the assumed lognormal distribution can be confirmed. Following their criteria, Myers and Pepin's arguments should then be applied to the delta lognormal model (more specifically to the density estimation component that models the nonzero catches) and to the current general linear model as well (if a lognormal distribution can be assumed for all observations, Nichols et al.[2]). In the bycatch database, there are a large number of cells with low number of observations (i.e. ≤40). Restricting the database to cases where the number of observations per stratum (year, area, season, depth, and dataset) were greater than 40, we were able to use cumulative CPUE distributions more approximate to lognormal

Table 4

Bycatch estimates from the general linear model and the delta lognormal model. Percentage of change is with reference to the bycatch general linear model estimates, negative percentages refer to lower estimates. The average values are over the 24-year period.

	Finfish			Atlantic croaker			Red snapper			Spanish mackerel		
	Millions of lbs.			Millions of fish			Millions of fish			Millions of fish		
Year	GLM	Delta	% change	GLM	Delta	% change	GLM	Delta	% change	GLM	Delta	% change
1972	1501.10	1305.45	−13	17,529.94	4736.80	−73	69.49	73.27	5	2.47	5.63	128
1973	1211.12	1093.34	−10	27,161.33	9034.68	−67	23.00	28.22	23	2.08	3.62	74
1974	934.85	826.66	−12	20,205.60	5396.10	−73	16.97	19.58	15	1.62	1.65	2
1975	1209.90	1098.10	−9	45,615.42	7337.83	−84	15.23	18.01	18	1.53	2.35	54
1976	1343.26	1177.58	−12	32,140.84	7806.93	−76	23.27	30.27	30	2.32	5.63	143
1977	843.11	772.07	−8	12,793.05	4405.55	−66	24.45	25.41	4	2.80	8.22	194
1978	1248.09	1113.57	−11	20,133.40	6648.36	−67	21.62	18.40	−15	3.43	6.27	83
1979	1045.06	957.10	−8	18,851.25	5121.00	−73	22.36	22.91	2	3.48	8.64	148
1980	1045.81	925.60	−11	24,707.77	5860.63	−76	34.07	38.35	13	4.24	16.93	299
1981	922.37	787.92	−15	10,431.83	4727.13	−55	34.21	37.99	11	2.57	5.94	131
1982	1028.24	878.77	−15	11,953.52	4264.06	−64	33.77	36.31	8	2.85	6.94	144
1983	790.33	680.57	−14	15,826.07	5940.60	−62	21.18	17.97	−15	2.58	3.08	19
1984	1217.03	1043.25	−14	22,381.82	7291.54	−67	16.44	13.57	−17	2.79	6.89	147
1985	975.74	821.60	−16	24,975.37	4558.15	−82	20.15	14.68	−27	2.79	2.17	−22
1986	606.40	513.85	−15	7453.91	2134.62	−71	18.80	14.31	−24	2.95	4.11	39
1987	656.50	556.19	−15	7778.19	1281.58	−84	23.88	11.99	−50	3.42	2.33	−32
1988	582.70	498.09	−15	8601.77	1732.06	−80	22.69	11.72	−48	3.94	8.33	111
1989	594.09	507.50	−15	10,286.57	2800.51	−73	27.51	18.10	−34	4.20	8.38	100
1990	748.97	639.65	−15	10,370.38	2414.03	−77	53.17	32.35	−39	3.77	6.64	76
1991	742.31	597.00	−20	20,449.99	3775.18	−82	46.93	27.03	−42	4.19	6.97	66
1992	684.74	430.25	−37	24,818.83	5298.03	−79	30.37	17.06	−44	5.05	10.74	113
1993	605.72	517.55	−15	11,556.16	1998.04	−83	33.71	18.77	−44	4.68	14.41	208
1994	729.20	660.36	−9	10,984.66	2177.96	−80	41.98	32.32	−23	3.01	4.11	37
1995	719.92	669.17	−7	8715.51	1500.90	−83	50.87	29.94	−41	3.06	5.32	74
Average	916.11	794.63	−14	17,738.47	4510.09	−74	30.26	25.36	−14	3.16	6.47	97

density function in the case of nonzero catches (i.e. delta lognormal model) than in the case when both zero and positive catches are included (i.e current general linear model). Thus, if departures from the assumed distribution produced biased lognormal estimates, certainly the current general linear model would be more prone to these biases than the delta lognormal model.

As stated by Pennington (1991) in his response to Myers and Pepin's (1991) article, the assumed lognormal data were contaminated with data from distributions that generated extremely small values, close to zero, which in a logarithmic scale become large negative values. These large negative values then biased estimates of the mean. In the case of the bycatch database this is not a problem because the smallest positive bycatch CPUE values are in most cases greater than 0.05.

Another point to consider when comparing the delta lognormal model and the current general linear model is the variance associated with the estimated bycatch. Smith (1988) described an exact variance for the delta lognormal distribution estimates. He also pointed out that the efficiency of the delta lognormal variance is a function of the sample size, the proportion of zero observations, and the variance within the nonzero observations. The variance of bycatch estimates are, however, restricted to the variance from the general linear model or the delta lognormal model because the shrimping effort multiplier is assumed to be exactly known (Nichols et al.[2]). Thus to compare true standard errors of bycatch estimates, one would require the variance of the shrimping effort and calculate an overall variance through a mathematical approach such as the delta method or use resampling techniques such as bootstrapping procedures. Because point estimates of bycatch are more frequently used in stock assessments of affected species rather than the confidence intervals, the present analysis focused on the point estimates of bycatch.

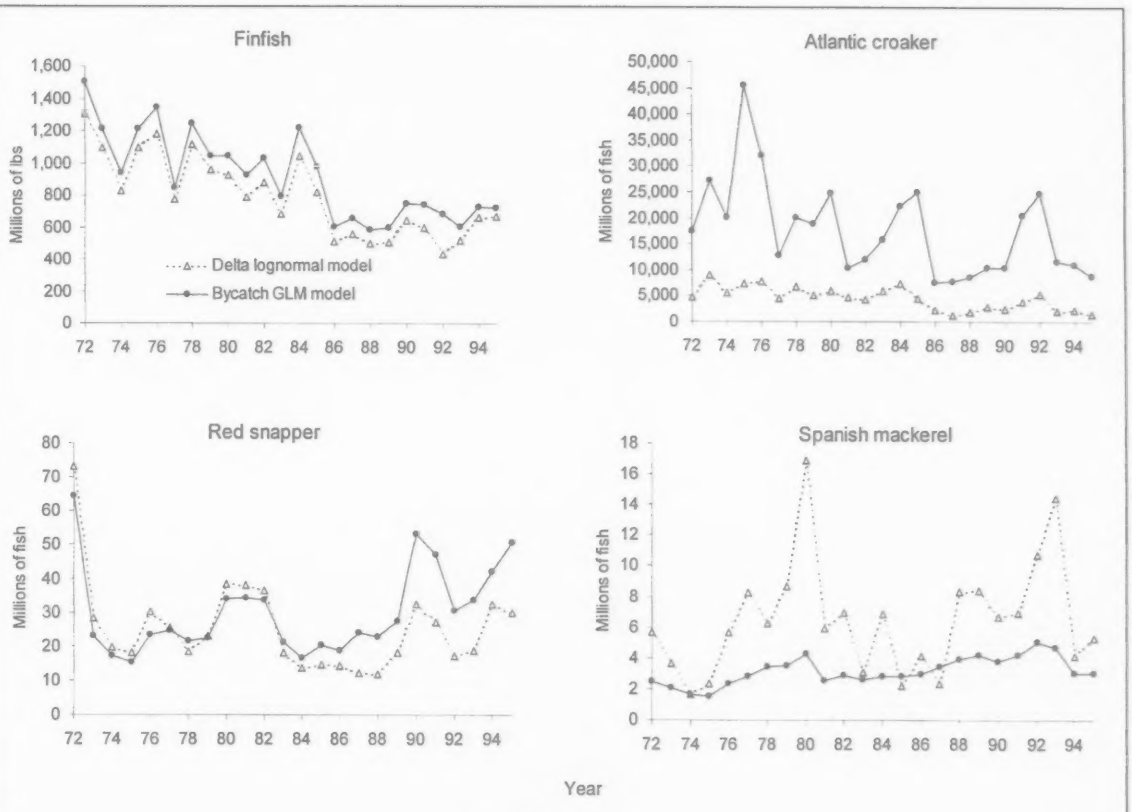

Figure 6

Estimates of total annual bycatch from the delta lognormal model and the current general linear model, for finfish (millions of pounds), Atlantic croacker, red snapper, and Spanish mackerel (millions of fish) 1972–1995.

Conclusions and recommendations

Analyses of the total finfish bycatch and the bycatch of Atlantic croaker, red snapper, and Spanish mackerel show that the delta lognormal model estimates differ both in magnitude and trends from those generated by the current general linear model. However, these differences are not consistent among species. In terms of absolute magnitude, they are substantially different for Atlantic croaker and Spanish mackerel over all years (1972–95), whereas for red snapper differences are greater in the most recent years of the time series (1987–95). Total finfish bycatch estimates are more similar in magnitude and trend for both models. Although the trends of bycatch in the time series from 1972 to 1995 are similar for the species examined, the absolute estimated values are highly variable. Because these estimates are included as additional catch (usually for age 0 and 1) in the stock assessments of directed fisheries, the uncertainty of the bycatch estimates will impact the results of these assessments. Further, this uncertainty will extend to management policies adopted from these assessment results for species like Spanish mackerel, king mackerel, and red snapper (Ehrhardt and Legault, 1997; Goodyear[7]).

As presented before, the general linear model estimates depend on choices about the constant added to the CPUE values prior to logarithmic transformation and on the standard time unit chosen for calculating CPUE values. These problems emerge from the noncompliance of the bycatch data with the assumptions associated with the general linear model. In particular, the observed CPUEs are not lognormally distributed owing to the significant proportion of zero observations within the data. In contrast, the delta lognormal model conforms better with the structure of the data and avoids the problems of choosing a c value for catches in the logarithm transformation and of selecting a standard time unit for the CPUE calculations. As

[7] Goodyear, C. P. 1995. Red snapper in U.S. waters of the Gulf of Mexico. Contribution report MIA 95/96-05, 171 p. Miami Laboratory, Southeast Fisheries Science Center, NMFS, NOAA, 75 Virginia Beach Dr., Miami, FL 33149.

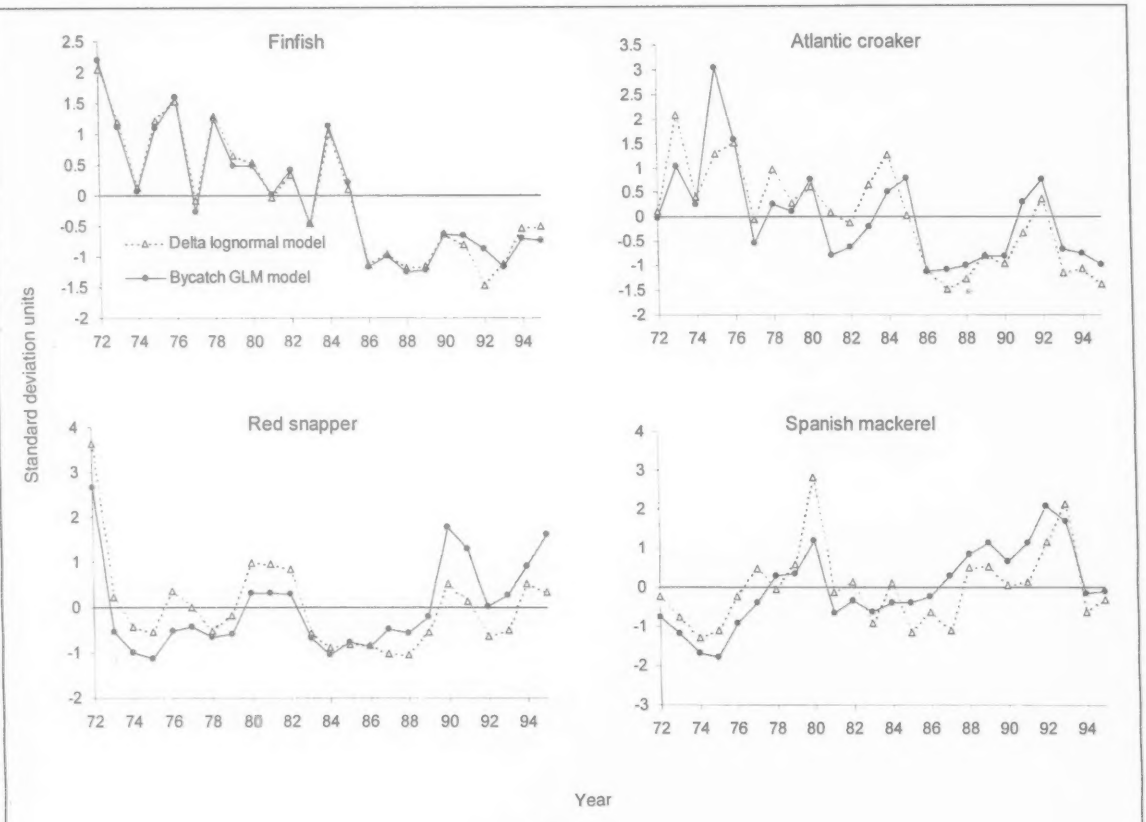

Figure 7

Normalized plots of bycatch estimates by species from the current general linear model and the delta lognormal model.

expected, both models agree better in the case of the finfish bycatch estimates where the proportion of zero CPUE values is the lowest (less than 3%).

Besides the problems related to zero observations, several other considerations must be addressed to generate annual bycatch estimates:

1 The matrix structure of area, season, year, and data source is inadequately covered by observations. This is true for any model that uses these same factors but in particular for the period 1985–90, when commercial observations were not available. It may be beneficial to limit the analysis to years, areas, and seasons where there are data from both commercial and research sources. This change, however, will require the redefinition of the objectives of the bycatch estimation procedure because the estimated annual bycatch will not be possible for the 1972–95 period.

2 Another important requirement is the standardization of the CPUE units for both the commercial and research observations. We feel that these CPUEs represent different units for each type of observation for each particular species and that a single linear relationship is not adequate. This standardization will require a thorough analysis of each fleet and additional information in order to convert the effort units from nominal to effective units for each fleet prior to bycatch estimation. It has been suggested that the more recent data obtained by the Bycatch Characterization Project (NOAA[1]) could be used for this type of analysis. As an alternative, we modified the delta lognormal model to incorporate the observed catch (i.e. numbers of fish) as the dependent variable, and we used the tow time (i.e. hours fishing) as a covariate in the systematic linear component of the delta lognormal model. With this modification, the total deviance explained by the model increased for red snapper. However, we would recommend standardizing the nominal CPUE instead of simply adding more variables to an already unbalanced matrix and avoid considering only goodness-of-fit as an indicator.

3 In the analysis of bycatch by species, it is presently assumed that estimated bycatch in number of fish belongs

to the same age class, usually the age-0 class. This may not be true for some species. Thus, bycatch estimates should take into account number of fish per age or size class.

Acknowledgments

This research was supported by a grant provided by MARFIN (NA57FF283-01); additional grants came from the Florida Sea Grant College Project (R/LR-8-37). We thank Victor Restrepo from the University of Miami RSMAS for his scientific advice, Scott Nichols from the Pascagoula laboratory of the NMFS for providing the bycatch database and algorithms, and Nancy Cummings from the NMFS Miami laboratory for her comments and suggestions. Three anonymous reviewers provided valuable comments on the final draft.

Literature cited

Berry, D. A.
1987. Logarithmic transformations in ANOVA. Biometrics 43:439–456.

Ehrhardt, N. M., and C. M. Legault.
1997. The role of uncertainty in fish stock assessment and management: a case study of the Spanish mackerel, *Scomberomorus maculatus*, in the US Gulf of Mexico. Fish. Res. 29:145–158.

Henwood, T. A., and W. E. Stuntz.
1987. Analysis of sea turtle captures and mortalities during commercial shrimp trawling. Fish. Bull. 85(4):813–17.

Lo, N. C., L. D. Jacobson, and J. L. Squire.
1992. Indices of relative abundance from fish spotter data based on delta-lognormal models. Can. J. Fish. Aquat. Sci. 49:2515–26.

McCullagh, P., and J. A. Nelder.
1989. Generalized linear models. Chapman & Hall, London, 512 p.

Myers, R. A., and P. Pepin.
1990. The robustness of lognormal-based estimators of abundance. Biometrics 46:1185–1192.
1991. Replay to: on testing the robustness of lognormal based estimators. Biometrics 47:1623–1624.

Pellegrin, G. J.
1982. Fish discards from the southeastern United States shrimp fishery: fish by-catch: bonus from the sea report of a technical consultation on shrimp by-catch utilization held in Georgetown, Guyana, 27–30 October 1981. International Development Research Center (IDRC), Ottawa, 163 p.

Pennington, M.
1983. Efficient estimators of abundance, for fish and plankton surveys. Biometrics 39:281–86.
1991. On testing the robustness of lognormal-based abundance estimators. Biometrics 47:1623.
1996. Estimating the mean and variance from highly skewed marine data. Fish. Bull. 94:498–505.

SAS Institute Inc.
1993. SAS/STAT® software: the GENMOD procedure, release 6.09. SAS® Technical Report P-243. SAS Institute Inc., Cary, NC, 88 p.

Shimizu, K.
1988. Point estimation. lognormal distributions: theory and applications. Department of Information Sciences, Faculty of Science and Technology, Science University of Tokyo, Japan Edwin L. Crow, and Kunio Shimizu. Marcel Dekker, Inc., New York, NY, 387 p.

Smith, S. J.
1988. Evaluating the efficiency of the Δ-distribution mean estimator. Biometrics 44:485–493.

Stefánsson, G.
1996. Analysis of groundfish survey abundance data: combining the general linear model and delta approaches. ICES J. Mar. Sci. 53:577–88.

Validation of annual growth increments in the otoliths of the lethrinid *Lethrinus mahsena* and the lutjanid *Aprion virescens* from sites in the tropical Indian Ocean, with notes on the nature of growth increments in *Pristipomoides filamentosus*

Graham M. Pilling
MRAG Ltd.
47 Prince's Gate
London SW7 2QA, United Kingdom
E-mail address: g.pilling@ic.ac.uk

Richard S. Millner
Michael W. Easey
Fisheries Laboratory
CEFAS
Pakefield Road
Lowestoft NR33OHT, United Kingdom

Christopher C. Mees
MRAG Ltd.
47 Prince's Gate
London SW7 2QA, United Kingdom

Shyama Rathacharen
Albion Fisheries Research Centre
Albion, Petite Riviere, Mauritius

Roland Azemia
Seychelles Fishing Authority
P.O. Box 449
Victoria, Mahe, Seychelles

Abstract.—The lutjanids *Pristipomoides filamentosus* and *Aprion virescens* and the lethrinid *Lethrinus mahsena* are commercially important demersal bank and deep slope reef fish from the central Indian Ocean. To obtain von Bertalanffy growth parameter estimates for management purposes, length-based methods are commonly applied by the fisheries institutions of the region. Because the relatively long-lived, slow-growing nature of these species results in a lack of distinct modal progression in length-frequency data, such estimates are unreliable. In an attempt to obtain more reliable growth estimates, the feasibility of age-based methods (where age is determined from annual increments in otoliths) was investigated. Successful validation of annual or daily increments has been reported in two of these species (*P. filamentosus* and *A. virescens*), but not for the target areas of our study: the banks of the Seychelles and Mauritius.

A range of methods was used in an attempt to ensure that the otoliths fulfilled the criteria for use in aging. Two methods are described in this paper: back-calculation and a combination of marginal increment and edge analysis. The results of validation are presented, along with a description of the problems encountered. Marginal increment and edge analysis both indicated that the increments present in the otoliths of *L. mahsena* are annuli. For *A. virescens*, no pattern was present in the marginal increment analysis of older individuals. However, edge analysis offered evidence that the increments present in the otoliths were annuli. The combined marginal increment and edge analysis proved inconclusive for *P. filamentosus*; therefore the increments present in the otoliths of this species could not be validated. Conclusions are drawn regarding the justification of assuming periodicity of increments on the basis of validation achieved in other locations.

Manuscript accepted 4 January 2000.
Fish. Bull. 98:600–611 (2000).

Examination of hard body parts, such as otoliths, frequently reveals the presence of "rings." Laid down incrementally (whether daily, monthly, or annually), these structures provide a means of aging fish. For tropical species, however, the use of otoliths has become relatively common only since the early nineteen eighties (e.g. Loubens, 1978; Morales-Nin and Ralston, 1990; Ferreira and Russ, 1992; Francis et al., 1992; Milton et al., 1995; see also Manooch, 1987, and Fowler, 1995, for reviews). The lack of studies before this time is frequently attributed to the expectation that tropical fish grow consistently in an aseasonal environment. Hence hard parts in tropical fish species were not expected to contain internal structures that relate to fluctuations in growth resulting from the environment.

The physiological basis for the formation of distinct zones in calcified structures of tropical species has not been established conclusively (Ferreira and Russ, 1994). The formation of such zones has been associated with both abiotic and biotic factors (Beckman and Wilson, 1995), such as regular seasonal variances in water temperature (e.g. Reay, 1972; Panella, 1980), photoperiod, feeding, reproduction, and spawning period (e.g. Morales-Nin and Ralston, 1990)

"Indeterminate increments" (increments not related to the annual time scale) are found in all hard parts. These need to be distinguished from increments formed at regular intervals (Fowler and Doherty, 1992). Before increments can realistically be used for aging, they need to be "validated" (Beamish and McFarlane, 1983) to ensure that the structures, such as the otoliths used in our study, can be used as accurate chronometers. They must therefore fulfill a number of criteria (Fowler and Doherty, 1992): 1) the otolith must grow throughout the lifespan of the individual fish; 2) the otolith must show an internal incremental structure; and 3) this structure must correspond to a regular time scale.

Our study concentrated on macro-increments. Aging through micro-(daily)increment counts (e.g. Ralston and Miyamoto, 1983) requires considerable investment in time and equipment and is generally constrained to younger ages, where daily increments remain distinct. These contraints render such techniques unfeasible for stock assessment purposes, particularly in developing countries.

The local fisheries institutions in the study locations of the central Indian Ocean are, to date, limited to the use of length-based methods for aging fish. The results of these methods are felt to be uncertain when applied to long-lived, slow-growing species such as snappers and emperors, owing to modal overlap and a general absence of modal progression (e.g. Langi, 1990). Our study aimed to validate as annual the macro-increments seen in the sagittal otoliths of two species of snapper, *Aprion virescens* (Valenciennes 1830) and *Pristipomoides filamentosus* (Valenciennes 1830), and one species of emperor, *Lethrinus mahsena* (Forsskål, 1775). Validation of the annual nature of increments seen in the otoliths of these species would allow age-based methods of stock assessment to be applied to these commercially important demersal bank and deep-slope reef-fish species from the central Indian Ocean.

Compliance with the three criteria for validation was examined by using two methods: back-calculation (e.g. Manooch, 1987; Van Leewen and Rijnsdorp[1]) and a combination of marginal increment and edge analysis (e.g. Mason and Manooch, 1985; Manooch and Drennon, 1987; Manickchand-Heileman and Philipp, 1996). Back-calculation was used to test the validity of the first two criteria for aging. Marginal increment analysis and edge analysis were then used to validate mark periodicity, fulfilling the third criterion.

Materials and methods

Otoliths of the study species were obtained from commercial fish catches. In waters off both Mauritius and the Seychelles, fishing is frequently limited by rough seas during the SE trade wind period from May to October. Samples of *Lethrinus mahsena* were obtained during excursions of the Mauritian mothership-dory vessels on Nazareth Bank of the Mascarene Ridge (15°S, 61°E). On the Mauritian banks, this species composes about 80–90% of the total catch (Ardil, 1986; Bertrand[2]). In the Seychelles, fishing occurs from smaller vessels, which generally remain on the Mahé Plateau (05°S, 55°E). Otoliths from both *P. filamentosus* and *A. virescens* were obtained from this area.

Two methods were used to examine whether the otoliths fulfilled the requirements for aging: 1) back-calculation of growth from otolith increments; and 2) marginal increment and edge analysis. A general description of these methods is provided in Blacker (1974) and Williams and Bedford (1974).

Sagittal otoliths were selected for examination because a number of studies have used these structures to age snapper and emperor species successfully elsewhere (e.g. Manooch, 1982; Mason and Manooch, 1985; Morales-Nin, 1989; McPherson and Squire, 1992; Newman et al., 1996), including *Aprion virescens* and *Pristipomoides filamentosus* (Loubens, 1980; Ralston and Miyamoto, 1981, 1983).

One otolith from each fish was embedded in black polyester resin, and a 0.5-mm transverse section taken through the center ("nucleus") of the otolith by using a diamond cutting blade (Bedford, 1983). Sections were then either mounted in clear resin on a microscope slide or stained with acidified neutral red (Richter and McDermot, 1990) and left unmounted. Otoliths were examined with a Zeiss compound microscope equipped with zoom lens and magnification up to 60×. Reflected or transmitted light was used as necessary to identify and count the increments.

In our study, terminology was based on that recommended in Secor et al. (1995). The term "opaque zone" refers to the area that appeared milky under reflected light or dark under transmitted light in unstained samples.

Back-calculation of growth by means of otolith increments

For back-calculation, snapper otoliths were most easily assessed unstained, whereas *L. mahsena* otoliths were most easily assessed stained. Only otoliths that showed clear increment patterns were used for measurements; as a result, seven *A. virescens* otoliths, in which it was difficult to distinguish the first or second increment, were omitted from the samples. Measurements of the total otolith radius, from the nucleus to outside edge, and the distance along the selected growth axis between suspected annual increments were made with the tools described in Millner and Whiting (1996). Unstained *P. filamentosus* and *A. virescens* otoliths were assessed along a growth axis close to the sulcus acousticus (Figs. 1 and 2). This area provides the most consistent and easily interpretable

[1] Van Leeuwen, P. I., and A. D. Rijnsdorp. 1986. The analysis of the growth of turbot by back-calculation of otoliths. ICES Council Meeting 1986/G:50

[2] Bertrand, J. 1986. Pour une evaluation des resources en capitaine/dame berri (*Lethrinus mahsena*) des bancs de Saya de Malha. *In* Rapport du Groupe Travaile, French Institute of Research and Exploitation of the Sea (IFREMER)/Albion Fisheries Research Centre (Mauritius). 23–25 Juillet 1985, 39 p. [Available from Albion Fisheries Research Centre, Albion, Petite Riviere, Mauritius.]

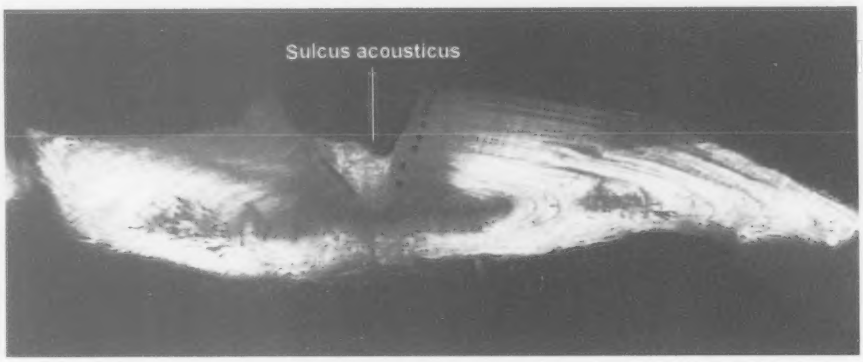

Figure 1

Unstained transverse 0.5-mm section through the sagittal otolith of *P. filamentosus* from Seychelles, viewed with transmitted light. Magnification: 16×. Black dots along sulcus acousticus mark are suspected annual increments.

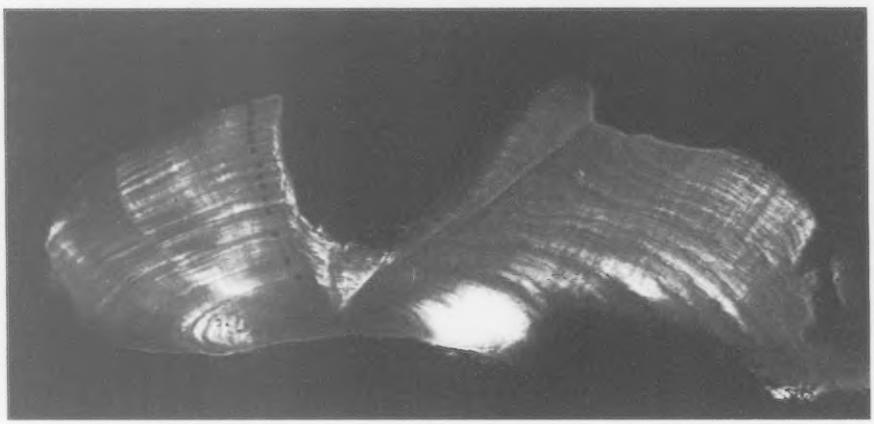

Figure 2

Unstained transverse 0.5-mm section through the sagittal otolith of *A. virescens* from Seychelles, viewed with transmitted light. Magnification: 32×. Black dots along sulcus acousticus mark are suspected annual increments.

incremental pattern. Measurements on stained *L. mahsena* otoliths were performed out to the tip of the dorsal lobe, at approximately 90° to the *sulcus* (Fig. 3). In all species, when the increment structure became too closely spaced to measure individual increments accurately, the thickness of further increments was estimated by interpolation based on the remaining distance from the last measured increment to the outside edge of the otolith, the number of years expected in this zone, and the pattern found in the previous increment widths.

Following the recommendations of Francis (1990) and Ricker (1992), we calculated the geometric mean regression (GMR) of fork length at capture from otolith radius at capture for each species. Back-calculated lengths-at-age for each individual were then derived with the following formula (Ricker, 1992):

$$FL_i = \left(\frac{FL_c - b}{O_c} \times O_i \right) \div b,$$

where Fl_i = the estimated fork length at age i;
Fl_c = the fork length at capture;
O_c = the otolith radius at capture;

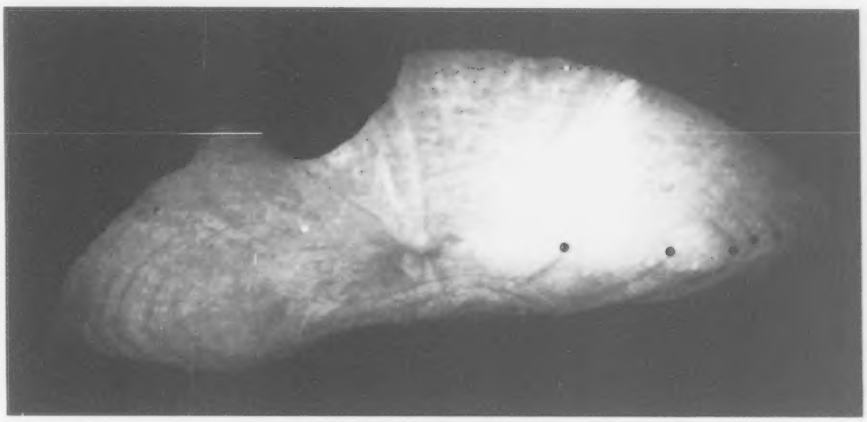

Figure 3

Transverse 0.5-mm section through the sagittal otolith of *L. mahsena* from Mauritius (Nazareth bank), stained with acidified neutral red (see text), and viewed with reflected light. Magnification: 23×. Black dots mark are suspected annual increments.

O_i = the otolith radius at age i; and
b = the intercept of the GMR calculated with the Ricker procedure.

For each species, a von Bertalanffy growth curve was fitted to the back-calculated mean length at age through least squares estimation.

Marginal increment analysis

The thickness of the outer zone in the otoliths was measured by using the image analysis system (see Millner and Whiting, 1996). Measurements were taken from the inside edge (start) of the last opaque band and the edge of the otolith. In stained *L. mahsena* otoliths (indeed in all three study species where otoliths were stained; see "Edge analysis," below), a band was stained on the border between the end of the "translucent zone," and the start of the next opaque zone. Measurements from the last stained band were therefore equivalent to those made for the snapper species. Because zones at the edge of sections taken from the unstained otoliths of both snapper species were not distinct, an average of four measurements was taken in the region of the sulcus (where zones were more easily distinguished). Zones at the edge of the stained *L. mahsena* otolith sections were clearly visible and, therefore, it was possible to obtain a single measurement along the same growth axis as that used for back-calculation.

The pattern expected in the marginal increment resulting from the development of an annual increment would be a minimal marginal increment at the start of the growth period, increasing with time until the measurement fell to a minimum again at the formation of the next period of growth.

The size of the growth zone varies both with time of sampling during the year and the age of the fish. Because younger fish grow faster than older individuals, a larger marginal increment is expected. For this reason, quantitative marginal increment analyses should be standardized for age. Our study was therefore carried out by age class. Owing to the wide range of ages encountered, however, there were insufficient samples to accomplish this standardization fully. It was necessary to combine the ages into two or three groups representing fast, moderate, and slow-growing individuals (Table 1). These classes were based on the growth curves derived from back-calculation, and hence on the assumption that the increments represented annual growth.

For *P. filamentosus*, because sample sizes were either small or because samples could not be obtained in specific months, data were grouped into bimonthly time periods. Sufficient *L. mahsena* and *A. virescens* samples were available to allow the analysis to occur on a monthly basis. For all three species, a mean marginal increment for each time period and growth category was calculated.

Edge analysis

The type of zone at the growing edge of the otolith was identified in each month of the year. Annuli were traceable as a developing single translucent and opaque zone on the edge of the otolith during that growth year.

Problems were encountered in identifying the edge type in unstained *P. filamentosus* and *A. virescens* from Seychelles because of poor resolution of the banding in otoliths, and what appeared to have been the seepage of resin either under or through the edge of the otolith. Staining trials were performed in an attempt to clarify the growth type at the edge of the otolith in these species, and stained otoliths were subsequently examined during edge analysis.

Thin sections of the stained otoliths were assessed for the presence of the band of stain on the growing tip of the

dorsal lobe. The percentage of otoliths with a stained band at the growing tip was calculated for each month. Although an extended data set was available for edge analysis, as a result of the seasonal nature of the Seychelles and Mauritius fisheries, sample sizes were either small or not available for certain months.

Results

Based on the assumption that the increments seen in the otoliths were annual, the length and age range of individuals from each species examined in each method is presented in Table 2. The sample size is also shown.

A greater number of samples were examined during edge analysis. This method was less intensive than that required for either back-calculation or marginal increment analysis, allowing more samples to be examined during the period of study and increased the range of lengths and ages examined.

Table 1

Age groups selected for marginal increment analysis, by species.

Species	Growth group	Age class (years)
L. mahsena	Fast	1–5
	Slow	6+
A. virescens	Fast	3–5
	Slow	6+
P. filamentosus	Fast	3–5
	Moderate	6–10
	Slow	11+

Back-calculation

A linear relationship existed between the fork length and otolith radius of fish in all three species, to which the geometric mean regression (GMR) of fork length from otolith radius was fitted (Figs. 4–6).

The von Bertalanffy growth parameters derived from mean back-calculated length-at-age data from *A. virescens*, *P. filamentosus* and *L. mahsena* are shown in Table 3. Initial L_∞ estimates for *L. mahsena* were low compared with the maximum lengths seen in length-frequency distributions from the region (52 cm). The asymptotic length, L_∞, was therefore constrained to levels in keeping with the maximum length found in the distributions, and the remaining von Bertalanffy growth parameters were re-estimated.

For the snapper species, both L_∞ and K estimates derived from the back-calculated length-at-age data were lower than those historical estimates derived with length-based methods. For *L. mahsena*, constraining L_∞ to a level in keeping with the maximum length found in catches resulted in estimates of K comparable to those estimated by Bautil and Samboo (1988).

Marginal increment and edge analysis

The number of individuals examined in marginal increment analysis are presented in Table 4 by species and time period.

Because the region between translucent and opaque zones took up the stain, the presence of a stained area at the otolith edge during edge analysis indicated the start of opaque band formation.

Table 2

The length range, age range, and sample size of individuals examined by method and species. Ages are based on the assumption that the increments identified in the otoliths are annuli.

	Method		
Species	Back-calculation	Marginal increment analysis	Edge analysis
L. mahensa			
Lenth range (cm)	22–42	22–42	20–50
Age range (yr)	3–14	3–14	3–16
n	222	220	568
A. virescens			
Lenth range (cm)	37–87	37–87	30–99
Age range (yr)	3–19	3–19	3–27
n	81	141	1259
P. filamentosus			
Lenth range (cm)	22–73	22–73	—
Age range (yr)	3–30	3–30	—
n	85	242	—

L. mahsena Marginal increment analysis indicated an overall increase in the marginal increment between January and May, falling in August (Fig. 7). This pattern was clearest in the younger, faster-growing growth group. A unimodal distribution was found in the plot of the proportion of stained edges found in each month, as well as a high proportion of individuals showing opaque growth commencing between May and August (Fig. 8).

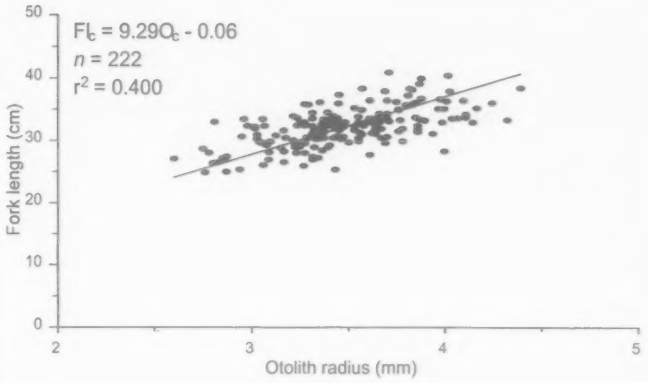

Figure 4

Geometric mean regression of fork length (cm) from otolith radius (mm) for *L. mahsena*.

A. virescens With relatively few samples at certain key times during the year, patterns in the marginal increment could not be identified clearly (Table 4). The width of the outer zone increased until June in younger, faster-growing individuals. In subsequent months, a lack of samples prevented the identification of an indicative pattern (Fig. 9). No pattern was found in the marginal increment of older individuals. Staining improved the clarity of the type of growth present on the edge of the otolith. Edge analysis of these specimens showed a unimodal distribution of the percentage of stained edges by month. A high proportion of individuals exhibited opaque zone formation in the period between October and March (Fig. 10).

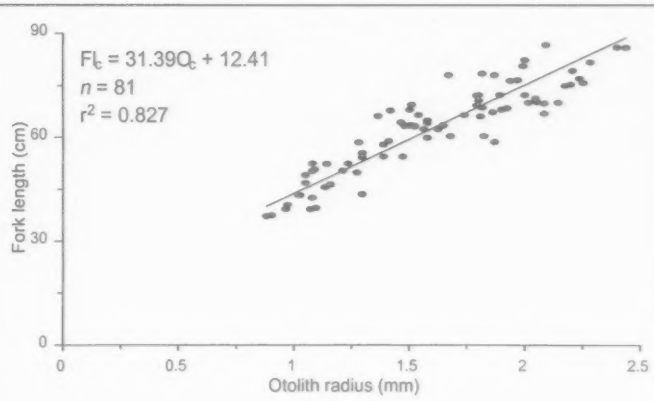

Figure 5

Geometric mean regression of fork length (cm) from otolith radius (mm) for *A. virescens*.

P. filamentosus No overall pattern of increase in the marginal increment was found (Fig. 11). This result was partly due to the lack of samples in the months of May and June. The legibility of the increments in the otoliths of this species was poor, and staining failed to improve the clarity of the otolith zones. Edge analysis was confused by indeterminate increments formed in the translucent growth period. Their presence on the edge of the stained otolith at the time of capture led to the misidentification of opaque zone formation and thus confused the identification of an overall pattern. As a result, validation could not be achieved with this method.

Discussion

Back-calculation indicated that there was a direct linear relationship between fork length and otolith radius. The otoliths of each species showed an internal structure, with increments widely spaced near the nucleus and narrower and more evenly spaced toward the edge. Growth curves derived from back-calculated length-at-age data indicated an exponential decrease in increment width with assumed increasing age. The otoliths of the three species therefore fulfilled the first two criteria for their use in aging, at least over the age range seen in the samples, in that the otolith grew throughout the life of the fish and showed an internal structure of increments. The pattern in *P. filamentosus* was, however, confused by the presence of indeterminate increments.

Confirmation of the third criterion (that increments seen in the otoliths corresponded to a regular time scale) was not demonstrated so readily. Validation could not occur through methods such as tetracycline injection owing to practical limitations imposed by the fisheries and to the depths inhabited by certain species. *Pristipomoides filamentosus*, for example, is caught at over 75 m depth. The majority of specimens would be dead or heavily stressed through barotrauma on reaching the surface (DeMartini et al., 1996) and useless for tagging programs. Marginal increment and edge analysis was therefore used.

Some evidence for the annual nature of the increments seen in the otoliths of *L. mahsena* was found in the pattern of the marginal increment through the year (Fig. 7). This evidence was confirmed by the unimodal distribution resulting from edge analysis (Fig. 8), indicating that opaque band formation was initiated once a year, from May to August.

For *A. virescens*, identification of the pattern in marginal increments (Fig. 9) was confused by the poor resolution of the unstained sections and the relatively small samples sizes, rendering the results inconclusive. However, the unimodal plot resulting from edge analysis on stained specimens from this species indicated that the transition between the translucent and opaque bands occurred once a year (Fig. 10), between October and March.

From this evidence, we considered the increments seen in the otoliths of both *L. mahsena* from Mauritius and *A. virescens* from Seychelles validated as annual deposits.

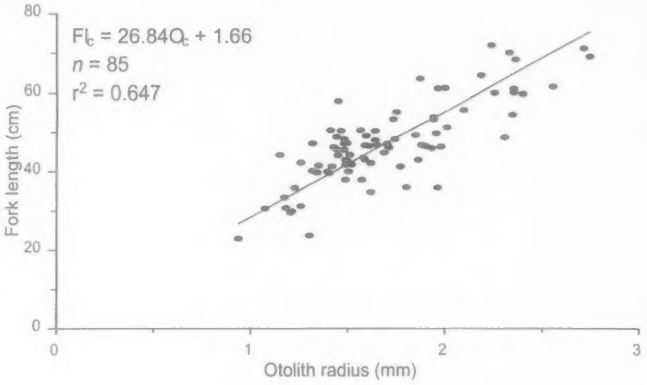

Figure 6

Geometric mean regression of fork length (cm) from otolith radius (mm) for *P. filamentosus*.

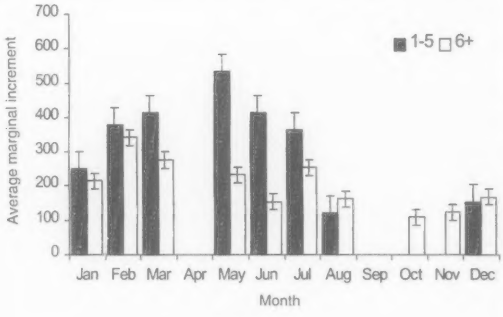

Figure 7

Marginal increment plot by month for *L. mahsena*. Marginal increment measured in VID units (pixels). Data segregated as in Table 1. Error bars denote one standard error.

Opaque zone deposition is thought to occur during periods of increased growth, whereas the corresponding "translucent zone" is formed during periods of low metabolic activity (Beckman and Wilson, 1995). The period of opaque zone initiation in *L. mahsena* from the Mauritian bank, from May to August, corresponded to the season of the southeast trade winds, a period of rough weather. The period of opaque zone deposition in *A. virescens* from Seychelles, from October to March, coincided with the northwest monsoon season from mid-November to mid-March.

In reviews of otolith studies in tropical latitudes, Beckman and Wilson (1995) and Fowler (1995) found that, for the majority of tropical species studied, the period of opaque growth coincided with spring and summer months, as seen in *L. mahsena* from the Mauritian bank. *Aprion virescens* from Seychelles appears to contradict this general pattern its opaque zone formation begins during winter months. The authors also performed edge analysis studies for 1090 *L. mahsena* individuals from Seychelles (not presented). These studies indicated that in this area, *L. mahsena* also exhibits opaque zone initiation during winter. Of the twenty-nine tropical species reviewed by Fowler (1995), only four showed opaque zone formation in the winter period. Timing of opaque zone formation in these two species may be driven by local phenomena. If opaque zone formation is linked with increased food availability, the monsoon periods experienced in Seychelles at this time, combined with local upwelling, may improve local productivity and feeding conditions. Although little empirical data exist to support this theory, algal blooms have been identified around Seychelles at this time of year.[3]

Although edge analysis indicated differences in the timing of opaque zone deposition at Nazareth bank (Mauritius), and Seychelles (Figs. 8 and 10), patterns in the marginal increment analysis for these locations were similar (Figs. 7 and 9). This similarity may result from the relatively small data sets available for marginal increment analysis, requiring ages to be grouped into age classes, and the difficulty experienced in measuring the marginal increment in *A. virescens* otoliths from Seychelles. Similarities may therefore result from inadequacies in the data that obscure the true pattern.

The results of marginal increment analysis for *P. filamentosus* were inconclusive because problems were experienced in identifying and measuring the outer zone in the otolith. Staining did not improve the clarity of the zones owing to the frequent appearance of "indeterminate increments." Validation was therefore considered to be unsuccessful for *P. filamentosus* in Seychelles and contrasts with that achieved in Hawaii where microincrements were used (Ralston and Miyamoto, 1981, 1983). During our study, ini-

[3] Tarbit, J. 1980. Demersal trawling in Seychelles waters. Fisheries Bulletin 5, Fisheries Division, Seychelles. Seychelles Fishing Authority, P.O. Box 449, Victoria, Mahé, Seychelles.

Table 3

Von Bertalanffy growth parameters estimated from back-calculated length data and published sources. Method: L = parameters derived through length-based methods, O = parameters derived from otoliths.

Species	K	L_∞ (FL)	n	Method	Reference
P. filamentosus	0.11	62.3	85	O	Our study
	0.29	81.7	—	L	Mees (1993)
	0.24	75.8	—	L	Mees and Rousseau (1997)
	0.146	78	—	O	Ralston and Miyamoto (1983)
	0.33–0.36	78-86	—	O	Hardman-Mountford et al. (1997)
A. virescens	0.13	79.0	81	O	Our study
	0.32	95-104	—	L	Mees (1993)
	0.31	65.6	—	O	Loubens (1980)
L. mahsena	0.38	34.1	222	O	Our study
	0.09	52.0	222	O	Our study, L_∞ = 52 cm
	0.1	61.7	—	L	Bautil and Samboo, (1988)
	0.32	58.9	—	L	Dalzell et al. (1992)

Table 4

Numbers of individuals examined for marginal increment analysis by monthly (*L. mahsena* and *A. virescens*) or bimonthly (*P. filamentosus*) interval.

	Age class						
	L. mahsena		*A. virescens*		*P. filamentosus*		
Month	1–5 yr	6+ yr	3–5 yr	6+ yr	3–5 yr	6–10 yr	11+ yr
Jan	14	8	—	4	95	29	20
Feb	13	5	—	—			
Mar	19	5	4	8	—	16	18
Apr	—	—	3	15			
May	15	9	10	17	—	—	—
Jun	4	11	6	11			
Jul	15	8	10	—	8	—	4
Aug	21	4	5	6			
Sep	—	—	—	8	11	19	5
Oct	—	17	—	4			
Nov	—	19	6	16	—	7	10
Dec	13	20	—	8			

tial examination of *P. filamentosus* otoliths was performed by using scanning electron microscopy, in an attempt to validate the "suspected" annuli through micro-increment counts (Brothers and Mathews, 1987). Unlike the results reported from studies in Hawaii, no consistent pattern of micro-increments was found, although it should be noted that our study was very limited in scope (n=4). Hardman-Mountford et al. (1997), also using specimens from the Seychelles, related assumed "monthly increments" to assumed annuli, finding approximately 12.4 monthly increments within each annual increment. Consistent banding of this type could not be found during our study for specimens collected from the same region, even though we had a larger sample size.

The lack of consistent annual increments in *P. filamentosus* may be due to the biology of the species. Spawning occurs throughout the year, with two peaks (Mees, 1993), and may not provide a sufficient stimulus for zone formation. *Pristipomoides filamentosus* is found at greater depths (between 75 and 150 m) than the other study species (around 30 m) in conditions that may be buffered against environmental change. Hardman-Mountford et. al. (1997), however, indicated that the 20–24.5°C temperature range at this depth (Mees, 1993) is sufficient to leave

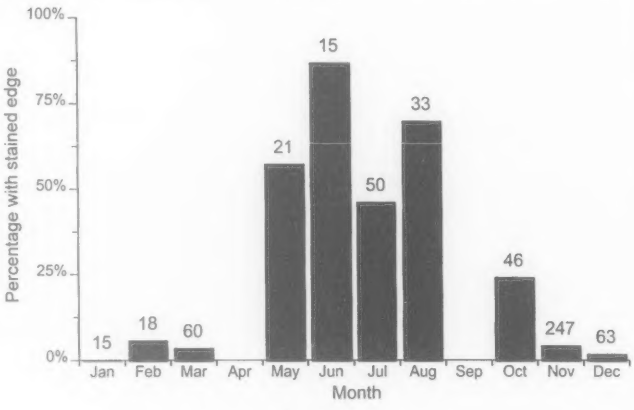

Figure 8

Proportion of *L. mahsena* otoliths with stained edges on the growing tip of the dorsal lobe, by month. Numbers denote sample size.

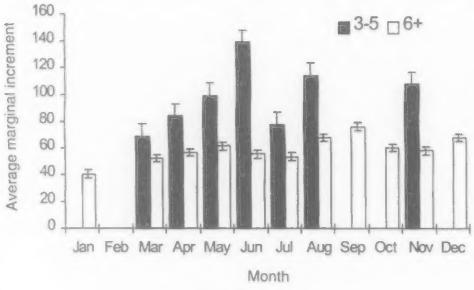

Figure 9

Marginal increment plot by month for *A. virescens*. Marginal increment measured in VID units (pixels). Data segregated as in Table 1. Error bars denote one standard error.

increments on scales in some species (Chey, 1933, in Panella, 1980). If this species is sensitive to relatively small changes in temperature, currents, food supply or food quality, relatively short periods of fluctuation in these factors may result in frequent "indeterminate increments." Even if validation had been achieved, *P. filamentosus* otoliths appear unsuitable for routine aging procedures owing to the difficulties in differentiating periodic increments from other increments not related to a regular time scale.

These difficulties highlight the dangers in assuming the periodicity of increments in otoliths on the basis of validation of that species or a similar species in another location (e.g. Smith and Kostlan, 1991) and also identify the need for thorough validation studies. For example, our study indicated that the assumption of annual, and possibly daily periodicity for increments in the otoliths for *P. filamentosus* in Seychelles, based on published data, would have been incorrect.

Published work (e.g. Sparre and Venema, 1998) suggests that consistent periodic increments do not form in otoliths of tropical species; this is particularly so in the case of low-latitude species. The validation results obtained by our study contrast sharply with this view; indeed, our results add to the expanding number of tropical species for which the validation of annual increments has been successful.

The results of models used in fisheries management, e.g. analytical yield per recruit models (Beverton and Holt, 1957), are sensitive to uncertainty in the estimates of input parameters such as the von Bertalanffy growth parameters (Mees and Rousseau, 1997). Current estimates of growth and mortality in fish in Seychelles and Mauritius

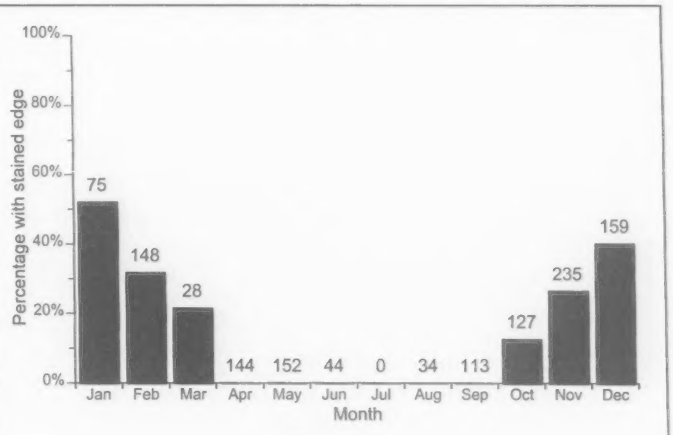

Figure 10

Proportion of *A. virescens* otoliths with stained edge on the growing tip of the dorsal lobe, by month. Numbers denote sample size.

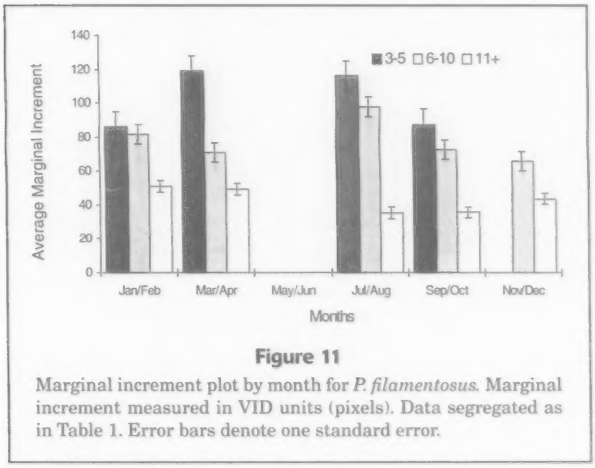

Figure 11

Marginal increment plot by month for *P. filamentosus*. Marginal increment measured in VID units (pixels). Data segregated as in Table 1. Error bars denote one standard error.

are derived through length-based methods, which for long-lived, slow growing species are considered uncertain. The preliminary back-calculated growth parameters from our study are the first otolith-based estimates of growth for the study species at these particular locations. Although these estimates are not definitive, they do suggest that current length-based growth estimates for *A. virescens* may have overestimated mean growth rate and asymptotic length. For *L. mahsena*, growth rate may have been underestimated, and asymptotic length overestimated. However, by constraining the value of L_∞ to levels in keeping with the maximum size found in length distributions from the region (52 cm), we obtained a similar growth rate to that identified by Bautil and Samboo (1988). If snappers do indeed have a longer life span than that indicated by length-based assessments, they may be more vulnerable to overfishing than previously thought. Future work will involve the estimation of more definitive growth parameters based on length-at-age data derived from otoliths.

Acknowledgments

The authors wish to thank the Directors and staff of CEFAS, Albion Fisheries Research Centre and the Seychelles Fishing Authority who collaborated on this project and provided the data necessary for this analysis. Three anonymous reviewers are thanked for their helpful comments on the manuscript. The project to which this paper relates was funded by the Department for International Development of the UK through the Fisheries Management Science Programme.

Literature cited

Ardil, J. D.
1986. Current status of the fishery in Mauritius. Food and Agriculture Organisation of the United Nations (FAO) Southwest Indian Ocean Project (SWIOP) document RAF/79/065/WP/37/87/E, 30 p.

Bautil, B., and C. R. Samboo.
1988. Preliminary stock assessment for the Mahsena emperor (*Lethrinus mahsena*) on the Nazareth Bank of Mauritius. *In* Proceedings of the workshop on the assessment of the fishery resources in the southwest Indian Ocean (M. J. Sanders, P. Sparre, and S. C. Venema, eds.), p. 260–267.

Beamish, R. J., and G. McFarlane.
1983. The forgotten requirement for age validation in fisheries biology. Trans. Am. Fish. Soc. 112:735–743.

Beckman, D. W., and C. A. Wilson.
1995. Seasonal timing of opaque zone formation in fish otoliths. *In* Recent developments in fish otolith research, no. 19 (D. H. Secor, J. M. Dean, and S. E. Campana, eds.), p. 27–43. The Bella W Baruch Library in Marine Science.

Bedford, B. C.
1983. A method for preparing sections of large numbers of otoliths embedded in black polyester resin. J. Cons. Int. Explor. Mer 41:4–12.

Beverton, R. J. H., and S. J. Holt.
1957. On the dynamics of exploited fish populations. Fish. Invest. Minist. Agric. Fish. Food GB (2 Sea Fish.) 19, 533 p.

Blacker, R. W.
1974. Recent advances in otolith studies. *In* Sea fisheries research (R. Harden-Jones, ed.), p 67–90. Elek Science, London.

Brothers, E. B., and C. P. Mathews.
1987. Application of otolith microstructural studies to age determination of some commercially valuable fish of the Arabian Gulf. Kuwait Bull. Mar. Sci. 9:127–157.

Dalzell, P., S. Sharma, and G. Naith.
1992. Estimation of exploitation rates in a multispecies emperor (Pisces: Lethrinidae) fishery in Fiji, based on length frequency data. *In* Papers on fisheries science from the Pacific Islands, vol. 1: Inshore fisheries research project, technical document 1, p. 43–50. South Pacific Commission, Noumea, New Caledonia.

DeMartini, E. E., F. A. Parrish, and D. M. Ellis.
1996. Barotrauma-associated regurgitation of food: implications for diet studies of Hawaiian pink snapper, *Pristipomoides filamentosus* (Family: Lutjanidae). Fish. Bull. 94:250–256.

Ferreira, B. P., and G. R. Russ.
1992. Age, growth and mortality of the inshore coral trout *Plectropomus maculatus* (Pisces: Serranidae) from the central Great Barrier Reef, Australia. Aust. J. Mar. Freshwater Res. 43:1301–1312.
1994. Age validation and estimation of growth rate of the coral trout *Plectropomus leopardus* from Lizard Island, Northern Great Barrier Reef. Fish. Bull. 92:46–57

Fowler, A. J.
1995. Annulus formation in otoliths of coral reef fish—a review. *In* Recent developments in fish otolith research, vol. 19 (D. H. Secor, J. M. Dean, and S. E. Campana, eds), p. 46–63. The Bella W Baruch Library in Marine Sciences.

Fowler, A. J., and P. J. Doherty.
1992. Validation of annual growth increments in the otoliths of two species of damselfish from the southern Great Barrier Reef. Aust. J. Mar. Freshwater Res. 43:1057–1068.

Francis, R. I. C. C.
1990. Back-calculation of fish length—a critical review. J. Fish Biol.:883–902.

Francis, R. I. C. C., L. J. Paul, and K. P. Mulligan.
1992. Ageing of adult snapper (*Pagrus auratus*) from otolith annual ring counts: validation by tagging and oxytetracycline injection. Aust. J. Mar. Freshwater Res. 43: 1069–1089.

Hardman-Mountford, N. J., N. V. C. Polunin, and D. Boullé.
1997. Can the age of tropical species be determined by otolith measurement? A study using *Pristipomoides filamentosus* (Pisces: Lutjanidae) from the Mahé Plateau, Seychelles. Naga 20:27–31.

Langi, S.
1990. The applicability of ELEFAN for use in analysing three species of deep-sea snappers (*Etelis corruscans*, *Pristipomoides flavipinnis* and *P. filamentosus*, Family Lutjanidae). Fishbyte 8(1):21–25.

Loubens, G.
1978. Biologie de quelque especes de poisson du lagon Neo-Caledonien. I. Determination de l'age (otolithometrie). Cahiers ORSTOM, Series Oceanographie 16:263–283.
1980. Biologie de quelques especes de poissons du lagon Neo-Caledonien III. Croissance. Cal. Indo-Pac. 2:101–153.

Manickchand-Heileman, S. C., and D. A. T. Philipp.
1996. Reproduction, age and growth of the Caribbean red snapper (*Lutjanus purpureus*) in waters off Trinidad and Tobago. *In* Biology, fisheries and culture of tropical groupers and snappers (F. Arreguín-Sánchez, J. L. Munro, M. C. Balgos, D. Pauly, eds.), p. 137–149. ICLARM, Manila, Philippines.

Manooch, C. S.
1982. Ageing reef fishes in the Southeast fisheries centre. *In* The biological basis for reef fishery management: proceedings of a workshop held October 7–10, 1980 at St. Thomas, Virgin Islands of the Unites States (G. R. Huntsman, W. R. Nicholson, and W. W. Fox, eds.), p. 24–43. U.S. Dep. Commer., NOAA, Beaufort, North Carolina 28516.
1987. Age and growth of snappers and groupers. *In* Tropical snappers and groupers: biology and fisheries management (J. J. Polovina and S. Ralston, eds.), p. 329–363. Westview Press Inc., Boulder, CO.

Manooch, C. S., and C. L. Drennon.
1987. Age and growth of yellowtail snapper and queen triggerfish collected from the US Virgin Islands and Puerto Rico. Fish. Res. 6:53–68.

Mason, D. L., and C. S. Manooch.
1985. Age and growth of the mutton snapper along the east coast of Florida. Fish. Res. 3: 92–104.

McPherson, G. R., and L. Squire.
1992. Age and growth of three dominant *Lutjanus* species of the Great Barrier Reef inter-reef fishery. Asian Fish Sci. 5 (1):25–36.

Mees, C. C.
1993. Population biology and stock assessment of *Pristipomoides filamentosus* on the Mahé Plateau, Seychelles. J. Fish Biol. 43:695–708.

Mees, C. C., and J. A. Rousseau.
1997. The potential yield of the lutjanid fish *Pristipomoides filamentosus* from the Mahé Plateau, Seychelles: Managing with uncertainty. Fish. Res. 33:73–87.

Millner, R. S., and C. L. Whiting.
1996. Long-term changes in growth and population abundance of sole in the North Sea from 1940 to the present. ICES J. Mar. Sci. 53:1185–1195.

Milton, D. A., S. A. Short, M. F. O'Niell, and S. J. M. Blaber.
1995. Ageing of three species of tropical snapper (Lutjanidae) from the Gulf of Carpentaria, Australia, using radiometry and otolith ring counts. Fish. Bull. 93(1):103–115.

Morales-Nin, B.
1989. Growth determination of tropical marine fishes by means of otolith interpretation and length frequency analysis. Aquatic Living Resources Nantes 2:241–253.

Morales-Nin, B., and S. Ralston.
1990. Age and growth of *Lutjanus kasmira* (Forsskål) in Hawaiian waters. J. Fish Biol. 36(2):191–203.

Newman, S. J., D. M. Williams, and G. R. Russ.
1996. Age validation, growth and mortality estimates of the tropical snappers *Lutjanus adetii* and *L. quinquelineatus* from the Central Great Barrier Reef, Australia. Mar. Freshwater Res. 47:575–584.

Panella, G.
1980. Growth patterns in fish sagittae. *In* Skeletal growth of aquatic organisms (D. C. Rhoads and R. A. Lutz, eds.), p. 519–560. Plenam Press, New York, NY.

Ralston, S., and G. T. Miyamoto.
1981. Estimation of the age of a tropical reef fish using the density of daily growth increments. *In* The reef and man (E. D. Gomez, C. E. Birkeland, R. W. Buddemeier, R. E. Johannes, J. A. Marsh, and R. T. Tsuda, eds.), p. 83–88. Proceedings of the fourth international coral reef symposium, Manila, 1981, vol. 1.
1983. Analyzing the width of daily otolith increments to age the Hawaiian snapper, *Pristipomoides filamentosus*. Fish. Bull. 81(3):523–535.

Reay, P. J.
1972. The seasonal pattern of otolith growth and its application to back-calculation studies in *Ammodytes tobianus*. J. Cons. P. Int. Explor. Mer 34:485–504.

Richter, H., and J. G. McDermot.
1990. The staining of fish otoliths for age determination. J. Fish Biol. 36:773–779.

Ricker, W. E.
1992. Back-calculation of fish lengths based on proportionality between scale and length measurements. Can. J. Fish. Aquat. Sci. 49:1018–1026.

Secor, D. H., J. M. Dean, and S. E. Campana.
1995. Recent developments in fish otolith research. Belle W. Baruch library in marine science no. 19, South Carolina Press, Columbia, SC, 735 p.

Smith, M. K., and E. Kostlan.
1991. Estimates of age and growth of Ehu *Etelis carbunculus* in four regions of the Pacific from density of daily increments in otoliths. Fish. Bull. 89:461–472.

Sparre, P., and S. C. Venema.
1998. Introduction to tropical fish stock assessment. Part 1, Manual, FAO Fisheries Technical Paper 306.1, rev 2. FAO, Rome, 407 p.

Williams, T., and B. C. Bedford.
1974. The use of otoliths for age determination. *In* Ageing of fish (T. B. Bagenal, ed.), p. 114–123. Unwin, Surrey, UK.

Age, growth, maturation, and protandric sex reversal in common snook, *Centropomus undecimalis*, from the east and west coasts of South Florida

Ronald G. Taylor
Florida Fish and Wildlife Conservation Commission
Florida Marine Research Institute
100 Eighth Avenue SE
St. Petersburg, Florida 33701-5095
E-mail address: ron.taylor@fwc.state.fl.us

James A. Whittington
Florida Fish and Wildlife Conservation Commission
Tequesta Field Laboratory
Florida Marine Research Institute
19100 SE Federal Highway
Tequesta, Florida 33469

Harry J. Grier
Florida Fish and Wildlife Conservation Commission
Stock Enhancement Research Facility
Florida Marine Research Institute
14495 Harllee Road
Port Manatee, Florida 34221

Roy E. Crabtree
National Marine Fisheries Service, F/SER23
9721 Executive Center Drive North
St. Petersburg, Florida 33702

Abstract.—During 1986–91, we examined 2088 common snook, *Centropomus undecimalis*, captured in Jupiter and Lake Worth inlets and adjacent waters on the east coast of Florida and 1784 common snook captured in Tampa Bay on the west coast of Florida. Of fish that were sexed, females ranged in length from 397 to 1105 mm FL, and males ranged from 124 to 925 mm FL. East coast fish were larger overall than west coast fish. Age of common snook was determined from sectioned otoliths. Results from the return of 80 oxytetracycline-marked otoliths combined with analyses of monthly patterns in marginal increments and the percentage of otoliths with an annulus on the edge, demonstrated that a single annulus is formed each year. Common snook can live to 21 years, but most of the fish in our sample were from 1 to 7 years old. The von Bertalanffy growth models were significantly different ($P<0.001$) for each coast and suggested that east coast snook grow faster than west coast snook. Common snook are protandric hermaphrodites. The gonads of 27 transitional specimens contained both degenerating spermatogenic and developing ovarian tissue, and sex reversal was observed in captive common snook. Common snook sex ratios and length-frequency distributions were also consistent with a diagnosis of protandric hermaphroditism. Females smaller than 500 mm FL were uncommon, and only one female less than 400 mm long was captured. The predicted lengths and ages at which 50% of the fish in the population would be females were 767 mm FL and 7.4 years for the east coast and 608 mm FL and 5.1 years for the west coast. Some males on both coasts were sexually mature at lengths less than 200 mm FL and at age 0; most age-1 males were mature on both coasts. All females were considered mature because they were derived from post-spawning males.

Manuscript accepted 6 January 2000.
Fish. Bull. 98:612–624 (2000).

Common snook, *Centropomus undecimalis*, (Perciformes: Centropomidae) are valuable euryhaline fishes that inhabit tropical and subtropical estuarine systems of the western Atlantic. They are abundant off the east coast of Florida from Cape Canaveral southward around the peninsula to Cedar Key off the west coast. They also inhabit waters off Galveston, Texas, south to Rio de Janeiro, Brazil (Gilmore et al., 1983; Rivas, 1986). They are commercially exploited throughout most of their range, except in Texas and Florida where they traditionally have supported large recreational fisheries (Matlock and Osburn, 1987). Snook are stenothermic: their northern range is limited by the winter 15°C isotherm (Shafland and Foote, 1983), similar to the distribution of mangroves which is their principal habitat (Marshall, 1958; Gilmore et al., 1983). Genetic studies of the stock structure suggest that in Florida, east coast and west coast populations are separate stocks (Tringali and Bert, 1996).

Anglers target common snook because of their fighting ability and culinary value (Tucker et al., 1985; Matlock and Osburn, 1987), and concerns about overfishing have resulted in a long history of regulation of the fishery off Florida (Bruger and Haddad, 1986). Size limits were first imposed on the fishery in 1953, and the sale of common snook in Florida has been prohibited since 1956. In 1994, a management goal was established to maintain a minimum spawning potential ratio (SPR) of 40% for

common snook stocks (Muller and Murphy[1]). In 1998, the Florida Marine Fisheries Commission enacted the current restrictive regulations to reduce the harvest of snook from Florida waters to maintain a 40% SPR.

Our study examined age, growth, maturation, and sex reversal of common snook which previously had not been diagnosed as being protandrous hermaphrodites. Earlier studies derived ages from either scales or whole otoliths, and ages were poorly validated (Volpe, 1959; Thue et al.[2]). Since these reports, studies on a variety of species have shown that scales are not reliable for aging long-lived fishes and that scale-derived and whole-otolith–derived age estimates are often lower than the validated estimates derived from sectioned otoliths (Beamish and McFarlane, 1983; Casselman, 1983; Lowerre-Barbieri et al., 1994; Crabtree et al., 1996). A validated method for aging snook is necessary to assess previous estimates of growth rates, mortality, and longevity. Our objectives were to describe validated aging techniques, length and age composition, and length and age at maturity of common snook populations from the east and west coasts of Florida. We also diagnosed common snook as protandrous hermaphrodites.

Methods

On the east coast of Florida, common snook were collected with hook-and-line gear during June–August 1987–91 in Sebastian, Jupiter, and Lake Worth Inlets. Young-of-the-year and juvenile common snook were collected on both coasts during April and May in 1989 and 1990 with a 3-m cast net (19-mm stretched mesh) from protected backwaters of coastal rivers. In December 1989, dead or moribund snook that had succumbed to low water temperatures were collected on both coasts. A detailed description of additional collections made with various nets on both coasts may be found in Taylor et al., 1998. Data, otoliths, and gonads collected and used in that study were used in the present study.

In the laboratory, total length (TL), fork length (FL), and standard length (SL) were measured to the nearest mm; all measurements reported in our study are fork lengths. Weights were measured to the nearest gram (g), and gonads were weighed to the nearest 0.01 g. Gonad samples were fixed in 10% buffered formalin for histological processing. Sagittal otoliths were removed and stored dry.

Age and growth

A Buehler Isomet low-speed saw was used to cut four sections approximately 0.5 mm thick that were mounted on a microscope slide (Chilton and Beamish, 1982). Annuli were counted on the section through the core by using compound microscopes and transmitted light. Two independent readers counted annuli on each otolith without knowledge of fish size or capture date. If the two readings disagreed, both readers read the otolith again, for a total of four readings. If three of the four readings agreed, then this reading was accepted as the annulus count; otherwise the otolith was excluded from further analysis.

An annual growth zone in a common snook otolith comprises a narrow, concentric opaque band, formed each winter as growth slows, and a wider, translucent band, formed each summer as growth increases. Opaque winter bands were enumerated as assumed annuli because they were the salient feature in each section. Ages were assigned to each fish on the basis of a 1 June birth date because most snook have completed annulus formation by 1 June and because June corresponds to the approximate beginning of the snook spawning season (Taylor et al., 1998). Annulus counts were adjusted on the basis of an assumed birth date of 1 June. All otoliths that had an annulus on the edge from fish captured between 1 December and 1 June were assigned an age of one less than the annulus count. Fish captured after 1 June and before 1 December were assigned ages equal to the annulus count.

In earlier studies (Volpe, 1959; Thue et al. 1982), whole otoliths or scales were used to estimate ages. To evaluate the validity of using these structures to estimate snook age, we examined whole and sectioned otoliths from 199 fish that included at least five individuals from each abundant age class and the oldest individuals. Whole otoliths were read three times by a single reader. Whole otoliths were submerged in glycerin and read over a dark background with reflected light. Scale impressions from 48 common snook of different ages and lengths were made on acetate slides and read under compound microscopes equipped with transmitted light. Ages from these scales were compared with ages derived from sectioned otoliths of the same fish.

The von Bertalanffy (1957) growth equation $FL_t = L(1 - e^{(-K(t-t_0))})$ was fitted to observed age-length data with nonlinear regressions. These predicted lengths at age were compared with the average observed lengths at age that included some seasonal growth that occurred after the formation of the final annulus. Likelihood-ratio tests were used to compare parameter estimates for males and females (Kimura, 1980). If coast had a significant effect, the equations were calculated for each coast. Length-weight regressions were calculated by linear regression of $\log_{10}$-transformed data. Length-length and length-weight regressions were calculated for common snook of both sexes with pooled data.

Age validation

We captured 754 common snook 327–961 mm and injected them with oxytetracycline (OTC) at a dosage of 25-mg OTC/kg of fish body weight. Fish were then double-tagged with dart and internal-anchor tags and released at the original capture site. We relied on anglers and our own fish-

[1] Muller, R. G., and M. D. Murphy. 1998. A stock assessment of common snook, *Centropomus undecimalis*. Rep. to the Florida Marine Fisheries Commission, Florida Dep. of Environ. Protection. Florida Marine Research Institute, 100 Eighth Ave. SE, St. Petersburg, Florida 33701, 53 p.

[2] Thue, E. B., E. S. Rutherford, and D. E. Buker. 1982. Age, growth and mortality of the common snook, *Centropomus undecimalis* (Bloch), in the Everglades National Park, Florida. U. S. National Park Service South Florida Research Center Report T-683, 32 p.

ery-independent sampling techniques to recapture tagged fish. Otoliths from recaptured OTC-injected common snook were processed, read, and measured according to Chilton and Beamish (1982) and Beamish and McFarlane (1983). The number of annuli formed after the OTC mark was then compared with the number of days since injection.

Measurements from the core to each assumed annulus and to the margin of the otolith were made with a digital image-processing system on an axis extending along the sulcal ridge to the proximal margin of each section. We expressed the distance from the final annulus to the edge of the otolith (the marginal increment) as a percentage of the distance between the last two annuli formed on the otolith, or for fish with only a single annulus, as a percentage of the distance between the otolith core and the first annulus. The monthly percentage of otoliths with an annulus on their margin was plotted by capture month to show when the annuli were formed and to reveal their repetitive seasonal trend in formation. The annularity of the assumed age mark was demonstrated for each age class by plotting monthly mean measurements for all ages pooled into three inclusive groups.

Reproduction

Sections of each gonad were prepared for histological analysis and scored according to the level of reproductive activity, or class. Gonad samples were processed with a modification of the periodic acid Schiff's (PAS) stain for glycol-methacrylate sections, with Weigert's iron-hematoxylin as a nuclear stain and metanil yellow as a counterstain (Quintero-Hunter et al., 1991). Seasonal spawning patterns and spawning frequency of the common snook that we examined were reported by Taylor et al. (1998). We considered common snook in Taylor et al.'s (1998) and Grier and Taylor's (1998) classes 2–5 to be sexually mature. For a more detailed description of common snook testicular maturation see Grier and Taylor (1998). These classes included snook that had testes with evidence of active spermatogenesis and regressed testes with evidence of previous gonadal development.

We diagnosed hermaphroditism in common snook by observing histological sections of transitional-sex-stage individuals and sex-specific age- and length-frequency distributions, according to the criteria of Sadovy and Shapiro (1987). We also conducted an experiment with captive snook to document sex reversal in individual fish. We raised common snook from eggs at the Florida Fish and Wildlife Commission's Stock Enhancement Research Facility. On 6 July 1995, 137 age-4 snook ranging from 445 to 608 mm (mean=534 mm) were identified as males on the basis of presence of flowing milt at the vent and were tagged with passive-integrated transponders (PIT tags). These fish were held for 13 months in a one-quarter acre outdoor pond that had constant exchange of ambient seawater. Water temperature and salinity ranged from 17 to 37°C and from 15 to 34‰, respectively. During December 1995 and January 1996, additional well water (17°C and 3‰) was added to maintain 17°C water temperature and to reduce the salinity to 15‰. Rations consisted of squid, sardines, and dried trout pellets. Fish were fed at the rate of 2% body weight per day.

These fish were examined and sexed on two occasions: after 2 months and after 13 months. Fish that could not be positively identified as males from the presence of flowing milt at the vent were sacrificed and examined by histological analysis.

A logistic function was fitted to the percentage of females in our samples by length and age to estimate the length and age at which 50% of the males in the population transformed into females. Regressions were performed with coast as a categorical effect. If coast was a significant effect, the equations were calculated for each coast. The inflection point of the logistic curves was used as an estimate of the length or age at which 50% of the population had undergone transition from male to female.

Results

The 3872 common snook that were examined ranged in length from 124 to 1105 mm (Fig. 1). Of the fish that we sexed, females ranged in length from 397 to 1105 mm (n=1448) and males ranged from 124 to 925 mm (n=2276; Fig. 2). East coast females were usually larger than west coast females (Fig. 2). East coast females ranged in length from 448 to 1105 mm (n=683), and west coast females ranged from 397 to 1032 mm (n=765; Fig. 2). East coast males ranged in length from 124 to 908 mm (n=1258) and west coast males ranged from 129 to 925 mm (n=1018; Fig. 2). The sex ratio (male to female) of the sample from the east coast (EC) was 1.8:1 and from the west coast (WC) was 1.3:1, significantly skewed towards males on both coasts (EC: χ^2=85, df=1, P<0.01; WC: χ^2=36, df=1, P<0.01). The length-length and length-weight regressions for common snook on each coast were significantly different (P<0.05); the relationship between SL, FL, and TL are presented in Table 1.

Age and growth

Common snook annuli are formed once each year, usually during late winter or spring. We recaptured 80 common snook that had been previously injected with OTC. At recapture, these fish ranged in length from 360 to 960 mm and ranged in age from 2 to 14 years. OTC-injected individuals were at large from 4 to 2505 days. All of the recaptured common snook that were at large long enough to have formed an annulus (n=51) showed the expected pattern of annulus formation: one per year. The fish at large for the longest period was 2 years old when it was injected and was recaptured 2505 days later (Fig. 3). This fish had formed seven annuli after the OTC mark and had been at large for 6 years and 11 months; thus the rate of annulus formation was consistent with our predicted rate of one annulus per year. The oldest fish recaptured was 8 years old when injected and was recaptured 5 years and 10 months later, at age 14. This fish had formed six annuli after the OTC mark.

Monthly patterns in marginal increments were also consistent with the formation of a single annulus each year. We plotted the monthly mean percentage of fish whose oto-

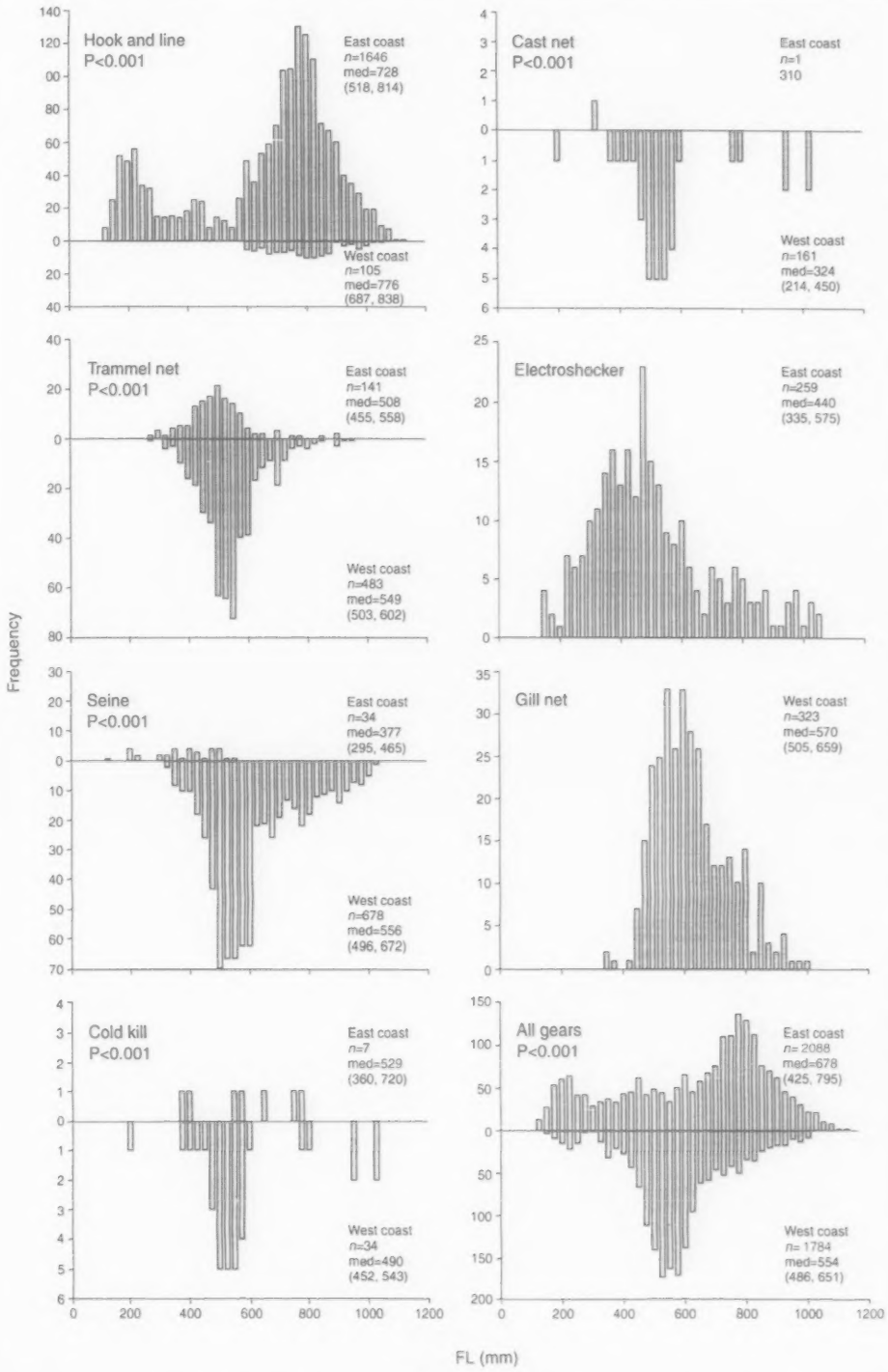

Figure 1

Length distributions, by gear type and coast, of common snook, *Centropomus undecimalis*, collected from South Florida waters during 1986–90. Med = median, numbers in parentheses are the 25th and 75th quartiles, and *P* is the Kolmogorov-Smirnov test value that compares the cumulative distribution of the two samples.

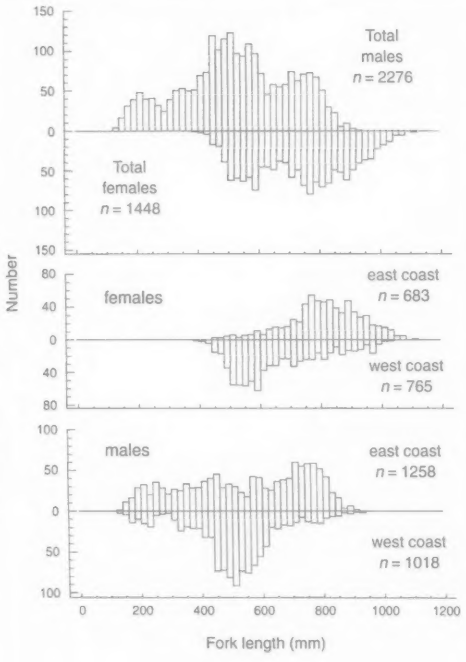

Figure 2

Lengths of male (n=2276) and female (n=1448) common snook, *Centropomus undecimalis*, sampled from South Florida waters.

liths had an annulus on the edge. The greatest percentages occurred during March–May of each year, confirming that annuli are formed then (Fig. 4). A cyclic annual pattern of margin deposition was consistent for common snook of all ages: three inclusive groups, with data pooled sufficient to reveal trends, showed a consistent annual cycle of narrowest margins during March–May and widest margins during late fall and early winter. By June, annulus formation was completed (Fig. 4).

Of the 3883 sectioned otoliths that we examined, 369 (9.5%) were rejected because of disagreements among readings. The length-frequency distribution of fish whose otoliths were rejected because they were unsuitable for age estimation was not significantly different from that of fish whose otoliths were readable (Kolmogorov-Smirnov two-sample test, two-sided test statistic=1.344, P=0.054).

Ages estimated from whole otoliths were significantly less than those estimated from sectioned otoliths (paired t-test, t=4.595, P<0.001). In addition, the slope of the regression of whole-otolith annulus counts on sectioned-otolith annulus counts was 0.873 (SE=0.014), which was significantly less than 1 (t-test=8.75, P<0.001; Fig. 5). Discrepancies between the ages estimated from the two structures were as great as five years, but usually the ages determined from whole otoliths were underestimated by 1–2 years for fish older than 10 years. Ages determined from the two structures agreed for 123 fish, whole-otolith-derived ages were greater for 15 fish, and sectioned-otolith-derived ages were greater for 72 fish. The oldest fish aged from the sectioned otoliths was estimated to be 21 years old and the oldest fish aged from whole otoliths was estimated to be 19 years old.

Table 1

The relationships between standard length, fork length, and total length and between length and weight of common snook, *Centropomus undecimalis*, from South Florida waters off the east and west coasts of Florida. *TL* = total length (mm), *FL* = fork length (mm), *SL* = standard length (mm), *WT* = whole weight (g). The fork length range for all length-length regressions was 112–1105 mm and for the length-weight regression was 124–1105 mm. Coast was a dummy variable equal to 1 for the east coast and 0 for the west coast used in the original regressions where both coasts were pooled, but only the simplified, two-parameter, coast-specific equations are presented here.

$Y = a + bX$						
Y	X	n	Coast	a	b	r^2
SL	*FL*	2416	east	–5.7186	0.8990	0.998
SL	*FL*		west	–14.7684	0.9338	
SL	*TL*	2023	east	–15.4246	0.8564	0.998
SL	*TL*		west	–21.8457	0.8566	
FL	*SL*	2416	east	7.1198	1.1109	0.998
FL	SL		west	20.0876	1.0630	
FL	*TL*	3343	east	–10.8259	0.9526	0.999
FL	*TL*		west	–14.8606	0.9512	
TL	*SL*	2023	east	19.3639	1.1652	0.998
TL	*SL*		west	26.5459	1.1648	
TL	*FL*	3343	east	11.826	1.0490	0.999
TL	*FL*		west	16.2241	1.0502	
$\log_{10}WT$	$\log_{10}FL$ 2919		east	–5.0821	3.0434	0.976
$\log_{10}WT$	$log_{10}FL$		west	–5.3564	3.1117	

Because scales were difficult to interpret, we were unable to obtain consistent readings. Ages determined from scales were always younger than ages determined from sectioned otoliths by 1 to 3 years for snook less than 10 years. We were unable to reach agreement for the ages of the ten older snook whose structures were compared. Because of the difficulties in interpreting the banding patterns on scales, we did not attempt to analyze counts derived from scales.

The oldest common snook in our sample was a 21-year-old, unsexed (i.e. sex not determined), east coast fish that was 890 mm long (Table 2). This fish was identified as a male in the field but because no gonad sample was taken, we could not confirm the sex of the fish by histological analysis; consequently, we considered the fish to be of undetermined sex in all analyses. The oldest east coast male, other than the unconfirmed 21-year-old fish, was 15 years old (865 mm); the largest east coast male was 908 mm long and 11 years old. The oldest east coast female was 18 years old (1025 mm), and the largest east coast female was 1105 mm long and 16 years old (Table 2). The oldest west coast male was 12 years old (810 mm), and the largest west coast male was 925 mm long and 4 years old. The oldest west coast female was 15 years old (982 mm), and the largest west coast female was 1032 mm long and 10 years old (Table 3).

Common snook grew rapidly until age 5–7 years after which growth slowed considerably (Fig. 6). The most abundant age classes of males were from 2 to 7 years old and those of females were from 3 to 8 years old (Tables 2 and 3). Only 10 east coast specimens were estimated to be older than 16 years, and no west coast fish were older than 16 years. The smallest and youngest female was a 397-mm west coast fish estimated to be 1 year old (Table 3). On the east coast, the smallest and youngest female was a 448-mm fish estimated to be 2 years old (Table 2). The sex-specific age-frequency distributions for the two coasts were significantly different, and east coast fish were older overall than west coast fish (Kolmogorov-Smirnov two-sample, $P<0.05$). The coast-specific differences in age were more pronounced for females than for males (Table 2, Fig. 2).

The von Bertalanffy growth models suggest that east coast fish grow more rapidly than do west coast common snook (Fig. 6, Table 4). Results of likelihood-ratio tests showed a significant difference in the overall von Bertalanffy growth models for east coast and west coast snook (χ^2=284.90, df=3, $P<0.001$). East coast estimates of K = 0.24, (95% confidence interval=0.22–0.25) and t_0 = –0.10 (95%CI=–0.01–(–0.19)) were significantly different from west coast estimates of K=0.18 (95% CI=0.14–0.21) and t_0 = –1.35 (95% CI=–1.68–(–1.01)), ($P<0.005$, $P<0.001$, respectively). The east coast estimate of L_∞ 989 mm (95% CI=966–1012) and 947 mm (95% CI=884–1010) for west coast fish were similar (P=0.342). For fish ages 1–2, the observed lengths at age of west coast fish were greater than those of east coast fish, but for fish in most of the older age classes, lengths of east coast fish were greater (Tables 2 and 3). Lengths at age predicted from the von Bertalanffy growth model for ages 0–2 were greater for west coast fish than for east coast fish, but those for all older age classes were greater for east coast fish than for west coast fish.

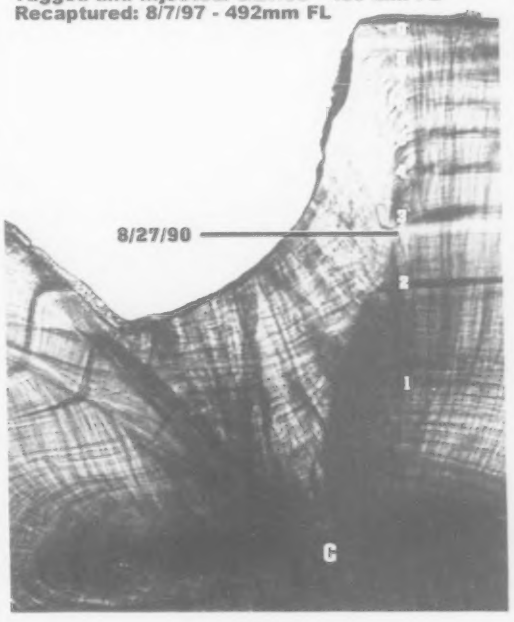

Figure 3

A transverse section of an otolith from an age-9 common snook, *Centropomus undecimalis*, that was injected with oxytetracycline (OTC) on 27 August 1990 and released at the entrance to Bishop's Harbor in lower Tampa Bay, Florida. The fish was recaptured 6 years and 11 months later at the same location and had formed seven annuli between the OTC mark and the otolith's edge.

Maturation and sex transition

Common snook present biological characteristics that are consistent with protandric hermaphroditism. We examined 27 wild-caught specimens that we considered were at the transitional-sex stage on the basis of simultaneous presence in the gonad of ovigerous lamellae and remnants of the dorsal sperm ducts that contained sperm. The mean length and age of these transitional-sex-stage common snook were 515 mm and 3.4 years. They ranged in length from a 240-mm, 1-year-old male specimen that had a prodigious number of ova in the peripheral portions of the testis, to an 824-mm, 7-year-old female with residual sperm in remnant sperm ducts. All ovaries, transitional and otherwise, contained remnants of the major dorsal sperm ducts, regardless of season or reproductive condition (Fig. 7). In addition, transitional gonads contained degenerating spermatogenic and developing ovarian tissue

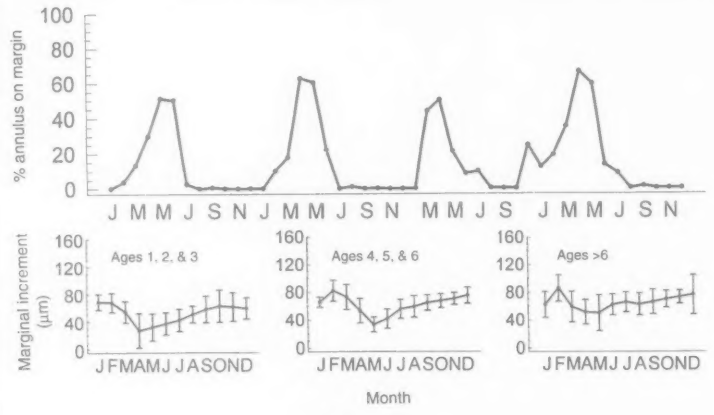

Figure 4

Percentage, by month, of otoliths with an annulus on the edge and mean monthly marginal increments with standard errors for all age classes pooled into three groups for common snook, *Centropomus undecimalis*, from south Florida waters.

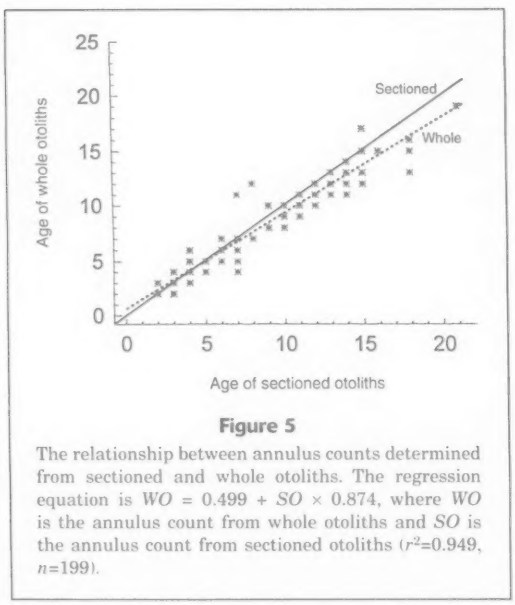

Figure 5

The relationship between annulus counts determined from sectioned and whole otoliths. The regression equation is $WO = 0.499 + SO \times 0.874$, where WO is the annulus count from whole otoliths and SO is the annulus count from sectioned otoliths (r^2=0.949, n=199).

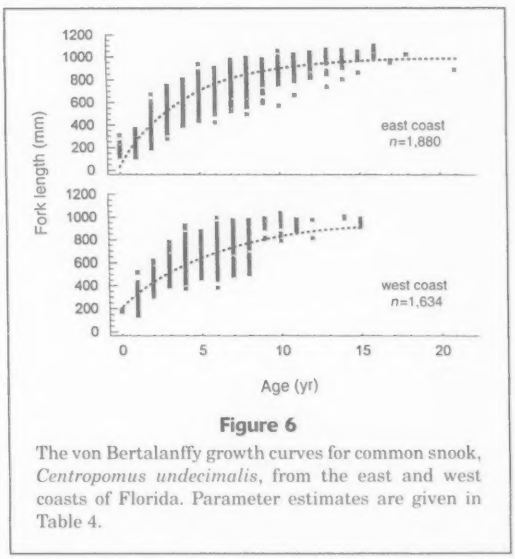

Figure 6

The von Bertalanffy growth curves for common snook, *Centropomus undecimalis*, from the east and west coasts of Florida. Parameter estimates are given in Table 4.

(Fig. 8). Most (74%) transitional-sex-stage fish were captured during September–November, shortly after the end of the spawning season, suggesting that sex reversal of postspawning males takes place shortly after spawning. The small number of transitional-sex-stage fish in our sample suggests that sex reversal occurs quickly.

During the 13-month experiment designed to document sex reversal, three males changed into females. The 137 four-year-old fish whose sex we monitored were initially sexed in July 1995 and ranged in length from 445 to 608 mm (mean=508 mm). In September 1995, we sexed the fish again and found that the largest individual (tag no. 96-344C, 617 mm) had completed sex reversal and that its ovary contained early vitellogenic oocytes. We examined these fish a final time on 17 August 1996 and found that they ranged in length from 467 mm to 649 mm (mean=534 mm). Two additional fish that were 622 mm (tag no. 10685C) and 584 mm (tag no. 13CB03) long had reversed sex, and their ovaries contained nonvitellogenic oocytes. The largest fish, a male, (tag no. 13BC2E) was

Table 2

Average observed and predicted (von Bertalanffy) fork lengths (mm) of east coast sexed and unsexed common snook, *Centropomus undecimalis*, and average observed lengths of females and males. The average observed length at age includes some seasonal growth that occurred after the formation of the final annulus. Values in parentheses are standard error and sample size.

Age (yr)	All snook		Females	Males
	Average observed	Predicted	Average observed	Average observed
0	185 (10.1;17)	22		228 (21.8;5)
1	211 (3.2;266)	225		231 (3.9;166)
2	359 (7.7;131)	385	580 (46.6;4)	357 (6.9;122)
3	514 (7.7;230)	511	644 (10.5;44)	484 (7.6;186)
4	629 (7.0;268)	611	695 (9.2;85)	597 (8.5;179)
5	698 (6.1;310)	690	760 (7.5;114)	661 (7.5;194)
6	755 (6.4;209)	753	809 (5.9;95)	711 (8.8;114)
7	792 (7.3;127)	802	841 (7.5;58)	748 (9.3;68)
8	820 (9.5;104)	841	874 (8.0;60)	747 (13.4;44)
9	849 (10.1;71)	872	902 (8.7;37)	782 (11.7;31)
10	903 (12.5;42)	897	936 (8.5;29)	807 (26.1;11)
11	911 (13.5;30)	916	943 (9.8;20)	832 (23.8;9)
12	948 (15.6;19)	932	973 (13.0;15)	854 (16.8;4)
13	959 (18.3;20)	944	989 (13.0;15)	832 (30.5;4)
14	960 (28.5;8)	953	994 (20.3;6)	857 (48.5;2)
15	987 (22.6;7)	961	1007 (11.8;6)	865 (1)
16	1048 (19.2;5)	967	1048 (19.2;5)	
17	961 (10.0;2)	971	961 (10.0;2)	
18	1024 (1.5;2)	975	1024 (1.5;2)	
19	978			
20	980			
21	890 (1)	982		

608 mm in 1995 and grew to be the largest fish in the study in 1996 (649 mm) but did not reverse sex. At the end of the experiment, the two fish that had reversed sex were the second-and third-largest snook.

Common snook sex ratios and length-frequency distributions were consistent with a diagnosis of protandric hermaphroditism. The overall sex ratio (male to female) for fish on both coasts, over the entire size range, was 1.6:1.0, significantly different from the expected 1:1 (χ^2=184, df=1, P<0.001). Females smaller than 500 mm were uncommon (4.63% of total observed), and only one female smaller than 400 mm was captured. Logistic curves were used to describe length- and age-related shifts in the common snook sex ratio. The predicted length at which 50% of the fish in the population were females was 767 mm on the east coast and 608 mm on the west coast (Fig. 9, Table 5). The predicted age at which 50% of the fish in the population were females was 7.4 years on the east coast and 5.1 years on the west coast (Fig. 9, Table 5).

Males reached sexual maturity at 150–200 mm on both coasts. The smallest mature east coast male was 175 mm long and the smallest mature west coast male was 152 mm long. The youngest mature male on both coasts was age 0. Our sample contained only 13 immature east coast males and 60 immature west coast males.

Discussion

We sampled common snook from a variety of fishery-independent and fishery-dependent sources. Some specimens were donated by recreational anglers, and others were caught by biologists using hook-and-line gear. We also used trammel and gill nets and haul seines to capture fish. On the east coast, most of the large common snook we sampled were caught by hook and line during the spawning season from spawning aggregations. In contrast, most west coast samples were collected with seines and trammel nets, and we did not regularly sample west coast spawning aggregations. We cannot quantify the potential biases resulting from the use of these different types of gears and sample sources, but our east coast material may have been biased towards larger fish because larger more aggressive individuals were harvested with hook and line. Our finding on the east coast of larger and older common snook and of larger observed and predicted lengths at age for most age classes

Table 3

Average observed and predicted (von Bertalanffy) fork lengths (mm) of west coast sexed and unsexed common snook, *Centropomus undecimalis*, and average observed lengths of females and males. The average observed length at age includes some seasonal growth that occurred after the formation of the final annulus. Values in parentheses are standard error and sample size.

Age (yr)	All snook		Females	Males
	Average observed	Predicted	Average observed	Average observed
0	179 (7.0;2)	200		179 (7.0;2)
1	272 (8.0;106)	320	460 (32.5;4)	264 (7.4;102)
2	442 (4.3;186)	421	487 (6.4;44)	428 (4.6;142)
3	521 (3.4;359)	505	548 (4.6;177)	494 (4.2;182)
4	587 (5.0;332)	576	623 (7.2;157)	555 (6.1;175)
5	625 (6.2;220)	636	664 (8.8;106)	589 (7.1;114)
6	651 (7.9;226)	686	720 (10.6;102)	594 (8.5;124)
7	719 (12.6;125)	728	796 (14.2;64)	637 (15.2;61)
8	751 (23.4;40)	763	827 (25.5;23)	647 (27.6;17)
9	928 (18.1;9)	793	928 (18.1;9)	
10	926 (24.7;10)	818	969 (15.1;7)	826 (19.1;3)
11	927 (12.0;10)	838	931 (12.6;9)	891 (1)
12	891 (81.0;2)	856	972 (1)	810 (1)
13	871			
14	995 (7.7;3)	883	995 (7.7;3)	
15	953 (12.6;4)	893	953 (12.6;4)	

Table 4

Parameter estimates of the von Bertalanffy growth model for common snook, *Centropomus undecimalis*, collected from the waters of South Florida. Values in parentheses are standard errors.

	n	L (mm FL)	K	t_0	Adjusted r^2
East coast	1880	989.3 (11.64)	0.235 (0.0076)	–0.0976 (0.04447)	0.835
West coast	1634	947.3 (32.15)	0.175 (0.0155)	–1.352 (0.1714)	0.610

Table 5

Relationships of percent female to fork length (mm) and age (years) for common snook, *Centropomus undecimalis*, from South Florida waters. *FL* = fork length (mm) and *Age* = age (years). P_{50} = the absolute value of $(a+b)/c$, which is the inflection point of the curve and is the length or age predicted by the logistic regression at which 50% of the common snook in our sample were females. Coast is a dummy variable equal to 1 for the east coast and 0 for the west coast. PD is the adjusted percentage of deviance explained by the model.

Percent female = $e^{(a+b(coast)+cX)}/(1 + e^{(a+b(coast)+cX)})$

X	n	a	b	c	PD	P_{50}
FL	3723	–5.713 (0.2114)	–1.495 (0.1006)	0.0094 (0.00035)	0.269	767 mm east coast 608 mm west coast
Age	3380	–1.578 (0.0900)	–0.705 (0.0778)	0.307 (0.0171)	0.093	7.4 years east coast 5.1 years west coast

may reflect sampling bias rather than a true difference in the maximum fish sizes reached on the two coasts.

Other comparative studies on two inshore (Florida) Sciaenidae species also have found that east coast fishes attain greater sizes or grow at faster rates than do west coast fishes (Murphy and Taylor, 1990; Murphy and Taylor, 1994). Although gear biases may have confounded growth differences in these comparative studies, there is some basis for physiological differences in common snook. Tringali and Bert (1996) have provided evidence that common snook in Florida comprise two genetically different populations: one population in Atlantic waters and one in Gulf waters. They have reported that mtDNA divergence, both in haplotype diversity and in nucleotide sequence, supports the hypothesis that the two populations are reproductively isolated, which may account for a portion of the observed differences in biological parameters.

Age and growth

Our findings suggest that scales and whole otoliths may not be suitable for aging common snook older than 6–9 years, the point at which our length-at-age data began to reach an asymptote. Ages derived from whole otoliths were reasonably accurate for snook younger than about 10 years, but ages of older snook were consistently underestimated. Furthermore, whole otoliths were more difficult to read than sectioned otoliths and therefore readers' counts from whole otoliths often varied, principally because the closely spaced annuli on the edge of whole otoliths were difficult to differentiate. Our observations of common snook scales led us to conclude that they were not suitable for use in age estimation. Whole-otolith–derived estimates of longevity reported by Volpe (1959) and scale-derived estimates by Thue et al. (1982) of 7–8 years are considerably less than our sectioned-otolith–derived estimate of 21 years. Both Volpe (1959) and Thue et al. (1982) examined fewer fish than we did; therefore their samples would be expected to contain fewer old individuals than ours did. Their samples were also collected many years before ours, and additional regulations have been imposed on the fishery since their studies; however, the magnitude of the discrepancies in ages between our study and theirs is so great that we suspect they underestimated the ages of many fish. Thue et al. (1982) reported von Bertalanffy growth parameters for common snook, but their growth model did not reach an asymptote; consequently, their estimate of $L = 1615$ mm for combined sexes is much greater than our estimate for either coast and is far larger than the length reported for any common snook. We suspect that their growth curve did not reach an asymptote because they consistently underestimated the ages of old common snook.

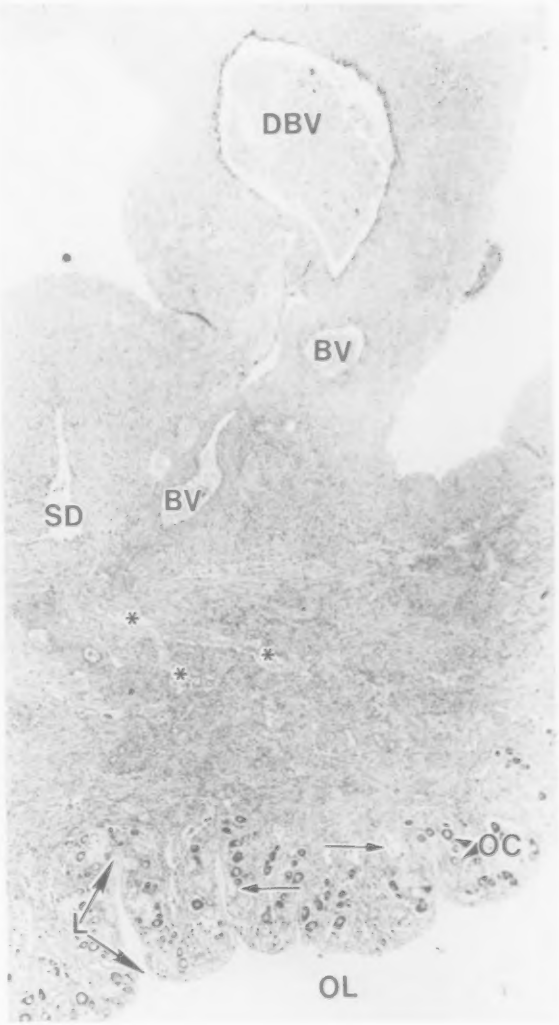

Figure 7

A histological section from a transitional-sex-stage common snook, *Centropomus undecimalis* (632 mm FL), captured in lower Tampa Bay in July 1989. Remnants of the major sperm duct (SD) and collecting tubules (*) are present in the dorsal matrix. Located throughout the peripheral ovigerous lamellae (L) are female germ cells that are either primary growth oocytes (OC) or meiotic and interphase oogonia (arrows). The dorsal (DBV) and lateral (BV) blood vessels are distinguished from the sperm ducts by the presence of red blood cells. OL = ovarian lumen.

Growth data for common snook in our study fitted the von Bertalanffy model well. The poor fit at age 0 for the east coast is explained by the collection of young-of-the-year fish in April and May, just prior to their first birthday when they were longest at age. The asymptotic values of

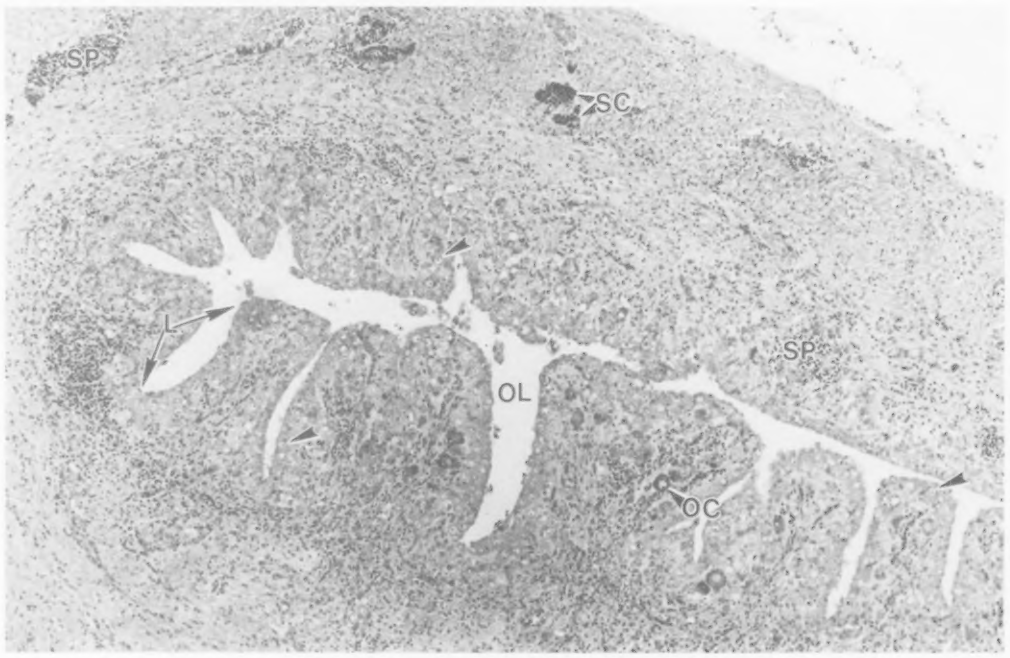

Figure 8

A histological section from a transitional common snook, *Centropomus undecimalis* (474 mm FL), captured in lower Tampa Bay in September 1989. Cysts that contain sperm (SP) and spermatocytes (SC) are visible in the peripheral wall of the gonad. Central lamellae (L) contain primary growth oocytes (OC) in addition to clusters of meiotic and interphase oogonia (arrow). OL = ovarian lumen.

approximately one meter may be a result of the difficulty of sampling large robust snook; trophy-size individuals are not uncommon in Florida and snook 1155–1194 mm are recorded (IGFA, 1998).

Maturation and sex transition

We based our determination that common snook are protandrous hermaphrodites on the following criteria presented by Sadovy and Shapiro (1987): 1) sex ratios shifted from exclusively male to predominantly female with increasing size and age, 2) transitional-sex-stage individuals were observed whose gonads contained both degenerating spermatogenic and developing ovarian tissue, and 3) sex change was documented in captive fish. Common snook have not previously been diagnosed as protandrous hermaphrodites, but another centropomid, the barramundi *Lates calcarifer*, has been diagnosed as a protandric hermaphrodite (Moore, 1979; Davis, 1982).

The male-to-female sex ratios previously reported for southwest Florida common snook (e.g. Volpe 1959, Thue et al.,1982), are similar to ours, with the exception of those reported by Marshall (1958). Thue et al. (1982) reported a 3:1 sex ratio for common snook smaller than about 500 mm and younger than age 2 in the Everglades National Park and a sex ratio 1:11 for common snook larger than 800 mm and older than age 8. Volpe (1959) reported a similarly skewed sex ratio of 1:3 for fish larger than 800 mm from southwest Florida. These shifts in the common snook sex ratio with increasing length and age are consistent with our diagnosis of protandrous hermaphroditism. In contrast, Marshall (1958) found that there were more females than males smaller than 500 mm (1.0:1.1) and that the overall sex ratio for common snook in southwest Florida was not significantly different from 1:1. It is possible that Marshall (1958) did not observe the actual sex ratio of the population he studied because 288 of the 531 total specimens in his sample had been gutted and were not included in the analysis.

Male common snook reach sexual maturity at surprisingly small lengths and ages, some at lengths less than 200 mm. We considered a fish to be sexually mature if mature sperm were present in the testis. According to this criterion, immature males made up <2% of our sample. Furthermore, most of the males we classified as immature were caught outside of the spawning season, and we may have misclassified some regressed mature fish as immature. Because our sample contained so few males that we could be certain were immature, we did not attempt to fit a logistic function to male maturity. The small mature

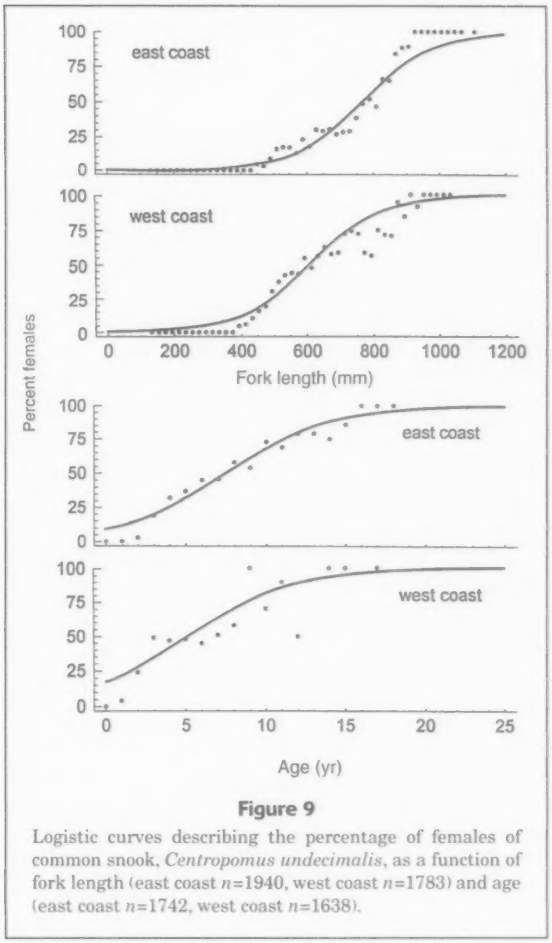

Figure 9

Logistic curves describing the percentage of females of common snook, *Centropomus undecimalis*, as a function of fork length (east coast n=1940, west coast n=1783) and age (east coast n=1742, west coast n=1638).

males we observed were smaller than those observed by previous workers; however, previous studies of maturation were based only on a macroscopic examination of gonads. Marshall (1958) examined 239 common snook from southwest Florida and concluded that 50% of the specimens of both sexes were mature at 400 mm and that all common snook, with few exceptions, were mature at 500 mm. Volpe (1959) used Marshall's lengths-at-maturity data to estimate the age at first maturity to be 3 years. It is unclear whether the small males we observed were spawning males, but they appeared to be capable of spawning; therefore we considered them to be sexually mature. Common snook typically spawn in large aggregations near passes and inlets (Taylor et al., 1998). We did not observe males smaller than 350 mm in spawning aggregations, and most spawning males were longer than 400 mm; however, we can not eliminate the possibility that some spawning involved smaller males outside these large aggregations. Additional research is needed to determine whether or not these small, precocious males are active members of the spawning population.

We considered all female common snook to be sexually mature on the assumptions that they develop directly from males that had previously spawned, that sex transition occurs shortly after spawning, and that they would be capable of spawning as females during the next spawning season. Among other centropomids, *L. calcarifer* also undergoes sex change near the end of the spawning season (Davis, 1982; Guiguen et al., 1994). Davis (1982) found that in *L. calcarifer*, oocytes first appear as the testes ripen for the final time and that sex reversal is completed shortly after spawning. This finding is consistent with our observations of common snook. Most transitional-sex-stage individuals were captured during September–November; we did not observe any transitional fish from April to June and only one transitional fish in February and one in March. Sex reversal appears to occur quickly and shortly after spawning, and we found no evidence to suggest that females do not spawn during their first spawning season after transition from male to female. This conclusion is supported by the captive fish that completed sex reversal and developed vitellogenic oocytes in only two months. Management decisions based on length and age at maturity of females should more appropriately focus on the size and age at sex transition, and all females should be included in estimates of spawning stock biomass.

Acknowledgments

We thank the many anglers and biologists who participated in this study. We especially thank Ed Irby, Kraig Krum, William Howard, and other staff at the Tequesta field laboratory. Iliana Quintero, Pamela Nagle, and Ruth Reese provided invaluable assistance. Buck Dennis, William Halstead, John Young, Patricia Hindle, and other staff at the Stock Enhancement Research Facility are kindly acknowledged. We thank David Harshany, Doug Haymans, Dan Merryman, Heather Patterson, Graham Gerdeman, and Connie Stevens for their assistance. This manuscript was greatly improved by the conscientious reviews of Jim Quinn, Judy Leiby, and Llyn French. This work was supported in part under funding from the Department of the Interior, U.S. Fish and Wildlife Service, Federal Aid for Sportfish Restoration, Project Number F-59.

Literature cited

Beamish, R. J., and G. A. McFarlane.
1983. The forgotten requirement for age validation in fisheries biology. Trans. Am. Fish. Soc. 112:735–743.

Bruger, G. E., and K. H. Haddad.
1986. Management of tarpon, bonefish, and snook in Florida. *In* Proceedings of the eleventh annual marine recreational fisheries symposium, Tampa, FL (R. H. Stroud, ed.), p. 53–57. National Coalition for Marine Conservation Inc., Savannah, GA.

Casselman, J. M.
1983. Age and growth assessment of fish from their calcified structures--techniques and tools. *In* Proceedings of the international workshop on age determination of oceanic pelagic fishes: tunas, billfishes, and sharks (E. D. Prince

and L. M. Pulos, eds.), p. 1–17. U.S. Dep. Commer., NOAA Tech. Rep. NMFS 8.

Chilton, D. E., and R. J. Beamish.
1982. Age determination methods for fishes studied by the groundfish program at the Pacific Biological Station. Can. Fish. and Aquat. Sci. Spec. Publ. 60, 102 p.

Crabtree, R. E., C. W. Harnden, D. Snodgrass, and C. Stevens.
1996. Age, growth, and mortality of bonefish, *Albula vulpes*, from the waters of the Florida Keys. Fish. Bull. 94:442–451.

Davis, T. L. O.
1982. Maturity and sexuality in barramundi, *Lates calcarifer* (Bloch), in the Northern Territory and south-eastern Gulf of Carpentaria. Aust. J. Mar. Freshwater Res. 33:529–545.

Gilmore, R. G., C. J. Donahoe, and D. W. Cooke.
1983. Observations on the distribution and biology of the common snook, *Centropomus undecimalis* (Bloch). Fla. Sci. 46:313–336.

Grier, H. J., and R. G. Taylor.
1998. Testicular maturation and regression in the common snook. J. Fish Biol. 53:521–542.

Guiguen, Y., C. Cauty, A. Fostier, J. Fuchs, and B. Jalabert.
1994. Reproductive cycle and sex inversion of the seabass, *Lates calcarifer*, reared in sea cages in French Polynesia: histological and morphological description. Environ. Biol. Fishes 39:231–247.

IGFA (International Game Fish Association).
1998. World record game fishes. IGFA, Ft. Lauderdale, FL, 352 p.

Kimura, D. K.
1980. Likelihood methods for the von Bertalanffy growth curve. Fish. Bull. 77:765–776.

Lowerre-Barbieri, S. K., M. E. Chittenden Jr., and C. M. Jones.
1994. A comparison of a validated otolith method to age weakfish, *Cynoscion regalis*, with the traditional scale method. Fish. Bull. 92:555–568.

Marshall, A. R.
1958. A survey of the snook fishery of Florida, with studies of the biology of the principal species, *Centropomus undecimalis* (Bloch). Fla. Board Conserv. Mar. Res. Lab. Tech. Ser. 22, 39 p.

Matlock, G. C., and H. R. Osburn.
1987. Demise of the snook fishery in Texas, USA. Northeast Gulf Sci. 9(1):53–58.

Moore, R.
1979. Natural sex inversion in giant perch, *Lates calcarifer*. Aust. J. Mar. Freshwater Res. 33:647–661.

Murphy, M. D., and R. G. Taylor.
1990. Reproduction, growth, and mortality of red drum *Sciaenops ocellatus* in Florida waters. Fish. Bull. 88:531–542.
1994. Age, growth, and mortality of spotted seatrout in Florida waters. Trans. Am. Fish. Soc. 123:482–497.

Quintero-Hunter, I., H. Grier, and M. Muscato.
1991. Enhancement of histological detail using metanil yellow as counterstain in periodic acid/Schiff's hematoxylin staining of glycol methacrylate tissue sections. Biotech. Histochem. 66:169–172.

Rivas, L. R.
1986. Systematic review of the perciform fishes of the genus *Centropomus*. Copeia 1986:579–611.

Sadovy, Y., and D. Y. Shapiro.
1987. Criteria for the diagnosis of hermaphroditism in fishes. Copeia 1987:136–156.

Shafland, P. L., and K. J. Foote.
1983. A lower lethal temperature for fingerling snook, *Centropomus undecimalis*. Northeast Gulf Sci. 6:175–178.

Taylor, R. G., H. J. Grier, and J. A. Whittington.
1998. Spawning rhythms of common snook in Florida. J. Fish Biol. 53:502–520.

Tringali, M. D., and T. M. Bert.
1996. The genetic stock structure of common snook (*Centropomus undecimalis*). Can. J. Fish. Aquat. Sci. 53:974–984.

Tucker, J. W., Jr., M. P. Landau, and B. E. Faulkner.
1985. Culinary value and composition of wild and captive common snook, *Centropomus undecimalis*. Fla. Sci. 48(4): 196–200.

Volpe, A. V.
1959. Aspects of the biology of the common snook, *Centropomus undecimalis* (Bloch) of southwest Florida. Fla. Board Conserv. Mar. Res. Lab. Tech. Ser. 31, 38 p.

von Bertalanffy, L.
1957. Quantitative laws in metabolism and growth. Q. Rev. Biol. 32:217–231.

Habitat associations of deep-water rockfishes in a submarine canyon: an example of a natural refuge

Mary M. Yoklavich

Pacific Fisheries Environmental Laboratory
National Marine Fisheries Service, NOAA
1352 Lighthouse Avenue
Pacific Grove, California 93950-2097
Present address: National Marine Fisheries Service
c/o Long Marine Laboratory
100 Shaffer Road
Santa Cruz, California 95060
E-mail address: mary.yoklavich@noaa.gov

H. Gary Greene
Gregor M. Cailliet
Deidre E. Sullivan

Moss Landing Marine Laboratories
8272 Moss Landing Road
Moss Landing, California 95039-9647

Robert N. Lea

California Department of Fish and Game
20 Lower Ragsdale Dr.
Monterey, California 93940

Milton S. Love

University of California Santa Barbara
Marine Science Institute
Santa Barbara, California 93106

Abstract.—A multidisciplinary assessment of benthic rockfishes (genus *Sebastes*) and associated habitats in deep water was conducted in Soquel Submarine Canyon, Monterey Bay, California. Rock habitats at depths to 300 m were identified by using bathymetric and side-scan sonar imaging, verified by visual observations from a manned submersible, mapped and quantified. Species composition, abundance, size, and habitat specificity of fishes were determined by using a video camera and parallel laser system along transects made by a submersible.

We counted 6208 nonschooling fishes representing at least 52 species from 83 10-min strip transects that covered an estimated 33,754 m^2. Rockfishes represented 77% of the total number of individuals, and included a minimum of 24 species. Six distinct habitat guilds of fishes were manifest from habitat-based clustering analysis: small species were associated with mud and cobble substrata of low relief, and larger species of rockfishes were associated with high-relief structures such as vertical rock walls, ridges, and boulder fields. There was remarkable concordance between some of the guilds identified in Soquel Canyon and the results of other habitat-specific assessments of fishes along the west coast of the United States from central California to Alaska. These generalities are valuable in predicting community structure and evaluating changes to that structure, as well as in applying small-scale species-habitat relationships to broader-scale fishery resource surveys. Additionally, establishment of these groups is critical when incorporating the concept of essential fish habitat (EFH), and negative impacts to it, into the management of fisheries in relatively deep water, as required by the Sustainable Fisheries Act of 1996.

High numbers of large rockfishes (e.g. *Sebastes chlorostictus*, *S. levis*, *S. rosenblatti*, and *S. ruberrimus*) were locally associated with rock ledges, caves, and overhangs at sites having little or no evidence of fishing activity. Abundance and size of several species were lower at fished than at unfished sites. We suggest that rock outcrops of high relief interspersed with mud in deep water of narrow submarine canyons are less accessible to fishing activities and thereby can provide natural refuge for economically important fishes, as exemplified in Soquel Canyon.

Manuscript accepted 17 December 1999.
Fish. Bull. 98:625–641 (2000).

Rockfishes (*Sebastes* spp.) are quite speciose, dominate coastal benthic fish assemblages on the west coast of the United States, and are among the most valuable fisheries in California. They have been harvested commercially in California as early as 1875 (Phillips, 1957). About 85% of the 57 or more rockfish species in California have some economic value, and landings have increased dramatically over the last 40 years (Lea, 1992). During the past decade (1988–97), commercial fishermen have landed an average of nearly 10,000 metric tons of rockfish at California ports per year, with an average exvessel value of $11.4 million per year (Thomson, 1999). During this period, recreational anglers on commercial passenger fishing vessels caught an additional 1.8 million individual rockfish per year (Thomson, 1999), at a value that far exceeds that of the commercial catch.

Many species of rockfishes are slow-growing, long-lived, and relatively old at maturity, making them particularly vulnerable to overfishing. Historically, rockfish landings have been especially high in Monterey (Phillips, 1939), and there are recent indications that numbers and sizes are decreasing for some species (Pearson and Ralston, 1990; Mason, 1995, 1998; Ralston, 1998). As with many coastal fisheries, the Monterey fleets have expanded their range to deeper and more remote areas as local stocks have become depleted in shallow water (Deimling and Liss, 1994; Karpov et al., 1995; Mason, 1995).

As increased fishing effort is applied to populations in deep coastal waters, it becomes critical to identify and protect areas of natural refuge for larger,

older individuals of valuable rockfish species. There is little information on the distribution, abundance, and habitat characteristics of mature rockfishes associated with deep-water benthic marine habitats off California. This type of habitat is below scuba depths (<30 m), and the rocky heterogeneous substrata inhabited by many rockfish species prohibit accurate estimates of fish abundance with conventional trawl surveys. Diversity, quality, and extent of habitat likely are among the most significant environmental determinants of distribution, abundance, and species richness of adult rockfishes (Larson, 1980; Richards, 1986; Pearcy et al., 1989; Carr, 1991; Stein et al., 1992). Characterizing and quantifying elements of suitable habitat, such as substratum type, texture, and relief, are therefore critical for evaluating the effectiveness of refugia, both natural and designated protected areas, to maintain regional marine resources.

Eight submarine canyons cut into the continental shelf off central California, placing deep-water habitats in close proximity to shore. We hypothesized that isolated rock outcrops in deep water along the steep walls of these canyons could serve as natural harvest refugia and allow certain rockfish species locally to attain large sizes and high abundances. Subsequent distribution of offspring from these mature fishes could help maintain viable populations and species diversity in adjacent areas of greater fishing activity.

Our general goal in this study was to characterize rockfish assemblages and their relationship to specific benthic habitats within submarine canyons by combining geophysical and *in situ* submersible surveys. Because temperate benthic habitats are often defined by geologic attributes, geophysical techniques are critical in determining habitat structure, depth, and lithology.

Within our general goal, this study had four specific objectives. Our first objective was to characterize the geomorphology of our study site in Soquel Canyon using bathymetric mapping and side-scan sonar imaging (i.e. sonographs) to classify the substrata and to locate rock outcrops on a spatial scale of 100s of meters to kilometers. Our second objective was to map and quantify the amount of exposed hard substrata at depths suitable to rockfishes within our study site. Third, using a manned submersible, we set out to verify our interpretations of the remotely sensed images of habitat on a smaller scale (i.e. 1 meter to 10s of meters) and determine frequency of occurrence, distribution and type of habitat that support assemblages of adult benthic rockfishes in Soquel Canyon. Our fourth objective was to estimate and compare species composition, abundance, size, and diversity of fishes among habitat types, depth zones, and locations that have been subject to various amounts of fishing activity within the canyon.

Materials and methods

Study site

Soquel Canyon (ca. 36°49′N, 121°59′W) is a submarine canyon of inactive sediment that cuts into the continental shelf in Monterey Bay nine miles south of Santa Cruz, at a water depth of 80 m. This canyon trends southwest for 10 km, at which point it intersects the larger Monterey Canyon at a depth of 915 m (Fig. 1A). Soquel Canyon is eroded from the generally flat-lying beds of the Pliocene Purisima Formation, a shallow-water marine deposit comprising interlayers of sandstone, mudstone, and shell hash (coquina). Previous undercutting of the canyon walls has caused extensive landslides and slumping; resultant rock exposures were the targets of our survey of rockfishes and their associated habitats.

Our study area covered about 17 km^2 of the headward part of the canyon, between 80 and 360 m water depth. This represents about two-thirds (6.7 km) of the length of the canyon's axis; at 6.7 km along the axis, the canyon is 3.5 km wide and 650 m deep.

Geophysical surveys

Side-scan sonar is a suitable method for distinguishing blocks of hard substrata from surrounding soft sediment by differences in intensity of reflected sound (Able et al., 1987; Greene et al., 1995; Yoklavich et al., 1997). Our sonographs of seafloor morphology resemble a black and white photographic negative. Topographic features such as ledges, vertical walls, and boulders produce dark and light images on the records, depending on the orientation and hardness of the feature. A strong signal or reflector (dark) is received from the side of a relatively hard feature facing the transducer, whereas a weak signal or shadow (light) is received from the side sloping away from the transducer.

We conducted a side scan sonar survey along 110 km of track lines using a 100 kHz acoustic signal with a swath width of 600 m (300 m per side). The sonographs along each track line were positioned precisely with navigational data from a differential global positioning system (GPS) to form a mosaic of rock type and texture within the canyon. Because of steep relief, only one side of the transducer received usable signals and 200% coverage was necessary to produce a complete mosaic.

We used the mosaic to quantify the amount of hard substrata at depths suitable to rockfishes. Our interpretations of the sonographs were verified by direct observations made by marine geologists (HGG and DS) during nine dives in the *Delta* submersible. Type, relief, and size and depth range of features were described; these field descriptions assisted the marine biologists in planning dives at each site and in assessment of habitat after the cruise.

We conducted a bathymetric survey of Soquel Canyon using a 3.5-kHz precision depth recorder integrated with Loran and GPS navigational data. The resultant high-resolution map (20-m intervals) was used to identify areas of high relief and potential slumps.

Fish and habitat surveys

We used the *Delta* submersible to assess benthic fish assemblages and associated habitat in Soquel Canyon in August 1992 and October 1993. The *Delta* is a small (4.75-m) submersible, accommodates one scientific observer and a pilot, has a maximum operating depth of 365 m, and a cruising speed of 1.5 knots. An acoustic track-point

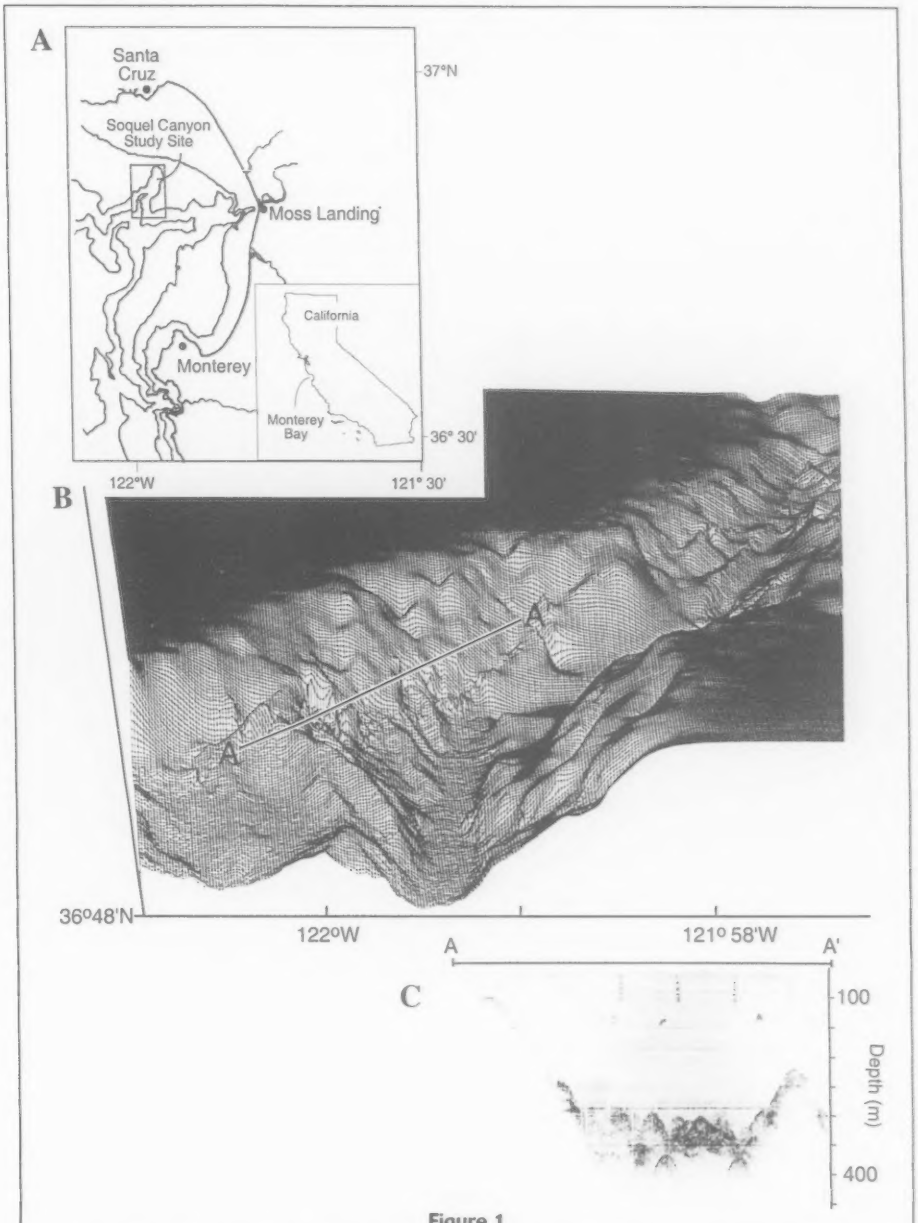

Figure 1

(**A**) Study area in Soquel Canyon, the northernmost tributary to the Monterey Submarine Canyon System. (**B**) A physiographic map of Soquel Canyon, produced from 3.5-kHz echo-sounding data. Transect A–A' is at the location of the seafloor profile (**C**), and displays the hummocky nature of slump deposits on the west wall of the Canyon.

system and differential GPS were used on board the support vessel to record the underwater location of the submersible. All dives were made during daylight to avoid potential bias due to diel activity patterns of some species (Hixon[1]; Yoklavich, pers. obs.)

To quantify fish abundance and habitat use, strip transects of 10-min duration were conducted 1–2 m off the

[1] Hixon, M. 1992. Personal commun. Department of Zoology, Oregon State University, Corvallis, OR 97331-2914.

bottom at 0.4–0.9 knots. Transects were purposely of short duration to maintain constant depth within the rock habitat at each station. Each transect was documented continuously with a high 8-mm video camera and associated lights that were externally mounted on the starboard side of the submersible. The scientific observer verbally annotated each videotape, identifying, counting, and estimating size of all fishes in front of the starboard viewing port. A hand-held dive sonar was aimed at objects (e.g. large fish and boulders) along the transects from inside the submersible to estimate distance from the observer to the object; this procedure helped us to estimate the width of the transect. After each dive, divers transcribed observations on fishes and habitat from video tapes into a computerized database on board the support vessel.

Two parallel lasers were mounted on either side of the external video camera at the fixed distance of 39.5 or 20.0 cm apart, in association with different laser systems each year. The laser spots were projected onto the seafloor habitats. They were visible to the observer, recorded onto the video tape, and were critical in accurately estimating the size of fishes, distance traveled along a transect and area of habitat patches. We made measurements by comparing the size of a fish or habitat feature to the known spacing of the two bright laser spots when the object was perpendicular to the camera and lasers (Tusting and Davis, 1993). We estimated the length of each transect, independent of submersible speed and bottom currents and type, by counting the number of laser-spot intervals as they moved along the substrata in the video transect (much like using a yardstick, end-over-end along the transect).

Microhabitat of each fish within the transect was characterized from the video tapes. Various combinations of substratum type, including mud, pebble, cobble, boulders, and rock ridge (see Greene et al., 1999, for definitions), were categorized according to primary (at least 50% of the area viewed) and secondary (>20% of the area viewed) microhabitat (conforming to Stein et al., 1992). Relief was categorized as flat (0–5°), low (5–30°), and high (>30°). Each surface area of uniform habitat (i.e. a patch) along the quantitative transect was measured to the nearest 0.1 m^2. Species-specific abundance was standardized per area of associated habitat patch. The habitat patch was used as our sample unit.

Data analyses

Similarity of assemblages of nonschooling fishes among the different combinations of substrata was evaluated with cluster analysis on the basis of abundance of each species standardized by area of associated bottom type in each patch. Only species representing ≥1% of the total abundance in each bottom type category and only bottom types representing ≥1% of the total area surveyed were used in this analysis. Only nonschooling (i.e. nonpolarized aggregations or solitary individuals) benthic fishes were included in our analyses because schooling fishes commonly were more abundant in midwater above our field of view and therefore could not be accurately enumerated. Clustering was performed with the average linkage method and with Euclidean distance as a measure of dissimilarity (SYSTAT, 1992). Dissimilarity among clusters ≥50% of the maximum overall distance was considered a major division and used to define distinct habitat guilds of fishes (*sensu* Root, 1967).

Further analyses were focused on nonschooling fish species that dominated the rock habitat guild, as defined by the cluster analysis. These are some of the species important in commercial and recreational catches (Weinberg, 1994; Mason, 1995, 1998). We used the incidence of fishing gear and associated debris, observed on the seafloor during the quantitative fish transects, as a relative index of fishing activity throughout our study area. Statistical differences in abundance (number of fish per 100 m^2 of habitat patch) of those species in the rock habitat guild were analyzed among five sites of varying fishing activity by using analysis of variance (ANOVA) with equal sample variances and otherwise by resampling statistics (Bruce et al., 1995). We used Cochran's test for homogeneity of variance (Winer, 1971).

Differences in size of selected dominant species were tested among two arbitrarily chosen 100-m depth categories (i.e. shallow [75–175 m] and deep [176–275 m]) and the five sites were tested by using two-factor ANOVA (with homogeneity of sample variances) where appropriate.

Overall species diversity was calculated as

$$H' = \sum_{i=1}^{s} [p_i][\ln p_i],$$

where s = number of species; and
p_i = proportional abundance of species i.

Richness (number of species), and evenness ($J' = H'/H'_{MAX}$), as well as species diversity, were evaluated for all habitat types (see Krebs, 1989) and then among sites just within the rock habitat guild in shallow and deep water. Sufficiency in the number of samples necessary to reliably characterize overall diversity for each habitat type was examined by plotting cumulative numbers of species against the sample unit (both for number of patches and area of habitat surveyed). These plots indicated that the number of samples was sufficient to yield a reliable estimate of diversity for comparisons among all habitats and for comparisons among sites in shallow and deep rock habitat (i.e. the number of samples evaluated for diversity always surpassed the number comprising 95% of the species; see data on Figs. 8 and 9).

Results

Geophysical mapping of habitats

A physiographic representation of the relatively high-resolution bathymetric data (Fig. 1B; production assisted by the U.S. Geological Survey, Menlo Park, CA) helped us to visualize canyon morphology, to identify areas of high relief and potential slumping, and to select submersible dive

sites for fish and habitat surveys. The bathymetry indicated that Soquel Canyon is steeper and more rugged than previously interpreted from NOAA's Seabeam data. From the 3.5-kHz bottom profiles we identified large slumps along both walls and in the axis of the canyon. These areas had a hummocky surface with little or no sediment cover and were bounded by sharp relief on either side (e.g. Fig. 1C); these characteristics indicated likely rockfish habitat.

Five study sites were defined (Fig. 2) on the basis of a series of side-scan images identified along the canyon walls. These images were interpreted as rock outcrops representing approximately 35 ha of the total area surveyed in Soquel Canyon. Area of rock outcrop in the five study sites ranged from 1.4 ha of isolated rocks in about 200 m water depth at site 5 to 19.6 ha of extensive rock in 90–350 m water depth at site 3. We considered these estimates to accurately represent the amount of exposed outcroppings within our study area.

From submersible observations we verified our interpretation of these reflectors as well-bedded rock outcrops of various resistance, lithologies, and bottom morphology (e.g., Fig. 3, A and B). Crescent-shaped slump scarps were imaged along the upper walls of the canyon, and extensive rockfalls comprising large (meters in diameter) angular to sub-rounded (having rounded corners but not spherical) blocks and smaller boulders (0.25–1.0 m diameter) were concentrated at the base and in the axis. Well-layered, friable sedimentary rocks were differentially eroded into overhangs (>90°), crevices, and caves. These rocks occurred as isolated outcrops (Fig. 3A), and as more extensive rock exposures (Fig. 3C) interspersed with soft mud along very steep walls from at least 150 to 330 m water depth.

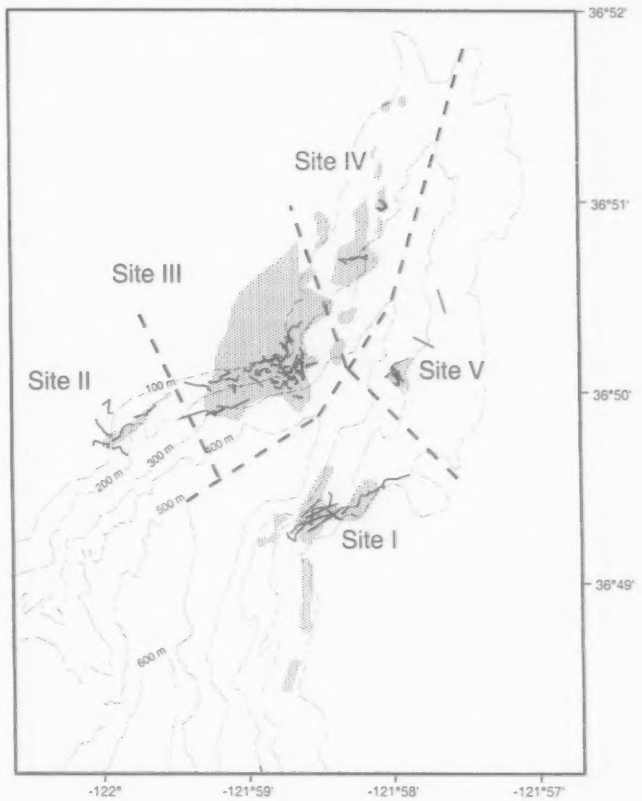

Figure 2

Schematic map constructed from interpretations of side-scan sonographs of rock outcrops (stippled areas) in Soquel Canyon. Submersible track lines during quantitative transects are mapped (lines), and the five main study sites are labeled.

Fish and habitat associations

Thirty-three submersible dives were made at five sites to assess rockfish assemblages and habitat associations in Soquel Canyon. We counted 6208 nonschooling fishes, representing at least 52 species (see Table 1 for both scientific and common names), from 83 10-min strip transects that covered an estimated 33,754 m^2. Rockfishes represented 77% of the total number of individuals, and included a minimum of 24 species. The 20 most abundant taxa (90% of total abundance) included 4540 individual rockfishes representing at least 12 species. Nonrockfish species were represented primarily by six species, which comprised 17.2% of the total abundance: *Microstomus pacificus*, *Ophiodon elongatus*, *Sebastolobus alascanus*, *Eptatretus stouti*, *Merluccius productus*, and an unidentified species (or possibly a complex of species) in the family Agonidae (most likely *Xeneretmus* spp.).

Major rockfish habitat types in Soquel Canyon included vertical cliffs with joints, fractures, and overhangs, small and large ledges, talus slopes, cobble, and boulder fields of exposed sandstone and mudstone interspersed with soft mud. Most rockfishes of all sizes were associated with some structure, including invertebrates such as crinoids, sea anemones and sponges, debris, and simple shallow depressions in the mud.

Cluster analysis (Fig. 4), which grouped standardized abundance of each fish species (number per 100 m^2) by bottom type, resulted in six habitat guilds. Most distinct were guild I, having small species found on uniformly mud bottom of flat or low relief, dominated by *S. saxicola* (42%) and to a lesser degree by *M. pacificus*, Agonidae, and *S. alascanus*, and guild VI, a rock-boulder habitat of low-to-high relief largely at 75–175 m depth, dominated by *S. wilsoni* (42%), and with less representation by *S. paucispinis*, *S. pinniger*, and *S. chlorostictus*.

The remaining four habitat guilds (guilds II, III, IV, and V; Fig. 4) were grouped two each into two clusters at Euclidian distances 0.058 and 0.063. Guilds II and III were characterized by combinations of mud and large-grain cobbles and pebbles that were of mostly flat or low relief (72% occurrence). These assemblages were relatively diverse,

evenly distributed (see results of diversity analysis that follows), and included mostly small species (i.e. *S. semicinctus*, *S. wilsoni*, and *S. elongatus*) and small members of a large species (*S. chlorostictus*). Most (88–95%) of habitat guild II occurred at shallow depth (75–175 m); about one-half of guild III occurred in water <175 m. Guilds IV and V represented habitats of large structure, high relief (78% occurrence), and both shallow and deep (>175 m) water. Although they both had similar top-ranked species, guild IV (boulder-mud) was much less diverse and was dominated by a single species (*S. helvomaculatus*). Economically valuable rockfish species made up most (52–77%) of guild V (rock habitat). The rock habitat guild, in particular, contained high numbers of large species up to 1 m in total length, such as *S. levis* (12% of total fish abundance in this habitat) and *S. ruberrimus* (5% total abundance). These fishes were closely associated with ledges, caves, crevices, and overhangs.

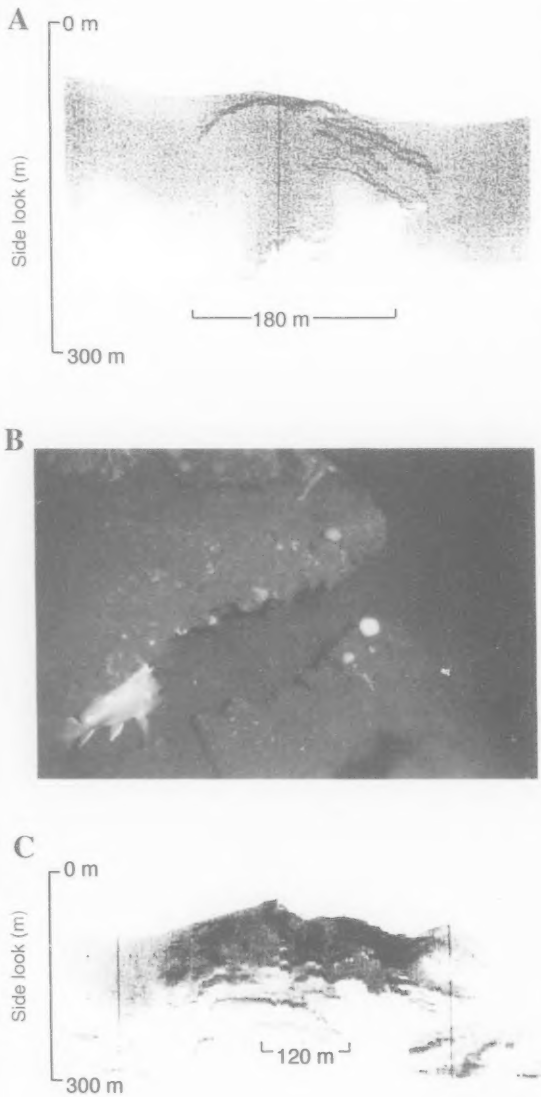

Figure 3

(**A**) Side-scan sonograph of isolated rock outcrop on steep wall of Soquel Canyon. Strong acoustic reflectors (dark areas) are from exposed bedding faces, white areas are shadows behind faces, and gray areas are nonreflective mud. (**B**) These eroded mudstone beds comprise habitat for benthic fishes, such as this adult greenspotted rockfish (*Sebastes chlorostictus*). (**C**) Side-scan sonograph of steep, well-bedded rock walls on southeast side of canyon from 150 to 330 m.

Fishes and habitat by site

In general, our study area in Soquel Canyon comprised five sites of exposed rock ridge, boulder, cobble, pebble, and mud bottom types (Fig. 5). From the mosaic of side scan sonographs, total area of outcrops ranged from 1.4 ha (site 5) to 19.6 ha (site 3), and the sampling effort (i.e. number of dives, transects) in these sites tended to vary accordingly. We quantitatively surveyed fish and habitat in 1025 sample patches (average area of a habitat patch was 34.0 m^2; SE=1.9 m^2), representing from 1285 to 13,626 m^2 per site. From analysis of 83 transects, 74–94% of the bottom types at these sites were characterized by mud, rock ridge, and combinations of both. Not surprisingly, nearly 50% of our survey was in areas of high relief, and almost all (97%) rock ridge was high relief. Mud habitats were largely (78%) of flat and low relief.

Site 1, located on the east canyon wall at a water depth from 98 to 305 m, was characterized as rock outcrop with moderate vertical fracturing, stepped rock ridges of 1–6 m height (habitat guild V), mud-cobble and mud-boulder fields (habitat guilds II and III), and mud terraces (habitat guild I). Directly opposite on the west wall, site 2 included a series of rock ledges, mud terraces, and vertical walls extending from 263 to 148 m depth; this site is heavily fished (see later criteria). Site 3 comprised small ledges interspersed with mud, boulder, cobble, and pebble slopes of low relief at 94–150 m, high-relief rock ledges with fractures cutting the bedding planes and massive vertical mudstone walls (150–250 m), and scattered boulder-mud fields at the base of the wall. Sites 4 and 5 were largely isolated outcrops of rock ridges surrounded by fields of mud at 152–226 m depth.

Rockfishes of various species ranked first in abundance at all of the five study sites (Table 1); over all habitat types and depth, at least three of the top five species were rockfishes (4–5 of 5 at most sites). Average abundance was highest at site 5 (42.4 fish per 100 m^2), 96% of which comprised economically valuable species (e.g. in rank order of abundance, *S. pau-*

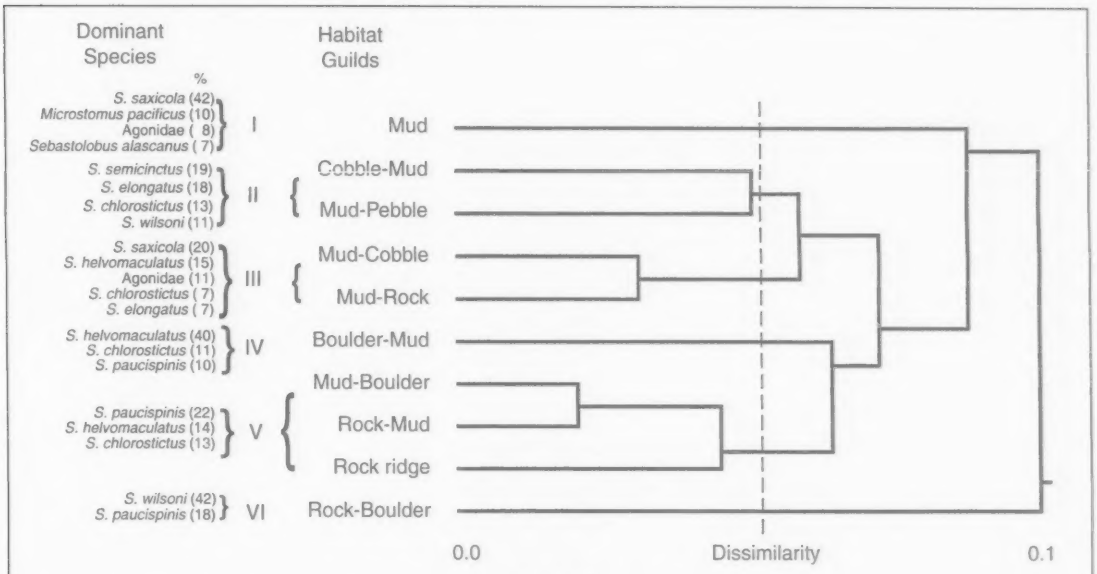

Figure 4

Cluster dendogram that groups standardized abundance (number per 100 m^2) of nonschooling benthic fish species in Soquel Canyon, based on associated type of bottom substrata. Dominant species (percent relative abundance in parentheses) of the six main habitat guilds are indicated. See Figure 8 for number of habitat patches sampled in each habitat.

cispinis, *O. elongatus*, *S. levis*, *S. rosenblatti*, *S. chlorostictus*, *S. ruberrimus*). These sedentary fishes were primarily sheltered under ledges, in crevices, and among large sea anemones (*Metridium giganteum*) on this isolated rock outcrop.

One objective of our study was to compare species composition, abundance, size, and diversity of fishes among sites receiving varying amounts of fishing pressure within the canyon. Seventy-five lines (polypropylene and monofilament; n=67) and cables (n=8) were observed on 83 transects during 13.5 h; no mesh nets, pots, or trawl tracks were found. Eighty-five percent of these sightings occurred at site 2, with 26.7 observations of gear made per hour of survey (or 0.9 sightings per 100 m^2). Observations of 1.5 and 0.7 per hour were made at sites 3 and 1, respectively. No evidence of fishing gear or activity was found at sites 4 and 5. These observations are supported by California Department of Fish and Game (CDFG) records of site-specific activities of commercial passenger fishing vessels (Reilly[2]).

From the cluster analysis, economically important rockfishes are largely represented by the rock habitat guild (V). After limiting statistical comparisons among sites to those species occurring on mud-boulder, rock-mud, and rock ridge bottom types (i.e. habitat guild V), we found abundance of each of the top eight species in this guild (Fig. 6) varied significantly among sites (ANOVA or randomization test; P<0.01). Large solitary and sedentary species, such as *S. chlorostictus, S. ruberrimus, and S. levis*, were most abundant at sites 1, 3, 4, and 5, which received minimal to no fishing pressure. Abundances of these three species were statistically less at site 2, the area of highest fishing activity.

Sebastes paucispinis, one of the most important species in commercial and recreational fisheries of Monterey Bay, occurred in high numbers at all sites but was significantly more abundant at site 5 (Fig. 6; randomization test, P<0.01). Although we limited our study to nonschooling individuals, *S. paucispinis* can be semipelagic and we sometimes encountered this species in loose groups of 50 or more fishes above rock outcrops. These groups were not included in our analysis but indicate that this species is more active and broad ranging than the solitary benthic rockfishes.

Interestingly, the most abundant species at the site most heavily fished (site 2) was *S. helvomaculatus*, a relatively small species and historically of minor interest to either commercial or recreational fisheries. This species also was significantly more abundant at this site than at any of the other four sites (Fig. 6; resampling test, P<0.01). *Sebastes crameri* and *S. rufus*, relatively important rockfish species in the commercial trawl fishery but rarely taken by hook and line, were abundant only at site 2 (ranking second and fifth, respectively). *Sebastes elongatus*, a relatively small species that was most abundant in the cobble-mud guild, was moderately abundant in the rock guild but only at sites 1–3.

Size of most of these species differed by site and depth category (shallow=75–174 m; deep=175–275 m; Fig. 7). Significantly smaller individuals of *S. chlorostictus*, *S. helvomaculatus*, *S. elongatus*, and *S. paucispinis* occurred

[2] Reilly, P. 1997. Personal commun. CDFG, 20 Lower Ragsdale Dr., Monterey, CA 93940.

Table 1

Abundance (mean number/100 m^2), total number and percentage, and mean total length of nonschooling fishes counted during 83 transects at five sites in Soquel Canyon. SE = standard error. Species names follow Robins et al. (1991).

		Site 1		Site 2		Site 3		Site 4		Site 5		Total[1]		Length (cm)	
Species	Common name	Mean	SE	Mean	SE	Mean	SE	Mean	SE	Mean	SE	No.	%	Mean	SE
Sebastes saxicola[1]	stripetail rockfish	3.6	0.6	2.7	0.7	3.7	0.7	0.2	0.2	0.3	0.2	1005	16.2	16.4	0.2
Sebastes paucispinis	bocaccio	2.5	0.8	2.5	0.6	0.7	0.3	1.9	1.2	18.2	5.6	712	11.5	55.3	0.5
Sebastes helvomaculatus	rosethorn rockfish	2.9	0.5	5.5	1.0	1.3	0.3	<0.1	<0.1	0.3	0.2	542	8.7	22.1	0.3
Sebastes chlorostictus	greenspotted rockfish	2.0	0.4	0.6	0.2	5.6	0.9	4.0	1.2	2.3	0.6	426	6.9	32.5	0.6
Sebastes spp	unidentified rockfishes	0.7	0.2	3.6	0.6	1.4	0.6	1.0	0.6	0.3	0.1	349	5.6	21.1	0.8
Agonidae	poachers	1.5	0.4	1.2	0.2	2.4	0.4	0.4	0.2	0.1	0.1	324	5.2	16.8	0.3
Sebastes elongatus	greenstriped rockfish	0.9	0.3	1.9	0.5	1.4	0.2	<0.1	<0.1	<0.1	<0.1	289	4.7	25.7	0.5
Sebastes crameri	darkblotched rockfish	—	—	4.7	0.8	<0.1	<0.1	0.4	0.4	—	—	259	4.2	21.3	0.3
Sebastes semicinctus	halfbanded rockfish	1.1	0.5	—	—	0.8	0.2	—	—	—	—	230	3.7	12.7	0.2
Sebastes levis	cowcod	0.6	0.4	0.1	0.1	0.2	0.1	0.4	0.4	5.1	1.1	202	3.3	58.6	1.1
Sebastes wilsoni	pygmy rockfish	1.9	1.4	0.2	0.1	0.7	0.3	—	—	—	—	201	3.2	16.2	0.3
Microstomus pacificus	Dover sole	0.7	0.3	0.1	<0.1	0.6	0.2	0.1	<0.1	0.3	0.2	199	3.2	24.5	0.7
Ophiodon elongatus	lingcod	<0.1	<0.1	0.3	0.1	1.4	0.4	0.3	0.2	6.4	1.8	171	2.8	57.8	1.5
Sebastolobus alascanus	shortspine thornyhead	0.6	0.3	<0.1	<0.1	1.3	0.3	—	—	<0.1	<0.1	171	2.8	19.8	0.6
Eptatretus stouti	Pacific hagfish	0.5	0.2	<0.1	<0.1	0.8	0.3	0.2	0.2	0.4	0.2	115	1.9	23.6	0.7
Sebastes ruberrimus	yelloweye rockfish	0.3	0.1	0.1	0.1	0.3	0.1	0.5	0.5	1.7	0.6	104	1.7	56.1	1.9
Merluccius productus	Pacific hake	0.2	0.1	0.1	0.1	0.1	<0.1	1.7	1.0	0.1	0.1	83	1.3	18.4	0.6
Sebastomus complex[2]	unidentified rockfishes	<0.1	<0.1	0.4	0.1	0.2	0.1	0.1	0.1	—	—	83	1.3	24.8	1.5
Sebastes pinniger	canary rockfish	—	—	—	—	0.5	0.2	—	—	—	—	73	1.2	37.5	0.5
Sebastes rosenblatti	greenblotched rockfish	0.1	<0.1	0.3	0.1	0.1	<0.1	0.9	0.3	5.0	3.3	65	1.0	42.7	1.4
Pisces	unidentified fish	0.2	0.1	0.3	0.1	0.3	0.2	—	—	<0.1	<0.1	56	0.9	17.6	2.6
Pleuronectiformes	unidentified flatfishes	0.3	0.2	0.3	0.1	0.1	<0.1	—	—	—	—	53	0.9	22.1	1.3
Sebastes rufus	bank rockfish	—	—	0.7	0.2	—	—	—	—	—	—	48	0.8	28.6	1.7
Sebastes entomelas	widow rockfish	—	—	0.1	0.1	—	—	—	—	1.4	0.6	45	0.7	45	1.8
Sebastes flavidus	yellowtail rockfish	—	—	—	—	0.4	0.1	—	—	—	—	36	0.6	40.3	1.2
Zaniolepis frenata	shortspine combfish	0.1	<0.1	0.1	<0.1	0.1	<0.1	—	—	—	—	31	0.5	21.6	0.7
Zalembius rosaceus	pink seaperch	0.1	<0.1	—	—	0.1	<0.1	—	—	—	—	30	0.5	15.9	0.6
Hydrolagus colliei	spotted ratfish	0.1	0.1	0.1	0.1	0.3	0.3	0.1	0.1	—	—	29	0.5	32.9	1.8
Sebastes chlorostictus and *S. rosenblatti*	greenspotted and greenblotched rockfish	<0.1	<0.1	—	—	0.2	0.1	—	—	0.2	0.1	29	0.5	41.3	1.1
Sebastes babcocki	redbanded rockfish	—	—	0.1	<0.1	<0.1	<0.1	—	—	0.3	0.1	24	0.4	39.3	3.5
Zoarcidae	unidentified eelpouts	0.1	0.1	0.1	0.1	<0.1	<0.1	—	—	<0.1	<0.1	24	0.4	24.4	1.6
Sebastes diploproa	splitnose rockfish	<0.1	<0.1	0.1	0.1	<0.1	<0.1	—	—	<0.1	<0.1	20	0.3	25.5	4.1
Lycodes cortezianus	bigfin eelpout	0.1	0.1	<0.1	<0.1	<0.1	<0.1	0.1	0.1	<0.1	<0.1	18	0.3	29.7	1.9
Zaniolepis spp	unidentified combfish	—	—	0.1	<0.1	<0.1	<0.1	—	—	—	—	17	0.3	22	2

continued

Table 1 (continued)

Species	Common name	Site 1		Site 2		Site 3		Site 4		Site 5		Total		Length (cm)	
		Mean	SE	Mean	SE	Mean	SE	Mean	SE	Mean	SE	No.	%	Mean	SE
Errex zachirus	rex sole	<0.1	<0.1	—	—	<0.1	<0.1	<0.1	<0.1	—	—	15	0.2	21	0.8
Pleuronectes vetulus	English sole	—	—	<0.1	<0.1	0.1	<0.1	<0.1	<0.1	—	—	12	0.2	26.3	1.7
Icelinus filamentosus	threadfin sculpin	0.1	0.1	<0.1	<0.1	<0.1	<0.1	—	—	—	—	11	0.2	14.3	1.9
Eopsetta exilis	slender sole	—	—	0.1	<0.1	—	—	0.1	0.1	—	—	11	0.2	20	4.5
Sebastes miniatus	vermilion rockfish	0.1	0.1	—	—	—	—	—	—	0.1	<0.1	11	0.2	47	3.4
Sebastes ensifer	swordspine rockfish	—	—	0.2	0.1	—	—	—	—	—	—	9	0.1	22.9	2
Cottidae[1]	unidentified sculpins	—	—	0.1	<0.1	<0.1	<0.1	—	—	—	—	9	0.1	13.3	3.3
Chilara taylori	spotted cusk-eel	<0.1	<0.1	—	—	<0.1	<0.1	—	—	—	—	8	0.1	20	
Plectobranchus evides	bluebarred prickleback	<0.1	<0.1	—	—	0.2	0.2	—	—	—	—	7	0.1	10.8	1.4
Synodus lucioceps	California lizardfish	—	—	—	—	<0.1	<0.1	0.2	0.2	—	—	6	0.1	32.5	5.9
Anoplopoma fimbria	sablefish	<0.1	<0.1	—	—	—	—	—	—	<0.1	<0.1	5	0.1	32	3.6
Bathymasteridae	unidentified ronquil	<0.1	<0.1	<0.1	<0.1	<0.1	<0.1	—	—	—	—	5	0.1	11	2.1
Coryphopterus nicholsi	blackeye goby	—	—	—	—	<0.1	<0.1	—	—	—	—	5	0.1	9	0.9
Raja rhina	longnose skate	<0.1	<0.1	—	—	<0.1	<0.1	—	—	<0.1	<0.1	5	0.1	42	7.5
Porichthys notatus	plainfin midshipman	<0.1	<0.1	—	—	—	—	—	—	—	—	4	0.1		
Sebastes goodei	chilipepper	—	—	—	—	<0.1	<0.1	—	—	—	—	4	0.1	28.3	6.7
Zaniolepis latipinnis	longspine combfish	—	—	<0.1	<0.1	<0.1	<0.1	—	—	—	—	4	0.1	20	
Sebastes ovalis	speckled rockfish	—	—	—	—	<0.1	<0.1	—	—	—	—	3	<0.1	40	
Argentina sialis	Pacific argentine	—	—	<0.1	<0.1	—	—	—	—	—	—	2	<0.1	25	
Raja spp	unidentified skates	<0.1	<0.1	—	—	—	—	—	—	<0.1	<0.1	2	<0.1	30	10
Sebastes rubrivinctus	flag rockfish	—	—	<0.1	<0.1	—	—	—	—	—	—	2	<0.1	10	
Eopsetta jordani	petrale sole	—	—	0.1	0.1	—	—	—	—	—	—	1	<0.1	60	
Hexanchus griseus	sixgill shark	<0.1	<0.1	—	—	—	—	—	—	—	—	1	<0.1	200	
Sebastes hopkinsi	squarespot rockfish	—	—	—	—	<0.1	<0.1	—	—	—	—	1	<0.1	15	
Sebastes jordani	shortbelly rockfish	—	—	<0.1	<0.1	—	—	—	—	—	—	1	<0.1		
Torpedo californica	Pacific electric ray	—	—	—	—	—	—	—	—	<0.1	<0.1	1	<0.1	45	
Sum		21.3		26.8		25.7		12.8		42.4		6208			
Number of taxa		31		35		38		20		22		52			
Number rockfish species		12		17		18		9		12		24			

[1] Observations of this small species could include *Sebastes zacentrus*, a species with similar color patterns and body shape.
[2] Rockfishes within the *Sebastomus* complex comprise seven species off central CA, several of which are difficult to identify without close examination.
[3] Likely *Icelinus* spp.

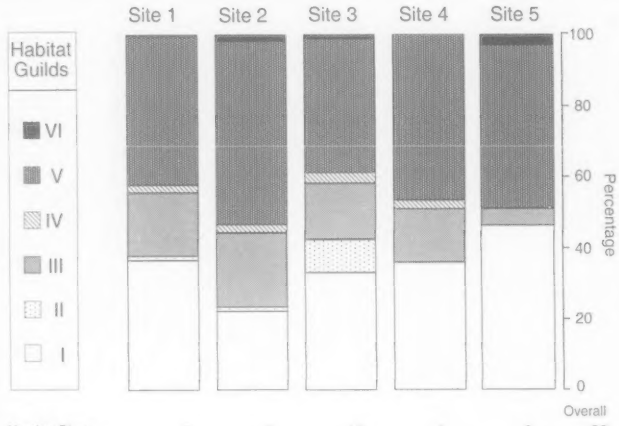

	Site 1	Site 2	Site 3	Site 4	Site 5	Overall
Number Dives	5	6	13	3	6	33
Number Transects	13	14	39	4	13	83
Number Habitat Patches	207	185	515	52	66	1,025
Depth Range (m)	98-305	148-263	94-296	153-210	152-226	94-305
Time Surveyed (h)	2.7	2.4	6.0	0.6	1.7	13.4
Area Surveyed (m^2)	7,638	7,256	13,626	1,285	3,949	33,754
Total Area (ha)	6.9	1.5	19.6	5.8	1.4	35.2

Figure 5

Percent cover of bottom types in habitat guilds (see Fig. 4 for identifications) at five study sites in Soquel Canyon. Number of dives, transects, and habitat patches, depth range, time and area covered, and total area (as estimated from mosaic of side scan sonographs in geographic information system) are listed for each site.

at shallow depths (ANOVA, $P<0.01$). Within depth category, site 2 generally had smaller fishes, and site 5 consistently had the largest fishes. *S. levis* and *S. ruberrimus* were abundant only in the deep category, and were significantly bigger at site 5.

Patterns of species richness (S), diversity (H′), and evenness (J′) were evident among the species assemblages associated with different bottom types (Fig. 8). The two most distinct habitat guilds in the cluster analysis (i.e. mud [guild I] and rock-boulder [guild VI]) ranked among the lowest in both H′ and J′, with a single species clearly dominating each guild. Diversity also was low in the boulder-mud guild (IV), although with somewhat more even proportions among species. The most diverse and evenly distributed assemblages were those in the remaining three guilds (II, III, and V).

Considering just the rock habitat guild (V), diversity measures were examined among sites having different fishing activity in both shallow and deep depth categories (Fig. 9). No patterns in diversity among the three sites in the shallow rock habitat guild were evident (Fig. 9A), although differences in relative abundance of each species were clear. In deep water, a shift in relative abundance occurred from site 2 to site 5, with large species playing a larger role at the less fished sites. The deep rock habitat guild at the iso-

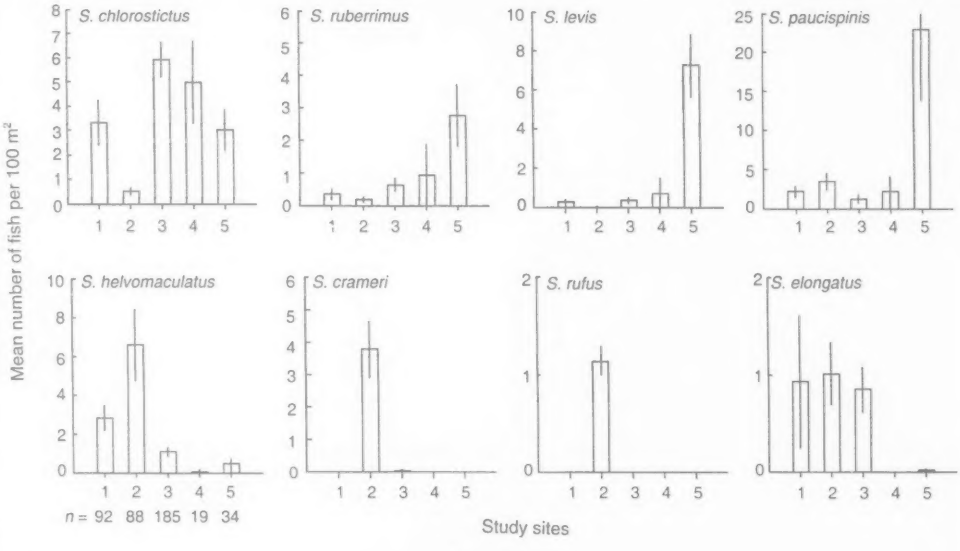

Figure 6

Index of abundance (mean number/100 m^2) of dominant species of nonschooling rockfishes in the rock habitat guild at five sites in Soquel Canyon. Vertical bars are 1 standard error; n = number of habitat patches at each site.

lated site 5 had the lowest diversity among all sites and depths, as measured by H′ and J′.

Discussion

Habitats

Several studies have described distinct fish-habitat associations for various species of benthic rockfishes during different stages of development (Carlson and Straty, 1981; Pearcy et al., 1989; Carr, 1991; Stein et al., 1992; O'Connell and Carlile, 1993). Although species composition may vary latitudinally, there is remarkable concordance between some of the habitat guilds identified in Soquel Canyon and the results of a habitat-based assessment of fishes using similar techniques and habitat characterizations on Heceta Bank off central Oregon (Stein et al., 1992). Mud, rock-boulder, and boulder habitats were most distinct in both studies and included the same dominant species; *M. pacificus*, *S. alascanus*, and Agonidae were abundant on mud, whereas *S. wilsoni* was the single most abundant species in the rock-boulder habitat of Soquel Canyon and the boulder habitat on Heceta Bank (Table 2). Fish assemblages in low relief, mixed habitats of mud, cobble, and pebble grouped together, and although dominant species were largely different (i.e. mud-cobble habitat dominated by *S. zacentrus* and *S. wilsoni* in Oregon and by *S. saxicola*, *S. helvomaculatus* and Agonidae in Soquel Canyon), the assemblages were made up of relatively small species in both studies. Several species common to both studies were characterized similarly in terms of habitats (e.g. associations of *S. pinniger* with rock-boulder combinations and *S. elongatus* with mud-cobble combinations).

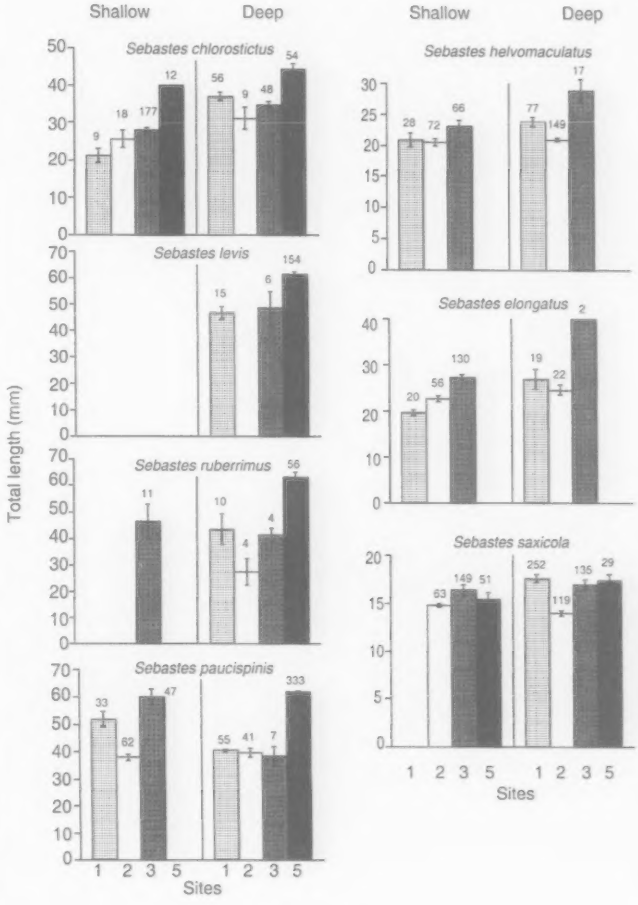

Figure 7

Mean size (vertical bars are 1 standard error) for dominant species in shallow and deep depth categories over all bottom types at study sites 1 to 3 and 5. Small numbers above bars are sample sizes.

Several of the species-habitat associations identified in Soquel Canyon also agreed with those described even farther north. From submersible observations off British Columbia, albeit made at shallower depths (21–150 m) and with less comprehensive habitat classifications than in Soquel Canyon or Heceta Bank, Murie et al. (1994) and Richards (1986) reported adult *S. ruberrimus* to be found exclusively on complex rock habitats, whereas *S. elongatus* was almost exclusively associated with sand-mud and mud-cobble substrata of low relief. In the eastern Gulf of Alaska, adult *S. ruberrimus* were found to be strongly associated with boulder fields, broken rock, overhangs, and crevices (O'Connell and Carlile, 1993), features similar to those of habitats described for this species in Soquel Canyon.

The generalities in habitat-specific associations, such as those described above for several rockfish species occurring along the entire west coast of the United States from central California to Alaska, can be valuable in predicting community structure and its response to perturbation. Identifying functional groups or habitat guilds that persist coastwide will be especially useful when applying these small-scale relationships between species and habitats to broader-scale resource surveys, potentially improving assessments of groundfish populations. Additionally, establishing these groups is critical to incorporating the concept of essential groundfish habitats, and negative impacts to them into the management of fisheries in relatively deep water, as required by the Sustainable Fisheries Act of 1996.

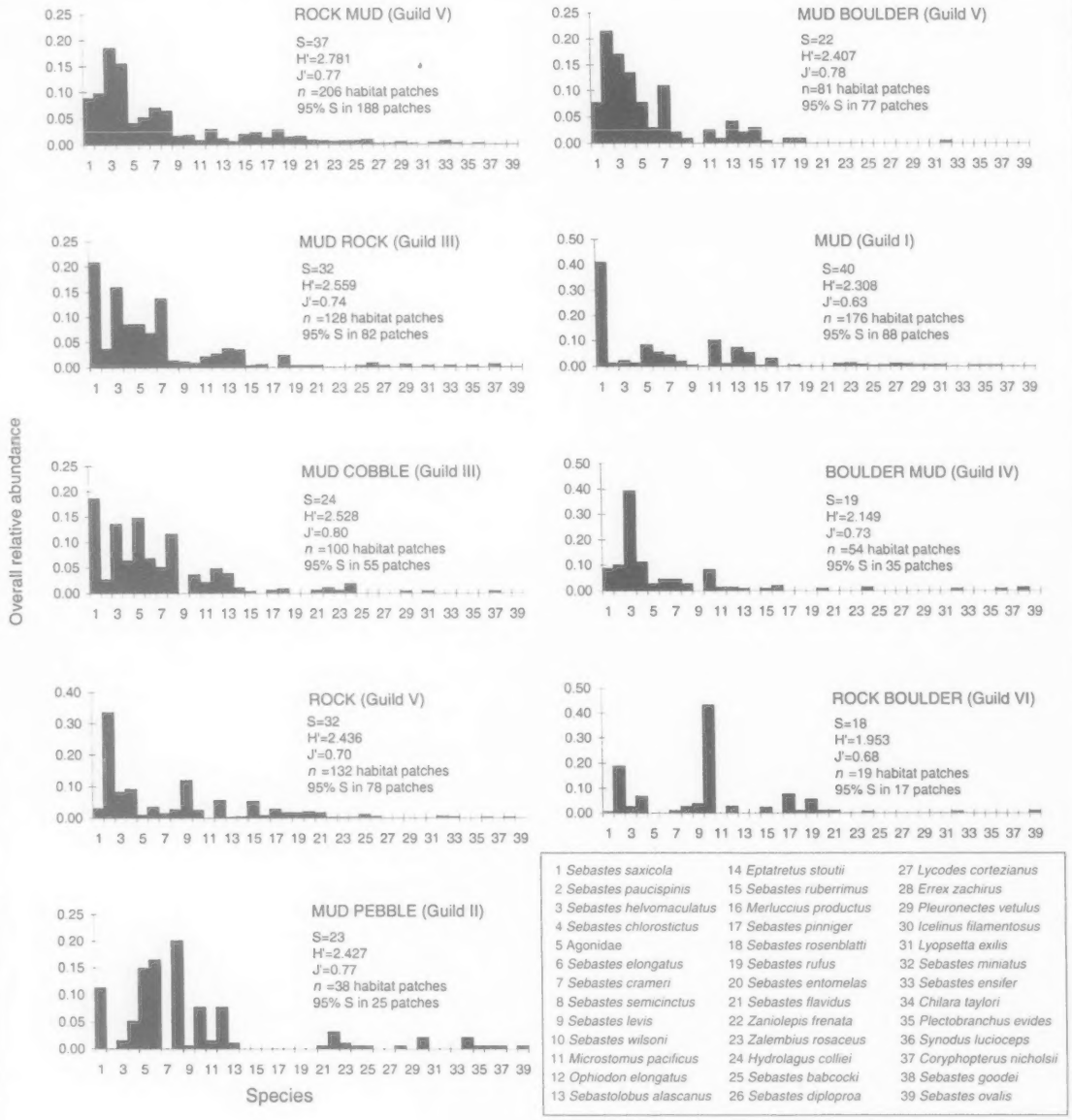

Figure 8

Overall relative abundance of each species associated with each type of habitat. Species richness (S), diversity (H'), and evenness (J') were calculated for each habitat guild (see Fig. 4 for identifications). n = the number of habitat patches sampled in each habitat. The number of patch samples required to detect 95% of the species is indicated.

Refugia

The high abundances of adult rockfishes associated with rock habitats along the sides of Soquel Submarine Canyon indicate that this canyon may in part serve as a natural harvest refuge, especially for those species of economic value. A comparison of average number of fish per hectare of habitat for the most abundant taxa in Soquel Canyon with the results of the habitat-based study on Heceta Bank (Stein et al., 1992), a longtime area of fishing activ-

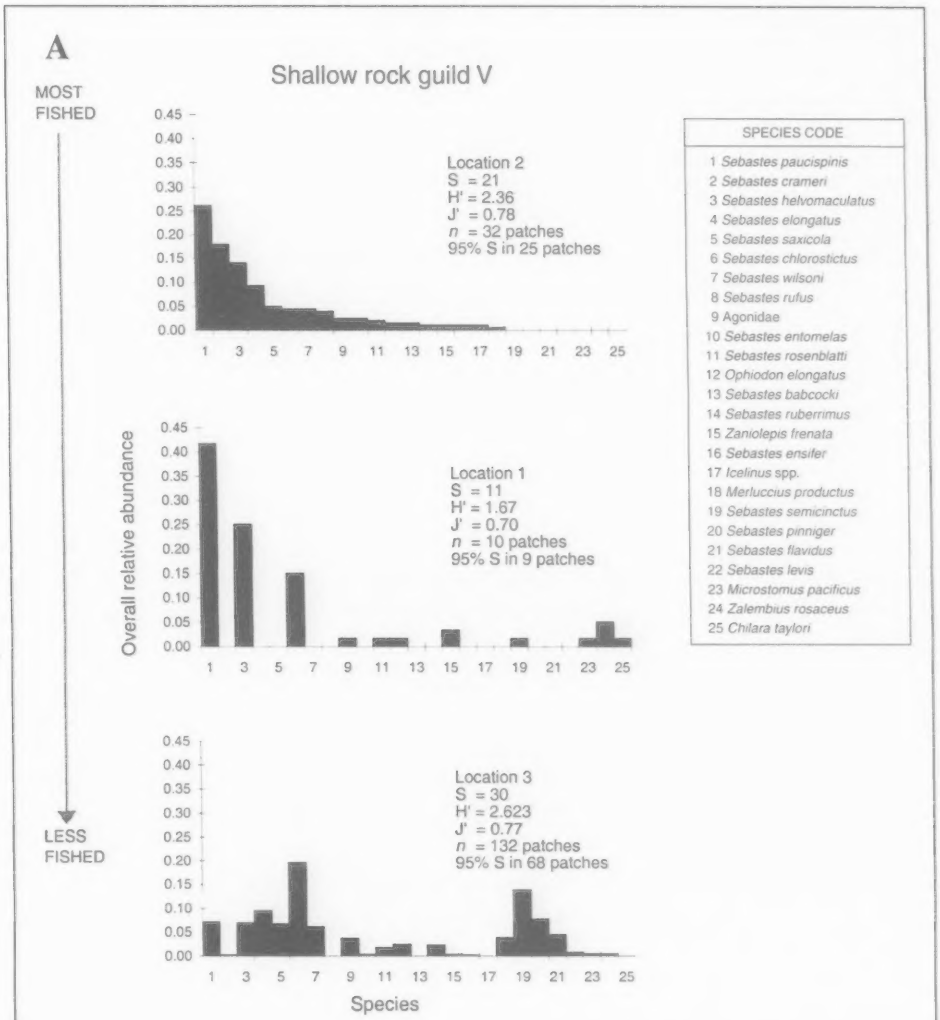

Figure 9

Overall relative abundance of each species in the rock habitat guild in (**A**) shallow (75–175 m) and (**B**) deep (176–275 m) water depths at locations with increasing relative levels of fishing activity in Soquel Canyon. Species richness (S), diversity (H'), and evenness (J') were calculated for each location at each water depth. *n* = the number of habitat patches sampled in each habitat. The number of patch samples required to detect 95% of the species is indicated.

ities, supports this conclusion. For example, our study site had several abundant, economically important benthic species (e.g. *O. elongatus*, *S. chlorostictus*, *S. levis*, *S. rosenblatti*, *S. ruberrimus*, *S. paucispinis*, *S. crameri*, and *S. rufus*; Table 2). These species generally dominated the rock, boulder, mud combination habitats in Soquel Canyon. Comparable habitats in Oregon were dominated by less valuable, small benthic rockfish species (e.g. *S. zacentrus*, *S. wilsoni* and *S. helvomaculatus*). The benthic species of highest abundance in the Oregon study were all in mud-cobble-boulder combination habitats, and most of these were not economically important. Large species of benthic rockfishes and *O. elongatus* did not occur in high numbers on Heceta Bank, Oregon. Although neither study estimated the abundance of active, semipelagic rockfishes, which generally aggregated above the submersible, commercially valuable species such as *S. flavidus* and *S. entomelas* occurred occasionally in high numbers in Soquel Canyon and more commonly over Heceta Bank.

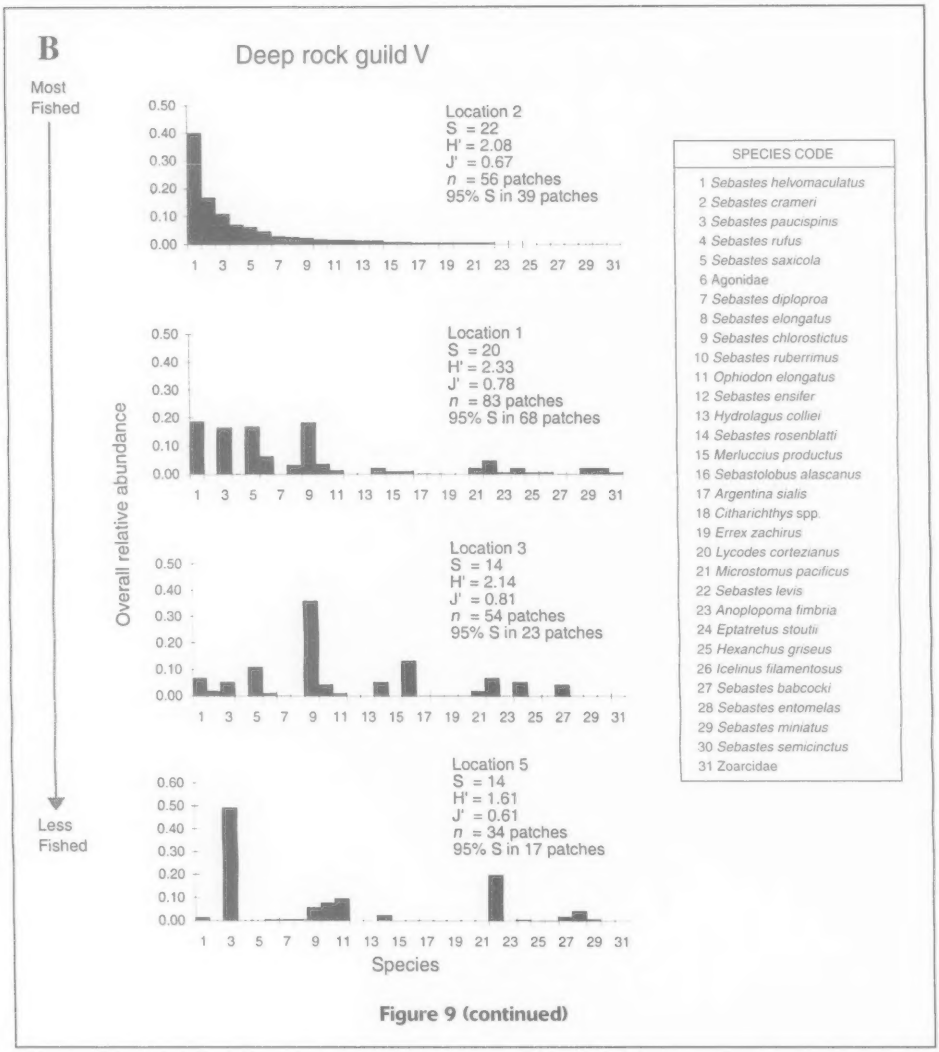

Figure 9 (continued)

The high abundances of large species of benthic rockfishes associated with complex habitats of rock, boulder, and mud combinations at several sites in Soquel Canyon are unique among other habitat-based groundfish assessments, lending further credibility to its designation as a natural harvest refuge. Other studies have reported relatively high numbers of various species of rockfishes associated with rock substrata (Richards, 1986; Stein et al., 1992; O'Connell and Carlile, 1993; Murie et al., 1994), but none have estimated abundances as high as those in Soquel Canyon. This is especially true when considering the extreme abundances of large fishes at site 5, an isolated outcrop on a steep section of the canyon wall surrounded by extensive fields of mud. For example, highest mean abundances of *S. ruberrimus* (number fish/100 m^2) on complex rock substrata were estimated to be about 0.3 off central Oregon (Stein et al., 1992), 0.9 in the Gulf of Alaska (O'Connell and Carlile, 1993), 1.4 off British Columbia (Richards, 1986), and 2.8 at site 5 in Soquel Canyon. Other economically valuable species (e.g. *S. paucispinis* and *O. elongatus*) had even higher abundances at some of the relatively unfished sites in the canyon (Table 1 and Fig. 6), but their abundances were not estimated in the other studies. Mean abundances of *S. elongatus*, a smaller species that is less frequently caught by anglers (Richards, 1986; Karpov et al., 1995), were similar off British Columbia, Oregon and in Soquel Canyon (about 1.5, 0.8, and 1.0 fish/100 m^2 of rock habitat, respectively).

The abundance of *Sebastes helvomaculatus*, another small species that is of minor value to regional fisheries, might be considered an indirect indicator of fishing activity. This benthic species was strongly associated with the same

Table 2

Average number of fish per hectare of habitat of most abundant taxa in Soquel Canyon study. Bold numbers are most common taxa in each habitat category. Number in brackets is abundance estimated in similar habitat off Oregon (Stein et al., 1992). Shading indicates economically valuable species that commonly occurred in relatively high abundance in Soquel Canyon but not off Oregon.

	Guild I	Guild II		Guild III		Guild IV	Guild V	Guild VI		
Species[1]	Mud	Cobble-mud	Mud-pebble	Mud-cobble	Mud-rock	Boulder-mud	Mud-boulder	Rock-mud	Rock-ridge	Rock-boulder
Agonidae	121 [186]	65 [-]	**228**	**251** [464]	110	53 [25]	147 [1122]	50 [-]	18 [18]	—
Eptatretus stouti	77	—	—	17	43	—	39	6	6	—
Merluccius productus	44	—	—	—	7	40	8	27	15	—
Microstomus pacificus	150 [499]	— [-]	24	34 [343]	27	26 [-]	46 [2295]	9 [-]	— [15]	—
Ophiodon elongatus	13 [-]	— [67]	118	81 [-]	33	26 [-]	15 [-]	35 [-]	117 [30]	123
S. chlorostictus and *S. rosenblatti*	5	—	—	—	3	13	15	11	18	20
Sebastes chlorostictus	19	**390**	78	106	110	237	**255**	**193**	**192**	328
Sebastes crameri	64	195	—	85	**176**	92	209	86	29	41
Sebastes elongatus	80 [64]	**325** [266]	**251**	115 [364]	87	92 [25]	54 [204]	64 [-]	74 [79]	—
Sebastes entomelas	1	—	—	—	3	13	—	18	42	41
Sebastes flavidus	— [-]	— [67]	8	8 [29]	3	— [176]	— [-]	9 [-]	34 [191]	41
Sebastes helvomaculatus	32 [26]	65 [933]	24	**229** [343]	**206**	**844** [161]	**325** [408]	**231** [474]	**172** [675]	123
Sebastes levis	5	—	8	—	13	—	15	20	**254**	184
Sebastes paucispinis	19	—	—	42	47	211	**410**	**122**	**714**	**922**
Sebastes pinniger	— [-]	— [-]	—	8 [14]	—	— [-]	— [102]	15 [158]	60 [82]	369
Sebastes rosenblatti	4	—	—	13	30	—	15	33	35	41
Sebastes ruberrimus	2 [-]	— [-]	—	4 [7]	3	13 [25]	54 [-]	23 [-]	111 [27]	102
Sebastes rufus	—	—	—	—	3	—	15	17	32	266
Sebastes saxicola[2]	**611** [60]	130 [133]	173	**314** [2930]	**270**	185 [-]	147 [2754]	109 [-]	62 [277]	20
Sebastes semicinctus	29	**325**	**306**	195	17	53	39	79	55	123
Sebastes wilsoni	1 [21]	260 [999]	118	59 [2129]	10	172 [2772]	— [8926]	21 [-]	51 [1785]	**2131**
Sebastolobus alascanus	108 [239]	— [-]	16	64 [443]	47	13 [-]	77 [2193]	14 [-]	2 [-]	—

[1] See Table 1 for common names.

[2] Comparison is made with *Sebastes zacentrus* in Stein et al. (1992) study.

complex rock habitats that harbor the larger, more valuable species, such as *S. ruberrimus*. *Sebastes helvomaculatus* ranked third in overall abundance both in Soquel Canyon and on Heceta Bank, Oregon (Stein et al., 1992). This was one of the dominant species in the complex rock habitats on Heceta Bank, as well as on site 2 (the area with the most fishing activity in Soquel Canyon). Interestingly, abundance of *S. helvomaculatus* was significantly lower in this same habitat at those sites having high numbers of larger species and less fishing activity in Soquel Canyon (i.e. sites 3–5; Fig. 6).

It is generally understood, especially in the broad literature on artificial and tropical reefs, that complex rock outcrops of high relief provide shelter and protection to reef fishes (Bohnsack, 1989; Potts and Hulbert, 1994, among others). O'Connell and Carlile (1993) noted that the occurrence of adult *S. ruberrimus* was higher in areas with more voids or refuge spaces, and that "extremely high" densities of this and other species were associated with isolated abrupt pinnacles comprising boulders and overhangs. This type of habitat, surrounded by fields of mud as is the case at Site 5 in Soquel Canyon, likely functions as a natural aggregating device for structure-oriented species such as many of the benthic rockfishes. Moreover, in seeking shelter near these rock outcrops in Soquel Canyon, large rockfishes may be excavating the semiconsolidated mudstone (Yoklavich, pers. obs.), thereby creating more of their own habitat (not unlike the construction of burrows in soft sediments by tilefish [*Lopholatilus chamaeleonticeps*; Able et al. 1982]). The extraordinary abundances estimated for several large species (*S. paucispinis*, *S. levis*, *S. rosenblatti*, *O. elongatus*) in a relatively small area of the canyon provide an insight into considerations of design and location when establishing protected areas as a management tool.

In addition to high abundances of valuable species on those rock outcrops in Soquel Canyon with little or no

evidence of fishing activities, the large sizes of individual fishes further support the concept of a natural harvest refuge in these areas. Although overall mean length of many species was similar and in some cases smaller in Soquel Canyon when compared with those on Heceta Bank (Stein et al., 1992), sizes were substantially larger for the large benthic species in the canyon (i.e. *S. ruberrimus, S. paucispinis, S. babcocki,* and *O. elongatus*).

Aggregations of young rockfishes were absent at any depth during our surveys of Soquel Canyon, leading us to conclude that although the canyon is likely a refuge for adult rockfishes it does not serve as a nursery ground. In contrast, from submersible observations of dense schools of young-of-the-year rockfishes associated with the shallow (100 m) ridge tops of Heceta Bank, Pearcy et al. (1989) suggested that rocky portions of the bank function as a nursery for young rockfishes. Heceta Bank is topographically isolated and located about 55 km off the Oregon coast; it is likely that there are no suitable nursery areas for rockfishes nearby. Soquel Canyon, however, is about 15 km offshore in Monterey Bay, and in close proximity to shallow rock outcrops, cobble fields, and kelp forests that function as nursery areas for many rockfish species (Carr, 1991; Johnson, 1997).

Aside from changes in population numbers and sizes, marine fisheries have been identified as one of the most critical environmental threats to marine biodiversity (Sobel, 1993; Boehlert, 1996), and it has been suggested that harvest refugia may contribute to the preservation of individual species, genotypes, and habitats (Bohnsack and Ault, 1996). Overall, the benthic fish assemblages in the various habitats of Soquel Canyon are relatively diverse; total species richness in the canyon was 52 (20 species comprising 90% of the total abundance) compared with 38 species on Heceta Bank (where only 10 species contributed to 90% of the abundance; Stein et al., 1992). Species diversity, as measured by H′ (Fig. 8), clearly varied among habitats; fish assemblages associated with complex habitats of rock, cobble, and mud maintained the highest diversity, whereas boulder habitats had lower diversity with a few dominant species. There was no clear influence of relative fishing activity on species diversity in the complex rock habitats of the canyon, but there was an influence on the relative abundance and sizes of the species themselves.

We conclude that some heterogeneous rocky habitats of high relief interspersed with soft mud in deep water of Soquel Submarine Canyon support high numbers of large adult rockfishes, in particular those species important to regional fisheries. These fishes are likely protected from excessive harvest because these habitat characteristics make them difficult to locate and target. These areas appear to function as a natural harvest refugium, potentially contributing new recruits to adjacent fished areas. We suspect that other such isolated high-relief rock habitat, as yet undetected or described, exists elsewhere in deep water on the continental shelf and slope of the west coast. The challenge now is to identify and characterize these habitats and associated fish assemblages, and to relate these small scale patterns to larger geographic areas relevant to benthic fishery stocks.

Acknowledgments

This multidisciplinary study required the time and effort of many people. In particular, we acknowledge the assistance of the following people: L. Browne, M. Ledbetter, G. Moreno, P. Reilly, R. Starr, P. Stipa, W. Wakefield, and D. Watters with field logistics and data collection; D. Caswell (Pelagos Corp.) with the side scan sonar survey; M. Boyle, T. Chase, C. Degnan, H. Lucky, and C. Steele (USGS) with geophysical data analyses and mapping; the captains and crews of the RVs *Jolly Roger, Cavalier,* and *Pt. Sur* for providing suitable research platforms; J. Barry and S. Etchemendy (MBARI) for logistical support; and all personnel from Delta Oceanographics, especially R. Slater, D. Slater, and C. Ijames, whose expertise and dedication provided for the safe and efficient use of the research submersible *Delta*. J. Mason, V. O'Connell, R. Parrish, P. Reilly, and three anonymous reviewers offered valuable comments on earlier drafts of this manuscript. This study was partially supported by NOAA's National Undersea Research Program, West Coast and Polar Regions Undersea Research Center, University of Alaska Fairbanks (grant nos. UAF-92-0063 and UAF-93-0036).

Literature cited

Able, K. W., C. G. Grimes, and J. R. Uzmann.
1982. Burrow construction and behavior of tilefish, *Lopholatilus chamaeleonticeps*, in Hudson Submarine Canyon. Environ. Biol. Fishes 7:199–205.

Able, K. W., D. C. Twitchell, C. G. Grimes, and R. S. Jones.
1987. Side scan sonar as a tool for detection of demersal fish habitats. Fish. Bull. 85:725–744.

Boehlert, G. W.
1996. Biodiversity and the sustainability of marine fisheries. Oceanography 9:28–35.

Bohnsack, J. A.
1989. Are the high densities of fishes at artificial reefs the result of habitat limitation or behavioral preference? Bull. Mar. Sci. 44:631–645.

Bohnsack, J. A., and J. S. Ault.
1996. Management strategies to conserve marine biodiversity. Oceanography 9:73–82.

Bruce, P. J. Simon, and T. Oswald.
1995. Resampling stats, version 4.0 edition. Resampling Stats, Inc., Arlington, VA, 127 p.

Carlson, H. R., and R. R. Straty.
1981. Habitat and nursery grounds of Pacific rockfish, *Sebastes* spp., in rocky coastal areas of Southeastern Alaska. Mar. Fish. Rev. 43:13–19.

Carr, M. H.
1991. Habitat selection and recruitment of an assemblage of temperate zone reef fishes. J. Exp. Mar. Biol. Ecol. 146: 113–137.

Deimling, E. A., and W. J. Liss.
1994. Fishery development in the eastern North Pacific: a natural-cultural system perspective, 1888–1976. Fish. Oceanogr. 3:60–77.

Greene, H. G., M. M. Yoklavich, R. M. Starr, V. M. O'Connell, W. W. Wakefield, D. E. Sullivan, J. E. McRea Jr., and G. M. Cailliet.
1999. A classification scheme for deep seafloor habitats. Oceanologica Acta 22(6):663–678.

Greene, H. G., M. M. Yoklavich, D. Sullivan, and G. M. Cailliet.
1995. A geophysical approach to classifying marine benthic habitats: Monterey Bay as a model. Alaska Fish Game Special Publication 9:15–30.
Johnson, K. A.
1997. Rockfish (*Sebastes* spp.) recruitment to soft bottom habitats in Monterey Bay, CA. M.S. thesis, California State University, Stanislaus, CA, 70 p.
Karpov, K. A., D. P. Albin, and W. H. Van Buskirk.
1995. The marine recreational finfishery in northern and central California: a historical comparison (1958–1986), status of stocks (1980–1986), and effects of changes in the California Current. Calif. Fish Game Fish Bull. 176:1–192.
Krebs, C. J.
1989. Ecological methodology. Harper and Row, Publishers, New York, NY, 654 p.
Larson, R. J.
1980. Competition, habitat selection, and the bathymetric segregation of two rockfish (*Sebastes*) species. Ecol. Monogr. 50:221–239.
Lea, R. N.
1992. Rockfishes: overview. *In* California's living marine resources and their utilization (W. S. Leet, C. M. Dewees, and C. W. Haugen, eds.), p. 114–116. Sea Grant Extension Publ. UCSGEP-92-12, University of California, Davis, CA.
Mason, J. E.
1995. Species trends in sport fisheries, Monterey Bay, California, 1959–86. Mar. Fish. Rev. 57:1–16.
1998. Declining rockfish lengths in the Monterey Bay, California recreational fishery, 1959–94. Mar. Fish. Rev. 60:15–28.
Murie, D. J., D. C. Parkyn, B. G. Clapp, and G. G. Krause.
1994. Observations on the distribution and activities of rockfish, *Sebastes* spp., in Saanich Inlet, British Columbia, from the *Pisces IV* submersible. Fish. Bull. 92:313–323.
O'Connell, V. M., and D. W. Carlile.
1993. Habitat-specific density of adult yelloweye rockfish *Sebastes ruberrimus* in the eastern Gulf of Alaska. Fish. Bull. 91:304–309.
Pearcy, W. G., D. L. Stein, M. A. Hixon, E. K. Pikitch, W. H. Barss, and R. M. Starr.
1989. Submersible observations of deep-reef fishes of Heceta Bank, Oregon. Fish. Bull. 87:955–965.
Pearson, D. E., and S. Ralston.
1990. Trends in landings, species composition, length-frequency distributions, and sex ratios of 11 rockfish species (Genus *Sebastes*) from central and northern California ports (1978–88). U.S. Dep. Commer., NOAA Tech. Memo. NMFS-SWFC-145, 65 p.
Phillips, J. B.
1939. The rockfish of the Monterey wholesale fish markets. Calif. Fish Game 25:214–225.
1957. A review of the rockfishes of California (Family Scorpaenidae). Calif. Fish Game Fish Bull. 104:1–158.
Potts, T. A., and A. W. Hulbert.
1994. Structural influences of artificial and natural habitats on fish aggregations in Onslow Bay, North Carolina. Bull. Mar. Sci. 55:609–622.
Ralston, S.
1998. The status of federally managed rockfish on the U.S. west coast. *In* Marine harvest refugia for west coast rockfish: a workshop (M. Yoklavich, ed.), p. 6–16. U.S. Dep. Commer., NOAA Tech. Memo. NMFS-SWFC-255, 159 p.
Richards, L. J.
1986. Depth and habitat distributions of three species of rockfish (*Sebastes*) in British Columbia: Observations from the submersible *PISCES IV*. Environ. Biol. Fishes 17:13–21.
Robins, C. R., R. M. Bailey, C. E. Bond, J. R. Brooker, E. A. Lachner, R. N. Lea, and W. B. Scott.
1991. Common and scientific names of fishes from the United States and Canada (5th ed.). Am. Fish. Soc. Spec. Publ. 20:1–183.
Root, R. B.
1967. The niche exploitation pattern of the blue-gray gnatcatcher. Ecol. Monogr. 37:317–350.
Sobel, J.
1993. Conserving biological diversity through marine protected areas. Oceanus 36:19–26.
Stein, D. L., B. N. Tissot, M. A. Hixon, and W. Barss.
1992. Fish-habitat associations on a deep reef at the edge of the Oregon continental shelf. Fish. Bull. 90:540–551.
SYSTAT.
1992. Statistics, version 5.2 edition. SYSTAT, Inc., Evanston, IL, 724 p.
Thomson, C. J.
1999. Economic and management implications of no-take reserves: an application to *Sebastes* rockfish in California. Calif. Coop. Oceanic Fish. Invest. Rep. 40:107–117.
Tusting, R. F., and D. L. Davis.
1993. Improved methods for visual and photographic benthic surveys. *In* Diving for science ... 1993. Proceedings of the American Academy of Underwater Sciences 13th Annual Scientific Diving Symposium, Pacific Grove, CA (J. N. Heine and N. L. Crane, eds.), p. 157–172. [Available from AAUS, 430 Nahant Rd., Nahant, MA 01908.]
Weinberg, K. L.
1994. Rockfish assemblages of the middle shelf and upper slope off Oregon and Washington. Fish. Bull. 92:620–632.
Winer, B. J.
1971. Statistical principles in experimental design. McGraw-Hill, Inc., New York, NY, 907 p.
Yoklavich, M., R. Starr, J. Steger, H. G. Greene, F. Schwing, and C. Malzone.
1997. Mapping benthic habitats and ocean currents in the vicinity of central California's Big Creek Ecological Reserve. U.S. Dep. Commer., NOAA Tech. Memo. NMFS-SWFC-245, 52 p.

Long-distance movement of a Nassau grouper (*Epinephelus striatus*) to a spawning aggregation in the central Bahamas

Stephania K. Bolden

Southeast Fishery Science Center
National Marine Fisheries Service, NOAA
75 Virginia Beach Drive
Miami, Florida 33133

E-mail address: stephania.bolden@noaa.gov

Smith (1972) first reported *Epinephelus striatus* (Nassau grouper) spawning aggregations. Since then, spawning aggregations from a few dozen individuals to perhaps 100,000 individuals have been reported from the Bahamas, Jamaica, Cayman Islands, Belize, the Virgin Islands, and Mexico (Olson and LaPlace, 1979; Colin et al., 1987; Carter, 1988; Colin, 1992; Aguilar-Perera and Aguilar-Davila, 1996). Colin (1992) investigated and documented actual spawning of *E. striatus* off Long Island, Bahamas. Colin et al. (1987) and Sadovy et al. (1994) have provided the only other observations of spawning aggregations of western Atlantic serranid species (*E. guttatus* and *Mycteroperca tigris*).

Epinephelus striatus spawning aggregation sites are transient, site specific, and are usually known by local fishermen who fish them intensely during the spawning period. *Epinephelus striatus* spawn in the southern Caribbean during the full moon of December and January (Smith, 1972; Olsen and LaPlace, 1979; Colin et al., 1987; Colin, 1992), and at more northern locales (i.e. Bermuda) from May to July (Bardach et al., 1958). Johannes (1978) suggested that the period and location of reef fish spawning is selected to favor larval survival; more recently Colin (1996) has suggested that aggregation sites may be "learned." Differing densities of *E. striatus* at spawning sites prior to, during, and following full moon periods indicate that individuals move to an aggregation site for a limited period of time (Colin, 1992). Timing, size, and sex composition of moving prespawning individuals are unknown.

Knowledge of the distance and direction of *E. striatus* movement to historic spawning sites is based on Colin (1992) where a single tagged specimen was recaptured by a fisherman at a known spawning site east of Long Island, Bahamas, after travelling approximately 110 km in two months. This contribution documents long-distance movement (220 km) of a tagged *E. striatus* to a spawning aggregation.

Materials and methods

The Exuma Cay Land and Sea Park (ECLSP, Fig. 1) was the study site for an investigation of the home range of *E. striatus*. The 456-km^2 ECLSP was established in the central Bahamas in 1958 and fishing was banned in 1986. A total of eleven individuals were captured by traditional Bahamian fish traps, tagged, and released for the home range study during summer 1997. An *E. striatus* (58.1 cm TL) captured on 24 June 1997, tagged on 25 June, held in a fish trap and released at 24°18.8′N and 76°33.6′W on 2 July 1997 was later recaptured by a fisherman.

Each fish had a unique Floy dart tag (Floy Tag & Manufacturing, Inc., Seattle, Washington) inserted below the anterior dorsal-fin rays, between the second and third scale rows.

Each fish also had an acoustic transmitter (VEMCO Limited, Nova Scotia, Canada) surgically implanted into its body cavity.

Daily water temperature data were obtained from Caribbean Marine Research Center (CMRC) at Lee Stocking Island (approximately 120 km NW of Long Island, Fig. 1) to correlate with spawning season. Mean monthly water temperature was calculated for the months of February 1998 (this investigation) and February 1989 (Colin, 1992). February 1988 data (Colin, 1992) were not available.

Fish were continuously tracked by their individual acoustic frequency 24 hours a day for a 3-week period. Subsequent daily diver observations identified individual fish by their external tags.

Results

The recaptured Nassau grouper was tracked by ultrasound at its presumed "home reef" from 2 to 31 July 1997. Daily visual observations (by divers) from 9 to 15 August confirmed the presence of the Nassau grouper at its home reef. The last observation was recorded at the tagging locale on 16 August 1997 at the end of the field season.

Three other individuals tagged during the summer 1997 investigation were observed at the exact patch reef where they were tagged in summer 1998. Two of these tagged individuals were considered to be mature adults when tagged (47.1 cm TL and 44.1 cm TL), and the third was deemed a juvenile (25.2 cm TL). Measurement of two individuals indicated an annual growth rate of 3–4 cm: from 47.1 to 50.1 cm TL, and from 25.2 to 29.0 cm TL. Seven other *E. striatus* tagged during summer 1997 were not observed during summer 1998.

A fisherman caught the tagged individual on 16 February 1998 in a fish trap at the Long Island, Bahamas, spawning location described by Colin (1992) as the "south point aggregation site" at 22°51.0′N and 74°51.5′W, approximately 220 km (in a straight ESE route) from the release point (Fig. 1). Physical features of the aggregation site are described by Colin (1992). The fish was at large for 185 days and was caught in 18–21 m of water. Because fishing was limited during the period "due to high seas and strong wind,"[1] the exact date the fish entered the trap or the soak time is unknown.

Manuscript accepted 16 February 2000.
Fish. Bull. 98:642–645 (2000).

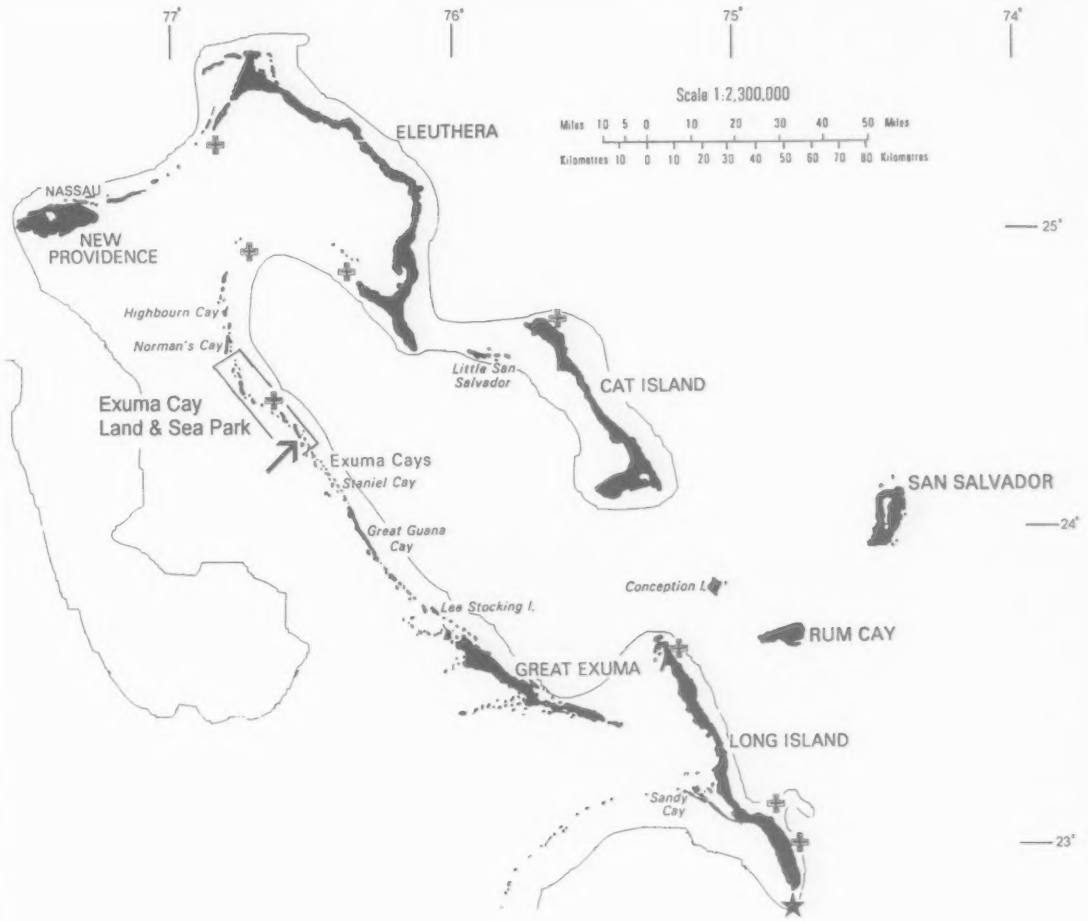

Figure 1

Map of the central Bahamas showing locations of tag and return sites of Nassau grouper (*Epinephelus striatus*). Longitude is west; latitude is north. The Exuma Cay Land and Sea Park is enclosed by a box. The site where the fish was captured, tagged, and released is designated by an arrow (↑); recapture site—denoted as the "south point aggregations site by Colin, 1992—by a star (★). Other possible *E. striatus* spawning sites noted by Bahamian government, local fishermen, and scientific literature are designated by a cross (✚). The 500-fathom depth contour, as determined by NOAA chart no. 23605, is designated by a solid line. This figure is modified with permission from a map produced by Department of Lands and Surveys for the Government of the Bahamas B.L.S. 1100.

Mean monthly water temperatures at CMRC dock were 23.94°C ±1.41 for February 1998, and $\bar{x}$ = 24.68°C ±0.75 for February 1989. Mean water temperature for the full moon period from 11 February 1998 to date of capture (16 February 1998) was 23.83°C ±0.63. The wide standard deviation for the February 1998 monthly mean was due to a 7-day (18–24 February) period of warm water temperature (>25°C every day).

[1] Cartwright, Capt. A. 1998. Personal commun. P.O. Box CB 11039, Nassau, Bahamas.

Discussion

Site fidelity for the recaptured Nassau grouper was 46 days; and perhaps a year for the three Nassau grouper at large, tagged in 1997 and resighted in 1998. Sexual maturity for *E. striatus* is reached at about 42 cm SL and 40 cm SL, for males and females respectively (Colin et al., 1987), thus the two larger fish seen again in 1998 were theoretically sexually mature. These two fish should have joined a spawning aggregation: they had either left the area and returned "home," or they were remarkably steadfast to that reef.

The south point aggregation site (where the tagged *E. striatus* was recaptured) has supported a seasonal fishery (fish trap, and hook and line) since before 1900 (Colin, 1992). During spawning aggregation periods, the site draws 2000–3000 *E. striatus*; density decreases during nonspawning periods (Colin, 1992). Notably, an *E. striatus* spawning aggregation site is known to have previously existed within the ECLSP boundaries at the "Wide Opening," approximately 20 km to the NNW of the tagging site.[2] However, it is not known if the site currently sustains spawning Nassau grouper. If this and other nearby spawning sites do exist (denoted by a cross (✚) in Fig. 1), one can only speculate as to why a fish would migrate a considerably greater distance to spawn.

I suggest that *E. striatus* learn the routes to historic spawning sites by local enhancement from older individuals (i.e. older animal directs attention of younger animal to a particular part or object in the environment), perhaps by socially transmitted traditions (see Helfman and Schultz, 1984, for definitions). The fact that traditions differ among subpopulations would account for both the number of spawning sites in an area and their historical nature. If spawning sites are learned from older individuals, then one could conjecture how this learning behavior affects recovering *E. striatus* populations; older individuals are required to socially transmit the location of spawning sites, and young adults need to be present to learn. Current and future studies of sensory systems and migration should provide insight into these hypotheses.

Because actual spawning was not observed and gonads were not available, the reproductive status of the recaptured *E. striatus* is unknown. Hence, fishermen reports and water temperature data were used to investigate the likelihood of *E. striatus* spawning at time of recapture. The recaptured fish was captured on 16 February from a spawning "school" five days after the full moon.[3] Local fishermen believe that spawning was occurring at this time because catches of *E. striatus* were abundant, the fishermen were targeting a known spawning site, and the fish were "full [of eggs]".[2] Spawning is usually synchronous with the full moon; thus it is speculated that the Nassau grouper use the moon as a visual cue in migrating to common spawning areas.

The geographic differences in spawning season of *E. striatus* are thought to correlate with water temperatures, of which optimal spawning temperature is most likely in the range of 25–26°C (Colin, 1992; Tucker et al., 1993). Mean monthly water temperature at the Long Island south point aggregation site was 24.68°C in February 1988 (no spawning; Colin, 1992) and 23.94°C in February 1998 (presumed spawning; present study). If spawning is correlated only with water temperature, then it is unlikely that the recaptured *E. striatus* grouper was actively spawning. However it is more likely that temperature is only one of many physical attributes influencing the spawning of *E. striatus* and if the fishermen reports are correct, it is entirely possible that the recaptured *E. striatus* was removed from a spawning aggregation.

ECLSP is a marine reserve for the preservation of animals, plant, and other marine life. For management purposes, the intent of a marine reserve is to provide spatial refuge from fishing, whereas the intent of traditional fishery restrictions on the resource is to allow a sufficient number of animals to reproduce. (Bohnsack, 1998). Evidence provided in the present study indicates that spatial refuge alone may be insufficient because the ECLSP reserve provided protection only until the animal migrated to spawn and thus was captured. If the Nassau grouper stock are to be preserved, protection throughout the animal's life history including spawning needs to be considered. Possible ways to provide this protection include closing documented spawning aggregation sites to fishing, enforcing seasonal closures, or providing protection for migrating and spawning individuals.

[2] Darville R. 1998. Personal commun. ECLSP Park Warden, P.O. Box N-4105 Nassau, Bahamas.

[3] Fishermen refer to the aggregations as "schools" because a large number of fishes are present in reproductive condition.

Acknowledgments

This research was conducted under a grant from NOAA Office of Protected Species, and a Research Permit from the Govt. of the Bahamas. I thank the National Marine Fisheries Service for financial support and the Nature Conservancy for field assistance. Special appreciation to Bell Island Ltd. and K. James for logistical support. Comments by W.J. Richards, J. Bohnsack, and three anonymous reviewers greatly improved the content. I would like to also thank Captain A. Cartwright and the Long Island fisherman who provided local fishing knowledge, L. Massey for creating the map, and N. Mehta of CMRC for temperature data. Field assistance by J. Kelly, H. Luciano IV, and K. Sullivan is appreciated.

Literature cited

Aguilar-Perera, A., and W. Aguilar-Davila.
1996. A spawning aggregation of Nassau grouper *Epinephelus striatus* (Pisces: Serranidae) in the Mexican Caribbean. Env. Biol. Fish. 45:351–361.

Bardach, J. E., C. L. Smith, and D. W. Menzel.
1958. Bermuda fisheries research program final report. Bermuda Trade Development Board, Hamilton, Bermuda, 59 p.

Bohnsack, J. A.
1998. Application of marine reserves to reef fisheries management. Aust. J. Ecol. 23:298–304.

Carter, J.
1988. Grouper mating ritual on a Caribbean reef. Underwater Natur. 17:8–11.

Colin, P. L.
1992. Reproduction of the Nassau grouper, *Epinephelus striatus* (Pisces: Serranidae) and its relationship to environmental conditions. Env. Biol. Fish. 34:357–377.
1996. Longevity of some coral reef fish spawning aggregations. Copeia 1996:189–191.

Colin, P. L., D. Y. Shapiro, and D. Weiler.
1987. Aspects of the reproduction of two species of groupers, *Epinephelus guttatus* and *E. striatus*, in the West Indies. Bull. Mar. Sci. 40:220–230.
Helfman, G. S., and E. T. Schultz.
1984. Social transmission of behavioural traditions in coral reef fish. Anim. Behav. 32:379–384.
Johannes, R. E.
1978. Reproductive strategies of coastal marine fishes in the tropics. Env. Biol. Fish. 3:65–84.
Olsen, D. A., and J. A. LaPlace.
1979. A study of a Virgin Islands grouper fishery based on a breeding aggregation. Proc. Gulf Carib. Fish. Inst. 31:130–144.
Sadovy, Y., P. L. Colin, and M. L. Domeier.
1994. Aggregation and spawning in the tiger grouper, *Mycteroperca tigris* (Pisces: Serranidae). Copeia 1994:511–516.
Smith, C. L.
1972. A spawning aggregation of Nassau grouper, *Epinephelus striatus* (Bloch). Trans. Am. Fish. Soc. 2:257–261.
Tucker, J. W. Jr., P. G. Bush and S. T. Slaybaugh.
1993. Reproductive patterns of Cayman Islands Nassau grouper (*Epinephelus striatus*) populations. Bull. Mar. Sci. 52:961–969.

Concurrent scavenging off a whale carcass by great white sharks, *Carcharodon carcharias*, and tiger sharks, *Galeocerdo cuvier*

Sheldon F.J. Dudley
Michael D. Anderson-Reade
Greg S. Thompson
Paul B. McMullen
Natal Sharks Board
P. Bag 2
Umhlanga Rocks 4320, South Africa
E-mail address (for S. Dudley): dudley@shark.co.za

The great white shark, *Carcharodon carcharias* (Lamnidae), and the tiger shark, *Galeocerdo cuvier* (Carcharhinidae), are two of the largest species of macropredatory sharks. Both are known to prey on dolphins (Delphinidae) off KwaZulu-Natal, South Africa (Cockcroft et al., 1989). Although scavenging off whale carcasses by white sharks (Carey et al., 1982; Pratt et al., 1982; McCosker, 1985; Long and Jones, 1996) and tiger sharks (Compagno et al., 1998) has been documented, the two species have not been recorded feeding concurrently on the same carcass. In August 1993, Natal Sharks Board (NSB) observers saw both species feeding on the carcass of a humpback whale, *Megaptera novaeangliae*, off Durban, but they were not seen scavenging concurrently (NSB[1]). In September 1997, elsewhere in the southwest Indian Ocean, tiger sharks were filmed feeding on a humpback whale carcass off the southern tip of Madagascar, but no white sharks were present. Compagno[2] subsequently viewed the footage and verified the identification of the tiger sharks.

This paper presents observations of white and tiger sharks scavenging off the floating carcass of a Bryde's whale, *Balaenoptera edeni*, off the coast of KwaZulu-Natal, South Africa. These observations are of a single event and hence should not be attributed more significance than they can support.

Methods

The National Sea Rescue Institute (NSRI) reported the presence of a Bryde's whale carcass to the NSB at midday on 26 April 1998. The NSRI, which had responded to a call reporting the carcass as a capsized yacht, found it floating 4 km east of the Durban harbor entrance (29°52′S, 31°24′E) with large sharks in its vicinity. The following day various reports were received that the carcass had drifted 25 km to the north and was several kilometers off the mouth of the Umdloti River (29°38′S, 31°07′E). Large sharks were reported to be feeding on it.

On 28 April, three of the authors launched a 5.5-m open-deck boat, equipped with photographic equipment and a shark cage, from the beach at Umhlanga Rocks (29°43′S, 31°05′E). The carcass was located 6 km offshore of the launch site and 10 km south of its position on the previous day. It was observed for 5 h. Conditions were excellent, with a glassy sea, light wind, little current, an estimated water temperature of 23°C and clarity of 15 m.

This account was written by S. F. J. Dudley (who did not witness the event) on the basis of separate interviews with the remaining authors and on viewing 27 min of video footage filmed by M. D. Anderson-Reade and an additional 4 min of footage filmed from another boat. All distances, times, and shark lengths (precaudal length, PCL) are approximate. The carcass was identified to species from the video footage, by the presence of prominent head ridges (Peddemors[3]).

Results

A white shark of 5 m was encountered 500 m from the carcass. The shark made numerous passes within 2 m of the stationary boat and just below the surface. This behavior continued for 15 min before the boat continued towards the carcass. This animal was not seen again.

Immediately upon reaching the carcass, two tiger sharks of 3.5 m were seen cruising 3 m below the surface. Two white sharks were present as well, one of about 4 m and the other a larger animal with a distinctive bite scar on the right side, located dorsolaterally and posterior to the first dorsal fin. A second boat was present and both shark species made approaches to each boat. The shark cage was deployed and occupied by two divers. A number of tiger sharks with distended abdomens were seen feeding on the carcass, usually singly but sometimes in groups of two or more. Their approaches to the carcass were leisurely and gave no evidence of intraspecific aggression. The white sharks, which were not seen feeding during this period, moved off soon after the cage was deployed and the animal with the bite scar was not seen again.

For 20 min the boat and cage were maneuvered around the carcass in an attempt to film the feeding process. Large quantities of organic debris reduced water clarity and because visibility was better from the surface, the divers returned to the boat and the cage was retrieved.

A 4-m female white shark, possibly the smaller animal seen at the carcass

[1] NSB (Natal Sharks Board). 1993. Unpubl. data. Natal Sharks Board, P. Bag 2, Umhlanga Rocks 4320, South Africa.

[2] Compagno, L. J. V. 1999. Personal commun. South African Museum, P.O. Box 61, Cape Town 8000, South Africa.

[3] Peddemors, V. M. 1998. Personal commun. Natal Sharks Board, P. Bag 2, Umhlanga Rocks 4320, South Africa.

Manuscript accepted 6 January 2000.
Fish. Bull. 98:646–649 (2000).

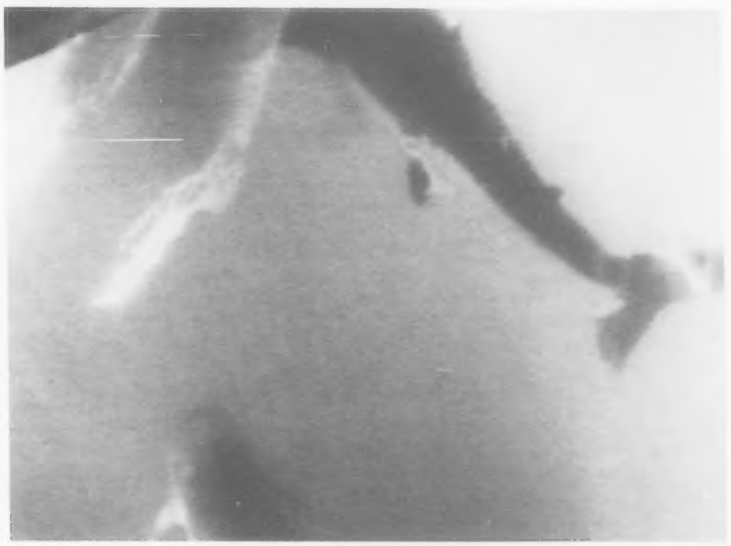

Figure 1

A 4-m PCL white shark feeding on the carcass of a Bryde's whale, and a 3.5-m tiger shark swimming below it. The head of the white shark, out of picture, is above water. The boat hull is at upper left, and strands of whale tissue are hanging beneath it. (Frame from Hi8 videotape).

initially, was observed surfacing 100 m from the carcass and regurgitating its stomach contents. It then circled the floating matter. While being approached by the boat, it began to feed on the regurgitated material. This was the only time that regurgitation was observed but, on other occasions, clouds of what appeared to be regurgitated matter were seen in the water near the carcass, indicating that regurgitation may have occurred more frequently.

Subsurface filming of the white shark was conducted over the gunwale. On five or six occasions the shark approached the camera (which was enclosed in a yellow housing) such that the cameraman was forced to lift the camera out of the water just prior to the shark's snout making contact. The shark would then mouth (lightly and briefly grasp) the boat or motors before moving off. On one occasion it damaged its head on the motor and the resulting laceration, immediately anterior to the right eye, was used subsequently as an identification mark.

A small (3–3.5 m), red, semirigid, inflatable boat arrived and the white shark immediately showed interest in it, approaching it from the rear several times and mouthing the motor.

After 40 min, the observers (coauthors) returned to close proximity of the carcass, where there now appeared to be between 7 and 10 tiger sharks, all 3.5 m. Feeding on the carcass continued, but the animals showed more interest in the boat than previously. Typically, a shark would leave the boat, feed on the whale and then return slowly to the vicinity of the boat. The motors were bumped three times and a propeller was mouthed once. As with the white shark, the tiger sharks approached the camera directly, and on several occasions the cameraman depended upon warnings from his co-observers to ensure timely evasion. Only one interaction between individual tiger sharks was observed. Two animals, swimming one above the other, converged slowly to within 1 m, at which point they diverged rapidly. Immediately prior to this event, one of the animals had been investigating the camera and it is possible that it had been unaware of the other shark's presence.

Soon after returning to the carcass, the observers noted the arrival of the white shark with the wounded snout. There appeared to be a slight increase in the swimming speed of the tiger sharks but no other reaction was observed. The white shark fed on three occasions and on each occasion one or more tiger sharks fed at the same time. On one occasion two tiger sharks swam within 3 m of the feeding white shark—one of these was captured on videotape, together with the white shark (Fig. 1). The white shark removed a piece from the carcass, then abandoned the piece and returned to the carcass. A tiger shark then fed on the piece but moved off when the white shark came back to it.

Both species fed on the carcass at the water line, but the tiger sharks fed below the water line as well. Tiger sharks were observed to thrust their heads out of the water to feed (Fig. 2) as has been observed previously (Gilbert, 1963;

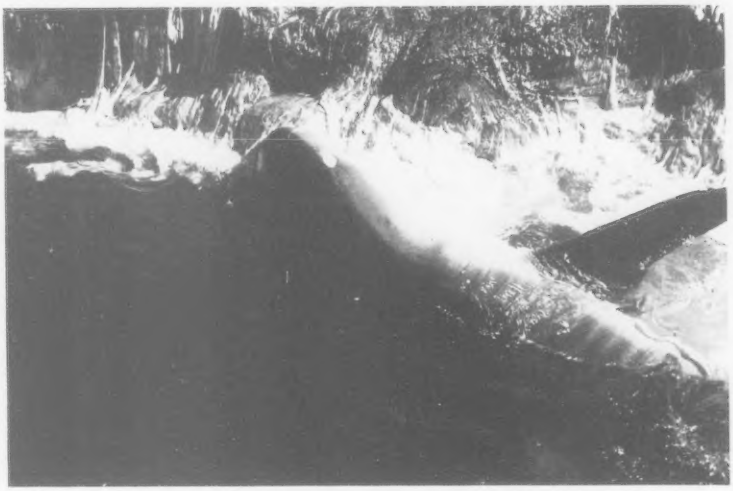

Figure 2

A 3.5-m PCL tiger shark feeding on a Bryde's whale carcass at the water line. The shark's eye is covered by the nictitating membrane.

Moss, 1972; Strong, 1991). One approach behavior exhibited by the white shark and captured on film conformed with that described by Tricas (1985) as an underwater approach, in which the shark approached the carcass just below the surface until approximately 1 m away and then attacked by deflecting the head upward, emerging out of the water to bite. When feeding above the water line, both species tended to bite twice in quick succession, apparently gaining better purchase with the second bite. This procedure was followed by slow and deliberate shaking, twisting, and turning to cut away the mouthful. The tiger sharks demonstrated more thrashing than the white shark, sometimes rolling onto their backs while biting. The white shark behavior described by Pratt et al. (1982), in which the shark bit a whale carcass ventral-surface-up before rolling upright to cut a mouthful, was not seen.

When tiger sharks fed below the surface, the carcass was penetrated vertically and a swaying motion of the body, rather than twisting, followed the bite. As many as five individual tiger sharks fed on the carcass at one time, some hanging below the carcass and some biting at the waterline.

The tiger sharks tended to remain at or near the carcass at all times, whereas the wounded white shark approached the carcass to feed and then moved off again, sometimes out of sight of the observers. A white shark of 3.5–4 m, believed to have been an individual not previously observed, made a brief appearance near the carcass during this period. The tiger sharks were generally more active than the wounded white shark, although both species were unhurried and deliberate. The white shark increased swimming speed only when investigating the camera.

The red inflatable boat which had been present earlier, returned, and the wounded white shark again showed particular interest in it. On one occasion the shark held the rear of the starboard pontoon in its mouth and kept the boat stationary despite the crew of the boat engaging gear and running the 40-hp motor at speed. After 10 sec the shark released the pontoon, the only damage to which was a single, small puncture, perhaps the result of exploratory mouthing behavior.

Discussion

White sharks feeding on whale carcasses appear to feed until satiated (McCosker, 1985). The observed regurgitation of food suggests that feeding may continue even after satiation.

Observations suggest agonistic encounters amongst white sharks when feeding on a whale carcass. Observers saw at least four and possibly up to nine different white sharks in the vicinity of a fin whale carcass, *Balaenoptera physalus*, over a 30-h period but never more than two together (Pratt et al., 1982). When two did co-occur their behavior appeared agonistic, and some of the sharks had tooth cuts and slashes (some previous wounds, some freshly inflicted). Similarly, Long and Jones (1996) reported that about five different white sharks fed on the carcass of a blue whale, *Balaenoptera musculus*, but only one fed at a time. McCosker (1985) observed an agonistic encounter between two white sharks feeding on horsemeat bait; the smaller shark was forced to depart after receiving a minor bite. Strong et al. (unpubl. data in Strong [1996]), also

noted that feeding attempts by individual white sharks may be thwarted by larger conspecifics. In our study, although three, possibly four, white sharks were seen at or near the carcass, only one was seen feeding. Although the observation period was brief, this type of behavior is consistent with the existence of intraspecific competitive exclusion. The animal seen feeding was smaller than at least two of its conspecifics, and it is possible that the larger individuals had fed previously.

The tiger sharks exhibited no evidence of intraspecific competition, despite the presence of up to 10 individuals in the vicinity of the carcass and up to five feeding concurrently. The abundance of food or the similarity in size of the sharks may have prevented the establishment of the size-dependent hierarchy discussed by Bres (1993).

Interspecific competition for food amongst reef-dwelling, carcharhinid species has been recorded (Nelson and Johnson, 1980), as have apparent interspecific hierarchies comprising 1) the silvertip shark, *Carcharhinus albimarginatus*, the Galapagos shark, *C. galapagensis*, and the blacktip shark, *C. limbatus*, (Limbaugh, 1963); 2) the oceanic whitetip shark, *C. longimanus*, and the silky shark, *C. falciformis*; and 3) hammerhead sharks (Sphyrnidae) and various other species (Springer, 1967). Pratt et al. (1982) noted that the locally abundant blue shark, *Prionace glauca*, and shortfin mako, *Isurus oxyrinchus*, were conspicuously absent from the vicinity of the fin whale carcass, and a fish spotter pilot observed no blue sharks within a 3.2-km radius. These authors suggested that this was a consequence of territorial exclusion by white sharks. Similarly, Long and Jones (1996) suggested that white sharks excluded blue sharks, a species known to scavenge on whale carcasses, from the blue whale carcass. McCosker (1985) observed a single white shark feeding on the carcass of a grey whale, *Eschrichtius robustus*, and saw no other shark species nearby. The white and tiger sharks, however, did not appear to compete at the Bryde's whale carcass. Springer (1967) noted that mixed-species feeding aggregations tend to consist of sharks of similar sizes. If it is hypothesized, therefore, that the single 4-m white shark would have competitively excluded a single 3.5-m tiger shark, the presence of several tiger sharks may have prevented this from occurring. McKibben and Nelson (1986) speculated that juvenile gray reef sharks grouping in a loose aggregation or as a polarized pack may obtain protection from larger sharks. The tiger sharks, attracted by a single stimulus, may have derived an incidental defensive benefit.

Literature cited

Bres, M.
1993. The behaviour of sharks. Rev. Fish Biol. Fish. 3:133–159.

Carey, F. G., J. W. Kanwisher, O. Brazier, G. Gabrielson, J. G. Casey, and H. L. Pratt.
1982. Temperature and activities of a white shark, *Carcharodon carcharias*. Copeia 1982(2):254–260.

Cockcroft, V. G., G. Cliff, and G. J .B. Ross.
1989. Shark predation on Indian Ocean bottlenose dolphins *Tursiops truncatus* off Natal, South Africa. S. Afr. J. Zool. 24(4):305–310.

Compagno, L. J. V., C. Simpfendorfer, J. E. McCosker, K. Holland, C. Lowe, B. Wetherbee, A. Bush, and C. Meyer.
1998. Sharks. (Reader's Digest explores). Reader's Digest, Pleasantville, NY, 160 p., illustr.

Gilbert, P. W.
1963. The visual apparatus of sharks. *In* Sharks and survival (P. W. Gilbert, ed.), p. 283–326. D.C. Heath and Co., Boston, MA.

Limbaugh, C.
1963. Field notes on sharks. *In* Sharks and survival (P. W. Gilbert, ed.), p. 63–94. D.C. Heath and Co., Boston, MA.

Long, D. J., and R. E. Jones.
1996. White shark predation and scavenging on cetaceans in the Eastern North Pacific Ocean. *In* Great white sharks: the biology of *Carcharodon carcharias* (A. P. Klimley and D. G. Ainley, eds.), p. 293–307. Academic Press, San Diego, CA.

McCosker, J. E.
1985. White shark attack behavior: observations of and speculations about predator and prey strategies. Mem. Southern Calif. Acad. Sci. 9:123–135.

McKibben, J. N., and D. R. Nelson.
1986. Patterns of movement and grouping of gray reef sharks, *Carcharhinus amblyrhynchos*, at Enewetak, Marshall Islands. Bull. Mar. Sci. 38(1):89–110.

Moss, S. A.
1972. The feeding mechanism of sharks of the family Carcharhinidae. J. Zool. Lond. 167:423–436.

Nelson, D. R., and R. H. Johnson.
1980. Behavior of the reef sharks of Rangiroa, French Polynesia. Natl Geog. Soc. Res. Rep. 12:479–499.

Pratt, H. L, J. G. Casey, and R. B. Conklin.
1982. Observations on large white sharks, *Carcharodon carcharias*, off Long Island, New York. Fish. Bull. 80(1):153–156.

Springer, S.
1967. Social organisation of shark populations. *In* Sharks, skates, and rays (P.W. Gilbert, R. F. Mathewson, and D. P. Rall, eds.), p. 149–174. Johns Hopkins Press, Baltimore, MD.

Strong, W. R.
1991. Instruments of natural selection: How important are sharks? *In* Discovering sharks (S. H. Gruber, ed.), p. 70–73. Am. Littoral Soc., Highlands, NJ.
1996. Repetitive aerial gaping: a thwart-induced behavior in white sharks. *In* Great white sharks: the biology of *Carcharodon carcharias* (A. P. Klimley, and D. G. Ainley, eds.), p. 393–400. Academic Press, San Diego, CA.

Tricas, T. C.
1985. Feeding ethology of the white shark, *Carcharodon carcharias*. Mem. Southern Calif. Acad. Sci. 9:81–91.

Validation of age estimates from otoliths of larval and juvenile spotted seatrout, *Cynoscion nebulosus*

Allyn B. Powell

Elisabeth H. Laban

Center for Coastal Fisheries and Habitat Research
National Ocean Service
National Oceanic and Atmospheric Administration
101 Pivers Island Road
Beaufort, North Carolina 28516-9722
E-mail address (for A. B. Powell): allyn.powell@noaa.gov

Scott A. Holt

G. Joan Holt

University of Texas Marine Science Institute
750 Channelview Drive
Port Aransas, Texas 78373

Otolith microstructure analysis has been shown to be valuable for relating biotic and abiotic factors to growth and survival (Crecco and Savoy, 1985; Thorrold and Williams, 1989; Maillet and Checkley, 1991; Jenkins et al., 1993) and determining size-specific mortality (Gleason and Bengtson, 1996; Sabo and Orth, 1996; Hare and Cowen, 1997) for the early life history stages of fishes. Prior to using otolith microstructure analysis, it is important that otolith validation studies be undertaken to examine the rate of increment formation and the timing of initial increment formation, and to check the interpretive skills of the otolith reader (Geffen, 1992).

Our validation study dealt with spotted seatrout, *Cynoscion nebulosus*, an economically important sciaenid. Otolith increment deposition rates from spotted seatrout have been validated by using tetracycline marking of wild-caught fish larvae and juveniles collected in Tampa Bay, Florida (McMichael and Peters, 1989). Because known-age larvae were not used, the timing of initial increment formation was not determined. The purpose of our study was to determine the rate of increment formation and timing of initial increment formation as well as to provide confidence to otolith readers by using known-age larvae and wild-caught juveniles. Our study is ancillary to spotted seatrout early life history studies in Florida Bay, Everglades National Park.

Materials and methods

Spotted seatrout eggs were obtained from the Texas Parks and Wildlife GCCA/CPL Marine Development Center hatchery from adults collected from upper Laguna Madre, Texas. Eggs were transported to the University of Texas Marine Science Institute (UTMSI), Port Aransas, Texas, in May 1997. Eggs were incubated in 600-L tanks at egg densities of 100 eggs/L. Tanks were held in greenhouses, illuminated with natural sunlight and 40-W overhead flourescent lights at a 24-h (15L:9D) photoperiod. A closed system was used, but water was continuously recirculated through a biofilter. During the rearing process, ambient temperatures ranged from 25.0 to 28.0°C; salinities, from 32 to 33 ppt. Larvae to age 12 d were fed rotifers (5/mL), which in turn were provided the algae *Isochrysis*. At age 13 d, brine shrimp nauplii, enriched with oil emulsion (Leger et al., 1986), were introduced (4 rotifers/mL; 2 nauplii/mL on a daily basis), and from age 15 d until the end of the experiment, 2–3 nauplii/mL were maintained on a daily basis. Food density was estimated twice a day and food added to the required density. Frozen adult brine shrimp and red drum, *Sciaenops ocellatus*, eggs were added on a daily basis from age 23 d to the end of the experiment. Otoliths of reared larvae were marked with alizarin complexone (ALC) at concentrations of 50 mg/L for four hours at age 9 and 16 d. Fifty larvae were sacrificed at ages 6, 9, 14, 20, 23, and 32 d and preserved in 95% ethyl alcohol. Larvae sacrificed at ages 6 and 9 d were not immersed in ALC.

Wild-caught juveniles were collected in Aransas Bay, Texas, in August 1997 with a 6-m bag seine (4.5-mm mesh in both the wings and the bag). Juveniles were placed in 45-L tanks and transported to the rearing facility at UTMSI, Port Aransas, Texas. Juveniles were held in 3-m raceways in 1100-L water at temperatures 27.0–28.0°C and a salinity of 36 ppt. Juveniles were segregated by size to avoid cannibalism. Two days after capture, otoliths were marked with ALC (100 mg/L for 4 h). Otoliths were similarly remarked 7 d later (9 d after capture). Mortality associated with the marking process was nil. All fish were sacrificed and preserved in 95% ethyl alcohol at 21 d after capture.

Otoliths were removed with probes and fine-tipped forceps. Polarized light was used to facilitate location of otoliths from fish <6 mm standard length (SL). All otoliths, except for the right sagitta, were placed on a slide, covered with mounting media and archived. The right sagittal otolith was embedded for transverse sectioning or polishing (or for both procedures). The left sagitta was embedded for transverse sectioning if the right was damaged during preparation.

Sagittae were read with a light microscope at 1000× magnification under oil immersion with blue light epifluorescence to detect ALC marks that fluoresce as reddish orange. The first increment was determined as that following the core increment, the latter a well-defined dark increment surrounding the core. Sagittae were read by one

Manuscript accepted 29 December 1999.
Fish. Bull. 98:650–654 (2000).

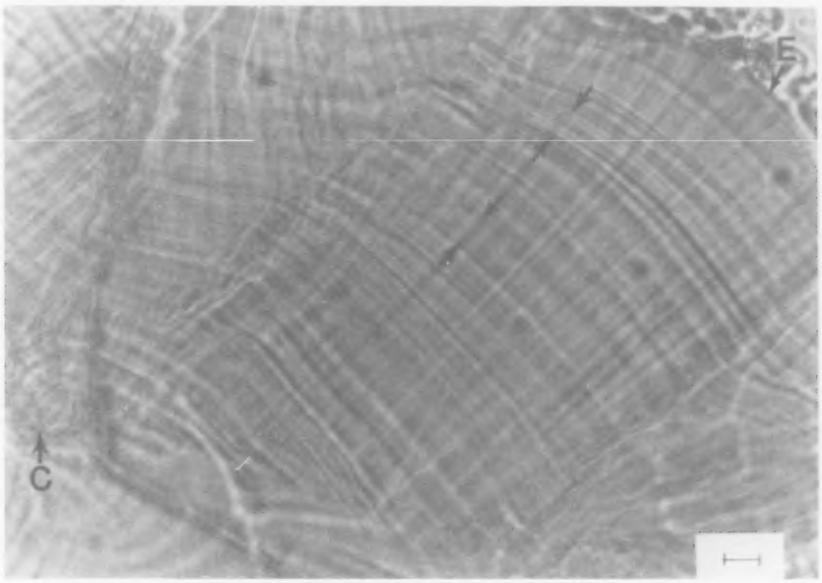

Figure 1

Photomicrograph of a transverse section of a spotted seatrout otolith from a 32-d-old laboratory-reared fish (SL=23.6 mm). C = the core; E = edge. The arrows point to daily increments that were determined as those rings that maintained relatively equal spacing as the fine focus was manipulated. The rings between the arrows were considered subdaily rings or optical artifacts. These rings did not maintain equal spacing when the fine focus was manipulated, were not continuous, and generally were poorly defined. Scale bar = 10 µm.

reader without knowledge of age of fish. Two to three readings were made and the counts averaged. Following Rice et al. (1985) and Ahrenholz et al. (1995), counts were regressed on age (SAS Institute, Inc., 1985), and Student's *t*-test used to determine if the slope was significantly different (α=0.05) than one. The null hypothesis is that the slope of increment counts on known age equals one. The null hypothesis is rejected if the slope is significantly different from one. A summary of the increment count data from known-age fish is shown in Table 1.

In our initial analysis, the slope of increment count regressed on known-age was significantly greater than one (α=0.05), but there were problems in aging the oldest juveniles (32 d)—problems that we related to variability in fish sizes (16.2 to 34.6 mm). Using linear regression, we examined the relation between increment count on size for all age groups. Only for the 32-d-old juveniles was the slope of increment count on size significantly different from zero (α=0.05), indicating that greater counts were observed as size increased. This result suggested that we interpreted subdaily rings as daily rings. We then examined otoliths from known-age juveniles in great detail to establish criteria to separate subdaily from daily rings. Although reading the older age (32-d-old) juveniles was difficult, daily rings maintained relatively equal spacing as the fine focus was manipulated. Subdaily rings or optical artifacts were not continuous, did not maintain equal spacing when focus was manipulated, and were not well defined (Fig. 1). Juvenile otoliths (23-d and 32-d-old) were reread (two blind readings per sagitta, with a hand counter). The reader avoided making mentally sequential counts, relying solely on the results of the hand counter.

Table 1

Mean, standard deviation (SD), number of fish (n), total number of readings (nr), and range of increment counts from known-age laboratory-reared *Cynoscion nebulosus*.

Age (days)	n	nr	Mean	SD	Range
6	10	25	4.7	0.7401	2–6
9	10	30	6.0	0.8383	5–8
14	10	30	12.1	0.6641	10–15
20	10	30	20.2	0.8409	17–24
23	12	24	21.9	1.3046	18–25
32	15	30	30.5	1.1568	28–33

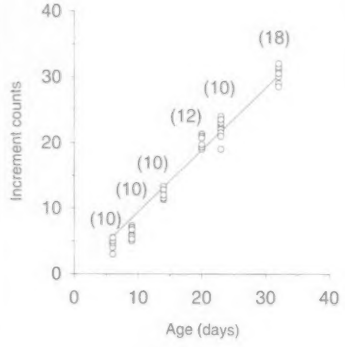

Figure 2

The relation between increment counts and known-age for spotted seatrout, *Cynoscion nebulosus*. Solid line represents regression line; dotted, 45° line. Values in parentheses indicate number of specimens.

Results

The slope of the line describing the relation between increment counts and known age was not significantly different from one (Table 2; Fig. 2). This result indicated that rings were being deposited daily and that we were correctly interpreting daily rings from subdaily rings or optical artifacts, a problem that was encountered with juveniles in our initial readings (see "Materials and methods" section).

A large percent of the laboratory-spawned and laboratory-reared fish that were marked with ALC failed to take up the stain on their otoliths. Only 15% (n=61) of the known-age fish exhibited a readable mark and only for two age groups. On the other hand, the majority (75%) of wild-caught juveniles exhibited a readable mark on their otoliths.

Increments were estimated to form at age 2–3 d. An inverse regression (counts regressed on age) yielded an intercept with a value of 2.3 d (Table 2). The intercept was significantly different from zero. Analysis of increment counts on ALC-marked otoliths from known-age larvae also revealed the first increment formed on day 2 or 3. For 14-d-old larvae marked at age 9 d, seven increments were counted; for 23-d-old larvae marked at age 9 d, six and seven were counted.

Increment counts on marked otoliths were fairly accurate. On 14-d-old larvae (n=4) marked at day 9, we counted seven increments from the core to the ALC mark, and four to six ($\bar{x}$=5.0; five expected) from the mark to the otolith edge. On 23-d larvae (n=5) that were marked on day 9 and day 16, we counted six to seven ($\bar{x}$=6.6) increments from the core to the first mark, 14 to 15 ($\bar{x}$=14.7) from the core to the second mark, and four to nine ($\bar{x}$=7.6) from the second mark (16-d-old) to the edge (23-d-old). For wild-caught larvae (n=12) (which ranged from 34.4 to 70.2 mm SL, were marked at 7-d intervals, and which were preserved 14 d after marking), we observed seven to eight ($\bar{x}$=7.0) increments between marks and 13–15 ($\bar{x}$=14.2) increments between the last mark and the edge.

Table 2

Analysis of variance results for increment counts versus age, and inverse regression for age versus increment counts (inverse regression) for all larvae and juveniles (n=69) of known-age spotted seatrout, *Cynoscion nebulosus*. SE = standard error.

Dependent variable	Slope	SE	Intercept	SE	P
Counts	1.0296	0.0172	−1.9867	0.3574	0.0001
Age	0.9538	0.0159	2.2273	0.3135	0.0001

Discussion

Our overestimation of ages, in our initial analysis (see "Materials and methods" section), from increment counts of older juveniles is difficult to relate to environmental factors. Overestimation of age is not common, although Fives et al. (1986) reported that larger bay anchovies, *Anchoa mitchelli*, in any known age group generally had more growth increments than smaller fish. Nielson and Geen (1982, 1985) noted that for salmonids, feeding frequency, exposure to warm or cool temperature cycles twice in a 24-h period, and an enforced increase in activity increased the rate of increment formation. Fish in our study did not undergo such cyclic events.

Campana and Moksness (1991), from a detailed appraisal of accuracy and precision of age estimates derived from otoliths, concluded that accuracy of age determination from validation experiments is probably "optimistic" owing in part to the constraints and limitations of validation studies done under laboratory conditions. The marked size difference of our known-age 32-d-old juveniles (16.2–34.6 mm SL) was undoubtedly a result of laboratory rearing conditions and indicated that even with appropriate photoperiod and feeding conditions, caution should be used when interpreting rings from older laboratory-reared juveniles, especially when size ranges are highly variable as in our study. For older known-age laboratory-reared material, multiple markings should be employed to discern those areas where interpretation is difficult and to discern subdaily rings.

Previous validation studies of spotted seatrout have indicated that rings are deposited daily, but central rings are difficult to interpret (McMichael and Peters, 1989). McMichael and Peters (1989) used otoliths mounted whole from tetracycline-marked wild-caught larvae and juveniles (7–10 mm). Although they were able to observe the formation of daily rings, they had difficulty in interpreting central rings. They used the average measurement to the tenth ring (50 µm, SD=2) taken from few exception-

ally clear juveniles. Our measurements from 23-d (n=12) and 32-d-old (n=15) juveniles averaged 52.4 µm (SD=8.1). Although our data were more variable, because we did not select only clear otoliths, our measurement to the tenth increment was similar to that of McMichael and Peters (1989), indicating we were interpreting the central increments fairly accurately.

Our relative lack of success in marking known-age larvae could be due to an inadequate concentration of ALC (50 mg/L) or insufficient immersion time at that concentration. Thomas et al. (1995) produced high mark quality on 6.0–9.0 mm red drum larvae at concentrations of 100 mg/L for as little as 2-h immersions. Fish mortality was minimal (and mark quality high) for immersion times up to 24 h at that concentration. A concentration of 50 mg/L for 4 h appears to be inadequate, however, for spotted seatrout larvae. Because of the relative lack of success in marking small larvae at 50 mg/L, larger juveniles were immersed in a concentration of 100 mg /L and marking success was relatively high after 4-h immersion, but still not 100%. Thomas et al. (1995) found that mortality of larvae was fairly high (>65%) at concentrations of 250 mg/L or higher; therefore longer immersion times are probably necessary for 100% marking success. Other investigators have had difficulties in marking larvae with tetracycline immersion that were related to divalent cations in full strength seawater (Campana and Nielson, 1982; Hettler, 1984; Gleason and Recksiek, 1990).

In conclusion, we caution investigators that our interpretation of increment counts for spotted seatrout may not be valid for other studies. The skill of the otolith reader is a critical component in otolith microstructure analysis (Campana and Moksness, 1991); therefore, microstructure analysis studies on spotted seatrout should require a separate validation study for each reader.

Acknowledgments

We are grateful to Cameron Pratt for collecting wild-caught fish, Patti Pickering for rearing and marking the fish, and Curtis Lewis for photographing and preparing the otolith figure. Dean Ahrenholz, Jon Hare, and two anonymous reviewers reviewed the manuscript and provided many valuable comments. This research was supported by the NOAA Coastal Ocean Program.

Literature cited

Ahrenholz, D. W., G. R. Fitzhugh, J. A. Rice, S. W. Nixon, and W. C. Pritchard.
1995. Confidence of otolith ageing through the juvenile stage for Atlantic menhaden, *Brevoortia tyrannus*. Fish. Bull. 93:209–216.

Campana, S. E., and E. Moksness.
1991. Accuracy and precision of age and hatch date estimates from otolith microstructure examination. ICES J. Mar. Sci. 48:303–316.

Campana, S. E., and J. D. Nielson.
1982. Daily growth increments in otoliths of starry flounder (*Platichthys stellatus*) and the influence of some environmental variables in their production. Can. J. Aquat. Sci. 39:937–942.

Crecco, V. C., and T. F. Savoy.
1985. Effects of biotic and abiotic factors on growth and relative survival of young American shad, *Alosa sapidissima*, in the Connecticut River. Can. J. Fish. Aquat. Sci. 42:1640–1648.

Fives, J. M., S. M. Warlen, and D. E. Hoss.
1986. Aging and growth of larval bay anchovy, *Anchoa mitchelli*, from the Newport River Estuary, North Carolina. Estuaries 9:362–367.

Geffen, A. J.
1992. Validation of otolith increment deposition rate. *In* Otolith microstructure examination and analysis (D. K. Sevenson and S. E. Campana, eds.), p. 101–113. Can. Spec. Publ. Fish. Aquat. Sci.

Gleason, T. R., and D. A. Bengtson.
1996. Size-selective mortality of inland silversides: evidence from otolith microstructure. Trans. Am. Fish. Soc. 125:860–873.

Gleason, T. R., and C. W. Recksiek.
1990. Preliminary field validation of daily growth increments in lapillar otoliths of juvenile cunner. *In* Fish marking techniques (N. C. Parker and five coeditors), p. 562–565. Am. Fish. Soc., Symposium 7, Bethesdsa, MD.

Hare, J. A., and R. K. Cowen.
1997. Size, growth, development and survival of planktonic larvae of *Pomatomus saltatrix* (Pisces: Pomatomidae). Ecology 78:2415–2431.

Hettler, W. F.
1984. Marking otoliths by immersion of marine fish larvae in tetracycline. Trans. Am. Fish. Soc. 113:370–373.

Jenkins, G. P., M. Shaw, and B. D. Stewart.
1993. Spatial variation in food-limited growth of juvenile greenback flounder, *Rhombosolea tapirina*: evidence from otolith daily increments and otolith scaling. Can. J. Fish. Aquat. Sci. 50:2558–2567.

Leger, P. H., D. A. Bengtson, K. L. Simpson, and P. Sorgeloos.
1986. The use and nutritional value of *Artemia* as a food source. Oceanogr. Mar. Biol. Rev. 24:521–623.

Maillet, G. L., and D. M. Checkley Jr.
1991. Storm-related variation in the growth rate of otoliths of larval Atlantic menhaden *Brevoortia tyrannus*: a time series analysis of biological and physical variables and implications for larva growth and mortality. Mar. Ecol. Prog. Ser. 79:1–16.

McMichael, R. H., and K. M. Peters.
1989. Early life history of spotted seatrout, *Cynoscion nebulosus* (Pisces: Sciaenidae), in Tampa Bay, Florida. Estuaries 12:98–110.

Nielson, J. D., and G. H. Geen.
1982. Otoliths of chinook salmon (*Oncorhynchus tshawytscha*): daily growth increments and factors influencing their production. Can. J. Fish. Aquat. Sci. 39:1340–1347.
1985. Effects of feeding regimes and diel temperature cycles on otolith increment formation in juvenile chinook salmon, *Oncorhynchus tshawytscha*. Fish. Bull. 83:91–101.

Rice, J. A., L. B. Crowder, and F. P. Binkowski.
1985. Evaluating otolith analysis for bloater, *Coregonus hoyi*: do otoliths ring true. Trans Am. Fish. Soc. 114:532–539.

Sabo, M. J., and D. J. Orth.
1996. Absence of size-selective mortality among larval smallmouth bass in a Virginia stream. Trans. Am. Fish. Soc. 125: 920–924.

SAS Institute, Inc.
1985. SAS/STAT guide for personal computers, version 6 ed. SAS Institute, Inc., Cary, NC, 378 p.

Thomas, L. M., S. A. Holt, and C. Arnold.
1995. Chemical marking techniques in larval and juvenile red drum (*Sciaenops ocellatus*) otoliths using different flourescent markers. *In* Recent developments in fish otolith research (D. H. Secor, J. M. Dean, and S. E. Campana, eds.), p. 703–717. Univ. South Carolina Press, Columbia, SC.

Thorrold, S. R., and D. M. Williams.
1989. Analysis of otolith microstructure to determine growth histories in larval cohorts of a tropical herring (*Herklotsichthys castelnaui*). Can. J. Fish. Aquat. Sci. 46:1615–1624.

Consumption of Pacific herring (*Clupea pallasi*) eggs by greenling (Hexagrammidae) in Prince William Sound, Alaska

Christopher N. Rooper

Lewis J. Haldorson

Juneau Center for Fisheries and Ocean Sciences
University of Alaska Fairbanks
11120 Glacier Hwy, Juneau, Alaska 99801
Present address (for C. N. Rooper: Fishery Sciences Building
Box 355020
University of Washington
Seattle, Washington 98195

E-mail address (for C. N. Rooper): rooper@fish.washington.edu

Predation is an important process regulating egg survival in marine systems (Bailey and Houde, 1989). Pacific herring (*Clupea pallasi*) spawn demersal adherent eggs on shallow subtidal and intertidal substrates. Consequently, their eggs are available to a variety of predators throughout incubation. Documented predators of herring eggs include birds, invertebrates, marine mammals, and fish (Palsson, 1984). Avian predators were responsible for over 95% of the herring eggs lost in the intertidal zone in Holmes Harbor, Washington, in 1946 (Cleaver and Franett, 1946), 39% of the intertidal herring eggs lost on the west coast of Vancouver Island from 1947 to 1950 (Outram, 1958), and 70% of the herring eggs lost in Yaquina Bay, Oregon, in 1970 (Steinfeld, 1971). Estimates of egg predation by birds at two sites in British Columbia in 1988 and 1989 were 3.0% and 3.5% of the total eggs deposited by herring (Haegele and Schweigert, 1989; 1991).

Much less is known about the effects of other predators because studies to quantify Pacific herring egg loss from predators other than birds have been rare. In Barkeley Sound, British Columbia, predation by invertebrates accounted for 13.0% of the total herring eggs deposited, whereas gray whales consumed 3.0% of the total eggs deposited (Haegele and Schweigert, 1989). In 1989, herring egg loss due to epibenthic invertebrates was 4.1% of the total eggs spawned in Georgia Strait, British Columbia (Haegele and Schweigert, 1991).

Fish predation on Pacific herring eggs has not been studied in the northeast Pacific, although some studies have been done on the deeper-spawning Atlantic herring (*Clupea harengus*). Historically, abundance of North Sea haddock (*Melanogrammus aeglefinus*) and saithe (*Pollachius virens*) with stomachs containing Atlantic herring eggs were used as indicators of the concentrations of herring eggs (Hempel and Hempel, 1971); in years of light spawning, cod and haddock can consume up to 60% of the total eggs deposited.[1] Stomachs of sand eels (*Ammodytes marinus*) have been observed to be full of Atlantic herring eggs (Rankine and Morrison, 1989), and perch (*Perca fluviatilis*) has been found to be the most important consumer of herring eggs in the Archipelago Sea (Rajasilta et al., 1993). For Atlantic herring off the coast of Norway, egg loss due to haddock consumption has been estimated at 4.2% of the total eggs spawned (Toreson, 1991). Total Atlantic herring egg loss due to consumption by winter flounder (*Pseudopleuronectes americanus*) was at least 7% of the total egg abundance at a site in the Northwest Atlantic (Tibbo et al., 1963).

[1] Johannessen, A. 1980. Predation on herring (*Clupea harengus*) eggs and young larvae. International Council for the Exploration of the Sea, Council Meeting/ 1980, H:33, 12 p.

Lack of knowledge about fish predation on Pacific herring eggs and the importance of herring as a forage fish in the Northeast Pacific Ocean, led us to study predation on herring eggs in Prince William Sound, Alaska. The objective of our study was to estimate total consumption of herring eggs by some fish predators with the Elliot-Persson model (Elliot and Persson, 1978).

Materials and methods

Our study was conducted after herring spawning was completed on northern Montague Island in Prince William Sound, Alaska (Fig. 1), during late April and early May, 1995. Two variable mesh gill nets, 30.5 m long and 2.4 m deep, were used to collect fish near incubating herring eggs in the subtidal and intertidal zones at eight transects. Stretched-mesh sizes ranged from 2.5 to 12.7 cm. Panels of same-size mesh were equal length and depth (6.1 m × 2.4 m), and a total of five panels per net were used. A standardized fishing plan was carried out from one to three transects per day. Two nets were set at the bottom parallel to the shoreline at each transect. Depths fished depended on tide stage; at high tide, depths fished were 0.0 m and –3.0 m, whereas at low tide, depths fished were –1.5 m and –3.0 m in relation to mean low water. Logistical constraints limited fishing to one series of gillnet samples centered around the daylight high tide, and one series of samples centered around the daylight low tide. Each series consisted of three one-hour sets of the two nets, for a total of six gillnet sets over each tide stage, and a total of 96 sets equally spread over the eight transects.

Fish captured were identified by species and measured for fork length. Time of catch, net soak time, and tide stage were also recorded for each fish. Fish stomachs were removed and preserved in 10% buffered formalin. Stomach contents were categorized by type of prey (herring eggs, vegetation, crustaceans, etc.) and weighed to the nearest 0.01 g. Wet weights of each group of stomach contents were recorded, and herring eggs were subsampled to determine the

Manuscript accepted 1 December 1999.
Fish. Bull. 98:655–659 (2000).

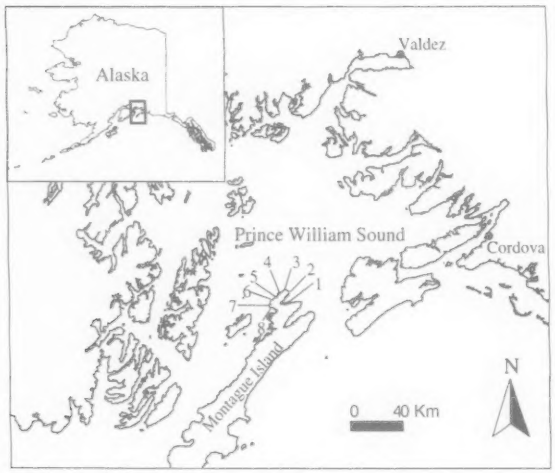

Figure 1

Study transects on Montague Island in Prince William Sound, Alaska, where gill nets were used to collect fish predators of herring spawn in 1995.

number of eggs per g. By multiplying the wet weight of herring eggs contained in each stomach by the number of eggs per g, the total number of herring eggs in each stomach was estimated.

Based on stomach-content analysis, estimates of daily ration were calculated only for greenling species. Because of the small number of each greenling species caught, these species were combined to estimate herring egg consumption. Estimates of daily ration were calculated by using the Elliot and Persson (1978) model,

$$C_t = \frac{(S_t - S_0 e^{-Rt}) \times Rt}{1 - e^{-Rt}}, \quad (1)$$

where C_t = food consumption during daylight hours;
R = the calculated gut clearance rate;
t = the number of daylight hours; and
S_0 and S_t = average stomach contents at time 0 and time t, respectively.

Estimates of stomach contents were obtained by examining fish caught during gillnet sampling and were assumed to be constant over daylight hours. The gut clearance rate (R) was calculated from a relationship of species evacuation rate versus temperature for marine and freshwater fish:

$$R = 0.0175T - 0.0442 \quad \text{(Worobec, 1984)}. \quad (2)$$

The average temperature (T) over the incubation period at a Montague Island transect was used in Equation 2. We had to extrapolate the equation in Worobec (1984) because their temperature range was warmer than ours. Initial consumption of food at the onset of daylight was calculated according to the Elliot-Persson model by using the equation

$$C_{initial} = S_{average} - S_0 e^{-Rt}, \quad (3)$$

where $S_{average}$ = the average eggs per stomach from gillnet samples; and
t = the nighttime hours.

Adding $C_{initial}$ and C_t gives an estimate of the daily consumption (C_d) of herring eggs over 24 h. Total consumption over the incubation period was then calculated by

$$C_{total} = C_d \times D \times I, \quad (4)$$

where C_d = the calculated daily consumption in numbers of eggs;
D = predator density; and
I = length of the incubation period in d.

Two previous studies estimated nearshore fish abundance on Montague Island. The first study estimated greenling density by using SCUBA surveys (Jewett et al.[2]) and the second study estimated nearshore fish biomass (Rosenthal[3]). We used both these estimates in separate calculations of Equation 4 to derive consumption estimates for greenling.

In the first calculation we used greenling density estimates in the subtidal zone from Jewett et al. (1995); total consumption per m^2 was compared directly with the average number of eggs per m^2 estimated in 1995. To use the biomass estimates from Rosenthal (1980), we changed the daily ration in egg numbers to a daily ration in egg biomass. Assuming isometric growth for greenling and using the end points of greenling length and weight ranges reported in Rosenthal (1980), we calculated the weight of each greenling caught during gillnet sampling. Using these two calculations for each fish sampled, we then estimated the daily ration as a percentage of body weight. Then, incorporating biomass estimates for greenling in Prince William Sound from Rosenthal (1980) and the number of incubation days for herring eggs in 1995, we calculated the total weight of eggs consumed per km^2 by converting Equation 4 to

$$C_t = B_g \times C_w \times I, \quad (5)$$

[2] Jewett, S. C., T. A. Dean, R. O. Smith, M. Stekoll, L. J. Haldorson, D. R. Laur and L. McDonald. 1995. The effects of the *Exxon Valdez* oil spill on shallow subtidal communities in Prince William Sound, Alaska 1989–93. *Exxon Valdez* Oil Spill Restoration Project Final Report (Restoration Project 93047; subtidal study number 2A), Alaska Dept. of Fish and Game, Habitat and Restoration Division, Anchorage, Alaska, 178 p.

[3] Rosenthal, R. J. 1980. Shallow water fish assemblages in the northeastern Gulf of Alaska: habitat evaluation, species composition, abundance, spatial distribution and trophic interaction. *In* Environmental assessment of the Alaskan continental shelf, p. 451–540. Final reports of principal investigators, 17: biological studies, NOAA/NOS, Office of Oceanography & Marine Services.

Table 1

Total gillnet hours fished and mean catch per hour for each fish species captured at Montague Island, Alaska, in 1995. Numbers in parentheses indicate total number of fish captured during sampling.

		Catch (no. of fish) per hour				
Transect	Hours fished	Greenling (two species)	Dolly Varden	Starry flounder	Red Irish lord	Great sculpin
1	13:48	(0)	0.435 (6)	0.072 (1)	(0)	(0)
2	14:26	(0)	0.069 (1)	(0)	(0)	(0)
3	13:28	0.446 (0)	(0)	(0)	(0)	(0)
4	13:52	0.072 (1)	(0)	(0)	(0)	0.072 (0)
5	13:32	0.296 (4)	(0)	(0)	0.074 (1)	0.074 (1)
6	12:15	0.082 (1)	(0)	(0)	(0)	(0)
7	14:34	0.069 (1)	0.069 (1)	(0)	(0)	(0)
8	14:39	(0)	(0)	(0)	(0)	0.068 (1)
Average CPUE		0.120 (13)	0.072 (8)	0.009 (1)	0.009 (1)	0.027 (1)

where C_t = the total biomass of eggs consumed per km^2;
B_g = the biomass of greenling;
C_w = the daily ration as a percentage of fish weight; and
I = the length of the incubation period in d.

This estimate of egg biomass consumed was applied to the biomass estimates of eggs spawned on Montague Island to obtain a percentage of the total herring eggs consumed by greenling.

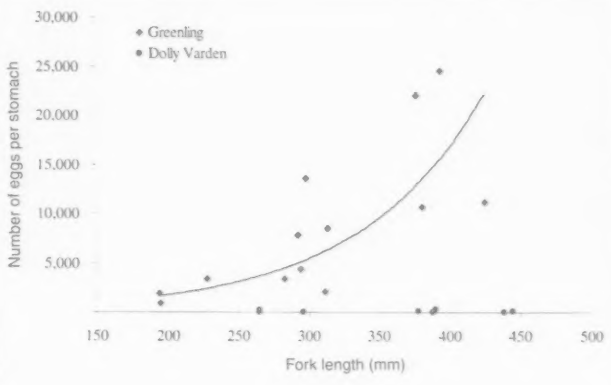

Figure 2

Number of eggs per stomach for combined greenling species (n=13) and Dolly Varden char (n=8) captured by gillnetting at herring spawning bed transects in 1995. The line represents the predicted exponential increase in eggs per stomach with increasing fork length; r^2 for the predicted versus the observed relationship was 0.55.

Results

Six fish species were caught during gillnet sampling: rock greenling (*Hexagrammos lagocephalus*), kelp greenling (*Hexagrammos decagrammus*), Dolly Varden char (*Salvelinus malma*), starry flounder (*Platichthys stellatus*), red Irish lord (*Hemilepidotus hemilepidotus*) and great sculpin (*Myoxocephalus polyacanthocephalus*). The most common fish caught were the two greenling species, followed by Dolly Varden and great sculpin; only one red Irish lord and one starry flounder were caught. Average catch for all species was relatively low, ranging from 0.009 fish per h (SE=0.008) for starry flounder and red Irish lord to 0.120 fish per h (SE=0.052) for the greenling species combined (Table 1). Only greenling and Dolly Varden consumed herring eggs; all 13 greenling stomachs contained eggs, whereas just 4 of 8 Dolly Varden stomachs contained eggs. Stomachs of other fish species contained a combination of unidentifiable fish and invertebrates. The average number of eggs per stomach was 87 (SE=40.4) for Dolly Varden, and 8785 (SE=2107.6) for greenling. The number of herring eggs per greenling stomach increased exponentially with length (Fig. 2).

A pattern in greenling and Dolly Varden catch distributions was apparent; Dolly Varden were caught exclusively in embayments, whereas all greenling, except one, were caught on the outer coast of Montague Island. The average temperature during incubation at –1.5 m depth was 5.8°C at transect 4, resulting in an estimated instantaneous evacuation rate of 0.057 per h. The daily ration calculated with that evacuation rate was 11,984 eggs per d (Table 2).

Subtidal surveys of fish abundance in Prince William Sound found an average of 0.0889 greenling per m^2 on

Table 2

Calculations for estimating daily consumption of herring eggs by greenling with the Elliot-Persson model.

Elliot-Persson model for estimating daily consumption (Eq. 1)	
1 Consumption during daylight hours (assuming constant stomach fullness), C	
t = average daylight hours from 29 April to 20 May 1995	16.67
Instantaneous evacuation rate (R)	0.057
S_0	9264
S_t	9264
C_t	8816
2 Initial consumption at onset of feeding, $C_{initial}$	
Decrease in stomach contents during night, $S_t = S_0 e^{-Rt}$	
S_0	9264
t = average nighttime hours from 20 April to 20 May 1995	7.33
Instantaneous evacuation rate (R)	0.057
S_t	6096
$C_{initial} = S_0 - S_t$	3168
3 Total consumption over 24 hours = $C_{initial} + C_t$	11,984

island points in shallow waters from 2 to 20 m deep on Montague Island (Jewett et al., 1995). According to the daily ration calculated above, daily consumption of herring eggs by greenling would be 1065 eggs per m^2. In 1995, the incubation period for herring eggs was 21 d in Prince William Sound; therefore total removal during incubation would have been 22,373 eggs per m^2. In 1995, the average number of eggs per m^2 was 606,831, on Montague Island.[4] Therefore, using the daily consumption above, we estimated that 3.7% of the eggs deposited were consumed by greenling over the course of incubation.

The weight of the estimated daily ration (11,984 eggs) for greenling was 38.3 g, or weight of the eggs in a greenling stomach multiplied by 1.29. From this conversion factor, daily ration as a percentage of greenling body weight was estimated as 6% per d. Results from dive surveys from Rosenthal (1980) have shown a greenling biomass at Zaikoff Point on Montague Island of approximately 35,000 kg/km^2. Multiplying this biomass estimate by the daily ration as a percentage of body weight and by the number of incubation days in 1995, yields an egg consumption estimate of 44,100 kg/km^2. In 1995, an estimated 5,922,673 kg of eggs were deposited over a 3.05-km^2 area on Montague Island.[2] If one assumes that all greenling move into subtidal and intertidal areas to feed on eggs deposited there, then greenling would have consumed 2.3% of the total eggs deposited.

Discussion

Calculation of daily ration by the Elliot-Persson method presented here assumes that greenling maintain a full stomach throughout the entire daylight period. The exponential increase in eggs per stomach with greenling length suggests that our assumption that greenling maintain a constant state of gut fullness is correct because greenling stomach volume should increase exponentially with body length. Our method for estimating total consumption of herring eggs by greenling also assumes that there is no numerical response to availability of eggs. If greenling move from deeper water to the band of herring eggs, the estimate of consumption may be higher. Migration of greenling to the spawning beds from areas where no spawn was deposited would also have increased the consumption estimate.

By sampling during slack tide periods, total consumption of eggs may have been underestimated. If greenling were actively feeding during the time when they encountered gill nets, their stomach contents may not have been representative of the entire daylight period. Greenling stomach contents may have been less during times of active feeding than during the rest of the day. Gill nets are also known to be both size selective and species selective (Hay et al., 1986; Methven and Schneider, 1998). Selectivity, therefore, probably influenced our results both on account of the nets selecting for a small range of greenling sizes and selecting only species that exhibited behaviors that made them susceptible to capture. If the average length of greenling captured during sampling was larger than the average length of greenling in the total population, we may have overestimated the total consumption of eggs. However, the estimate of total consumption of herring eggs is likely to have been underestimated for Prince William Sound, because the estimate is only for two species of fish. Because greenling make up only 56% by number and 59% by biomass of the fish species at Montague Island (Rosenthal, 1980), many other species inhabiting the zone covered by herring eggs would have access to the rich food source the eggs provide. Our results are similar to other studies in the Atlantic where predation on herring eggs by fish has typically been estimated at less than 10% of the total herring eggs (Tibbo et al., 1963; Toreson, 1991).

A concurrent study of egg loss in Prince William Sound has shown that herring egg loss from spawning beds increases at shallower depths (Rooper et al., 1999). Consumption of eggs by bird species indicate avian predators may be responsible for removals of large numbers of eggs (27%),[5] most of which are lost in the intertidal zone. The different levels of predation in the intertidal and subtidal zones by birds and fish may be the underlying cause of the higher egg loss rates observed at shallower depths. If predation is an important factor regulating survival of eggs to time of hatching, then herring behavior may lend itself to depensatory mortality. Concentration of herring

[4] Wilcock, J., and K. Hyer. 1998. Personal commun. Alaska Department of Fish and Game, P.O. Box 669, Cordova, AK 99754.

[5] Bishop, M. A., and P. Green. 1998. Unpubl. data. USFS-CRDI, PO Box 1460, Cordova AK 99574.

stocks into a relatively small area during spawning and the resulting spatial concentration of eggs in the spawning beds could lead to high egg losses owing to predation even in years of low herring biomass. This in turn could drive the abundance of herring eggs even lower, as predators continued to concentrate on an ever-dwindling resource.

In summary, our study estimated that two greenling species consumed between 2.3% and 3.7% of the total herring eggs deposited on Montague Island in Prince William Sound in 1995. Greenling represent only a portion of the fish species in Prince William Sound; therefore predation by other fish species would probably increase the consumption estimates. Although consumption of herring spawn by fish species has not been extensively studied in the Pacific, the results of our study indicate the importance of predation by fish species on the mortality of herring eggs in spawning beds.

Acknowledgments

We thank John Wilcock and Karen Hyer, Alaska Department of Fish and Game, for providing the egg abundance data, as well as Dr. Terrance Quinn II and Jennifer Boldt, University of Alaska Fairbanks, for their technical support. Funds for this study were provided by the Exxon Valdez Trustee Council through the Alaska Department of Fish and Game, Herring Natal Habitats Project no. 95166.

Literature cited

Bailey, K. M., and E. D. Houde.
1989. Predation on eggs and larvae of marine fishes and the recruitment problem. Adv. Mar. Biol. 25, 82 p.

Cleaver, F. C., and D. M. Franett.
1946. The predation by sea birds upon the eggs of the Pacific herring (*Clupea pallasi*) at Holmes Harbor during 1945. Washington State Dept. Fish. Biol. Rep. 46B, 18 p.

Elliot, J. M., and L. Persson.
1978. The estimation of daily rates of food consumption for fish. J. Animal Ecol. 47:977–991.

Haegele, C. W., and J. F. Schweigert.
1989. Egg loss from Pacific herring spawns in Barkeley Sound in 1988. Can. Manage. Rep. Fish. Aquat. Sci. 2037, 40 p.
1991. Egg loss in herring spawns in Georgia Strait, British Columbia. *In* Proceedings of the International Herring Symposium, Anchorage, Alaska, October 23–25, 1990, p. 309–322. Univ. Alaska, Fairbanks, AK.

Hay, D. E., K. D. Cooke, and C. V. Gissing.
1986. Experimental studies of Pacific herring gillnets. Fish. Res. 4:191–211.

Hempel, I., and G. Hempel.
1971. An estimate of mortality in eggs of North Sea herring (*Clupea harengus* L.). Rapp. P.-V. Reun. Cons. Int. Explor. Mer 160:24–26.

Methven, D. A., and D. C. Schneider.
1998. Gear-independent patterns of variation in catch of juvenile Atlantic cod (*Gadus morhua*) in coastal habitats. Can. J. Fish. Aquat. Sci. 55:1430–1442.

Outram, D. M.
1958. The magnitude of herring spawn losses due to bird predation on the west coast of Vancouver Island. Fish. Res. Board Can. Pac. Biol. Stat. Prog. Rep. 111:9–13.

Palsson, W. A.
1984. Egg mortality upon natural and artificial substrata within Washington state spawning grounds of Pacific herring (*Clupea harengus pallasi*). M.S. thesis, Univ. Washington, Seattle, WA, 191 p.

Rajasilta, M., J. Eklund, J. Hanninen, M. Kurkilahti, M., J. Kaaria, P. Rannikko, and M. Soikkeli.
1983. Spawning of herring (*Clupea harengus membras* L.) in the Archipelago Sea. ICES J. Mar. Sci. 50:223–246.

Rankine, P. W., and J. A. Morrison.
1989. Predation on herring larvae and eggs by sand-eels *Ammodytes marinus* (Rait) and *Hyperoplus lanceolatus* (Lesauvage). J. Mar. Biol. Assoc. U. K. 69:493–498.

Rooper, C. N., L. J. Haldorson, and T. J. II Quinn.
1999. Habitat factors controlling Pacific herring (*Clupea pallasi*) egg loss in Prince William Sound, Alaska. Can. J. of Fish. Aquat. Sci. 56:1133–1142.

Steinfeld, J. D.
1971. Distribution of Pacific herring spawn in Yaquina Bay, Oregon, and observations on mortality through hatching. M.S. thesis, Oregon State University, Corvallis, OR, 75 p.

Tibbo, S. N., D. J. Scarratt, and P. W. G. McMullon.
1963. An investigation of herring (*Clupea harengus* L.) spawning using free-diving techniques. J. Fish. Res. Board Can. 20:1067–1079.

Toreson, R.
1991. Predation on the eggs of Norwegian spring-spawning herring (*Clupea harengus* L.) on a spawning ground on the west coast of Norway. ICES J. Mar. Sci. 48:15–21.

Worobec, M. N.
1984. Field estimates of the daily ration of winter flounder, *Pseudopleuronectes americanus* (Walbaum), in a southern New England salt pond. J. Exp. Mar. Biol. Ecol. 77:183–196.

Superintendent of Documents **Publications** Order Form

*5178

☐ YES, please send me the following publications:

____ Subscriptions to *Fishery Bulletin*
for $50.00 per year ($62.50 foreign)

The total cost of my order is $ _____ . Prices include regular domestic postage and handling and are subject to change.

_____
(Company or Personal Name) (Please type or print)

_____
(Additional address/attention line)

_____
(Street address)

_____
(City, State, ZIP Code)

_____
(Daytime phone including area code)

_____
(Purchase Order No.)

Charge your order. IT'S EASY!

VISA

MasterCard

Please Choose Method of Payment:

☐ Check Payable to the Superintendent of Documents
☐ GPO Deposit Account ☐☐☐☐☐☐☐–☐
☐ VISA or MasterCard Account
☐☐☐☐☐☐☐☐☐☐☐☐☐☐☐☐
☐☐☐☐ (Credit card expiration date)

To fax your orders (202) 512-2250

_____
(Authorizing Signature)

Mail To: Superintendent of Documents
P.O. Box 371954, Pittsburgh, PA 15250-7954

Thank you for your order!

Fishery Bulletin

Guide for Contributors

Content

Articles published in *Fishery Bulletin* describe original research in fishery marine science, engineering and economics, and the environmental and ecological sciences, including modeling. Articles may range from relatively short to extensive.

Notes are reports of 5 to 10 pages without an abstract and describing methods or results not supported by a large body of data.

Although all contributions are subject to peer review, responsibility for the contents of papers rests upon the authors and not upon the editor or the publisher. It is therefore important that the contents of the manuscript are carefully considered by the authors.

Submission of an article is understood to imply that the article is original and is not being considered for publication elsewhere. Manuscripts should be written in English. Authors whose native language is not English are strongly advised to have their manuscripts checked by English-speaking colleagues prior to submission.

Preparation

Title page should include authors' full names and mailing addresses, the corresponding author's telephone, FAX number, and e-mail address, and a list of key words to describe the contents of the manuscript.

Abstract should not exceed one double-spaced typed page. It should state the main scope of the research but emphasize its conclusions and relevant findings. Because abstracts are circulated by abstracting agencies, it is important that they represent the research clearly and concisely.

Text must be typed double-spaced throughout. A brief introduction should portray the broad significance of the paper; the remainder of the paper should be divided into the following sections: Materials and methods, Results, Discussion (or Conclusions), and Acknowledgments. Headings within each section must be short, reflect a logical sequence, and follow the rules of multiple subdivision (i.e. there can be no subdivision without at least two items). The entire text should be intelligible to interdisciplinary readers; therefore, all acronyms, abbreviations, and technical terms should be spelled out the first time they are mentioned. The scientific names of species must be written out the first time they are mentioned; subsequent mention of scientific names may be abbreviated. Follow Scientific Style and Format: the CBE Manual for Authors, Editors, and Publishers (6th ed.), for editorial style, and the most current issue of the American Fisheries Society's Common and Scientific Names of Fishes from the United States and Canada, for fish nomenclature. Dates should be written as follows: 11 November 1991. Measurements should be expressed in metric units, e.g. metric tons as t; if other units of measurement are used, please make this fact explicit to the reader. The numeral one (1) should be typed as a one, not as a lower-case el (l). Use of appendices is discouraged.

Text footnotes should be numbered with Arabic numerals and inserted at the bottom of text. Footnote all personal communications, unpublished data, and unpublished manuscripts with full address of the communicator or author, or, as in the case of unpublished data, where the data are on file. Authors are advised to avoid references to nonstandard (gray) literature, such as internal, project, processed, or administrative reports. Where these references are used, please include whether they are available from NTIS (National Technical Information Service) or from some other public depository.

Literature cited comprises published works and those accepted for publication in peer reviewed literature (in press). Follow the name and year system for citation format. In the text, cite as follows: Smith and Jones (1977) or (Smith and Jones, 1977). If there is a sequence of citations, list alphabetically by author(s): Smith, 1987; Smith and Jones, 1985; Smith and Peterson, 1986. Abbreviations of serials should conform to abbreviations given in Serial Sources for the BIOSIS Previews Database. Authors are responsible for the accuracy and completeness of all citations.

Tables should not be excessive in size and must be cited in numerical order in the text. Headings within tables should be short but ample enough to allow the table to be intelligible on its own. All unusual symbols must be explained in the table legend. Other incidental comments may be footnoted with italic numerals. Use the asterisk only to indicate probability in statistical data. Zeros should precede all decimal points for values less than one.

Figures must be cited in numerical order in the text. The senior author's last name and the figure number should be written on the back of each one. Hand-drawn illustrations should be submitted as originals and not as photocopies. Submit photographs as glossy prints or slides with good contrast, otherwise we cannot guarantee a good final printed copy. Graphs should be submitted as laser-printed copies, not as photocopies. Label all figures with Helvetica typeface and capitalize the first letter of the first word in axis labels. Italicize species name and variables in equations. Use zeros before all decimal points. Use uppercase Times Roman bold typeface to label the parts of a figure, e.g. A, B, C, etc. Each figure legend should explain all symbols and abbreviations in the figure and should be double-spaced and placed at the end of the manuscript.

Copyright law Government publications are not copyrighted; they fall within the public domain. If an author reproduces any part of a government publication in his work, reference to source is appreciated.

Submission

Send printed copies (original and three copies without staples) to the Scientific Editor:

Dr. John V. Merriner
Southeast Fisheries Science Center
National Marine Fisheries Service
101 Pivers Island Road
Beaufort, NC 28516

Once the manuscript has been accepted for publication, you will be asked to submit an electronic copy of your manuscript to the Managing Editor. The electronic copy should be submitted in WordPerfect or Microsoft Word text format and placed on a 3.5-inch disk that is double-sided, double or high density, and that is compatible with either DOS or Macintosh systems.

A copy of page proofs will be sent to the author for final approval prior to publication.
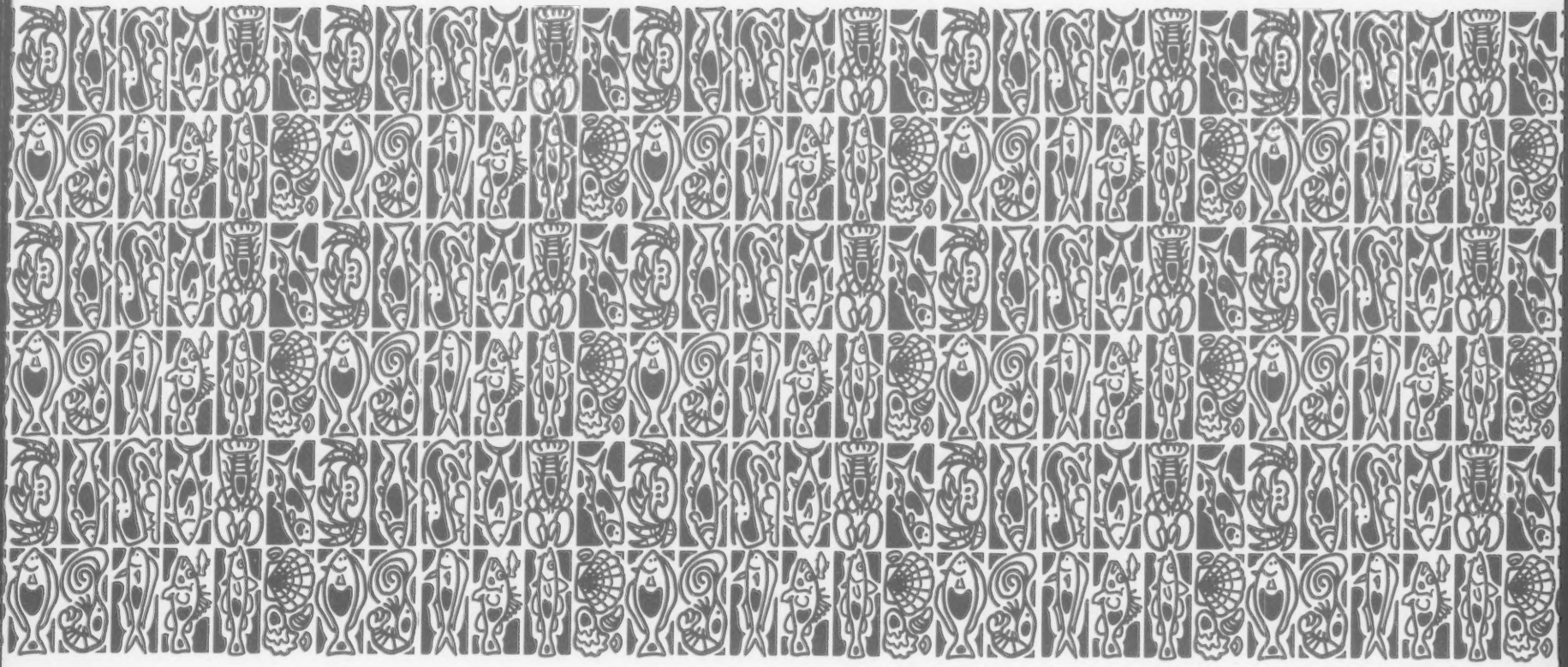
Reprints (copies of published articles and notes) are available free of charge to the senior author (50 copies) and to his or her laboratory (50 copies). Additional copies may be purchased in lots of 100 when the author receives page proofs.